APPALACHIAN DELTA PLAIN PALEOECOLOGY OF THE CRETACEOUS WOODBINE FORMATION AT THE ARLINGTON ARCHOSAUR SITE NORTH TEXAS

by

DEREK JASON MAIN

Presented to the Faculty of the Graduate School of

The University of Texas at Arlington in Partial Fulfillment

of the Requirements

for the Degree of

DOCTOR OF PHILOSOPHY

THE UNIVERSITY OF TEXAS AT ARLINGTON

May 2013

DEDICATION

This dissertation is dedicated in loving memory to my father:

Norman A. Main 1938-2003.

"Come my friends, tis not too late to seek a newer world. Push off and sitting well in order smite the sounding furrows, for my purpose holds to sail off the bathes of all the western stars,
until I die. To pursue knowledge like a sinking star. To strive, to seek, to find and not to yield. "

Alfred Lord Tennyson

"The Cosmos is full beyond measure of elegant truths, of exquisite interrelationships, the awesome machinery of nature."

Carl Sagan

ACKNOWLEDGMENTS

I thank my parents Norman and Jannie Main for their support of my education that culminated in this doctorate; they never gave up on me, regardless of how exceptionally unexceptional my academic efforts were for many years. My friend and love Deborah Nixon for her encouragement and support over the course of this doctorate. I thank my advisor Christopher R. Scotese for his support of the Arlington Archosaur Site project and all things dinosaur while at UTA. Over the course of my graduate education, Scotese was a great mentor and friend. I could not have done this project without him. I thank my friends and colleagues George E. Bennett (Geb) and Christopher R. Noto; they provided guidance, support and insightful knowledge on many occasions (and sometimes they just listened when needed). Equally, I thank Chris Brochu, Jack Horner, Thomas Holtz, Jim Kirkland, Darren Tanke and Dave Weishampel for their responses to my many questions via email, Facebook and in the hallways at SVP meetings; their patience and willingness to answer questions and offer advice were beyond kind and most helpful to this project.

I thank Huffines, HC-LOBF of Arlington and Robert Kimball from JC, KPL, LLC and the Viridian Project for granting land access at the Arlington Archosaur Site (AAS). I thank AAS discoverers Phil Kirchhoff, Art Sahlstein and Bill Walker for reporting the AAS to UTA and donating fossils. I thank the AAS volunteers: Kevin Anderson, David Angel, John Beeck, Kim (“B-rex”) Bell,

Coralyn Bingman, Rachel Brown, Anissa Camp, Ronnie Colvin, Nathan Campbell, Brad Carter, Roger Fry, Jeremy Greene, Amanda Hankins, Pat and Marge Kline, Angela Maxwell, Albert Miramontes, Austin Motheral, Stewart & Travis Nolan, Angie Osen, Rachell Peterson, Jason Rich, Phil Scoggins, Darlene Sumerfelt, Nathan Van Vranken, and Jan Weisner for their many dedicated hours of digging in the field and working on fossils in our AAS fossil lab at UTA. The AAS volunteers ("*The Archosaurs*") were the backbone of the AAS Project. I thank my UTA intern-assistant Albert Miramontes, without his many hours, many AAS fossils would not have prepared for study. Of special note, I thank Pat and Marge Kline for bringing back to life the "Flying Turtle" in the AAS-UTA lab.

I thank my AAS research colleagues, as much of this work was born of my interaction with them; Eric Allen, Kevin Anderson, George Bennett, Stephanie Drumheller, Barbara Grandstaff, Christopher Noto, David Parris and Dave Weishampel. The intellectual professionalism we shared greatly enriched my work, knowledge and abilities. I thank Glenn Hadsall for designing the AAS webpage, a wonderful conduit of public outreach for the AAS. I thank Clinton Crowley, Tracy Ford, David Killpack and Jacek Major for donating their artwork that demonstrates what the AAS ecosystem may have looked like long ago.

I would be remiss not to thank my graduate committee. I thank my mentor Christopher Scotese, and committee; Arthur Busbey, Jim Grover, Merlynd Nestell, Eric Smith and David Weishampel. Each provided guidance which I

appreciate. Prior to graduate school, I had experiences that significantly improved my knowledge and influenced my thinking. My earliest experiences in paleontology involved working on the excavation of an *Alamosaurus* in the Cretaceous of Big Bend National Park. I thank my undergrad Dinosaurs professor Dr. Montgomery for allowing me to work the dig. Equally of great influence was my time spent working at local museums. As an undergraduate, my years working in the Paleontology Department at the Dallas Museum of Nature and Science (now the Perot Museum) as well as in the fossil prep labs at the Shuler Museum of Paleontology at SMU were of great benefit. At SMU, under the supervision of Louis Jacobs and Kent Newman, I learned about the Texas Cretaceous, the Woodbine Formation. Equally, under the supervision of Tony Fiorillo and George Bennett at the DMNS, I had my first opportunities at learning fossil preparation, as well as doing research and presenting research at meetings.

Coming full circle, I thank my father, Norman Main. He was an insurance salesman by trade, but a scholar at heart. His encouragement and support of my education resulted in this doctorate. He always pushed me forward throughout the years, encouraging me to continue on with my studies, even when he was terminally ill. The AAS was reported to UTA the month that he passed away. Within a week of my first visit to the AAS, he passed on. The last ten years of work are dedicated to him.

November 16, 2012

ABSTRACT

APPALACHIAN DELTA PLAIN PALEOECOLOGY OF THE
CRETACEOUS WOODBINE FORMATION AT THE
ARLINGTON ARCHOSAUR SITE
NORTH TEXAS

Derek J. Main, PhD.

The University of Texas at Arlington, 2013

Co-supervising Professors: Merlynd Nestell and Christopher R. Scotese

The Arlington Archosaur Site (AAS) is a North Texas fossil locality that preserves a mid- Cretaceous ecosystem along a low lying coastal plain. The site lies within the Cenomanian (94-96 Mya) rocks of the Woodbine Formation in North Arlington, Tarrant County, TX. The depositional environment of the AAS is a coastal delta plain, principally a peat bog. The vertebrates recovered from the AAS include dinosauria (ornithopod and theropod), crocodyliform, chelonian and dipnoan. A large, nearly complete crocodyliform was excavated in the summer of 2009, and proved to be a new taxon; *Deltasuchus motherali*. The name of the new taxon was based upon an adult crocodyliform skeleton that was recovered, along with the remains of numerous juveniles. Of the AAS dinosaurs, ornithopods are more common and theropod quite rare, represented only by scant isolated teeth

and claws. The ornithopod material is predominantly hadrosauroid post crania from a single adult individual and includes; an axis, cervical, dorsal and caudal vertebrae, a scapula, coracoid, a left femur and a near complete left pelvis (ilium, ischium and prepubis). Of equal importance is the first juvenile ornithopod (hadrosauroid) material recovered from the Woodbine Formation at the AAS. The AAS juvenile hadrosauroid material is principally post crania and represents multiple individuals of variable growth stages.The AAS ornithopod (hadrosauroid) material represents the most recovered from the Woodbine Formation to date and was used to describe the post cranial anatomy of a primitive hadrosauroid; *Protohadros*.

Other components of the coastal plain ecosystem include a new species of lungfish. The new dipnoan is represented by one pterygopalatine and five prearticular tooth plates. The AAS lungfish is significant as it represents a new species that is unique to Texas, as well as it extends the biostratigraphic range of *Ceratodus* into the Cenomanian. The new species was named *Ceratodus carteri* in honor of the fossil collector that discovered it, Brad Carter.

Numerous trace fossils were documented and recovered from the AAS, of particular interest were coprolites that preserved data on the regional ecology. Over 150 coprolites were recovered that demonstrate a variety of morphologies suggestive of multiple taxa. The morphologies are Cylindrical, Spiral and Ovoid. The cylindrical coprolites were interpreted as crocodyliform intestinal tract

material (Thulborn, 1991). Spiral coprolites are typically indicative of marine taxa; shark and fish (Coy, 1995). Ovoid coprolites are indicative of reptiles; dinosaurs and crocodyliforms. The most common coprolite found at the AAS was attributed to crocodyliforms. The mapped locations of the coprolites show that most of the crocodyliform coprolites were found with broken and bitten turtle remains along with numerous crocodyliform teeth. The coprolites were used to propose a paleobiological model for the AAS as being a coastal crocodyliform feeding ground.

Examples of paleobiological behavior in extinct organisms are rare. This study presents fossils from the Woodbine Formation that exhibit tooth marks consistent with predation by large crocodyliforms (*Deltasuchus*). The feeding traces consist of pits, scores, and punctures that occur on multiple turtle shell fragments and two dinosaur limb bones. The pattern of marks and breakage on turtle carapaces and plastra suggests they were crushed, whereas marks on the dinosaur bones indicate possible dismemberment. Marks are consistent with those produced by living crocodylians exhibiting similar behavior.

The morphology of the new crocodyliform, *Deltasuchus* and distribution of bite marks indicates it was likely a generalist; an opportunistic predator that fed on a variety of prey, including turtles and dinosaurs. Given this evidence and the paleoenvironmental setting, the ecology of large crocodyliforms from the Woodbine Formation was likely most similar to that of fossil and living

crocodylians inhabiting delta-plain environments. Not only were these crocodyliforms likely apex predators in the AAS ecosystem, they also played an important taphonomic role in the assembly of vertebrate remains from the coastal AAS community. This analysis of the Woodbine Formation at the AAS brings forth more data on the dynamics of Cenomanian coastal ecosystems in North America with regard to Cretaceous paleogeography, as the AAS represents the most complete ecosystem discovered in southwest Appalachia.

TABLE OF CONTENTS

.

APPENDIX

LIST OF ILLUSTRATIONS

LIST OF TABLES

CHAPTER 1

INTRODUCTION:
THE ARLINGTON ARCHOSAUR SITE

"Somewhere there is something incredible waiting to be discovered"

Carl Sagan

1.1 The Arlington Archosaur Site

The Arlington Archosaur Site (AAS) is a North Texas fossil locality that preserves a Mid- Cretaceous ecosystem along a low lying coastal plain. The site lies within the Cenomanian (95-96 Mya) rocks of the Woodbine Formation in North Arlington, Tarrant County, TX. The depositional environment of the AAS is a coastal delta plain, or swamp. The vertebrates recovered from the AAS include dinosauria (ornithopod and theropod), crocodyliform, chelonian, salamander, shark, fish (dipnoan) and mammal (multituberculate). A large, nearly complete crocodyliform skeleton was excavated and proved to be an interesting new taxon; *Deltasuchus motherali*. The name of the new taxon was based upon a nearly complete adult crocodyliform skeleton that was recovered, along with the remains of numerous juveniles. The adult and juvenile material was laser scanned and digitally scaled to build a composite reconstruction of the crocodyliform.

Of the AAS dinosaurs, ornithopods are more common and theropod quite rare. The ornithopod material is predominantly hadrosauroid post crania from multiple individuals of varying ontogentic stages and includes; an axis, cervical, dorsal and

caudal vertebra, a scapula, coracoid, a humerus, a left femur and a near complete left pelvis (ilium, ischium and prepubis). Of equal importance is the first juvenile ornithopod (hadrosauroid) material recovered from the Woodbine Formation at the AAS. The AAS juvenile hadrosauroid material is principally post crania and represents multiple individuals of variable growth stages.The AAS hadrosauroid represents the most complete skeletal material recovered from the Woodbine Formation to date and was used to describe the post cranial anatomy of *Protohadros*.

Other components of the AAS ecosystem include a new species of lungfish. The new dipnoan was assigned to the genus *Ceratodus* and is represented by one pterygopalatine and five prearticular tooth plates. The AAS lungfish is significant as it represents a new species that is unique to Texas. The AAS lungfish is equally important as it extends the biostratigraphic range of *Ceratodus* into the Cenomanian and increases the biogeographic range of the genus in North America.

Numerous trace fossils were recovered; of particular interest were coprolites that preserved data on the regional ecology. Over 150 coprolites were recovered that demonstrate a variety of morphologies suggestive of multiple taxa. Sizes range from 3cm to 30cm in diameter, with fish being smallest and dinosaur and crocodyliform being the largest. The coprolites were noted to occur with shed crocodyliform teeth, along with broken and bitten turtle shell. This pattern of

deposition implies crocodyliform feeding behavior and evidence of the coastal plain once being used as a feeding ground.

1.2 Discovery of the Arlington Archosaur Site

The AAS was discovered independently by UT-Arlington students and local fossil collectors in 2003. UT-Arlington students Phil Kirchhoff and Bill Walker are credited with discovering the site along with fossil collector Art Sahlstein. Local resident and fossil collector, Art Sahlstein discovered fossils exposed on a hillside near his home while on a nature walk. He collected numerous osteoderms and teeth from a crocodyliform. Sahlstein later presented the fossils he found to the Fort Worth Museum of Nature and Science (FWMNS) curator Jim Diffly, who identified the material as belonging to *Woodbinesuchus.* The museum however, did not investigate.

At approximately the same time, Kirchhoff and Walker were prospecting exposures of the Woodbine Formation near the Trinity River in the far north part of Arlington when they came upon fossils on a hillside (Main, 2004). The area that they were prospecting was a hillside near an open field located off South Main St., where South Main St. dead ends south of Trinity Blvd (GPS: N 32˚48.635 and W 097˚ 04.757) (Fig. 1.1). While prospecting the site, Kirchhoff found a dinosaur tooth and Walker found several small vertebrae and teeth on the hillside Woodbine exposures (Main, 2004). Kirchhoff presented the material they found to Dr. Christopher Scotese at UTA. Scotese in turn contacted the author,

who was a new graduate student at UTA. The author determined the material was from a hadrosauroid and a crocodyliform, possibly *Protohadros* and *Woodbinesuchus* (Main and Fiorillo, 2003; Main, 2004). The author visited the AAS in October of 2003, in order to ascertain its importance, samples were collected and photos taken (Main, 2004) (Fig 1.2). The full excavation and study of the site was however delayed by the landowner's refusal to grant land access. From 2003-2007, the 2,200 acres of fossil rich land in Arlington was unavailable to exploration and scientific study.

Figure 1.1 Location of the Arlington Archosaur Site (AAS) in North Arlington. The AAS is situated in a field, south of Trinity Blvd and east of South Main St at the intersection of Calloway Cemetery Rd. and Main. The fossils occur on a hillside where the Woodbine Formation is exposed in outcrops facing south. AAS coordinates: N 32˚48.635 and W 097˚ 04.757 (image from Google Earth).

In 2007, Kirchhoff contacted the River Legacy Living Science Center in Arlington and approached the director Phyllis Snyder about the AAS. Kirchhoff learned from Snyder that new owners, the Huffines family, purchased the land in 2006 for commercial development. Due to the close proximity of their development to the Nature Center's wetlands, the new owners contacted the Nature Center. Snyder arranged a meeting at the Nature Center with the new land owner, the AAS discoverers Phil Kirchhoff and Art Sahslstein, along with representatives from UTA, Dr. Christopher Scotese and the author. The Huffines representative suggested that a contract be drafted between the land owner and the university that granted students access to the land. Thus the AAS became open to excavation and study.

Figure 1.2 Location and outcrop photo of Woodbine Formation exposures at the Arlington Archosaur Site when the site was reported in 2003 prior to excavation.

1.3 Stratigraphy of the Woodbine Formation

The Woodbine Formation is a middle Cretaceous (Cenomanian: 93-99 Mya) stratigraphic unit that occurs in North Central Texas (Fig. 1.3). The Woodbine Formation of North Texas was mapped and named by R. T. Hill for the village of Woodbine in Cooke County (Hill, 1901). Hill originally subdivided the Woodbine into two units, the upper "Lewisville beds", and the lower "Dexter beds" (Hill, 1901). The Woodbine Formation is about 100 meters thick and consists predominately of sandstones and shales (Johnson, 1974). The Woodbine

occurs in outcrops in North Central Texas and southern Oklahoma. It is the oldest Upper Cretaceous unit in the Gulf Coastal Plain (Hedlund, 1966; Oliver, 1971).

In Texas, the Woodbine outcrops along a line from Temple in central Texas, northward to Lake Texoma near the Red River (Main, 2005; Oliver, 1971; Trudel, 1994) (Fig. 2.1). The Woodbine outcrop belt occurs as an irregular and narrow band, up to 20 miles wide extending from Cooke County to Johnson County (Johnson, 1974; Oliver, 1971) (Fig. 2.1). In the subsurface, the Woodbine underlies a 45 county area in Texas, bounded by outcrop on the north and west, and by the Sabine uplift to the east (Oliver, 1971; Trudel, 1994). Woodbine sediments weathered from the Ouachita Mountains in southern Oklahoma and settled in a series of near shore environments in the subsiding northeast Texas basin (Oliver, 1971). The Woodbine deposits are primarily terrigenous near shore and shallow marine depositional systems and include fluvial, deltaic and shelf deposits (Main, 2005; Oliver, 1971; Trudel, 1994). The Woodbine unconformably overlies the Grayson Formation of the Washita Group and is unconformably overlain by the strata of the Eagle Ford Group (Johnson, 1974; Lee, 1997; Oliver, 1971; Trudel, 1994) (Fig. 2.2). A period of marine deposition lasting about ten million years separates the Woodbine from the earlier terrestrial depositional environments of the Trinity Group (Winkler et al., 1995).

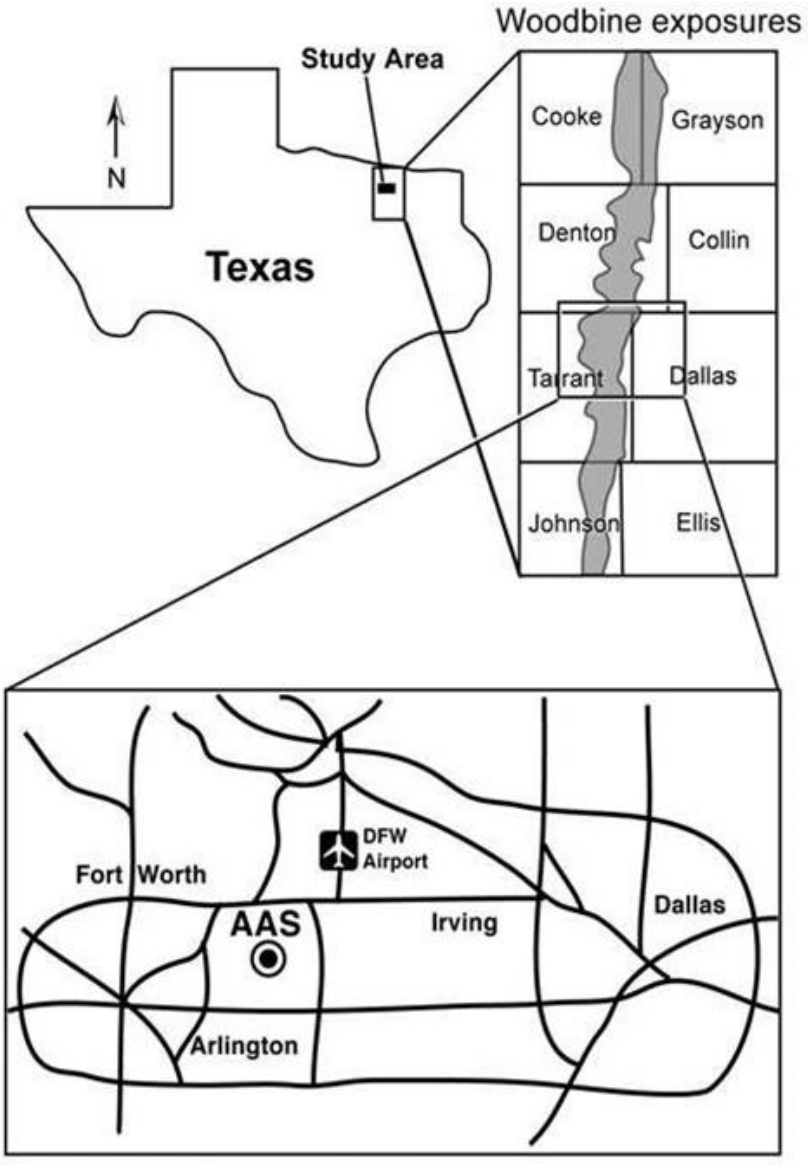

Figure 1.3 Texas map with outline of counties in which Woodbine Formation exposures occur. AAS Woodbine Formation study area in northeastern Tarrant County and southern Denton County denoted with circle south of DFW airport (Woodbine exposure data modified from Main, 2005).

Dodge (1968) proposed four units, or members, for the Woodbine Formation, in ascending order they are; the Rush Creek Member, Dexter Member, Lewisville Member and the Arlington Member (Fig 1.4). The Rush Creek Member was first noticed by Bergquist (1949) as a shale unit that occurred between the overlying Dexter Member of the Woodbine Formation and the underlying Grayson Formation. Bergquist (1949) defined the Dexter Member of the Woodbine Formation lithologically as fluvial ferruginous and siliceous sandstone with silty clay lenses with some carbonaceous clay at the members base (Oliver, 1971).Overlying the fluvial sandstone of the Dexter Member is the coastal, shallow marine Lewisville Member (Fig. 1.4).

The Lewisville Member consists of mudstone and shale deposited along a coastline, marginal to active deltaic depositional systems, an extensive delta plain with distributary channels (Main, 2005; Oliver, 1971; Trudel, 1994). The AAS lies within the coastal delta plain sediments of the Lewisville Member (Fig. 1.4). The final, uppermost member of the Woodbine Formation is the Arlington Member. Murlin (1974) defined the Arlington Member of the Woodbine Formation as a fluvial sandstone that occurs in North Texas as exposures in Denton, Johnson and Tarrant counties that directly overlie the carbonaceous shale beds of the Lewisville Member (Fig. 1.4). He described the Arlington Member as a thin (< 3 m) unit that consisted of thin beds of laminated siltstone interbedded with massive beds of fine grained, oxidized sandstone from distributary channels.

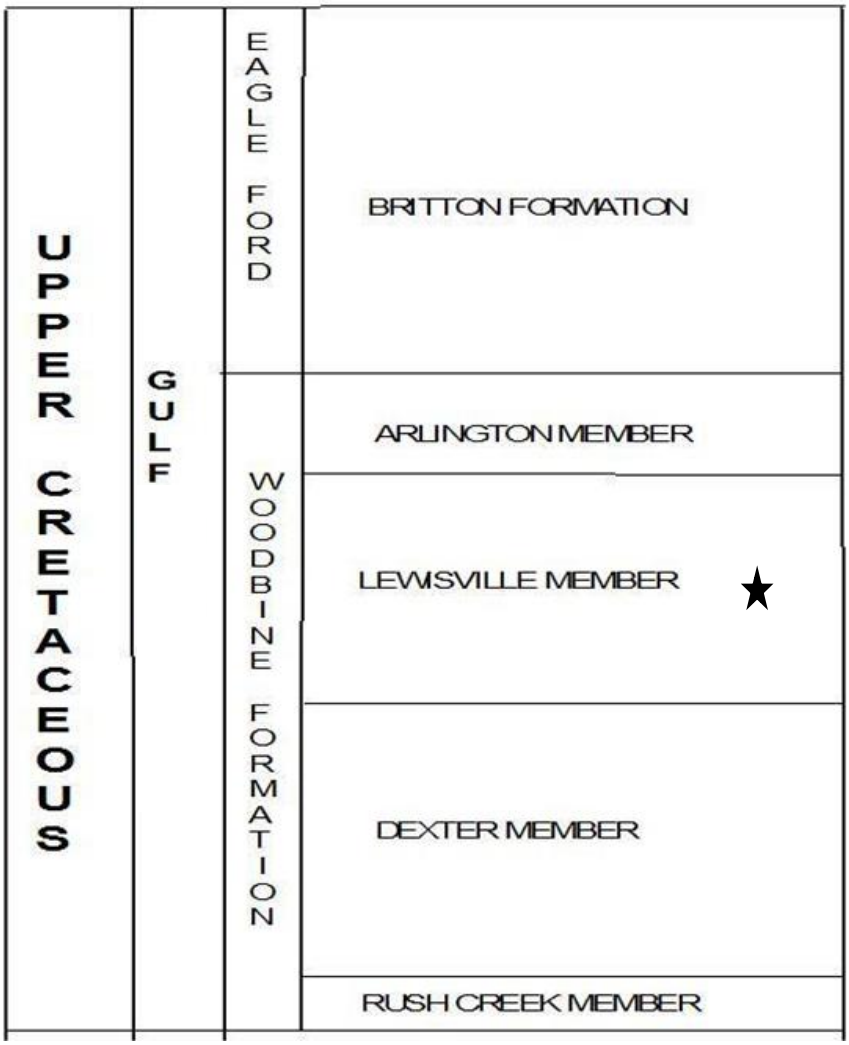

Figure 1.4 Woodbine Stratigraphy, stratigraphic position of the four members in relation to overlying Eagle Ford Group, stratigraphic location of the AAS denoted within the Lewisville Member with a star (modified from Main, 2005).

1.4 AAS Woodbine Stratigraphy and Paleoenvironments

The Woodbine Formation exposures at the AAS are relatively thin, with <5 m of total outcrop present on the hillside. The AAS Woodbine outcrops preserve four stratigraphic beds that are defined by distinct facies that are denoted by changes in lithology (lithofacies), fossils (biofacies) and sedimentary structures (Fig. 1.5). The four beds are described and referred to herein as Facies A-D utilizing the modern facies concept defined by de Raaf et al. (1965) and Walker (1983 and 1984). The modern facies concept that is used herein was best defined by de Raaf et al. (1965) as "Facies are distinguished by lithological, structural and organic aspects that are detectable in the field. The facies may be given informal designations such as Facies A, followed by a brief description of the designation (laminated siltstone facies) and given an environmental interpretation." All of the AAS beds, or facies, represent coastal deltaic paleoenvironments, many of which are be attributed to delta plain (floodplain/swamp), the intermittently flooded lowlands between coastal distributary channels that consist of organic rich sediments.

The first AAS Woodbine bed, Facies A, is a shallow marine near shore sandstone that is distinguished by trace fossil burrows attributed to the Skolithos ichnofacies, and a siderite rich horizon with a charcoal conglomerate. The second bed, Facies B is an organic debris rich peat that is highly fossiliferous, containing

the mixed remains of numerous vertebrate fossilss in association with coprolites and carbonized logs. It was within this stratigraphic horizon that the majority of the AAS fossil fauna described herein was recovered (Table 1.2). The third bed, Facies C is a poorly developed clay rich paleosol. It was classified as a Histic Gleysol utilizing the soil classification scheme of Mack et al. (1993); it is distinguished by a dull blue-grey hue, slickensides and large siderite concretions that imply seasonal wetting and drying. Histic Gleysols are typical of floodplain environments that are periodically inundated with varying levels of water. The fourth bed is Facies D, a heterolithic mudstone bed with multiple crevasse splay sand lenses (Fig. 1.5). Each stratigraphic bed, its distinct facies and representative paleoenvironments will be discussed in further detail in chapter 2.

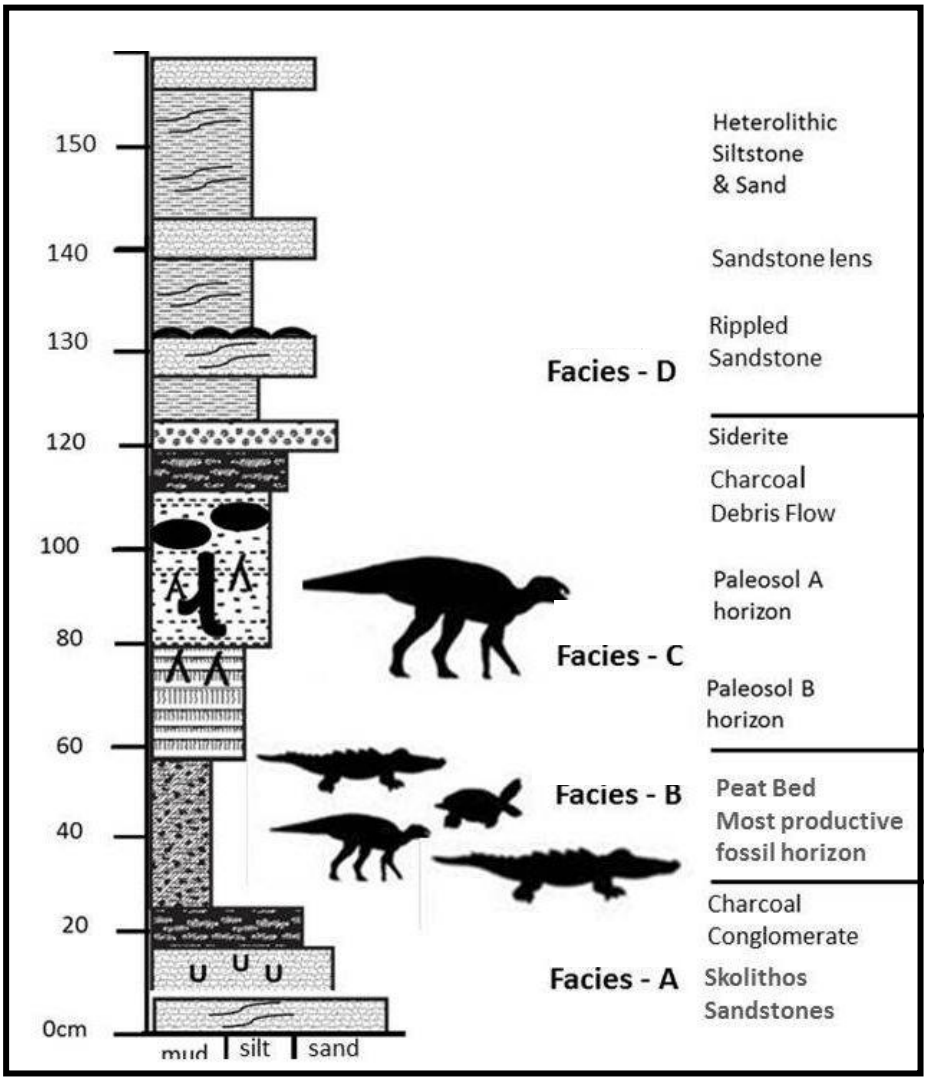

Figure 1.5 Stratigraphy and paleontology of the AAS Woodbine exposures. A composite stratigraphic section with the sedimentology of each bed defined and fossil discoveries denoted with shadow characters in relation to the stratigraphic bed/facies that produced them. The Facies B peat horizon produced most of the AAS fossil fauna.

1.5 AAS Paleoenvironments and Paleoecology

The AAS Woodbine strata preserve a wide range of vertebrates including; fish, lungfish, shark, amphibian, marine reptile, turtle, crocodyliform, dinosaur (theropod and ornithopod), and mammals, along with numerous coalified logs and minor plant leaf remains belonging to the angiospermidae. Among the AAS fauna are several animals that are new to science; a new species of lungfish *Ceratodus carteri*, a new chelonian, a new amphibian, a new multituberculate mammal, a new taxon of crocodyliform, *Deltasuchus motherali*,and a basal hadrosauroid (Main et al., 2012; Main et al., in press; Noto et al., 2012). The AAS hadrosauroid and crocodyliform remains form the core of the AAS Woodbine fauna, due totheir prominent occurrence at the site and roles within the coastal ecosystem (Fig. 1.7). All of the AAS fauna are relict in nature and denote the transition between older Early Cretaceous forms to those characteristic of the Late Cretaecous.

The AAS fossil fauna principally occur within a small two meter section of Woodbine sediments. From this small section of strata over 1,120 fossils were recovered and catalogued for this study (see collections database in Appendix A). All of the fossils were mapped in a grid system by AAS volunteer Roger Fry (Fig.1.6). A Cartesian coordinate system was used to plot the locations of all fossils in 2D space. Each fossil within the grid was given an (x, y) coordinate; for example (4.5) or (-18.12), and drawn onto the maps with a brief note about the type of fossil found. This method was used in an effort to document both the

initial identification and location of all fossils. The mapped positions of the fossils allowed for a more accurate study of the sites taphonomy and paleoecology (see chapter 8). For more information on the AAS maps made by R. Fry and a full display of the mapping grid, see Appendix B.

Most of the AAS fossils recovered and studied were recovered from the organic rich peat bed at the base of the section, with only a minor amount of material found in the overlying paleosol and heterolithic strata (Table 1.2). The AAS peat bed produced numerous crocodyliform, turtle, and dinosaur (juvenile orithopod) fossils along with prolific amounts of carbonized wood (logs, branches and twigs) (Table 1.2). The overlying paleosol bed also produced crocodyliform and turtle fossils, but in smaller proportions than that of the underlying peat bed (Table 1.2). The AAS paleosol principally produced the remains of an adult hadrosauroid. The nature and size of which were never again found in any of the other AAS strata, as the lower beds only produced juvenile remains.

Paleogeographically, the AAS Woodbine ecosystem was located on a peninsula that projected into the interior seaway in southwestern Appalachia. The margin of the peninsula formed an extensive coastal flat, part of which was associated with a delta plain swamp or mangrove-like bog. The AAS fossil fauna was recovered from the delta plain as evidenced by the sedimentology of the site; the organic rich peat beds and clay and organic rich paleosol beds. The AAS ecosystem was possibly isolated on the peninsula by the mid-Cretaceous

paleogeography, a eustatic highstand. This hypothesis supported by paleogeographic studies of the Greenhorn interior seaway and by the relatively primitive or relict nature of the AAS fauna (Elder and Kirkland, 1994; Main et al., in press). For a complete faunal list by bed/facies of the AAS Woodbine fossil ecosystem, see Table 1.2.

The scientific importance of the AAS is that it preserves multiple components of a middle Cretaceous (Cenomanian) ecosystem along an ancient coastal plain. Of greatest importance is the age of this ecosystem. The Cenomanian is a poorly known, and relatively little studied point in Earth History. Thus, the AAS presents a rare opportunity to study not only one animal from this time, but a nearly complete coastal system fauna. The diverse ecosystem with the presence of dinosaurs and crocodyliforms, and the location, was the basis for the name, the Arlington Archosaur Site (Fig. 1.7). This name seemed appropriate as the first fossils reported to the author were dinosaur and crocodyliform, members of the ruling reptiles of the Mesozoic; the Archosauria.

Table 1.1 AAS Woodbine Faunal List (fossils and facies).

AAS Fauna-Taxanomy	Bed/Facies	Reports in the litereature
Chondrichthyes		
Hybodontiformes		
Hybodus sp.	A	McNulty and Slaughter, 1968.
Ptychodus sp.	A	
Laminformes		
Cretodus sp.	A/B	McNulty and Slaughter, 1968.
Squalicorax sp.	A	McNulty and Slaughter, 1968.
Rajiformes		
Onchopristis dunklei	A	McNulty and Slaughter, 1968.
Myliobatiformes		
Pseudohypolophus (*Hypolophus mcnultyi*)	A	McNulty and Slaughter, 1968.
Osteichthyes		
Ceradontiformes		
Ceratodus carteri	A/B	Main et al., 2012
Pycnodontiformes		
cf. *Paleobalistum geiseri*	A	McNulty and Slaughter, 1968.
Pycnodontidae indet.	A/B	McNulty and Slaughter, 1968.
Semionotiformes		
Lepidotes sp.	A	McNulty and Slaughter, 1968.
Tetraodontiformes		
Stephanodus sp.	A	
Lissamphibia		
Caudata		
Caudata indet	B	Winkler and Jacobs, 2002
Cryptobranhidae indet	B	
Anura		
Anura indet	B	Winkler and Jacobs, 2002
Reptilia		
Chelonia		
Baenidae indet	B	
Glyptops sp.	A/B	
Trionichidae indet	A/B/C/D	Noto et al., 2012
Trionichid new gen. sp.	B	

Table 1.1 cont.

Squamata		
Plesiosauridae (?)	A	
Crocodyformes		
Bernessartia sp.	A/B	Lee, 1997a
Deltasuchus motherali	A/B/C	Main et al., in press
Goniophilidae indet	A/B/C/D	Noto et al., 2012
Woodbinesuchus sp.	A/B	Lee, 1997a
Dinosauria		
Theropoda		
Allosauroid	A/B	Noto and Main, in press
Dromaeosaurida indet	B	Noto and Main, in press
cf. Richardoestesia	A/B	Noto and Main, in press
Tetanurae indet	B	Noto and Main, in press
Ornithopoda		
Hadrosauridae indet	A/B/C/D	
Protohadros	B/C	Main et al., in press
Protohadros byrdi.	B/C	Head, 1998
Mammalia		
Multituberulata		
Multituberculate indet	B	Jacobs and Winkler, 1998

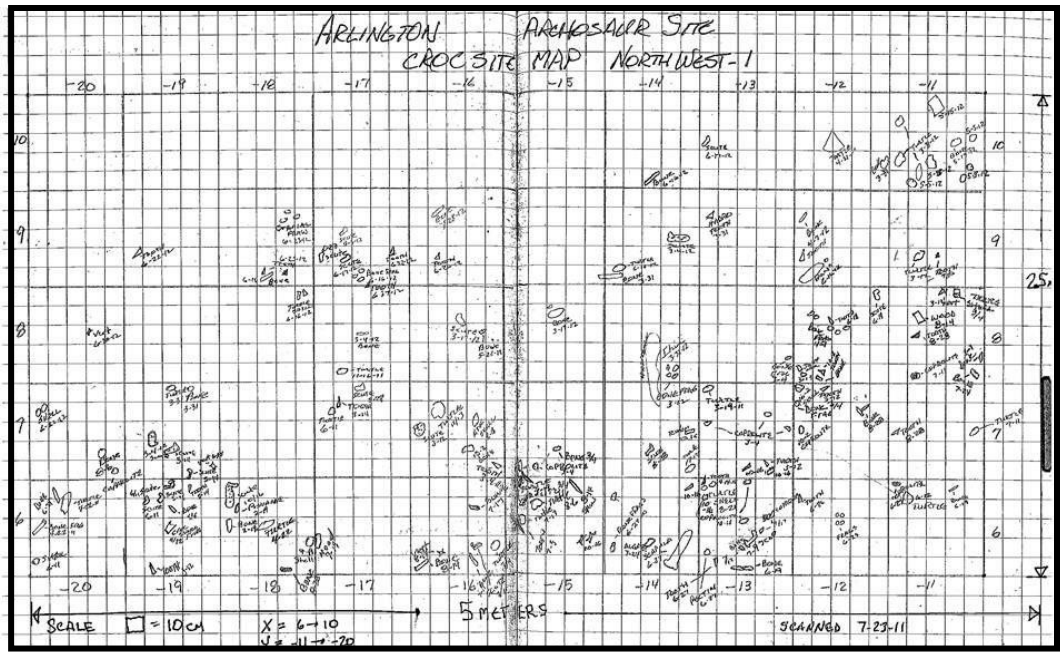

Figure 1.6 AAS Northwest 1 map, a representative section of the AAS map grid developed by Roger Fry with fossils plotted in 2D space using a Cartesian coordinate system (x,y), all fossils shown in map were recovered from a single stratigraphic horizon (peat bed).

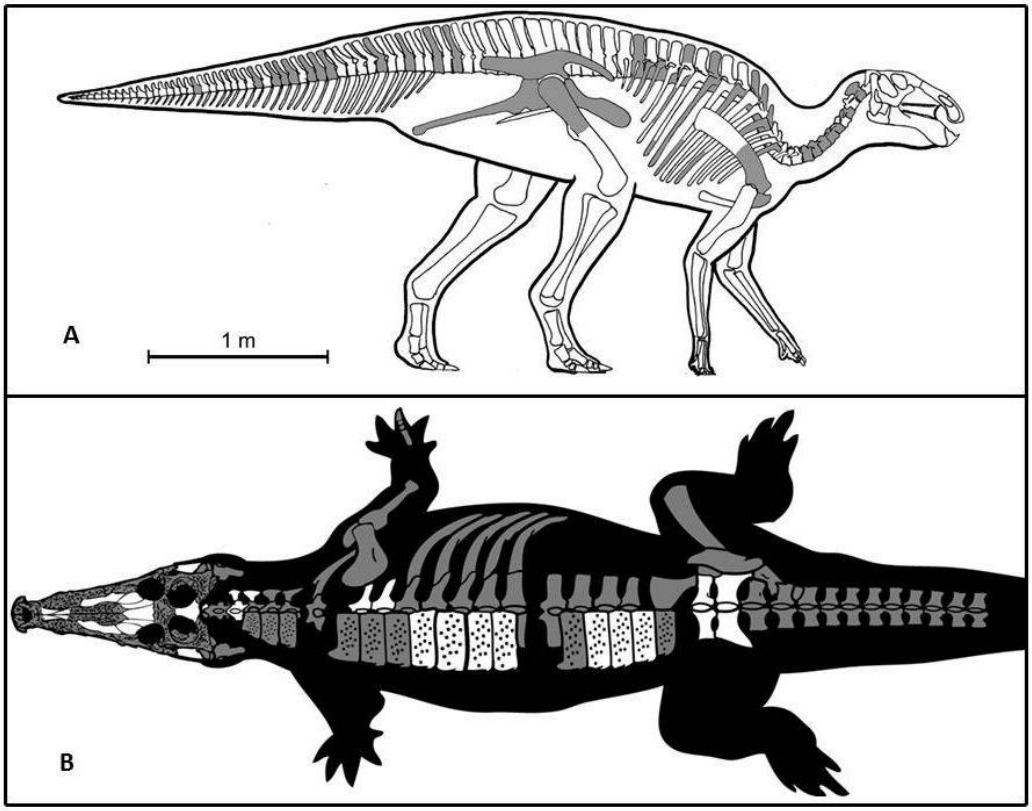

Figure 1.7 Composite image of skeletal reconstructions representing the core of the AAS coastal fauna and the basis for the name of the site; A) hadrosauroids and B) crocodyliforms. Hadrosauroid artwork courtesy of Tracy Ford (Main et al., in press). Crocodyliform artwork modified from Sereno et al. (2001).

CHAPTER 2

STRATIGRAPHY AND PALEOENVIRONMENTS OF THE WOODBINE FORMATION: A CRETACEOUS COASTAL SYSTEM FROM SOUTHWEST APPALACHIA

"They flow from form to form, and nothing stands. They melt like mist, all lands."

Alfred Lord Tennyson

2.1 Introduction and Overview of Woodbine Stratigraphy

The Cenomanian stage of the mid-Cretaceous is an important time frame within Earth history that is rarely studied due to the lack of exposed outcrops from this time. This project presents a study of Cenomanian age outcrops from North Texas that discusses a coastal depositional system in relation to a well preserved fossil ecosystem. The study area is in North Central Texas; at a diverse fossil site called the Arlington Archosaur Site (AAS) that occurs within outcrops of the Cretaceous (Cenomanian) Woodbine Formation. The Woodbine Formation was deposited along a low lying delta plain on the southwestern coast of Appalachia, which at the time protruded into the interior seaway forming a peninsula.

The studied sections are from the northwestern coast of the ancient peninsula and consist of a series of distinct horizons that were subdivided into four facies (Facies A-D) utilizing the facies concept as defined by de Raaf et al. (1965), Walker (1983 and 1984). The studied section begins with a bed (Facies A) of nearshore tidal flat sandstone that preserves a ripple bed that is extensively burrowed with *Skolithos* trace makers. The *Skolithos* ichnofacies bed is overlain

by delta plain deposits, predominantly by organic rich peat and clay rich mudstone. The peat bed (Facies B) is a fossil rich horizon, containing remains of turtles, crocodyliforms, dinosaurs and carbonized logs. Over 20 carbonized, or coalified logs were mapped within Facies B, the majority having a common SW-NE trend of deposition. Overlying the Facies B peat/lignite bed is a clay rich mudstone bed (Facies C), and a fossil horizon containing mixed remains of vertebrates, this bed is a delta plain paleosol. The paleosol is a well developed, rooted Histic Gleysol that contains calcareous concretions. Within the concretions occur charcoal fragments and several large charcoal tree stumps and roots. Concretion formation is indicative of seasonal dryness, and the charcoal tree stumps are evidence of wildfires. The vertebrates occurring within the Facies C horizon include dinosaur and crocodyliform. The uppermost bed is Facies D, a heterolithic delta plain mudstone that has a series of thin, rippled lenticular crevasse splay sand beds that represent distributary channel avulsion, possibly driven by coastal storms. This record is the first of Cenomanian avulsion deposits from an ancient delta plain and among only a few Cenomanian coastal plain systems known to support a variety of dinosaurs and crocodyliforms, all of which were impacted by coastal processes. The AAS Woodbine strata were correlated to similar Woodbine exposures at other documented fossil localities; Bear Creek, Lake Grapevine and the *Protohadros* type locality in Grapevine.

2.2 Geologic Background

The Cretaceous has received great attention by geologists over the years due to the significant volumes of porous clastic sediment in the western United States basin and range province that hold reservoirs for petroleum, and for the many known formations that produce the fossil remains of dinosaurs. Many of the dinosaur bone bearing Cretaceous strata in North America are from rock formations that were deposited by either braided or meandering river systems that once migrated across the plains, or along deltaic coasts where the rivers once met the coast of the Western Interior Seaway. Among the more notable Cretaceous formations known for producing dinosaurs and related fauna in North America are; the Aguja Formation, Antlers Formation, Cedar Mountain Formation, Dinosaur Park Formation, Fruitland Formation, Glen Rose Formation, Hell Creek Formation, Judith River Formation, Oldman Formation, Ojo Alamo Formation and the Two Medicine River Formation to name but a few (Brinkman et al., 1998; Brinkman et al., 2004; Brown, 1907; Eberth et al., 1990; Eberth, 2005; Farlow, 1976 and 1993; Fiorillo, 1989; Gilmore, 1919; Horner, 1983; Horner et al., 2011; Kirkland et al., 1997; Kirkland, 2005; Kirkland and Madsen, 2007; Ostrom, 1961; Rowe et al., 1992 and Sankey, 2007). Although fossil rich, the strata of many of these dinosaur bone bearing formations were deposited along the western border of the interior sea, and not on the eastern margin. The Woodbine Formation is unique not only for its chronostratigraphic position within the Cretaceous, the

Cenomanian, but also its paleogeographic location, on the eastern coast of the interior seaway.

Previous studies of North American Cenomanian stratigraphy and paleoecology have focused on stratigraphic units from Alaska, Canada, Colorado, New Mexico, Wyoming and Utah (Table 2.1). The Chandler Formation of Alaska is a Cenomanian unit known to produce fossil remains of turtles, dinosaurs and birds (Gangloff, 1998). The Dunvegan Formation is an unfossiliferous, but well studied, river dominated delta from the Cenomanian of Canada (Bhattacharya and Walker, 1991). The upper most part of the Mussentuchit Member of the Cedar Mountain Formation of Utah is a late Albian-Early Cenomanian aged unit that preserves the remains of a diverse fauna of dinosaurs (Cifelli, et al., 1999; Garrison et al., 2007; Kirkland, 1996; Kirkland et al., 1997 and 1999; Kirkland, 2005; Kirkland and Madson, 2007; McDonald et al., 2010 and 2012).

The Mussentuchit Member is important, as it is stratigraphically close in age to the Woodbine Formation with similar paleoenvironments and a similar fauna; of note are *Dakosuchus* and *Eolambia* (Cifelli et al., 1999; Kirkland, 2005; Kirkland and Madson, 2007; and McDonald et al., 2012). The Mussentuchit Member was however situated on the opposite side of the Greenhorn interior seaway, and provides for an interesting correlation. The Dakota Group and overlying Graneros Shale of the American southwest (Colorado, New Mexico, Utah) are mid-Cretaceous rock units (Albian –Cenomanian) that roughly correlate

with the Woodbine Formation in Texas and record the Late Albian-Early Cenomanian transgressive sequence (Ende, 1991; Holbrook and Dunbar 1992; Holbrook, 1996 and 2001).

The previously mentioned Cretaceous stratigraphic units principally occur on the western coast of the Greenhorn interior sea, along the eastern coasts of Laramidia. The geologic record of the Cenomanian in eastern North America, Appalachia, is relatively scant and poorly studied. In Texas, the only stratigraphic unit that preserves a record of Cenomanian coastal environments and ecosystems of southwestern Appalachia is the Woodbine Formation of North Central Texas. Thus, the Woodbine Formation, and its sedimentary and fossil record are important to science.

Table 2.1 North American Cenomanian Stratigraphic Units

(Bhattacharya and Willis, 2001; Bhattacharya and Walker, 1992; Cobban and Hook, 1984; Gangloff, 1998; Holbrook, 2001; Kirkland, 1996; Kirkland et al., 1997; Kirkland and Madsen, 2007; Main, 2005; Oliver, 1971):

Stratigraphic Unit	**Geographic Occurrence**
Chandler Formation -	Alaska
Corwin Formation -	Alaska
Dunvegan Formation -	Alberta, Canada
Frontier Formation -	Wyoming
Graneros Shale -	New Mexico / Colorado
Mancos Shale -	New Mexico / Colorado
Greenhorn Limestone -	New Mexico / Colorado
Dakota Formation -	New Mexico / Colorado / Utah / Arizona
Cedar Mountain Fm. -	Utah
Muddy Formation -	New Mexico / Colorado (Dakota Group)
Romeroville Sandstone -	New Mexico (Dakota Group)
Pajarito Formation -	New Mexico (Dakota Group)
Mesa Rico Sandstone -	New Mexico (Dakota Group)
Woodbine Formation -	Texas
Grayson Formation -	Texas

The “Father of Texas geology”, R. T. Hill was the first geologist to map and define the Cretaceous of North Texas (Hill, 1901). The Woodbine Formation was named by Hill for the village of Woodbine in Cooke County (Hill, 1901). Hill originally subdivided the Woodbine into two units, the upper "Lewisville beds", and the lower "Dexter beds" (Hill, 1901). The Woodbine Formation is about 100 meters thick and consists predominately of sandstone and shale (Johnson, 1974). The Woodbine occurs extensively in outcrops in North Central Texas and southern Oklahoma, in which it tapers to the east and pinches out. It is the oldest Upper Cretaceous unit in the Gulf Coastal Plain (Hedlund, 1966; Oliver, 1971).

In Texas, the Woodbine outcrops along a line from Temple in central Texas, northward to Lake Texoma near the Red River (Main, 2005; Oliver, 1971; Trudel, 1994) (Fig. 2.1). It occurs as an irregular and narrow band, up to 20 miles wide extending from Cooke County to Johnson County (Johnson, 1974; Oliver, 1971) (Fig. 2.1). In the subsurface, the Woodbine underlies a 45 county area in Texas, bounded by outcrop on the north and west, and by the Sabine uplift to the east (Oliver, 1971; Trudel, 1994). Woodbine sediments weathered out from the Ouachita Mountains in southern Oklahoma and settled in a series of near shore environments in the subsiding northeast Texas basin (Oliver, 1971). The Woodbine deposits are primarily terrigenous near shore and shallow marine depositional systems and include fluvial, deltaic and shelf deposits (Main, 2005; Oliver, 1971; Trudel, 1994). The Woodbine unconformably overlies the Grayson

Formation of the Washita Group and is unconformably overlain by the Eagle Ford Group (Johnson, 1974; Lee, 1997; Oliver, 1971; Trudel, 1994) (Fig. 2.2). A period of marine deposition lasting about ten million years separates the Woodbine from the earlier terrestrial depositional environments of the Trinity Group (Winkler et al., 1995).

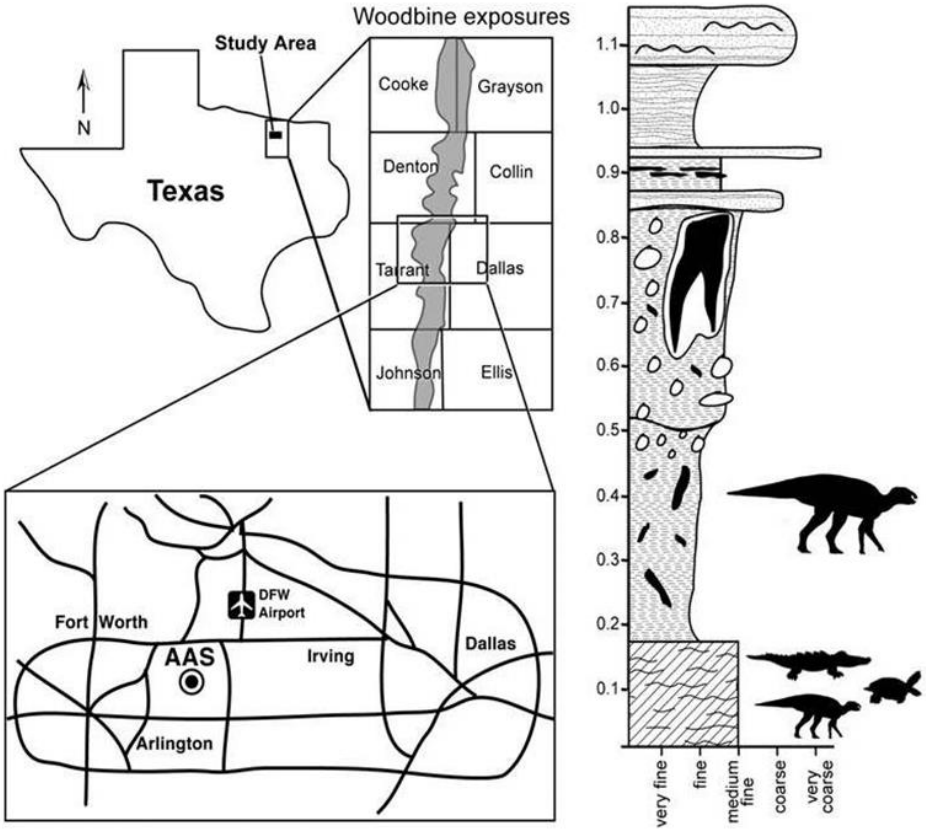

Figure 2.1 Texas map with outline of counties in which Woodbine Formation exposures occur. Woodbine Formation study area in northeastern Tarrant County and southern Denton County with a generalized stratigraphic section of the exposures at the Arlington Archosaur Site (Woodbine exposure data modified from Main, 2005 and Trudel, 1994) (Noto et al., 2012).

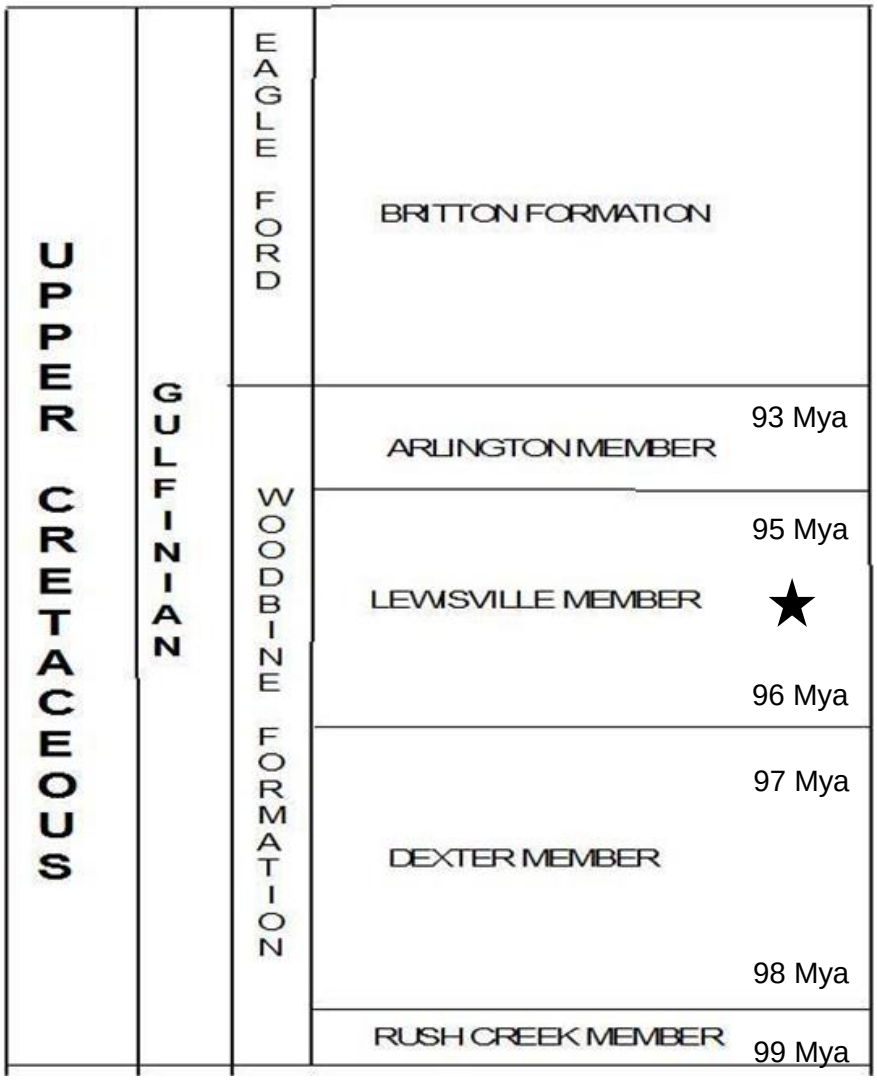

Figure 2.2. Woodbine Stratigraphy, stratigraphic position of the four members in relation to overlying Eagle Ford Group with relative ages of each member noted and the position of the AAS within the Lewisville Member denoted with a star (modified from Main, 2005).

Dodge (1968) proposed four units for the Woodbine Formation, in ascending order they are; the Rush Creek Member, Dexter Member, Lewisville Member and the Arlington Member (Fig 2.2). The Rush Creek Member was first

noticed by Bergquist (1949) as a shale unit that occurred between the overlying Dexter Member of the Woodbine Formation and the underlying Grayson Formation. Johnson (1974) later studied the depositional environments of the Rush Creek Member as part of his UT-Arlington graduate work. Johnson (1974) noted that the Rush Creek Member consisted of interfingering shale and sandstone, divided into two provinces at the Denton–Tarrant County line. The southern province is distinguished by offshore bars and lagoonal deposits (Johnson, 1974). The northern province is distinguished by lower shoreface siltstone and sandstone, lower shoreface shale and clay, and estuarine sandstone (Johnson, 1974). Johnson's work on the stratigraphy of the lower portion of the Woodbine Formation identified the environments of deposition and facies variation for the basal Rush Creek Member.

Bergquist (1949) defined the Dexter Member of the Woodbine Formation lithologically as fluvial ferruginous and siliceous sandstone with silty clay lenses with some carbonaceous clay at the member's base. The uppermost part of the Dexter is composed of a varicolored clay unit that was mapped and considered as a different member of the Woodbine by Bergquist (1949). This uppermost clay was called the Rainbow Clay by Bergquist, but was later included as part of the Dexter Member by Dodge (1969). The Dexter fluvial deposits comprise 1/3 of the northern Northeast Texas basin and consist of tributary facies and coarse-grained meander belt facies (Oliver, 1971). The Dexter outcrops principally in Grayson

County, with some southern outcrops occurring in Tarrant Co. (Trudel, 1994). In Tarrant County, the Dexter deposits are principally fluvial-deltaic in nature (Oliver, 1971).

Overlying the fluvial sandstone of the Dexter Member is the coastal, shallow marine Lewisville Member (Fig. 2.2). The Lewisville Member consists of mudstone and shale deposited along an extensive coastline, marginal to active deltaic depositional systems (Main, 2005; Oliver, 1971; Trudel, 1994). The Lewisville member of the Woodbine is highly fossiliferous, containing mollusks, ammonites and arenaceous foraminifers (Trudel, 1994). Among the ammonite fauna of the Lewisville Member is the ammonite *Conlinoceras tarrantense,* a biostratigraphic zonal marker for the base of the middle Cenomanian (Kennedy and Cobban, 1990). The presence of *C. tarrantense* thus establishes an age constraint for the unit (Kennedy and Cobban, 1990). In outcrop the Lewisville Member consists of 23-29 meters of fossiliferous, glauconitic sand lenses, mudstone and shale (Oliver, 1971; Trudel, 1994). The dominant lithologies of the Lewisville Member, however, are mudstone and shale, with sandstone occurring as lenticular bands between the mud and shale beds. The shale tends to be blue-gray or black, is finely laminated to massive bedded, contain numerous fossils, and principally represents a coastal facies (Main, 2005; Oliver, 1971). The Lewisville Member is characterized by numerous shallow marine fossils, principally the oyster; *Ostrea soleniscus* (Bergquist, 1949; Trudel, 1994). The

Lewisville Member includes what was called by Bergquist (1949) as the Red Branch Member. The Red Branch Member is a basal unit of lenticular, cross-bedded ferruginous sandstone with localized lignite beds (Trudel, 1994). The Red Branch Member was later included in the Lewisville Member by Dodge (1969) and is still recognized as such today.

Oliver (1971) classified the Woodbine deltas as a destructive deltaic system of progradational channel- mouth bar facies. Oliver (1971) classified the Woodbine deltaic systems as marine influenced due to the poor development of constructional sequences, the formation of embayments and associated strandplains, well developed coastal barriers proximal to areas of maximum discharge, relatively thin prodelta facies and high sand-mud ratio with poor muddy delta plain aggradational deposits. Oliver (1971) did not place these deltaic deposits directly in the Lewisville Member; rather he referred to these deposits as the Freestone Delta System. In this work, the Woodbine deltas are not referred to as the Freestone Delta System and are not classified as marine influenced. The Woodbine deltas are recognized for this work as occurring within the Lewisville Member. The AAS was placed within the Lewisville Member of the Woodbine Formation based upon the lithology of the unit as defined in the literature and on the biostratigraphy of the site. The presence of the invertebrates *Anchura* and *Gyrodes* biostratigraphically place the AAS to strata within the lower to middle part of the Lewisville Member (Stephenson, 1952). The

palynomorphs *Dichastopollenites* and *Stellatopollis*, recovered from the AAS, affirm a mid-Cenomanian age (May, 1975).

Overlying the Lewisville Member is the fluvial sandstone of the Arlington Member. Murlin (1974) defined theArlington Member of the Woodbine Formation as a fluvial sandstone that occurs in North Texas as exposures in Denton, Johnson and Tarrant counties and include strata that directly overlie the carbonaceous shale of the Lewisville Member. He described the Arlington Member as a thin (< 3 m) unit, that consists of thin beds of laminated siltstone interbedded with massive beds of fine grained, heavily oxidized, cross bedded sandstone (Murlin, 1974). The paleoenvironments preserved within the Arlington Member are non-marine delta plain deposits that are marginal to a distributary system (Murlin, 1974). Head (1998) placed the type locality for *Protohadros* within the Arlington Member of the Woodbine Formation. Previously, Lee (1997) placed the heterolithic strata of the Woodbine Formation at the Bear Creek SMU fossil site within the Arlington Member. With this work, the heterolithic strata of the Woodbine documented at the AAS are placed within the Lewisville Member, as the studied exposures lack thick (>1 m) beds of cross bedded sandstone.

Previously, the work of Main (2005) presented a stratigraphic study of the delta deposits of the Woodbine Formation at the Arlington Archosaur Site and at Lake Grapevine along the north shore in Rock Ledge Park. The Woodbine

Formation exposures at Lake Grapevine preserve a nearly complete delta sequence (Main, 2005). The AAS Woodbine exposures in contrast principally preserve paleoenvironments from a coastal delta plain. Deltas are recognized as being cyclic, either constructional (progradational) or destructional (Bhattacharya and Walker, 1992). Progradational systems are river dominated and destructional phases are principally marine dominated. The AAS Woodbine delta is classified as a cyclic climate (allocyclic) driven system that was fluvial influenced due to the amount of sand observed in the delta front and delta plain environments. The AAS Woodbine section is considered as progradational due to the amount of sand observed in the delta front and to a lesser extent in the delta plain environments. Principally the presence of sand lenses implies the tangential presence of distributary channels building out across the plain via channel avulsion similar to processes documented today in the Cumberland Marshes of Canada and Mississippi Delta of the Gulf (Edmonds et al., 2009; Roberts, 1998; and Smith et al., 1989).

The AAS Woodbine delta plain correlates to other Woodbine sites, and can be stratigraphically traced across North Texas. The Lewisville Member exposures at the AAS can be traced 6 km northeast to the SMU Bear Creek locality (Site 245) near DFW International Airport. The Bear Creek Woodbine exposures occur in a creek that has exposed Woodbine Formation sediments via weathering and erosion along the south entrance of the airport and Texas Hwy

183. The Bear Creek exposures consist of an organic rich mudstone overlain by nearly two meter thick heterolithic bed that is capped with three meter thick cross-bedded sandstone (Fig. 2.17). These strata correlate directly to those of the AAS and are both placed within the delta plain deposits of the Lewisville Member (Fig. 2.17). Lee (1997b) placed the heterolithic beds exposed in Bear Creek within the Arlington Member; the author disagrees with this assignment based on sections studied in the creek and their correlation to other studied sites. Using the classification of the Woodbine established by Dodge (1969) and Oliver 1971), the lower heterolithic beds of the Bear Creek strata are placed within the upper part of the Lewisville Member, rather than in the Arlington Member.

The Arlington Member contact is present in Bear Creek where it was observed and studied in a tributary of Bear Creek in 2012. It is a thick 3.6 m sequence of fluvial cross-bedded sandstone found overlying heterolithic beds in a tributary of Bear Creek ~2.5 km west of the SMU 245 Bear Creek fossil locality. The Bear Creek sandstone sequence begins as a fL, grey (Munsell Soil Chart value of 2.5YR-5/1) rippled to cross bedded sandstone that coarsens upwards in section to a fU-mL tan (Munsell Soil Chart value of 7.5YR-7/8) cross-bedded sandstone (Fig. 2.17). The cross-bedded sand of the upper most part of the section are interbedded with thin shale beds and siderite nodules as well as thin, iron rich bands or lenses (Fig. 2.17). The cross-bedded sandstone sequence of Bear Creek

is interpreted as being the lower most section of the Arlington Member, thus representing the uppermost member of the Woodbine Formation.

The Lewisville Member of the Woodbine Formation also occurs in outcrop 15 km due north of DFW International Airport at Rock Ledge Park on the north shore of Lake Grapevine (Fig. 2.17). The Lake Grapevine beds were correlated to Bear Creek and the AAS (Fig. 2.17). The lower AAS exposures of burrowed and rippled sandstone correlates to the lower prodelta beds at Lake Grapevine and the mid-section AAS delta plain peat bed and paleosols correlate to the mid- section delta plain deposits of the Woodbine exposures at Rock Ledge Park and Murrell Park at Lake Grapevine (Main, 2005) (Fig. 2.17). All of these stratigraphic intervals belong to the lower part of the Lewisville Member. The Lake Grapevine section coarsens upwards from fine grained rippled sandstone and burrowed mudstone at the base, to delta plain siltstone, paleosols and carbonaceous shale (clay rich peat) in mid-section, then capped by cross bedded fluvial sandstone (Main, 2005) (Fig. 2.17). The delta plain siltstone and carbonaceous shale of the Lake Grapevine exposures correlate to the heterolithic beds of the AAS and Bear Creek (Fig. 2.17). The sandstone intervals at Lake Grapevine are a thin sequence in this section, but exhibit cross-beddeding, with noted iron content and a similar buff tan (Munsell Soil Chart value of 7.5YR-7/8) as those that were observed in Bear Creek. These strata are attributed to fluvial, delta channel deposits (Main, 2005). Thus, the Lake Grapevine Woodbine

sections, the lower Bear Creek section and the AAS sections belong to the Lewisville Member, with the upper cross-bedded sandstones documented at Lake Grapevine and Bear Creek representing the Arlington Member. At the AAS, the upper exposures of ripple laminated heterolithic mudstone and sandstone correlate to the mid-section of Woodbine exposures at the SMU Bear Creek locality near DFW Airport (Fig. 2.17).

These strata were further correlated to another important Woodbine fossil locality, SMU 303, the *Protohadros* type locality. The *Protohadros* type locality is located on Texas FM 2499 at the edge of the towns of Grapevine and Flower Mound, the Flower Mound city limit is drawn at the Texas FM 2499 roadside, once on the outcrop, you've entered Grapevine. The Texas FM 2499 SMU 303 locality is ~2 km northwest of Grapevine Mills Mall and 1 km northeast of Rock Ledge Park and the Lake Grapevine spillway; N 32˚ 59.181 and W 097˚ 03.046 with an elevation of 156 m. The Texas FM 2499 road side exposures are outcrops that were excavated by highway construction in the early 1990's.

The Texas FM 2499 Woodbine exposures consist of ~5 meters of silty-sandy shale interbedded with siderite lenses and overlain by a peat bed. The elevation of the roadside exposures is ~156 meters (± 2 meters). The lower sandy siltstones and shales are light tan in color (Munsell Soil Chart value of 7.5 YR -8/4) with occasional sulfur stains, and interbedded with siderite (hematite) rich lenses and

common siderite concretions (Fig. 2.17). The peat bed is organic rich, with a high clay content and is fissile. Due to the high clay content and the fissile or platey structure, it should be considered as carbonaceous shale, rather than peat. The lower SMU 303 strata are similar in appearance to the coastal delta plain deposits studied from the exposures at Rock Ledge Park at Lake Grapevine (Main, 2005) (Fig. 2.17). The Lewisville Member was previously described as a coastal plain sequence by Dodge (1968), Main (2005) and Oliver (1971), with the Arlington Member consisting of fluvial, cross-bedded sandstone (Dodge, 1969; Murlin, 1974; Oliver, 1971). Therefore, the lowermost section of the *Protohadros* type locality is interpreted as being within the delta plain deposits of the upper part of the Lewisville Member, with the contact of the lower part of the Arlington Member occurring at the top of the section, south of the Texas FM 2499 exposures (Fig. 2.17).

The Arlington Member was observed at a ~4 m section of cross bedded sandstones 1 km south of Texas FM 2499. The SMU 303 *Protohadros* type locality sandstones occur in the upper portion of exposed outcrops across a field that lies tangential to the roadside exposures. The upper sandstones of site SMU 303 are located along the edge of a field, near lands maintained by the Army Corps of Engineers at N 32˚ 59.083 and W 097˚ 03.064, elevation ~158 m (± 2 meters). A peat bed was noted at the base of the studied sandstone section and was used to correlate the outcrops to the upper part of the section of the FM 2499 exposures (Fig. 2.17). The Arlington Member exposures consisted primarily of cross bedded

sandstone that are buff tan in color, interbedded with wavy-ripple laminated sandy siltstone and intermediate siderite concretion beds (Fig. 2.17).

The Arlington Member sandstone beds are a buff tan (Munsell Soil Chart value of 7.5YR-7/8) sand that is a fL, wavy laminated sandstone at the base that grades into a cross-bedded fU sandstone at the top with sulfur concretions occurring periodically in section (Fig. 2.17). The sandstone beds are similar in structure and appearance to the upper sandstone beds observed at Bear Creek and Lake Grapevine, and although thinner in outcrop, are similar to the definition of those within the Arlington Member as used by Dodge (1969), Murlin (1974) and Oliver (1971). Thus, the upper sandstone beds of SMU 303 are placed within the Arlington Member of the Woodbine Formation (Fig. 2.17). Head (1998) placed the *Protohadros* type locality within the Arlington Member of the Woodbine Formation. Of interesting note, the description of this section by Head (1998) made no mention of the separation of the two outcrops, or of the placement of Arlington Member contact with the Lewisville Member at this location. Based upon this section correlation, the SMU 303 *Protohadros* type locality straddles the contact of the upper most part of the Lewisville and the lower most part of the Arlington Member (Fig. 2.17). Thus the AAS Woodbine delta plain can be traced ~24 kilometers northwards across North Texas; from Arlington, to DFW International Airport, to the shores of Lake Grapevine and to roadside outcrops in the towns of Grapevine and Flower Mound.

2.3 Cretaceous Eustasy and Paleogeography

During the Cretaceous global sea level rose in a eustatic highstand that covered much of the continental interiors with shallow seas. In North America, this eustatic highstand is best recorded in strata of late Albian, Cenomanian and middle Turonian in age and is referred to as the Greenhorn cyclothem (Kauffman, 1969; Kirkland, 1996; Kirkland and Madsen, 2007). The Greenhorn cyclothem, or cycle, is recorded in the Cenomanian strata of the Dakota Formation of Colorado, New Mexico and Utah, the uppermost members of the Cedar Mountain Formation of Utah and the Woodbine Formation of North Texas (Holbrook, 2001; Johnson, 1974; Kirkland, 1996; Kirkland and Madsen, 2007; and Main, 2005). Although the Woodbine Formation is a prominent stratigraphic unit in North Texas, it is largely either buried in the subsurface, or obscured from study by urban sprawl. This lack of good outcrops is unfortunate, as many areas of North Texas once held vast exposures of Woodbine sediment at the surface, but the rapid expansion of the Dallas Fort Worth metroplex has covered many of the Woodbine exposures with apartment buildings, shopping malls and parking lots. The AAS is important as it represents a unique opportunity to study the Greenhorn cycle in Texas as AAS Woodbine exposures occur on ~2,000 acres of private land, currently undeveloped. The only other areas in North Texas where the upper members of the Woodbine may easily be viewed in outcrop are within Bear Creek at the south

entrance to DFW Airport, the north shore of Lake Grapevine and at intermittent roadside outcrops along Texas FM 2499 in Grapevine and Flower Mound.

Paleogeographically, North Texas was an emergent, but low lying coastal plain along a peninsula that protruded into the Greenhorn interior seaway of southeastern Appalachia (Elder and Kirkland, 1994; Hancock and Kauffman, 1979; Scotese, 2005) (Fig. 2.3). The peninsula was formed during the eustatic highstand of the mid-Cretaceous that flooded much of the North American continental interior, and presented a stable platform for deltaic deposition for much of the middle to late Cenomanian and early Turonian (Elder and Kirkland, 1994; Hancock and Kauffman, 1979; Haq et al., 1987; Kirkland, 1996; Main, 2005; Oliver; 1971). To the north the peninsula was a high topographic relief due to the Oklahoma highlands via the Arbuckle and Ouachita Mountains (Elder and Kirkland, 1994; Oliver, 1971; Scotese, 2005) (Fig. 2.3). To the south the peninsula was a low coastal plain composed of multiple river-delta channels migrating across acoastal plain depositing sediment via river avulsion and bifurcation (Main, 2005; Oliver, 1971; Trudel, 1994) (Fig. 2.3).

For this work, the North Texas Cenomanian peninsula is referred to as Rudradia, named so in honor of Rudra the ancient Hindu god of storms; also known as the "the Howler" (Basham, 1989). The name Rudra (or Rudradia) was chosen due to the position of the peninsula within the Greenhorn interior seaway, and for its potential for experiencing storms along its coasts. During the

Cenomanian stage of the Greenhorn cycle, what is now Florida would have been submerged, leaving the southern coast of Appalachia open to substantial impact from potential hurricanes (Scotese, 2005) (Fig. 2.3).

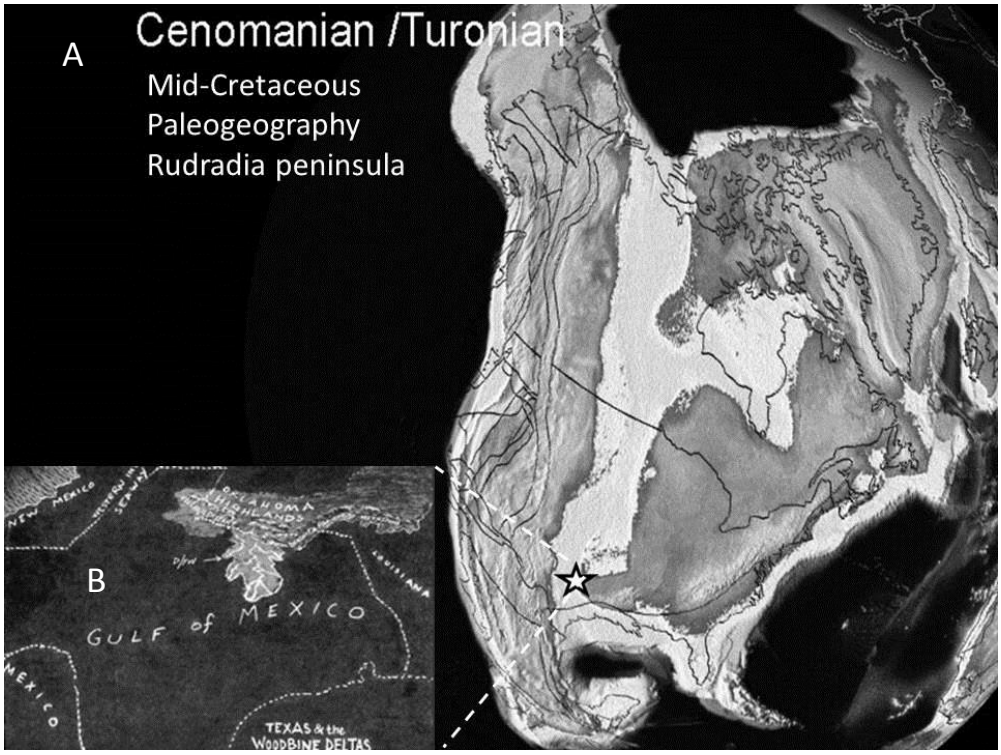

Figure 2.3 A. Cretaceous (Cenomanian-Turonian) North American paleogeographic map, AAS denoted with a star on the Rudradian peninsula of ancient North Texas (modified from Scotese, 2005). B. Expanded view of Rudradia and the Woodbine delta system (art courtesy of Clinton Crowley).

2.4 AAS Woodbine Paleoenvironments

The Woodbine Formation exposures at the AAS preserve distinct stratigraphic beds, or facies, that are denoted by changes in lithology (lithofacies), fossils (biofacies) and sedimentary structures. The AAS stratigraphic beds were subdivided into facies utilizing the facies concept previously defined and utilized by Collinson (1969) to describe deltaic facies, and de Raaf et al. (1965) and Walker (1983 and 1984) to describe facies models within a sequence stratigraphic framework. The AAS beds or facies are referred to as Facies A-D, each representing a different depositional environment within the coastal plain system. All of the AAS facies represent coastal deltaic paleoenvironments, many of which could be attributed to either estuarine or delta plain. However, they vary somewhat through the studied section based upon their placement within the system, most of which represent delta plain/floodplain environments, some of which could represent estuary environments.

Pritchard (1967) defined estuaries as semi-enclosed coastal bodies of water that have access to the ocean and within which seawater is measurably diluted by freshwater from land drainage. The AAS Woodbine sections are generally attributed to delta plains/floodplains that existed between distributary channels, however some horizons could have been part of an estuary system of mixed marine-fluvial sediments. As estuarine systems are a common part of the coastal system that interfaces with the delta plain, the AAS beds/facies are simply

referred to as delta plain with the understanding that there is a mix of fresh and brackish waters within the system.

The first bed, Facies A is a shallow marine near shore sand distinguished by trace burrows, and a siderite horizon of charcoal conglomerate, the second bed, Facies B is an organic and fossil rich peat bed, the third bed, Facies C is a paleosol, and the fourth bed Facies D a heterolithic mudstone bed with multiple crevasse splay sand lenses. Each distinct bed and its facies (lithologic and biofacies) will be discussed in further detail.

Bed 1-Facies A is classified as a shallow marine, near shore environment based upon the presence of trace fossil burrows, principally U-shaped back fill burrows of *Rhizocorallium* occurring with *Arenicolites* and branching *Thalasinoides* burrows (Seilacher, 2007) (Fig. 2.4). A prominent trace fossil bed was mapped ins a sandstone located 65 meters southwest of the AAS Dinosaur Quarry (UTM 3631846). This one bed was heavily burrowed with multiple *Rhizocorallium* exposed at the surface (Fig. 2.4).Within this same horizon, the fossils of a new taxon of decapod has also been recovered along with pycnodont tooth palates and shark teeth assigned to the relatively common Cretaceous shark genera *Cretodus* (Fig. 2.4). The ichnofacies are attributed to shallow water, marine environments of the lower to middle shoreface in which organisms burrow in into the sediment to form feeding structures (Seilacher, 2007). The trace fossils present in this bed are attributed to the *Skolithos* ichnofacies, or nearshore

environments and structures (Seilacher, 2007). Thus, the presence of the trace burrows, along with decopod fossils, fish and shark teeth recovered from Facies A, places it within a shallow, nearshore marine setting along the lower to middle shoreface (Fig. 2.4).

The lower facies studied at the AAS are attributed to a broad coastal tidal flat. This interpretation is supported by a large ripple bed found at the same horizon as the *Skolithos* trace fossil bed. The ripple bed is large, but covered periodically with rain-washed sediment and over grown with weeds in many places. Thus, it appears as sporadic exposures throughout the field south of the AAS hillside dig. One prominent bed is exposed at the site, and is located southwest of the AAS Dinosaur Quarry by 146 meters (UTM 0679750). The AAS ripple bed is 14.6 m L x 8.8 m W in size.

The ripples are preserved in a fine grained (fL) arenaceous sandstone that is burrowed heavily with horizontal and vertical trace makers (Fig. 2.5).The horizontal burrows are branching and attributed to *Thalasinoides*, the vertical burrows occur as parallel openings and are attributed to *Arenicolites* (Seilacher, 2007). The ripples are exposed at the surface and eroded, but are preserved well enough to identify the wavelength, morphology and paleoflow. The AAS tidal flat ripples are symmetric (some are slightly asymmetric), with peaked crests and rounded troughs with a wavelength of 8-10 cm (Fig. 2.5). Due to the general symmetric morphology and deep rounded troughs, the AAS ripples are considered

as formed under oscillatory conditions, as is typical of a tidal flat (Prothero, 1990). A paleoflow reading was taken from some of the best preserved ripples; the paleoflow along the ancient tidal flat was N76˚E/S250˚W (Fig. 2.5). The presence of ripples, numerous trace maker burrows along with decapod fossils are all indicative of a broad, nearshore shallow water tidal flat.

Although dinosaur tracks were not mapped within these beds, it is conceivable given the environment and common occurrence of tracks within the Lower Cretaceous Glen Rose Formation that tracks could be found within the AAS tidal deposits (Farlow, 1993; Main and Fry, 2009; and Shuler, 1917). The tracks of Dinosaur Valley State Park at Glen Rose are situated along an ancient coastline where herds of sauropods migrated along the open flats (Farlow, 1993). Sauropods are well documented within the Lower Cretaceous and Upper Cretaceous strata of Texas (Lehman and Coulson, 2002; Lehman et al., 2006; Rose, 2007) However, sauropods have not yet been reported from the mid-Cretaceous of Texas. Hadrosauroids are well documented in the Woodbine, and are known to have lived and migrated in herds (Head, 1998; Farlow, 1993; Lee, 1997b; Lockley et al., 1982; Main, 2005; Main and Fry, 2009). Previous researchers have reported ornithopod tracks occurring in the Woodbine Formation. Lee (1997b) reported numerous ornithopod (hadrosauroid) tracks in Woodbine Formation deposits along the north shore of Lake Grapevine at Murrell Park. The Murrell Park tracksite is ~2 km west of the SMU 303 *Protohadros* type

locality on Texas FM 2499, and within <1 km of the hadrosauroid site reported by Main (2005). Thus it is possible for tracks to be found at Woodbine fossil sites.

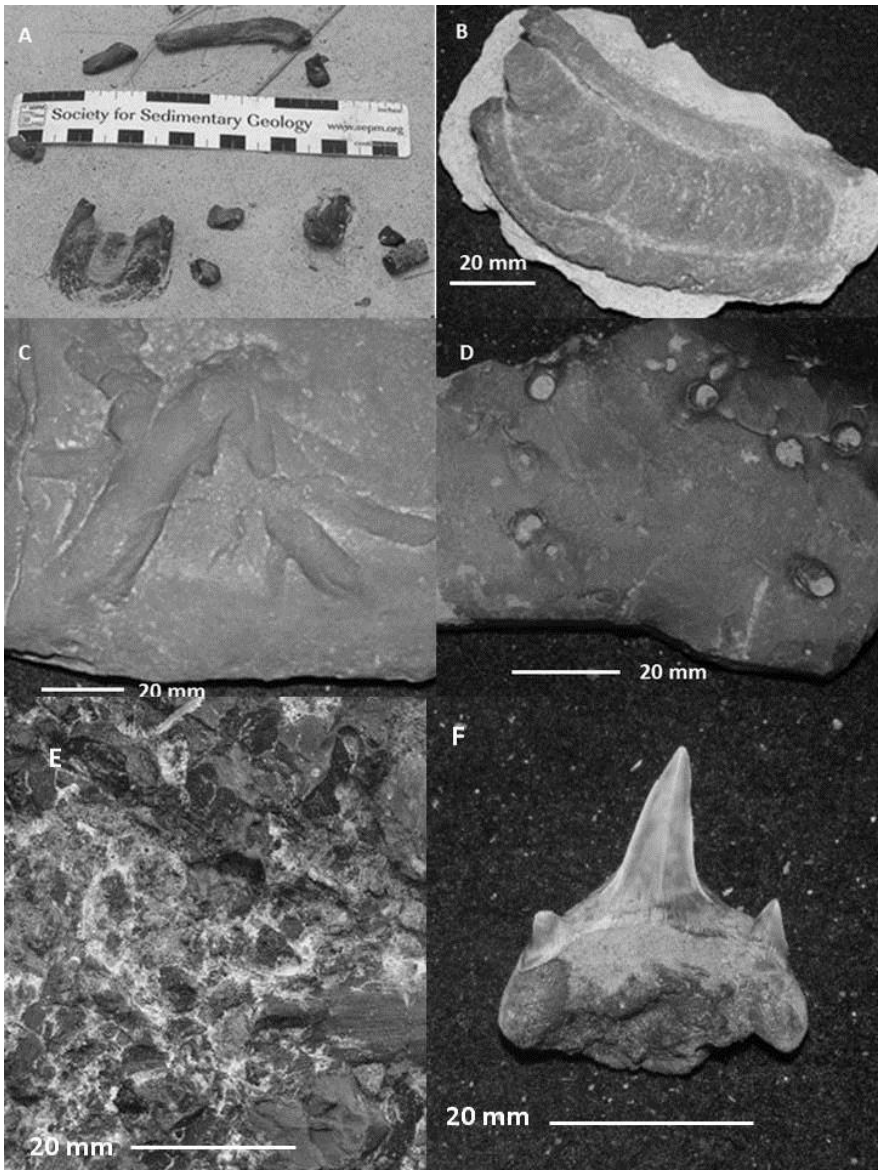

Figure 2.4 Facies A features. A. A weathered *Rhizocorallium*. B. A collected *Rhizocorallium* specimen, C. Thalasanoides D. *Arenicolites* and E. Charcoal conglomerate, charcoal clasts mixed with fossil wood in a siderite sandstone. F. *Cretodus* shark tooth from the nearshore sandstone of Facies A.

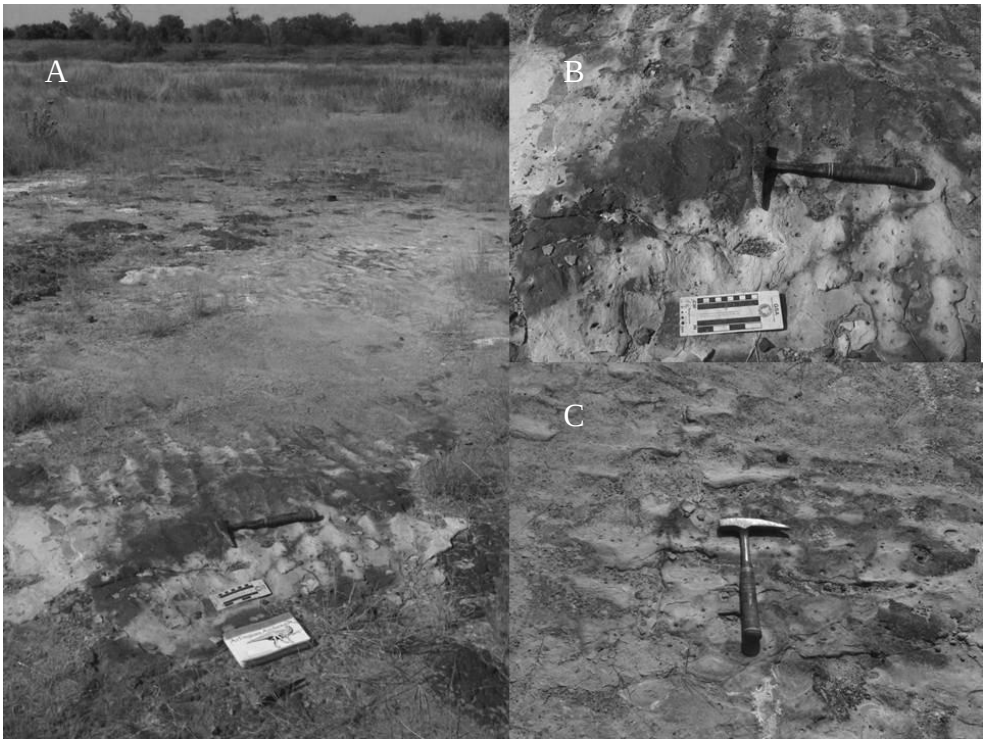

Figure 2.5 The AAS ripple bed. A. North facing image showing the 14.6 m length of the ripple bed and the NE paleoflow, hammer for scale. B. Oblique view of ripples with geologic hammer aligned perpendicular to the ripples to show paleoflow, GSA scale bar for scale (cm) of ripples and wavelength. C. Ripples in plan view, hammer for scale.

Included within Facies A is a siderite bed with charcoal inclusions that was classified as a charcoal conglomerate and showing evidence of forest fires. Fossil charcoal was observed in three distinct horizons in the Woodbine Formation exposures at the AAS (Fig. 2.4). The charcoal conglomerate in Sequence A is the first of the three forest fire horizons and will thus be notated as FFB1 for clarity. FFB1 occurs laterally contemporaneous to the burrowed trace fossil bed, although 120 meters to the northwest. It consists of multiple small

fragments of fossil charcoal bound in a siderite rich sandstone bed with petrified wood. The fossil charcoal fragments range in size from 0.5 cm -2.4 cm L, and the petrified wood varies from 6.4 cm -24.2 cm L (Fig. 2.5). The binding matrix of the wood and charcoal in FFB1 is siderite. Wells (2000) noted that siderite was common in the Woodbine Formation and was indicative of organic rich environments where sphaerosiderite and pyrite provided a source of iron.

FFB1 occurs at the base of the studied section, and is exposed at the surface to the west of the AAS Dinosaur Quarry (Fig. 2.5). It is 6.4 m L x 2.7 cm W at its mid-point it tapers to ~1 m W at each end to the east and west. The charcoal conglomerate is interpreted as part of a coastal, deltaic system where burned materials fell into a distributary channel and were later transported to the nearshore coastal environment and deposited. The dominant presence of siderite in FFB1 supports the paleoenvironmental model of an organic rich, swampy delta plain. Although FFB1 is the only charcoal conglomerate found in situ that was stratigraphically mapped, fragmentary hand samples of charcoal conglomerate are quite commonly found throughout the AAS. The contact between Facies A and the overlying Facies B was not accurately mapped due to erosion and talus from the nearby AAS hillside. Therefore, the age and stratigraphic relationship between the two Facies cannot be ascertained precisely.

Bed 2 –Facies B overlies the nearshore deposits of Facies A. Facies B is a lithologically and ecologically distinct bed (Fig. 2.14 and 2.15). Facies B and the overlying Facies C and D all occur on the AAS hillside outcrops. The AAS hillside outcrops occur at N32˚ 48.633 and W 097˚ 04.746 and at an elevation of ~148 meters (±2 meters). The hillside outcrops have a south facing, sloping, weathered profile and a gentle 10-12˚ eastwards dip. Facies B consists of an organic rich peat bed that is intermittently high in clay content, sulphur and pyrite. The Woodbine peat could be the result of continued sea level rise during the Cenomanian that led to a higher water table and extensive coal swamps across the Appalachian delta plain. Today peat forms in isolated areas on low lying plains, away from fluvial deposition and are typical of wetlands, bogs or fen meadows in the inland fluvial Cumberland Marshes of Saskatchewan Canada and the coastal Mahakam Delta of Kalimantam Indonesia and the Mississippi River Delta of the Gulf Coast (Davies-Vollum and Smith, 2008; Day et al., 2000; Gostaldo and Huc, 1992; Roberts, 1998; Smith et al., 1989).

The AAS peat is a laterally continuous, but a vertically thin bed (50-60 cm) that occurs along the base of the hillside exposures (Fig. 2.14 and 2.15). It is organic rich and highly fossiliferous, containing the mixed remains of numerous vertebrates, carbonized wood (branches and twigs) and fallen logs. The AAS peat is a laterally continuous bed, but thin (<1 m) and dark brown-black in hue, with a Munsell Soil Chart value that varies from 7.5 YR-3/1 to 7.5 YR- 3/2. It is

somewhat platy or shale like with a Munsell Soil Chart platy structure classification of Medium to Coarse (5 mm-10 mm thickness). The platy structure of the AAS Woodbine peat could almost place it within the classification of carbonaceous shale using the classification of Pettijohn (1957). But the peat is not easily friable; it is well lithified and does not easily crumble. The Woodbine peat is indicative of an inundated, standing water delta plain that formed from a distributary channel switching away from the site and allowing for anoxic still water deposition. Thus, Facies B represents calm, swamp deposition, likely a coastal inland fen or bog similar to the modern day Mississippi coastal plain, or the more mangrove style coast seen in the Mahakam Delta of Indonesia (Gostaldo and Huc, 1992; Roberts, 1998).

This Facies B horizon is highly fossiliferous, containing the mixed remains of several vertebrate taxa, including; fish, amphibian, mammal, turtle, crocodyliform, and dinosaur (ornithopod and theropod) (Fig. 2.15 and 2.17). The primary fossil horizon at the AAS occurs within this facies, and has produced the remains of a new taxon of crocodyliform, along with numerous turtle remains, some of which record the feeding behavior of a large crocodyliform (Allen et al., 2011; Main and Fry, 2011; Noto et al., 2012). Many of the fossils occur from along the mapping grid from (32.10) to (-26.8), from the Crocorama, the Turtle Buffet and the Nursery sites. The peat bed in the Dinosaur Quarry did not yield as many vertebrate fossils, as it did logs. Although some remains of a sub adult

hadrosauroid were recovered from the edge of the quarry at (-28.7) along with some crocodyliform material and fragmentary turtle shell. The sub adult hadrosauroid recovered from the peat bed consisted of a complete ilium and near complete sub-adult dentary.

The peat of Facies B also contains abundant carbonized or coalified logs, the largest of which were recovered from the AAS Dinosaur Quarry. The coalified logs are classified as vitrain coal using the British classification scheme utilized by Pettijohn (1957). The AAS peat logs are jet black and glassy in cross section, and relatively structure less with intermittent conchoidal fractures, and extremely brittle to the touch. The first log was discovered at the southern most edge of the Dino Quarry by Phil Scoggins in the fall 2008 dig season (Fig. 2.7). The log was so large, that it was initially mistaken for a dinosaur limb bone (Fig. 2.6 and 2.7). After a long excavation, it was uncovered and revealed to be over 4 meters long (Table 2.2). Later in the spring of 2009 another twenty logs were excavated from the Dino Quarry peat bed, where they principally occurred within a 6 m L x 5 m W area within the middle of the quarry (Fig. 2.7). The logs vary in size from 0.34 m – 4.2 m and follow a distinct depositional trend, as many of the logs are lined up in a common NE to SW compass bearing (Table 2.2) (Fig. 2.6). Few, if any of the carbonized logs at the AAS represent complete trees, all of them are fragmentary and therefore are considered as debris. Of particular interest, the logs occur within a peat bed, and not within a lithologic unit, such as

sandstone, siltstone or a silty-mudstone, which could be linked to a log jam, typical of a channel deposit.

Many of the world's deltas are associated with dense, coastal vegetation that form peatlands, marshes and coastal mangroves. The Mahakam Delta of East Kalimantan, Indonesia is well documented for its dense coastal mangroves and low lying trees, as is the Rhine Meuse Delta of the Netherlands. The Amazon River basin of South America is well known for its dense coastal jungles and equally the Mississippi River delta of the North American Gulf Coast for its extensive marshlands (Dunbar, et al., 1994; Gastaldo, 1992; Storms et al., 2005; Stouthhammer and Berendson, 2000). The Mississippi River delta plain has a record of fallen wood debris that is attributed to hurricanes that date back several centuries (Dunbar et al., 1994; and Kolb and Van Lopik, 1958). In the Atchafalaya River, log jams have been documented as a cause for channel avulsion and diversion (Roberts, 1998). However, the Atchafalaya log jams occurred within the river channel, not on the delta plain (Roberts, 1998). The AAS peat is lithologically uniform, lacking sand content, pebbles or gravel that would imply an influx of water flow. Therefore, it is interpreted that the alignment of the logs is potentially related to coastal storms, possibly blown down in a common direction during a hurricane or other coastal climate driven process.

It should however be noted that some coasts are mud dominated, with little sand deposited either on the plain or the coast. The modern Mississippi River has been documented to have distributary channels that are silt, mud and clay dominated, not all channels are sand dominant (Aslan et al., 2005; Dunbar, et al., 1994; Tornqvist and Bridge, 2002). Within the Mississippi River floodplain, numerous factors have been attributed to river avulsion (Aslan et al., 2005). Most studies focus on channel pinch out due to sand aggradation, which leads to channel splays, avulsion and bifurcation across the delta plain (Aslan et al., 2005; Slingerland and Smith, 2004; Tornqvist and Bridge, 2002). However, it is plausible that the AAS Dinosaur Quarry logs represent an ancient mud dominated coastal channel that became blocked with downed drift wood and logs that effectively jammed, closed of the channel and lead to avulsion of the channel across the delta plain similar to the modern Atchafalaya River, log jams (Roberts, 1998).

The effects of climate driven coastal processes such as cold fronts and hurricanes are well documented along the Gulf coast, and the Atchafalaya and Mississippi Rivers in particular (Dunbar et al, 1994; Liu and Fearn 1993; 2000a and 2000b; Liu, 2004; and Roberts, 1998). In the Atchafalaya River, coastal sedimentation and delta plain deposition are significantly affected by seasonal cold fronts and hurricanes. The strong northerly winds of the fall season have been documented to disrupt prevailing westwards transport of suspended

sediment and create a westward drift referred to as the "mudstream" (Roberts, 1998). The wind driven fluid mudstream deposits significant amounts of mud that accumulates to form extensive mudflats along the Atchafalaya coastal plain (Roberts, 1998). In the case of the AAS, there is no evidence of wind driven mudstreams.

The presence and possible influence of hurricanes along the Cretaceous coast of North Texas is also supported by the multiple beds of fossil charcoal at the AAS, as prehistoric wildfires were likely ignited by the lightning strikes (Scott, 2010). Lighting strikes are generated by storms. The study of the geologic record of storms, or hurricanes, is a relatively new field that was referred to as Paleotempestology by Liu (2004). Paleotempestology relies principally upon the Quaternary record of storms, as the more recent geologic record provides more data (Liu, 2004). Although tracing the record of Gulf storms from the Quaternary to the Cretaceous present's challenges, it holds the potential to answer broader questions about coastal systems through time.

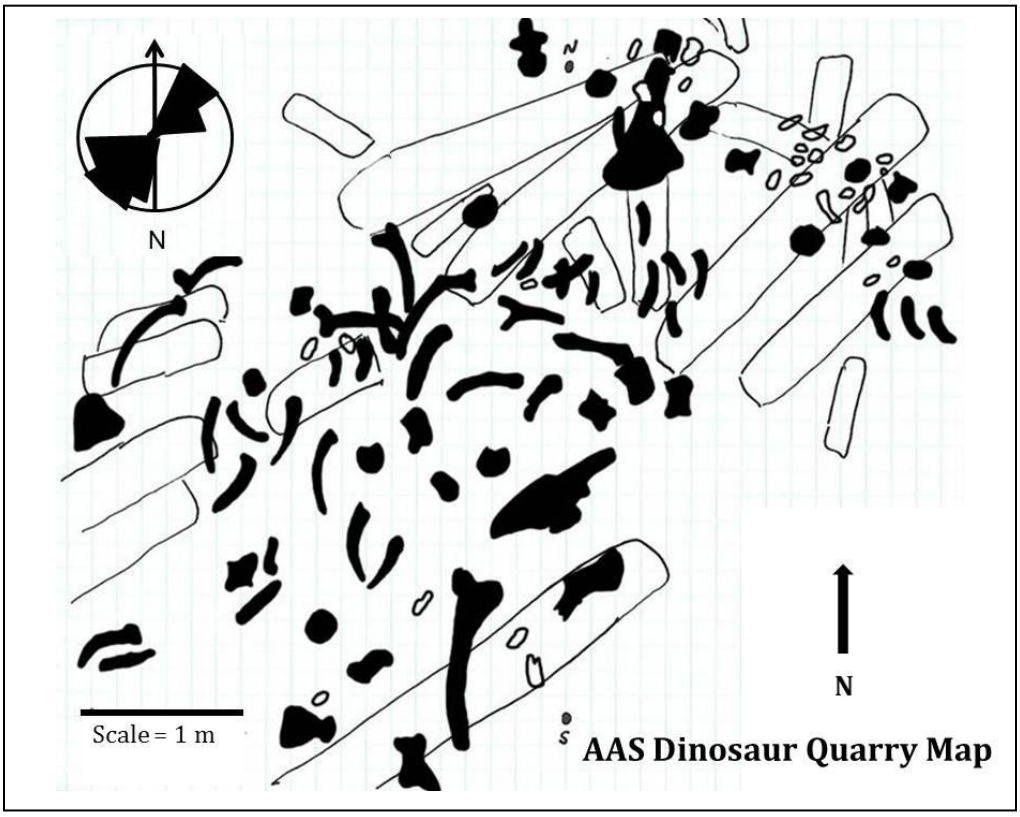

Figure 2.6 AAS Dinosaur Quarry map of "Logs and Bones" showing the NE-SW alignment of the fossil logs in the quarry peat bed (note Rose Diagram). The overlying dinosaur fossils are black; the carbonized logs are white. Dino Quarry log dimensions, compass and map data are in Table 2.

Table 2.2 Measurements of carbonized logs mapped within the AAS Dinosaur Quarry (measurements in centimeters: N/A = no data available).

Specimen	Position in Quarry	Compass data	Measurements: L x W
AAS-2008A	North grid	N50˚E /S240˚W	420 L x 28 W
AAS-2009B	West grid	N50˚E/S240˚W	72 L x 22 W
AAS-2009C	West grid	N55˚E/S245˚W	70 L x 21 W
AAS-2009D	West grid	N40˚E/S235˚W	68 L x 24 W
AAS-2009E	West grid	N65˚E/S255˚W	108 L x 26 W
AAS-2009F	West grid	N/A	54 L x 21 W
AAS-2009G	West grid	N/A	82 L x 24 W
AAS-2009H	North grid	N55˚E/S245˚W	48 L x 22 W
AAS-2009I	North grid	N45˚E/S240˚W	204 L x 26 W
AAS-2009J	North grid	N35˚E/S230˚W	176 L x 24 W
AAS-2009K	North grid	N/A	55 L x 21 W
AAS-2009L	North grid	N.A	62 L x 22 W
AAS-2009M	North grid	N35˚E/S230˚W	58 L x 22 W
AAS-2009N	East grid	N35˚E/S225˚W	165 L x 24 W
AAS-2009O	East grid	N30˚E/S220˚W	128 L x 22 W
AAS-2009P	East grid	N25˚E/S210˚W	34 L x 18 W
AAS-2009Q	East grid	N20˚E/S210˚W	46 L x 20 W
AAS-2009R	East grid	N20˚E/S200˚W	228 L x 24 W

Figure 2.7 Images of carbonized logs excavated the peat bed of the AAS Dinosaur Quarry A. Dig crew excavating logs from the quarry; 2009. B. Exposed carbonized logs. C. Wood knot in a log .D. First log found at AAS in 2008. E. D. Main plastering the first log found in the quarry to protect it.

Bed 3-Facies C overlies the fossiliferous peat bed of Facies B and is a thicker stratigraphic horizon. Facies C is an organic and clay rich paleosol. The paleosol is a heavily rooted, organic and sulfur rich fossil soil, with intermittent swale structures and numerous concretions (Fig. 2.8 and 2.15). It is dull grey in color, with a Munsell Chart hue of Gley 10GY-5/1 that lightens in hue upwards in section into Gley 5PB-7/1. The paleosol is mud and clay rich, with slickensides and swale structures that are an indication of periodic wetting, followed by drying (Mack et al., 1993). The paleosol is classified as a Histic Gleysol, a fossil soil that forms in tropical climate belts (Mack et al., 1993; Goswami, 2011). It is characteristic of swamps, or peatlands (often referred to as a peatland soil) where the water table fluctuates, but is typically high and drainage is poor (DiMichele, et al., 2006; Mack et al., 1993). The Gleysol classification is based upon the grey, blue-brown (gley) appearance in outcrop with patches of red and yellow-brown staining (sulfur), the high clay and organic content, along with the presence of sulphur and numerous concretions (Collins and Kuel, 2001; Mack et al., 1993).

The presence of concretions and root structures was used to differentiate the paleosol into two horizons; an A horizon and a B horizon. The lower B horizon was a clay rich mudstone, darker in hue (10GY-5/1), organics were sparse and it lacked concretions. The paleosol B horizon exhibited slickensides and swale structures that are indicative of wetting and drying, possible indicators of seasonal variation on the delta plain. Of ecological interest, it was within the B

horizon of the paleosol that the remains of a large hadrosauroid (Dinosauria: Ornithischia) were recovered (Fig. 2.17). The remains were disarticulated but associated, and consisted of the post crania of a single side of a lone individual: cervical, dorsal and caudal vertebrae, a scapula and coracoid, an ilium, ischium and prepubis (Fig. 2.6 and 2.17). The fossils were excavated from the lower most B horizon at the contact with the peat (Fig. 2.6). Two hypotheses are proposed for the deposition of the dinosaur remains.

The first taphonomic hypothesis assumes that the dinosaur was deposited near the location of death, with little or no transport. This hypothesis is supported as the remains recovered were not broken or fragmentary and represented one side of the body. It is likely that one side of the animal settled into the mud, under its own massive weight and was preserved (Main, 2010). The author refers to this hypothesis as the "Fat and Flat" hypothesis, as the animal sank into the mud under its own weight.The second hypothesis assumes transport of the skeletal remains along the delta plain. This hypothesis is supported by the partial post cranial skeleton and the lack of cranial material. Dinosaur skulls are composed of numerous individual bones, many of which are thin and fragile. If transported a given distance under turbid flow conditions, the skull would be disassembled, broken and destroyed. The second deposition hypothesis would require that the paleosol B horizon have been deposited as a mudflow, likely under storm conditions with high winds. Similar deposits have been documented along the

modern Mississippi River delta plain by Roberts (1998) and referred to as storm related mudflows. Cases of “Bloat and Float” have been recorded in which dinosaurs have died along a coastline and were later carried out to sea by the tides, then burst and settled to the seafloor (Main, 2010; Schwimmer, 1997). With the second taphonomic hypothesis, the dinosaur remains were carried across the delta plain, not out to sea. The dinosaur remains were mapped and later noted to follow a similar depositional trend of NE-SW that was documented in the underlying peat bed and carbonized logs (Main, 2010) (Fig. 2.7). The alignment of the dinosaur remains in a similar compass bearing as the numerous carbonized logs possibly implies transport. Due to the accumulation of large bones within a single, distinct fossil horizon, the site was named the Dinosaur Quarry.

The upper A horizon was organic rich, lighter in hue (5PB-7/1), with numerous concretions (Fig. 2.14 and 2.15). The concretions observed within the upper paleosol horizon A, were numerous, some of which were quite large (>25 cm diameter). The concretions did not react to hydrochloric acid (HCL) when tested, thus they are not composed of calcium carbonate. They are stained red, and thus interpreted to have either siderite or hematite included in their composition. Organic rich, sulfate soils bearing siderite concretions are typical of coastal plains, or swamps where the water table is high and the soil is saturated (Calder et al., 2006; Collins and Kuel, 2001; DiMichele, et al., 2006; Mack et al., 1993; Main, 2009; van Breeman, 1982). The upper A horizon lacked the numerous

dinosaur fossils that were recovered from the lower B horizon, though some scattered, fragmentary remains of dinosaur bone were recovered sporadically throughout the horizon, as well as rare crocodyliform teeth and minor amounts of turtle shell.

A second forest fire bed (FFB2) occurs within the concretions of the upper paleosol horizon, some of which were noted to contain vertical, columnar charcoal roots, or stumps (Main et al., 2010) (Fig. 2.8). Concretions that form around roots are generally referred to as *Rhizoconcretions*, or more specifically as *Glaebules* in the case of concretion formation within soils (Brewer and Sleeman, 1964). The charcoal roots, or stumps in FFB2 were interpreted to be plant remains as they were vertical, not horizontal, and columnar to conical in shape; thick on top and tapering at the bottom (Main et al., 2010). Over a dozen root structures were documented in the Dinosaur Quarry paleosol, they are columnar, Medium to Coarse (40-150 mm width) on the Munsell Chart Prismatic Scale and ranged in length from 10 cm L-42 cm L (see Table 2) (Fig. 2.8). As many of the charcoal structures documented in the quarry paleosol were within 10-20 cm in length and within 10 cm in width, they were interpreted as root structures rather than stumps (Table 2.3). Only three charcoal structures were documented in the quarry at over 30 cm in length and 12 cm in width. These three charcoal structures could be considered as small stumps, or simply large roots (Table 2.3). Concretion formation can be indicative of climate, seasonal dryness or precipitation, as well

as an indicator of organic material in the environment and the burned tree roots and stumps are considered as evidence of wildfires (Brewer and Sleeman, 1964; Ludvigson et al., 1998; Wells, 2000; White et al., 2001).

The top of the Facies C ends with a thin charcoal bed that unconformably overlies the paleosol horizon, and is overlain by a siderite rich lag deposit. The charcoal bed occurs in outcrop primarily along the east wall of the AAS Dinosaur Quarry (Fig. 2.8). It is a thin lenticular bed that tapers and pinches out to the west. It is ~22 cm at its thickest point, is sand rich and has gravel inclusions throughout the bed. The gravel inclusions vary in size from 4 mm – 16 mm L; all are subrounded-rounded, implying abrasion via tumbling during transport. Paleosols with overlying charcoal beds have been reported previously from the Hell Creek Formation, and were interpreted as being representative of seasonally dry swamps from subhumid climates (Retallack et al., 1987). However, the presence of sand and rounded gravel inclusions within the charcoal, led to the interpretation of this horizon as a debris flow, or a charcoal avulsion deposit that can occur on delta plains (Davies-Vollum and Smith, 2008; Kraus, 1996; Main et al., 2010, Roberts, 1998).

Delta switching and avulsion within the modern Atchafalaya River in the Mississippi River delta plain and in the Cumberland Marshes of Saskatchewan, Canada are well documented as a cause for the significant displacement of

sediments across low lying floodplains in the modern world (Davies-Vollum and Smith, 2008; Roberts, 1998). Thus, the FFB3 horizon is interpreted as being representative of a wildfire that burned further inland, reducing the coastal foliage to a surficial charcoal that was later transported across the delta plain (Main et al., 2010). The mode of transport could have been by stage 1 avulsion of a channel, using the classification of Smith et al. (1989) and Stouthhamer (2001). The unconformable base of the debris flow bed is likely an erosional feature, and supports the interpretation of FFB3 being a debris flow deposit.

Table 2.3
Measurements of fossil charcoal roots and stumps found in the AAS Woodbine Paleosol (all measurements in centimeters).

Specimen	Position in Quarry	Length x Width
AAS-2010-E1	East grid (-32. 9)	10 L x 4 W
AAS-2010-E2	East grid (-32. 9)	12 L x 5 W
AAS-2010-E3	East grid (-34. 9)	14 L x 6 W
AAS-2010-E4	East grid (-36. 10)	18 L x 8 W
AAS-2010-E5	East grid (-38.10)	22 L x 9 W
AAS-2010-N1	North grid (-42.10)	28 L x 12 W
AAS-2010-N2	North grid (-44.10)	32 L x 11 W
AAS-2010-N3	North grid (-44. 10)	24 L x 10 W
AAS-2010-N4	North grid (-45. 10)	36 L x 14 W
AAS-2010-N5	North grid (-46. 10)	42 L x 15 W
AAS-2011-N6	North grid (-46. 10)	18 L x 8 W
AAS-2011-N7	North grid (-48. 11)	11 L x 5 W
AAS-2011-N8	North grid (-48. 11)	26 L x 12 W
AAS-2011-W1	West grid (-52.10)	12 L x 5 W
AAS-2011-W2	West grid (-53. 10)	16 L x 6 W

Figure 2.8 A cross sectional image of the Woodbine Formation outcrops seen in the AAS Dino-Quarry with images of burned roots (A-D) found in the Hisitic Gleysol, or FFB2 horizon. Dashed line denotes the boundary of the last forest fire horizon (FFB3).

Bed 4 –Facies D overlies Facies C, and is a thick heterolithic bed of mudstone and siltstone interbedded with wavy laminated thin sandstone sheets that represent levee and stage 1 avulsion deposits of a coastal delta plain. Facies D varies in thickness from .70 cm to 1.5 cm (based upon the slope of the hillside); it begins with a thin siderite and fossil rich sandstone bed that overlies the debris

flow bed of Facies C with an unconformable erosional base. The sandstone lag deposit varies in thickness from 5 cm to 12 cm. It is graded, siderite rich and variably composed of pebbles, and frequent gravel (0.6-2.2 cm L), some of which are phosphatic and occur with fragmentary fossil debris (Fig. 2.9). This bed is graded, with ripple laminated sandstone at the base that grades into a pebble conglomerate at the top. The gravel and fossil rich siderite bed is interpreted as a lag deposit. Previously, a similar bed was reported from the Woodbine by Lee (1997) at SMU locality 254, which he classified as transgressive lag. However, based upon the classification scheme used by Rogers and Kidwell (2000), marine transgressive lag deposits should have invertebrate shell debris and little to no terrestrial vertebrate fossil content.

The AAS lag deposit lacks invertebrate shell debris, and vertebrate fossils along with charcoal debris are common. The presence of phosphate nodules could be used to support a marine origin of the lag deposit, however, phosphate nodules may also form in brackish water, or calm stagnant waters typical of peat forming swamps (Pettijohn, 1957). Due to the thickness of the bed (< 0.5 m), its composition and fossil content, and it's position within a section bound by terrestrial strata, this lag is not interpreted as a transgressive lag, but rather a form of tempestite, or episodic deposit as described by Dott (1983), Kumar and Sanders (1976), and Marsaglaia and Klein (1983). The episodic, or storm lag deposit interpretation is supported by the presence of charcoal fragments and terrestrial

fossils sampled within the bed (dinosaur teeth and turtle shell), with only a minor component of marine fossils; shark and ray teeth. Thus, this bed is interpreted as an episodic deposit, or basal lag associated with possible storm conditions along the Cretaceous coast (Dott, 1983; Kumar and Sanders, 1976).

Figure 2.9 AAS Woodbine lag deposit. Note hummocky erosional base, ripple laminated, micro-hummocky sandstone grading into a gravel conglomerate at the top of the bed
(SEPM 15 cm scale bar for scale).

Overlying the lag deposit are a series of heterolithic deposits included within Bed 4-Facies D. The Facies D heterolithic strata are composed of rhythmically interbedded muddy-siltstone and sandstone bodies that were ~1.5 m (146 cm) in thickness, although the bed could be thicker as the uppermost section

was weathered and covered with talus (Fig. 2.14 and 2.15). The section is composed of lenticular bedded rhythmites with thin (0.8-1.2 cm thick) siderite bands and thin (0.2 -1.4 cm thick) sand lenses that are ripple laminated, thus demonstrating fluctuating hydrodynamic conditions that are typical of delta plain-floodplain crevasse complexes, as well as lakes, coastal estuaries and tidal mudflats (Boggs, 1995; Prothero, 1990) (Fig. 2.10 and 2.11). Rhythmically deposited nontidal sediments consisting of alternating sandstone and carbonaceous laminae are common in modern wetlands and have been noted in the famous Dinosaur Park Formation from the Late Cretaceous of Alberta (Eberth, 2005). Facies D is bioturbated with small (< 1 cm) horizontal burrows that appear as round to compressed ovoid structures in outcrop (Fig. 2.10 and 2.11). Floodplain/delta plain environments such as crevasse splay complexes, can demonstrate a variety of horizontal burrowing invertebrates ranging from freshwater clams to beetles and spiders (Hasiotis, 2002). The first section of lenticular beds are capped by a large, 10 cm thick rippled to hummocky bedded sandstone lens, with a ripple wavelength of ~10 cm (Fig. 2.10).

Figure 2.10 Hummocky bedded sandstone lens observed in Facies D of the AAS Dino Quarry. Arrows denote ripple crests and show wavelength (10 cm) (SEPM scale bar for scale).

Three sand lenses of variable thickness were observed in the upper heterolithic strata of Facies D (Fig. 2.10 and 2.11). They decrease in thickness upwards in section and are interpreted as crevasse splay. The first sand lens overlies the first sequence of heterolithic sediments; it is ~10 cm thick and composed of well sorted, tan arenaceous fine grained (fL-fU) sand. It is bioturbated with roots and burrows and was found to contain some fossils, consisting of a minor amount of mixed terrestrial and brackish water faunas; principally crocodyliform teeth and fragmentary turtle shell along with shark teeth. The sand lens has ripples throughout, and is capped with symmetric ripples

with 1.5-2 cm height and 10 cm wavelength at the top (Fig. 2.10). The presence of ripples within the bed, along with the mixed brackish water fauna, and the rippled-hummocky cap led the author to interpret the bed as a possible episodically influenced avulsion deposit. The interpretation of these rhythmically bedded, heterolithic strata as fluvial in origin as opposed to a tidally influenced mudflat is supported by the amount of sand in the section, sedimentary structures and bioturbation. The rippled sands are fairly uniform, not bidirectional as what would be expected from a tidal flat due to variation of tidal current speed (Dalrymple, 1992).

Heterolithic beds of fluvial or coastal plain origin are well documented within the geologic record, and from notable fossil sites. Eberth (2005) noted rhythmically deposited heterolithic beds in the Cretaceous (Campanian) Dinosaur Park Formation of Canada and related them to fluvial channel avulsion across a floodplain rather than tidal flat deposits. He based his interpretation upon the lack of claystone in the beds, the abundance of coalified plant remains and the amount of sand and silt associated with the mudstones. Hatcher (1893 and 1903) described ceratopsian sites within heterolithic deposits of the Cretaceous Lance Formation in Wyoming. Kirkland and Madsen (2007), Kirkland (1998 and 2005), Kirkland et al. (1997) and McDonald et al. (2010 and 2012) documented numerous vertebrate bearing fossil sites from the floodplain deposits of the upper members of the Cretaceous Cedar Mountain Formation of Utah. Brown (1907),

Bakker et al. (1988), Fastovsky (1987), Horner and Lessem (1993) Horner et al. (2011), Osborn (1905) and many others, have reported numerous important vertebrate fossil sites from the heterolithic, or floodplain deposits of the Hell Creek Formation, most notable of course being the infamous *Tyrannosaurus rex.* Previously, Lee (1997b) reported important vertebrate fossil bearing sites occurring within the Woodbine Formation at Bear Creek. Similar paleoenvironments to the Woodbine were described by Carr (1991) for the heterolithic beds in the Late Cretaceous (Coniacian-Santonian) Wepo Formation of Arizona and by Calder et al. (2006) for heterolithics at the famous Joggins Fossil Site within the Pennsylvanian Joggins Formation of Nova Scotia.

In the Wepo Formation, the sediments are nearly identical to those of the Woodbine; carbonaceous shale/peat beds overlain by heterolithic sequences of interbedded mudstone and sandstone with thin rippled sandstone sheets occurring throughout (Carr, 1991). Carr (1991) interpreted the heterolithic strata of the Wepo Formation as coastal plain deposits with avulsion driven sandstone sheets occurring throughout the section. Of interesting note, the Wepo Formation occurs along the southwestern margin of the interior seaway, due west on the opposite side of the seaway from the Woodbine in North Texas. At the Joggins Fossil Site, the stratigraphy described by Calder et al. (2006) is nearly identical to that of the AAS. The Joggins Fossil Site is famous for its abundant lycopsid trees preserved within interdistributary wetland deposits, principally heterolithic mudstone and

sandstone, overlying peat with common siderite (Calder et al., 2006). Similar to the AAS delta plain system represented in Facies D, the Joggins Fossil Site heterolithic beds contain interbedded mudstone alternating with planar-lenticular sandstone beds that vary in thickness, are current ripple-cross laminated and have erosional bases (Calder et al., 2006).

The rhythmically deposited upper heterolithic beds observed in the Woodbine Formation at the AAS are similar in nature to those reported previously by Calder et al. (2006), Carr (1991), and Eberth (2005) in that they are coastal, but with fluvial origins and influence, as the studied sections were likely in the distal delta plain, away from the tidal flats. It is worth noting however, that the thickness and scale of the Joggins Formation deposits are much greater than those of the Woodbine Formation, as the entire AAS section was ~ 2.5 meters (with the heterolithic deposits representing ~1.5 meters) and the Joggins sections were composed of 30 meter exposures (Calder et al., 2006). Regardless of the volume of sediment, there are similar patterns recognized between the two sites. Calder et al. (2006) noted the presence of siderite within the Joggins Formation. Siderite concretions, as well as thin bands of siderite were observed in the strata of the AAS Dinosaur Quarry (Fig. 12B). Calder et al. (2006) noted the pervasive presence of siderite in the Joggins Formation as an indicator of persistently water logged substrate, typical of a wetland or marsh. Of particular interest, Calder et al. (2006) noted the ripple-cross laminated sandstone and heterolithic beds as

evidence of episodic deposition. Similarly, the ripple-hummocky bedded sandstones interbedded within the laminated siltstone/mudstone of Facies D are interpreted as delta plain deposition that were potentially episodically influenced, a reflection of coastal processes and climate.

Invertebrate fossils were collected from the heterolithic deposits of Facies D, as well as the underlying mudstone of the Facies C paleosol (Fig. 2.12). The invertebrate fossils represent brackish coastal environments, all of which are attributed to the Lewisville Member (Dodge, 1968; Johnson, 1974; and Stephenson, 1952). The invertebrates collected include; UTA-AASI-020 the gastropod *Anchura whitneyensis* (a negative mold), UTA-AASI-017 *Carota pendula*, UTA-AASI-010 *Paladmete tubiform*,UTA-AASI-003-005, and UTA-AASI-011-015 *Gyrodes sp*., UTA-AASI-006 *Natica striaticosta* and UTA-AASI-007 *Lunatia pendernails* (Conrad, 1860; Cragin, 1893; Roemer, 1849; Stephenson, 1952) (Fig. 2.12). The most common genus recovered from the AAS was *Gyrodes,* a fresh water to intertidal carnivore that feeds on detritus, decayed matter (Stephenson, 1952).

The paleoenvironments of these genera range from fresh water, to brackish intertidal coastal waters and nearshore marine waters (Stephenson, 1952). As these specimens were collected from Facies C and D, the AAS paleosol and heterolithic bed, they are interpreted as a brackish water fauna from the Woodbine delta plain swamps (Fig. 2.12). Of greatest importance, is the

biostratigraphic utility of the Woodbine invertebrates in ascertaining an age range for the AAS. The Facies C and D invertebrates biostratigraphically place the AAS in the lower to middle strata of the Lewisville Member (~95 Mya) (Stephenson, 1952) (Fig. 2.12). *Anchura* and *Gyrodes* are here used to establish a biostratigraphic zone for the lower to middle Lewisville Member, which was then compared to the SMU 245 Bear Creek site at the south entrance to DFW airport, then north to Rock Ledge Park at Lake Grapevine and then to the *Protohadros* type locality SMU 303 on Texas FM 2499 (Fig. 2.16). Thus, the AAS invertebrate data allows the AAS Woodbine strata to be correlated to other Woodbine fossil sites in North Texas and to establish a relative age date between the sites, which is important in order to ascertain the unique age at which the AAS Woodbine exposures represent.

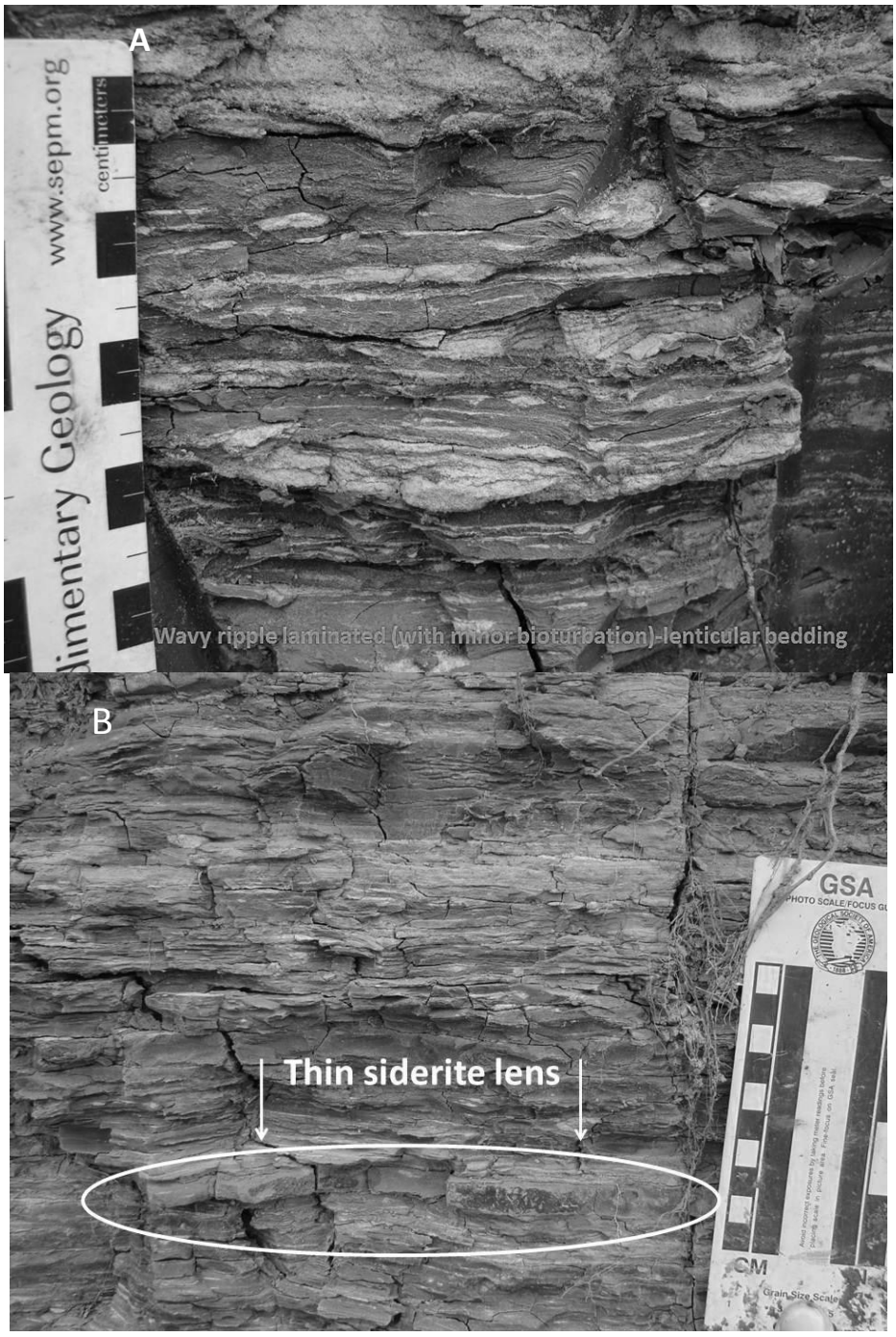

Figure 2.11 Heterolithic bed of Facies D as observed in the upper Woodbine strata of the AAS Dino Quarry. A. Note small scale ripples and oblate burrows (SEPM Scale bar for scale). B. Thin siderite lens within heterolithic strata.

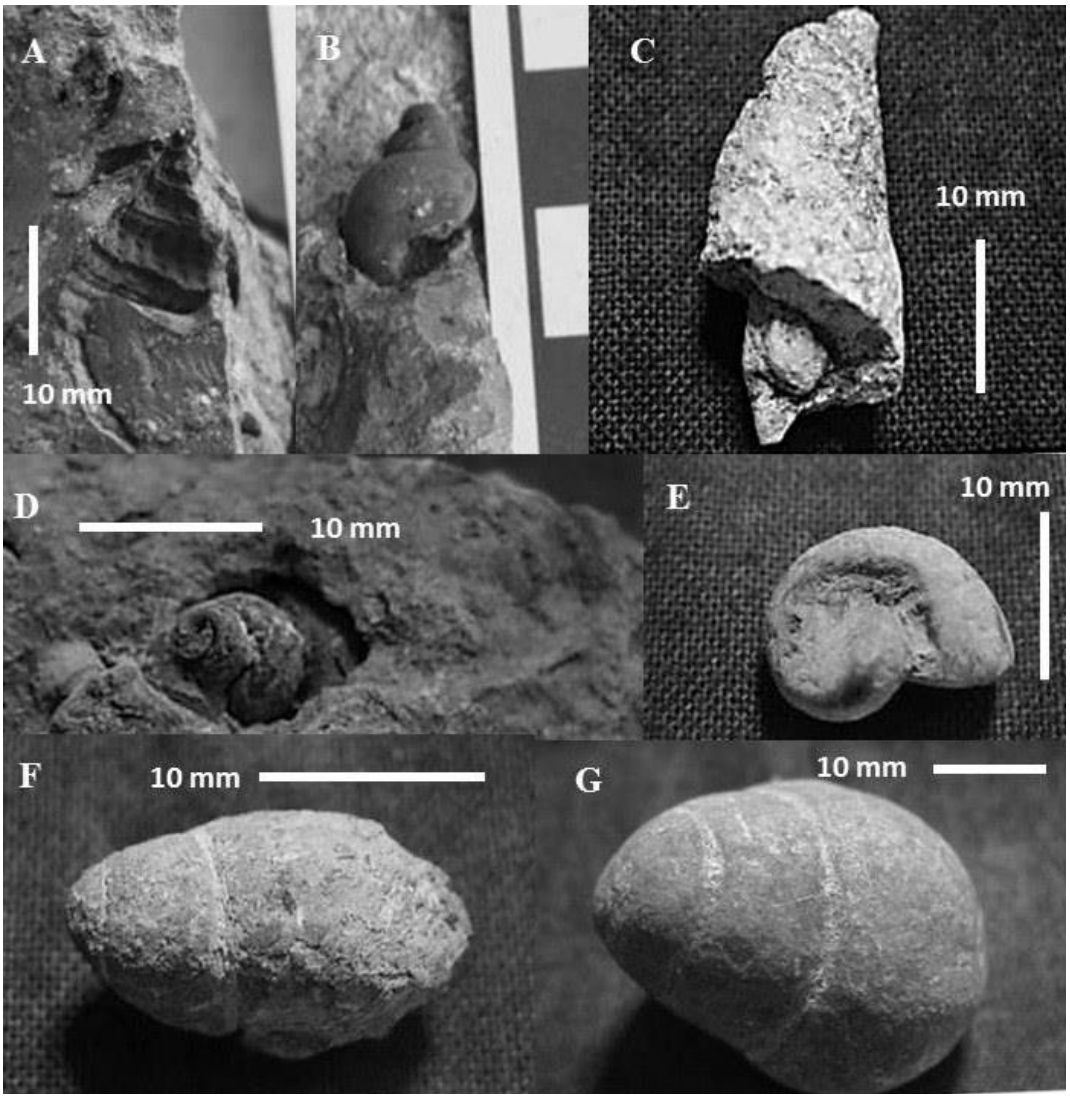

Figure 2.12 AAS Woodbine invertebrates collected from heterolithic Facies D and the lower mudstone horizon of the Facies C Paleosol. All of which are associated with the coastal fresh to brackish water environments of the Lewisville Member (Dodge, 1968; Johnson, 1974; Stephenson, 1952). A. UTA-AASI-020a *Anchura whitneyensis*, negative mold. B. UTA-AASI-020b *Anchura whitneyensis* (Stephenson, 1952). C. UTA-AASI-017 *Carota pendula* (Stephenson, 1952) D. The common Woodbine gastropod UTA-AASI-009 *Paladmete tubiform* (Stephenson, 1952). E. UTA-AASI-005 *Gyrodes sp*. (Stephenson, 1952). F. UTA-AASI-006 *Natica striaticosta* (Stephenson, 1952). G. UTA-AASI-007 *Lunatia pendernails* (Stephenson, 1952) (Photos courtesy Nathan Van Vranken).

Table 2.4 AAS Woodbine Facies Summary

Bed/Facies	Description	Features	Thickness	Interpretation
1-Facies A	Rippled sandstone	Skolithos burrows and ripples, crab pellets, shark teeth, FFB1.	< 50 cm	Tidal flat
2-Facies B	Carbonaceous shale and peat.	Organic debris and fossil rich with logs and vertebrate remains.	45-80 cm	Delta plain floodplain swamp
3-Facies C	Mudstone/Paleosol	Clay rich with slickensides, organic debris, roots and logs, FFB2.	60-110 cm	Delta plain floodplain swamp
4-Facies D	Heterolithic sequence of interbedded sandstone, siltstone and mudstone.	Parallel wavy-ripple laminations, sand lenses, mudstone and organic debris, FFB3.	90-125 cm	Delta plain crevasse splay

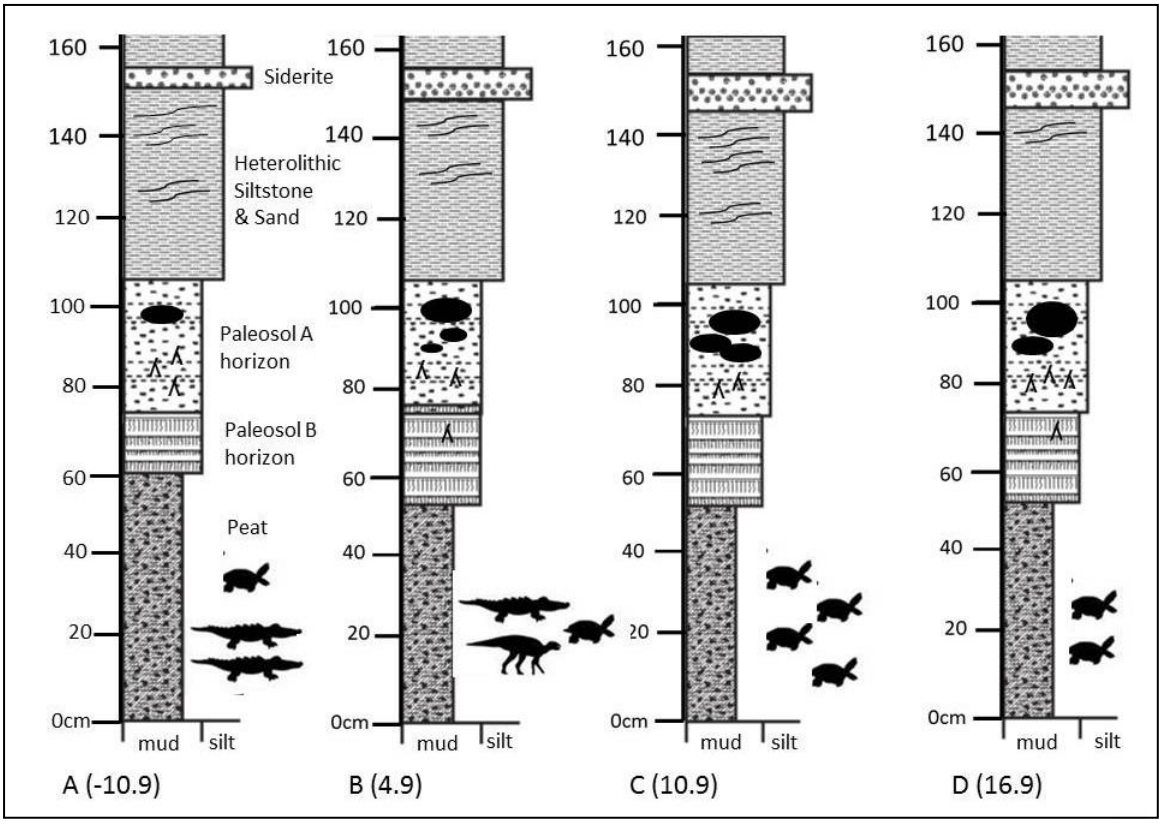

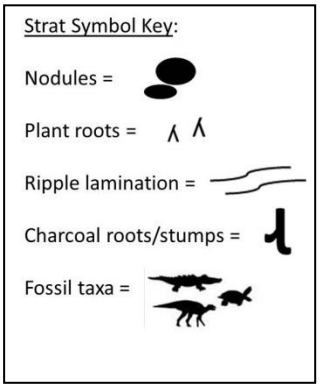

Figure 2.13 AAS stratigraphic sections A-D taken along the map grid from (-10.9) to (16.9), Corocorama and the Turtle Buffet. The lower peat beds are fossil rich with carbonized logs and numerous turtle and crocodyliform fossils. The paleosol bed is subdivided into two horizons (A and B) based upon increase in plant roots and concretions in the upper horizon. Each section is capped with a siderite lag deposit.

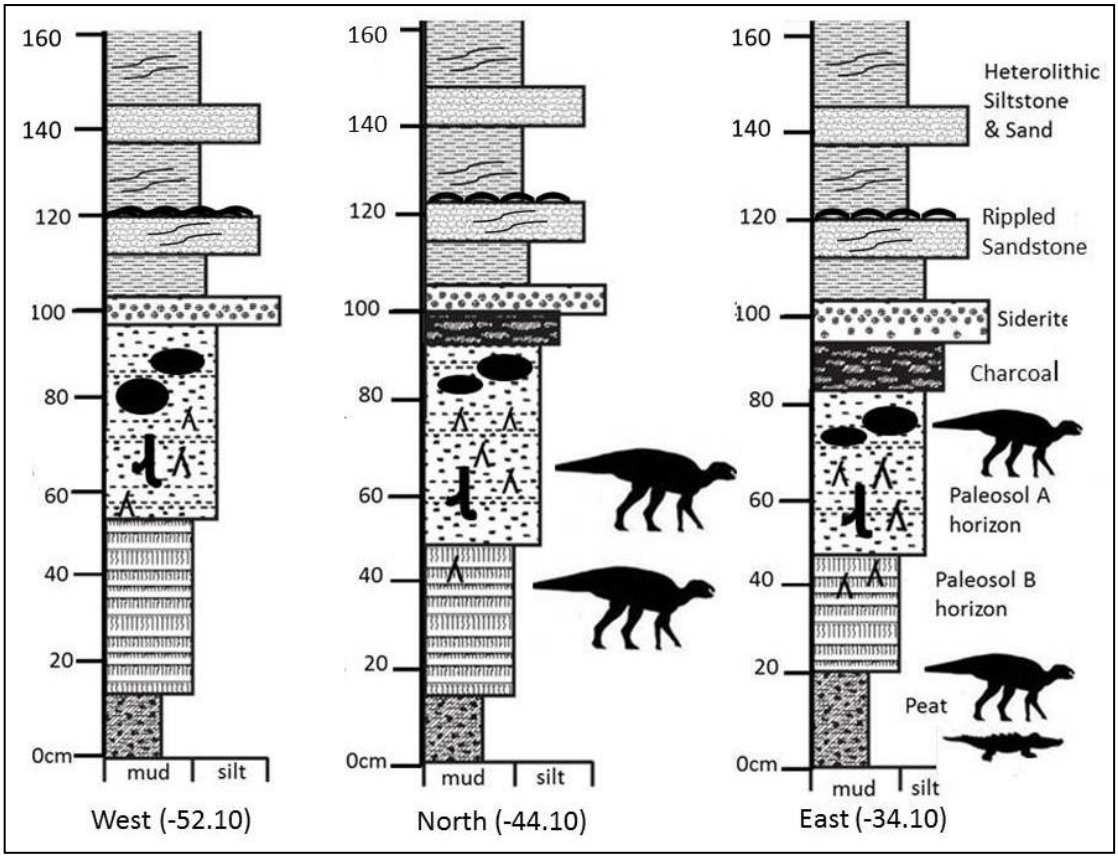

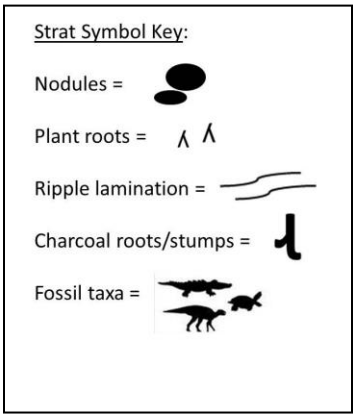

Figure 2.14 AAS Dino Quarry stratigraphic sections West-East taken along the map grid from (-52.10) to (-34.10). The lower peat beds are fossil rich with carbonized logs and numerous turtle and crocodyliform fossils. The paleosol bed is subdivided into two horizons (A and B) based upon increase in plant roots and concretions in the upper horizon. The AAS hadrosauroid was excavated from the paleosol A horizon.

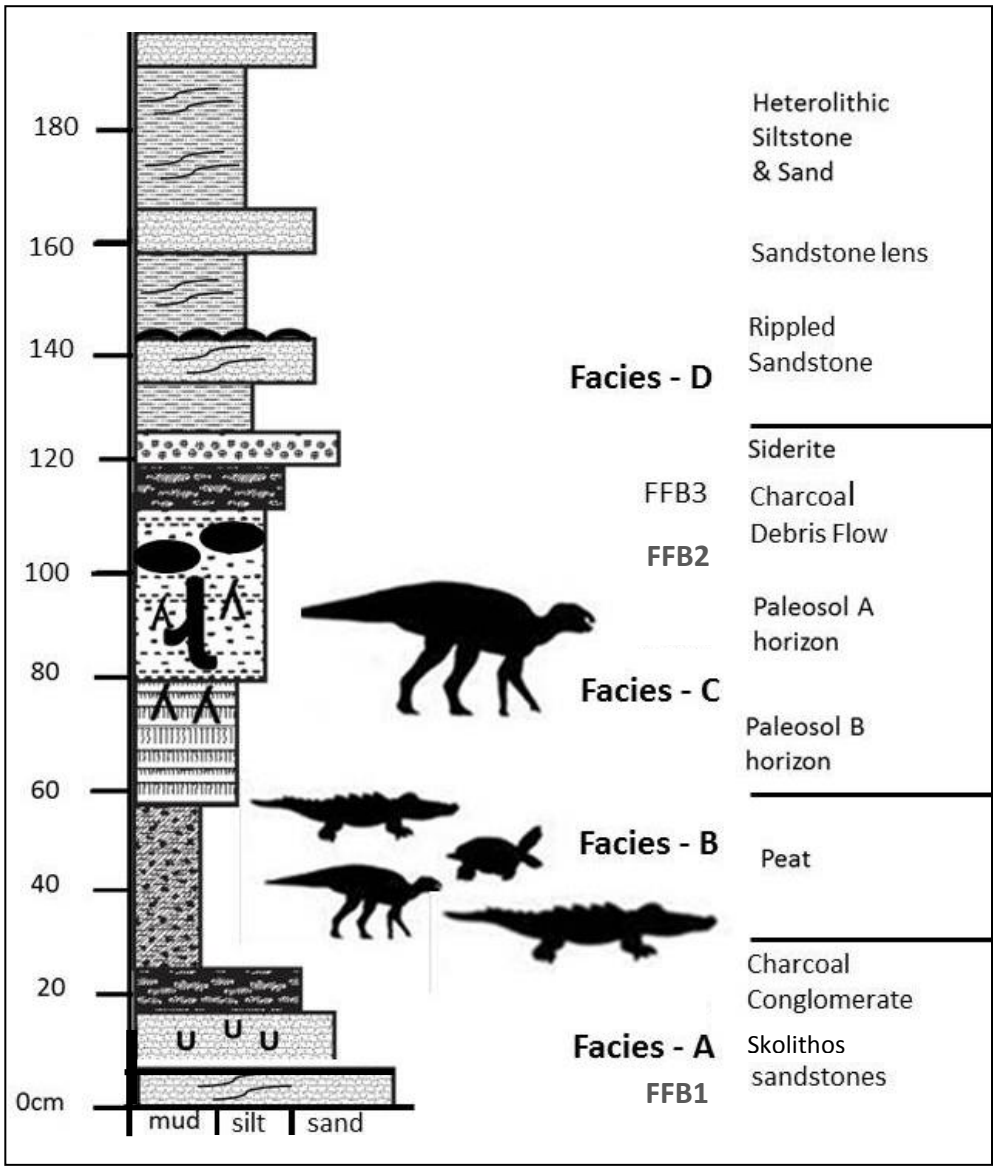

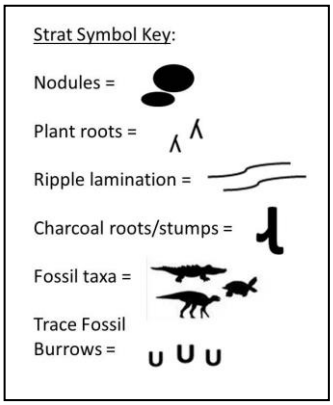

Figure 2.15 AAS composite stratigraphic section. The lower peat beds are fossil rich with carbonized logs and numerous vertebrate fossils. The paleosol bed is subdivided into two horizons (A and B) based upon an increase in plant roots and concretions. The AAS hadrosauroid was excavated from the A horizon. Facies A-D and FFB1-FFB3 denoted to the side.

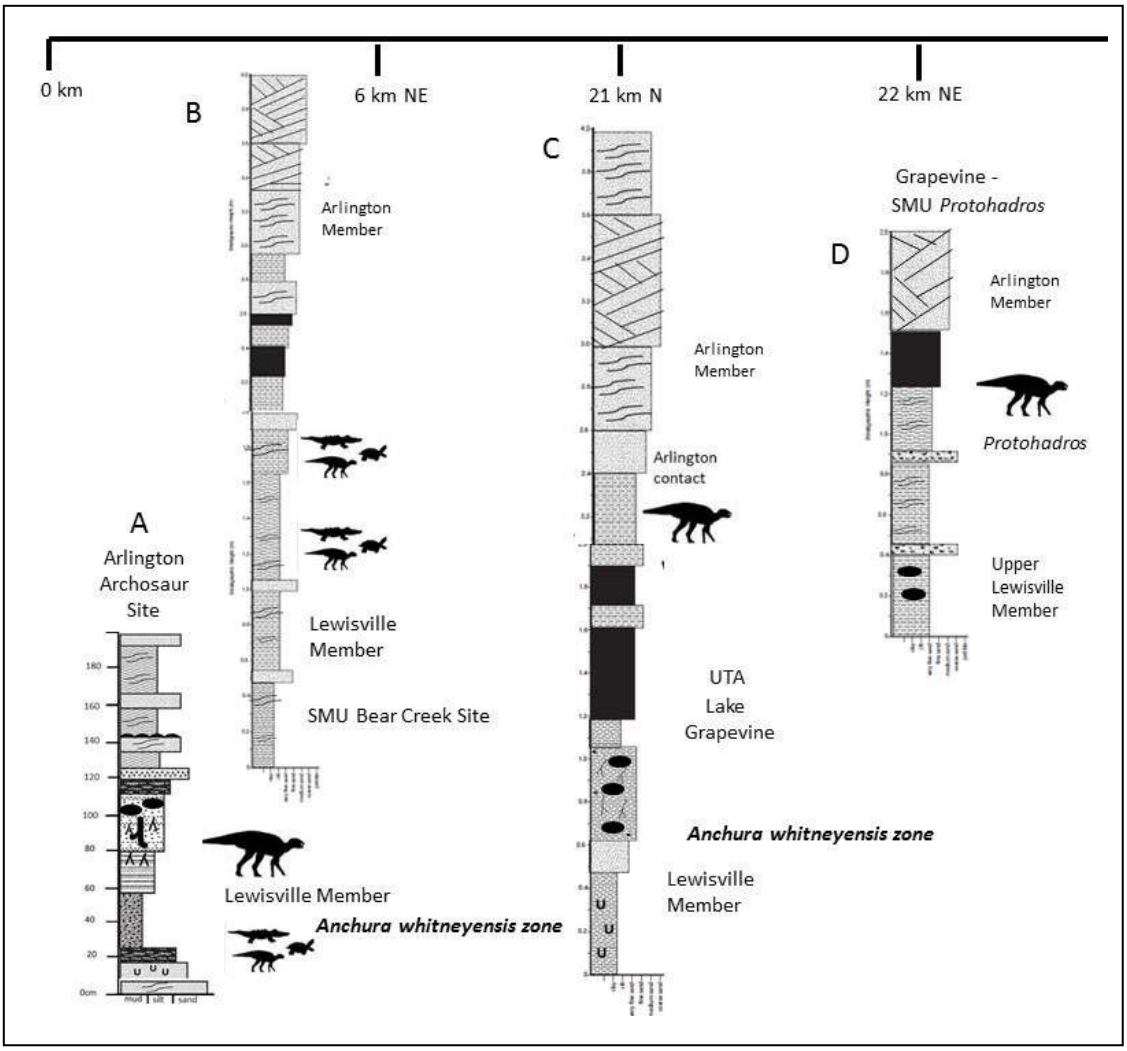

Figure 2.16 Woodbine stratigraphic correlations across North Texas from the AAS (A) to the SMU 245 site at Bear Creek (B) near the south entrance to DFW International Airport, to Rock Ledge Park along the north shore of Lake Grapevine (C), to the SMU 303 *Protohadros* site (D) on Texas FM 2499 in Grapevine/Flower Mound. Distance between areas studied denoted with scale bar (in kilometers at top).

2.5 Conclusions

The Cenomanian of North America is represented by only a few stratigraphic units, one of which is the Woodbine Formation of North Texas. The Cenomanian Woodbine Formation is a sequence of sediments occurring in North Texas that preserves a deltaic depositional system along an ancient paleogeographic peninsula, herein named Rudradia. The Woodbine Formation represents coastal paleoenvironments that range from nearshore facies, to estuary, and extensive delta plain (Fig. 2.14). The delta plain is the emergent portion of the deltaic system, where sedimentation occurs in distributary channels, levees, splays, lagoons, tidal flats and marshes (Prothero, 1990). Woodbine Formation exposures representing primarily an inundated delta plain were examined along hillside outcrops at a productive new fossil site located in Tarrant County, the Arlington Archosaur Site (AAS).

At the AAS, nearshore Woodbine environments are represented by *Skolithos* burrowed and rippled sandstone from an ancient tidal flat. Coastal estuary or delta plain swamp environments are represented by a peat bed, a paleosol and heterolithic deposits consisting of mudstone and sandstone. The AAS paleosol is classified as a Histic Gleysol, a soil that is typical of marshlands and swamps. It represents deposition in a subtropical climate, with swale structures and slickensides within the paleosol suggesting seasonal wetting and drying. Paleoclimate models for this time show a high rate of precipitation, which

correlates to the sedimentological data preserved in the Woodbine (Goswami, 2011). Three distinct charcoal beds were observed at the AAS, a charcoal conglomerate, charcoal roots and stumps in the paleosol and a charcoal debris flow (Fig. 2.14). The charcoal beds found throughout the AAS Woodbine exposures are interpreted as representing evidence of wildfires that were possibly ignited by lightning strikes. The Woodbine heterolithic deposits are ripple laminated with ripple-hummocky cross laminated sand bodies that are interpreted as the result of delta channel avulsion that was possibly related to episodic events (periodic coastal storm systems) (Fig. 2.11).

The Woodbine deposits at the AAS are fossil rich preserving a near complete coastal ecosystem with a variety of organisms ranging from small fish and lizards, to lungfish, turtles, crocodyliforms and dinosaurs (ornithopod and theropod) (see Table 2.3) (Main, 2009, Noto et al., 2012). The AAS dinosaur fauna was dominated by large herbivorous ornithopods, principally a basal hadrosauroid (Main et al., 2011). The AAS coastal ecosystem also supported a variety of small to medium range of carnivorous theropods that hunted along the coastal plain. Although theropods were present along the Rudradian coast, crocodyliforms were more common and therefore thought to be the apex predator of the system. This interpretation is supported by numerous turtle shell remains found at the site with a variety of crocodyliform bite marks and feeding traces (Noto et al., 2012). The AAS Woodbine peninsula was located on the Rudradian

peninsula in southwestern Appalachia. The AAS ecosystem was possibly isolated on the peninsula, representing an endemic ecosystem, and the only mid-Cretaceous coastal system preserved along the southeastern side of the Greenhorn interior seaway.

The Woodbine Formation can be correlated to other mid-Cretaceous (Cenomanian) stratigraphic units in North America. Among them are; the Cedar Mountain Formation's upper Mussentuchit Member of Utah, the Chandler Formation of Alaska, the Dakota Formation of Arizona, Colorado, New Mexico and Utah, the Dunvegan Formation of Alberta, as well as the Frontier Formation of Wyoming, the Mancos Shale of Colorado, the Greenhorn Limestone of Colorado and New Mexico, the Muddy Formation, and the Mesa Rico and Romeroville Sandstones from the Dakota Group of New Mexico (Bhattacharya and Willis, 2001; Bhattacharya and Walker, 1992; Gangloff, 1998; Holbrook and Dunbar, 1992; Holbrook, 2001; Kirkland, 1996 and 2005; Kirkland et al., 1997; Kirkland and Madsen, 2007). Of these formations, only the Cedar Mountain Formation has produced numerous fossils, many of which may be correlated to the AAS Woodbine ecosystem. Of particular interest are the Cedar Mountain iguanodontids and the hadrosauroid *Eolambia,* as it demonstrates anatomical similarities to the Woodbine hadrosauroids (Kirkland 1998, McDonald et al., 2012). Unique among these formations, the AAS Woodbine coastal system is the first to be studied along a peninsula on the southern Appalachian coast. Of equal

importance, Rudradia and the Woodbine coastal system were potentially influenced by allocyclic processes, Cretaceous climate and coastal storms.

Rudradia protruded into the continental interior seaway of the Cretaceous Greenhorn Cycle, similar to the Florida peninsula of the modern world (Kirkland, 1996; Kirkland et al., 1997; and Scotese, 2001) (Fig. 2.3). The modern Gulf of Mexico has experienced hurricanes for centuries, although seasonal hurricanes are increasing in frequency, and worsening in effect and impact, due to current trends in global climate change (Dunbar et al., 1994; Emanual, 2005; Karl et al., 2009). The effects of hurricanes on coastal deposition have been studied by geologists for decades in order to understand coastal processes and how wetlands are impacted by storm events (Dunbar et al., 1994; Liu, and Fearn 1993, 2000a and 2000b; Liu, 2004; and Saucier, 1994). Among coastal system depositional systems studied, the Mississippi delta plain is among the best documented (Dunbar et al., 1994; Gould, 1970; Kolb and Van Lopik, 1958; Roberts, 1998; and Saucier, 1994).

The Mississippi River delta plain and the associated Atchafalaya River floodplain experience significant changes in suspended sediment bedload, high velocity mudflows and wind forced changes in water levels along the plain under storm conditions (Dunbar et al., 1994; Gould, 1970 and Roberts, 1998). In the geologic past, storm systems may have had an affect on coastal sedimentation. The record of episodic sedimentation has been addressed by numerous geologists

interested in understanding allocyclic sedimentation and the relationship between climate and deposition; Algner (1985); Caceres, and Alsina (2012); Dyson (1996); Liu, and Fearn 1993, 2000a and 2000b; Liu, 2004; McCloskey and Keller, 2009; Mawamba and Torres (2002), Palangues et al. (2008); Pepper and Stone, (2004); Ralston and Stacey (2007); Williams and Rose (2001) and Yang et al. (2006) to name but a few. Marsagalia and Klein (1983) at the time of their work cited 69 documented examples of ancient storm sequence in the geologic record and helped establish a list of criteria in which to use to recognize episodic deposits. Thus, there is a significant body of work conducted on the subject of ancient storm deposits, or Paleotempestology, and the effects of storms on coastal systems prior to this work.

In the mid-Cretaceous, the Florida peninsula was submerged beneath the Greenhorn Cycle transgression (Scotese, 2005). Thus, Florida would not have provided a barrier to incoming hurricanes during the mid-Cretaceous.Without such a barrier to block or slow incoming hurricanes, it is theoretically conceivable that large storm systems could have migrated up the shallow Greenhorn Cycle interior seaway, following the southern Appalachian coast and impacting along the Rudradian peninsula. These storms were likely seasonal and could have effected not only coastal sedimentation but may have also periodically disrupted the coastal AAS ecosystem. Evidence of storm influenced systems are documented at other famous fossil localities, in particular, the Joggins Fossil Site

of Nova Scotia. In the case of the Joggins Fossil Site, it is a well documented coastal wetland in which peat formation was periodically disrupted by deposition of organic rich heterolithic beds of mudstone and sandstone with common siderite. At Joggins, the siderite was attributed to a diminished dry season, the heterolithic beds, and the sandstone bodies in particular, were attributed to episodic deposition; storms (Calder et al., 2006). The episodic interpretation of the Joggins beds relied principally upon the erosive base of the noted beds, and the current ripple cross-laminations (Calder et al., 2006). The Woodbine heterolithic beds studied at the AAS also show evidence of current ripple cross laminations in section, with erosional bases at the onset of the heterolithic sequence (sequence boundary).

The Woodbine Formation exposures studied at the AAS match the criteria for episodic influenced deposition noted by previous workers on the topic; Algner (1985), Dyson (2007), Hunter and Clifton (1982), Liu and Fearn (2000a and 2000b) and Marsagalia and Klein (1983). Ancient storm deposits may be recognized by; erosional surfaces, intraformational conglomerates, periodicity of bioturbation, graded bedding, hummocky stratification/lamination, parallel laminations, shell lag deposits and Bouma sequences (Marsagalia and Kein, 1983). In the Woodbine at the AAS, several of the diagnostic storm influence features may be recognized; erosional surfaces, intraformational conglomerates, bioturbation, and hummocky to parallel laminations. In the case of the AAS in

particular, evidence of wildfires may be added to the criteria for storm deposit recognition via a preserved record of multiple charcoal horizons.

The AAS Woodbine deposits do not show signs of catastrophic deposition; on the contrary, the Woodbine deposits are herein interpreted as showing signs of reoccurring coastal processes that united the regional system to a broader system of change due to external forcing mechanims. These mechanisms were possibly climate driven seasonal storms, or at least seasonal variations in precipitation that represent broader allocyclic controls on the nature of deposition in the Woodbine delta system. The presence of multiple charcoal beds at the AAS is supportive of the storm hypothesis, as charcoal is indicative of fire, and wildfires are commonly caused by lightning strikes (Scott, 2000). The presence of peat deposition and siderite at the AAS is an indicator of standing bodies of shallow water, typical of low lying coastal plains in humid climate belts. The presence of swelling in the AAS paleosol, along with charcoal roots and stumps is interpreted as an indicator of a change in seasonality from wet to dry.

The AAS Woodbine delta sequence is classified as a cyclic climate driven delta system, that was fluvial influenced due to the amount of silt and sand observed in the delta front and delta plain environments. The onset of prolonged periods of peat formation at the AAS that were punctuated by soil formation and heterolithic deposition denotes changes from prolonged wet seasons and a high

water base to shorter wet seasons followed by long dry seasons and possible coastal storms. The proposed storms would have impacted the coast of Rudradia, the paleogeographic peninsula of North Texas, initiating wildfires and driving distributary channels to flood their banks leading to avulsion across the delta plain. The strata of the Woodbine Formation, as studied at the Arlington Archosaur Site, represents a coastal system that principally preserves components of a delta plain that was influenced by broad, allocyclic factors that may be traced to the regional paleogeography, global paleoclimate and coastal storms. Although tracing the record of Gulf storms back to the Cretaceous present's challenges, this approach holds the potential to answer broader questions about the link between paleogeography, paleoclimate, paleoecology, and the dynamic nature of our planet's past.

2.6 Acknowledgements

The author thanks the Huffines family, Robert Kimball at Viridian Properties and HC LOBF of Arlington for access to the land in which the Woodbine Formation exposures at the Arlington Archosaur Site occur. Kevin Anderson, Geb Bennett, Anissa Camp, Brad Carter, Tim Dalby, Roger Fry, Albert Miramontes, Chris Noto, Nathan Van Vranken and Richard Zack for assisting with data collection that aided in the stratigraphic sections. Nathan Van Vranken for providing photos and information on Woodbine invertebrates. TCU geologist Bo Henk for his insightful discussions on Woodbine Formation stratigraphy and

ichnology. Steve Hasiostis for presenting an excellent workshop on trace fossils at UT-Arlington and taking time afterwards to discuss trace fossils with the author. Richard Zack and Brad Carter for showing the author Woodbine Formation exposures along Bear Creek near DFW airport and Brad Carter in particular for showing the author the location of the AAS Cruiziana trace fossil site. Chris Noto for introducing the author to the Illustrator program and showing him how to generate stratigraphic columns. John Holbrook for introducing the author to the study of rivers and the use of a Munsell Soil Chart (and showing him how to use it), as well as detailed discussions on coastal depositional systems and the effects of hurricanes. A special thanks to Janok Bhattacharya for encouraging the author to study stratigraphy, years ago when he was a mere undergraduate and for giving him a chance to spend a summer doing field work in Wyoming as a grad student. Also a special note of thanks to the AAS dig crew chief Roger Fry, if not for his many tenacious discussions about the possibility of prehistoric coastal storms, the author likely would never have considered the topic.The Arlington Tomorrow Foundation, the Dallas Paleontological Society, the Earthwatch Institute, the Jurassic Foundation, the Paleomap Project, the UTA Graduate Studies Office for providing a Dissertation Fellowship and the Western Interior Paleontological Society for providing funding in support of this work.

CHAPTER 3

A NEW LUNGFISH (DIPNOI: CERATODONTIDAE) FROM THE CRETACEOUS WOODBINE FORMATION, ARLINGTON ARCHOSAUR SITE, NORTH TEXAS.

"The beauty of homology echoes through eternity."

D. J. Main

3.1 Introduction

A significant number of lungfish dentitions are now known from the Cretaceous (Cenomanian) Woodbine Formation, primarily from one new locality, the Arlington Archosaur Site of northeast Tarrant County, Texas. The Arlington Archosaur Site preserves a diverse coastal ecosystem within exposures of the Woodbine Formation, principally from a thin section of peat, mudstone and a clay rich paleosol from a delta plain environment. The new lungfish specimens pertain to previously undescribed species from the Cenomanian. Previously recorded from but one specimen, this taxon is now represented by both prearticular and pterygopalatine dental plates of sectorial aspect. This species is similar to, and presumably descended from, one that has been previously recorded from various formations of Albian age. Measurements of the angles of the dental plate margins and crests confirm that it is distinct. Two small specimens appear to represent an earlier ontogenetic stage. Although dipnoan evolution generally appears to have proceeded slowly, the taxa from the Cretaceous (Albian – Cenomanian) of Texas may possibly provide some stratigraphic indices, based on what is now known.

The new Woodbine lungfish is herein referred to a new species; *Ceratodus carteri.*

Lungfish tooth plates are biogeographically widespread throughout Late Jurassic to middle Cretaceous strata in North America, but are nonetheless uncommon at any one site (Kirkland, 1987). They are preserved in freshwater to brackish marginal marine environments, typically associated with deposits of the Western Interior Sea (Kirkland, 1987 and 1998). The North American fossil record of Cretaceous Dipnoi is scant, with few reports from the Cenomanian, other than *Ceratodus gustasoni* from the Dakota Formation of southern Utah (Kirkland, 1987). With this paper, seven lungfish tooth plates recovered from Cretaceous (Cenomanian) Woodbine Formation exposures at the Arlington Archosaur Site in North Central Texas are reported (Fig. 3.1).

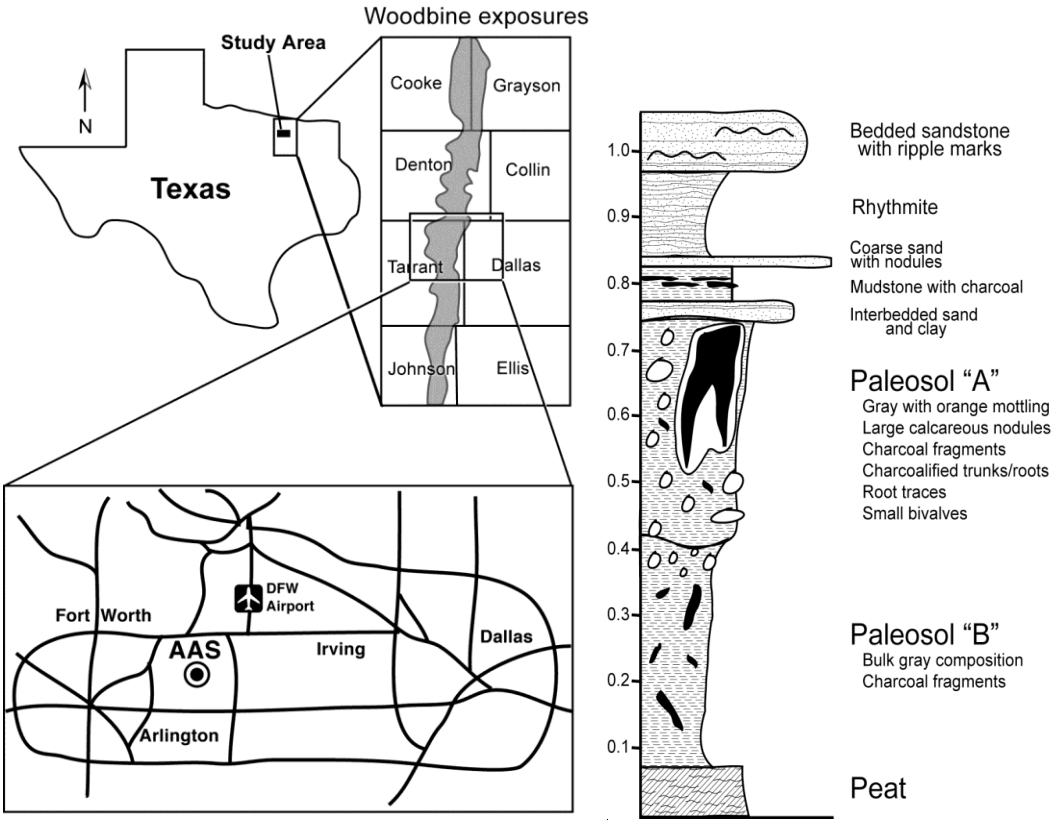

Figure 3.1. Texas map with outline of counties in which Woodbine Formation outcrops occur. Woodbine Formation study area in northeastern Tarrant County noted as AAS, generalized composite stratigraphic column showing Woodbine stratigraphy at the Arlington Archosaur Site.

The Woodbine Formation of North Central Texas, named by R. T. Hill (1901) is a Cenomanian age, or middle Cretaceous unit. The age of the Woodbine Formation was established biostratigraphically by Kennedy and Cobban (1990) using ammonites from marine members in the lower part of the formation. The lower members of the Woodbine Formation range from fluvial, to marginal marine, then fully marine, and consist of the Rush Creek, Dexter, and Lewisville

Members (Bergquist, 1949; Dodge, 1952, 1968 and 1969; Oliver, 1971; and Johnson, 1974). The uppermost member is a coastal deltaic unit referred to as the Arlington Member (Oliver, 1971; Main, 2009). The new lungfish tooth plates discussed herein were recovered from Lewisville Member exposures occurring at a productive new Texas fossil locality; the Arlington Archosaur Site (Fig. 3.1).

The Arlington Archosaur Site (AAS) preserves a coastal mid-Cretaceous ecosystem along a low - lying delta plain on the southeastern margin of the interior seaway. Previous researchers have discussed various components of the Woodbine coastal faunas. The first investigations of the fossil vertebrate fauna of the Woodbine Formation were published by McNulty and Slaughter (1962, 1968). Since this initial work, additional studies have been conducted on the vertebrate faunas of the Woodbine Formation, most notably on the Woodbine dinosaurs (Lee, 1997; Head, 1998; Winkler and Jacobs 2002). Dinosaurs and crocodyliforms are documented within the Cretaceous rocks of North Central Texas (Winkler et al., 1995; Lee, 1997; Head, 1998; Jacobs and Winkler, 1998; Winkler and Jacobs 2002; and Main, 2005). Woodbine outcrops along Bear Creek near the south entrance to Dallas-Fort Worth International Airport have produced crocodyliform, theropod, nodosaurid and hadrosaurid remains (Lee, 1997). Ornithopod dinosaur cranial and postcranial material has been reported from the Woodbine Formation at sites in Flower Mound and along the shores of Lake Grapevine (Lee, 1997; Head, 1998; Main, 2005).

The fauna recovered from the AAS is representative of a coastal wetland. The fossils include lungfish, gar, shark, turtle, dinosaur and crocodyliform remains along with numerous carbonized logs. The fossils primarily occur within a 1.5 m section of organic-rich sediment (peat) dominated by finely commutated plant matter with prominent carbonized logs that grades upward into a muddy, organic-rich paleosol (Fig. 3.1). The environment of deposition is interpreted as a delta plain or coastal wetland. Prior to this work, a single lungfish tooth plate (SMU 73202) was reported from coastal deposits of the Woodbine Formation (Parris et al., 2007). This report significantly expands what is known of Woodbine lungfish and provides a comprehensive study of Cenomanian lungfish in North America. Preservation of lungfish tooth plates in the geologic record is strongly facies controlled (Parris et al., 2007). Dipnoans are typically associated with freshwater environments of intermittent stress, and more rarely with coastal or paralic settings (Bruton, 2003). This new material from the AAS is the first reported occurrence of lungfish tooth plates recovered from a Cenomanian delta plain environment, whereas the Utah examples are from a coastal plain behind a possible barrier coastline (Kirkland, 1987; Eaton et al., 1999 and Titus et al., 2005). All specimens discussed herein were surface collected from Woodbine exposures at the AAS by Brad Carter (Fig. 3.2). Some of the collected specimens were found at the AAS hillside excavation; however ,the first specimen was found

south of the AAS hillside at an area near Birds Fort where Woodbine exposures are extensive (Fig. 3.2).

Figure 3.2 AAS lungfish sites at the Birds Fort micro-sites, south of the AAS hillside excavation. A. Photo of Woodbine outcrops where surface collecting was conducted. B. Lungfish discoverer Brad Carter pointing to the location of where the first tooth plate was surface collected.

3.2 Locality and Horizon

The new lungfish specimens discussed herein were recovered from a new fossil locality in North Central Texas known as the Arlington Archosaur Site (AAS). The AAS occurs within the Cretaceous (Cenomanian) sediments of the Woodbine Formation in northern Arlington, Tarrant County, TX. The "Father of Texas geology" R. T. Hill was the first geologist to map and define the Texas Cretaceous ranging from North Texas to the Big Bend region (Alexander, 1976). The Woodbine Formation of North Texas was named by Hill in 1901 for Cretaceous age sediments occurring near the village of Woodbine in Cooke

County (Alexander, 1976). Hill originally subdivided the Woodbine into two units, the upper "Lewisville beds", and the lower "Dexter beds" (Hill, 1901). The Woodbine Formation is about 100 meters thick and consists predominately of sandstone, mudstone and shale (Johnson, 1974). The Woodbine occurs in outcrops in North Texas and southern Oklahoma. It is the oldest Upper Cretaceous unit in the Gulf Coastal Plain (Hedlund, 1966; Oliver, 1971).

In Texas, the Woodbine outcrops from Temple, to Lake Texoma on the Red River (Oliver, 1971) (Fig. 1). It occurs as an irregular and narrow band, extending from Cooke County to Johnson County (Johnson, 1974) (Fig. 3.1). In the subsurface, the Woodbine underlies a 45 county area in Texas, bounded by outcrops on the north and west, and by the Sabine Uplift to the east (Oliver, 1971). Woodbine sediments weathered out from the Ouachita Mountains in southern Oklahoma and settled in a series of near shore environments in the subsiding East Texas basin (Oliver, 1971). Woodbine deposits primarily represent near shore terrestrial and shallow marine depositional systems and include fluvial, deltaic and shelf deposits (Dodge, 1952; Oliver, 1971; Trudel, 1994). The deltaic paleoenvironments of the Woodbine Formation at Lake Grapevine and the AAS were discussed by Main (2005). The Woodbine Formation overlies the Grayson Formation of the Washita Group and is unconformably overlain by the strata of the Eagle Ford Group (Dodge, 1952; Oliver, 1971). A period of marine deposition

lasting ~10 million years separates the Woodbine from earlier age strata and paleoenvironments (Winkler et al., 1995).

The depositional environments preserved within the Woodbine exposures at the Arlington Archosaur Site (AAS) are fluvio-deltaic along a low lying coastal delta plain. The Woodbine AAS outcrops range from nearshore marine environments, to brackish embayments, and delta plain ecosystems. The Crocorama excavation occurred at the base of the hillside outcrops in a peat bed. The peat deposits are organic rich with carbonized logs and plant debris. Peat deposits are associated with ancient swamps, bogs or mires.

3.3 Discussion

Five families of Mesozoic Dipnoi were recognized by Martin (1982a, 1982b and 1984), with only three represented by North American tooth plates; Arganodontidae, Ptychoceratodontidae and Ceratodontidae. Martin (1982a) recognized the Ptychoceratodontidae and Ceratodontidae based on lungfish tooth plates consisting of four to six ridge crests. The Ptychoceratodontidae are characterized by high, narrow cutting ridge crests and the Ceratodontidae are characterized by relatively low, broad crushing crests (Martin, 1982a). Kirkland (1987) reviewed the occurrences of lungfish from the Mesozoic of North America and referred all North American Cretaceous lungfish to *Ceratodus*. Until the report of a Campanian lungfish plate from New Jersey (Parris et al., 2004), it was

thought that lungfish became extinct in North America in the Cenomanian (Kirkland, 1987). It is now known that they endured until nearly the end of the Cretaceous. However, the Cenomanian remains a time of interest in the evolution of dipnoans, specifically of *Ceratodus*.

Ceratodus was recovered from strata of the middle member of the Dakota Formation within the Grand Staircase-Escalante National Monument near the town of Cannonville. It is likely that middle member is middle to lower upper Cenomanian based on the age of the overlying marine invertebrate faunas in the upper member and a radiometric age of 95.97 +/-0.22 Mya within this member below the Dakota microvertebrate sites on Bulldog Bench (Kirkland, 1987; Eaton et al., 1999; Dyman et al., 2002; Titus et al., 2005).

The new Woodbine lungfish is represented by seven tooth plates from the Arlington Archosaur Site; four adult prearticular plates, two juvenile prearticulars and one adult pterygopalatine plate. The Arlington Archosaur Site lungfish tooth plates were surface collected and found isolated from other material. As the new specimens were surface collected, the precise stratum within the Woodbine Formation from which they are derived is uncertain. Lungfish tooth plates are scant in the North American fossil record, thus it is unusual to find so many from a single locality. Heretofore, five valid lungfish species were known from the Late Jurassic to middle Cretaceous of the North American Western Interior. The

Woodbine lungfish tooth plates discussed herein expands this species count to six and represents the largest assemblage of lungfish recovered from a single site in the eastern subcontinent. Previous reports of North American ceratodontids suggests that crushing toothed lungfishes dominated Cretaceous Interior Seaway coastal systems. However, the sectorial plates of the Woodbine specimens suggest a cutting – slicing form of feeding typical of invertebrate predation was also present among Western Interior lungfishes during the Cretaceous (Kirkland, 1987 and 1998).

The lungfish tooth plate anatomical terms used in this paper follow Kemp (1997 and 1998) (Fig. 3.3). Standardized reference points and angles are those used by Vorob'yeva and Minikh (1968), Martin (1980, 1982a, and 1982b), and Kirkland (1987) (Fig. 3.3). Vorob'yeva and Minikh (1968) utilized the angles of ridge crests to diagnose lungfish species. Martin (1980, 1982a and 1982b), Kirkland (1987), Kemp (1997) and Parris et al. (2004 and 2007) have also used this method, and the same technique was applied to the new Woodbine lungfish tooth plates (Fig. 3.3). Five of the seven tooth plates are figured. One plate is badly weathered. The weathered tooth plate was identifiable as a lungfish, however the ridges are eroded and the angles between C1 and Cp were not measurable. The figured tooth plates include one pterygopalatine plate, three adult prearticular plates and one juvenile prearticular.

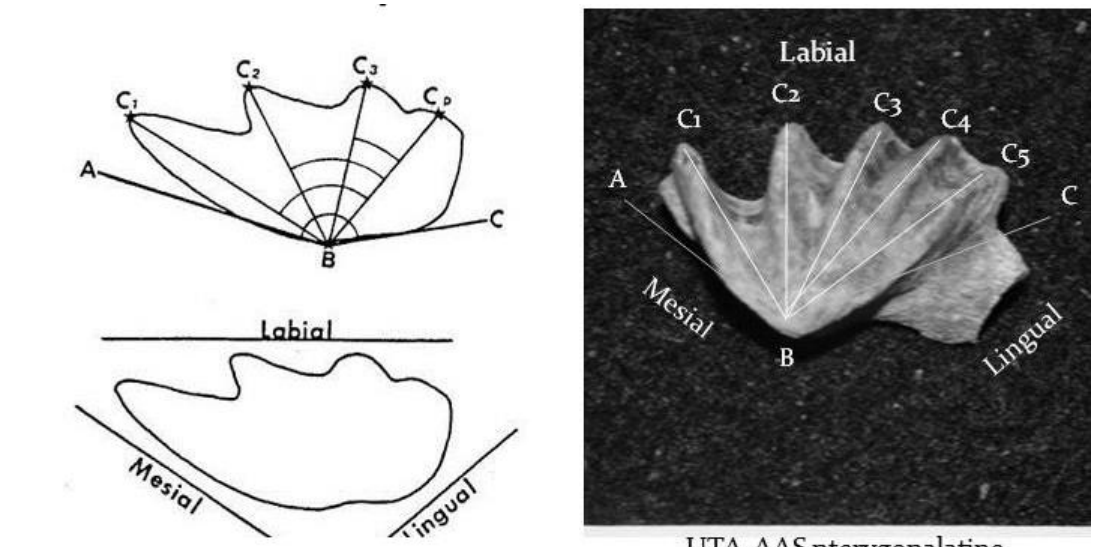

Figure 3.3 Diagram of tooth plate biometrics and angles used to identify lungfish tooth plates in this study, modeled after Kemp (1997).

All of the tooth plates are relatively small (<4 cm) and compare with previous descriptions of Early Cretaceous (Albian) lungfish recovered in Texas (Thurmond, 1974; Kirkland, 1987; Winkler et al., 1990 and Parris et al., 2007). The new Woodbine tooth plates are considered to be from a single species, with two specimens (one figured) belonging to an early ontogenetic stage. Along with their small size (less than 4 cm in any occlusal dimension), other diagnostic characters of the new plates are sharp ridge crests that narrow toward the occlusal surface.

3.4 SYSTEMATIC PALEONTOLOGY

DIPNOI, Muller, 1845.

CERADONTIFORMES Berg, 1940

CERATODONTIDAE Gill, 1872

CERATODUS Agassiz, 1837

CERATODUS CARTERI n. sp.

Material—The new lungfish is represented by seven tooth plates (5 figured) from the middle Cretaceous (Cenomanian) Woodbine Formation at the Arlington Archosaur Site, northeastern Tarrant County, Texas and one SMU specimen from Woodbine exposures in the Lake Grapevine spillway.

Holotype —UTA-AASL006: a right pterygopalatine plate.

Paratype — UTA-AASL 001, a left prearticular plate.

Referred material—five prearticular plates: UTA-AASL 002 is a right prearticular plate, UTA-AASL 003 a left prearticular plate and UTA-AASL 001 a left prearticular plate, and UTA-AASL 004 a juvenile left prearticular plate and UTA-AASL 007 a juvenile right prearticular and SMU 73202 a right prearticular from Lake Grapevine.

Locality and horizon—Lewisville Member of the Woodbine Formation at UTA Location 50, the Arlington Archosaur Site (AAS).

Etymology—The species is named for Bradley Carter, the discoverer of the tooth plates recovered from the Woodbine Formation at the Arlington Archosaur Site.

Diagnosis—A small ceratodontid with tooth plates ranging from 18 mm to 33 mm long. There are five ridge crests on the upper tooth plate and four on the lower tooth plate. The tooth plates have diagnostic high, sharp ridge crests, obtuse inner angles and relatively straight lingual margins. The new species is diagnosed based on its small size relative to other Cretaceous North American ceradontids, obtuse angulation of inner crests, high crest ridges, and lack of a flattened crushing platform. This species is close to *C. guentheri* but differs in size. It is most similar in size and morphology to *C. texanus*, as it is likely a descendant of this Trinity Group species (Parris et al., in press).

3.5 Description

Holotype; UTA-AASL006 A medium sized (<30 mm length) ceratodontid upper right tooth plate with attached entopterygoid, Paratype and referred prearticular tooth plates range from 18 mm to 33 mm long (C1-CP), and 8 mm to16 mm in width, internal angles (<ABC) range from 94-118 degrees with

five crests on the upper plate and four crests on the lower plates radiating from this internal angle (Table 3.1). All specimens have distinct high, sharp ridge crests. The unworn tooth plates are covered with a thin enamel layer. The lingual margin is relatively straight on the pterygopalatine. The mesial margin displays a slight curvature. The first crest (C1) of the pterygopalatine is tall, relatively straight with a slight mesial curvature (Fig. 3.4). The angle between the first and second crest is greater than that of crest three and four.

The general morphology of *C. carteri* is similar to *C. guentheri,* with obtuse inner angles, although lacking the flattened crushing platform associated with the third and fourth crests. The ridge crests are high and sharp, similar in morphology to *C. guntheri*. The size of the upper tooth plate is relatively small compared to other North American ceratodontids, smaller than *C. frazeri, C. guentheri* and *C. gustasoni* (Kirkland, 1987). The cutting portion of the ridge crest is sharp, suggesting a slicing or cutting mode of feeding rather than crushing.

The prearticular plates are the only dental elements in the lower jaws of lungfishes. The prearticulars of *C. carteri* range in size; the paratype (specimen UTA-AASL001) is 33 mm long (C1-CP) and 16 mm wide, UTA-AASL002 is 28 mm long and 15 mm wide, UTA-AASL003 20 mm is long and 12 mm wide, juvenile specimen UTA-AASL004 is 18 mm long and 8 mm wide (Fig. 3.4). Specimens 001 and 002 have the attached pterygoid extending caudal to the tooth

plate (Fig. 3.4). The pterygoid of specimen 002 is slightly broader than that of 001 (Fig. 3. 4). All Woodbine prearticulars are similar in size to *C. guentheri*, but relatively small compared to the ceratodontids *C. fossanovum* and *C. gustasoni* (Kirkland, 1998). The prearticulars of *C. carteri* have slender, elongate crests with C1 being of greatest length (Fig. 3.4). Crests C2-CP are of subequal length, with the fourth crest (CP) being the smallest. All of the prearticulars have sharp ridge crests that narrow toward the occlusal surface (Fig. 3.4). Lingual margins of the prearticular plates are slightly curved, but not to the extant seen in *C. frazieri* (Kirkland, 1987).

TABLE 3.1 Biometrics; crest angle and L x W measurements taken on Woodbine specimens. *holotype, **paratype. All measurements in mm.

Lungfish plates:	ABC	C1Cp	C2Cp	C3CP	L x W
UTA-AASL006*	110	65	36	18	24x10mm
UTA-AASL001**	114	84	42	24	33x16mm
UTA-AASL002	118	86	56	32	28x15mm
UTA-AASL003	98	88	44	22	20x12mm
UTA-AASL004	94	78	56	36	18x8mm
SMU 73202	118	91	49	22	N/A

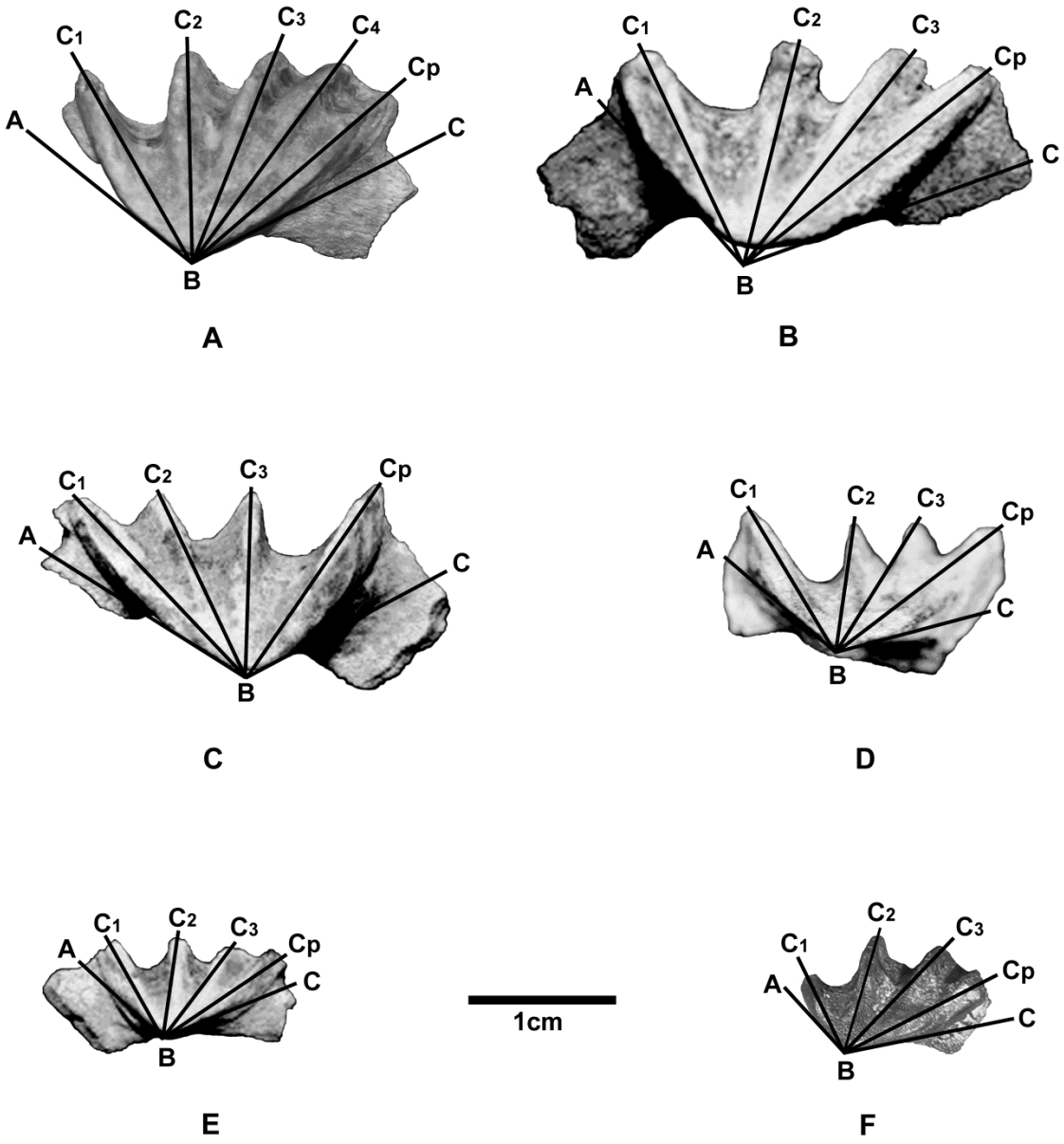

Figure 3.4 A. Holotype UTA-AASL-006 right pterygopalatine., B. Paratype UTA-AASL-001 left prearticular plate. C. UTA-AASL-002 right prearticular plate. D. UTA AASL-003 left prearticular plate. E. UTA-AASL-004 left prearticular plate, juvenile. F. SMU 73202 right prearticular plate from Woodbine exposures at Lake Grapevine spillway. Scale in centimeters.

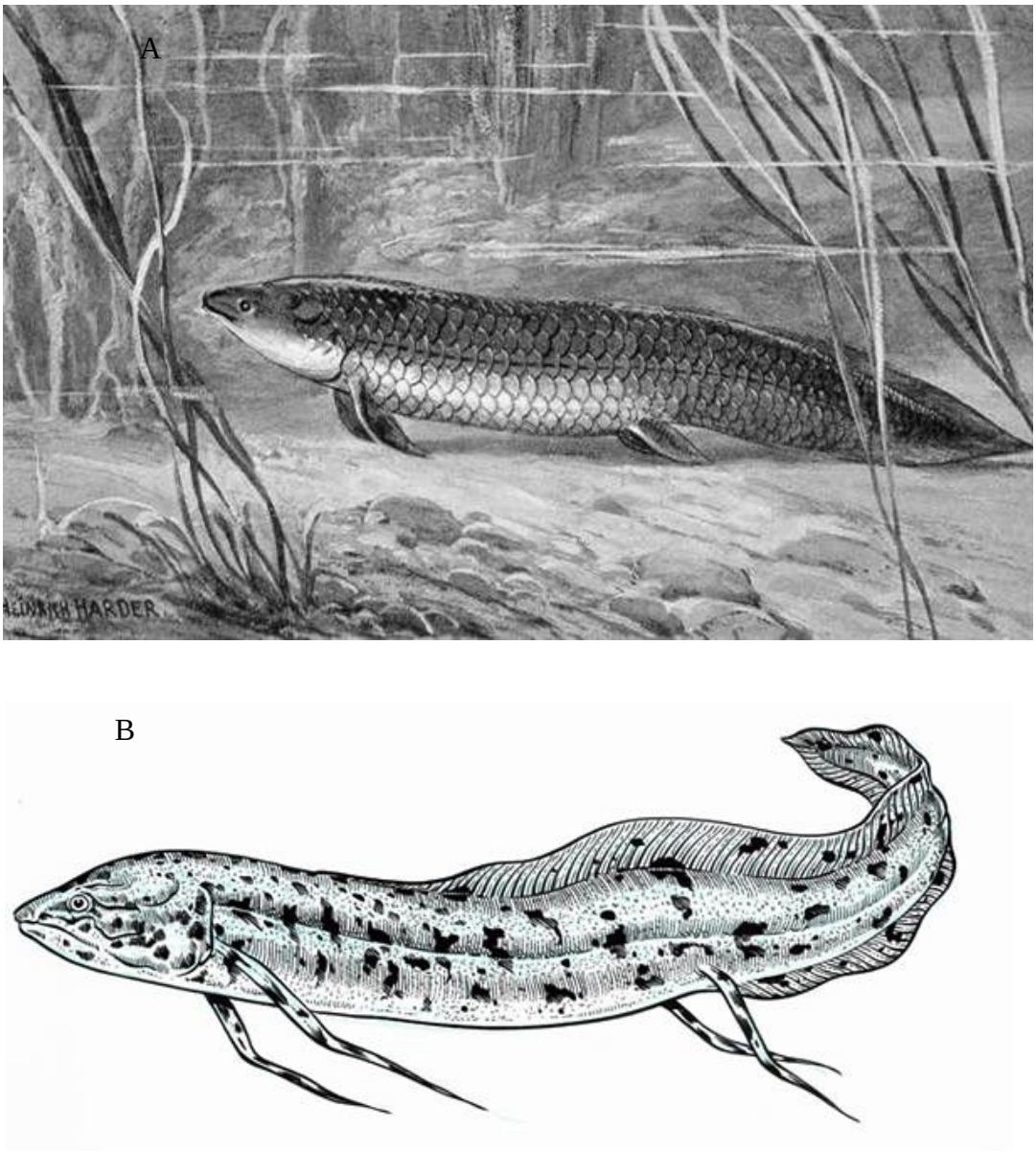

Figure 3.5 Images of ancient and modern lungfish, possible analogs for the AAS Woodbine lungfish. A. Artwork reconstruction of *Ceratodus* by Heinrich Harder. B. An artist reconstruction of the modern African lungfish, *Protopterus annectens* (art courtesy of the Queensland Department of Agriculture, Fish and Wildlife).

3.6 Conclusions

A new species of Cretaceous (Cenomanian) lungfish, *Ceratodus carteri* is named in honor of the discoverer Brad Carter and represented by seven tooth plates: the holotypic adult pterygopalatine plate, four adult prearticular plates, and two juvenile prearticular plates (Fig. 3.4). Most of the tooth plates were recovered from a single Woodbine Formation fossil locality, the Arlington Archosaur Site in northeastern Tarrant County, Texas. One of the tooth plates was recovered from the Lake Grapevine spillway, Denton County, Texas. The depositional model for the type locality is a coastal delta plain. The biometrics of the Woodbine specimens (Table 3.1) supports the interpretation of these specimens as a single species. The lingual margin is relatively straight on the pterygopalatine with a slight curvature to the mesial margin. However, the lingual margins of the prearticular plates are slightly curved, but not to the extant seen in *C. frazieri* (Kirkland, 1987). The general morphology of *C. carteri* is similar to *C. guentheri,* with obtuse inner angles, although lacking the flattened crushing platform associated with the third and fourth crests. All of the Woodbine specimens discussed have high, sharp ridge crests that are interpreted as an adaptation for a slicing, or cutting feeding style. The upper tooth plate is relatively small compared to those of other North American ceratodontids, smaller than *C. guentheri*. However, the primitive morphology of *C. carteri* is reminiscent of earlier North American ceratodontids such as *C. guentheri*, but differs in size. It is

most similar in size and morphology to the newly described *C. texanus*, as it is likely a descendant of this Early Cretaceous Trinity Group species (Parris et al., in press).

With the work of Pardo et al. (2010) newly discovered cranial material of *Ceratodus guentheri* from the Upper Jurassic of Colorado, has justified referral of that species to a new genus, *Potamoceratodus*. It has been suggested that all Mesozoic lungfishes from North America may belong to this new genus with the possible exception of *C. robustus* (Pardo et al., 2010). This assignment follows Martin's (1981) earlier inclusion of North America's Jurassic and Cretaceous lungfish in the genus *Ptychoceratodus* based on a tooth form with the distinctive *C. robustus* retained in *Ceratodus*. As noted by Parris et al.. (in press), this species was potentially ancestral to the Texas lineage that includes *C. texanus* and *C. carteri*, a clade with cutting-chopping adaptations. However, because knowledge of *C. texanus* and *C. carteri* are limited to dental plates, referral of any Texas specimens to the new genus is unjustified. Therefore, we maintain the practice of assigning isolated lungfish tooth plates found in the Cretaceous of North America to the genus *Ceratodus* until their taxonomy, systematics and phylogenetic relationships to Mesozoic dipnoans outside North America are properly examined (Martin et al., 1981; Martin, 1982).

Lungfish typically live in fresh water habitats; however, the AAS Woodbine lungfish likely lived on a delta plain. The modern South American lungfish *Lepidosiren paradoxa* lives in the Amazon River basin and delta marshes. Thus, it is not unreasonable to use it as a modern analog for the AAS Woodbine lungfish. Lungfish are typically conservative vertebrates; however, the lack of change in the Texas specimens may suggest a relict form that hints at biogeographic isolation or endemism. The Texas specimens differ from contemporaneous Cretaceous lungfishes on the western side of the seaway and more closely resemble lungfish taxa from the Jurassic Morrison Formation (Kirkland 1987; 1998). Early to middle Cretaceous eustatic fluctuations could have isolated the Texas ceratodontid faunas on the southeastern coast of the epicontinental seaway, producing a primitive endemic fauna. Further work in the Cenomanian of North America will no doubt elucidate these paleogeographic and paleobiogeographic scenarios.

3.7 Acknowledgements

The author thanks the Huffines family, Robert Kimball at the Viridian Properties and HC LOBF of Arlington for granting land access to conduct work at the Arlington Archosaur Site, Brad Carter for finding, reporting and donating the specimens discussed herein, colleagues David Parrish and Barbara Grandstaff for their collaboration on this project, C. R. Scotese and the PaleoMap Project for

providing research funds and facilities, the Dallas Paleontological Society for providing a scholarship to the author, the Jurassic Foundation and the Western Interior Paleontological Society for providing research grants to support this work, Geb Bennett for proofreading an early version of the manuscript and offering comments, Chris Noto for providing comments and assisting with figures, Jim Kirkland for providing comments, reference materials and advice, and Arlington Archosaur Site project members; Brad Carter, Roger Fry, Art Sahlstein, Richard Zack, Kevin Anderson, Anissa Camp, Rachell Peterson and Darlene Sumerfel for their assistance at the AAS, Carl Franklyn and Eric Smith of the UT-Arlington Amphibian and Reptile Diversity Research Center for allowing the author to view modern lungfish and take out specimens on loan that aided in this study, and Dale Winkler at the Shuler Museum of Paleontology at Southern Methodist University for providing SMU specimen information.

CHAPTER 4

NEW THEROPOD MATERIAL FROM THE CRETACEOUS CENOMANIAN) WOODBINE FORMATION AT THE ARLINGTON ARCHOSAUR SITE, PALEOECOLOGIC AND PALEOBIOGEOGRAPHIC IMPLICATIONS.

"There is more to theropod evolution than the origins of birds!"

"Homoplasy, thy name is Theropod!"

Thomas Holtz

4.1 Introduction

New theropod material was recovered from the mid-Cretaceous (Cenomanian) Woodbine Formation exposures at the Arlington Archosaur Site in North-Central Texas (Fig. 4.1). As Theropod fossils are virtually unknown from the Woodbine Formation, the new material reported herein is a significant advancement. The Woodbine Formation was named by R. T. Hill (1901) and a Cenomanian age (95 Mya) for the formation was established biostratigraphically by Kennedy and Cobban (1990) using ammonites from lower marine members. The lower members of the Woodbine Formation range from fluvial, to marginal marine, then fully marine, and consist of the Rush Creek, and Dexter Members (Bergquist, 1949; Dodge, 1952, 1968 and 1969; Johnson, 1974; Oliver, 1971). The uppermost members represent a coastal delta plain and associated fluvial environments with strata referred to as the Lewisville and Arlington Members (Oliver, 1971; Main, 2005; Murlin, 1975). The new theropod material discussed

herein was recovered from Lewisville Member exposures occurring at a productive North Texas fossil locality: the Arlington Archosaur Site (Fig. 4.1).

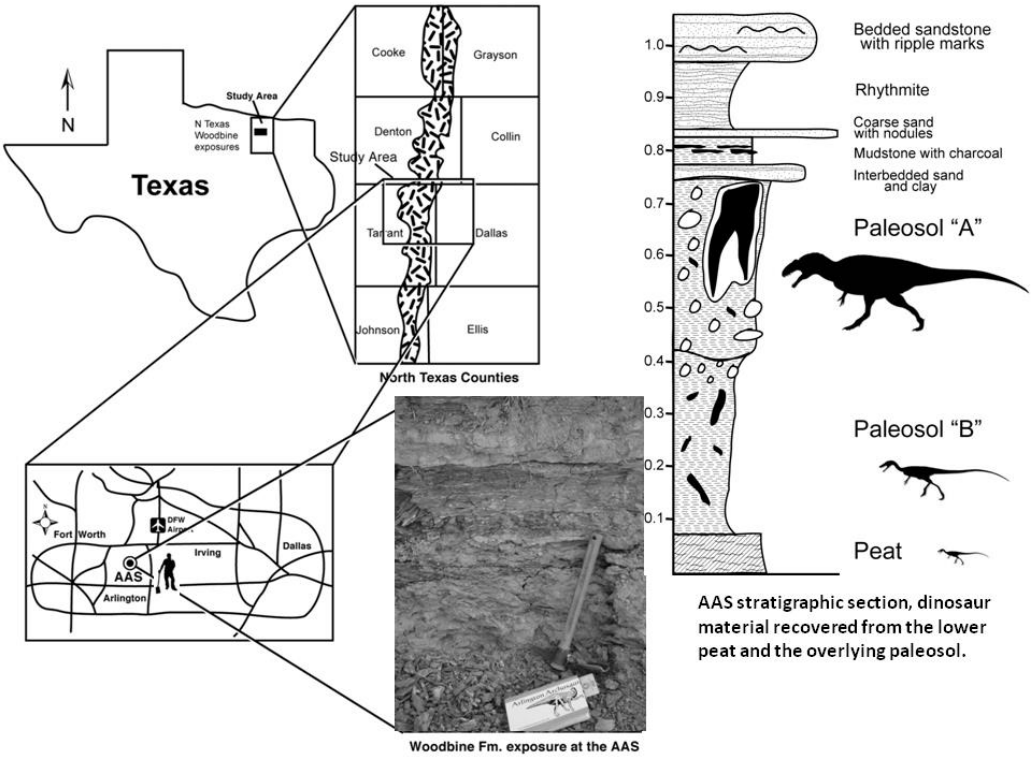

Figure 4.1 The occurrence of Woodbine Formation exposures in North Texas and location of the Arlington Archosaur Site (AAS) in Tarrant County. Photo and stratigraphic section shows Woodbine Formation stratigraphy, as viewed within the AAS Dinosaur Quarry; an organic rich delta plain paleosol overlain by a lag deposit and heterolithic deposits.

The Arlington Archosaur Site (AAS) preserves a coastal Cretaceous delta plain ecosystem along the southeastern margin of the interior seaway. Previous researchers have discussed components of the Woodbine coastal faunas. The first

investigations of the fossil vertebrate fauna of the Woodbine Formation were published by McNulty and Slaughter (1962, 1968). Since their work, additional studies have been conducted on the vertebrate fauna of the Woodbine Formation, most notably on the Woodbine dinosaurs (Lee, 1997; Head, 1998; Winkler and Jacobs, 2002; Main, 2005). Dinosaurs and crocodyliforms are documented within the Cretaceous rocks of north-central Texas (Winkler et al., 1995; Lee, 1997; Head, 1998; Jacobs and Winkler, 1998; Winkler and Jacobs 2002; and Main, 2005). Woodbine outcrops along Bear Creek near the south entrance to Dallas-Fort Worth International Airport have produced crocodyliform, theropod, nodosaurid, and hadrosaurid remains (Lee, 1997). Ornithopod cranial and postcranial material has been reported from the Woodbine Formation of Flower Mound and Lake Grapevine (Lee, 1997; Head, 1998; and Main, 2005).

The fauna recovered from the AAS represents a coastal wetland or delta plain ecosystem. The fossils include a new species of lungfish, gar, dinosaur (ornithopod and theropod), a new taxon of crocodyliform, and turtle remains, some of which demonstrate a record of feeding behavior from the AAS crocodyliform (Noto et al., 2012; and Main et al., 2012). The fossils primarily occur within a 1.5 m section of organic-rich sediment (peat) dominated by plant matter and prominent carbonized logs that grades upward into a muddy, organic-rich paleosol that is overlain by a transgressive lag sand bed and heterolithic deposits from a tidal flat (Fig. 4.1). The environment of deposition is interpreted

as a coastal delta plain (Main, 2009). Prior to this work, several theropod teeth were reported from the Woodbine by Lee (1997) and referred to *Richardoestesia.* Previously, no theropod postcrania have been reported from the Woodbine Formation, until now.

The Woodbine theropod teeth, phalange, manual ungual and limb shaft were all found isolated from other material at the AAS. The theropod pedal ungual was excavated from a carbonaceous peat bed and found associated with juvenile crocodyliform material by C. R. Noto. As most of the new specimens were surface collected, the precise stratum within the Woodbine Formation from which they are derived is uncertain. Although, all specimens show signs of oxidation and siderite staining, and are therefore thought to originate from the siderite rich paleosol horizon (Facies C). Regardless, much work has been conducted with theropod teeth (Currie, 1987; Currie et al., 1990; Fiorillo and Currie, 1994). Theropod teeth are common in the North American fossil record, however, scant material has been reported from the Woodbine Formation.

4.2 SYSTEMATIC PALEONTOLOGY

SAURISCHIA Seeley, 1887

THEROPODA Marsh, 1881

DROMAEOSAURIDAE indet. Matthew and Brown, 1922

Material—Woodbine theropod UTA-AAST-001 is represented by a small tooth.

Description—UTA-AAST-001 is a small dromaeosaurid tooth (11 mm length) (Table 4.1). The tooth is broad and triangular in lateral view, oval in cross section with anterior and posterior carinae, each possessing denticles (Fig. 4.2A). The denticles are small (0.2-0.3 mm), short, wide, and square. Denticles are distinctly visible along the posterior carinae, however, the anterior denticles are visible but worn. The anterior carinae are close to the midline at the tip, but twists toward the lingual surface proximally. This twist is a character typically associated with the maxillary and dentary teeth from *Dromaeosaurus*, although not restricted to the genus (Currie et al., 1990).

Discussion—This report is the first of dromaeosaurids from the Woodbine Formation. Although isolated teeth are common in the fossil record, theropods are scant in the Woodbine Formation. Biostratigraphically and biogeographically this report demonstrates a consistent record of dromaeosaurids in Texas through the

Aptian to the Cenomanian of North Central Texas, on into the Campanian and Maastrichtian of southwest Texas (Sankey et al., 2005; and Weishampel et al., 2004).

SAURISCHIA Seeley, 1888

THEROPODA Marsh, 1881

ALLOSAURIDAE Marsh, 1878

Material—Woodbine theropod UTA-AAST-002 is represented by a medium sized tooth.

Description—UTA-AAST-002 is a medium sized (16 mm) (Table 4.1), partial tooth that is weathered with the proximal and distal ends missing (Fig. 4.2B). It has a laterally compressed, oval base, typical of carnosaurs. The tooth is tall, narrow, and slightly recurved. Only the posterior carinae are visible, with a small series of denticles completely preserved. The denticles are square and wide as they are tall, with accompanying blood grooves between the bases of the denticles that curve proximally toward the base of the tooth. This character is shared with *Acrocanthosaurus* and tyrannosaurs (Currie and Carpenter, 2000, Currie et al., 1990; Harris, 1998, Sankey et al., 2005). The extent of lateral compression, and small denticle size precludes assignment to a tyrannosaur.

Discussion—This report is the first of an allosauroid from the Woodbine Formation. The presence of allosauroids in the Woodbine of North Texas extends the biostratigraphic range of this taxa into the Cenomanian and presents interesting biogeographic and ecologic implications. This tooth suggests that allosauroids were a consistent component of southern North American ecosystems that were later isolated via Cenomanian high stands and potentially integrated into a southeastern endemic coastal fauna at the Arlington Archosaur Site. Of interesting note, the similarity in denticles and blood groove morphology suggests the possibility of ecological convergence between tyrannosaurs and acrocanthosaurs.

SAURSICHIA Seeley, 1888

THEROPODA Marsh, 1881

ALLOSAURIDAE Marsh, 1878

Material—Woodbine theropod UTA-AAST-006 is represented by a small tooth.

Description— UTA-AAST-006 is a small tooth (11.4 mm) (Table 4.1). It has a laterally compressed, oval base, typical of carnosaurs (Fig. 4.2C). The tooth is tall, narrow, and slightly recurved. Both anterior and posterior carinae are visible. Posterior carinae extend all the way to the base, whereas anterior carinae end

approximately 1 mm from the base. Anterior denticles are visible but worn. A series of posterior denticles are completely preserved, yet slightly obscured by matrix making further identification difficult.

Discussion—The morphology of this specimen is similar to UTA-AAST-002, thus this specimen may represent a juvenile tetanuran similar to *Acrocanthosaurus*.

SAURSICHIA Seeley, 1888

THEROPODA Marsh, 1881

THEROPODA indet.

Material—Woodbine theropod UTA-AAST-003 is represented by a small pedal phalanx.

Description—UTA-AAST-003 is a medium sized pedal phalanx that preserves most of the shaft, and missing the proximal end (Fig. 4.2D). The preserved length is 32 mm, with a 8.8 mm minimum shaft width. The distal end is 11.8 mm wide and about 11 mm high. The preserved articular surface is strongly ginglymoid, with deep lateral pits for ligament attachment. The broken proximal shaft exposes a hollow interior, typical of theropods.

Discussion—Despite its fragmentary nature, the size of the phalange implies a medium sized theropod, demonstrating that these predators were present in the Woodbine fauna of North Texas. This thin element suggests a gracile, cursorial animal within southeastern coastal plain ecosystems (Fig. 4.6).

SAURSICHIA Seeley, 1888

THEROPODA Marsh, 1881

THEROPODA indet.

Material—Woodbine theropod UTA-AAST-005 is represented by a small pedal claw.

Description—UTA-AAST-005 is represented by a well preserved small pedal claw. It is 9.8 mm long and moderately curved with a sharp intact tip. It has a prominent lateral grove on the left side and a partial lateral groove on the right side. The flexor tubercle is weakly developed, and bears some resemblance to basal coelurosaurs such as *Compsognathus*, *Coelurus* and *Tanycolagreus* (Carpenter et al., 2005a,b, Peyer, 2006).

Discussion—The small size of the claw suggests a light, gracile predator, possibly juvenile. This specimen is the only theropod material found to date *in situ* at the AAS and associated with a site known to primarily produce crocodyliform remains. With its close association with juvenile crocodyliform remains, there is the distinct possibility that the element may be crocodyliform

and not theropod. At the time of this writing the identification is considered problematic.

SAURSICHIA Seeley, 1888

THEROPODA Marsh, 1881

THEROPODA indet.

Material—Woodbine theropod UTA-AAST-004 is represented by a partial limb shaft.

Description—UTA-AAST-004 is represented by a partial limb shaft with a distinctly hollow medullary cavity (Fig. 4.2F). The preserved portion of the shaft is 42.5 mm long, 15.7 mm wide and 18.4 mm deep. The hollow interior space tapers to one end, suggesting that it was approaching the end of the limb. It has a slight curvature, and is oval in cross section. Worthy of mention, another partial limb shaft with similar preservation and character states was recovered from the same area at the AAS as this chapter was under preparation.

Discussion—The slight curvature and the hollow space implies that is a long bone from one of the limbs. It shares a similar type of preservation as specimen UTA-AAST-003, and may belong to the same individual or taxon.

SAURSICHIA Seeley, 1888

THEROPODA Marsh, 1881

TETANURAE *indet.* Gauthier, 1986

Material—Woodbine theropod UTA-AAST-007 is represented by a large partial proximal end of a claw.

Description—UTA-AAST-007 is a large partial manual ungual (Fig. 4.2G and 4.3). The preserved portion measures 65.4 mm from the dorsal surface to the tip of the flexor tubercle. The joint surface is 43.3 mm tall and 26 mm wide. These measurements correspond to a claw that would be 150-160 mm long (Fig. 4.3). The estimated size of the claw and morphology of the flexor tubercle suggests a relationship to allosauroid or spinosauroid tetanurans, in particular *Allosaurus*, *Suchomimus* and *Acrocanthosaurus*.

Discussion—The partial manual ungual demonstrates that a taxon of large theropod was a component of the Woodbine ecosystem, as would be expected with the presence of a large ornithopod at the AAS (Fig. 4.3). In the modern African savannah, large predators typically hunt prey that are at least equal in size, if not more than double the size of the predator. Current size estimates of the AAS hadrosauroid places them at approximately 8 - 9 meters in length. Thus, a large carnivore would fit well into the ecosystem. In Late Cretaceous ecosystems

such as those preserved within the Hell Creek Formation, large tyrannosaurs are the dominant predator (Holtz, 2002; Russel, 1970; Snively, et al., 2006).

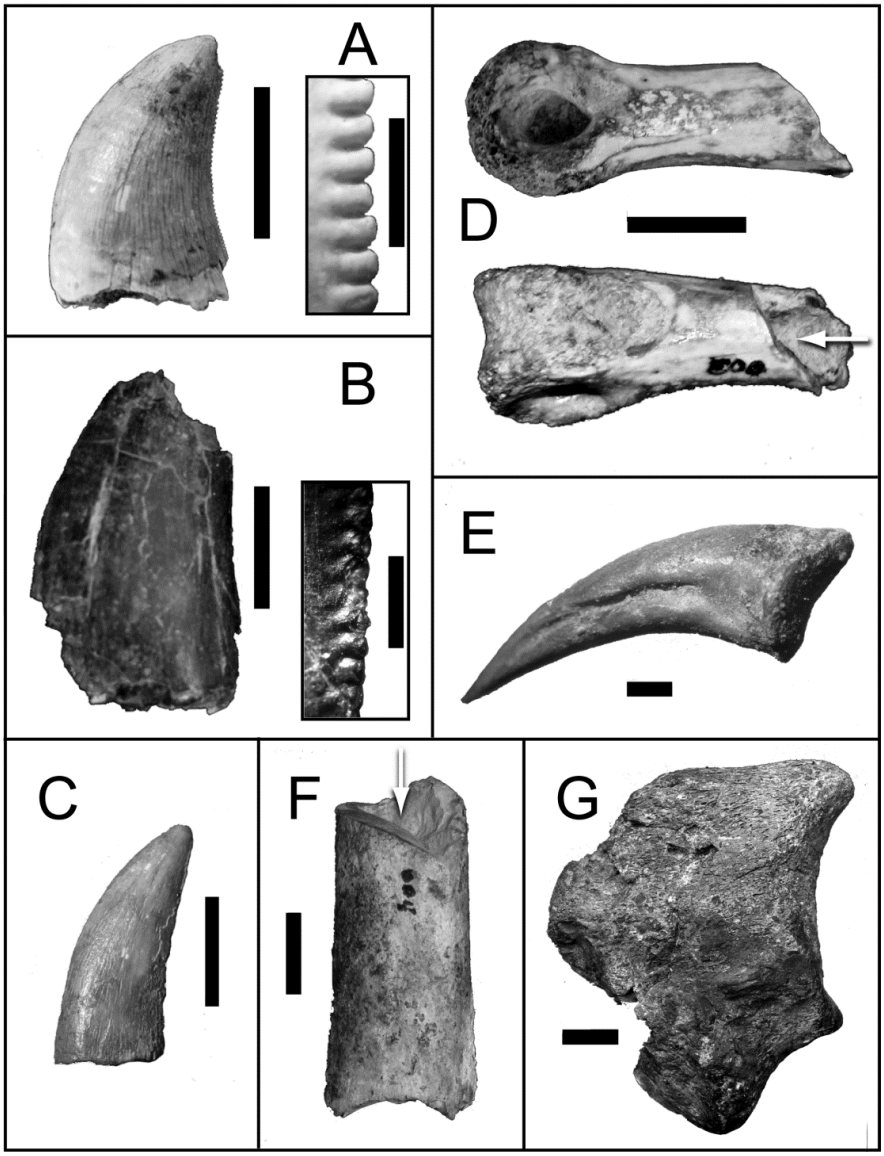

Figure 4.2 AAS theropod material. A. UTA-AAST-001 tooth, Scale bar=1 cm, denticles on posterior carinae. Scale bar=1 mm; B. UTA-AAST-002, denticles on posterior carinae. Scale bar=1 mm; C, UTA-AAST-006, juvenile tooth. Scale bar= 5 mm; D. UTA-AAST-003 phalanx in lateral and dorsal views. Scale bar=1 cm; E. UTA-AAST-005, a pedal ungual lateral view. Scale bar=1 mm; F. UTAAAST-004 a partial shaft. G. UTA-AAST-007, partial manual ungual in lateral view. Scale bar=1 cm.

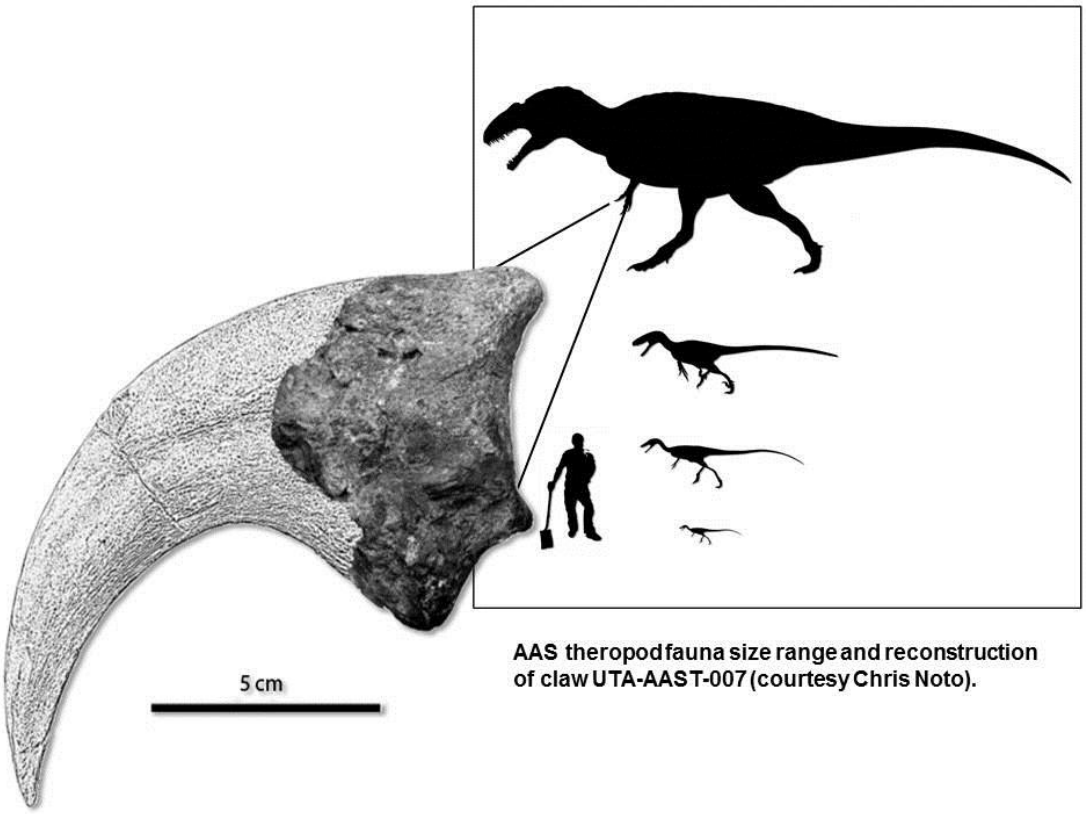

Figure 4.3 Reconstruction of claw UTA-AAST-007 (fossil material to the posterior, overlain with claw reconstruction of an *Acrocanthosaurus*). AAS theropods set to scale to elaborate the size range of Woodbine theropods (paleontologist D. J. Main for scale, shadow dinosaurs courtesy of Scott Hartman, claw art courtesy of Chris Noto).

Table 4.1 AAS Theropod tooth measurements

Specimen Field Number	Height	Width	FABL	DPM
UTA-AAST001	16.4	6.2	11	4
UTA-AAST002	26.6 (35*)	8	16	4
UTA-AAST006	11.4	2.6	4.8	N/A

H (Height), W (Width), FABL (Fore, Aft Basal Length), DPM (Denticle per mm), *Estimated

4.3 Discussion and Conclusions

The theropod teeth and postcrania discussed herein were recovered from a single Woodbine Formation fossil locality, the Arlington Archosaur Site (AAS) in northeastern Tarrant County, Texas. The AAS yielded the first significant theropod material to be recovered from the Woodbine, which documents the transitional nature of Cenomanian coastal ecosystems in Texas. This new material increases known dinosaur diversity from mid-Cretaceous Texas to include multiple taxa of small, medium, and large theropod predators (Fig. 4.3). Small dromaeosaurids are typically associated with Campanian and Maastrichtian North American ecosystems, not Cenomanian. The new Woodbine fossils demonstrates the transitional nature of Cenomanian dinosaur communities, as large, non-

coelurosaur tetanurans (NCTs) still appear to be the dominant terrestrial predators in northern mid-Cretaceous ecosystems, later to be replaced by tyrannosaurs (Fig. 4.4).

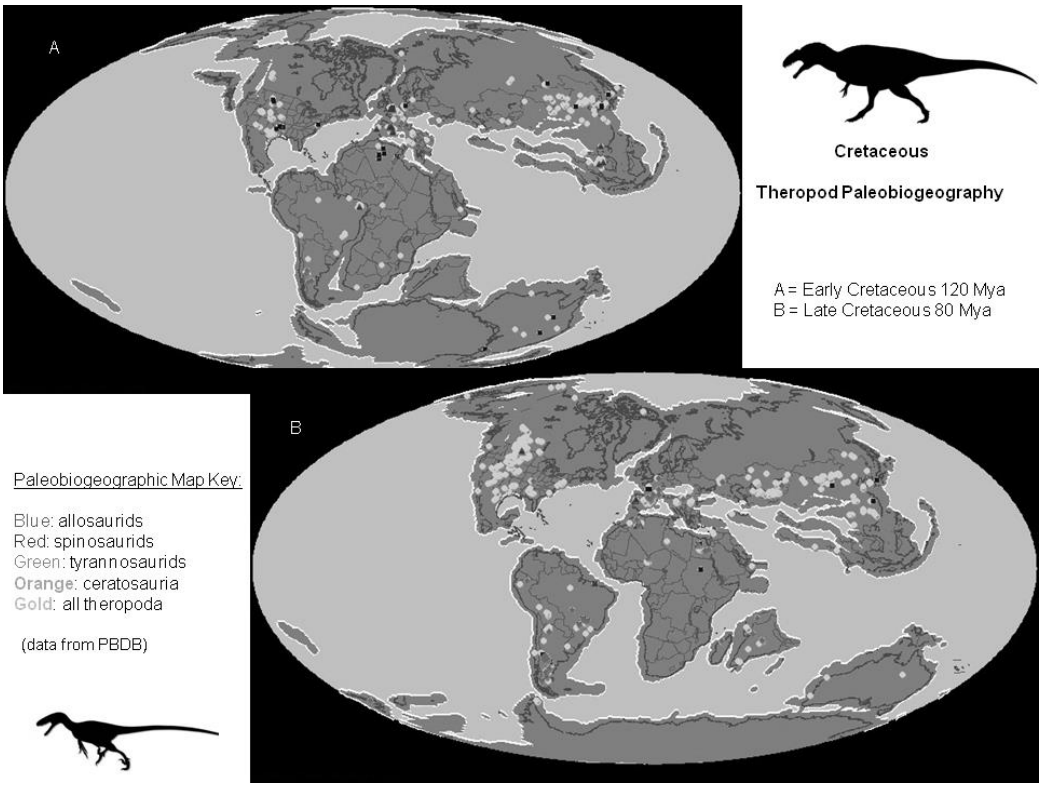

Figure 4.4 Global Late Cretaceous theropod paleobiogeography. Distributions plotted on two stage maps; A. Early Cretaceous (Aptian-120) and B. Late Cretaceous (Turonian-80 Mya). Paleobiogeographic maps created using data from the Paleobiology Database (PBDB).

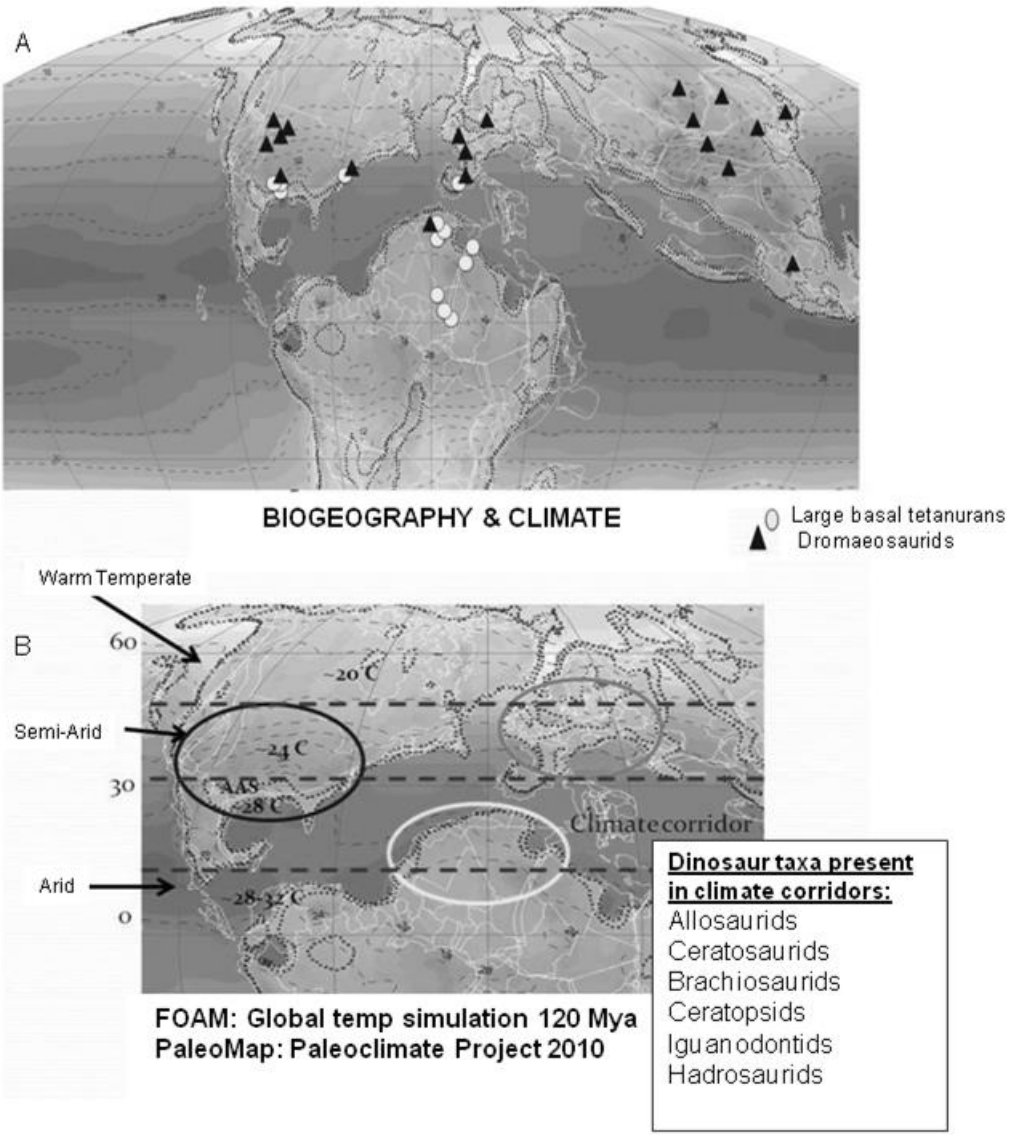

Figure 4.5 Theropod paleobiogeography and climate. A. Theropod dinosaur locations plotted on a paleogeographic map and overlain with a FOAM climate simulation. B. Paleogeographic map and FOAM simulation demonstrate a semi-arid climate corridor between 30° paleolatitude and the equator (Scotese, 2010). The AAS fauna existed within the same climate corridor as those of Central America, NW Africa and southern Eurasia.

Figure 4.6 Artist reconstruction of AAS theropods stalking hadrosauroid prey along the North Texas Woodbine coastal plain (paleo-art courtesy of Clinton Crowley, 2009).

The Woodbine NCT theropod suggests that this group possibly endured as an important part of southern North American faunas well into the Cenomanian. mid-Cretaceous Texas was potentially ecologically more similar to Gondwanan faunas than later Cretaceous Javelina, Judith River, or Lance Formation ecosystems. This ecological scenario is similar to that reported by Amiot et al. (2004) from the Cenomanian of Morocco. The presence of NCTs in the Woodbine lends support to the biogeographic model proposed by Galton and Taquet (1982), Buffetaut and Ouaja (2002) and Amiot et al. (2004), where the interchange of faunas between Laurasia and Gondwana occurred at some point in the Early Cretaceous. The presence of NCTs such as *Suchomimus*,

Carcharodontosaurus, and *Spinosaurus* in Gondwanan ecosystems and large allosauroids, perhaps something similar to *Acrocanthosaurus*, in southern North America during the Cenomanian suggests that NCTs were the large land predators of the equatorial latitudes through the mid-Cretaceous. It should be noted, however, that there is also the potential for the existence of tyrannosauroids in the Cenomanian of Texas, the presence of which would alter this interpretation.

Kirkland et al. (1997) and Zanno and Mackovicky (2011) discussed the presence of tyrannosauroids in the Early to mid-Cretaceous of North America. Kirkland (1997) reported the presence of a tyrannosauroid tooth in the mid-Cretaceous Mussentuchit Member of the Cedar Mountain Formation of Utah. Zanno and Mackovicky (2011) reported a tyrannosauroid premaxillary tooth from the Early Cretaceous (Albian) Clovery Formation of Wyoming. The presence of tyrannosauroids in the Early Cretaceous (Albian) of North America was used by Zanno and Mackovicky (2011) to support an Asiatic origin for the clade via Beringian land bridge dispersal. As the AAS Woodbine theropod material is both scant and fragmentary, the identification and assignment of the material is difficult at best. If the AAS theropod material is representative of tyrannosauroids, then it too would support an Asiatic origins and Beringian dispersal into North America model.

Paleogeographic and paleoclimatic models demonstrate a semi-arid (~28° C) climate belt existing from 15° to 30° latitude and extending from Texas to Morocco and Niger during the Cenomanian (Scotese, 2010), linking the ecosystems of these regions within a single climate envelope, or corridor (Fig. 4.5). It appears that during the Cretaceous large NCTs had an ecological and climatic preference to semi arid equatorial and near equatorial biomes all of which fall within a mid latitude climate corridor (Fig. 4.5). This observed pattern of climate corridor biogeography may represent a broader influence of climate on dinosaur distributions than previously noted. Further research into dinosaur distributions in relation to climate patterns generated by advancing paleoclimate programs will no doubt elucidate this matter. Equally, continued work on the fossil faunas of the Woodbine Formation and correlative stratigraphic units may shed more light upon the paleoecology and paleobiogeography of Cenomanian dinosaur communities.

4.4 Acknowledgments

I thank the Huffines family, Robert Kimball of Viridian Properties and HC LOBF Arlington for granting land access. I thank my coauthor, colleague Chris Noto for his invaluable input on this project, Noto's knowledge of theropod teeth and claws made this project possible. I thank Brad Carter and Art Sahlstein for finding and donating the specimens discussed herein, C. R. Noto for providing

line drawings of claws. C. R. Scotese for reviewing an early draft of this work and the PaleoMap Project for providing research funds. Artists Clinton Crowely and Scott Hartman for providing paleo artwork. The Dallas Paleontological Society for providing a scholarship to the author and the Jurassic Foundation and Western Interior Paleontological Society for providing research grants. Special thanks to AAS project members: Kevin Anderson, GebBennett, Brad Carter, Anissa Camp, Albert Miramontes, Rachell Peterson, Art Sahlstein, Richard Zack and countless others for their assistance.

CHAPTER 5

A BASAL HADROSAUROID (DINOSAURIA: ORNITHOPODA) FROM THE CRETACEOUS (CENOMANIAN) WOODBINE FORMATION OF NORTH CENTRAL TEXAS.

"*The study of dinosaurs is a labor of love. Amateur and professional alike collect and preserve the data needed to tell dinosaur stories in full, for the benefit of everyone."*

Jack Horner

"*What do you mean that they're just like modern cows? Ornithopods, especially hadrosaurs, have majesty of their own!"*

David B. Weishampel

5.1 Introduction

New ornithopod material recovered from the Woodbine Formation at the Arlington Archosaur site is the most complete basal hadrosauroid (Dinosauria: Ornithopoda) recovered from the Woodbine Formation. The new fossil material is important, as it allows for the most detailed study of the anatomy of basal hadrosauroids from Texas. The AAS hadrosauroid is herein described based upon fossils recovered from the Arlington Archosaur Site (AAS), a North Texas fossil locality that preserves a mid-Cretaceous (Cenomanian) ecosystem along a coastal plain. The site occurs within Woodbine Formation exposures in North Arlington,

Tarrant County, TX. The depositional environment of the AAS is a coastal delta plain, fine grained mudstone overlying an organic rich peat bed. Among the hadrosauroid fossils recovered are: a dentary and shed teeth, cervical, dorsal and caudal vertebrae, a scapula and coracoid, an ilium, ischium and pubis, humeri and femora. The new Woodbine fossils demonstrate a unique mix of plesiomorphic hadrosaurid characters with derived iguanodontian features that places this taxon near the base of hadrosauroid evolution.

The relative lack of change in the AAS hadrosauroid and other AAS specimens, hints at biogeographic isolation or endemism. The primitive-transitional nature of the AAS hadrosauroid may represent a broader ecological pattern in the fossil record. North American middle Cretaceous faunas were likely sourced by Early Cretaceous Eurasian faunas migrating across the Beringian land bridge and later isolated by Cenomanian eustatic high stands. The endemic nature of the AAS hadrosauroid and other Cenomanian forms provides an evolutionary bridge between Early and Late Cretaceous ecosystems in North America.

The only known Woodbine ornithopod, *Protohadros byrdi,* was discovered by Dallas Paleontological Society member Gary Byrd along Texas FM 2499 in Flower Mound in the early 1990's and later named by Head (1998) in his honor. *Protohadros byrdi* was based upon a nearly complete skull and little to no post crania found in strata that was assigned to the Arlington Member of the Woodbine Formation.

Formation (Head, 1998). The Woodbine exposures from which *Protohadros* was recovered consists of delta plain siltstone overlain by carbonaceous shale, with intermittent siderite concretions (Head, 1998). To date, no other fossil material has been recovered from this site.

The new material discussed herein was recovered from the Arlington Archosaur Site (AAS) intermittently between the years 2003 to 2012. The AAS occurs within a lower member of the Woodbine, the Lewisville Member and represents a stage that is possibly up to a million years older than the *Protohadros byrdi* type locality. This analysis describes the anatomy of a primitive hadrosauroid and further explores the plesiomorphic nature of the Woodbine hadrosauroid fauna. As the AAS taxon is based primarily upon post cranial elements and *Protohadros* is based upon crania, it is difficult to ascertain with complete certainty that the two taxa are either the same taxon, or independent. As the AAS is an ongoing excavation, future recovered cranial material could further clarify the diversity of the Woodbine hadrosauroid fauna. The fossils recovered and described from the AAS to date demonstrates the transitional nature of the Cenomanian and represents a broader ecological pattern in the fossil record, in which middle Cretaceous faunas present an evolutionary bridge between Early and Late Cretaceous ecosystems.

By the Late Cretaceous, hadrosauroids were the most common herbivores, and among the best documented of the ornithopods. Although hadrosauroid postcrania are common in the fossil record, little work had been done to use them due to the belief that they were of little systematic value. Brett-Surman (1975 and 1989) was among the first to publish a detailed discussion of post cranial characters useful in distinguishing hadrosaur taxa. Followed by the work of Davies (1983), Maryanska and Osmolska (1984), Casanovas et al. (1999), Brett-Surman and Wagner (2007), Prieto Marquez et al. (2006), Poole (2008) and McDonald et al. (2010). Their pioneering work with post crania established the utility of the post cranial skeleton for identifying key characters in hadrosauroid taxa, and was the basis of much of this work, as the majority of the AAS hadrosauroid is represented by post cranial elements.

5.2 Geolgic Setting

The father of Texas geology, R. T. Hill was the first geologist to map and define the Texas Cretaceous ranging from North Texas to the Big Bend region (Alexander, 1976). The Woodbine Formation of North Texas was named by Hill for the village of Woodbine in Cooke County (Alexander, 1976). In North Central Texas, the Woodbine outcrops from Temple, to the Red River (Oliver, 1971) (Fig. 5.1). It occurs as an irregular and narrow band, extending from Cooke County to Johnson County (Johnson, 1974) (Fig. 5.1). In the subsurface, the Woodbine

underlies a 45 county area in Texas, bounded by outcrops on the north and west, and by the Sabine Uplift to the east (Oliver, 1971). Woodbine sediments weathered out from the Ouachita Mountains in southern Oklahoma and settled in a series of nearshore environments in the subsiding East Texas basin (Oliver, 1971). Woodbine deposits primarily represent terrigenous nearshore and shallow marine depositional systems and include fluvial, deltaic and shelf deposits (Dodge, 1952; Main, 2005; Murlin, 1975; Oliver, 1971; Trudel, 1994). The Woodbine overlies the Grayson Formation of the Washita Group and is unconformably overlain by the strata of the Eagle Ford Group (Dodge, 1952, Oliver, 1971). A period of marine deposition lasting ~10 million years separates the Woodbine from earlier environments (Winkler et al., 1995).

Dodge (1968 and 1969) proposed four units for the Woodbine Formation, in ascending order they are: the Rush Creek Member, Dexter Member, Lewisville Member and the Arlington Member. The Rush Creek Member was first noticed by Bergquist (1949) as a shale unit that occurred between the overlying Dexter Member of the Woodbine Formation and the underlying Grayson Formation. Johnson (1974) later studied the depositional environments of the Rush Creek Member as part of his UT-Arlington graduate work. He noted that the Rush Creek Member consisted of interfingering shale and sandstone, divided into two provinces at the Denton –Tarrant County line. The southern province is distinguished by offshore bars and lagoonal deposits (Johnson, 1974). The

Northern Province is distinguished by lower shoreface silts and sand, lower shoreface shale and clay, and estuarine sand (Johnson, 1974). Johnson's work on the lower Woodbine stratigraphy identified the environments of deposition and facies variation for the basal Rush Creek Member.

Bergquist (1949) defined the Dexter Member of the Woodbine Formation lithologically as fluvial ferruginous and siliceous sandstone with silty clay lenses with some carbonaceous clay at the base of the member. The uppermost Dexter is composed of a varicolored clay unit that was mapped and considered a different member of the Woodbine by Bergquist (1949). This uppermost clay was called the Rainbow Clay by Bergquist, but was later included as part of the Dexter Member by Dodge (1969). The Dexter fluvial deposits compromise 1/3 of the northern Northeast Texas basin and consists of tributary facies and meander belt facies (Oliver, 1971). The Dexter outcrops principally in Grayson County, with some southern outcrops in Tarrant County that are principally fluvial-deltaic in nature (Oliver, 1971).

Overlying the fluvial sand of the Dexter Member is the marine Lewisville Member which consists primarily of marine mud and shale deposited along an extensive coastline, marginal to active delta systems (Oliver, 1971; Trudel, 1994). The Lewisville Member is highly fossiliferous, containing mollusks, ammonites and foraminifers (Trudel, 1994). In the ammonite fauna of the Lewisville

Member is *Conlinoceras tarrantense,* a biostratigraphic zonal marker for the base of the middle Cenomanian (Kennedy and Cobban, 1990). The presence of *C. tarrantense* thus establishes an age constraint for the unit. In outcrop the Lewisville Member consists of 29 meters of fossiliferous sand lenses, mudstone and shale (Oliver, 1971). The dominant lithologies of the Lewisville Member, however, are mudstone and shale, with sandstone occurring as lenticular bands between mud and shale beds (Main, 2005). The shale tends to be blue-gray or black, finely laminated to massive bedded, contain numerous marine fossils, and principally represent shelf facies (Oliver, 1971). The Lewisville Member is characterized by numerous marine fossils, principally small reefs with the oyster *Ostrea soleniscus* (Bergquist, 1949). The Lewisville Member includes what was called by Bergquist (1949) as the Red Branch Member. The Red Branch Member is a basal unit of lenticular, cross bedded sand with localized lignite beds that was later included in the Lewisville Member by Dodge (1969) and is still recognized as such today (Beall, 1964; Trudel, 1994).

Murlin (1974) defined the Arlington Member of the Woodbine Formation as a fluvial sandstone that occurs in North Texas as exposures in Denton, Johnson, and Tarrant Counties that directly overlie the carbonaceous shale of the Lewisville Member. He described the Arlington Member as a thin (< 3 m) unit that consists of thin beds of laminated siltstone interbedded with massive beds of fine grained, heavily oxidized, cross bedded sandstone (Murlin, 1974). The

paleoenvironments preserved within the Arlington Member are non-marine delta plain deposits that are marginal to a distributary system (Murlin, 1974). Head (1998) placed the type locality for *Protohadros* within strata of the Arlington Member of the Woodbine Formation.

Oliver (1971) classified the Woodbine deltas as destructive deltaic systems of progradational channel-mouth bar facies that are marine influenced due to the poor development of constructional sequences, the formation of embayments and associated strandplains, well developed coastal barriers proximal to areas of maximum discharge, relatively thin prodelta facies and high sand - mud ratio with poor muddy delta plain aggradational deposits. Oliver (1971) did not place these deltaic deposits directly in the Lewisville Member, but referred to these deposits as the Freestone Delta System. In this work, the Woodbine deltas are not referred to as the Freestone Delta System and are placed within the Lewisville Member of the Woodbine, based on observations made by the author at the AAS, Bear Creek and Lake Grapevine (Main, 2005). The AAS was placed within the Lewisville Member of the Woodbine Formation based upon the lithology of the unit as defined in the literature and on the biostratigraphy of the site. The presence of the invertebrates *Anchura* and *Gyrodes* biostratigraphically place the AAS within the lower to middle strata of the Lewisville Member (Stephenson, 1952). The palynomorphs *Dichastopollenites* and *Stellatopollis*, recovered from the AAS, affirm a mid-Cenomanian age (May, 1975).

The AAS occurs within strata of the Lewisville Member of the Woodbine Formation and preserves a migrating coastal plain that experienced several eustatic events. The lowermost section consists of a rippled nearshore sandstone that is heavily burrowed with *Diplocraterion, Thalasinoides* and *Arenicolites* trace makers from the *Skolithos* facies (Seilacher, 2007). The hadrosauroid fossils discussed herein were recovered from an overlying heavily carbonaceous peat and an organic rich paleosol (Fig. 5.1). Overlying the paleosol is a lag deposit and a series of heterolithic strata consisting of mudstone, and finely laminated and rippled sandstone from a low lying delta plain (Fig. 5.1). The depositional model of the AAS is a coastal system consisting of fine grained sediments, rich with organic material from an inundated delta plain. Within the clay and mud, numerous coprolites and fossil wood have been recovered that can be used to study the ecosystem dynamics of the region. The amount of plant and wood found at the site is indicative of a dense coastal wetland, a fen or mangrove. Several large (>3 m) and numerous partial (<2 m) logs were excavated from a peat bed that immediately underlies the primary dinosaur bonebed in the AAS Dinosaur Quarry (Fig. 5.3). The hadrosauroid fossils were recovered from the peat and organic rich paleosol of the mid section sequence in the AAS Dinosaur Quarry. The hadrosauroid fossil remains were recovered disarticulated but associated from an approximately 6 meter square horizontal area and about 0.6 meters of vertical relief (Fig. 5.1 and 5.4).

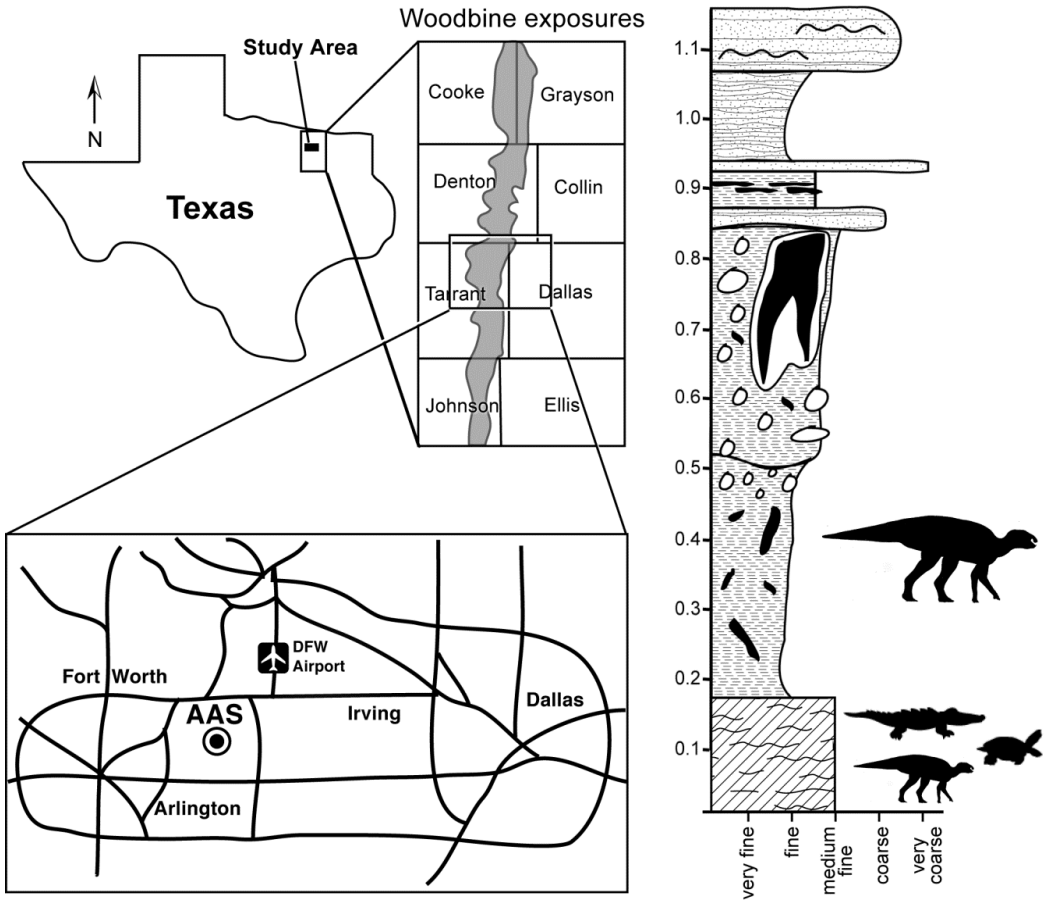

Figure 5.1. Texas map with outline of counties in which Woodbine Formation exposures occur. Woodbine Formation study area in northeastern Tarrant County with AAS study area denoted. Stratigraphic column shows relative position of AAS ornithopod to other AAS fossils.

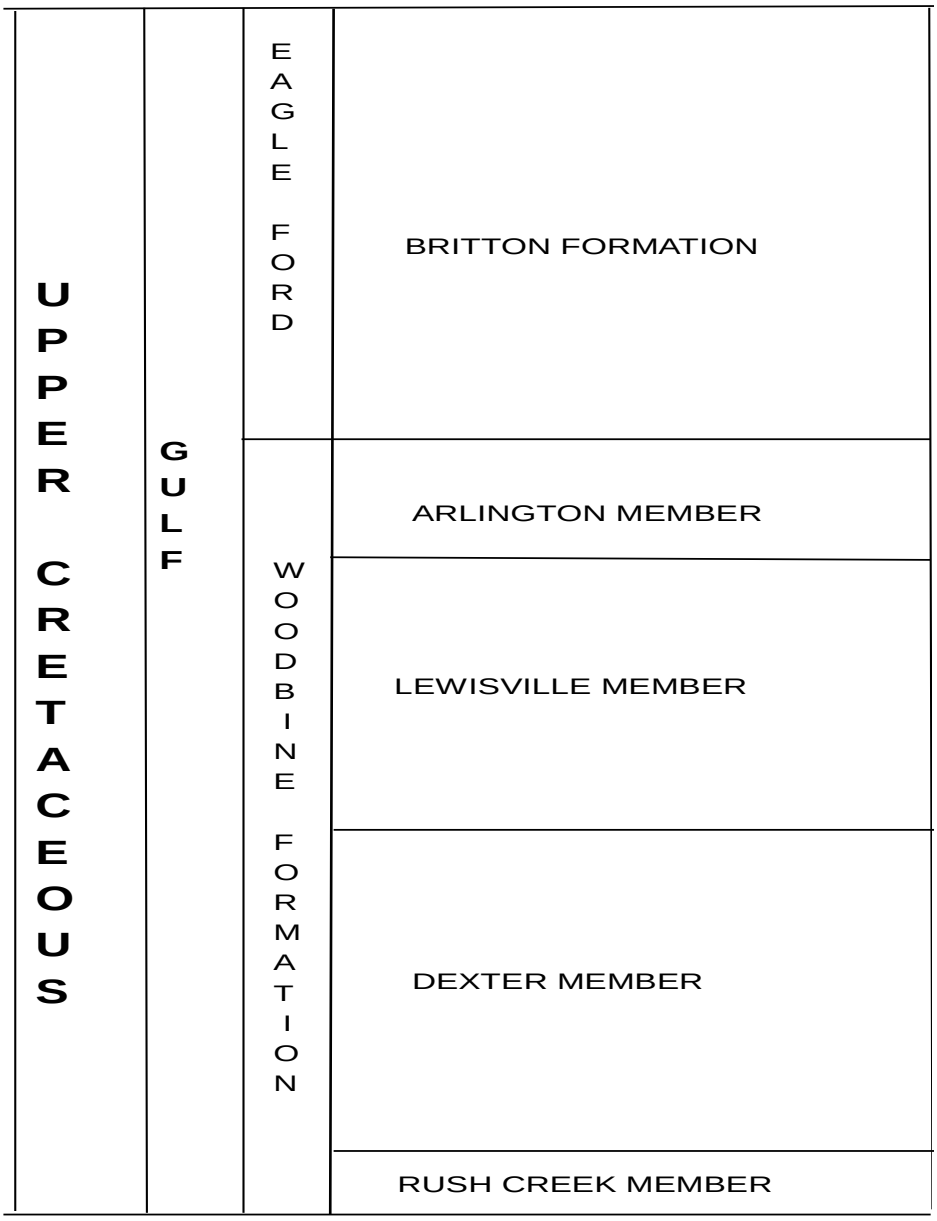

Figure 5.2 North Texas Cretaceous stratigraphy in relation to the members of the Woodbine Formation; Rush Creek, Dexter, Lewisville and Arlington. Stratigraphic position of the Arlington Archosaur Site lies in the upper part of the Lewisville Member of the Woodbine Formation.

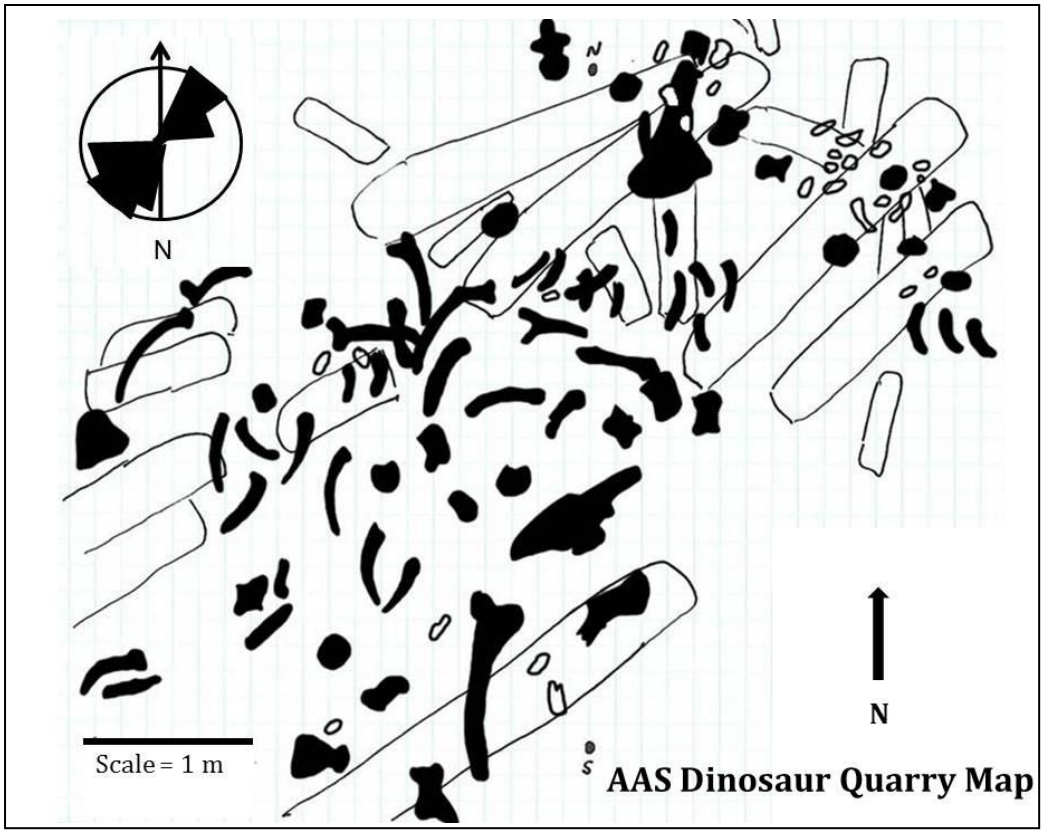

Figure 5.3 AAS Dinosaur Quarry map of showing the distribution of hadrosauroid fossils and carbonized logs. All fossils demonstrate a NE-SW alignment in the quarry (note Rose Diagram). The overlying dinosaur fossils are black; the lower underlying carbonized logs are white.

Figure 5.4 Image of the eastern wall of the AAS Dinosaur Quarry as it appeared in 2010. The hadrosauroid material was recovered from middle of the quarry (left) toward the Northeast quarry (middle–right). The adult material was recovered from the lower, mudstone horizon of a Histic Gleysol (denoted with hammer). Sub adult hadrosauroid material was recovered from the lower peat bed that occurs in the floor of the quarry
(bottom of image).

Figure 5.5 Images of the early excavations of the AAS Dinosaur Quarry. A. First large excavation in August 2008 with Dallas Paleontological Society (DPS) volunteers. B. View inside the tent during the first dig, 2008. C. Author D. Main working in the Dino Quarry with UTA Dinosaurs students and DPS volunteers, spring 2009. D. Outcrop photo of AAS Dino Quarry exposures, hammer and arrow denotes dinosaur fossil horizon in paleosol.

5.3 Locality and Horizon

Material— The AAS hadrosauroid is represented by four individuals from two horizons, a juvenile, sub-adult and an adult; a partial juvenile dentary with isolated teeth, a femur and humeri, isolated adult teeth, a scapula, coracoid, ilium, ischium and prepubis, a juvenile femoral condyle, a partial adult femur, cervical and dorsal ribs, an axis, cervical, dorsal and caudal vertebrae. The material was recovered from the middle Cretaceous (Cenomanian: 95-100 Mya) Woodbine Formation at the Arlington Archosaur Site, northeastern Tarrant County, Texas.

Locality and horizon—Specimens of four individuals were recovered from two bone bearing horizons within strata of the Lewisville Member of the Woodbine Formation (Cenomanian) at UTA Location 50, the Arlington Archosaur Site (AAS) in Arlington, Tarrant Count, TX. The AAS is located in northern Arlington, off Texas Hwy 360 and Trinity Blvd at Main St., several kilometers due north of the Dallas Cowboys Stadium. The exact GPS coordinates of the location are on file with the University of Texas at Arlington.

5.4 Description

5.4.1 Cranial Material

Dentary – UTA-AASO-161 is a partial right dentary from a sub adult individual. The dentary is 220 mm in length and preserves 19 alveoli (Fig. 5.6). Along the length of the dentary, the dorsal and ventral margins are parallel for nearly half

the total length of the specimen, diverging toward the rostral ramus (which is not preserved in this specimen) (Fig. 5.6). It is unfortunate that the rostral ramus is not preserved in this specimen, as it is an important character noted in *Protohadros* and *Eolambia* (McDonald et al., 2012). The ventral margin preserves a partial, but distinct Meckelian groove that is best observed beneath the 12th alveolus (Fig. 5.6). The posterior most ventral margin also preserves a deep adductor fossa beneath the terminal point of the alveoli at the base of the coronoid (Fig. 5.6).

The alveoli range in size from approximately 9 mm to 10 mm wide, and are relatively shallow (Fig. 5. 6). Together they are set parallel to one another and do not show impressions from the teeth, a derived hadrosaur trait. Although the dentary is not complete, as the rostral ramus is missing, the anterior dorsal margin is complete and preserves the rostral most alveolus (Al1) and to the posterior the alveoli clearly terminate near the base of the coronoid process, similar to *Eolambia*, *Protohadros* and *Telmatosaurus* (Head, 1998; McDonald et al., 2012; and Weishampel et al., 1993;). In derived iguanodontians, the alveoli typically terminate at the base of the coronoid process. A defining synapomorphy of hadrosaur dentaries is a termination of the alveoli caudolateral to the coronoid process (Horner et al., 2004). The base of the coronoid rises up vertically from a broad, concave lateral shelf that forms a distinct horizontal margin between the coronoid and the dentition (Fig. 5.6). The coronoid process is a robust element

that has a caudally deflected rostral expansion of the coronoid process that is subtriangular in lateral view, similar to *Eolambia* and *Protohadros* (Head, 1998; and McDonald et al., 2012) (Fig. 5.6). An important feature of the dentary is the lack of a ventral convex bulge beneath a prominent lateral convex groove seen along the base of the coronoid, and a distinct subrectangular blade like process projecting to the posterior (Fig. 5.6). Although the dentary is not complete, and this process is broken along the posterior most margin, it appears to be prominent process not observed in either *Eolambia* or *Protohadros* (Head, 1998; and McDonald et al., 2012) (Fig. 5.6). This variance, and others could possibly be attributed to ontogeny, as this specimen was not from an adult. Overall, the similarities between the AAS dentary and the type specimen of *Protohadros* were striking. Based upon the comparison of the sub-adult dentary found at the AAS and that of *Protohadros*, the AAS specimen may likely be assigned to *Protohadros sp*., although more material is needed to clarify this relationship.

Teeth – Over forty hadrosauroid teeth were recovered from the AAS, however, most were worn, shed remnants. UTA-AASO-002, 003 and 004 isolated teeth, are worn but preserve margins with denticles present (Fig. 5.6). The teeth are distinctly hadrosaurid, demonstrating an overall diamond shape and single median carinae and lack the secondary ridges seen in many iguanodontians (Horner et al, 2004; Norman, 2004) (Fig. 5.6). The teeth with preserved roots have rounded apices that gradually expand outwards toward the crown (Fig. 5.6). The teeth

possess a single median carinae, with an obtuse labial (~70°) angle between the root and crown (Fig. 5.6). The denticles are somewhat eroded, forming a series of ridges along the margins, enlarging (widening) slightly toward the occlusal surface. The maxillary crowns are slightly asymmetric, laterally compressed with a very slight lingual curve.

The dentary teeth are larger than the maxillary teeth, with long tapering roots and broad, wide crowns (Fig. 5.6). The dentary teeth have an average 14 mm medial width compared to the maxillary teeth that average an 8 mm medial width. The lingual surface of each dentary crown is raised and covered with a thick enamel shield (Fig. 5.6). The angle of the lingual surface, near the resorption facet, is unusually sharp (~20°) (Fig. 5.6). The dentary teeth show signs of close compaction within the dental battery via grooves along the buccal surface and a concave resorption facet on the distobuccal surface (Fig. 5.6). The close compaction of the teeth is a feature typically associated with hadrosaurid dental batteries (Horner et al., 2004). Unfortunately, the teeth were found isolated and not in place within the dentary, thus no observations may be made on the number of teeth per tooth position. Hadrosaurids typically have 3-5 teeth per tooth position (Horner et al., 2004). However, the teeth do show indications of close compaction within the dental battery, which implies a hadrosaurid state (Horner et al., 2004). UTA-AASO-002 and 004 are similar to those of *Protohadros.*

Figure 5.6 AAS hadrosauroid dentary and dentition. A. UTA-AASO-161 a right sub adult dentary in lingual view. B. UTA-AASO-161 a right sub adult dentary in labial view. Abbreviations used: Alveolus 1 (Al1), Adductor fossa (Adf), Lateral convex buldge (Lcb), Lateral shelf (Ls), Meckelian groove (Mg), Rostral expansion of coronoid process (Rcp). C-F. UTA-AASO-002, 003, 004 shed teeth, dentary and maxillary.

5.4.2 Post Cranial Skeleton

Post Crania – The axial skeleton is represented by approximately twenty five vertebrae from the axial column; including numerous partial centra, nearly five complete cervicals, including the axis, several dorsals and caudals along with numerous cervical and dorsal ribs (Fig. 5.17).

Axis–UTA-AASO-090 is relatively complete, with minor deformation to the neural spine. The centrum is longer than tall and shorter than the large neural spine. It is 96 mm long laterally and 92 mm in vertical height and strongly opisthocoelous with a pronounced odontoid condyle on the anterior articular surface and a broad keel on the ventral surface (Fig. 5.7). The pronounced odontoid process is similar in form to *Zalmoxes, Camptosaurus, Bactrosaurus*, and *Telmatosaurus*, although larger than *Camptosaurus*, and lacking the dorsal deflection of *Bactrosaurus* (Carpenter and Wilson, 2008; Dalla Vecchia, 2006; Godefroit et al., 1998; Weishampel et al., 1993; and Weishampel et al., 2003). The pronounced odontoid process and broad ventral keel are features typical of iguanodontians, and absent in most hadrosaurids (although present in *Telmatosaurus;* Weishampel et al., 1993). The prezygapophyses are oblong structures that sit flush with the sides of the neural spine and extend cranially above the centrum (Fig. 5.7). However, they do not extend beyond the cranial condyle. Caudal to the prezygapophyses are small rounded transverse processes.

The neural arch and spine are robust, extending dorsally 156 mm above the centrum. The cranio-dorsal margin is blade-like in lateral view and thins dorsally to a rounded point. In lateral view the neural spine has a gentle slope (~60°) that rises caudally, most starkly at its dorsal most prominence, forming an elongated S- shape (Fig. 5.7). The curved slope of the neural spine is similar to the iguanodontians *Tenontosaurus* and *Camptosaurus*, and is a feature not seen in hadrosaurids. The axis of Late Cretaceous (Campanian-Maastrichtian) hadrosaurids typically have rounded, crescent or blade like neural spines that expand outwards dorsally, as seen in *Kritosaurus*, *Gryposaurus* and *Edmontosaurus* (Davies, 1983; Lull and Wright, 1942; Parks, 1920). Caudally, the neural arch bifurcates into separated broad postzygapophyses that are arched and stout with pronounced flattened ventral articular facets. The caudal articular surface of the centrum is deeply concave and appears slightly reniform. In caudal view, the axis centrum and neural spine appears roughly hour glass in shape. The overall morphology of the axis is similar to the iguanodontians *Camptosaurus* and *Bactrosaurus* with some affinities to the primitive hadrosaur *Telmatosaurus* (Carpenter and Wilson, 2008; Dalla Vecchia, 2006; Godefroit et al., 1998; and Weishampel et al., 1993).

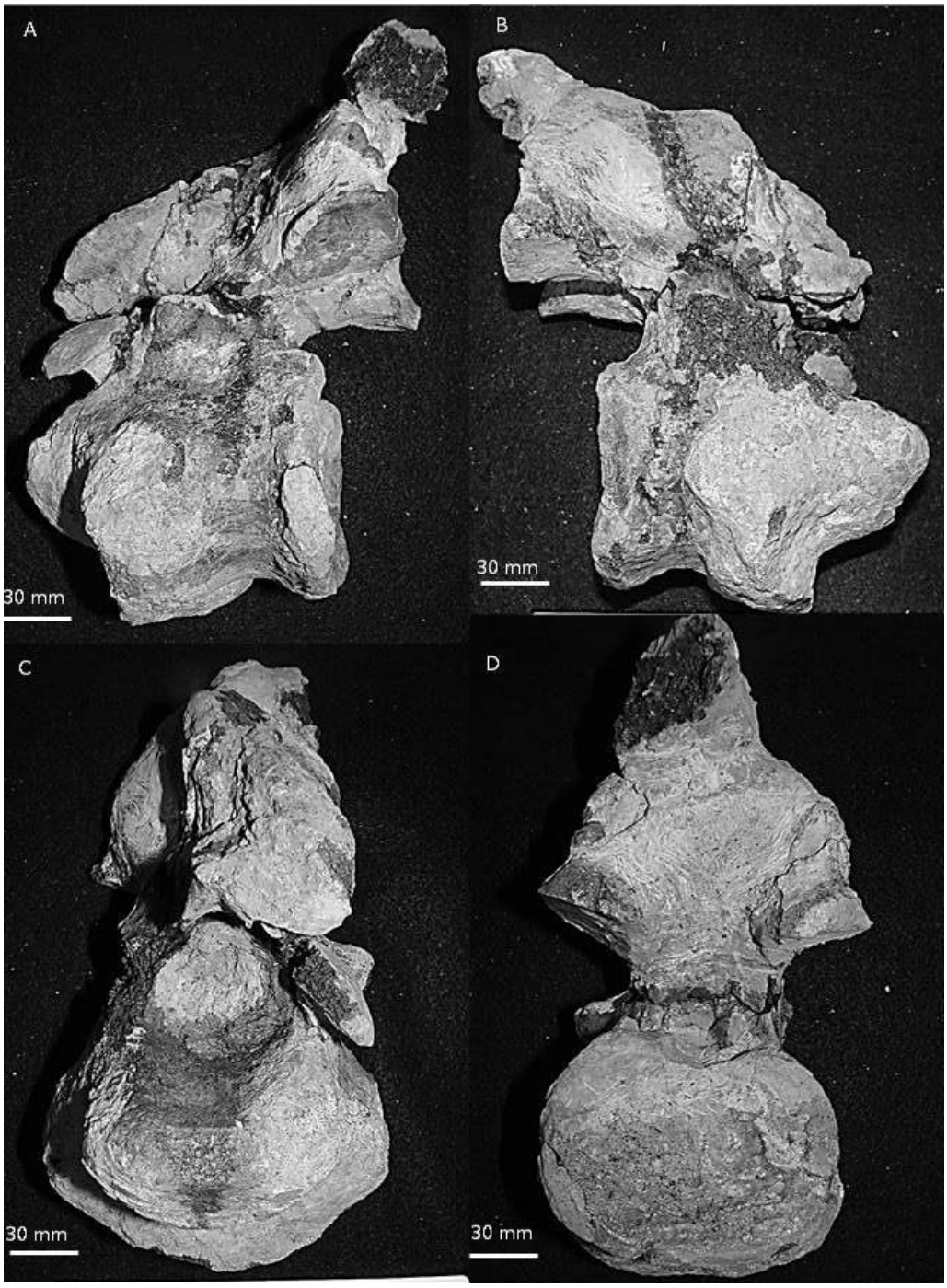

Figure 5.7 UTA-AASO-090 axis. A. Axis in left lateral view. B. Axis in right lateral view. C. Axis in anterior view. D. Axis in posterior view.

Post axial cervicals–All recovered cervical vertebrae were disarticulated, but associated from a single fossil horizon within the AAS Dinosaur Quarry. All are roughly equal in length with strongly opisthocoelus centra, a character typical of hadrosauroids (Horner et al., 2004). The cervical centra are broad transversely and elongate axially, with a slight constriction in the middle of the centra and deeply concave caudal articular surfaces. Both in cranial and caudal view, the centra appear reniform. The mudstone matrix on the posterior face of the centrum of UTA-AASO-091 has slickensides preserved, typical of shrinking and swelling of a clay rich soil, an indicator of climate influenced depositional deformation. UTA-AASO-091 a cranial cervical is deformed, with a neural spine that deflects to the right (Fig 5.8). The neural arch and spine are a complex structure, vertically short, and elongate (Fig. 5.8). The neural spine slopes caudodorsally, with a gentle (~40°) rise, thickening caudally into a bifurcated wedge at the postzygapophysis on the cranial cervical series. The neural arch and spine broadens and widens on the cervicals caudally as they approach the dorsals (although the most caudal cervicals are incomplete). The prezygapophyses of UTA-AASO-091 are incomplete, with only a partial left prezygapophysis preserved. The left prezygapophysis is elongate laterally and extends cranially over the centrum with an ovoid articular facet. The length of cranial extension of the prezygapophysis over the centra of the cranial cervicals is greater in iguanodontians than in hadrosaurids. A single diapophysis is preserved on UTA-

AASO-091; it is a rounded process that deflects away from the laterally directed right transverse process, the cervical rib is broken and incomplete. The postzygapophyses are elongate, and wedge shaped that sweep caudolaterally at a wide angle over the caudal centrum. The right lateral twist is only observed in UTA-AASO-091. All other cervicals lack this deformation. The ventral articular surfaces of the postzygapophysis are broad, ellipsoidal surfaces that are flattened and expand caudally for articulation with the prezygapophysis. The right transverse process is thin, set craniolaterally on the neural arch and deflects ventrally (Fig. 5.8). Cervical ribs were found disarticulated and thus collected separate from the AAS cervicals.

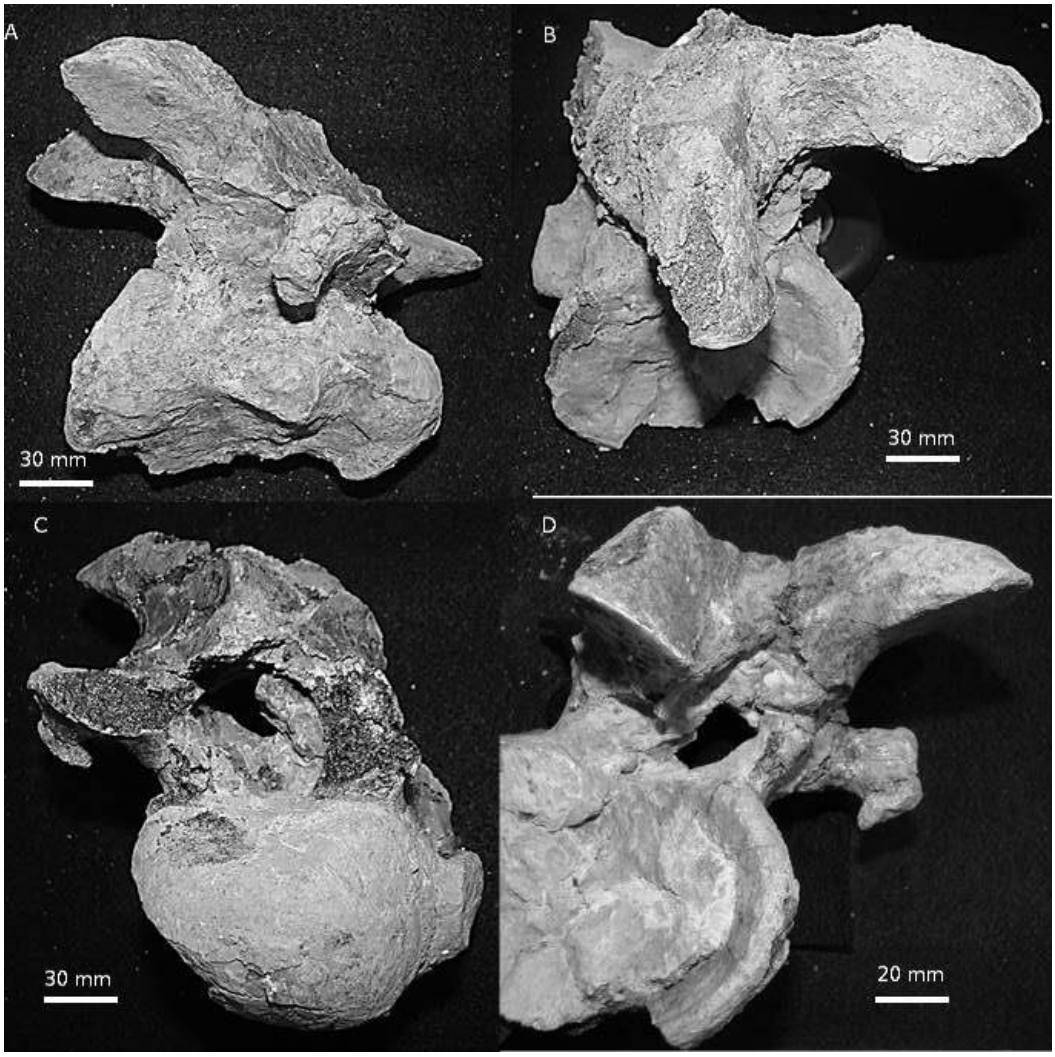

Figure 5.8 UTA-AASO-091 a cranial cervical that is deformed. A. UTA-AASO-091 in right lateral view. B. UTA-AASO-091 in oblique dorsal view, note that the neural spine deflects to the right. C. UTA-AASO-091 in anterior view, note deflection of neural spine. D. UTA-AASO-091 in posterior view.

Cervical and Dorsal ribs–The cervical ribs are represented by partial, disarticulated elements from the caudal cervical series. The cervical ribs are similar in general morphology to those of *Tethyshadros* and *Iguanodon* (Dalla

Vecchia, 2009; and Norman, 1980). The tuberculum is shorter than the capitulum and the shaft in the most caudal cervical ribs are long and ventrally rather than caudolaterally situated (Fig. 5.9). In UTA-AASO-017, a small cranial dorsal rib, the capitulum is rod like and the tuberculum is broken at the shaft-tuberculum intersection (Fig. 5.9). The dorsal ribs are more elongate than the cervicals and project proximally and ventrolaterally. They are curved ventrolaterally and appear triangular in cross section. UTA-AASO-050 is a proximal dorsal rib with a well preserved capitulum and tuberculum, which are much larger and better defined in the dorsal series (Fig. 5.9). In UTA-AASO-050 the tuberculum is a small, rounded process that projects vertically away from the surface of the rib, terminating after ~1 cm. The capitulum is a thin, rectangular projection that extends away from the tuberculum at a 30° angle, ending in a flattened articular surface for attachment to the vertebra (Fig. 5.9). The length of separation between the capitulum and the tuberculum, the extended rectangular shape and gentle angle, or slope descending ventrally to the rib shaft are features that are morphologically similar to *Iguanodon bernissartensis*, and not seen in derived hadrosaurids such as *Edmontosaurus* (Lambe, 1920; Lull and Wright, 1942; Norman, 1980).

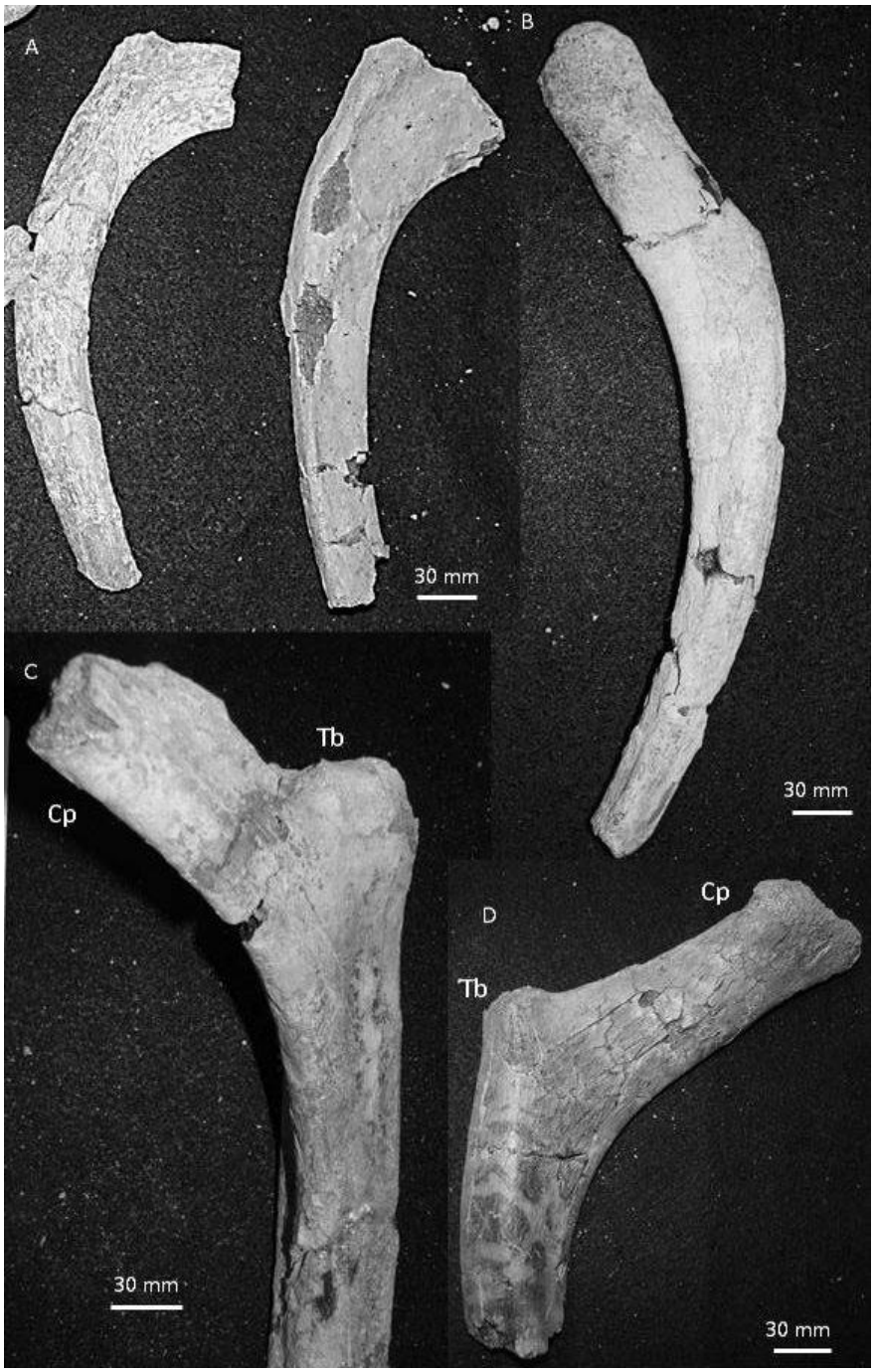

Figure 5.9 Dorsal ribs. A. UTA-AASO-017 and 018 cranial dorsal ribs. B. UTA-AASO-062 a cranial dorsal rib. C. UTA-AASO-056 a dorsal rib with well preserved capitulum (Cp) and tubercle (Tp). D. UTA-AASO-050 a partial dorsal rib.

Dorsal vertebrae–The dorsal vertebrae recovered from the AAS are more numerous than the cervicals, consisting of eight complete specimens, and approximately ten with miscellaneous fragments included. Due to the fragmentary nature of the vertebrae, the complete number of dorsals is unknown. However, 16 or more vertebrae in the dorsal series are typical of *Iguanodon* and hadrosauroids (Norman, 2004; Della Vecchia, 2009). The cervico-dorsal transition is seen in the proximal most dorsals, as they are low with small centra and dorsolaterally directed transverse processes. The neural arch and spines thicken along the dorsal series, with the neural spines increasing in height and straightening dorsoventrally (Fig. 5.17). The neural spines dwarf the dorsal centra, which are approximately 1/3 the length of the elongate neural spines, a character typically associated with the Hadrosauridae (Prieto-Marquez, 2007).

UTA-AASO-103 is a partial dorsal vertebra from the cranial dorsal series. It is composed of a complete centrum with neural arch and a right transverse process, the neural spine is missing (Fig. 5.10). The centrum is slightly opisthocoelous and subrounded, broadening to the posterior in lateral view. Above the neurocentral suture, two thin ridges of bone form an arch rising dorsally to the transverse process, within this arch is the parapophysis, which is small and sits at mid height laterally beneath the right transverse process (Fig. 5.10). The presence and small size of the parapophysis places this dorsal vertebra within the cranial dorsal vertebral series. The right transverse process rises

dorsolaterally, outwards away from the neural arch at a near vertical angle. It is rectangular in lateral view, ending in a thick, subrounded diapophysis. The vertically arched transverse process is typical of the cranial dorsal series in hadrosauroids. The pre and postzygapophyses are not present on this specimen.

UTA-AASO-104 a partial dorsal vertebra from the middle to posterior dorsal series is composed of a complete centrum with neural arch, a partial neural spine and partial transverse processes (Fig. 5.10). The centrum is amphiplatyan, as is typical of hadrosauroid dorsal vertebrae, rounded in cranial and caudal view, then broadening to the posterior in lateral view. The transverse processes are situated at a near 90° angle to the neural spines and project laterally outwards, a feature that is typical of the middle to sacral dorsal vertebrae (Fig. 5.10). The exact lengths of the transverse processes are unkown as the specimen is incomplete. The neural spine is partial, rectangular in lateral view and projects dorsally, rather than dorsocaudally, as seen in the cranial dorsal series. The prezygapophyses project dorsomedially from the base of the neural arch, but do not extend far over the centra. The prezygapophyses are subrounded with ellipsoidal facets that face lateroventrally. The postzygapophyses are not present on this specimen. The remainder of the dorsal vertebrae are represented by centra only. All specimens are amphiplatyan and relatively rounded in cranial and caudal view. They do not demonstrate the hexagonal, or heart shape typical of hadrosaurid caudal vertebrae (Horner et al., 2004).

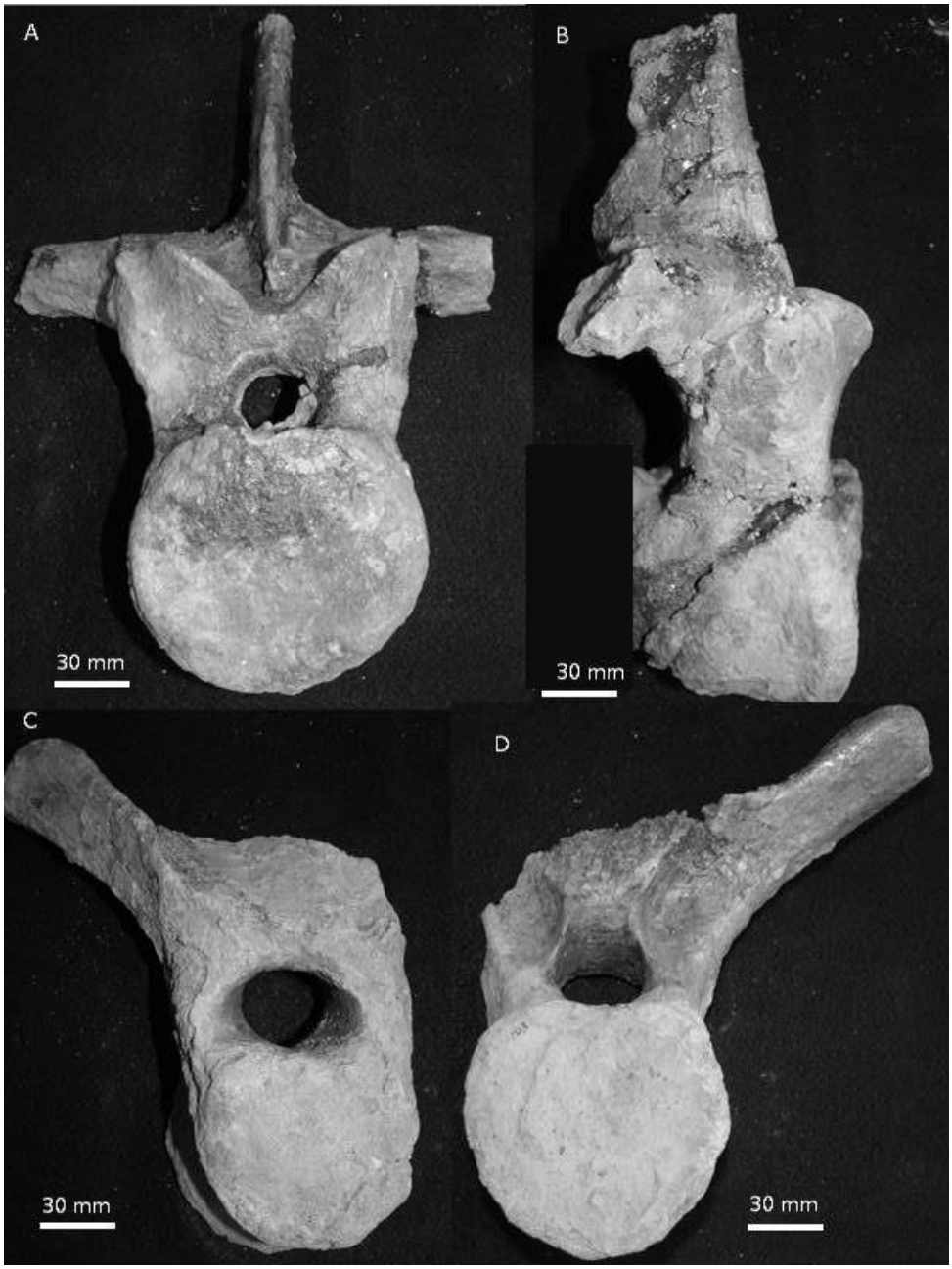

Figure 5.10 Dorsal vertebrae. A. UTA-AASO-104 posterior dorsal vertebra in anterior view. B. UTA-AASO-104 posterior dorsal vertebra in right lateral view. C. UTA-AASO- 103 cranial vertebra in anterior view. D. UTA-AASO- 103 cranial vertebra in posterior view.

Caudal vertebra–Six disarticulated, but associated caudal vertebrae were recovered from the AAS, two proximal and several distal caudals along with miscellaneous fragmentary partial centra (Fig. 5.17). The centra are broad and amphiplatyan with a neural spine that is three times the length of the centrum. The ventral surface of the centra is rounded, with a pronounced hemapophyseal facet for chevron (hemal arch) attachment deflected ventrally. The dorsal surface of the caudals is defined by broad, triangular neural arches. The prezygapophyses project obliquely proximally on all proximal caudals. The postzygapophyses are raised and directed ventrolaterally with oblong facets. The neural spines on UTA-AASO-100 and 098 are rectangular in lateral view, tall (>30) cm long and deflected distally by ~45°-60° (Fig. 5.11). The transverse processes are lost distally down the tail. At the same time, the centra become less rounded and more heart shaped distally. Heart shaped centra of the caudal vertebrae are typical of hadrosaurids, more so than iguanodontians.

UTA-AASO-100 is from the proximal caudal series as the centrum is round in proximal view, not heart shaped, is proximomedially compressed and it lacks prominent prezygapophyses. The prezygapophyses are small ovoid facets that deflect ventrolaterally away from the base of the neural spine. The neural spine is rectangular in lateral view and deflects distally at a sharp angle (~45°) (Fig. 5.11). UTA-AASO-098 is from the middle caudal series, as the centrum is heart-shaped in proximal view and prominent prezygapophyses are present. The

zygapophyses are small pedestals with ovoid articular facets.The postzygapophyses project ventrolaterally from the neural arch, with the ovoid articular facets that are visible in lateral view. The neural spine is deflected distally, but at a reduced angle (~60°) than UTA-AASO-100 and the opening for the neural canal is quite small (Fig. 5.11). The remaining caudals are from the middle to distal series; the middle caudals are incomplete, all have heart-shaped centra and lack neural spines and zygapophyses. The distal most caudals have more elongate centra in lateral view.

Ossified tendons- Ossified tendons were recovered, they were found isolated away from the caudal vertebrae. None were recovered on or associated with the caudal series. They are thin, cylindrical elements, pencil like in appearance. They are thicker along the cranial surface and thin caudally.

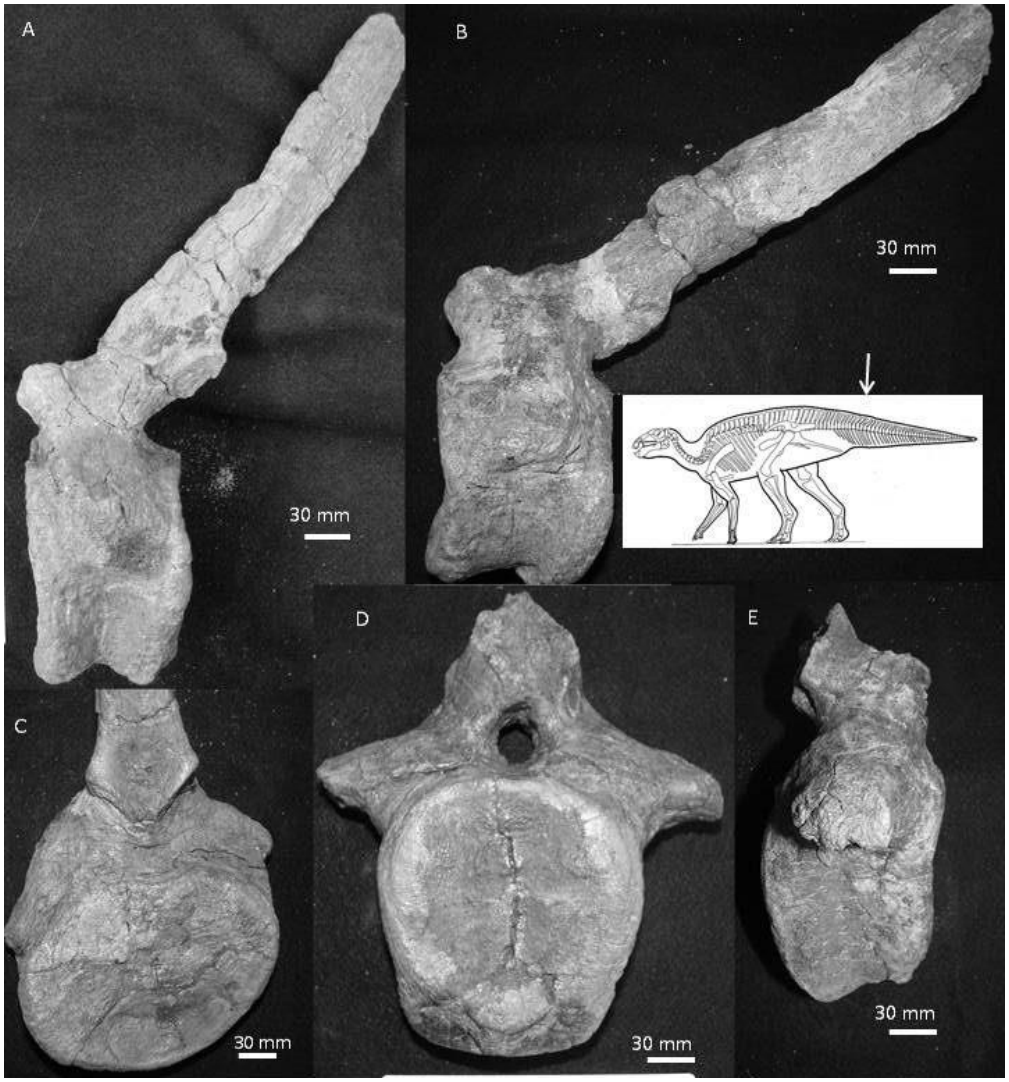

Figure 5.11 Caudal vertebrae. A. Caudal vertebra UTA-AASO-100 in lateral view. B. Caudal vertebra UTA-AASO-098 in left lateral view. C. UTA-AASO-100 in posterior view. D. UTA-AASO-107 in anterior view, note hadrosauroid heart shaped centrum. E. UTA-AASO-107 in right lateral view.

Scapula – UTA-AASO-008 is a broad, robust scapula, 356 mm in length from the ventral margin to the mid-shaft. The blade of the specimen was damaged during excavation, and the complete length is indeterminable (Fig. 5.12). The

partial blade is straight in lateral aspect with a mild medial curvature to accommodate the rib cage. It is thick and rounded (ovoid) proximally and thins distally. It is unfortunate that the distal blade is incomplete, as hadrosaurs typically have a rectangular blade, whereas the blade of iguanodontians diverges posteriorly along the dorsal and ventral margins, a character worthy of note (Brett-Surman and Wagner, 2007). The cranial edge of the blade rises gently into the pseudoacromial process (Fig. 5.12). The latter is a convex, rounded ridge that thins cranially and folds dorsoventrally toward the coracoid suture, similar to that of *Eolambia*, and is a character typically associated with hadrosaurs. However, the pseudoacromial process is rather broad and not as angular as compared to *Eolambia* (Kirkland, 1998; and McDonald et al., 2012). The pseudoacromial process curves ventrally into the coracoid suture.

The coracoid suture is convex and bifacetted into two thick, prominent surfaces in transverse view, similar to *Camptosaurus* and *Mantellisaurus* (Carpenter and Wilson, 2008; and Paul, 2007). The coracoid suture is thick (94 mm), then thins and curves into the scapular part of the glenoid. In transverse view, the cranial margin is distinctly asymmetric, with a shallow medial concavity (Fig. 5.12). The proximal blade expands ventrally to produce a deep, pronounced contribution to the glenoid, which is a robust (60 mm wide x 150 mm long), thick crescentic depression that terminates in a broad buttress that projects laterally from the body. It is similar in form to the iguanodontians *Camptosaurus* and

Iguanodon (Carpenter and Wilson, 2008; and Norman, 2004). The scapula labrum is rather broad, extending ventrally away from the shaft at a steep, near right angle. The steep angle of ascent of the scapula labrum away from the shaft is similar in form to *Eolambia* (Kirkland, 1998; and McDonald et al., 2012).

The extensive glenoid-buttress form and broad cranial margin is typically seen in non-hadrosaurid iguanodontians rather than hadrosaurids. The glenoid and coracoid suture are approximately equal in size. However, the division of the coracoid suture and glenoid along the midline at the coracoid fossa is worth noting. This division creates a near bilaterally symmetric fan shape similar to *Camptosaurus* and *Iguandon*. Morphologically, the scapula is distinctly iguanodontian, similar in form to *Camptosaurus*, *Iguanodon* and *Eolambia* (Carpenter and Wilson, 2008; Kirkland, 1998; and McDonald et al., 2012; and Norman, 1980 and 2004).

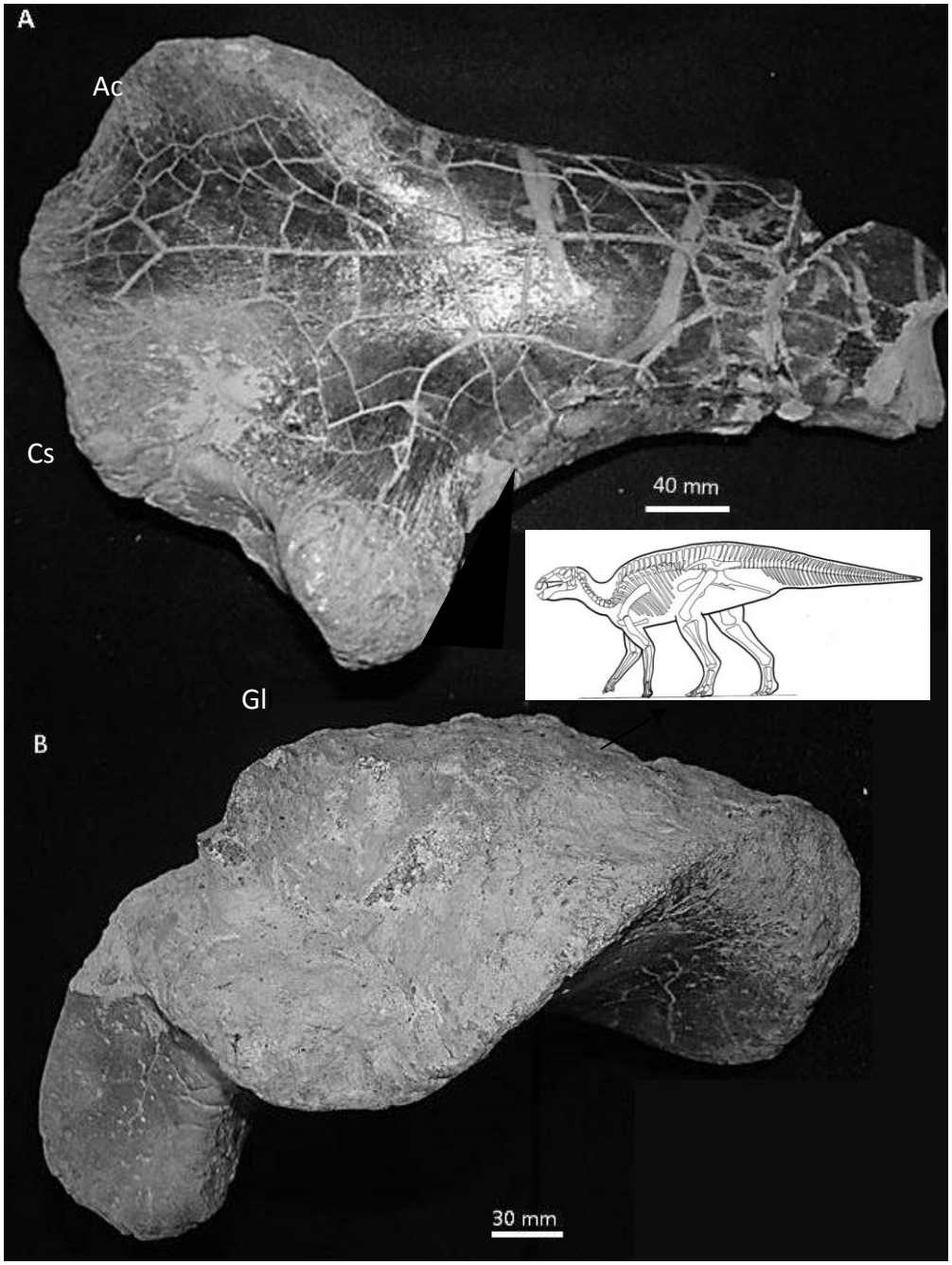

Figure 5.12 Scapula. A. UTA-AASO-008 in lateral view with prominent glenoid buttress (Gl), expanded cranial margin and coracoid suture (Cs) and broad acromion ridge (Ac)(dino-art T. Ford). B. UTA-AASO-008 in cranial view.

Coracoid – UTA-AASO-009 is a complete left coracoid, it is subtriangular in planar view, and convexoconcave in lateral view with a small (36 mm) coracoid foramen at the junction of the glenoid and the sternal suture (Fig. 5.13). The coracoid foramen is ovoid, piercing the coracoid as a ventrolateral opening located 36 mm dorsocranially to the glenoid. The coracoid is 200 mm long from the distal to proximal end, with minor weathering distally. The glenoid suture faces caudoventrolaterally, it is a large (74 mm x 48 mm) concave, ovoid depression that serves as an articular facet for the proximal humerus. It is nearly twice the thickness as that of the dorsal most surface. The scapular suture is a thin, elongate surface that thins proximally and thickens distally, terminating at the sternal suture. The sternal suture is a broad and rugose at the glenoid contact, and tapers cranially into a subtriangular form, as viewed ventrally. The coracoid body thickens proximally from the glenoid and the scapular suture (60 mm) to a thin ridge along the dorsal most surface (8 mm). It has a concave curve medially, that produces a twisted tear drop shape in lateral view. It is thickest along the ventral surface at the glenoid, thin and blade-like at the pseudoacromial ridge. The coracoidal ridge is gently deflected, curving in towards the sternum, and lacks the large hook-like process typical of hadrosaurs (Brett-Surman and Wagner, 2007).

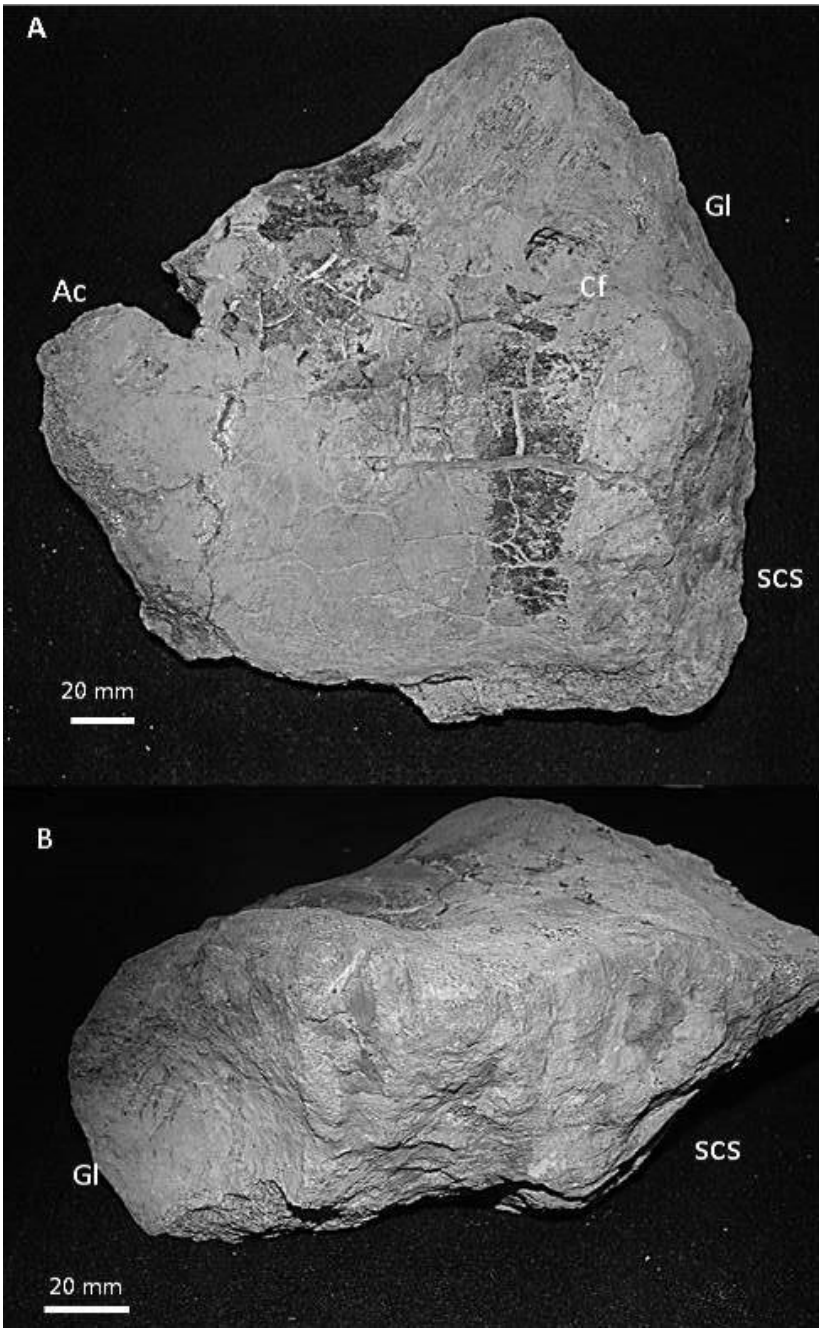

Figure 5.13 A. UTA-AASO-009 is a complete left coracoid in lateral view; glenoid (Gl), coracoid foramen (Cf), scapular suture (SCS). B. UTA-AASO-009, view of the broad glenoid and scapular suture.

Humerus – The humerus is represented by two elements from juvenile individuals; UTA-AASO-149 and UTA-AASO-137 (Fig. 5.14). UTA-AASO-149 is represented by a somewhat gracile, complete juvenile specimen (Fig. 5.14). It is 122 mm long, broader proximally and thins distally, with a mid-shaft width of 26 mm (Fig. 5.14). The articular head and lateral tuberosity are flattened, with a caudally sloping medial tuberosity that descends at a gentle 15° angle and terminates as a subrounded process (Fig. 5.14). The humerus has a reduced deltopectoral crest that is not as pronounced as that of Late Cretaceous hadrosauroids (Fig. 5.14). The reduced deltopectoral crest could be an ontogenetic feature, as this is a juvenile specimen. Thus, the deltopectoral crest could be more pronounced in adults. However, the deltopectoral crest is a reduced, subrectangular feature similar in form to *Camptosaurus, Eolambia* and *Telmatosaurus*, although lacking the medial fold seen in *Camptosaurus* (Carpenter and Wilson, 2008; McDonald el al., 2012 and Weishampel et al., 1993). The humeral shaft is relatively narrow and straight,.then terminates with a gently subrounded radial and ulnare condyles (Fig. 5.14). For a list of complete measurements see Table 5.1.

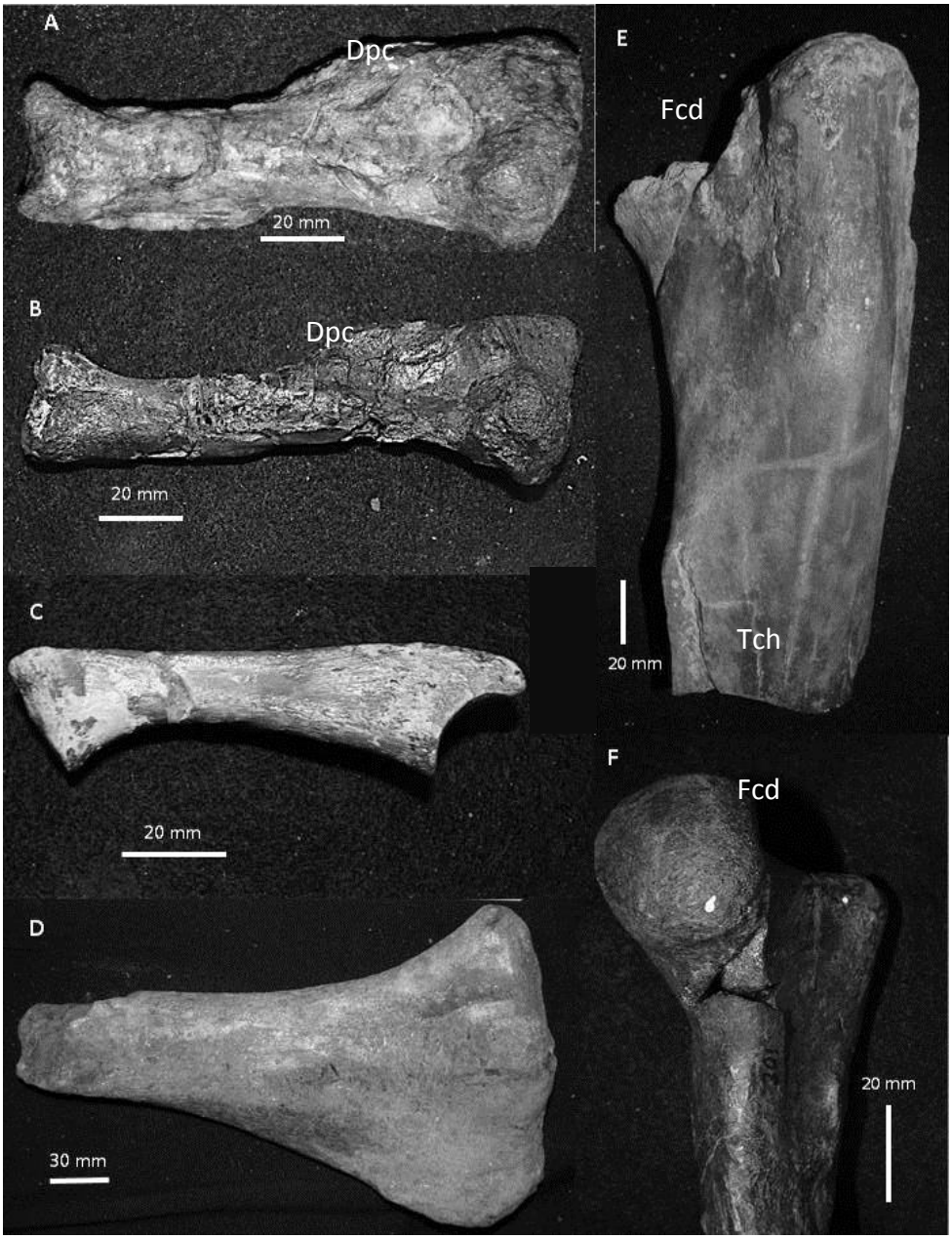

Figure 5.14 Limb elements. A. UTA-AASO-149 a juvenile humerus in lateral view, deltopectoral crest denoted as (Dpc). B. UTA-AASO-137 a juvenile humerus in lateral view. C. UTA-AASO-158 a juvenile ulna. D. UTA-AAS-162 a partial tibia. E. UTA-AASO-125 a partial adult femur in lateral view (trochanter: Tch). F. UTA-AASO-201 a partial proximal juvenile femur in oblique, condyle denoted (Fcd).

Ilium – UTA-AASO-012 is represented by a left well preserved, broad and robust element that has a vertical height of 212 mm and a length of 604 mm from the pre to post acetabular process (Fig 5.15). The preacetabular process is incomplete and thus relatively short (~160 mm). It is stout and rounded dorsally with a thinned cranioventral margin giving the process a nearly triangular appearance in cross section (Fig. 5.15). It is gently deflected ventrolaterally, similar to *Eolambia*, *Bactrosaurus* and *Camptosaurus*, but not as extensive as *Bactrosaurus* (Godefroit et al., 1998; Kirkland, 1998; McDonald et al., 2012; and Carpenter and Wilson, 2008). The ventral deflection of the preacetabular process is typical of derived iguanodontians (Norman, 2004). The cranial margin of the preacetabular process is incomplete, damaged during excavation. The preacetabular notch is open (Fig. 5.15).

The pubic peduncle is short (3.6 cm), subrounded with a slight inclination cranially (Fig. 5.15). It is similar to *Bactrosaurus, Probactrosaurus,* and *Eolambia,* although much more reduced in size (Godefroit et al., 1998; Kirkland, 1998, McDonald et al, 2012; and Norman, 2002) (Fig. 5.15). Lull and Wright (1942) and Maryanska and Osmolska (1984), have noted that the light, reduced form of the pubic peduncle as a character associated with hadrosaurs. Maryanska and Osmolska (1984) specifically noted this character in their detailed study of the post crania of the hadrosaurine *Saurolophus angustirosbris.* The presence of a reduced pubic peduncle is considered an interesting character, as the ilium

principally demonstrates an overall iguanodontian form. The ischial peduncle is 176 mm in length, broad and rectangular (Fig 5.15). The broadness of the ischial peduncle is typically associated with lambeosaurines, including *Eolambia* (Brett-Surman and Wagner, 2007; Kirkland, 1998; and Mcdonald et al., 2012). The acetabular margin is 93 mm in length and relatively shallow.

The supracetabular crest, or "antitrochanter", is 220 mm in length, broad and rises above the preacetabular process at a near perpendicular angle (Fig. 5.15). It thickens dorsally, with a thick (20 mm) curved ridge that deflects caudoventrally, it thickens (4 cm) medially, appearing triangular in caudolateral view and roughly reniform in dorsal view. A triangular suprailiac crest is distinctive of early hadrosaurids (Brett-Surman and Wagner, 2007). The suprailiac crest thins (~10 mm) and curves gently into the supracetabular process caudally (Fig. 5.15). The dorsal surface is relatively flat, similar to *Zalmoxes*, *Eolambia* and *Probactrosaurus,* yet has a unique cranial dorsal deflection that forms a near perpendicular rise from the preacetabular process in lateral view (Kirkland, 1998; McDonald et al., 2012; Norman, 2002; Weishampel et al., 2003) (Fig. 5.15). *Mantellisaurus* and *Eolambia* have a similar dorsal deflection, although it is a much gentler rise and more caudal (Kirkland, 1998; McDonald et al., 2012; and Paul, 2007). Thus, the dorsal deflection of the cranial supracetabular process is a character that is unique to this taxon (*Protohadros sp.?*).

In dorsal view, the supracetabular crest is deflected laterally over the ischial peduncle by 6 cm, similar to *Mantellisaurus* and *Probactrosaurus* (Fig. 5.15). The postacetabular process is 75 mm wide cranially at the supracetabular process and thins to 44 mm to a subrounded caudal margin (Fig. 5.15). It has a slight ventral deflection and is more pronounced than that of *Cedrorestes, Mantellisaurus* or *Probactrosaurus,* but not as elongate as *Bactrosaurus* (Gilpin et al., 2007; Godefroit et al., 1998; and Paul, 2007). It is broad, and roughly triangular in lateral view, as is typical of derived iguanodontians (Norman, 2004). The lateral surface of the ilium is concave, with the deepest portion overlying the ischial peduncle (Fig. 5.15).

The AAS ilium is morphologically similar to *Bactrosaurus, Probactrosaurus, Cedrorestes* and *Eolambia* (Gilpin et al., 2007; Godefroit et al., 1998; Kirkland, 1998; McDonald et al., 2012; and Norman, 2002). The postacetabular process is elongate, triangular in lateral view, rounded in caudal view, then tapers caudoventrally. It is less elongate than what is typically seen in hadrosaurids. It is similar in form to *Eolambia, Probactrosaurus* and *Camptosaurus,* although more elongate than *Probactrosaurus,* and *Camptosaurus* (Carpenter and Wilson, 2008; Kirkland, 1998; McDonald et al., 2012; and Norman, 1986). The postacetabular process is distinctly triangular in lateral view, similar to *Camptosaurus*, *Cedrorestes, Eolambia* and *Mantellisaurus* (Carpenter and Wilson, 2008; Kirkland, 1998; Gilpin et al., 2007; McDonald et al., 2012; and

Paul, 2007). Although the preacetabular process is incomplete, it does not show the ventral deflection seen in *Bactrosaurus* and Late Cretaceous hadrosaurids such as *Gryposaurus* (Godefroit, et al., 1998; and Horner et al., 2004). The preacetabular process is commensurate with *Camptosaurus*, *Eolambia* and *Mantellisaurus* (Carpenter and Wilson, 2008; Kirkland, 1998; McDonald et al., 2012; and Paul, 2007). Overall, the horizontal preacetabular process, the broad, flattened supracetabular process and triangular postacetabular process places the AAS ilium morphologically within Iguanodontia and basal hadrosaurids. It is similar in form to *Bactrosaurus* and *Probactrosaurus*, with affinities to *Eolambia* and *Mantellisaurus* (Godefroit et al., 1998; McDonald et al., 2012; Norman 2002 and Paul, 2007). The ilium fits well into the first iliac morphotype recognized by Chapman and Brett-Surman (1990).

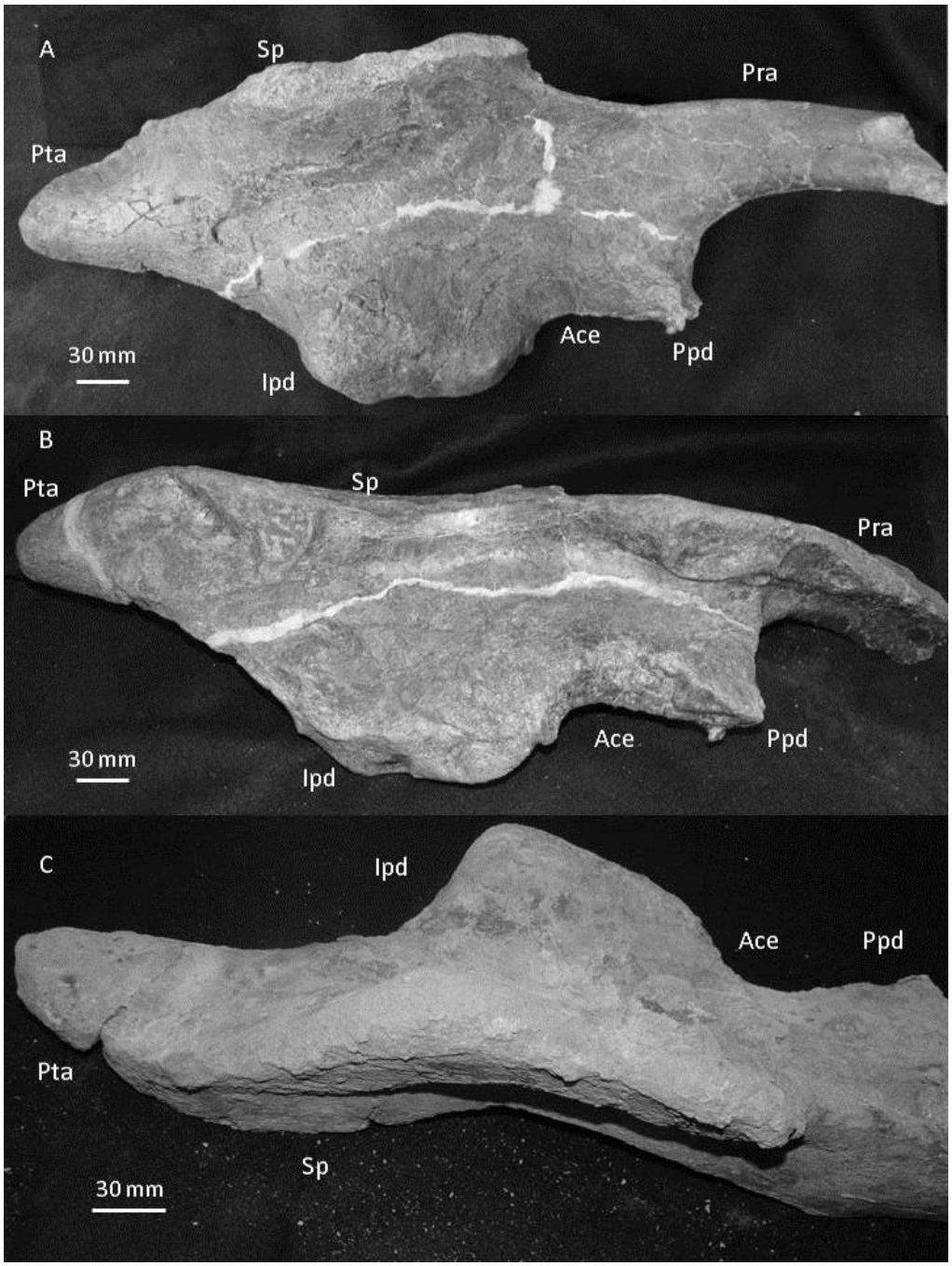

Figure 5.15 A. UTA-AASO-012 a left ilium in lateral view, key processes labeled: Preacetabular process (Pra), Suprailiac crest (Sp), Postacetabular process (Pta), Ischial peduncle (Ipd), Acetabulum (Ace), and Pubic peduncle (Ppd). B. UTA-AASO-012 in sacral view. C. UTA-AASO-012 in dorsal view.

Ischium – UTA-AASO-012 is a complete ischium, demonstrating the typical triradiate ornithopod form, although it shows multiple fractures along the shaft (Fig. 5.16). The ischium is 720 mm long and ranges in width from 76 mm to 52 mm from the obturator process to the caudoventral margin of the element. The width of the ischium is 256 mm from the pubic peduncle to the iliac peduncle with a 128 mm opening for the acetabulum. The acetabulum is denoted by a gentle sloping, shallow concavity. The pubic peduncle is smaller than the iliac peduncle, similar to the ratios seen in *Bactrosaurus* and *Eolambia* (Godefroit et al., 1998; Kirkland, 1998 and McDonald et al., 2012). The iliac peduncle is broad (98 mm cranial width), rising above the shaft at nearly 90 degrees (Fig. 5.16). It is a flattened and thick (40 mm) subrectangular process. The pubic peduncle is small (50 mm cranial width), thin and rectangular, similar to *Probactrosaurus* and *Eolambia* (Kirkland, 1998; McDonald et al., 2012 and Norman, 2002). On the caudoventral part of the proximal blade, the obturator process is subrounded and small (16 mm), with a shallow obturator foramen. The obturator process is proximally placed, a character typical of iguanodontians. Although, the obturator is a small process, and not as pronounced as that of *Mantellisaurus* and *Bactrosaurus*, but rather reduced as seen in *Eolambia* (Godefroit et al., 1998; Kirkland, 1998; McDonald et al., 2012; and Paul, 2007). A ridge extends dorsolaterally away from the obturator process down the length of the shaft, flattening distally. This tapering ridge is similar to the ischial ridge noted in

Probactrosaurus, although more sublime (Norman, 2002). The shaft is columnar, and elongate, thickening distally with a gentle bowed distal curve (of which the ridge follows) (Fig. 5.16). The distal end of the shaft terminates in an ischial knob or boot, an iguanodontian character (Norman, 2004). The ischium fits within the Type 1 *Gilmoreosaurus* classification used by Brett–Surman and Wagner (2007).

Pubis – UTA-AASO-010 is a prepubis is 420 mm long and primarily represented by a left prepubic process, as the pubis is shattered along the caudal shaft and acetabular margin (Fig. 5.16). The prepubic process is shallowly concave along the ventral margin and relatively flat along the dorsal margin. The ventral margin is fractured and broken along the midline caudally. The prepubic process is 180 mm in vertical height, twice that of the minimum constriction of the neck. It is dorsoventrally wide, laterally compressed and thins cranially with an axe-like cranial margin that thins dorsally into a blade like process, similar to *Eolambia* (Kirkland, 1998; and McDonald et al., 2012). As it is thin, the margins of the prepubic process are not completely preserved. However, it is clear that it does not have parallel dorsal and ventral margins that mirror one another. Rather, they angle outwards and expand into an axe like blade, similar in form to *Eolambia* (Kirkland, 1998; and McDonald et al., 2012). This relatively equal distal expansion of the prepubic process into a blade like process is a synapomorphy of iguanodontians (Norman, 2004). Caudally, the ventral margin of the prepubic process thickens towards the shaft with a mild sinuosity.

The prepubic neck is relatively long, 12 cm and thin, similar in form to *Eolambia* and *Tethyshadros* (Dalla Vecchia, 2009; Kirkland, 1998 and McDonald et al., 2012). The dorsal margin of the neck is thick and rounded, whereas the ventral margin is thin and terminates into a distinct longitudinal line. The middle shaft of the prepubic process narrows dorsoventrally (90 mm height), then thickens laterally caudally, into the peduncles. The ischial peduncle is broken and partially missing (Fig. 5.16). The iliac peduncle is a short, subrounded triangular boss, beneath which lies the oblique curve of the acetabular margin. The acetabular margin is broken with approximately 20% missing directly above the ischial peduncle (Fig. 5.16). The pubis proper bows ventrally with much of the pubic bar broken and missing. The AAS prepubic process is morphologically similar to *Tethyshadros* and *Eolambia* (Dalla Vecchia, 2009; Kirkland, 1998 and McDonald et al., 2012).

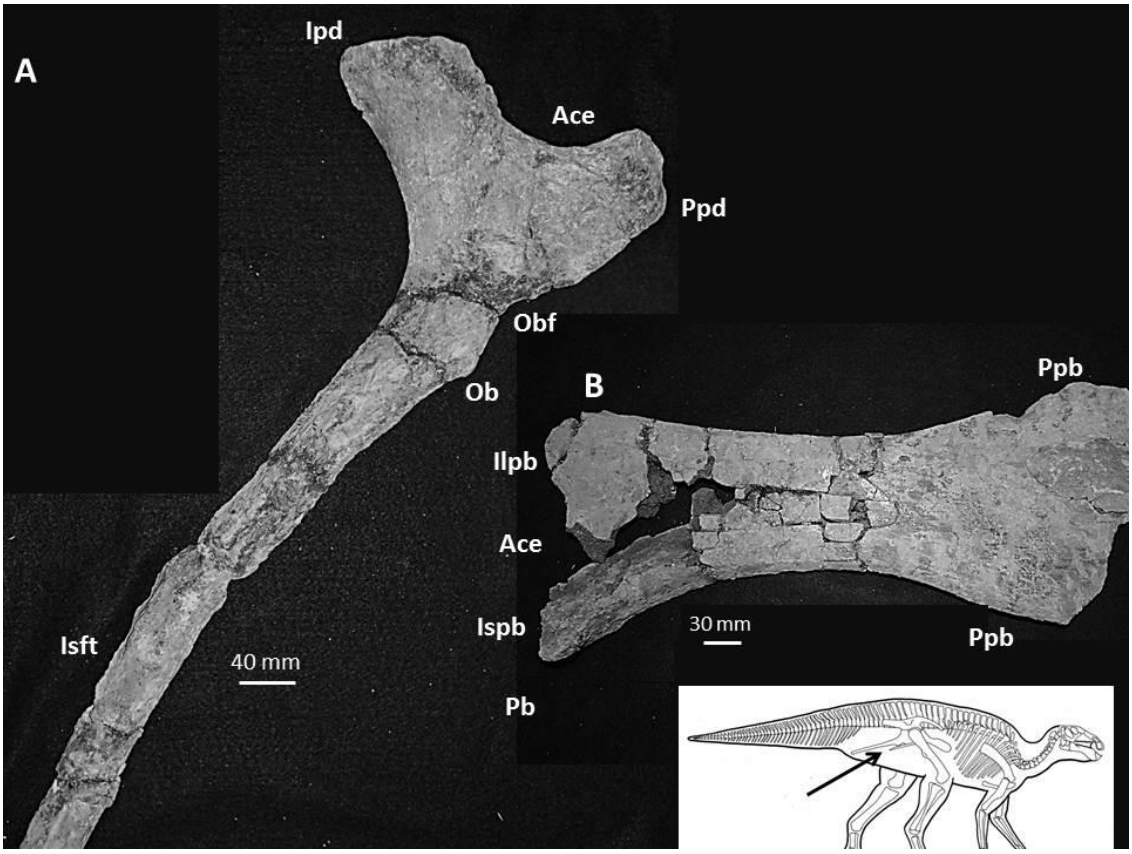

Figure 5.16 Pelvic elements. A. UTA-AASO-011 a left ischium; Ischial peduncle (Ipd), Acetabulum (Ace), Pubic peduncle (Ppd), Obturator foramen (Obf), Obturator process (Ob), Ischial shaft (Isft). B. UTA-AASO-010 a left prepubis; Iliac peduncle (Ilpb), Acetabulum (Ace), Ischial peduncle (Ispb), Pubic bar (Pb), Prepubic blade (Ppb). Pelvic elements denotes with arrow on diagram (dinosaur skeletal diagram courtesy T. Ford).

Femur-UTA-AASO-125 is a partial proximal adult femur that is broken along the upper shaft (~1/3) and preserves the greater and cranial trochanter, the fourth trochanter and a partial femoral head (Fig. 5.14). The femur is gently bowed laterally, with the head leaning toward the body at a slight angle (~15°)

(Fig. 5.14). The partial element is 260 mm long and 110 mm wide proximally with a broad subrounded head (Fig. 5.14). The femoral head is missing, with only a fragmentary partial base with exposed trabeculae. The femoral head is preserved in a separate element, from a juvenile individual; specimen UTA-AASO-201 (Fig. 5.14). The greater trochanter is pronounced in UTA-AASO-125; it is a subrounded element similar in form to *Telmatosaurus*, although not as angular in lateral view (Weishampel et al., 1993). The greater and cranial trochanters are separated by a 62 mm vertical cleft. The cranial trochanter is a weathered and small, with no signs of grooves for insertion of *m. iliofemoralis*. The fourth trochanter is a small, poorly developed caudomedial feature of the shaft that is situated 120 mm below the femoral head (Fig. 5.14). It is not as pronounced a feature as seen in *Telmatosaurus* and *Bactrosaurus* and Late Cretaceous hadrosaurids (Godefroit et al., 1998 and Weishampel et al., 1993). The fourth trochanter does not extend prominently away from the shaft, but rather gently rises over the surface as a triangular lateral protrusion (Carpenter and Wilson, 2008; and Godefroit et al., 1998) (Fig. 5.14). The femoral shaft is broken just beneath the fourth trochanter. Of interesting note, this element preserves evidence of predatory behavior via two pit marks along the proximal shaft. A prominent bite (pit) mark is present on the shaft, 102 mm below the greater trochanter, and another on the opposite side of the shaft below the cranial trochanter. The pit

marks are round impressions in the bone surface attributed to the feeding behavior of a large crocodyliform, discussed in detail in Noto et al. (2012).

UTA-AASO-201 is a partial juvenile femur with a well preserved femoral head and greater trochanter (Fig. 5.14). Unlike element UTA-AASO-125, juvenile specimen 201 has a well preserved femoral head. It is a large, pronounced bulbous feature in lateral view and crescentric in dorsal view (Fig. 5.14). The degree of roundness is a feature generally lacking in adult hadrosauroids, and may be a feature of ontogeny (Horner et al., 2004). The femoral head sits on a stout neck and is set at a sharp angle along a slightly bowed neck. The cranial features of the femur are similar in form to *Eolambia* and *Telmatosaurus,* and other basal hadrosaurids (McDonald et al., 2012; Weishampel et al., 1993).

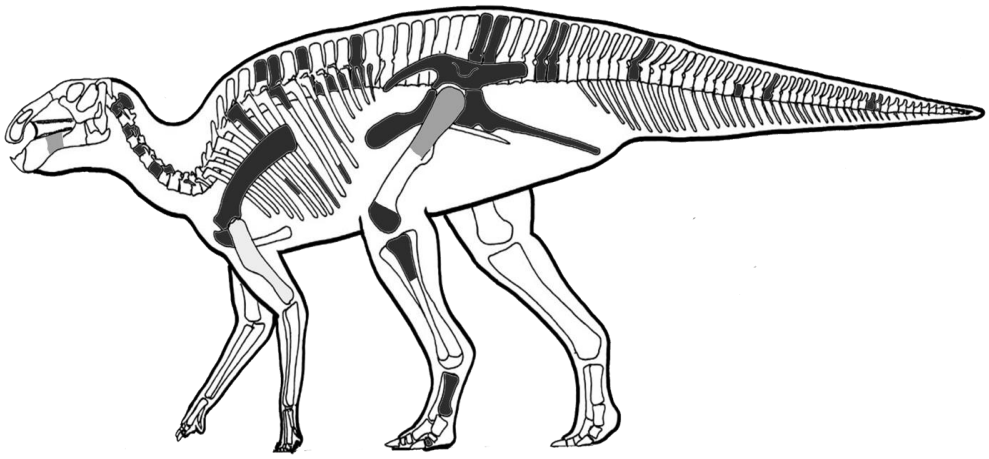

Figure 5.17 Generalized skeletal reconstruction, recovered fossils are shaded. Darker bones are from an adult individual, the more lightly shaded bones are from sub adult individuals (artwork courtesy Tracy Ford).

Table 5.1 Measurements (axial lengths) in millimeters of elements recovered from the Arlington Archosaur Site.

Element	AAS Number	Length	Width (Height)
dentary	UTA-AASO-161	220 mm	58 mm
tooth	UTA-AASO-002	28 mm	14 mm
axis	UTA-AASO-090	120 mm	96 mm
cervical	UTA-AASO-091	140 mm	92 mm
cervical	UTA-AASO-095	111 mm	60 mm
dorsal	UTA-AASO-103	88 mm	84 mm
dorsal	UTA-AASO-104	124 mm	111 mm
caudal	UTA-AASO-100	140mm	102 mm
caudal	UTA-AASO-098	138 mm	140 mm
caudal	UTA-AASO-107	108 mm	136 mm
scapula	UTA-AASO-008	356 mm	300 mm
coracoid	UTA-AASO-009	200 mm	185 mm
prepubis	UTA-AASO-010	420 mm	90 mm
ilium	UTA-AASO-012	604 mm	212 mm
ischium	UTA-AASO-011	720 mm	256 mm
humerus	UTA-AASO-149	121 mm	26 mm
femur	UTA-AASO-125	260 mm	110 mm

5.5 Discussion

Paleoecologically, hadrosauroids were a diverse group of dinosaurs that occupied a wide range of ecological niches from the Early to Late Cretaceous. Their remains have been found in different biotopes which include; marine basins, terrestrial foredeeps, and intermontanes (Weishampel and Horner, 1990; Horner et al., 2004). Hadrosauroid skeletal material has been recovered from coastal plain deposits, lower coastal plain channels, overbank and deltaic paleoenvironments (Norman, 2004; and Weishampel and Horner, 1990). It has been suggested that some Campanian hadrosaurids had specific ecological preferences. The presumed ecological preferences are based upon morphological adaptations found in specimens recovered from specific paleoenvironments. The hadrosaurines *Kritosaurus* and *Brachylophosaurus* have transversely extended snouts and arched facial regions (Weishampel and Horner, 1990; Horner et al., 2004). As these taxa are found exclusively in deltaic or near marine deposits, it is presumed that the extended snouts were an adaptation for deltaic environments (Weishampel and Horner, 1990). Head (1998) described the deflected snout of *Protohadros* and cited it as an adaptation for living in delta environments. With the discovery of a basal hadrosarauroid at the AAS in a delta plain environment, living within a coastal setting similar to that reported for *Protohadros*, Head's

(1998) interpretation of *Protohadros byrdi* may also be applied to the AAS hadrosauroid.

Head (1998) named *Protohadros byrdi* based on a nearly complete skull and minor, incomplete post crania. This analysis describes the post cranial anatomy of a basal Woodbine hadrosauroid, possibly attributable to *Protohadros,* and further explores the primitive nature of the Woodbine hadrosauroid fauna. As the AAS hadrosauroid is based primarily upon post cranial elements and *Protohadros byrdi* is based upon crania, it is difficult to verify the relationships. However, it should be mentioned that the juvenile dentary recovered from the AAS has substantial characters in common with the dentary from the *Protohadros* type specimen. Variance in character data between the two is likely due to ontogeny. As the AAS is an ongoing excavation, future recovered cranial material could further clarify the nature of the AAS hadrosauroid, as well as the diversity of the Woodbine hadrosauroid fauna. Until that time, the the author proposes that the two be treated as synonymous taxa for the sake of further analysis. However, for the sake of distinguishing the AAS specimen from the SMU type specimen, the author suggests using the common name "Olivia" for the AAS *Protohadros*. The name "Olivia" is in honor of the daughter of one of the AAS discoverers, Art Sahlstein.

Head (1998) used the primitive cranial characters of the skull to place *Protohadros byrdi* within a basal position of Hadrosauridae as a predecessor to the primitive *Gilmoreosaurus* and *Telmatosaurus* at the base of the hadrosaurid evolutionary tree. Prior to that, Weishampel et al. (1993) considered the European hadrosaur *Telmatosaurus* as the most basal hadrosaur, based upon its primitive cranial characters, principally a dorsoventrally expanded jugal and accessory ridges on the dentary teeth. Weishampel el al. (1993) used *Telmatosaurus* to establish a Eurasian origins model for the hadrosaurids. Before Weishampel et al. (1993) worked with *Telmatosaurus*, the Asian hadrosaur *Gilmoreosaurus* from the Iren Dabasu Formation was considered the basal hadrosaurid, due to its primitive cranial characters, principally the presence of symmetrical dentary teeth and its early Tuonian age (Head, 1998; Horner et al., 2004; Gilmore, 1933a).

The primitive nature of the AAS hadrosauroid (*Protohadros sp?*) and *Protohadros byrdi*, implies ecological isolation, or endemism. The Woodbine coastal plain ecological community could represent yet another instance of endemically influenced evolution, similar to what has previously been reported for the Late Cretaceous hadrosaurs *Tethyshadros* and *Telmatosaurus* (Dalla Vechia, 2009; Weishampel et al., 1993; and Weishampel and Jianu, 2011). As *Tethyshadros* and *Telmatosaurus* were isolated in Europe by the Alpine Tethys,

the AAS hadrosauroid was likely isolated in southwestern Appalachia by geographic barriers presented by the Rudradian peninsula.

The AAS hadrosauroid, or its predecessors, could have migrated from a point in Eurasia in the Early Cretaceous via the Beringian land bridge (Fig. 5.18). An Asian progenitor fauna could have migrated across Beringia in the Early Cretaceous and seeded North America with a new hadrosauroid fauna as is represented by the derived iguanodontians of the Cedar Moutnain Formation (McDonald et al., 2012). Hadrosauroids of the upper part of the Cedar Mountain Formation (*Eolambia*) could have easily migrated from Laramidia to Appalachia during the late Early Cretaceous lowstand of the Albian (Kirkland et al., 1996). This Asian origins model is similar to the biogeographic model propoposed by Brett-Surman (1979) and Weishampel and Weishampel (1983). Once established in southern North America, this taxon could have become isolated by mid-Cretaceous eustatic fluctuations (eustatic high stand) and continued Atlantic rifting that created barriers to migration to either western North America or a return to Eurasia. The paleogeography of the Cretaceous changed significantly from the Early Cretaceous to the middle Cretaceous, as the Barentsian land bridge and North Atlantic Corridor closed by the Aptian and the interior seaway divided North America into Laramidia and Appalachia by the Cenomanian (Fig. 5.18). Other components of the Woodbine fauna currently under study support this model for an endemic, primitive fauna.

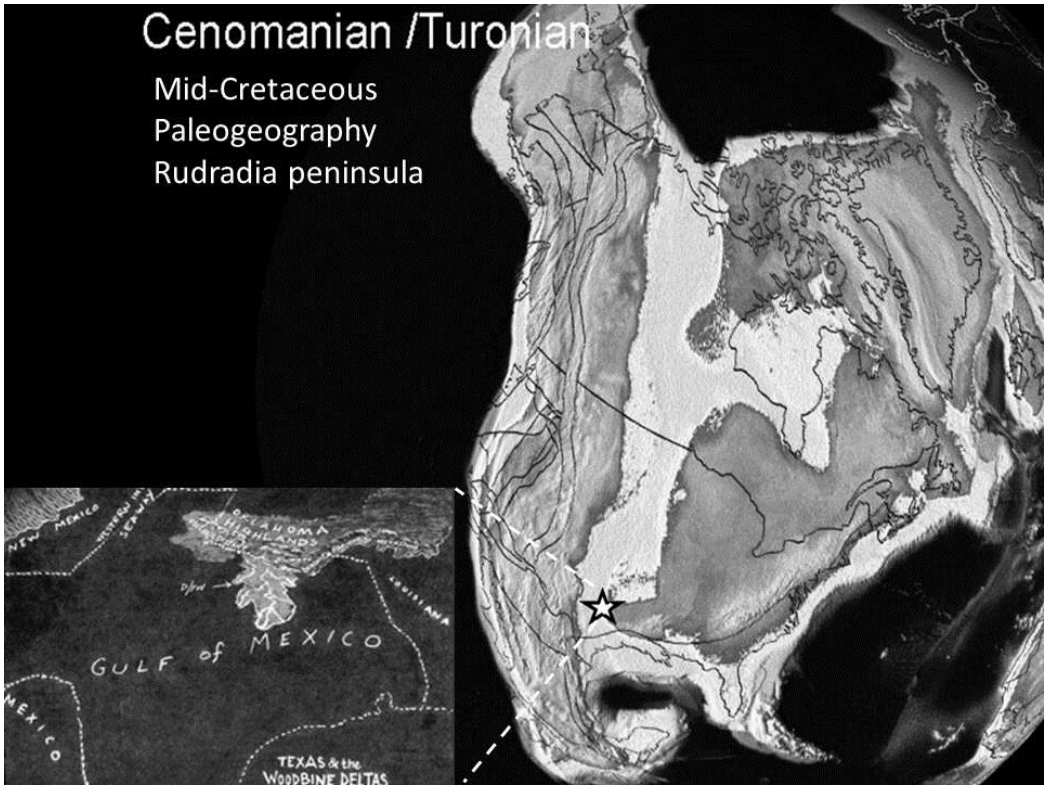

Figure 5.18 AAS location denoted with star on the southeastern coast of the Interior Seaway on the Rudradian peninsula. Woodbine fauna separated from the Upper Cedar Mountain fauna by the interior seaway. The Beringian land bridge was well established to the north, connecting North America to Asia. Cretaceous (Cenomanian) North American paleogeographic map by Scotese (2005).

5.6 Paleobiogeography and Paleoecology

Weishampel and Weishampel (1983) proposed an Asiatic origins for hadrosaurids based upon the Iran Dabasu faunas, with a later dispersal to North America. Head (1998) used the discovery of *Protohadros* to propose North

American origins for Harosauridae in the Cenomanian. Utilizing dispersal – vicariance analysis, Preito Marquez (2010) proposed multiple biogeographic events for the dispersal of Hadrosauridae, with North American origins dating back to the Santonian. Weishampel and Jianu (2011) tentatively suggest Europe sometime prior to the Cenomanian.

The primitive characters retained within the post crania of the AAS hadrosauroid suggest a biogeographically isolated Woodbine fauna. Weishampel et al. (1993) noted the isolated nature of *Telmatosaurus* in Europe and related the primitive characters to its endemism via isolation caused by the Alpine Tethys, although Weishampel and Jianu (2011) did not relate these characters to exclusively to endemism. Dalla Vecchia (2009) discussed the primitive characters retained within the hadrosauroid *Tethyshadros* from an isolated carbonate platform within the Tethys Ocean. A relative lack of change is noted in the AAS hadrosauroid and other AAS specimens hints at biogeographic isolation or endemism. For example, the primitive tooth plate morphology of the Woodbine lungfish *C. carteri* is reminiscent of earlier North American ceradontids such as *C. guentheri* (Main et al, 2012). Lungfish are typically conservative vertebrates; but the lack of change in the Texas specimens may suggest a relict form. Other components of the AAS fauna demonstrate signs of endemism, as the theropods recovered from the site include cf. *Acrocanthosaurus*, typically an Early Cretaceous carnosaur (Noto and Main, in review). The Woodbine theropod

suggests that this group endured as a part of southwestern Appalachian faunas well into the Cenomanian.

The mid-Cretaceous Texas fauna was ecologically similar to Early Cretaceous Laurasian ecosystems. The Woodbine fauna lends support to the biogeographic model proposed by Brett Surman (1979) and Weishampel and Weishampel (1983), where the interchange of faunas between Laurasia and North America occurred at some point in the Early Cretaceous, likely in the late Albian or early Cenomanian after the Beringian land bridge formed. The proposed timing of these dispersal events is supported by the paleogeography, specifically availability of the Beringian land bridge (Fig. 5.18). The Early to middle Cretaceous eustatic fluctuations could have then isolated the AAS faunas between the southeastern coast of the epicontinental seaway and the Ouachita Mts. The regional paleogeography of the Rudradian peninsula produced an endemic relict fauna at the AAS. The characters noted in the Cenomanian Woodbine hadrosauroid fauna, *Protohadros byrdi* and the AAS hadrosauroid (*Protohadros sp*.) supports a scenario of paleogiogeographic endemism and ecological isolation.

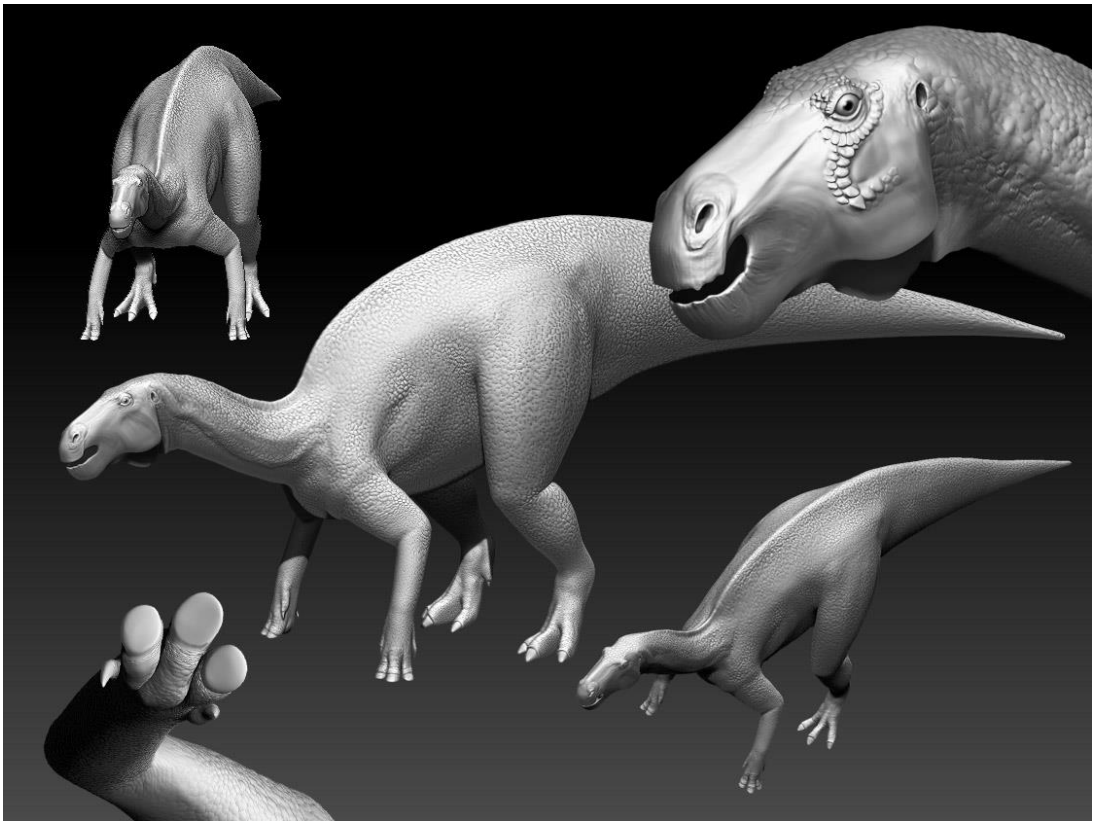

Figure 5.19 AAS hadrosauroid (*Protohadros*) digital reconstructions courtesy of medical illustrator David Killpack.

5.7 Acknowledgments

I thank the Huffines family, Robert Kimball at the Viridian Properties and HC LOBF of Arlington for granting land access to conduct work at the Arlington Archosaur Site. I thank my colleagues on this project; Chris Noto, Karen Poole, and David Weishampel. I thank Brad Carter, Phil Kirchhoff, Art Sahlstein and Bill Walker for donating the specimens discussed herein, the Earthwatch Institute, the PaleoMap Project and the Jurassic Foundation for providing research funds,

the Dallas Paleontological Society, the UT-Arlington Graduate School for providing a dissertation fellowship and the Western Interior Paleontological Society for providing scholarships and grants. I thank Arlington Archosaur Site project volunteers; Art Sahlstein, Roger Fry, Albert Miramontes, Darlene Sumerfelt, Angie Osen, Ronnie Colvin, Richard Zack, Phil Scoggins, Nathan Van Vranken, Tim Dalbey, Stewart and Travis Nolan along with members of the Dallas Paleontological Society and UTA Dinosaurs class students for their assistance excavating the Dinosaur Quarry at the AAS. Fabio M. Dalla Vecchia and Jim Kirkland for providing literature references and advice, Andrew McDonald for viewing images of AAS fossils and offering his insight, and for providing data and literature on *Eolambia*, Darren Tanke for reviewing AAS fossils and providing useful comments, Tracy Ford for providing a hadrosauroid dinosaur skeletal diagram and medical illustrator Dave Killpack for providing life like reconstructions of our AAS hadrosauroid, and Louis Jacobs and Dale Winkler at the Shuler Museum of Paleontology at Southern Methodist University for providing access to the *Protohadros* type specimen.

CHAPTER 6

AN ENIGMATIC NEW CROCODYLIFORM FROM THE CRETACEOUS (CENOMANIAN) WOODBINE FORMATION AT THE ARLINGTON ARCHOSAUR SITE, NORTH CENTRAL TEXAS.

"If I had missed that fossil, it would have rested there beneath the hot sun, to be disintegrated, within a week, or perhaps a month or two. At any rate, that skeleton would not have been there the following year. We got to it just at the right time."

Edwin H. Colbert

6.1 Introduction

A new crocodyliform was recovered from a fossil locality within the mid-Cretaceous (Cenomanian) Woodbine Formation of North Central Texas. The Arlington Archosaur Site (AAS) is a productive vertebrate fossil locality within the Woodbine Formation that represents a Cretaceous delta plain ecosystem preserving a diverse coastal fauna including sharks, lungfish, turtles, dinosaurs (ornithopods and theropods), and crocodyliforms. Herein, we report on the discovery of a new large mesoeucrocodylian crocodyliform. The new taxon is based on multiple disarticulated but associated cranial and post cranial elements of both adult and juveniles representing a wide ontogenetic range. As such, it represents an ecomorphotype not previously reported from the Woodbine. Remains consist predominately of a disarticulated partially complete skull and considerable postcranial material from a single large (~6 m) adult individual and additional disarticulated material from a second adult, at least one subadult, and

several juveniles, elucidating a partial growth series. Phylogenetic analysis of the AAS taxon was conducted following Turner and Buckley (2008) and Allen (2010), and recovers the AAS crocodyliform as a sister to Eusuchia and Goniopholididae, united primairly by gross skull shape and squamosals that overhang the temporo-orbital opening. This result is weakly supported as the taxon retains numerous pleisomorphic and homoplastic characters, such as "goniopholidid-style" paravertebral osteoderms and extensive polygonal ventral osteoderms, which make precise phylogenetic placement difficult. The taxon may represent a previously unsampled lineage of mesoeusuchian diversity and help to elucidate relationships among crocodyliforms, particularly the placement of problematic clades such as the goniopholidids.

The crocodyliforms are among the longest lived and only surviving non-avian archosaurs with a fossil record extending from the early Mesozoic, and throughout the Cenozoic (Brochu, 2003; Salisbury, 2006). The term crocodyliform is inclusive of the Triassic protosuchians, the Jurassic and Cretaceous mesoeusuchians ("mesosuchians"), and the Cretaceous and Cenozoic eusuchians (Brochu, 2003). Within the mesoeusuchians lies an enigmatic family of crocodyliforms, the Goniopholidae. Richard Owen, best known for naming the Dinosauria, named the first species of *Goniopholis*, (*G. crassidens*) (Owens, 1841). Owen noted a distinct feature first seen in this specimen; rectangular osteoderms with a well defined processus articularis that extends anteriorly from

the osteoderm at a 90° angle (Owen, 1841). These rectangular osteoderms with their distinct "spikes" were the basis of Owen (1841) choosing a name for the genus. *Goniopholis* literally translates into "angle scale" (Owen, 1841; Salisbury et al., 1999).

The Goniopholididae were later classified by Cope as a distinct group of crocodyliforms (Cope, 1875). Since then, discoveries have revealed a near global biogeographic distribution and a broad biostratigraphic range, from the Late Jurassic to the Mid- Late Cretaceous (Salisbury et al., 1999). The oldest species reported to date is *G. baryglyphaeus* from the Late Jurassic of Portugal (Schwarz, 2002) (Fig. 6.2). In North America, goniopholidids are rare. The oldest goniopholidids recovered from North America are *G. gilmorei* and *G. stovali* from the Late Jurassic and Early Cretaceous deposits of the continental interior. As a group, they tend to be semi-aquatic, similar in life style to modern alligators and typically range in size from 2-4 m long (Salisbury et al., 1999).

Crocodyliforms have been documented within the Woodbine Formation intermittently, with reports of isolated teeth and osteoderms commonly occurring along with other fossils (Adams et al., 2011). Prior to this work, the only confirmed crocodyliform taxa reported in the literature for the Woodbine Formation were *Terminonaris* (Adams et al., 2011) and *Woodbinesuchus* (Lee, 1997). Herein, we report a new taxon of crocodyliform from the Woodbine

Formation, represented by numerous cranial and post–cranial elements recovered from a single locality known as the Arlington Archosaur Site (AAS). The AAS is located in Tarrant County, in the middle of the burgeoning Dallas-Fort Worth metropolitan area, within the city of Arlington just a few kilometers north of the Dallas Cowboy Stadium and Rangers Ballpark (Fig. 6.1). To date, the AAS has produced the fossil remains of a variety of mid-Cretaceous vertebrates that include dinosaur (ornithopod and theropod), and crocodyliforms, cheloniana, amphibians, a mammal, teleosts, chondrichthyans, and a new species of dipnoan (Main et al., 2012). Crocodyliform and chelonian remains are the most common. All of the AAS material was recovered from strata of the Lewisville Member of the Woodbine Formation (Cenomanian).

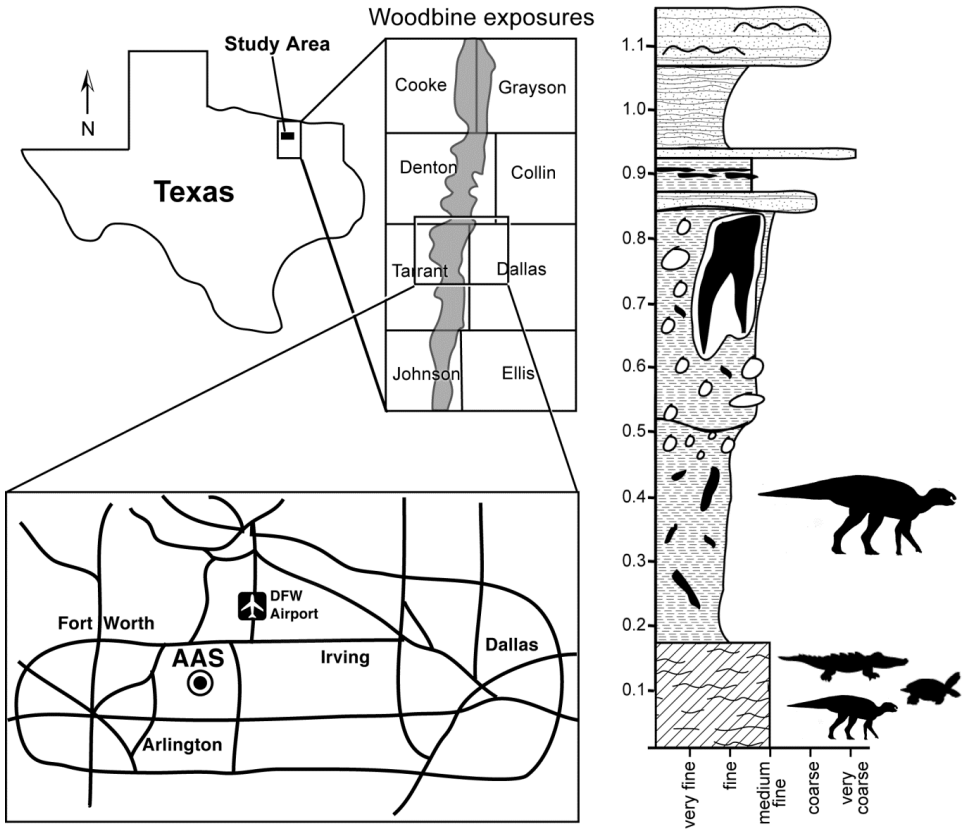

Figure 6.1 Map of Woodbine Formation exposures in North Texas and location of the AAS with the new crocodyliform locality. Stratigraphic column of Woodbine exposures along the AAS hillside with fossil fauna noted at approximate horizons.

The Woodbine Formation of North Central Texas was mapped and named by R. T. Hill (1901). The age of the Woodbine Formation was established biostratigraphically using ammonites as zonal markers, principally *Conlinoceras tarrantense* (Kennedy and Cobban, 1990). The lower members of the Woodbine Formation consist of the Rush Creek, Dexter, and Lewisville Members, parts of which are fluvial, marginal marine, or fully marine (Bergquist, 1949; Dodge,

1969; Johnson, 1974; Oliver, 1971a). The uppermost Arlington Member of the Woodbine Formation is a coastal fluvial unit composed of bifurcating channel sandstone and splay deposits (Main, 2005; Oliver, 1971b). The AAS is located within strata of the upper part of the Woodbine Formation, which places it firmly in the Cenomanian (~ 95-96 Mya). The paleoenvironments of the strata of the Woodbine at the AAS are are interpreted as low lying coastal delta plains. The total measured section of the studied area is ~ 2.5 meters and consists of a heterolithic mudstone bed with sand lenses that overlies a poorly developed paleosol, with an organic rich peat bed at the base of the section (Fig. 6.1).

During the 2009 summer AAS field season, a large adult crocodyliform was excavated from the lower section of the peat bed. In the following summer field season of 2010, new elements from multiple juvenile crocodyliforms were recovered from the same peat horizon, approximately 8 m west of the adult skeleton found in the Crocorama site. Both the adult and juvenile material recovered from the AAS was included in this study in order to fully reconstruct the new taxon and assess ontogenetic change during the growth of an individual. The remains include a disarticulated partially complete skull and considerable postcranial material from a single large (~6 m) adult individual and additional disarticulated material from a second adult, at least one subadult, and several juveniles. Recovered AAS crocodyliform elements include: crania (premaxilla, maxilla, dentary, mandible, palatine, nasals, jugal, post orbital, surangular,

angular, quadrate, spleenial, frontal, exoccipital and basioccipital), and post crania (an atlas, axis, dorsal and caudal vertebrae, a scapula, femur, radius, ilium, ischium and osteoderms). For a complete list of recovered AAS crocodyliform material see Table 6.1.

Skeletal elements including those of the skull were completely disarticulated and in some cases incomplete. In order to produce the most accurate reconstruction of this taxon as possible, select individual elements were scanned at high resolution using a NextEngine Scan Studio 3-D laser scanner (NextEngine, Inc.). All scanned elements are listed in Table 6.1. Elements were then processed and assembled virtually using the open source program Blender (blender.org). Depending on the element, processing included resizing, cropping and or mirroring in order to produce the necessary elements for the reconstruction. Juvenile elements were enlarged isometrically. Because the scale could not be held constant between scans due to variations in size between elements and limitations of the scanning apparatus, all elements were scaled to fit each other based on comparisons of articular surfaces. If an element was incomplete, a composite was created from existing partial elements by matching overlapping morphological structures. If only a left or right element were recovered, the element was copied and mirrored to create the opposite side. In some cases, as with juveniles or distorted or partial material, parts of the element conflicted in overall shape with other elements and were cropped for clarity. If an

element was missing from the collection entirely, it was not included in the reconstruction. The detailed 3D scans allowed for a more thorough morphologic study of the material and virtual reconstruction of the new taxa from individuals of different sizes and ages.

Inistitutional Abbreviations — UTA; University of Texas at Arlington, AAS; Arlington Archosaur Site.

6.2 SYSTEMATIC PALEONTOLOGY

CROCODYLIFORMES Hay, 1930

MESOEUCROCODYLIA Whetstone and Whybrow, 1983

GONIOPHIOLIDIDAE Cope, 1875

Genus *DELTASUCHUS* new gen. et sp.

Type Species — *Deltasuchus motherali*, sp. nov.

Etymology — In the generic name, *Delta* refers to the coastal delta plain deposits of the Woodbine Formation in which the new taxa was found, *suchus* for crocodile, and the species name, *motherali* was chosen to honor the discoverer; Austin Motheral, hence the name: "Mother of all delta crocodiles."

Holotype—UTA-AASC-2009 a partial adult skull and associated post crania, from the AAS Crocorama site discovered by Austin Motheral. The elements of

the holotype are numbered individually, but the collections number is

UTA-AASC-2009

Referred Material — UTA-AASC-2011; associated but disarticulated post crania of a sub-adult individual. UTA-AASC-2010; disarticulated but associated juvenile crania and post crania, all from the same horizon as UTA-AASC-2009, although from separate localites within the AAS; the Nursery and Crocorama East.

Horizon and Type Locality —The Lewisville Member of the Woodbine Formation; the *Conlinoceras tarrantense* zone denotes the base of the mid Cenomanian (~95-96 Mya) (Kennedy and Cobban, 1990). All fossils were recovered from a single locality in northwest Arlington, Tarrant County, Texas; the Arlington Archosaur Site (AAS). The AAS is located off of Trinity Blvd at Main St., between Texas Hwy 157 and Texas Hwy 360 several kilometers due north of the Dallas Cowboys Stadium. The exact location, including latitude and longitude coordinates is on record with the University of Texas at Arlington.

Diagnosis —*Deltasuchus* is a large crocodyliform characterized by a robust, triangular skull, moderately enlarged supratemporal fenestrae, a short dentary symphasis, paired double pseudocanines on both the dentary and maxilla, a robust premaxilla that overhangs the dentary, and a broad angular process of the mandible, rectangular dorsal osteoderms with a prominent articularis processes

and hexagonal ventral osteoderms associated with the sternum, a broad ilium with an expanded supracetabular ridge.

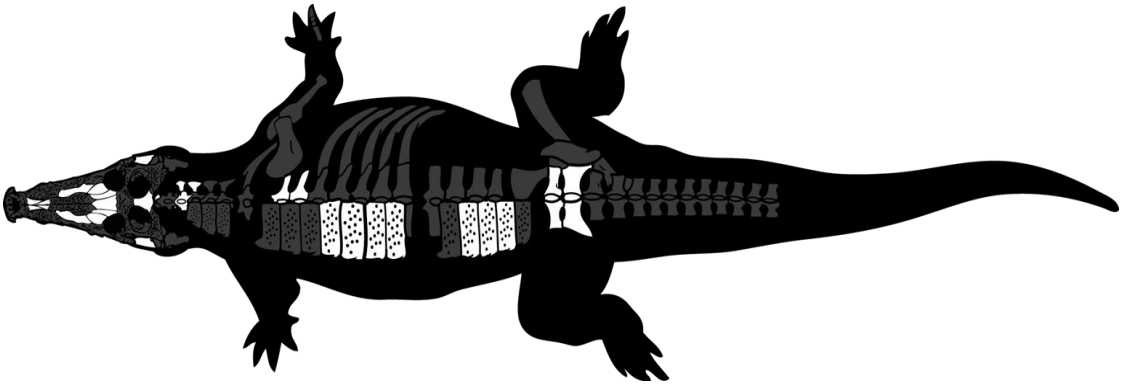

Figure 6.2 Generalized *Deltasuchus s*keletal reconstruction with fossils found denoted by grey shading, modified from Sereno et al. (2001).

6.3 Description

6.3.1 The Skull

The description of the skull of *Deltasuchus* is based upon a digital composite created from elements of adult, sub-adult and juvenile specimens. All elements were associated but disarticulated and found within a single stratigraphic horizon of organic rich peat. All specimens recovered from this horizon were relatively well preserved with no signs of post depositional deformation. The laser scan composite of the elements allowed for a detailed view of the taxon that would not otherwise be possible (Fig. 6.3). This initial model resized, but did not

distort or reshape cranial elements (for a list of individual specimen numbers and measurements see Table 6.1. Therefore, this model is considered tentative and may be revised following more detailed study. In dorsal view the skull is wide, broad and triangular, falling within the generalized alligatorid morphotype discussed used by Brochu (2001). This morphotype is broader than the Woodbine Formation pholidosaur *Terminonaris* and the Woodbine goniopholidid, *Woodbinesuchus*. It is similar in form to the stratigraphically older goniopholidids; *Goniopholis simus*, *G. crassidens*, and *G. stovali*, with striking similarities to the stratigraphically younger pholidosaur *Denazinosuchus* (Lee, 1997; Lucas and Sullivan, 2003; Mook, 1964; Owens, 1878 and Salisbury et al., 1999). The broad, generalist morphology of the skull is considered a unique ecomorphotype within the coastal Woodbine delta plain ecosystem, as *Woodbinesuchus* and *Terminonaris* were likely specialized for feeding on fish, whereas *Deltasuchus* was a generalist adapted to a wider range of feeding (Adams et al., 2011; Brochu, 2001; and Lee, 1997).

In dorsal view, the skull has external sculpturing in the form of deep subrounded to elongate pits, 4 - 16 mm long and 2 - 6 mm wide, that are irregularly spaced from the anterior to the posterior, similar in form to *Goniopholis simus*. The rostrolateral corner of the cranial table is subrectangular or squared, similar to *Denazinosuchus* and *G. simus* (Lucas and Sullivan, 2003; Salisbury et al., 1999). The supratemporal fenestrae are quite large, forming a

significant feature of the cranial table (Fig. 6.3). The supratemporal fenestrae of *Deltasuchus* are much larger in diameter than those of the goniopholids. Enlarged supratemporal fenestrae are absent from the goniopholidids and are more common in pholidosaurs, such as *Oceanosuchus* and *Denazinosuchus* and quite typical of thalattosuchians, such as *Dakosaurus, Metriorhynchus* and *Geosaurus*, as well as *Anglosuchus* (Frey et al., 2002; Gasparini et al., 2006; Hue et al., 2007; Leeds, 1908; Lucas and Sullivan, 2003; and Mook, 1942a). *Deltasuchus* has a distinctly robust, triangular snout that differentiates this taxon from the slender snouts of *Woodbinesuchus* and *Terminonaris* (Adams et al., 2011; and Lee, 1997).

Both upper and lower jaws possess two pairs of prominent pseudocanines, a potentiallyunique trait among crocodyliforms. A similar condition may exist in *G. crassidens* but is not developed to the same degree. The upper pair is found in the maxilla and the lower pair in the dentary. The lower pair of pseudocanines form a laterally concave depression directed toward the suture of the nasals and the premxilla, similar to *G. simus* and *Leidyosauchus* (Salisbury et al., 1999 and Wu et al., 2001). The premaxilla of *Deltasuchus* over hangs the dentary in a prominent beak like manner, similar in form to pholidosaurs such as *Oceanosuchus* and *Sarcosuchus* (Hua et al., 2007; and Sereno et al., 2001). The teeth of *Deltasuchus* are homodont, conical and slightly recurved with carinae present on the labial and lingual surfaces, some have faint longitudinal ridges.

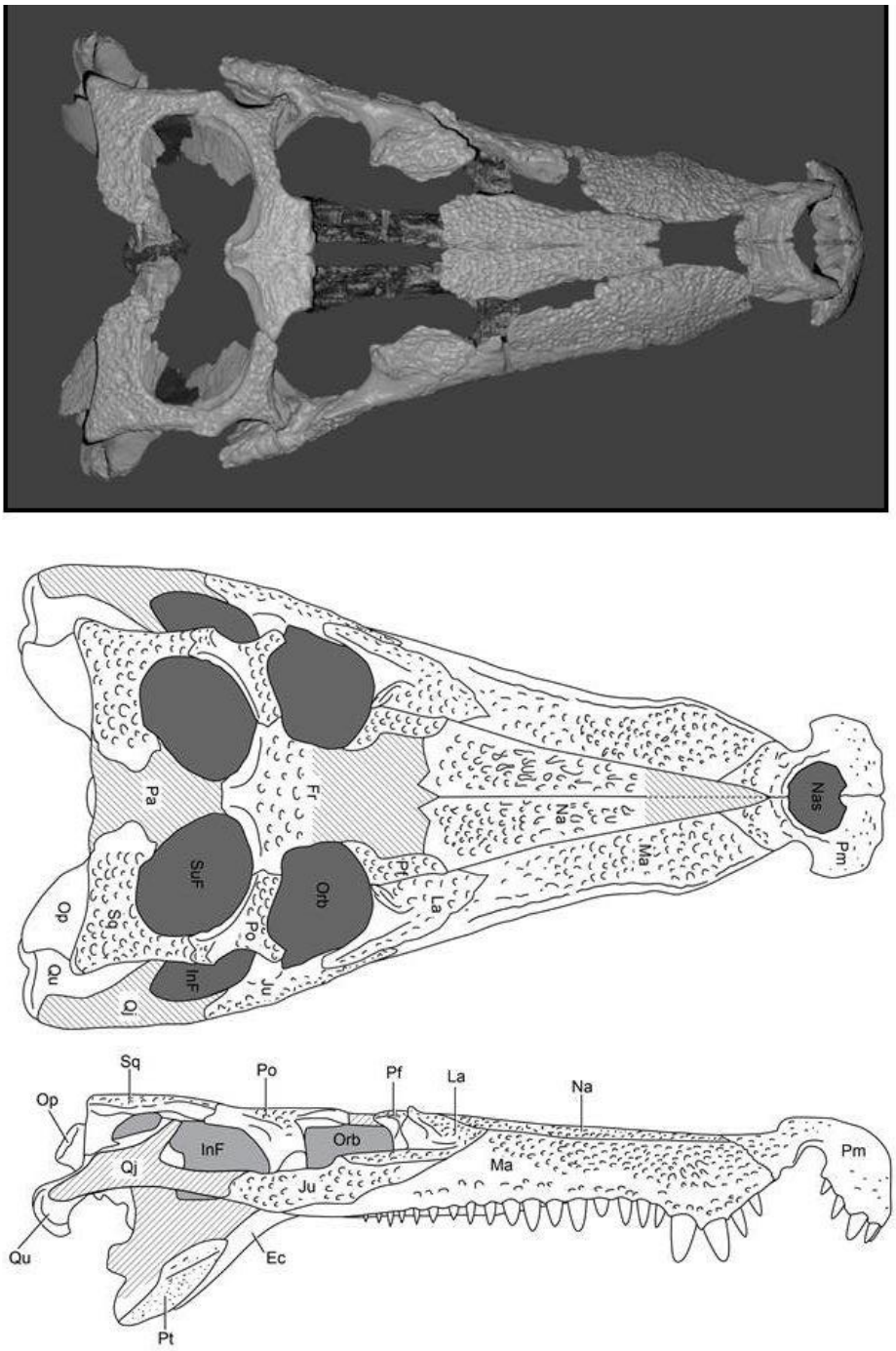

Figure 6.3 A. *Deltasuchus* digital skull reconstruction, digital composite of adult and juvenile fossils. B. *Deltasuchus* skull line drawing in dorsal view. C. *Deltasuchus* line drawing in lateral view (courtesy C. R. Noto).

Premaxilla—The premaxilla is represented by a near complete posterior left adult premaxilla and a partial right adult and complete right juvenile premaxilla. These elements were scanned and utilized in the digital composite of the skull (Fig. 6.3). UTA-AASC-448 is a left premaxilla and is the most complete, although it only has one alveolus preserved with the anterior most margin missing. In dorsal view, the premaxilla has external sculpturing in the form of deep subrounded pits and a concavity for the dentary pseudocanines that forms a deep indention along the lateral margin.

The pseudocanines are directed toward the suture of the nasals and the premaxilla, similar in form to *Leidyosuchus* and the goniopholids *G. simus* and *G. stovali* (Mook, 1964; Salisbury et al., 1999 and Wu et al., 2001). In dorsal view, the premaxilla is sub-rounded and laterally flared into a blade like shape similar to those of *G. simus and G. kiplingi*, although the external naris is heart shaped and proportionally larger than *G. simus* and extends further caudally (Fig. 6.3) (Andrade et al., 2011; and Salisbury et al., 1999). In lateral view, they are expanded into a rounded, convex beak shape that drapes down ventrally, a character noted in the goniopholids *G. simus* and *G. stovali* (Mook, 1964; Owen, 1878; Salisbury et al.. 1999). The ventral drape is more pronounced than that of the goniopholids however, extending down and prominently over hanging the dentary, completely covering it in dorsal view (Fig. 6.3). The prominent ventral

drape of the premaxilla is a character noted in the pholidosaurids *Oceanosuchus* and *Sarchosuchus* (Hua et al., 2007 and Sereno et al., 2001).

In ventral view, the premaxilla exhibit two prominent depressions. Although prominent, the dentary teeth do not fit into these depressions, a condition also seen in *Sarchosuchus* (Sereno et al., 2001). The third alveolus is enlarged, nearly twice the diameter of the other premaxillary alveoli. The external naris is broad, undivided and subrounded (heart shaped) in dorsal view with a prominent ridge (a 1-1.5 cm rim, the naris vallatus) that defines the external naris. similar to that noted in both goniopholidids and pholidosaurids; *G. simus*, *Sarchosuchus* and *Terminonaris* (Fig. 6.3) (Adams et al., 2011; Owen, 1878; Salisbury et al., 1999; Sereno et al., 2001). The external naris is contained entirely within the premaxilla. The premaxilla and maxilla contact one another at a notch for the psdeudocanine (Fig. 6.3). The premaxillary-maxillary suture forms an M shape with the nasals across the posterior margin of the premaxilla, similar to that of *G. simus*, although more sublime (Fig. 6.3) (Salisbury et al., 1999).

Maxilla—The maxilla consists of four specimens used in this study; UTA-AASC-286 and 250 and UTA-AASC-251 and 404 for measurements see Table 6.1. The general morphology is similar to that noted for *Denazinosuchus* and *Goniopholis*, (*G. simus* and *G. stovali*), with an overall length of 420 mm that equals >50% of the total skull length (Lucas and Sulllivan, 2003; Mook, 1964; Owen, 1878 and

Salisbury et al., 1999). Anterioriorly, the maxillae are separated dorsomedially by the premaxillae, and posteriorly by the nasals. The maxillae have an anteriolateral protrusion, or swell, that later curves in for a dorsomedial constriction that tapers at the suture for the premaxillae.

The general morphology is similar in form to *Crocodylus depresifrons* and *Denazinosuchus,* as well as to the goniopholidids; *G. crassidens, G. gilmorei, G. simus,*and *G. stovali* (Delfino and Smith, 2009; Holland, 1905; Hooley, 1907; Lucas and Sullivan, 2003; Mook, 1964; Owens, 1878; Salisbury et al., 1999). The maxillae (and all cranial elements) have deep, rounded to elongate pits, 4 -16 mm long and 2 - 6 mm wide (Fig. 6.4 and 6.5).

The left anterior maxillae are the most complete, with ten alveoli preserved. The alveoli are divided internally by thin interdental plates and vary in size, with the largest occurring at the anterior maxillary protrusion. The posterior left maxilla is a partial element, broken mediolaterally with only nine alveoli preserved (nineteen total alveoli for both left maxilla specimens), the alveoli vary in diameter from 8 to 18 mm.

Both the right and left maxilla preserve at least 19 alveoli, similar in number to the goniopholidids *G. stovali* and *G. simus* (Mook, 1964; Owen, 1878; and Salisbury et al., 1999) (Fig. 6.4). The maxillae have a pronounced lateral

swell associated with alveoli 3 and 4 that are associated with the anterior lateral protrusion of the maxillae (Fig. 6.4 and 6.5).

The vascular foramina form a distinct line dorsally over the alveoli on the left maxilla, of which 20 are distinguishable. The absence of sculpturing, or pitting, along the alveolar margin on the lateral surface, is a character state associated with pholidosaurids and therefore considered as a unique character trait of this taxon (Fig. 6.4 and 6.5).

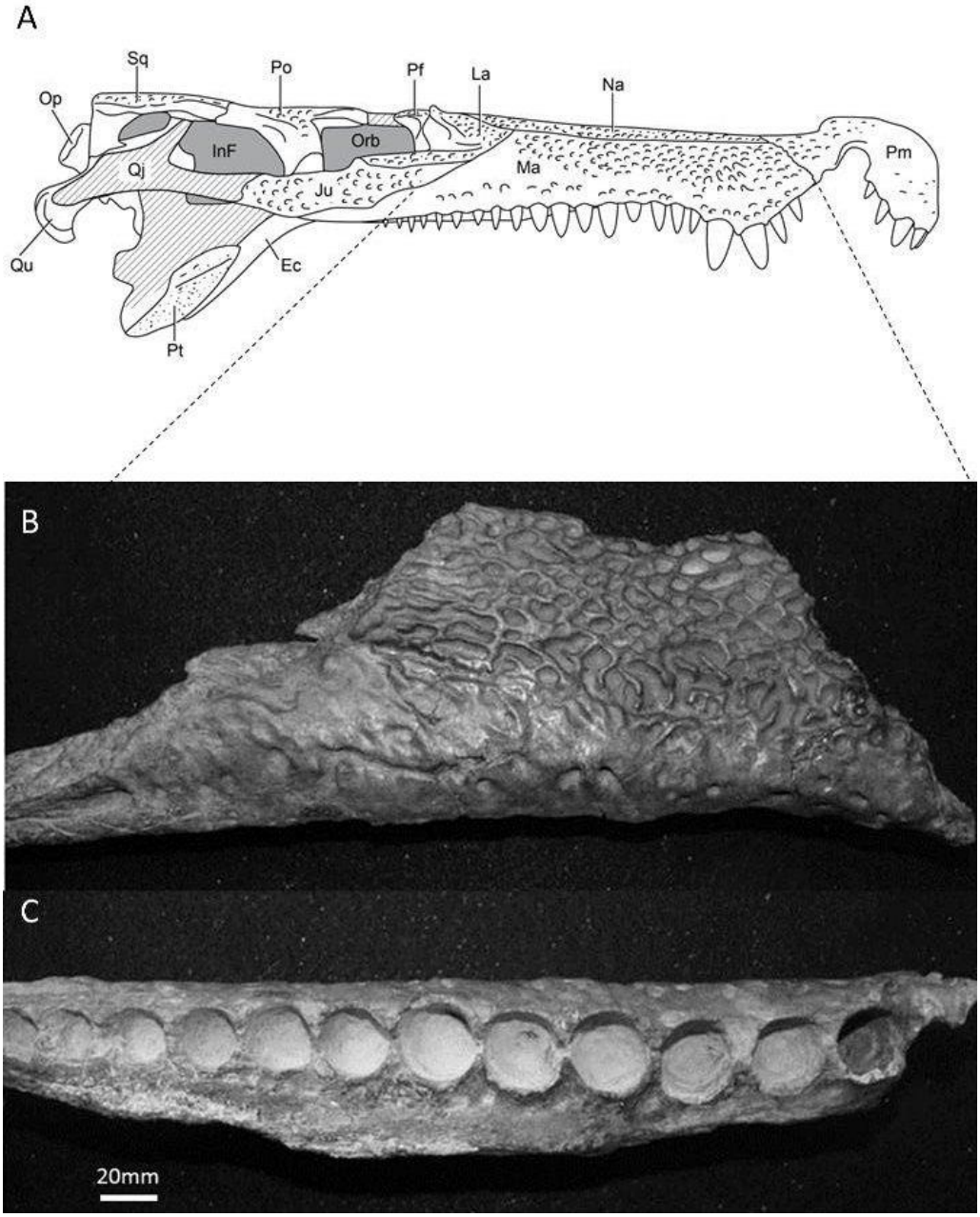

Figure 6.4 A. *Deltasuchus* skull diagram in lateral view. B. UTA-AASC-250 right maxilla in lateral view. C. UTA-AASC-250 in ventral view with depth and size variation of alveoli clearly shown.

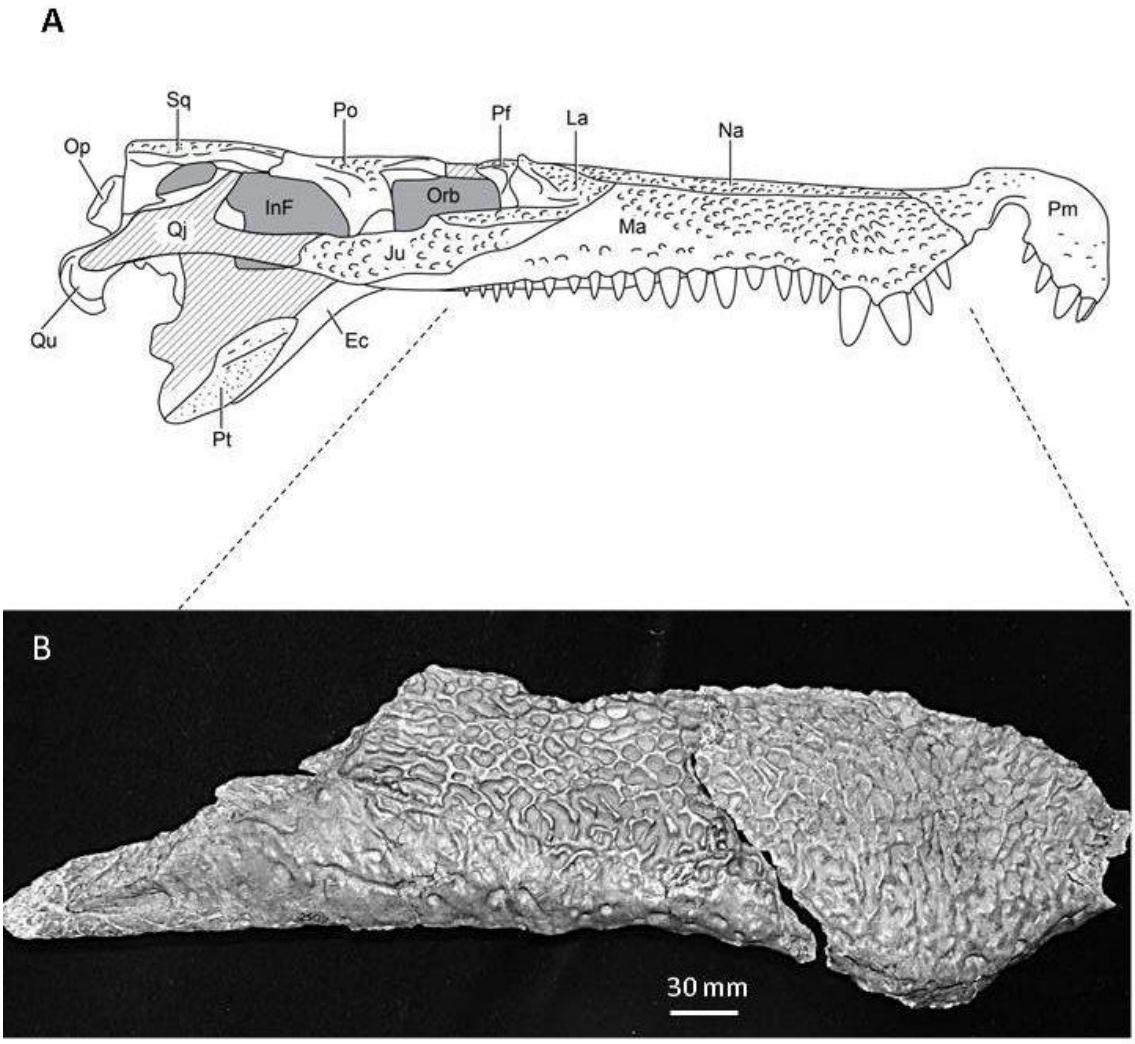

Figure 6.5 *Deltasuchus* maxilla. A. *Deltasuchus* skull line drawing for context B. UTA-AASC-250 and 286 right maxilla in lateral view (artwork courtesy C. R. Noto).

Palatine — UTA-AASC-389 is represented by a nearly complete left juvenile specimen, approximately half the full adult size (Fig. 6.6). The palatine is gently convex on the ventral surface, with a slight bend resulting from deformation (Fig. 6.6). The lateral edges of the palatine are parallel and bear a process along the interior margin that project into the suborbital fenestra. The palatine joins with the maxilla at the anterior base of the suborbital fenestrae with a sharp right angle that slightly extends beyond the anterior end of the suborbital fenestrae (8 mm), thus giving the palatine-maxilla a distinct U-shaped form (Fig. 6.6). The palatine – pterygoid suture appears to terminate at the posterior suborbital fenestrae with a slight medial deflection.

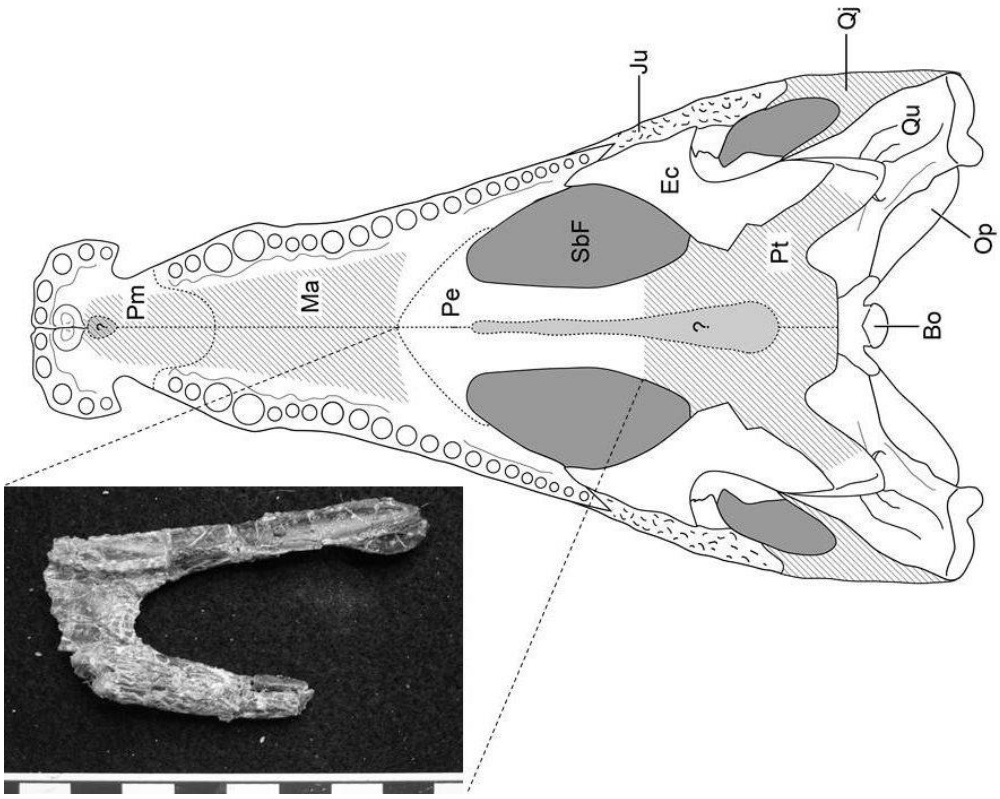

Figure 6.6 *Deltasuchus* palatine UTA-AASC-389 in ventral view with skull diagram in ventral view (palatine labeled as "Pe" on skull diagram) (scale bar in cm).

Nasals— UTA-AASC-328 is a left and UTA-AASC-327 a right nasal. The nasals are from an adult individual with the rostral part of each nasal absent (Fig. 6.7). The right is better preserved and thus more complete than the left, and measures 212 mm in length (Fig. 6.7). In dorsal aspect, the nasals are elongate, subtriangular elements that taper gently toward the premaxillae, and widen posteriorly with a gentle ventral curve at the lacrimals (Fig. 6.7). The nasals

contact the premaxilla, but do not touch the external naris, similar to *Goniopholis* and *Sarchosuchus* (Owen, 1878; Salisbury et al., 1999; and Sereno et al., 2001).

The nasals are elongate, with the preserved portions nearly four times as long as they are wide (Fig. 6.7). The nasals are subtriangular in dorsal view and do not have the tapering tear drop form seen in *G. simus*. They have deep rounded, oblong pits in the dorsal surface that are larger and more pronounced than those of the maxillae (Fig. 6.7). The posterior margin terminates in a V shape, presumably at the suture with the frontals. The nasals terminate approximately above tooth position 22 of the maxilla.

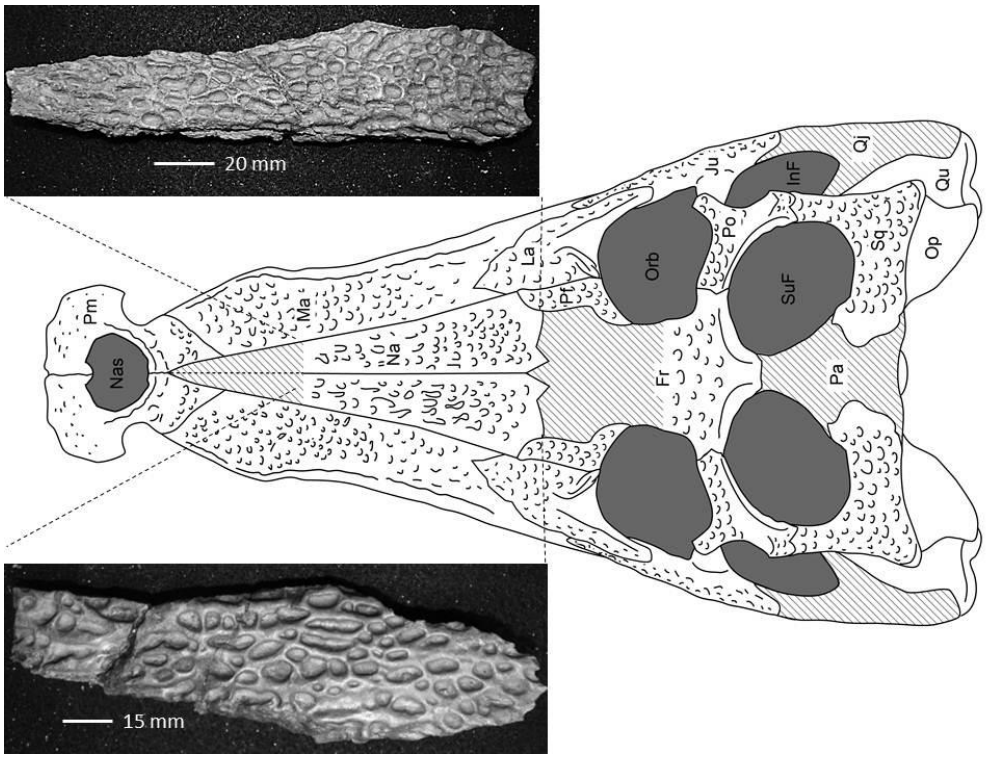

Figure 6.7 *Deltasuchus* nasal bones. UTA-AASC-327 and UTA-AASC-328 nasals; left (on bottom) and right (on top).

Frontal— UTA-AASC-409 is a partial juvenile element. The posterior section is preserved lacking the nasal process and sutural contacts (Fig. 6.8). When complete, the frontal is likely subtriangular in dorsal view. The lateral sides of the frontal form the posteromedial border of the orbit and anteromedial border of the supratemporal fenestra. The margin of the supratemporal fenestrae has a gentle concave ridge, with a smooth superior surface. The left orbit has a distinct flat rim (Fig. 6.8). The frontal is heavily pitted on the dorsal surface, although the pits are

smaller and shallow than those of the nasals and posterior skull table (Fig. 6.3). This feature is likely related to the juvenile state of the specimen.

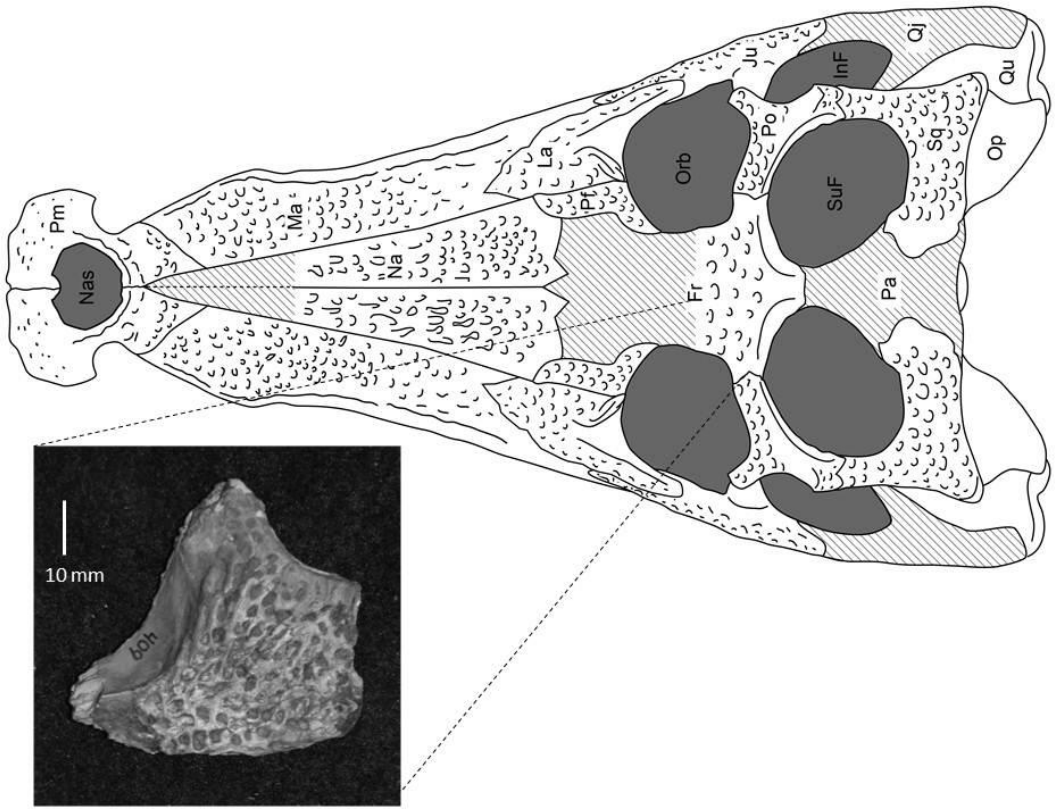

Figure 6.8 *Deltasuchus* frontals, UTA-AASC-409 frontal in dorsal view with skull diagram for orientation.

Quadrate— UTA-AASC-218 is a right adult quadrate and UTA-AASC-429 a left adult specimen. The quadrate is laterally smooth, with well preserved sutures on the medial margin. A well developed otic recess is present on the dorsal anterior margin, forming a near vertical surface dropping ventrally away from the exoccipital suture (Fig. 6.9). The quadrate has a roughly reniform medial

hemicondyle, with a sharply inset concavity that separates it from the lateral hemicondyle, which is relatively flat and elongate (Fig. 6.9). The ventral surface is defined by a prominent quadrate crest that displays a distinct ridge that projects ventrally away from the surface and is deeply concave dorsally (Fig. 6.9). This feature is an autapomorphy of the new taxon. The general morphology is similar to that of the goniopholidids *G. simus* and *G. stovali,* although larger and broader, a trait noted in the pholidosaur *Sarchosuchus* (Mook, 1964; Salisbruy et al., 1999; Sereno et al., 2001). All measurements are listed in Table 6.1.

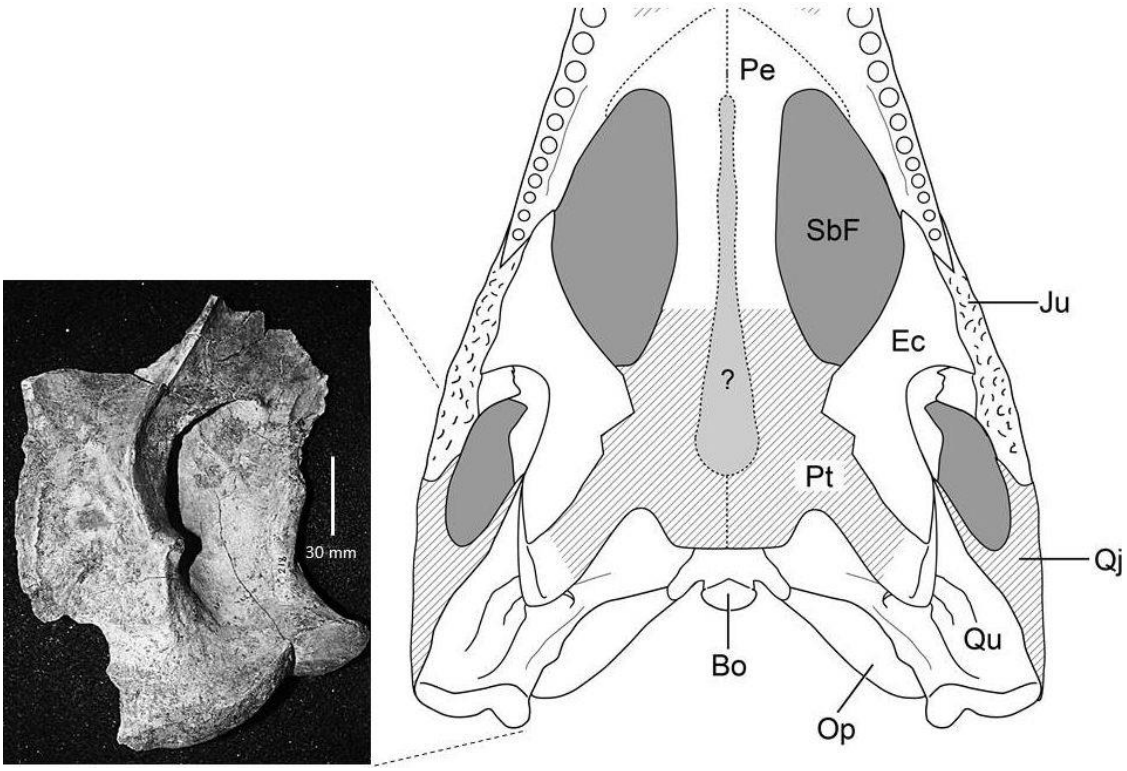

Figure 6.9 *Deltasuchus* quadrate, UTA-AASC-218 right quadrate with partial skull diagram in ventral view.

Jugal— UTA-AASC-248 is an adult specimen, complete but moderately weathered. The jugal is elongate and slightly sigmoid in lateral view, with the dorsal surface defining the posteroventral margin of the orbit and the anteroventral margin of the infratemporal fossa (Fig. 6.10). The prominent, anteromedially curved post-orbital process separates the two features. The medial jugal foramen is absent, possibly weathered away. The medial post-orbital process has a recessed suture surface that deepens ventrally. The anterior margin of the jugal is subtriangular at the suture surface of the maxilla and lacrimal (Fig. 6.10). The jugal–lacrimal suture is partially preserved in *Deltasuchus*, although the posterior maxillary margin is missing. The lateral surface is covered with deep, rounded to oblong pits, similar to *G. simus* (Salisbury, 1999). The medial surface has a rounded, gentle curve towards the lacrimal suture. The maxillary suture is weathered, as is a substantial portion of the ectopterygoid and quadrate suture surfaces. The posterior jugal is subrounded, and terminates with the suture for the quadrate (Fig. 6.10).

Postorbital — UTA-AASC-214 **is** a complete adult specimen that is moderately weathered, covered with deep, rounded pits on the dorsal surface (Fig. 6.10). The supratemporal fenestra is defined by a rim that has a gentle anterolateral curve. The anterolateral margin of the postorbital is rounded and curved ventrally. The postorbital bar is thick, with a slight anterior ridge that projects into the orbit (Fig. 6.10). The postorbital-jugal suture is well defined and forms a strong articulation

with the jugal (Fig. 6.10). The posterior margin of the postorbital is subrounded. The squamosal suture is situated ventrally, with much of the suture missing.

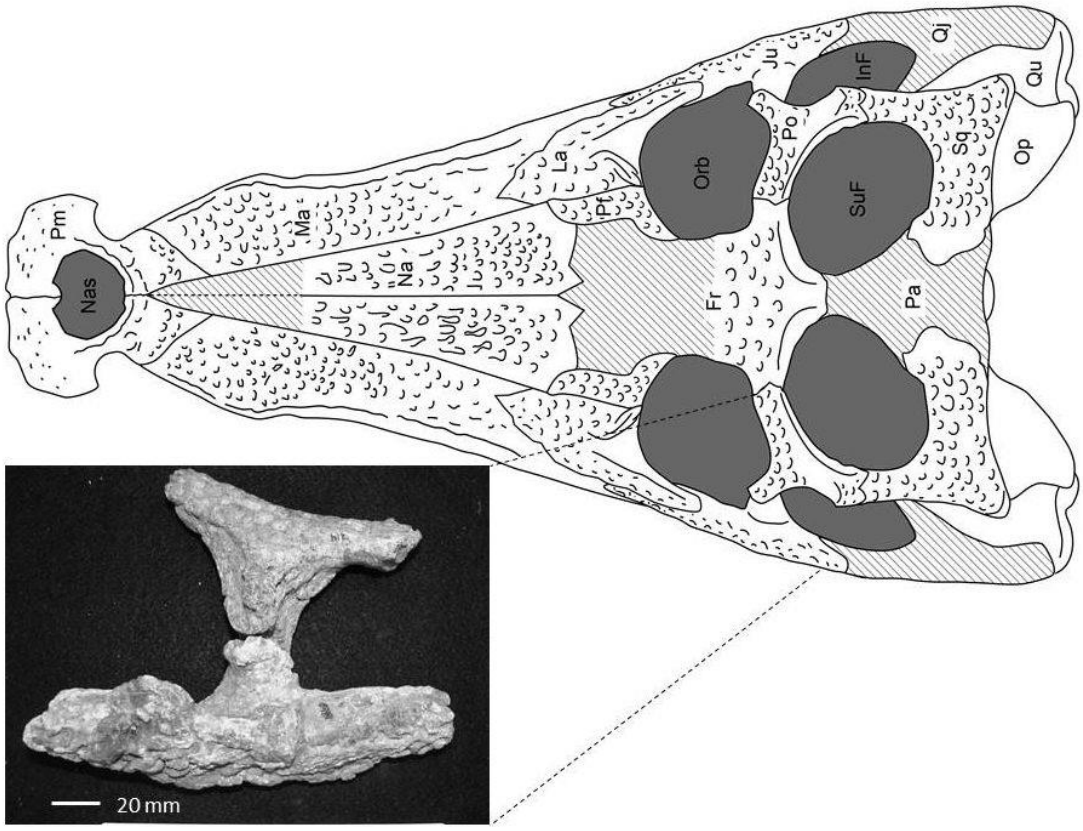

Figure 6.10 *Deltasuchus* post orbital and jugal. UTA-AASC-214 and UTA-AASC-248 a post orbital and jugal in dorso-lateral view with skull diagram in doral view.

Squamosal— UTA-AASC-431 is a complete right sub-adult specimen. The dorsal surface is deeply pitted with small (1-3 mm) rounded pits (Fig. 6.11). The medial margin is concave, forming the posteriolateral border of the supratemporal fenestrae. The lateral margin over the recessus oticus externus is concave, with a deep groove extending along the lateral surface (Fig. 6.11). The squamosal-quadrate sutures extend ventrally at an oblique angle from the squamosal prong, which is supported by a relatively thin and short process (Fig. 6.11). The squamosal prong is short and subtriangular in form, not posteriorly extended as in *Terminosaris* or *Sarcosuchus* (Adams et al., 2011). The short, subtriangular morphology of the squamosal prong is similar in form to *G. simus*, although not as pronounced (Salisbury et al., 1999). The posterior squamosal rim is shallow and does not extend beyond the occipital surface (Fig. 6.11). Element specimen data can be referenced in Table 6.1.

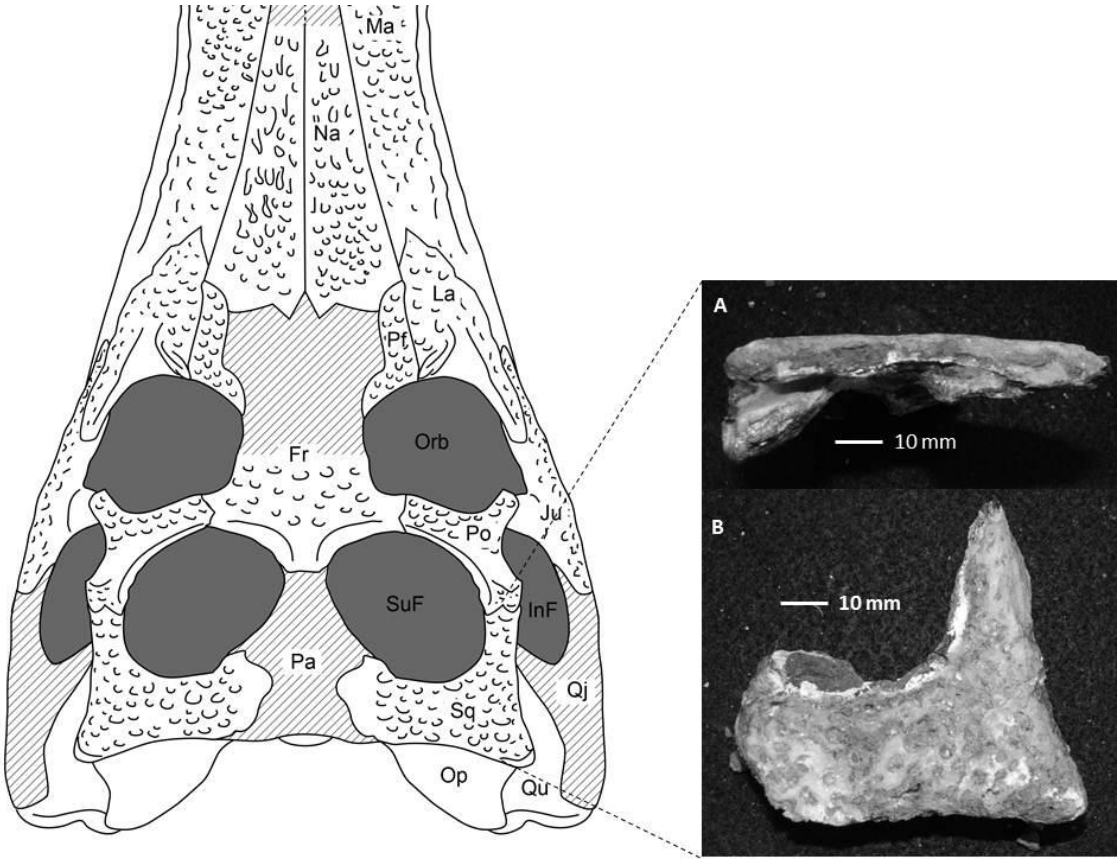

Figure 6.11 *Deltasuchus* squamosals. A. UTA-AASC-431 right squamosal in lateral view. B. Right squamosal in dorsal view with partial skull diagram for reference.

Exoccipital — UTA-AASC-287 is a left adult specimen and UTA-AASC-406 a right adult specimen. The exoccipitals are twice as wide as they are high and form the lateral and dorsal boundaries of the foramen magnum. The paroccipital processes are wide, and wing-shaped (Fig. 6.12). In the left exoccipital, the foramina for cranial nerves IX-XI and XII and the internal carotid artery are visible and located close to the foramen magnum, which is the condition seen in

Terminonaris and *Oceanosuchus* (Adams et al., 2011; Hua et al., 2007; Wu et al., 2001). The interior exoccipital suture is elevated into a raised ridge that forms a shallow shelf over the foramen magnum (Fig. 6.12). The exoccipital –quadrate suture is well preserved in UTA-AASC-406; it is a deeply concave suture with a narrow lateral ridge (Fig. 6.12). The exoccipital most likely did not extend beyond the lateral margin of the squamosal, a condition similar to *G. simus* (Salisbury et al., 1999).

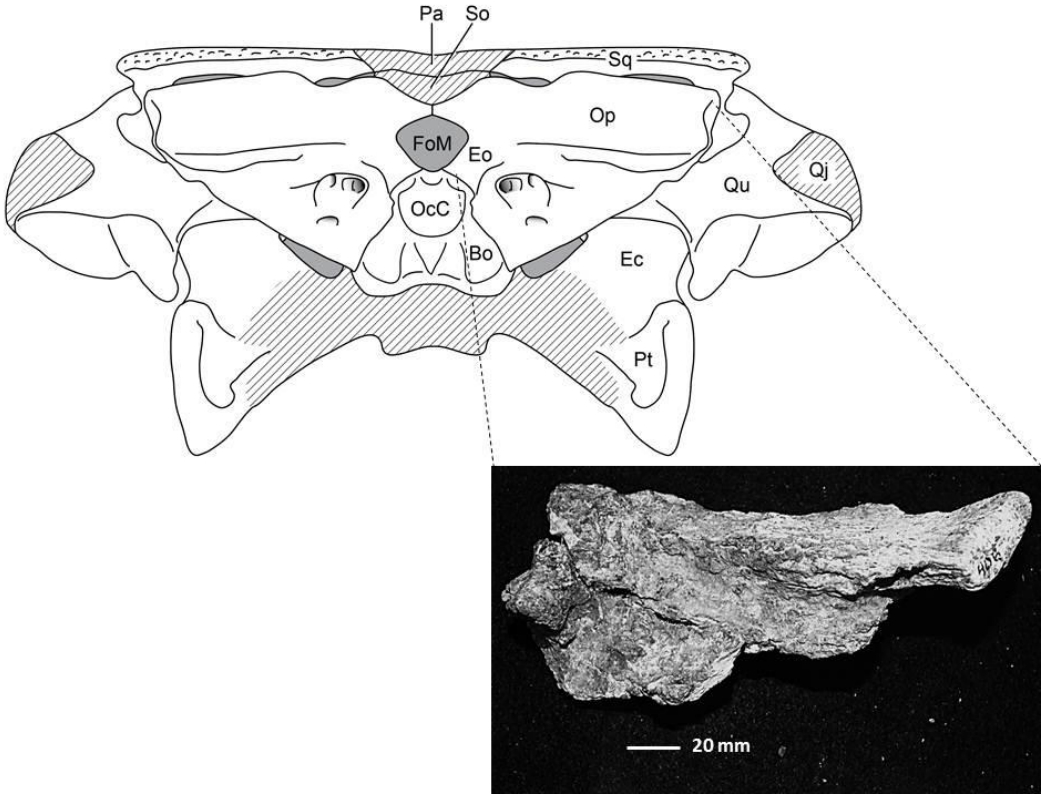

Figure 6.12 *Deltasuchus* exoccipitals. UTA-AASC-406 a right exoccipital in posterior view with *Deltasuchus* line drawing for reference (exoccipital denoted on skull as "Eo").

Basioccipital— The basioccipital is represented by an adult, a subadult and two juvenile specimens. UTA-AASC-414 is a near complete adult basioccipital; it forms the occipital condyle and ventral margin of foramen magnum (Fig. 6.13). The occipital condyle is a subhexagonal structure in posterior view, much broader on the adult specimen than the juvenile, and similar in general morphology to *G. kiplingi* (Andrade et al., 2012) (Fig. 6.13). A distinct groove forms the ventral surface of the foramen magnum. Of interesting note, ontogenetic variation was observed in the posterior margin of the basioccipital. A foramen directly ventral to the condyle is present in juvenile specimens, yet this feature is absent from the adult. Equally, two distinct ridges are present along the posterior ventral margin in the adult that are absent from the juveniles. This feature is similar to the W shaped ridge noted in *Eosuchus* (Delfino et al., 2005).

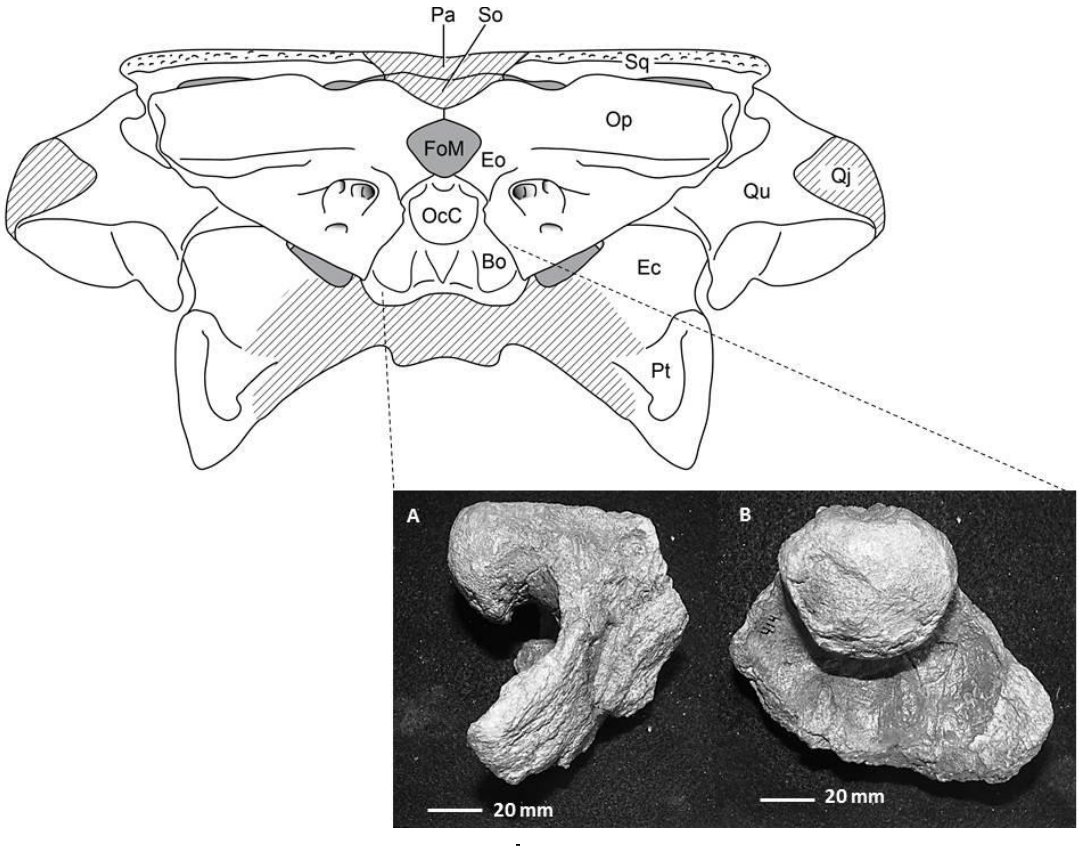

Figure 6.13 *Deltasuchus* basioccipital. UTA-AASC-414 basioccipital condyle in lateral view (A) and posterior view (B).

Mandible—The mandible of *Deltasuchus* is represented by juvenile left and right dentaries, a partial left and right adult dentaies, two right angulars (adult and juvenile), a juvenile right surangular and an adult left surangular, and a left adult splenial (for a list of element data see Table 6.1). Only the adult dentary symphysis, angular and splenial occur as individual elements. The mandible is a gracile element, relatively narrow in dorsal view, thinning medially into a blade like process (Fig. 6.14 and 6.15). Cranial to this, the symphysis slightly expands

laterally producing a near spatulate outline in dorsal view and terminating at a concavity near the sixth alveolus, similar to *G. simus* (Fig. 6.14). The mandible of *Deltasuchus* is similar in form to *G. simus* in dorsal view; however, in lateral aspect it is more slender to the posterior, lacking the broad expanse of the angular (Fig. 6.14) (Salisbury et al., 1999). It is noticeably broader than the other Woodbine crocodyliforms; *Woodbinesuchus* and *Terminonaris* (Fig. 6.14) (Adams et al., 2011; Lee, 1997).

The dentitions of the mandible are broad, and rounded, a morphology associated with crushing and breaking (Noto et al., 2012; Sereno et al., 2001). This feature distinguishes *Deltasuchus* from *Woodbinesuchus* as having a more gereralist diet than that of a gharial like animal that subsisted on hunting fish. Of interesting note, the tooth rows are essentially flat and not sinuous (Fig. 6.14). The measurements of each element are included in Table (6.1). When viewed with the reconstructed skull, the mandible is noticeably shorter than the upper jaw, with the premaxilla overhanging the mandible in a manner most similar to the pholidosaur *Sarchosuchus* (Sereno, et al., 2001) (Fig. 6.19).

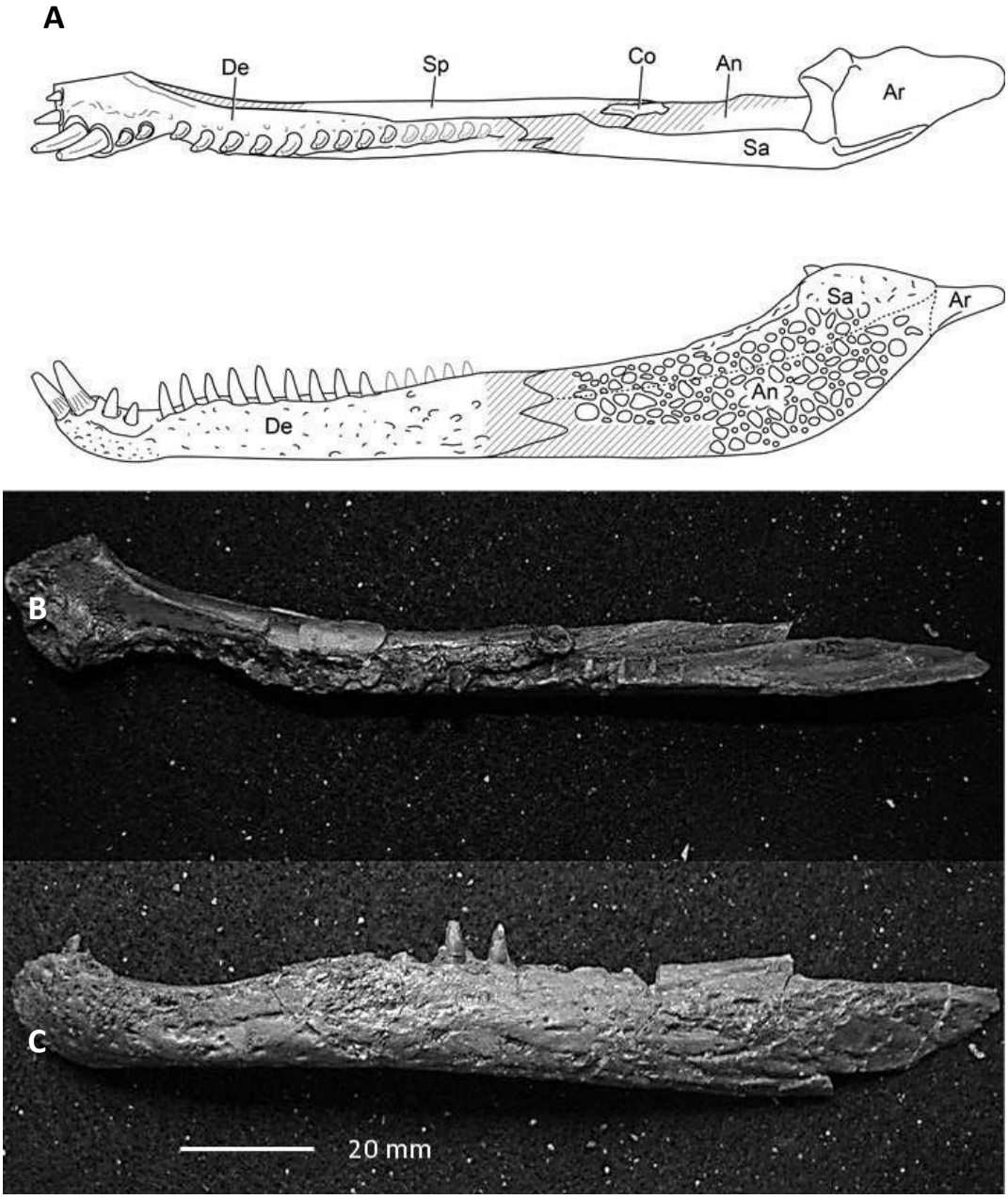

Figure 6.14 *Deltasuchus* mandible. A. Line drawings of the mandible; De = dentary, Sp = Splenial, An = Angular, Ar = Articular, Sa = Surangular . B. UTA-AASC-354 juvenile mandible in dorsal view. C. UTA-AASC-354 in lateral view.

Dentary— UTA-AASC-326 is a partial right adult dentary, UTA-AASC-256 and UTA-AASC-304 are the left and right dentary symphasis from an adult individual, UTA-AASC-207, 306, 346 and 430 are four juvenile dentaries. All specimens were collected from a single bonebed and the same horizon, an organic rich peat. *Deltasuchus* has a short symphysis that is laterally expanded with a rostral bulge, paired pseudocanines, and a robust triangular snout. Although robust, the dentary is twice as long as it is tall (Fig. 6.15). A goniopholidid character, which differentiates this taxon from the longirostrine goniopholid *Woodbinesuchus*, and the pholidosaur *Terminonaris*, both reported from the Woodbine Formation (Adams et al., 2011; Lee, 1997; Owen, 1878; Salisbury, 1999).

Though the adult specimens are incomplete, comparison with the more complete juvenile specimens indicate that each dentary contained 19-22 alveoli. The dentary alveoli are asymmetric, approximately equal in diameter until the pseudocanines, at which they are greatly expanded, nearly doubling in size along the lateral margin (from 1.2 cm to 2.3 cm) and producing a pronounced lateral swelling that extends beyond the lateral border of the maxilla and premaxilla (Fig. 6.14 and 6.15). The fourth and fifth alveoli are raised along the rim of the pseudocanines, similar in position to *G. simus* (Salisbury et al., 1999). Three replacement teeth are clearly visible in the alveoli of the right adult dentary (Fig.

6.15). There are nine vascular foramina preserved along the lateral margin from the pseudocanines to the symphysis (Fig. 6.15).

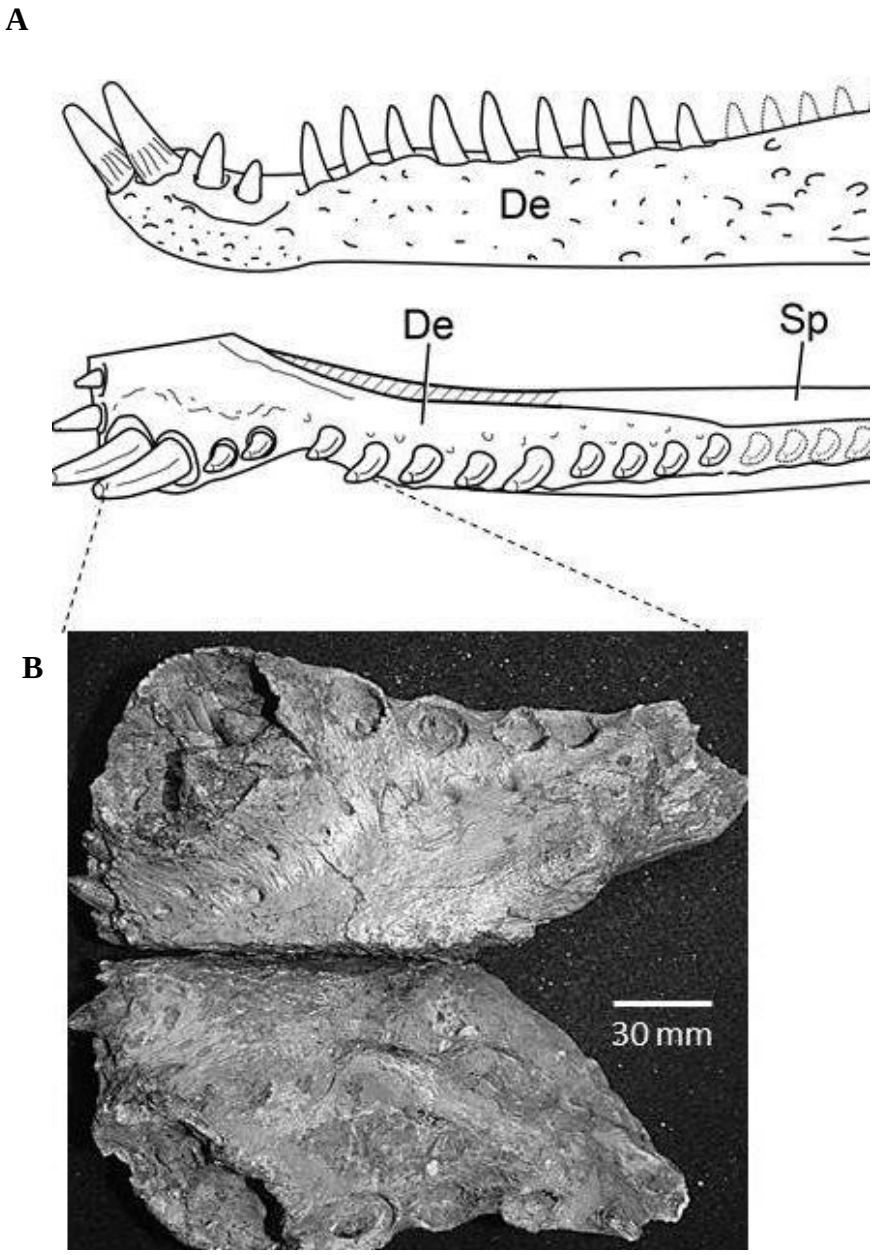

Figure 6.15 *Deltasuchus* dentary. A. *Deltasuchus* dentary line drawings in lateral and dorsal view. B. UTA-AASC-256 and 304 right and left adult dentary in dorsal view.

Splenial — UTA-AASC-430 is a near complete left adult specimen. It is a thin process that is thicker ventrally and slightly concave medially. It widens posteriorly, forming a wedge or subtriangular shape. The posterior does not appear to show a foramen mandibularis oralis, which may be missing as the element is incomplete posteriorly. The splenial lacks surface texture and has minor, if any, participation in the symphysis. For specimen data see Table 6.1.

Angular — Represented by UTA-AASC-314 an adult right angular and UTA-AASC-355 a partial juvenile angular (Fig. 6.16 and 6.17). The lateral surface is pitted with deep, subrounded pits (Fig. 6.16). It is worth noting that only the lateral surface has deep pittings. The angular is crescent shaped, widening posteriorly. A broad ridge is present along the interior–dorsal margin denoting the position of the mandibular fenestra. The proximal most surface is partially eroded; however, the dorsal surface at the midline for what appear to be the mandibular fenestrae preserves a surface for articulation with the surangular (Fig. 6.16). Measurements are listed in Table (6.1).

Surangular — Represented by UTA-AASC-201 is a juvenile right surangular and UTA-AASC-224 an adult left surangular (Fig. 6.17). The adult surangular is a relatively stout and robust element with a lateral surface that is covered with shallow, rounded pits (Fig. 6.17). It should be noted that only the lateral surface is covered with pittings. The juvenile surangular is partial, but preserves the

articular surface with the angular, which is relatively flat, although rounded at the ventral edge. The ventral surface terminates into a thin, leading edge for the mandibular fenestrae (Fig. 6.17). The dorsal surface is broad and flat, with a slight cranial concavity forming an articular surface for the quadrate (Fig. 6.17).

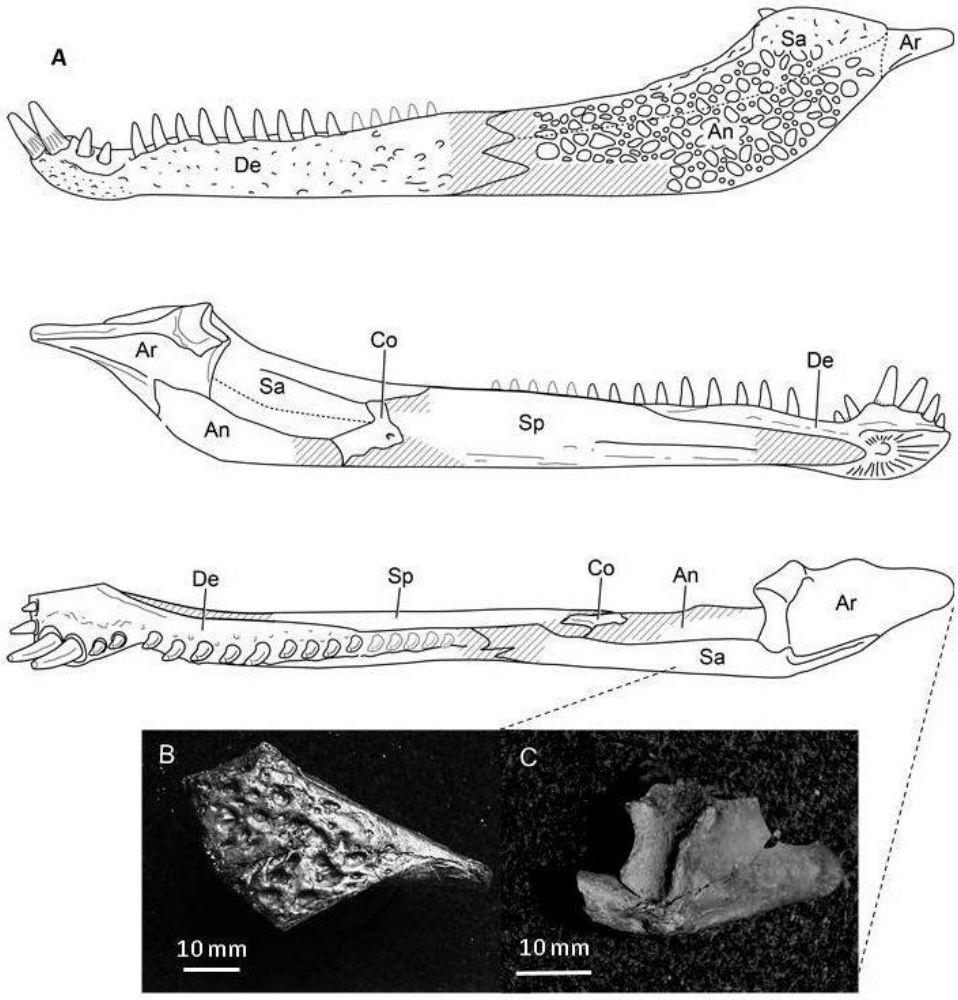

Figure 6.16 *Deltasuchus* angular and surangular. A. Line drawings of *Deltasuchus* mandible in left lateral, right lateral and dorsal views. B. UTA-AASC-355 a juvenile angular and surangular in lateral view. C. UTA-AASC-355 in articular view.

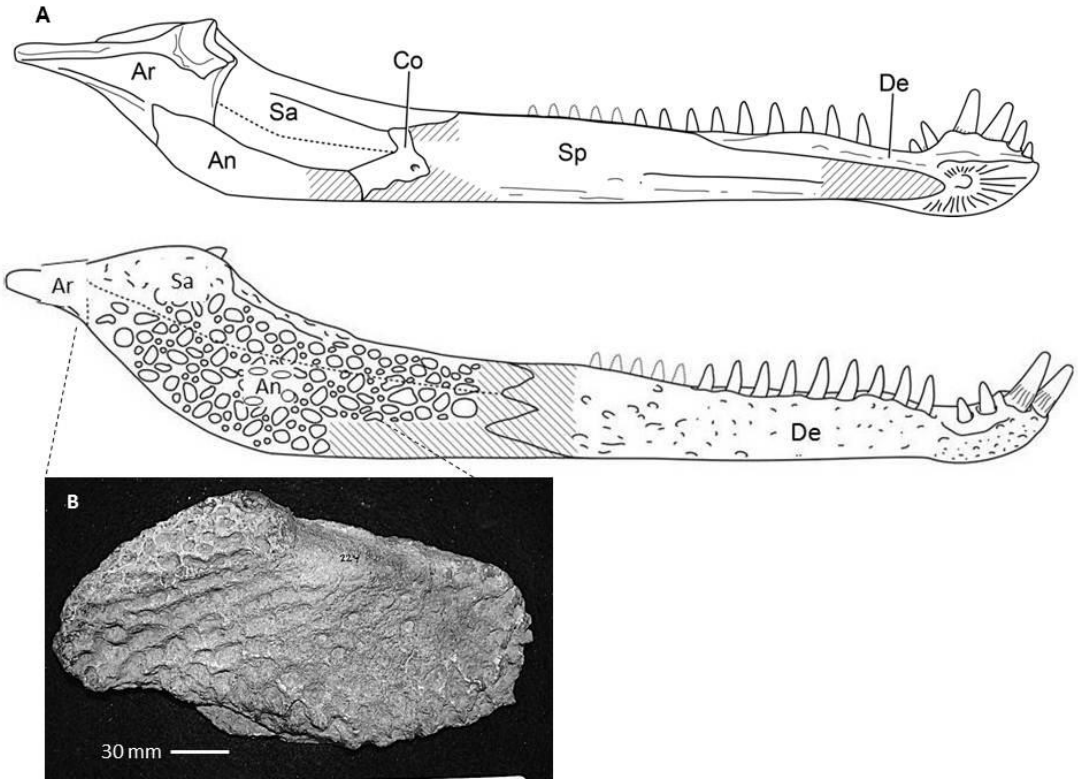

Figure 6.17 *Deltascuchus* angular. A. Line drawings of *Deltasuchus* mandible in lateral view. B. UTA-AASC-224 adult left surangular in lateral view.

Pterygoid — UTA-AASC-432 is a partial right adult specimen representing the lateral pterygoid process. The pterygoid is broad, and elongate along the lateral surface with rounded edges. The lateral surface is raised in a prominent ridge to the anterior that tapers to the posterior. Irregular small pits are visible on the anterior surface, though much smaller than on other regions of the skull (1 mm), providing points for muscle attachment. The pterygoid plate is broken and missing, thus little can be said of the choanae.

Ectopterygoid—UTA-AASC-447 is a partial right adult specimen and UTA-AASC-331 a complete left juvenile specimen. The superior ramus of the ectopterygoid articulates with both the jugal and postorbital in the region of the postorbital bar as a large subrectangular plate. It tapers posteroventrally forming a stout bar that widens into a broad process that articulates with the pterygoid posteromedially.

Dentition— Dozens of isolated teeth were found associated with the cranial and post cranial elements along with some in situ teeth found preserved within the jaws. The teeth are homodont, broad at the base, conical, with a slight curve towards the crown (Fig. 6.18). The teeth all have lateral striations on both the labial and lingual surfaces (Fig. 6.18). As the teeth are broad, not gracile, it is inferred that *Deltasuchus* was a generalist, feeding upon a variety of prey (Noto et al., 2012). Complete juvenile dentary specimens indicate that each dentary contained at least 19-22 teeth. The adult maxilla have approximately 22 teeth (total count based on eroded alveoli), similar in number to the goniopholidids *G. simus* and *Sunosuchus* (Salisbury et al., 1999; and Wu et al., 1996a). The teeth vary in diameter along the length of the jaw. In the maxilla, the teeth broaden to the anterior, doubling in diameter with the largest occurring at the anterior maxillary protrusion. Along the length of the dentary, the teeth also increase in size, until the psdeudocanines, in which they nearly double in size along the lateral margin at a pronounced lateral swelling that extends beyond the lateral

border of the maxilla and premaxilla. The raised alveoli and broad teeth of the pseudocanines are similar to *G. simus* (Salisbury, 1999). The premaxilla has approximately five alveoli, suggesting a similar number of premaxillary teeth as the pholidosaur *Sarchosuchus* (Sereno et al., 2001).

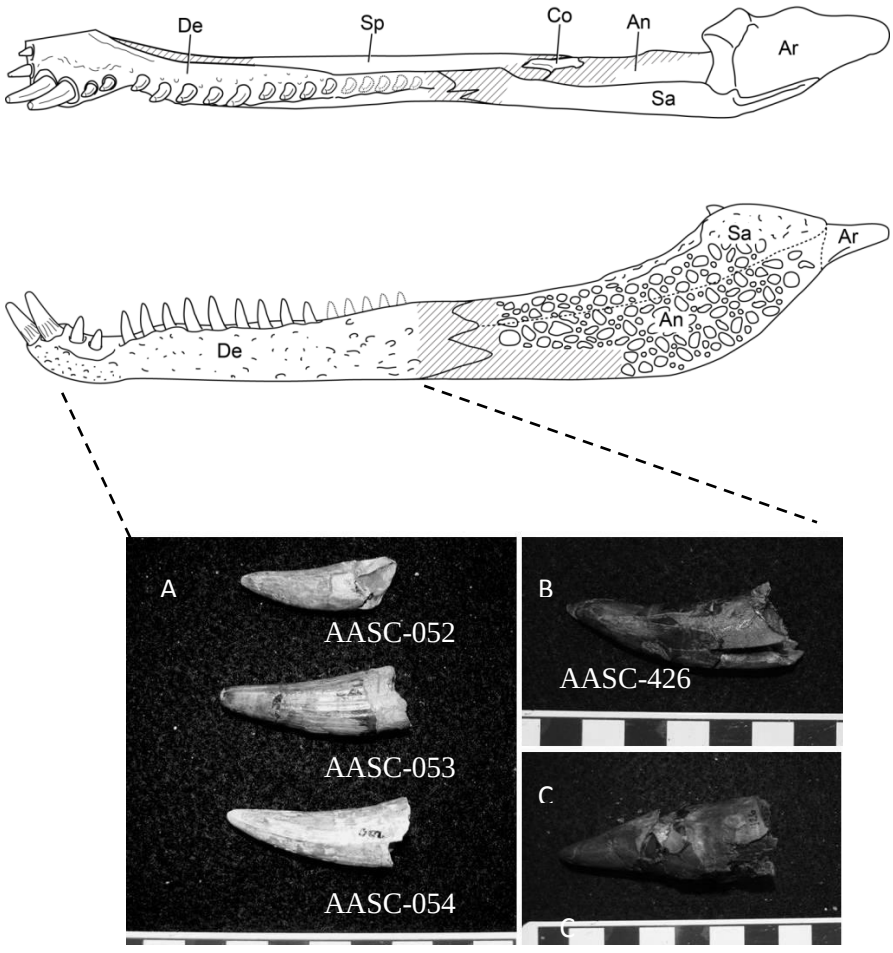

Figure 6.18 *Deltasuchus* teeth. A. UTA-AASC-052, 053 and 054 isolated crocodyliform teeth attributed to *Deltasuchus.* B. UTA-AASC- 426 an isolated tooth from *Deltasuchus* right lateral view. C. UTA-AASC- 426 an isolated tooth from *Deltasuchus* left lateral view.

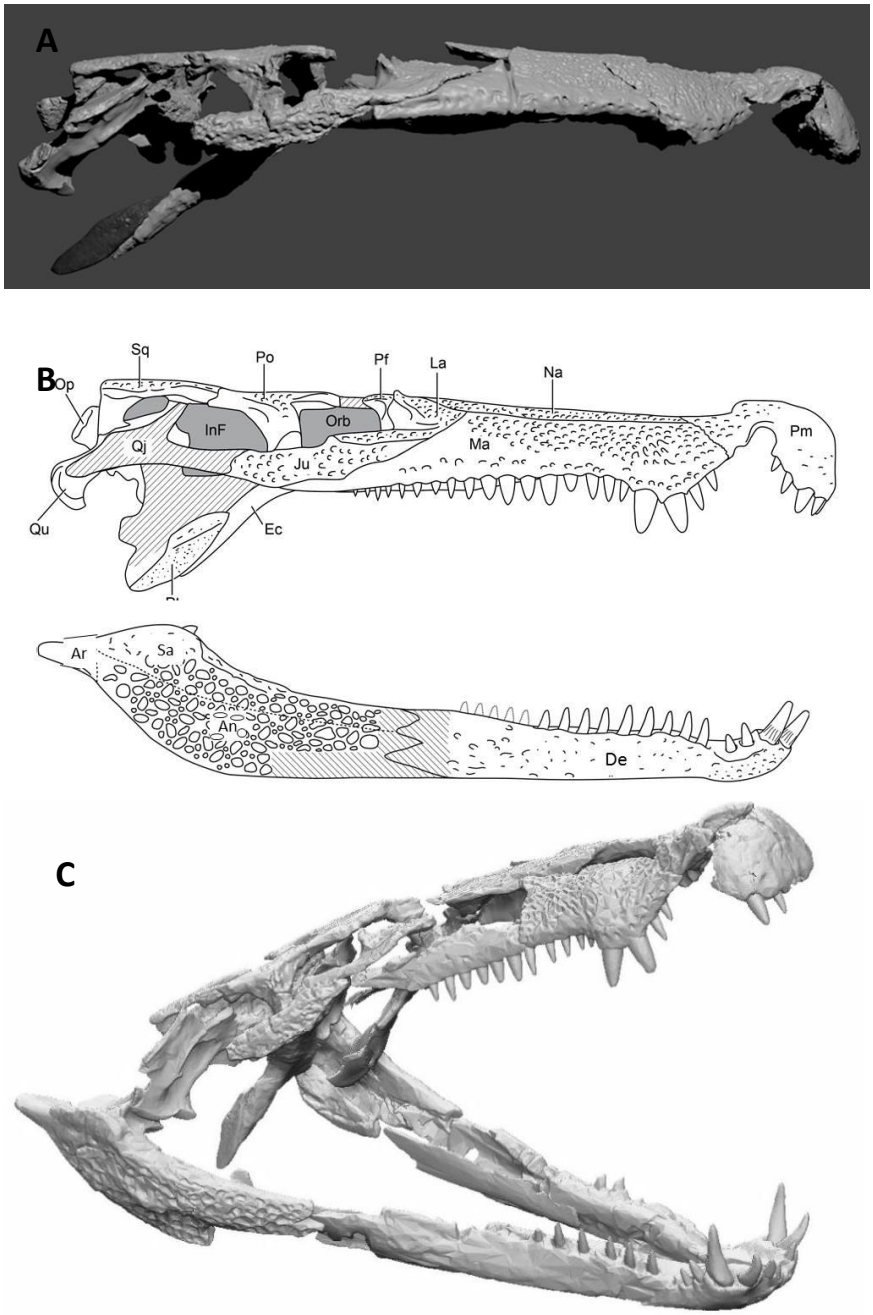

Figure 6.19 A. Digital composite of the skull of *Deltasuchus* constructed from laser scans of multiple individuals, in right lateral view. B. Line drawing of skull in right lateral view based upon laser scans (courtesy C. R. Noto). C. Digital reconstruction of the skull of *Deltasuchus* in right lateral view (reconstruction courtesy of David Killpack).

6.3.2 Post Cranial elements

Cervical vertebra — The cervicals are represented by UTA-AASC-309 a partial atlantal arch, UTA-ASSC-293 an axial centrum, UTA-AASC-280 an odontoid and UTA-AASC-267 a cervical rib. UTA-AASC-039 is a partial left atlal arch that has a broad, rounded pedicle and tapers to a thin blade ventrolaterally. UTA-AASC-293 is an adult axis; it lacks the neural arch and zygopophyseal processes, only the centrum is present. The axial centrum is amphicoelus and has the hourglass shape that is typical of mesosuchians (Salisbury et al., 1999) (Fig. 6.20). Of interesting note, the ventral surface of the centrum has an unusual robust tuberosity that is not seen in goniopholidids, and only reported in the pholidosaur *Oceanosuchus* (Hua et al., 2007). UTA-AASC-280 is an odontoid, the axis and odontoid process (dens) are unfused, as are many of the large cervical vertebrae but most of the largest caudal vertebrae are fused, suggesting that the largest AAS individuals were not yet completely morphologically mature. This feature does not necessarily have a direct relationship with growth though. However, it may be an indication of rapid growth to attain adult size, similar to *Sarcosuchus* (Sereno et al., 2001). The cervical rib UTA-AASC-267 preserves both the tuberculum and the capitulum. The tuberculum is more gracile than the capitulum, which is shorter than the tuberculum and flares laterally into a subtriangular articular facet

(Fig. 6.21). The rib is ventrolaterally deflected, with a prominent caudal surface that terminates in a V shape (Fig. 6.21).

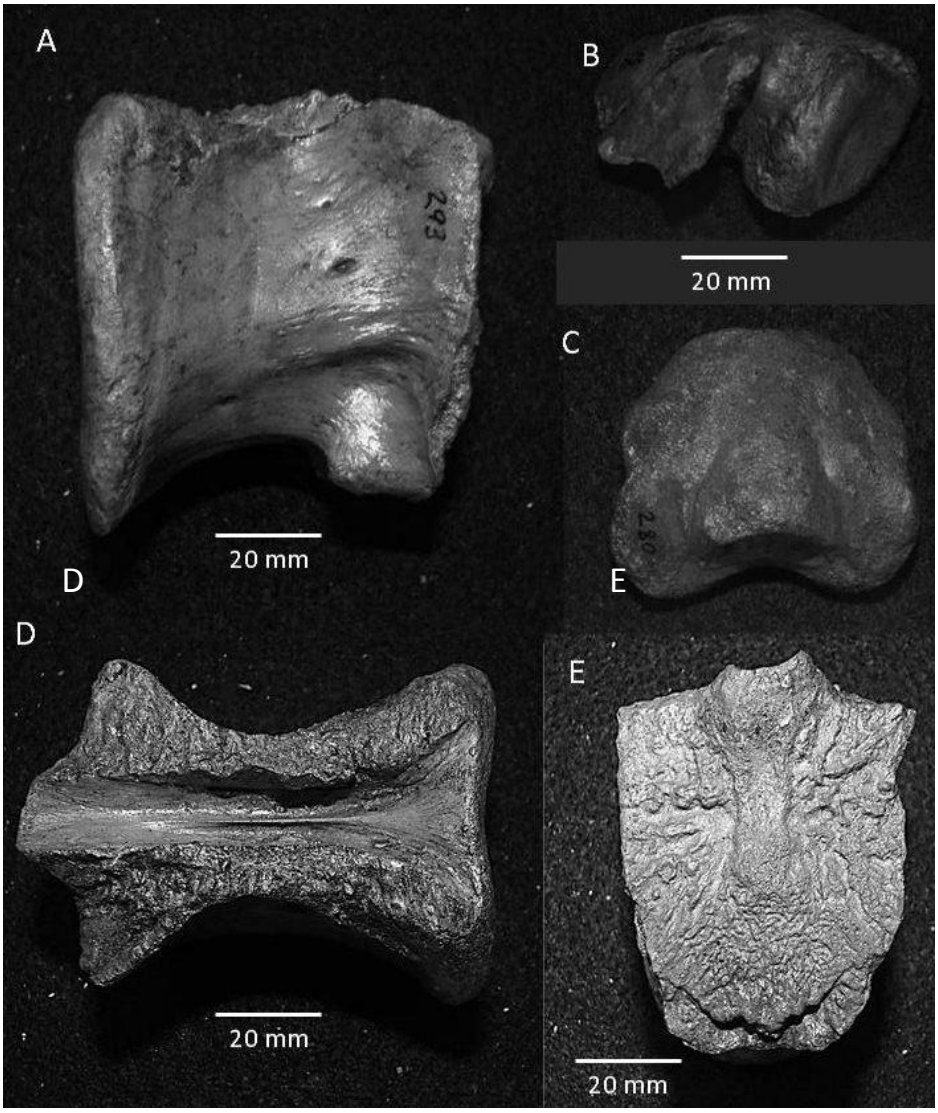

Figure 6.20 *Deltasuchus* cervical vertebrae. A. UTA-AASC-293 axis centrum in lateral view, B. UTA-AASC-039 a partial atal arch. C. UTA-AASC-280 an odontoid. D. UTA-AASC-293 axis neural arch sutures in dorsal view. E. UTA-AASC-293 axis in cranial view.

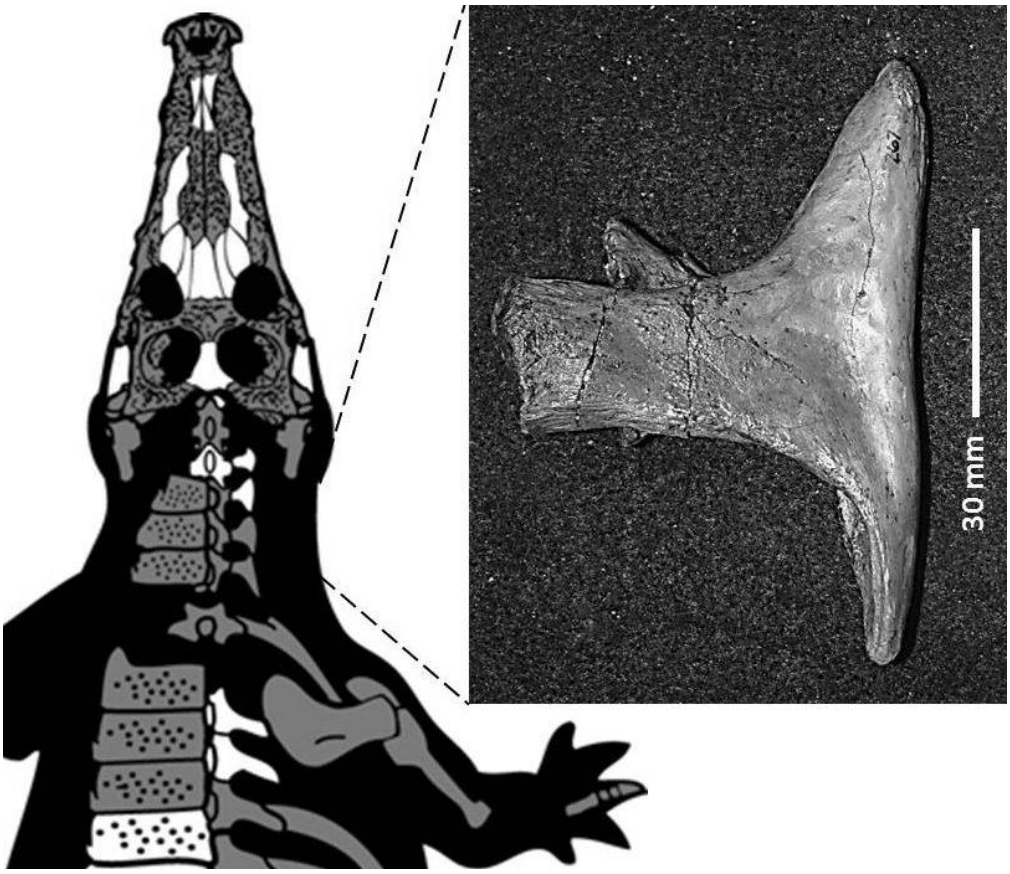

Figure 6.21 *Deltasuchus* ribs. UTA-AASC-267 an adult cervical rib in lateral view (crocodyliform skeletal diagram modified from Sereno et al., 2001).

Dorsal vertebra — The dorsal vertebrae are represented by eight partial adult elements and numerous juvenile elements, many preserved only as centra, with one complete adult specimen that is assigned to the mid thoracic vertebrae. UTA-AASC-102 is one of seven adult dorsal centra; it is amphicoelus and hour glass shaped (Fig. 6.22). UTA-AASC-356 is a juvenile dorsal vertebral centrum; it is amphicoelus, hour glass shaped and ¼ the size of the adult vertebrae (Fig. 6.22).

UTA-AASC-332 is a near complete adult dorsal, with one transverse process missing. The centra are amphicoelus and hourglass shaped, similar to the cervical vertebrae (Fig. 6.22). In anterior and posterior view the centra are rounded and have a distinct keel present on the ventral surface. Only UTA-AASC-332 preserves a neural arch and partial spine. The neural arch and spine are broad with long transverse processes that are ventrally deflected (Fig. 6.22). The neural spine is thick at the base, subrectangular in lateral view at the base and missing the distal half. It is anteroposteriorly wider, more so than what would be expected for the cervicals, and what is seen in the caudals (Fig. 6.20 and 6.22). The pre and postzygapophysial processes are well developed with preygapophysial processes that extend well beyond the centrum. The zygapophysial processes occur high on the neural arch and have slightly oblique, horizontal angles of orientation (Fig. 6.20). The horizontal orientation of the facets is distinct and similar to *Terminonaris robusta* and *Dakotasuchus kingi* (Wu et al., 2001). UTA-AASC-367 is a complete neural arch-spine complex from a juvenile indidual, although smaller than the adult vertebrae, it demonstrates these features more clearly (Fig. 6.22). Vertebral measurements are listed in Table 6.1.

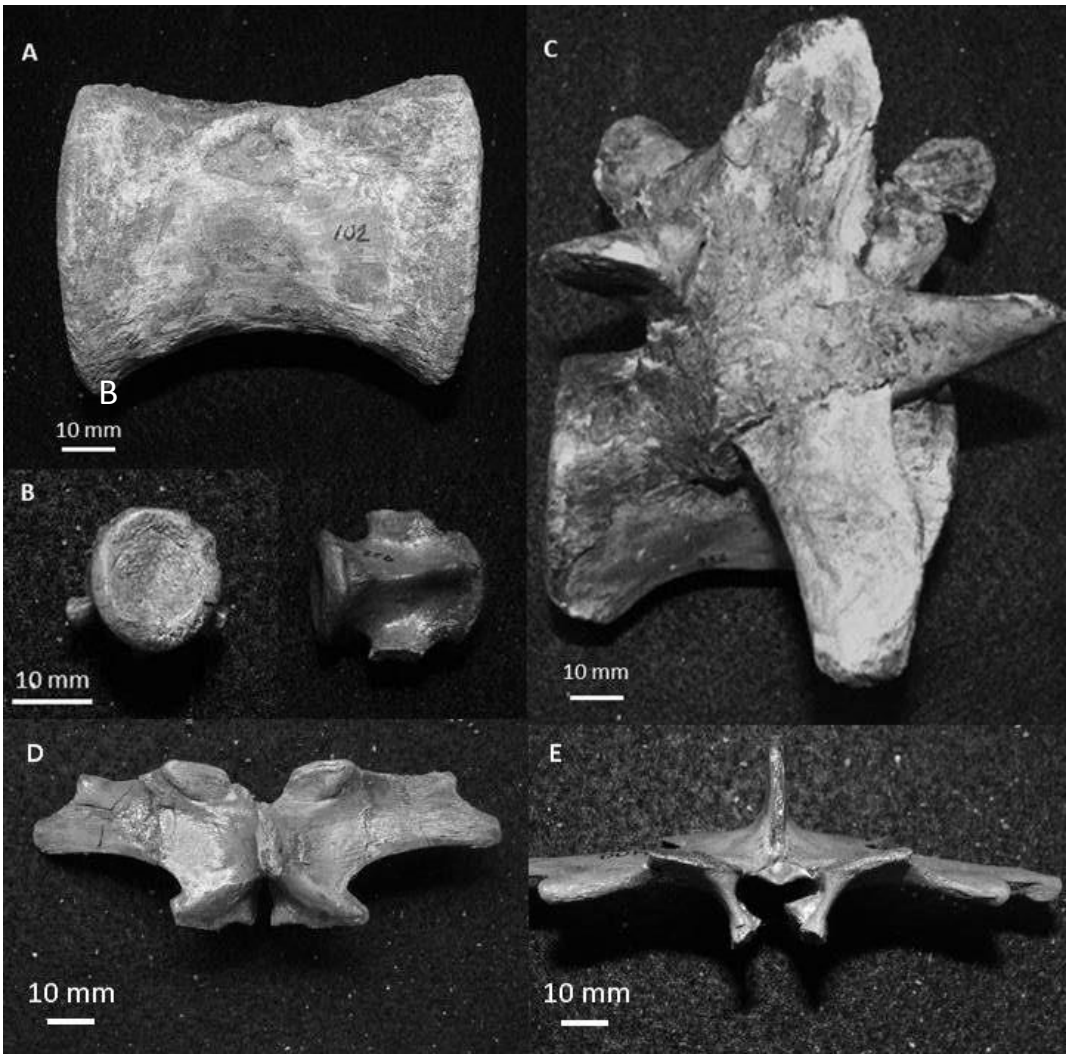

Figure. 6.22 *Deltasuchus* dorsal vertebrae. A. UTA-AASC-102 in lateral view. B. UTA-AASC-356 a juvenile dorsal vertebra in anterior and ventral view. C. UTA-ASSC-332 dorsal vertebrae in lateral view. D. UTA-AASC-367 neural arch with transverse processes in dorsal view. E. UTA-AASC-367 neural arch with transverse processes in anterior view.

Caudal vertebra — The caudals are represented by twelve adult vertebrae. The centra are amphicoelus and elongate, becoming progressively longer distally. The largest are unfused, suggesting that the largest AAS individuals were not yet completely morphologically mature. In anterior view the proximal caudal centra have a distinct heart shape that is not seen in either goniopholidids or pholidosaurs. UTA-AASC-249 and 278 are proximal caudals, they have broad, tall neural spines, long thin transverse processes and reduced zygapophyseal processes (Fig. 6.23). Although reduced in size, the prezygapophysial processes still extend beyond the centrum. The proximal neural spines are tall and subtriangular in lateral view; the spines shorten and become more slender to in the posterior caudals (Fig. 6.22). UTA-AASC-249 and 258 are from the mid-caudal series. The centra are more elongate than the proximal caudals and are gently bowed dorsoventrally (Fig. 6.23). UTA-AASC- 235, 240, 260, 278 and 290 are distal caudals that become more elongate, and narrow with reduced neural arches and zygopophysial processes (Fig. 6.24). The prezygapophysial processes extend well beyond the centrum as seen in the proximal caudals; however the transverse processes are greatly reduced. A longitudinal groove is present on the ventral surface of the caudal centra. Vertebral measurements are listed in Table 6.1.

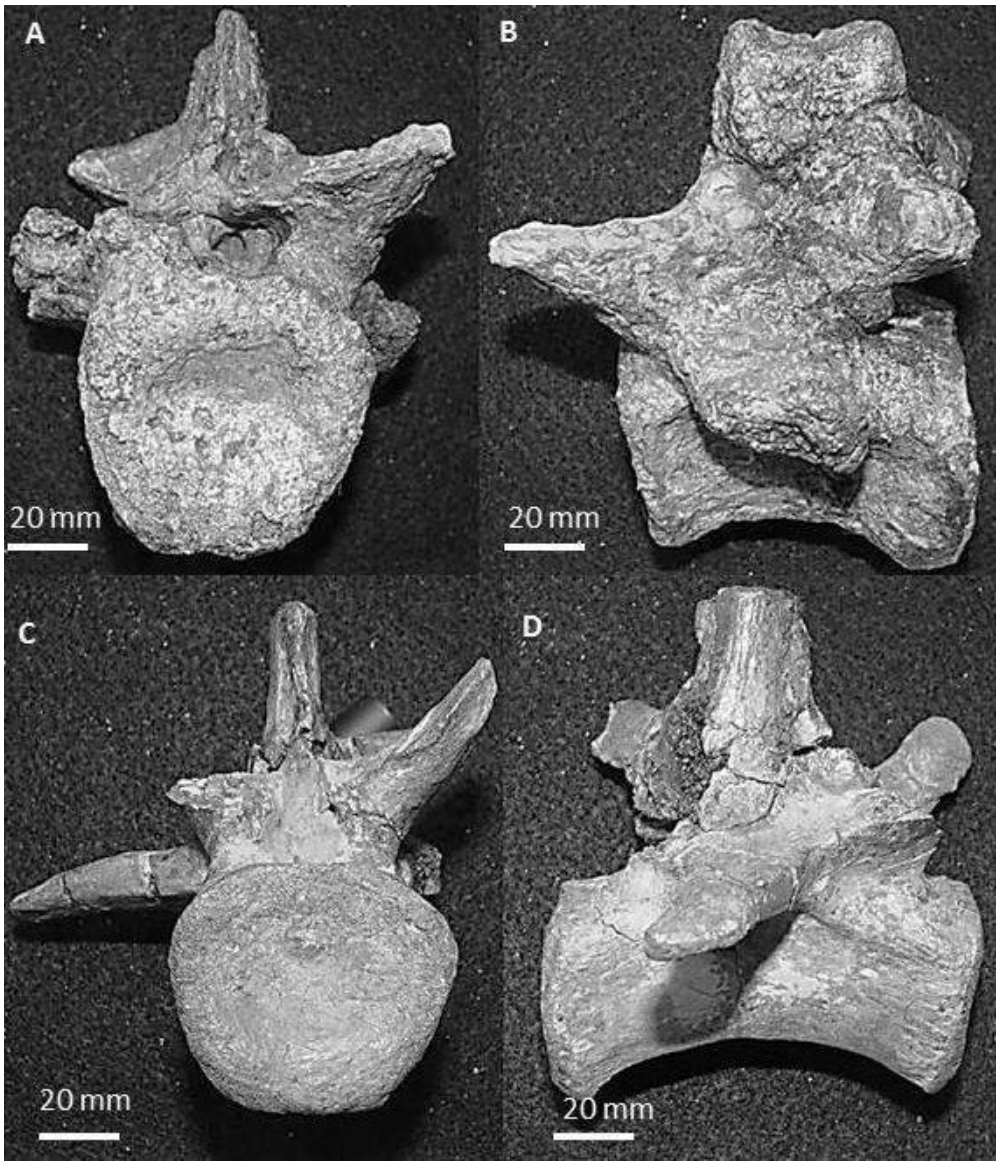

Figure 6.23 *Deltasuchus* caudal vertebrae. A. UTA-AASC-249 proximal caudal vertebrae in anterior view. B. UTA-AASC-249 proximal caudal vertebrae in lateral view. C. UTA-AASC-278 proximal caudal vertebrae in anterior view. D. UTA-AASC-278 proximal caudal vertebrae in lateral view.

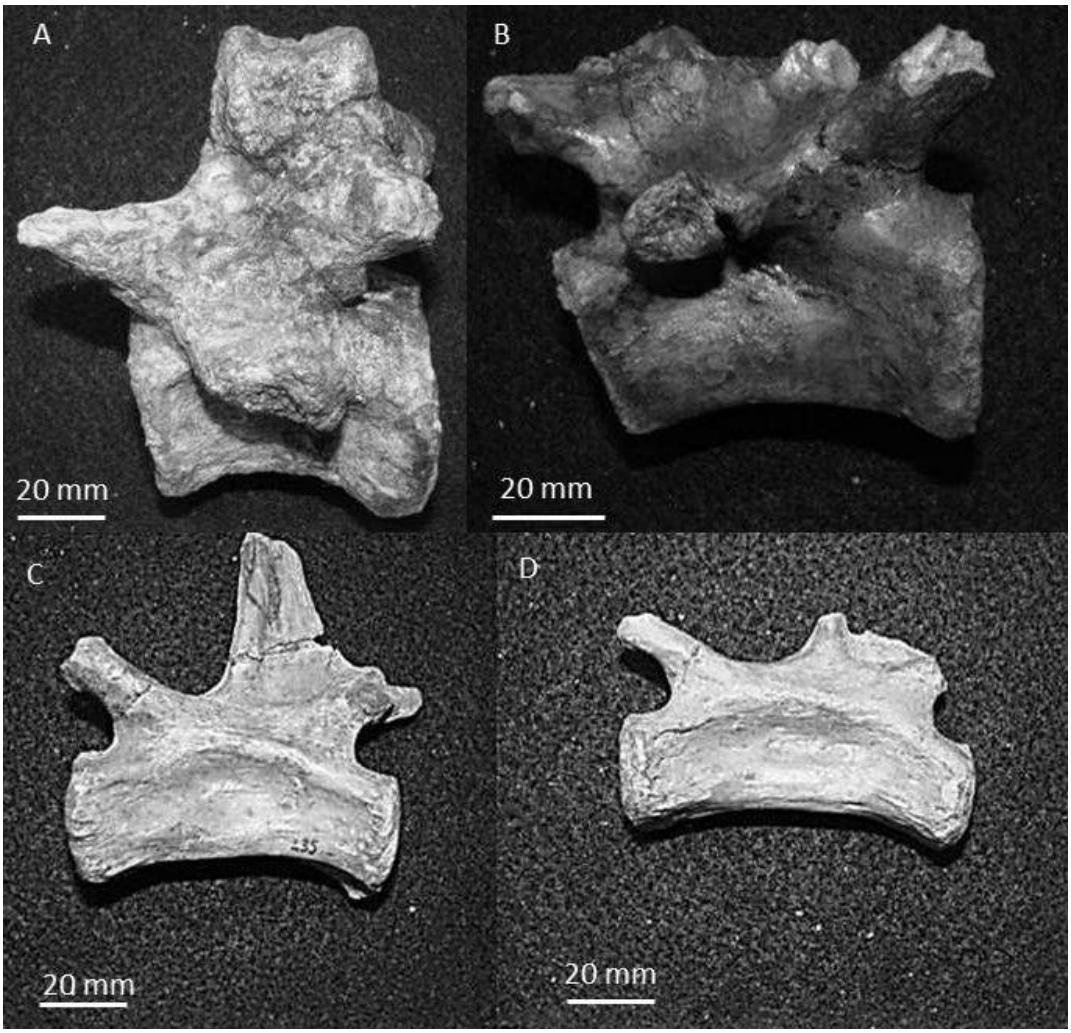

Figure 6.24 *Deltasuchus* caudal vertebrae. A. UTA-AASC-249 proximal caudal. B. UTA-AASC- 290 mid caudal vertebra. C. UTA-AASC-235 distal caudal vertebrae D. UTA-AASC-240 distal most caudal. Centra become progressively elongate.

Scapula — UTA-AASC-340 is a complete juvenile element. It is asymmetric in lateral view with a gently concave cranial surface that expands into a blade like cranial edge and broad, dorsoventrally expanded glenoid (Fig. 6.25). The glenoid broadens distally with a ventral flare, and the sutures are prominent and unfused, a condition typical of juveniles. The shaft is flat and asymmetric, narrowing anteriorly near the glenoid, then gradually widening, leading to a subtriangular caudal surface that is thin, flat and broken dorsally (Fig. 6.25). It is similar in form to *Goniopholis*, but starkly differs from other Woodbine Formation goniopholidids such as *Woodbinesuchus,* which is symmetric in form and lacks the anterior concavity and fan like shape along the cranial edge (Fig. 6.25) (Lee, 1997; Owen, 1878). Measurements listed in Table 6.1.

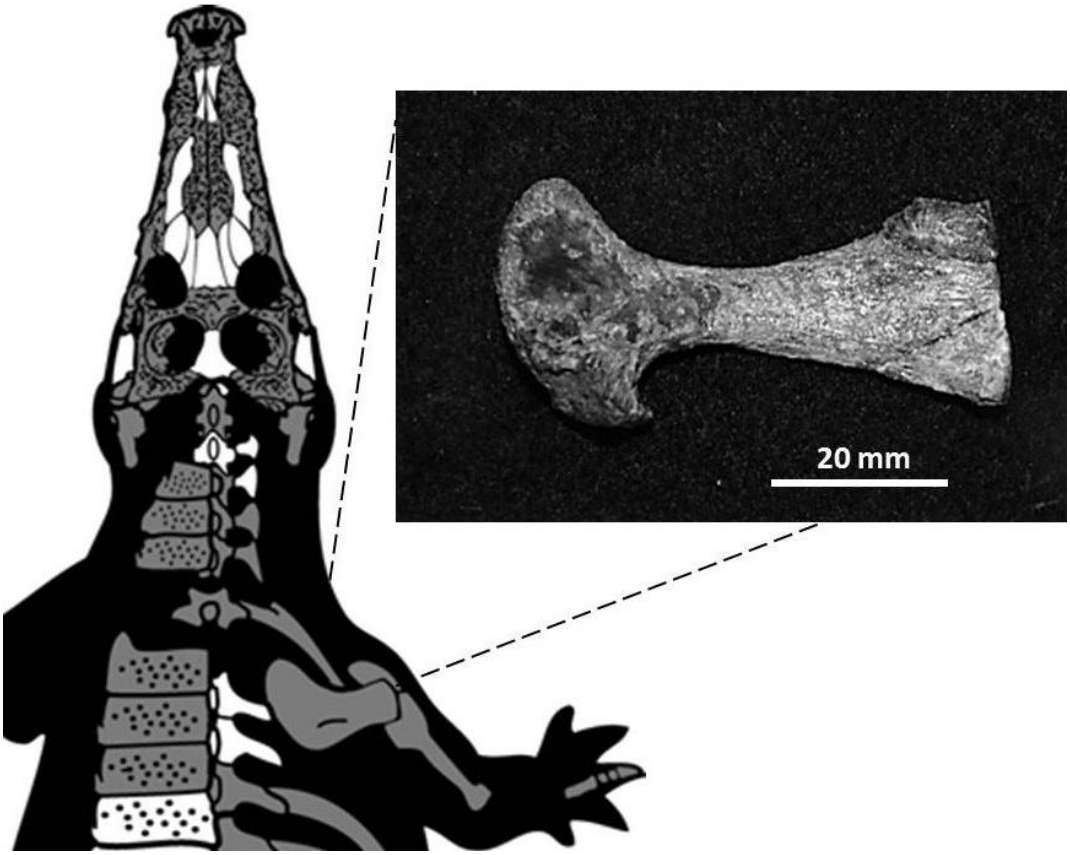

Figure 6.25 *Deltasuchus* scapula. UTA-AASC-340 a juvenile scapula in lateral view, crocodyliform diagram modified from Sereno et al. (2001).

Ilium — UTA-AASC-200 is a near complete right adult specimen (Fig. 6.26). The ilium is a stout, heavy element, much broader than modern crocodylians and having a robust form similar to the goniopholid *G. crassidens* and the pholidosaurs *Sarcosuchus* and *Oceanosuchus* (Hua et al., 2007; Owen, 1878; Sereno et al., 2001). An interesting feature of the ilium is a triangular process that rises over the antitrochanter, forming a right triangle caudally (Fig. 6.26).

A similar feature was noted in *Sarcosuchus* by Sereno et al. (2001). The preacetabular process is greatly reduced and represented by a small anterodorsally oriented triangular process (Fig. 6.26). The ilium has a prominent ridge along the antitrochanter that terminates into a rounded postacetabular process (Fig. 6.26). The postacetabular region of the ilium is incomplete, although what is preserved indicates the postacetabular process is large and robust, possibly triangular to subrectangular in shape. The ischial peduncle is rounded and thicker dorsally than ventrally (Fig. 6.26). The pubic peduncle is a broad process that has two facets and appears subtriangular in ventral view. The acetabular cavity is deep and prominently occupies most of the lateral surface of the bone. Ventrally, the ilium terminates into a thin, concave ridge between the pubic and ischial peduncles.

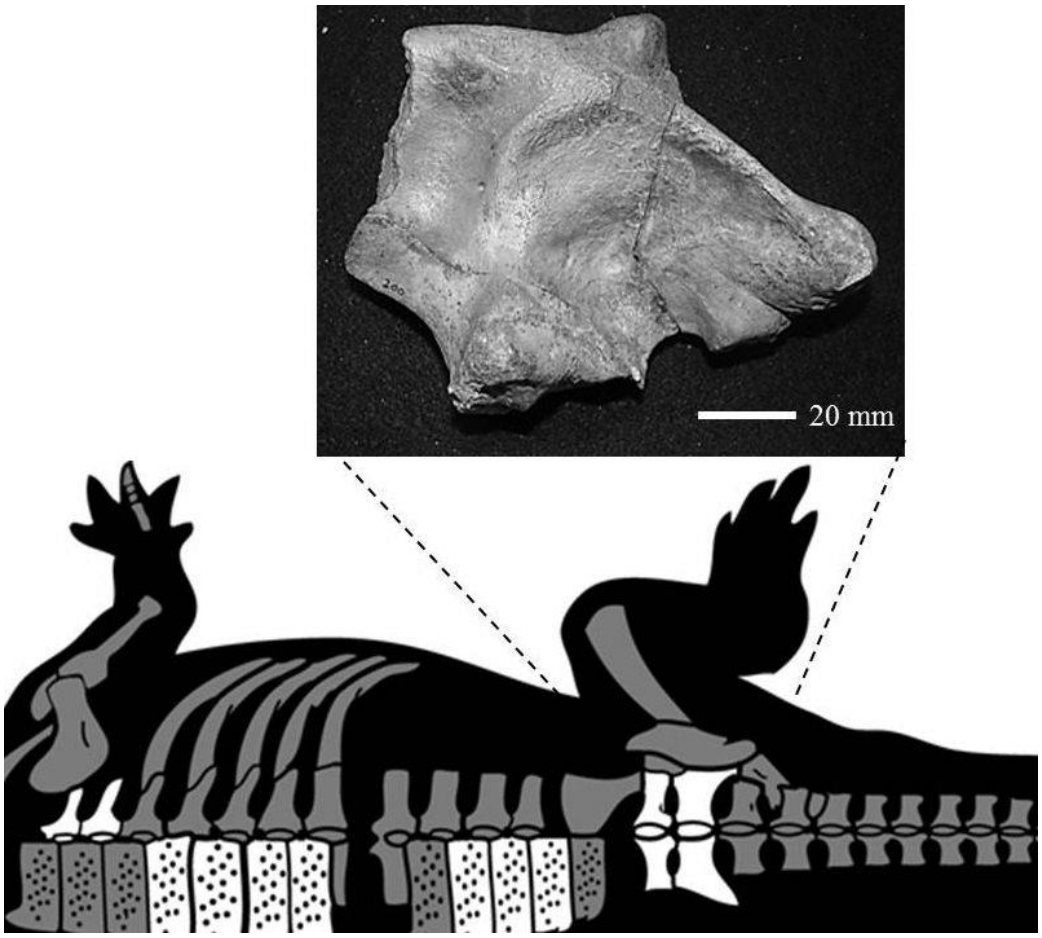

Figure 6.26 *Deltasuchus* ilium. UTA-AASC-200 a left adult ilium in lateral view, crocodyliform diagram modified from Sereno et al. (2001).

.

Ischium — UTA-AASC-405 is a complete left adult, or sub-adult element; it is robust proximally and thins distally (Fig. 6.27). Although it thins distally, the proximal surface is not constricted, as is seen in many mesosuchians, similar in form to *Oceanosuchus* and *Sarcosuchus* (Hua et al., 2007; Sereno et al., 2001). The peduncle has a deep mid-line groove and unfused suture surfaces. Distally,

the ischium broadens into a subtriangular blade that terminates with a thin, flat ridge (Fig. 6.27). Measurements of the pelvic elements are listed in Table 6.1.

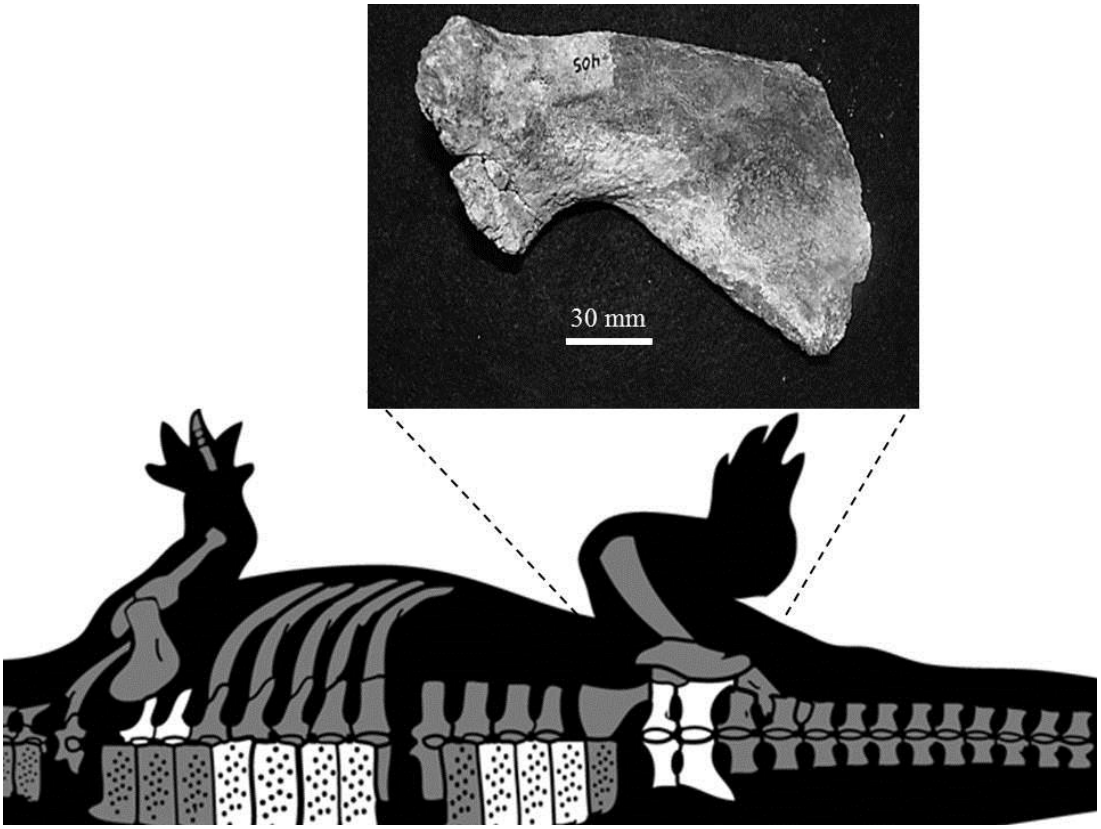

Figure 6.27 *Deltasuchus* ischium. UTA-AASC-405 left adult ischium in lateral view. Crocodyliform skeletal diagram modified from Sereno et al. (2001).

Radius — UTA-AASC-217 is a complete adult radius. It is a gracile, elongate element with a length of 152 mm. The proximal end is thin and fan shaped, with a subtriangular head that gently tapers along the medial surface (Fig 6.28). The

head tapers into a long cylindrical shaft.The distal end is defined by a prominent dorsal tubercle and extensor grooves. As the shaft is thin, it is broken proximally and distally with significant fractures. Limb bone measurements are listed in Table 6.1.

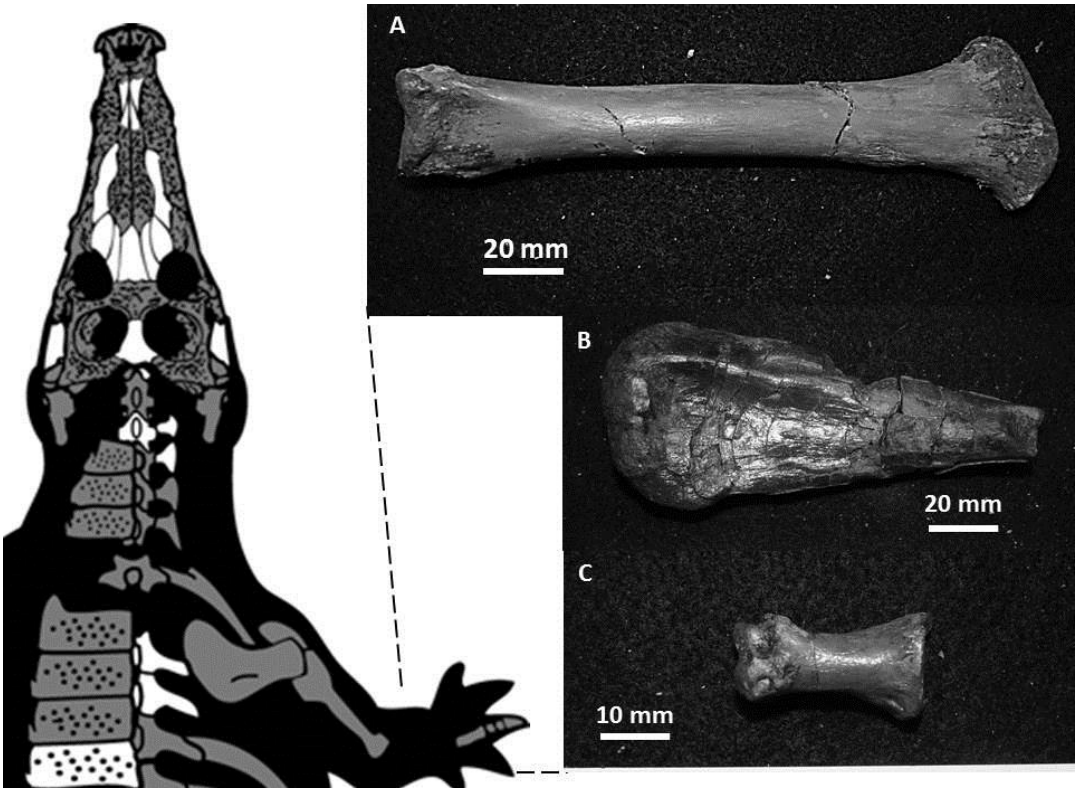

Figure 6.28 *Deltasuchus* limb elements. A. UTA-AASC-217 an adult radius in lateral view. B. UTA-AASC-205 a partial proximal ulna .C. UTA-AASC-212 an adult phalange in dorsal view (crocodyliform skeletal diagram modified from Sereno, 2001).

Humerus — UTA-AASC-285 is a complete, isolated left adult humerus found associated with numerous adult elements from the Crocorama excavation (Fig. 6.29). UTA-AASC-285 is a robust element, it is 33.2 cm long and 3.50 cm wide (Fig. 6.29). It has a broad, large condyle that is deflected ventrally with a gentle 45˚ slope rising away from the shaft and terminating in a flattened, reniform articular surface that has a medial slant (Fig. 6.29). It is much larger proximally than distally. In lateral view the crest is sub-triangular in shape and convex. The deltapectoral crest is a prominent sub-rounded process that sits laterally along the shaft consuming nearly 1/3 of the length of the shaft and gently deflects mediolaterally at a 90˚ angle (Fig. 6.29). The shaft is flattened proximally, fractured in the middle, with a slight curve that terminates with a distal process that turns 45˚ away from the shaft and terminates into broad articular condyles that are not equally developed (Fig. 6.29). The capitellum is large, rounded and broader anteriorly creating an anterolateral to medial slant to the articular surface (Fig. 6.29). The two distal condyles are separated by a shallow, concave trochlea which continues the depressed structures of the supracondylar ridges of the humerus (Fig. 6.29). The ridges are subequal with the lateral ridge being more prominent. The humerus articulates with the pectoral girdle at an angle that would produce a sprawling gait typical of the crocodyliforms.

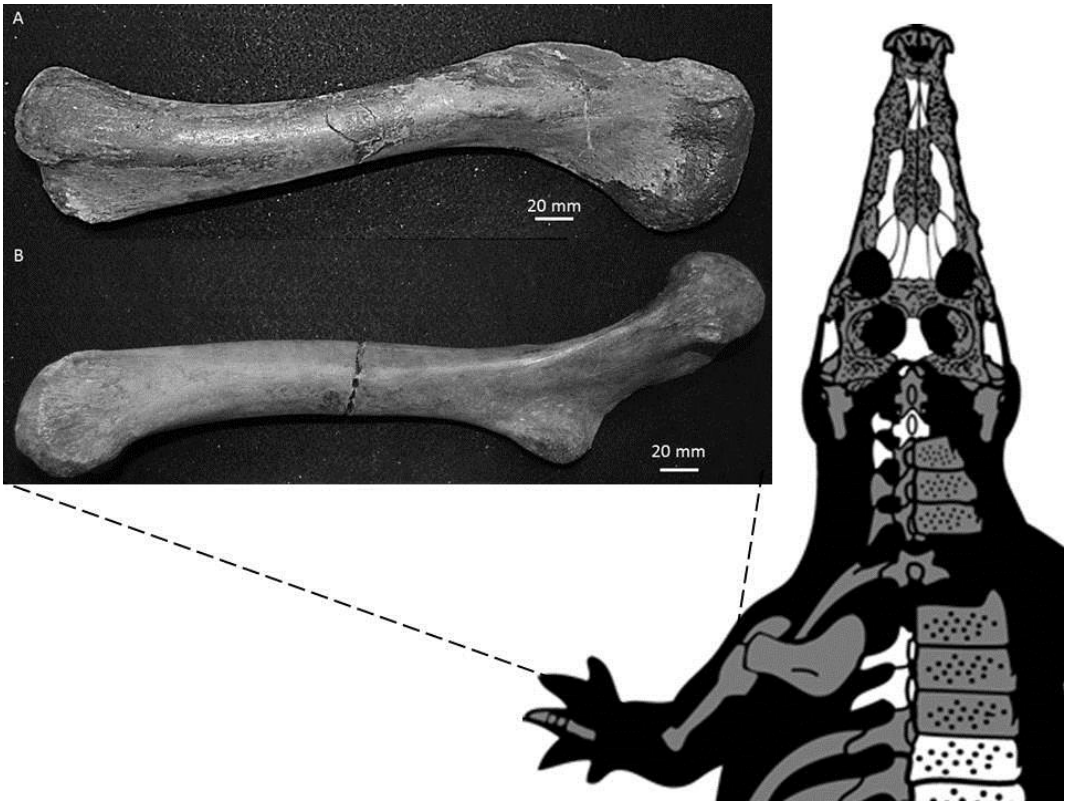

Figure 6.29 *Deltasuchus* humerus. A. UTA-AASC-285 an adult humerus in dorsal view view. B. UTA-AASC-285 in posterior view with the deltapectoral crest denoted (Dpc). Crocodyliform skeletal diagram modified from Sereno et al. (2001).

Femur —UTA-AASC-444 is a complete juvenile femur, it is 24 cm long and 2.8 cm wide at mid-shaft. The femur is sigmoidal in anterior view with an elongate shaft that expands into a pronounced femoral head, greater trochanter and medial condyle (Fig. 6.30). The proximal end of the femur is subtriangular in outline. The femoral head is well developed and sits upon an elongated proximal shaft that is dorsoventrally flattened and directed medially towards the acetabulum (Fig.

6.30). The prominent fourth trochanter is situated distally from the proximal end, and it is subrounded, gently merging into the shaft. The shaft is elongate and stout, with a smooth surface. The shaft is rounded medially, with a slight flattening associated with the proximal curvature of the shaft (Fig. 6.30). The distal end terminates with a pair of prominent condyles. The medial condyle is robust, subangular in anterior view and larger than the lateral condyle, with a small medial depression (Fig. 6.30). The lateral condyle is small and flattened with a narrow lateral groove for muscle attachment. Measurements of the limb bones are listed in Table 6.1.

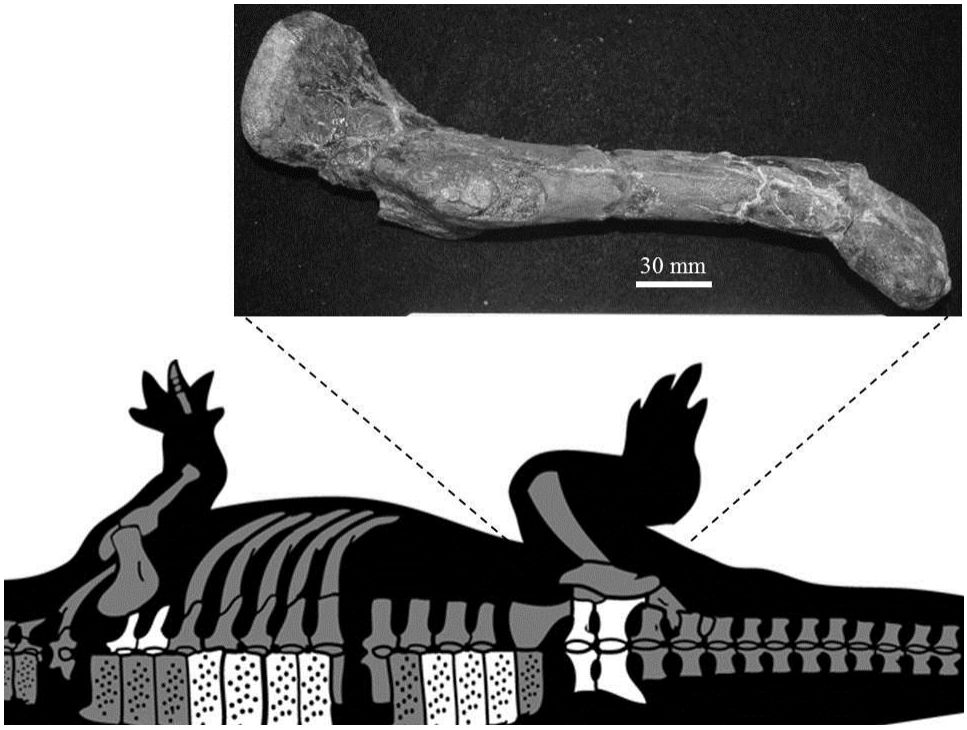

Figure 6.30 *Deltasuchus* femur. UTA-AASC-444 juvenile femur in lateral view. Crocodyliform skeletal diagram modified from Sereno et al., (2001).

Osteoderms — Numerous associated juvenile and adult osteoderms were recovered, primarily from the dorsal series, with very few recovered from the ventral series. All of the osteoderms have deep, subrounded to elongate pits on the dorsal surface. UTA-AASC-001, 234 and 276 are among the largest, best preserved adult osteoderms that were recovered and belong to the dorsal series (Fig. 6.31) (see Table 6.1 for data). Numerous juvenile osteoderms were recovered; all were small, thin and fragile. UTA-AASC-341, 394 and 408 were among the best preserved, with UTA-AASC-394 representing the most complete ventral osteoderm (Fig. 6.31).

The dorsal osteoderms are rectangular, have overlapping articular surfaces along the anterior and posterior edges, and the distinct hook shaped processus articularis that extends outward from the anterolateral end at 90° first noted in *Goniopholis* by Owen (1841). The processus articularis underlies the adjoining osteoderm so that they are longitudinally locked. The processus articularis is subrounded in comparison to goniopholidids *G. simus* and *G. crassidens*, in which the process terminates in a sharp, angled projection (Fig. 6.31). It is similar in comparison to pholidosaurs, in which a short subrounded keel leads into an angled edge along the distal ends of the largest dorsal osteoderms. This feature is similar in form to the osteoderms of *Sarcosuchus* (Sereno et al., 2001). The caudal osteoderms are smaller than the dorsal series, they are subrounded in form and

lack the distinct hook shaped processus articularis. The ventral osteoderms are small and hexagonal in form with shallow, rounded pits on the surface (Fig. 6.31).

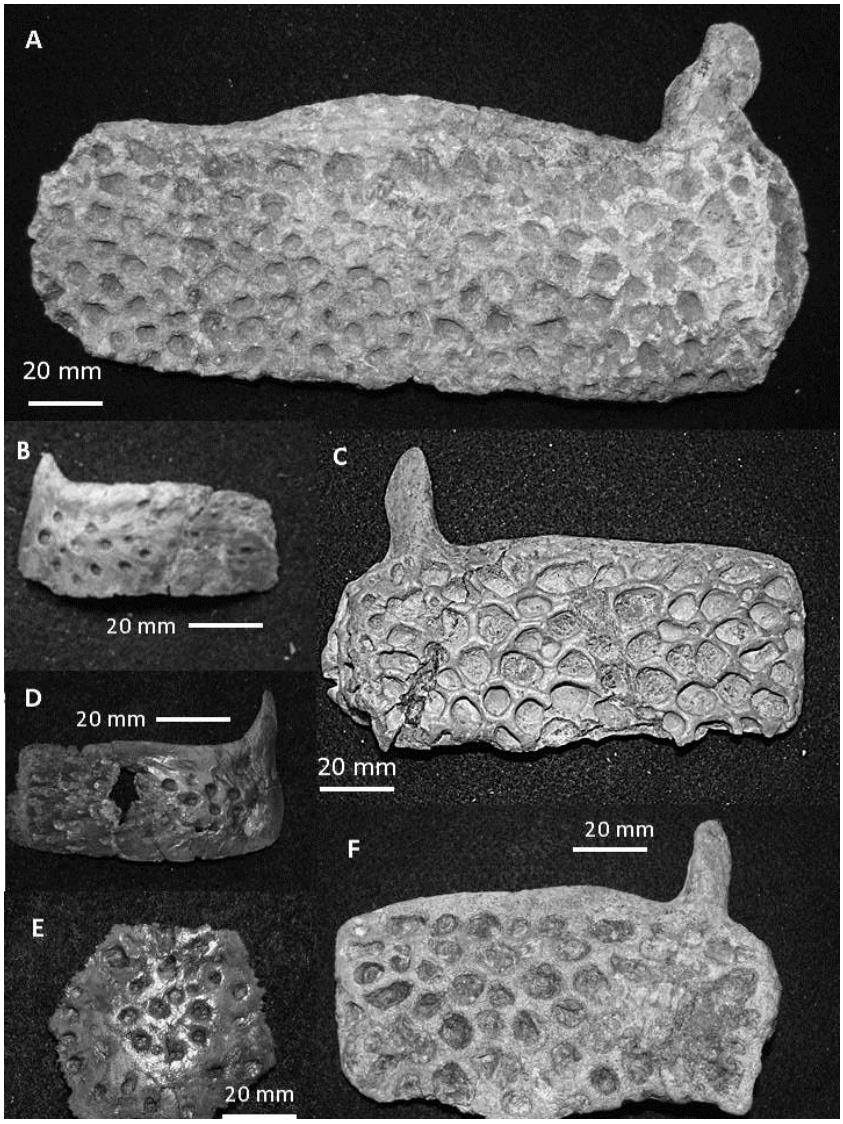

Figure 6.31 Osteoderms of *Deltasuchus*, adult and juvenile. A. UTA-AASC-234 an adult dorsal osteoderm (lumbar). B. UTA-AASC-341 a juvenile dorsal osteoderm. C. UTA-AASC-276 an adult osteoderm from the dorsal series. D. UTA-AASC-408 a juvenile dorsal osteoderm. E. UTA-AASC-394 a juvenile ventral osteoderm. F. UTA-AASC-001 an adult osteoderm, distal dorsal series.

Table 6.1 – *Deltasuchus* element data (in cm), for map data see Appendix B.

UTA Specimen #	Element ID	L x W	Site and Grid #
Crania:			
UTA-AASC-304	Right Dentary	4.8 L x 4.4 W	Crocorama (-6.6)
UTA-AASC-256	Left Dentary	12 L x 7 W	Crocorama (5.5)
UTA-AASC-257	Right Dentary	14 L x 7 W	Crocorama (9.5)
UTA-AASC-448	Left Premax	10.6 L x 4.8 W	Crocorama (5.5)
UTA-AASC-286	Right Maxilla	19 L x 9.5 W	Crocorama (4.4)
UTA-AASC-250	Right Maxilla	29.5 L x 8.4 W	Crocorama (5.4)
UTA-AASC-404	Left Maxilla	20 L x 9.8 W	Crocorama (4.4)
UTA-AASC-251	Left Maxilla	21.5 L x 5 W	Crocorama (5.4)
UTA-AASC-389	Left Palatine (j)	7.4 L x 0.8 W	Nursery (-21.2)
UTA-AASC-327	Right Nasal	20.4 L x 4.6 W	Crocorama (4.4)
UTA-AASC-328	Left Nasal	12 L x 4.5 W	Crocorama (4.4)
UTA-AASC-326	Mandible	12.4 L x 4 W	Crocorama (5.4)
UTA-AASC-346	Right Mand (j)	11 L x 1.5 W	Nursery (-19.3)
UTA-AASC-306	Left Mandible (j)	12 L x 1.6 W	Crocorama (-6.8)
UTA-AASC-354	Left Mandible (j)	15.4 L x 1.6 W	Nursery (-20.2)
UTA-AASC-207	Left Mandible (j)	11.4 L x 1.2 W	Crocorama (14.6)
UTA-AASC-430	Right Mandible (j)	18.4 L x 2.6 W	Crocorama (-5.5)
UTA-AASC-270	Tooth	4.8 L x 2 W	Crocorama (6.5)
UTA-AASC-220	Tooth	5.0 L x 2.5 W	Crocorama (8.5)
UTA-AASC-426	Tooth	5.6 L x 2.2 W	Crocorama (-5.5)

Table 1 continued

UTA-AASC-248	Left Jugal	17.8 L x 4 W	Crocorama (5.3)
UTA-AASC-214	Rht Post Orbital1	1.1 L x 6.5 W	Crocorama (8.4)
UTA-AASC-201	Rht Surangular (j)	5.0 L x 2.4 W	Crocorama (10.9)
UTA-AASC-218	Right Quadrate	13.6 L x 9 W	Crocorama (8.5)
UTA-AASC-429	Left Quadrate	12.8 L x 9.4 W	Crocorama (8.5)
UTA-AASC-314	Right Angular	9.4 L x 4 W	Crocorama (-9.3)
UTA-AASC-430	Left Splenial	18.6 L x 2.6 W	Crocorama (-5.5)
UTA-AASC-409	Right Frontal	4.25 L x 3.9 W	Crocorama (11. 9)
UTA-AASC-287	Left Exoccipital	11.8 L x 6.2 W	Crocorama (5.5)
UTA-AASC-406	Rt Exoccipital	14.6 L x 4.8 W	Crocorama (7.4)
UTA-AASC-431	Right Squamosal (j)	6.0 L x 2.5 W	Crocorama (15.8)
UTA-AASC-440	Left Squamosal (j)	6.2 L x 3.5 W	Crocorama (13.10)
UTA-AASC-414	Basioccipital	6.0 L x 7 W	Crocorama (5.3)
UTA-AASC-311	Basioccipital	5.0 L x 4.5 W	Crocorama (-8.6)
UTA-AASC-439	Basioccipital	2.5 L x 3.4 W	Crocorama (18.5)
UTA-AASC-360	Basioccipital	2.4 L x 2.2 W	Crocorama (-18.5)
UTA-AASC-447	Ectopterygoid	4.4 L x 1.2 W	Crocorama (-20.6)
Post-Crania:			
UTA-AASC-285	Humerus	33.2 L x 3.5 W	Crocorama (4.4)
UTA-AASC-444	Femur	24 L x 2.8 W	M. Turtle (-155, 10)
UTA-AASC-217	Radius	14.4 L x 1.5 W	Crocorama (8.5)
UTA-AASC-405	Ischium	11 L x 4 W	Crocorama (5.4)

UTA –AASC-200	Ilium	14.5 L x 12 W	Crocorama (10.5)
UTA-AASC-309	Atlas neural arch	5.0 L x 2.1 W	Crocorama (-7.5)
UTA-AASC-280	Axis odontoid	5.0 L x 3.6 W	Crocorama (3.6)
UTA-AASC-293	Axis centrum	5.7 L x 4.2 W	Crocorama (4.6)
UTA-AASC-249	Vertebra (caudal)	6.2 L x 8.4 W	Crocorama (5.3)
UTA-AASC-258	Vertebra (caudal)	6.6 L x 5.5 W	Crocorama (6.3)
UTA-AASC-235	Vertebra (caudal)	6.0 L x 6.5 W	Crocorama (7.5)
UTA-AASC-278	Vertebra (caudal)	6.8 L x 7.4 W	Crocorama (2.10)
UTA-AASC-290	Vertebra (caudal)	6.1 L x 4.8 W	Crocorama (4.6)
UTA-AASC-240	Vertebra (caudal)	5.6 L x 3 W	Crocorama (7.7)
UTA-AASC-260	Vertebra (caudal)	5.7 L x 3 W	Crocorama (6.4)
UTA-AASC-332	Vertebra (dorsal)	6.4 L x 9.2W	Crocorama (11.8)
UTA-AASC-267	Cervical rib	8.7 L x 6.2 W	Crocorama (6.5)
UTA-AASC-234	Osteoderm	22.2 L x 8.4 W	Crocorama (7.4)
UTA-AASC-276	Osteoderm	14.6 L x 6.2 W	Crocorama (2.5)
UTA-AASC-340	Scapula (j)	5.6 L x 1 W	Crocorama (-18.3)

Most fossils are adult elements from the AAS Crocorama site, unless otherwise stated. Juvenile specimens are denoted with a (j). Element data: L = length and W = width.

6.4 Discussion

Deltasuchus is a distinct new taxon of crocodyliform from the Woodbine Formation of North Central Texas. It has a robust, triangular snout, which differentiates it from other Woodbine crocodyliforms, the longirostrine goniopholidid *Woodbinesuchus*, and the pholidosaur *Terminonaris*. The broad, generalist alligatorid morphotype suggests that *Deltasuchus* was a generalist that had a broad range of feeding habits and represents a unique ecopmorphotype within coastal Woodbine ecosystems (Brochu, 2001; and Noto et al., 2012). The skull shares general morphologic similarities referable to the goniopholids *G. simus* and *G. crassidens*, along with specific features of the pholidosaurs *Denazinosuchus* and *Sarchosuchus* (Lucas and Sullivan, 2003; Owens, 1878; Salisbury et al., 1999; and Sereno et al., 2001). It is distinguished by a broad, robust skull with deep pitting across the dorsal surface, enlarged supratemporal fenestrae, a strong concavity along the lateral surface of the premaxilla-maxilla suture for the reception of the pseudocanines, an undivided external naris, elongate nasals and broad triangular mandibles (Fig. 6.32).

Deltasuchus was a broad snouted predator that sought a variety of prey along a low lying coastal plain. Within the Woodbine Formation, *Deltasuchus* is one of several reported taxa, but likely represents an apex predator among the Woodbine crocodyliforms. When they co-occur, crocodyliforms tend to have variable ecomorphotypes (Brochu, 2001). Other Woodbine Formation

crocodyliforms, *Woodbinesuchus* and *Terminonaris*, had long, relatively thin snouts (Adams et al., 2011; Lee, 1997). Ecomorphologically, long snouted forms typically represent coastal piscivores. *Deltasuchus*, with its broad crushing snout, likely filled a different ecological role. Both in the modern world and in the deep past, when multiple taxa live in the same region, each taxon will fill a different ecological niche, reducing competition for resources (Brochu, 2001). Bite mark feeding traces found on both turtle shell and dinosaur bones recovered from the AAS support the generalist feeding ecomorphotype (Noto et al., 2012). Specific evidence of turtle crushing feeding behavior, as well as dinosaur bone gnawing was documented at the AAS was discussed in further detail in Noto et al. (2012).

The co-occurrence of remains and bite marks of different crocodyliform ages suggests that the AAS, or immediate vicinity, may have been a crocodyliform nesting area that was revisited over multiple breeding seasons. Adult crocodyliforms collected prey in the surrounding area, potentially storing some captured prey items in caches for future feeding. Juveniles could then feed on this carrion as well as other small prey, with prey preference changing through ontogeny (Milàn et al., 2010; Njau and Blumenschine, 2006; Sullivan and Lucas, 2003).

The AAS has demonstrated a paucity of theropod material to date. The lack of material and diagnostic theropod tooth marks on recovered bitten bones

suggests that crocodyliforms were the likely apex predators of the AAS coastal ecosystem (Noto et al., 2012; Noto and Main et al., 2012). In modern ecosystems crocodylians are known to feed upon a diversity of prey from the surrounding community (Cott, 1961; Delany and Abercrombie, 1986; Nopsca, 1902; Weigelt, 1989). Whereas the cranial and dental morphology of the AAS crocodyliform could be interpreted as adaptations for a crushing diet, comparison with fossil and living crocodyliforms supports a more generalized diet. The bite marks described by Noto et al. (2012) from the AAS provide additional evidence of crocodyliform predation on dinosaurs and represents the best evidence for this behavior outside of Late Cretaceous communities (Rivera-Sylva et al., 2009; Schwimmer, 2002; Schwimmer and Harrell, 2010).

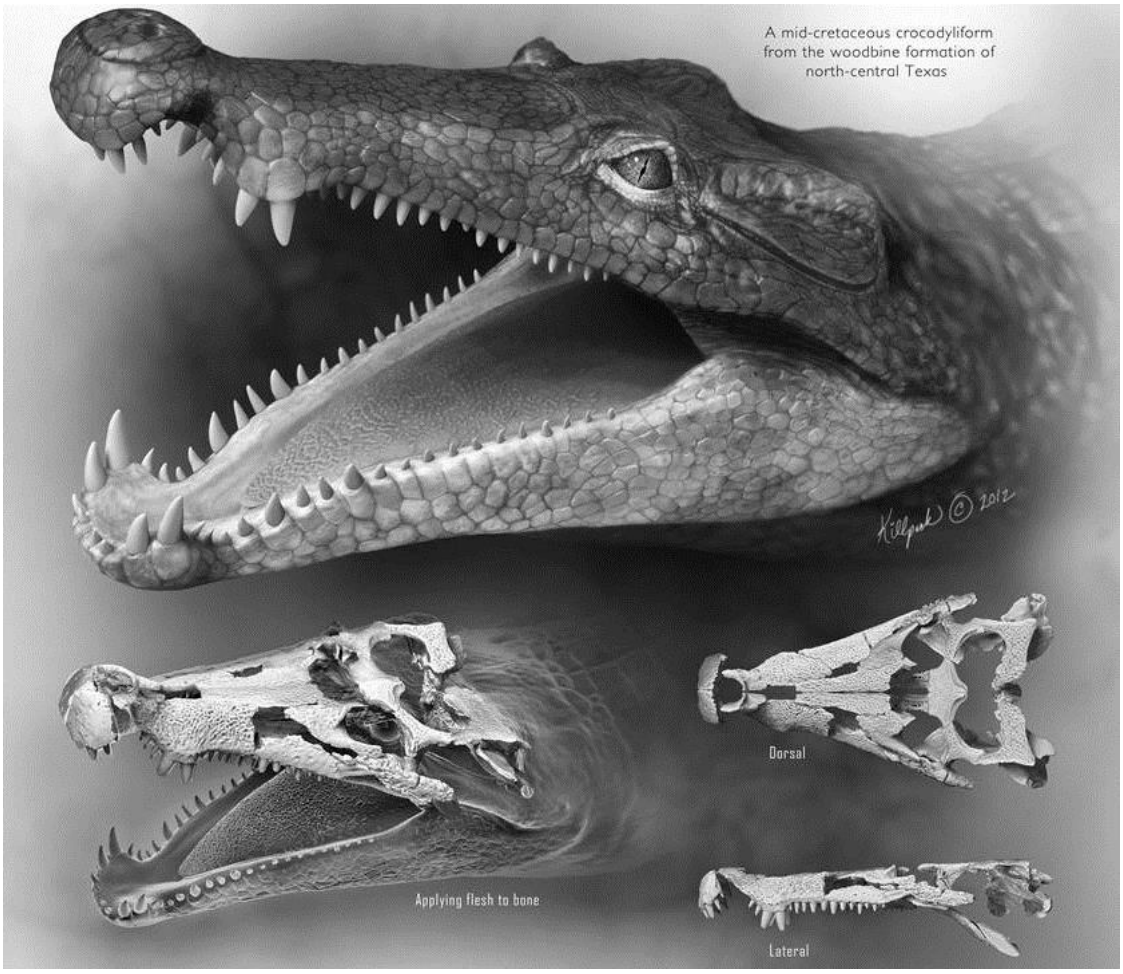

Figure 6.32. Artist reconstruction of *Deltasuchus*, the cranial anatomy and surficial appearance in lateral, dorsal and oblique views (artwork courtesy of medical illustrator David Killpack, 2012).

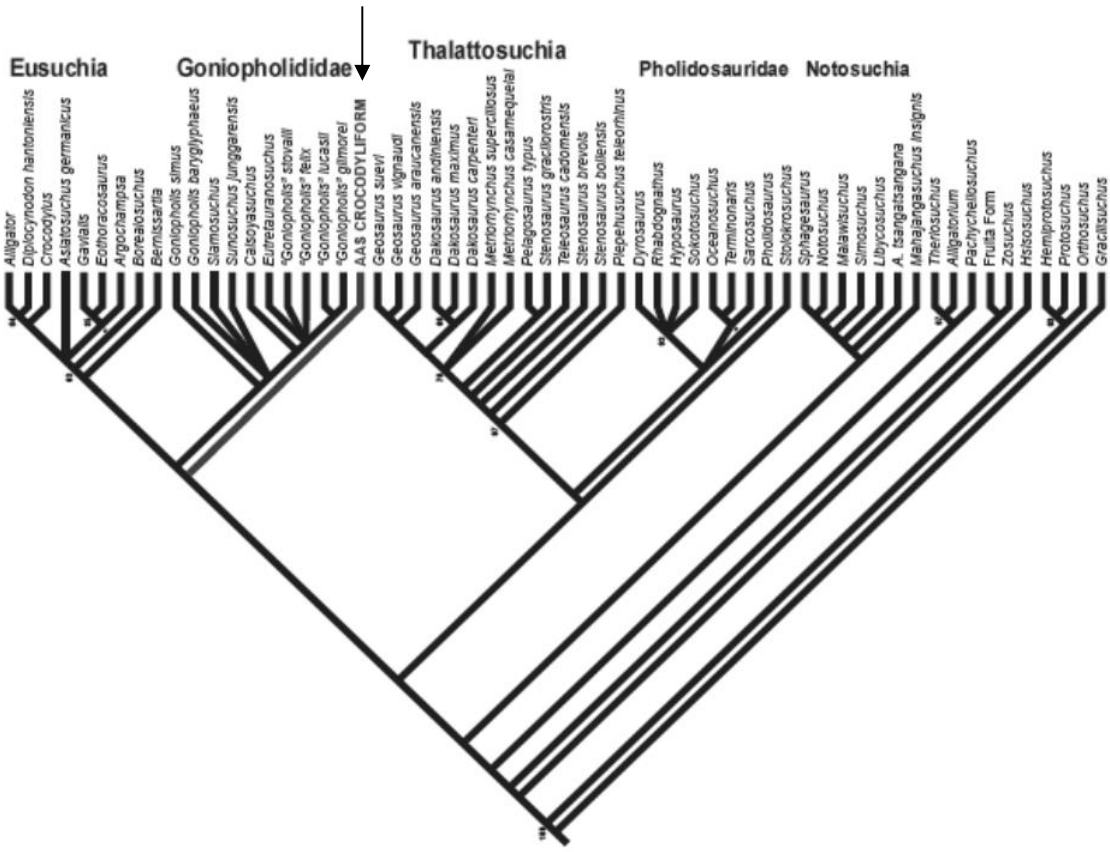

Figure 6.33 Phylogenetic analysis of the AAS crocodyliform. A strict consensus tree of 540 equally-optimal trees. Length=718, C.I. = .36 R.I. =.68. Numbers indicate bootstrap support. Matric incorporates 210 characters (172 cranial, 38 postcranial). Analyzed using TNT (Goloboff et al., 2003) and modified from Allen et al. (2011).

A phylogenetic analysis following Turner and Buckley (2008) and Allen (2010) recovers *Deltasuchus* as a sister taxon to Eusuchia and Goniopholididae (Fig. 6.33). The analysis was primairly based upon the general broad shaped skull morphology and squamosals which overhang the temporo-orbital opening and the broad premaxilla that overhang the dentary. This result is weakly supported as the

taxon retains numerous pleisomorphic and homoplastic characters, such as "goniopholidid-style" paravertebral osteoderms and extensive polygonal ventral osteoderms, which make precise phylogenetic placement difficult. *Deltasuchus* is an interesting taxon as it preserves a mix of characters that may be attributed to both the goniophoidids and to the phlidosaurs, characters that may reflect the paleobiogeography of the taxon. Equally, *Deltasuchus* may represent a previously unsampled lineage of mesoeusuchian diversity and help to elucidate relationships among crocodyliforms, particularly the placement of problematic Mesozoic clades such as the goniopholidids and the pholidosaurs.

6.5 Acknowledgements

I thank the Huffines, Robert Kimball at the Viridian Properties and HC LOBF Arlington for granting access to the land in which the fossils were found, the Motheral family for reporting the discovery and assisting with the excavation. I thank my research colleagues; Chris Noto, Eric Allen, Stephanie Drumheller, Art Busbey, and Rachell Peterson for their assistance. Chris Noto's laser scans of the skeletal material, and the line drawings produced from them, were of tremendous value to this project. The following diggers are but a few that helped at the excavation: Austin Motheral, Roger Fry, Art Sahlstein, Tommy Diamond, Richard Zack, Darlene Sumerfelt, Tom Green, Ronnie Colvin, Angie Osen, Brad Carter, Doug Penny, Tim Dalbey, Todd Betz, Kim Richardson, and Brandi Clark. Anissa Camp, Ronnie Colvin, Albert Miramontes, and Angela Maxwell for

assistance with fossil preparation. Darren Tanke of the Royal Tyrrell Museum of Paleontology for providng key literature, Carl Franklyn for allowing the author to view modern crocodile skeletons in the collections of the UTA Amphibian and Reptile Diversity Research Center, Louis Jacobs and Dale Winkler for allowing the author to study the type specimen for *Woodbinesuchus* at the Shuler Museum of Paleontology at SMU. The PaleoMap Project, the Jurassic Foundation, The Earthwatch Institute, the Western Interior Paleontological Society and the Arlington Tomorrow Foundation for providing funds in support of this work.

CHAPTER 7

THE FEEDING TRACES AND PALEOBIOLOGY OF A CRETACEOUS (CENOMANIAN) CROCODYLIFORM: AN EXAMPLE FROM THE WOODBINE FORMATION OF NORTH TEXAS

"Because when they strike it can be that quick that if they're in range, you're dead, you're dead in your tracks."

Steve Irwin (Crocodile Hunter)

7.1 Introduction

In the study of vertebrate paleobiology, inferences regarding behavior must often rely on skeletal material. Direct evidence of behavior in the vertebrate fossil record is exceedingly rare (Varricchio et al., 2007), especially for interspecific interactions like predation (e.g. Carpenter, 1998; Varricchio, 2001). In terrestrial ecosystems, the most abundant evidence of behavior consists of ichnofossils such as trackways (Wright, 1999; Milner et al., 2009) or coprolites (Chin et al., 2003; Chin, 2007). Tooth marks, when attributable to a particular taxon, can provide direct evidence of carnivore feeding behavior and information on the trophic structure of the community (Fiorillo, 1991a; Chure et al., 1998; Erickson and Olson, 1996; Schwimmer, 2002; Rogers et al., 2003; Reisz and Tsuji, 2006). Numerous broken remains of turtle shell and dinosaur bones were recovered from a productive Cretaceous fossil locality in Texas, the Arlington Archosaur Site, that preserves taphonomic indicators of crocodyliform feeding.

7.2 Crocodyliform Feeding Behavior

Crocodyliforms exhibit thecodont dentition, with most taxa possessing conical teeth. Teeth are continually replaced throughout life, preventing precise occlusion, but do interlock between upper and lower jaws. Tooth shape varies depending on ontogenetic stage of the individual and eruption age of the tooth. As tooth roots are resorbed and shed each successive tooth grows larger than its predecessor, with replacement slowing through life (Poole, 1961; Lubkin, 1997; Njau and Blumenschine, 2006). Teeth possess anterior and posterior carina that may have small denticles. Newly erupted teeth are typically more pointed and sharp, becoming rounded and blunt with age and use. Prey preferences change with ontogenetic stage, mainly reflecting changes in body size (Cott, 1961; Delany and Abercrombie, 1986; Erickson et al., 2003). Juveniles use their teeth for piercing and grasping small, fast prey such as insects, crustaceans, amphibians, and fish. As they grow, the development of stronger jaws and robust teeth in adults are used for crushing and tearing of larger prey items. Along with the variation in tooth wear and eruption pattern, the tips of new teeth are easily chipped, which can lead to a variety of tooth mark morphologies being created by even a single individual (Njau and Blumenschine, 2006).

Nopsca (1902) was among the first to note crocodylian feeding grounds as a potential source of bone accumulation in the fossil record. He attributed the

accumulated remains of reptiles in Upper Cretaceous sediments of Romania to the feeding habits of crocodyliforms (Nopsca, 1902). Otherwise, the taphonomic contribution of crocodyliform feeding behavior to vertebrate assemblages in wetland, riverine, and lacustrine ecosystems has only recently regained attention (Njau, 2006). Living crocodylians usually attack prey in water or at the water's edge, dragging the carcass into water to be consumed (Cott, 1961; Weigelt, 1989; Njau and Blumenschine, 2006). They may even travel inland to capture or scavenge prey. Most bones and teeth consumed by crocodylians are likely to be destroyed through digestion, removing them from the fossil record (Fisher, 1981). Remains too large to swallow may simply be ignored, dismembered, or cached for later consumption. Such activities introduce vertebrate remains to an active depositional environment, thus enhancing their preservation potential. As opportunistic predators, crocodylians act as wide samplers of the surrounding fauna, especially smaller and/or juvenile individuals (Cott, 1961; Delany and Abercrombie, 1986; Weigelt, 1989). This vertebrate material may be aggregated into relatively small areas (Weigelt, 1989; Njau, 2006), possibly forming bone beds that eventually attract the attention of paleontologists. In many ways then, crocodyliforms play a positive role in the formation of the vertebrate record of the areas they inhabit.

7.3 Fossil Locality

All fossil material was recovered from a productive new locality in north-central Texas dubbed the Arlington Archosaur Site (AAS) (Fig. 7.1) and currently housed in the Earth and Environmental Sciences Department at the University of Texas at Arlington. The AAS is part of the Lewisville Member of the Woodbine Formation (Dodge, 1952; 1968; 1969; Oliver, 1971; Johnson, 1974; Main, 2005) and is Cenomanian in age (approximately 95 Mya) (Kennedy and Cobban, 1990). Woodbine exposures in Texas extend from Lake Texoma on the Red River to the Edwards Plateau near Austin and occur as an irregular and narrow north-south band (Hill, 1901; Bergquist, 1949; Oliver, 1971; Johnson, 1974). Woodbine deposits primarily preserve nearshore terrestrial and shallow marine depositional systems, and include fluvial, deltaic and shelf deposits (Dodge, 1952; Oliver, 1971; Main, 2005). The AAS represents a coastal ecosystem from a delta plain along the southeastern margin of the Western Interior Seaway. The diverse biota recovered so far includes lungfish, gar, shark, ray, turtle, amphibian, mammal, dinosaur (ornithopod and theropod), and crocodyliform remains along with numerous carbonized logs (Main, 2009). The fossils primarily occur within a 1 m section of organic-rich sediment (peat) with prominent carbonized wood remains (Main, 2009). The crocodyliform remains represent a new taxon, distinguished from the Woodbine crocodyliform *Woodbinesuchus byersmauricei* primarily by

its wide, A-shaped skull and occurrence in much younger strata than the latter. Description of this new Woodbine taxon was detailed in the previous chapter.

Here we describe tooth marks and bone breakage patterns on the fossil remains of turtles and ornithopod dinosaurs that are consistent with feeding by a large crocodyliform. These marks differ substantially from those produced by other potential carnivores and are attributed to a new taxon of crocodyliform from the same locality. The presence of large, predatory crocodyliforms in the extinct biota has important paleoecological and taphonomic implications for the fossil locality and our understanding of this ancient ecosystem.

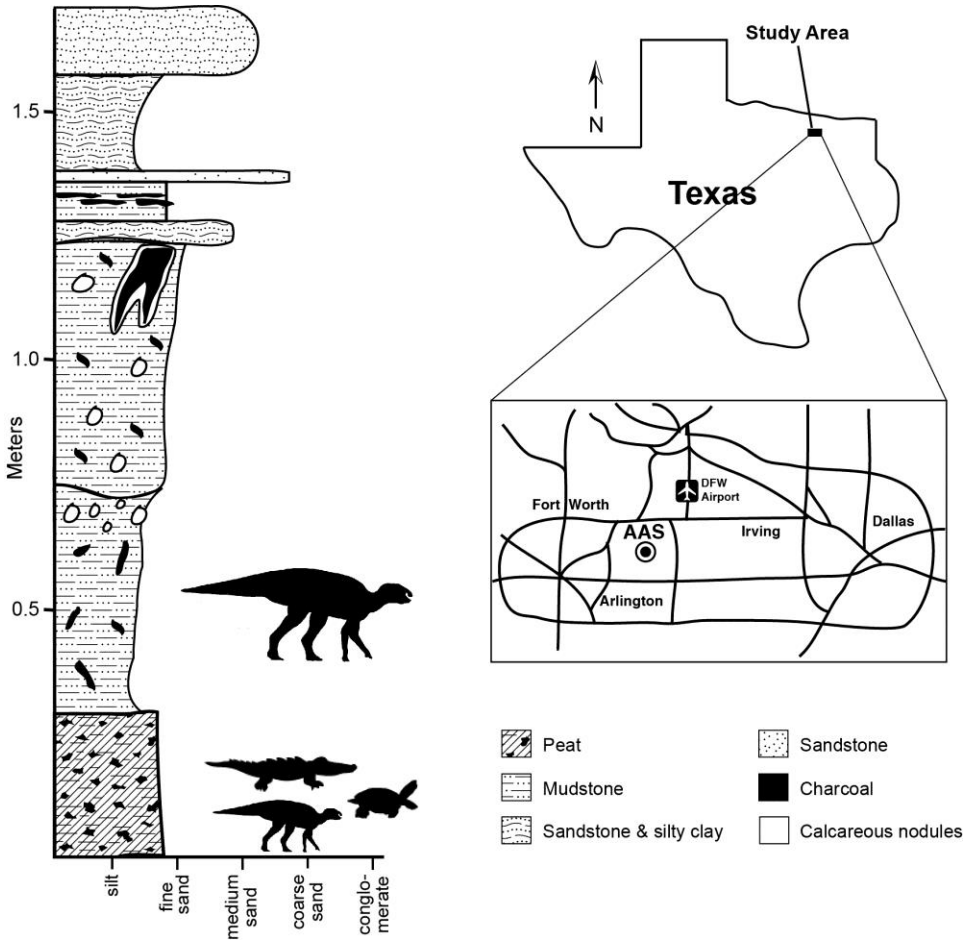

Figure 7.1. Location of the Arlington Archosaur Site (AAS). At left a composite stratigraphic column. The lowermost horizon is the peat bed containing the crocodyliform, turtle, and juvenile ornithopod remains. The horizon above contained the bitten adult ornithopod bone in a paleosol, which also contained carbonate nodules and charcoal fragments.

7.4 Taphonomic Analysis

As part of ongoing work at the Arlington Archosaur Site, a preliminary taphonomic analysis was done, focusing on the sedimentary environments represented, quality of macrofossil preservation, and spatial distribution of fossils

recovered so far. Because the quarry remains active, with new fossils recovered on a weekly basis, more detailed taphonomic analyses (e.g., MNI, taxonomic diversity/evenness, etc.) remain to be completed. Sedimentological analysis consisted of detailed study of vertical and horizontal changes in lithology throughout the entire exposure forming the walls and floors of the quarry. A large proportion of sediment removed from the quarry has been screen washed for microfossils following generally practiced methods (McKenna, 1962; Jamniczky et al., 2003). Preservation quality was assessed through a survey of over 100 bones. Bone surface features and breakage patterns were noted and compared to published features for identification (Behrensmeyer, 1978; Fiorillo, 1991a and 1991b; Fiorillo et al., 2000; Bader et al., 2009).

7.5 Fossil Specimens and Documentation

Over two hundred dinosaur bones and 29 turtle shell fragments were examined for tooth marks. The specimens described here include 17 fragments of turtle shell and two partial dinosaur limb bones (Table 7.1). Turtle shell fragments include pieces of carapace and plastron referable to at least two individuals and smaller fragments of several others. All represent relatively large individuals (35–45+ cm carapace length), and include at least two different taxa. The turtle material was found in close association to the remains of a large adult crocodyliform and in a nearby concentration that produced numerous juvenile

remains (Fig. 7.2). Dinosaur bones are the proximal ends of femora from one adult and one juvenile ornithopod. Note that the adult bone was recovered from the paleosol layer directly overlying the peat bed (Fig. 7.1).

Most specimens required modest preparation with hand tools due to the relatively friable matrix. Probable tooth marks were examined with a 10X hand lens or microscope, photographed, and measured with digital calipers. Marks were identified following the criteria of Binford (1981) and include pits, scores, and punctures. Special attention was paid to features diagnostic of crocodyliforms (Njau and Blumenschine, 2006). In addition, measurements of alveoli and isolated teeth were taken from four adult and two juvenile jaw elements recovered from the site and compared to the marks as well as visually assessing the congruence between spacing of jaw elements, teeth and bite marks (after Rogers et al., 2003).

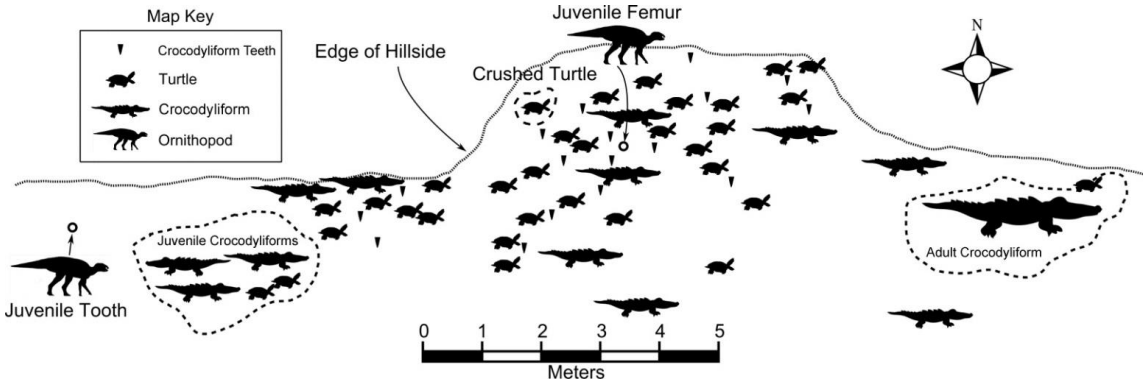

Figure 7.2. Diagram-map of the quarry showing locations of crocodyliform, turtle, and ornithopod dinosaur remains. Dense collections of material referable to one or more individuals are surrounded by dotted lines.

7.6 Paleoenvironment and Taphonomy

Fossils in the AAS are derived almost exclusively from the two lowest beds exposed in the quarry (Fig. 7.1). The lowermost bed is a carbonaceous silty shale (or peat) with occasional fine sand mixed in the matrix. Pyrite growths and siderite nodules are common throughout the bed. Some clay is present, as shown by the presence of occasional slickensides. Plant remains are abundant, including coalified plant parts 10–40 cm in length, most likely the remains of large branches. Some faint root casts are also visible. Turtle, dinosaur, and crocodyliform are the most common macrovertebrates. Bones are mainly disarticulated and unassociated, with the remains of several species and individuals mixed throughout the exposed area, although some associated bones do occur (Fig. 7.2). Bones appear to show no preferred horizontal orientation and

occur at a variety of vertical angles within the layer, most likely from shrink-swell cycles and/or bioturbation. The survey of more than 200 bones from this layer show most fall within weathering stages 0 or 1 (Behrensmeyer, 1978) with little evidence of sediment abrasion from aqueous transport or surface pitting from acidic soil conditions. Many bones are complete or nearly complete. Incomplete bones are often separated at growth plates or, if broken, exhibit transverse fracturing associated with breakage after fossilization (Fiorillo et al., 2000). A diverse assemblage of microvertebrates has been recovered representing mainly aquatic or semi-aquatic taxa known to have freshwater, brackish, or marine distributions.

The layer above the peat bed represents a thick, well-developed paleosol, although its exact type has yet to be determined. The upper horizons are well-drained and consist of red-gray mottles, carbonate nodules, and charcoalified plant remains (Fig. 7.1). The lower horizon is a gray siltstone where the majority of the ornithopod dinosaur remains were recovered. Because only one bone from this layer was found with tooth marks, detailed taphonomic analysis will be saved for a future paper. That being said, bones from this layer do demonstrate evidence of greater surface exposure prior to burial than bone from the peat layer below.

7.7 Tooth Marks

A total of 31 bone fragments demonstrated tooth marks (2 ornithopod, 29 turtle). Eighty definitive tooth marks were identified along with numerous possible marks (Table 7.1). Nearly 60% of turtle fragments showed tooth marks (17 of 29), whereas only 1% of ornithopod bones were similarly marked (2 of 202).

Pits.—A total of 54 pits were observed on 16 different fragments (52% of fragments). Pits appeared as bowl-shaped or irregular depressions in the bone surface, varying in diameter from 1–11 mm (Fig. 7.3 and Table 7.1). Few bisected pits were observed as described in Njau and Blumenshine (2006) and is most likely due to varying states of wear between teeth when the bite took place (Njau and Blumenschine, 2006). Only one pit was observed to have a small notch that potentially represents a partial bisect (Fig. 7.3). Pits were observed on carapace and plastron fragments from both turtle taxa, some of which led into scores. At least two pits sit at the center of a 40 mm wide concave oval with edges cracked and depressed towards the center, likely representing bone failure (Fig. 7.3). Two pits were identified on the adult dinosaur femur and six smaller, questionable pits on the juvenile femur (Fig. 7.4). On both femora pits appear oriented transversely across the greater trochanter. Pits on the adult specimen are about twice the size of those on the juvenile. In addition, a large flake (30 mm long by 25 mm wide)

and associated pit are present on the lateral side of the broken end of the adult femur (Fig. 7.4).

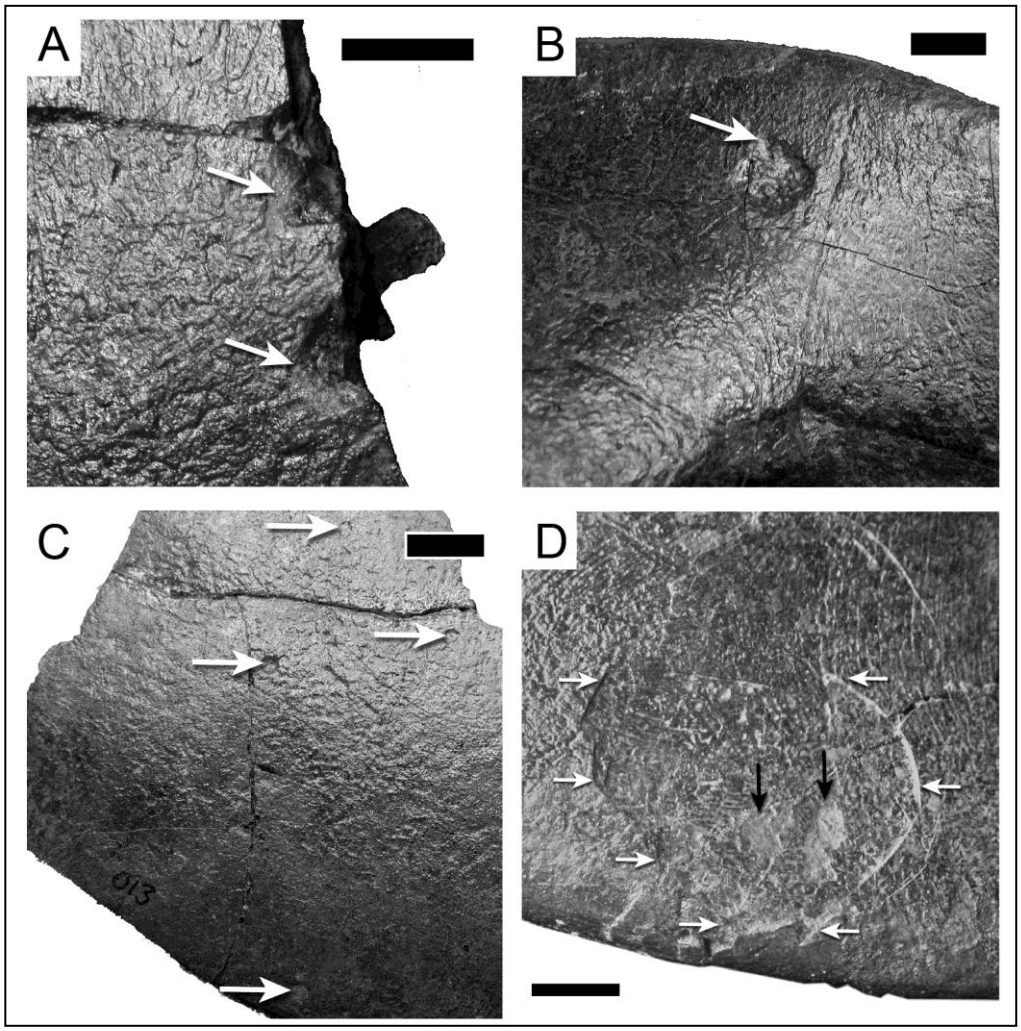

Figure 7.3. Examples of pit marks on AAS specimens. A. Two pits along broken edge of turtle shell UTA-AASTL-012 (arrows). B. Pit on underside of turtle carapace piece UTA-AASTL-003 Arrow points to possible partial bisect. C. Turtle shell with small circular pits (arrows).

Scores.—Twenty-six scores were observed on 12 fragments (39% of fragments), ranging from 6–94 mm in length and 2–20 mm in width (Fig. 7.5). Multiple score marks are present on most turtle specimens, but absent from the dinosaur bones. Score shapes vary substantially. Many are shallow and U-shaped in cross-section, whereas a few are deeply bisected. They are singular or occur as serial tooth marks. One large score is significantly hooked, which may be diagnostic of inertial feeding behavior (Njau and Blumenschine, 2006; D'Amore and Blumenschine, 2009). Some marks end at fractured edges or bone margins. A small subset of scores exhibits bisections along their length. These bisected scores tend to be narrow (≤4 mm) and elongate. One exception occurs on the underside of one turtle specimen (UTA-AASTL 006) where two large, bisected scores have crushed and distorted the underlying bone, with the larger (20 mm wide) leading into a fractured edge.

Punctures.—Only one potential puncture mark was observed on a turtle specimen (UTA-AASTL 001). It is oval in shape and approximately 3 mm wide.

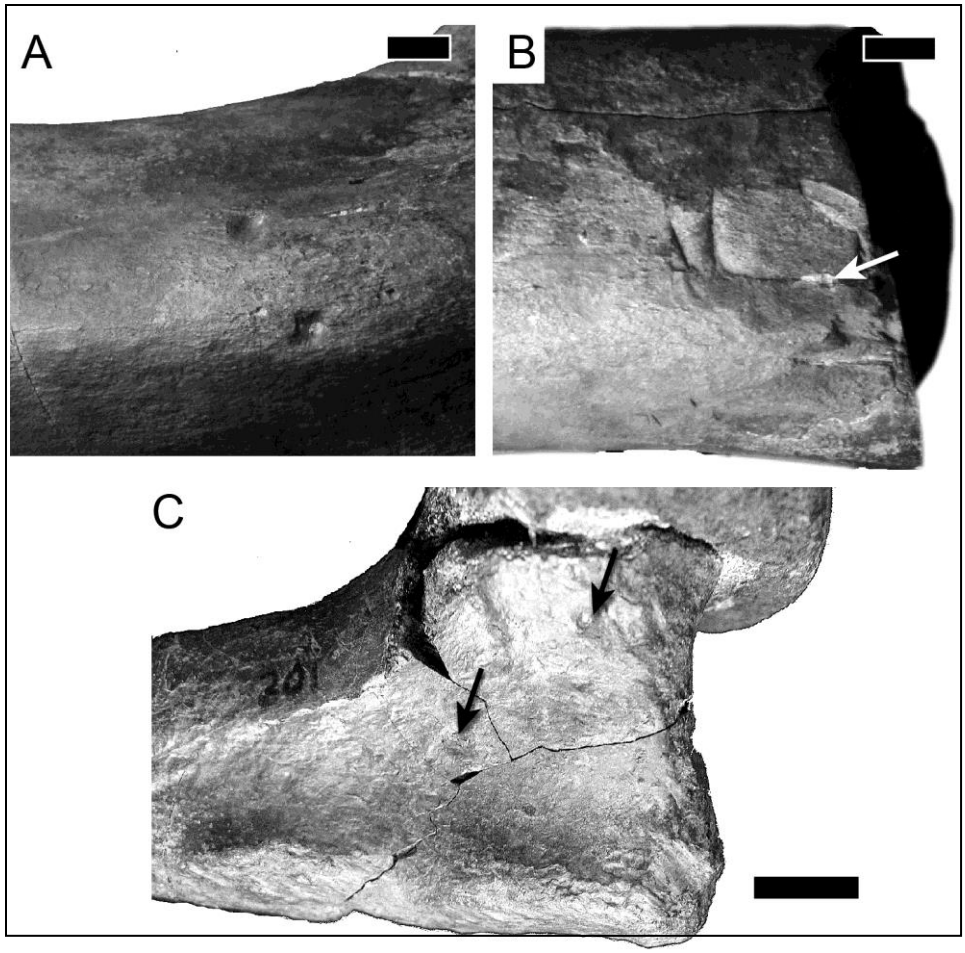

Figure 7.4 A. Proximal end of adult ornithopod femur UTA-AASO-125 showing two pit marks. B. Large flake in broken distal end of same adult ornithopod femur. Arrow points to pit along midline of flake. C. Proximal end of juvenile ornithopod femur UTA-AASO-201 showing two potential pits (arrows). D. Pits (black arrows) on turtle carapace section UTA-AASTL-001. White arrows are arranged along fractured edges. All scale bars
equal 1 cm.

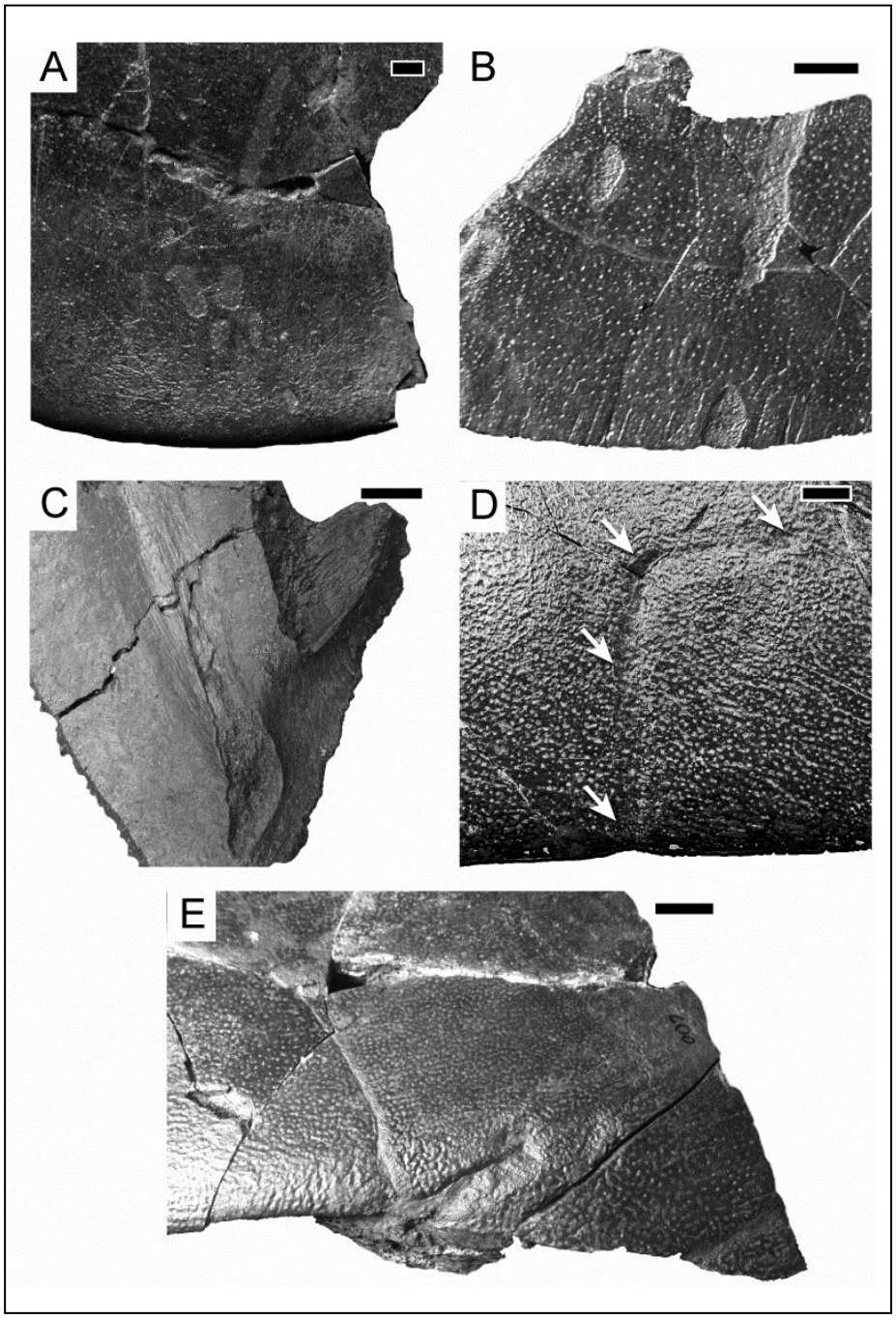

Figure 7.5 Score marks on AAS turtle specimens. A. Carapace section UTA-AASTL-002 with multiple scores. B. Carapace section UTA-AASTL-006 with serial scores. C. Underside of specimen in B, showing two deep bisected scores. D. Carapace section UTA-AASTL-007 with hook score. E. Bisected scores along edge of D. All scale bars equal 1 cm.

7.8 Distribution Patterns and Comparisons

All three types of bite marks were observed on the turtle specimens, although there is no specific pattern in their distribution. Pits were by far the most commonly observed traces, followed by scores, with punctures the least prevalent (or absent). In the most complete associated turtle specimen, most visible pits and scores surround the edges and sides of the carapace and plastron; the center of each is largely missing (Fig. 7.6).

The width of the large bisected scores on the underside of turtle specimen UTA-AASTL 006 closely match the diameter of the largest crocodyliform teeth collected from the site, which range from 19–24 mm. Furthermore, the distance between the start of both marks is nearly identical to the distance between the centers of the two largest dental alveoli, about 31–32 mm (Fig. 7.7).

Only pits but no scores were observed on the dinosaur bones. Although the femora are incomplete, these pits appear to be concentrated proximally, nearer the femoral head. The large flake and associated single pit are the only other identifiable marks on the broken distal end of the larger femur.

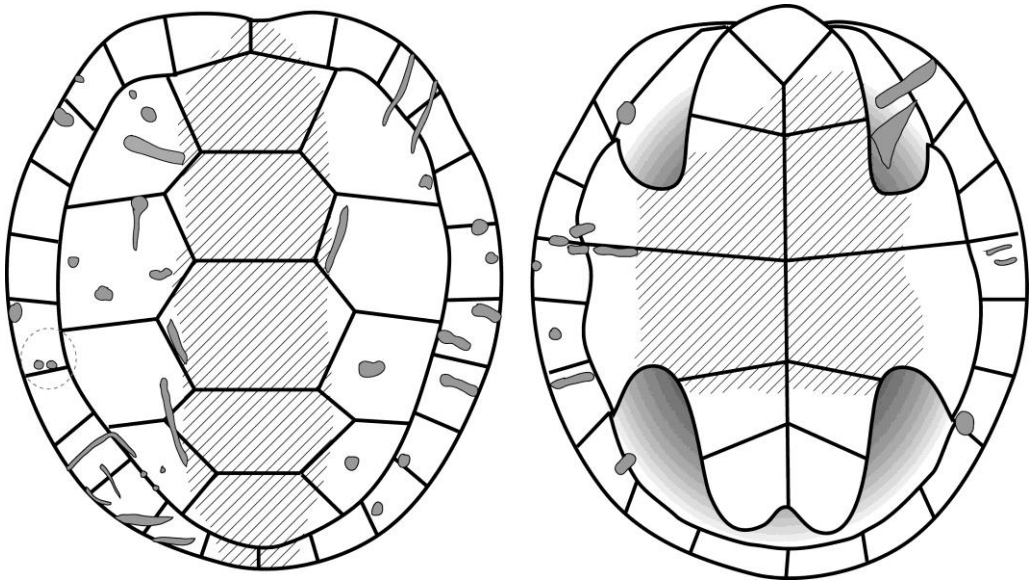

Figure 7.6 Distribution of tooth marks from shell fragments placed on a generalized turtle shell. Hatched area represents missing portions of shell material recovered so far. In some cases, exact placement of marks on shell can only be estimated.

Figure 7.7 Alignment of AAS crocodilian jaw elements and tooth marks.

7.9 Discussion

The taphonomy of the lowermost carbonaceous (peat) bed indicates it is an attritional assemblage formed in a low-energy environment. The lack of surface modification (i.e., abrasion), size disparity between sediment particles and bones, and relatively random orientation of bones suggests they underwent little, if any, aqueous transport (Fiorillo et al., 2000). Most bones were buried within a few years of deposition as indicated by minimal amounts of weathering. The moist, swampy conditions would have further delayed surface weathering as seen in similar environments, allowing bones to accumulate for a period of years before complete burial (Behrensmeyer et al., 1979; Tappen, 1994). The extremely disassociated nature of the macrovertebrate assemblage is likely a combination of decay and disarticulation at the surface prior to burial and/or the shrink-swell cycles and bioturbation of the sediment following burial. As such, the macrovertebrate remains at the AAS are most likely parautochthonous, having undergone little transport from the location of death, and representative of dominant taxa from the surrounding area. On the other hand, the mixed terrestrial, freshwater, brackish, and marine nature of the microfossil assemblage suggests a largely allochthonous origin and indicating the close proximity of the AAS to the paleocoastline. Estimating the time of formation for a fossil assemblage is difficult, however, comparisons with taphonomic studies of modern and fossil bone accumulations suggests the remains constituting the AAS assemblage

accumulated most likely over a period of decades, but not more than a century (Potts, 1986; Fiorillo, 1988; Lyman and Fox, 1989; Behrensmeyer et al., 1992; Fiorillo et al., 2000). Following burial, organic preservation was enhanced by a locally high water table, which promoted anoxic and reducing conditions, as shown by widespread siderite and pyrite formation. The data as a whole paint the picture of a coastal, possibly seasonal, marsh that was periodically influenced by marine incursions.

Theropod feeding traces are fairly common in the literature (e.g. Carpenter, 1998; Fiorillo, 1991a; Fowler and Sullivan, 2006; Horner and Lessem, 1993; Erickson and Olson, 1996; Chure et al., 1998; Jacobsen, 2001), and are generally described as being reflective of the clade's ziphodont dentition. The pronounced denticles on theropod teeth often leave striations in bite marks (Fig. 8A-B). The laterally compressed shape of ziphodont teeth tend to create marks that are more deeply V-shaped in cross section than the more conical teeth of crocodyliforms. Edge marks, where the recurved surface of the posterior tooth edge contacts a sharp surface on the prey bones, are also present. All of these traces have been found through actualistic work with modern komodo dragons, a group that, while only distantly related to theropod dinosaurs, has similar ziphodont dentition (D'Amore and Blumenschine, 2009).

Paleontological examples of bite marks attributed to crocodylian and non-crocodylian crocodyliforms, particularly on turtles (e.g. Fuentes, 2003; Mead et al., 2006; Steadman et al., 2007) and dinosaurs (e.g. Schwimmer, 2002; Rivera-Sylva et al., 2009), are well documented. Actualistic experiments focusing on members of *Crocodylus niloticus* have revealed a number of novel bite marks and feeding patterns (Njau and Blumenschine, 2006). Tooth marks tend to be wide and oval or U-shaped in cross-section. A lack of extensive furrows or scalloped edges, which have been associated with mammalian-style chewing or gnawing (Binford, 1981), and the presence of hook scores, which are L- or J-shaped structures (Njau and Blumenschine, 2006) both have been associated with animals which exhibit inertial feeding behavior (D'Amore and Blumenschine, 2009). Bisected pits, scores, and punctures, which are caused by the prominent carina present in relatively newly erupted, unworn crocodyliform teeth, were first identified among specimens of *C. niloticus* (Njau and Blumenschine, 2006), but have since been observed in many extant (Drumheller, 2007) and extinct (Rivera-Sylva et al., 2009; Brochu et al., 2010) crocodylians. These marks, identified by subscores within the body of the bite mark and/or notches on the margin of pits and punctures, are considered to be diagnostic of crocodyliforms (Fig. 7.8). Pathological sources of these marks, such as shell disease, can be excluded due to secondary alterations, i.e., fracturing and crushing, related to impact damage (Byers, 2005; Hernandez-Divers et al., 2009).

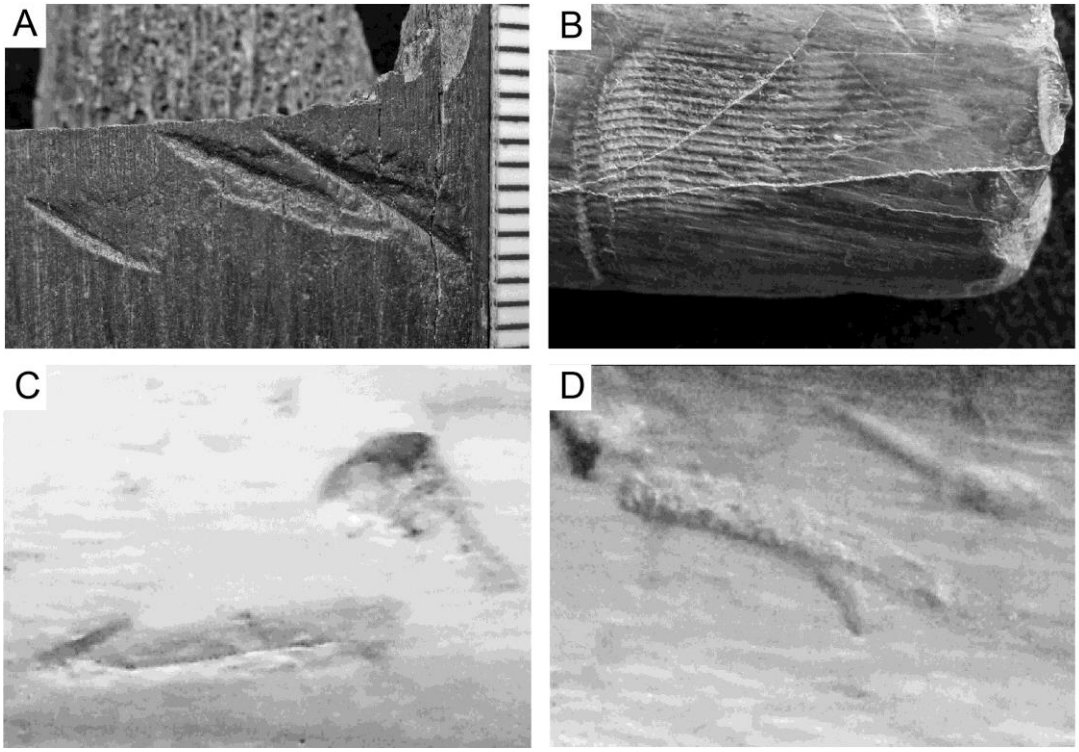

Figure 7.8 Comparison of theropod tooth marks exhibiting ziphodont condition (A, B) and tooth marks produced by a crocodylian (C, D).

The traces discovered at the Arlington Archosaur Site closely match the above morphologies and are therefore attributed to a crocodyliform agent. Most important are the presence of bisections, a diagnostic trait of crocodyliform feeding. In addition, the size and spacing of many marks closely matches the skull and dental morphology of AAS crocodyliform fossil remains. All tooth marks lack features created by ziphodont teeth. Theropod material from the AAS and vicinity is extremely rare, amounting to only a few teeth and fragments, none of which could have produced the observed tooth mark morphology (Noto and Main,

in review). Therefore theropod dinosaurs may be excluded as the source of the tooth marks present at this locality. Furthermore, no fossil evidence of any other crocodyliform taxa, such as the goniopholidid *Woodbinesuchus,* has yet been recovered from the site. The new crocodyliform taxon discovered at the AAS is thus inferred to be the primary trace-maker.

Tooth marks and related damage inflicted on bone are traces of feeding behavior (Njau and Blumenschine, 2006). Numerous studies exist on bone modification by extant mammals, but comparatively little actualistic work has been done on reptiles. Crocodyliform feeding traces have been documented on a variety of recent vertebrates, including turtle, cow, horse, small mammal, and human remains (Fisher, 1981; Davidson and Solomon, 1990; Mead et al., 2006; Njau and Blumenschine, 2006; Steadman et al., 2007). There is a growing record of fossil crocodyliform feeding traces from the Mesozoic and early-mid Cenozoic (Fisher, 1981; Schwimmer, 2002; Forrest, 2003; Mikuláš et al., 2006; Hua et al., 2007; Bader et al., 2009; Rivera-Sylva et al., 2009; Schwimmer and Harrell, 2010). The feeding traces described here, in the context of the AAS, provide important data on the paleobiology of a large Cretaceous crocodyliform and gives insight into their role in forming this unique fossil assemblage.

The pattern of bite marks and damage to turtle shell and dinosaur bone specimens suggests that the AAS crocodyliform fed in a manner very similar to

living, generalist representatives (Cleuren and De Vree, 2000). Based on personal and published observations of crocodylian feeding behavior, the AAS crocodyliform likely fed in the following manner: the entire turtle body is grasped in the mouth, then quick inertial motions of the head and jaws position the turtle either parallel or perpendicular to the jaws, at which point the shell is rotated to one side, where it is crushed between the jaws (Fig. 7.9). This pattern of feeding takes advantage of potential weak points in the turtle shell where bone is thinnest, targeting the hinges laterally and mid-sagittal axis of the shell. Such behavior potentially obliterates the central portions of the shell while leaving thicker marginal portions relatively intact. Continuing motion of the jaws may then be used to further fragment the shell before ingestion (Cleuren and De Vree, 2000). It has been shown in some cases that the body of the turtle can be consumed while leaving the carapace and plastron intact (Milàn et al., 2010). The abundance of shell remains and paucity of other turtle skeletal material at the AAS may reflect this feeding behavior, although preservation bias in favor of robust shell elements cannot be discounted.

Living crocodylians are known to consume turtles, which have been found to make up the majority of stomach contents in some large alligators and crocodiles (Cott, 1961; Delany and Abercrombie, 1986; Milàn et al., 2010). Multiple healed bite marks on turtle and mammal bones are known from the recent fossil record of the Bahamas and Costa Rica (Mead et al., 2006; Steadman

et al., 2007). Weigelt (1989) discussed the feeding grounds of crocodylians and noted the presence of turtle remains occurring with them in the Gosau Formation of Austria as well as the German Weald. The preponderance of both marked and unmarked turtle remains suggest turtles were both plentiful and diverse in the ecosystem, and likely formed a portion of the AAS crocodyliform's diet.

Figure 7.9 Two examples of feeding behavior by the American alligator, *Alligator mississippiensis*, on turtles. In both cases the shell is being crushed transversely, shattering the shell along the midline. Photos by Jessie Dickson, used with permission.

The AAS crocodyliform skull is mostly complete, with at least one element represented from most skull bones, including the frontal, nasal, maxilla, premaxilla, angular, dentary, and quadrate. These bones show that the skull was broad and triangular in shape with a laterally expanded and overhanging premaxilla similar to *Sarcosuchus* (Main et al., in prep). The rostrum is tall and robustly built with a large dentary symphysis, blunt or rounded teeth, and a flat

superior alveolar margin. These last three features are shared with the Late Cretaceous alligatoroid *Brachychampsa montana*, which is thought to have included turtles as part of its diet (Carpenter and Lindsey, 1980; Sullivan and Lucas, 2003). The extremely blunt posterior teeth of *Brachychamspa* and related alligatoroids suggests turtle consumption was likely common among crocodyliforms, but the lack of correlation between tooth morphology and chelonivory in living crocodylians implies these taxa were not specialized turtle predators (Sullivan and Lucas, 2003).

Living crocodylians will take a variety of prey, depending on availability, body size, and ontogenetic stage of the individual (Njau and Blumenschine, 2006; Milàn et al., 2010). Bitten remains likely resulted from a combination of predation and scavenging. The transverse or oblique orientation of pits to the long axis of both femora is consistent with crocodyliform feeding behavior (Njau and Blumenschine, 2006). The proximal position of pits and large flake associated with a break on the adult dinosaur femur suggest the AAS crocodyliform dismembered larger prey (such as dinosaurs) in a manner similar to living crocodiles: by grasping the limb near the joint and shaking, pulling, or death rolling to separate it from the socket (Njau and Blumenschine, 2006) (Fig. 7.9 and 7.10).

Tooth-marked remains occur with the bones of adult and juvenile crocodyliforms, including numerous teeth, in a single, well mapped horizon (except for the adult ornithopod femur). All bones are well-preserved and lacked any pitting or etching that would indicate they had passed through a crocodile's digestive system. Crocodylians are notorious for their strong stomach acids, which can completely dissolve bone (Fisher, 1981). Small fragments of etched turtle shell were described by Carpenter and Lindsey (1980) as possible scat remnants of *Brachychampsa*, but the large size and good condition of the remains described here precludes a digestive- or scat-residue origin. Instead, we propose that a portion of the fossil bones in this large accumulation were produced during feeding by resident AAS crocodyliforms (Njau, 2006). Some of the associated skeletal remains may even represent preserved caches; however, a conclusive determination remains difficult. This site was part of an active feeding area, possibly a breeding/feeding ground for an extended time as shown by the over 350 isolated crocodyliform teeth and numerous feeding traces recovered to date, a feature typical of localities with intense crocodylian activity (Njau, 2006).

Figure 7.10 Paleo-artist interpretation showing the method of crocodyliform feeding discussed herein, with a prey turtle being crushed by an attacking crocodyliform (art by Jude Swales).

In modern ecosystems crocodylians are known to feed upon a diversity of prey from the surrounding community (Nopsca, 1902; Cott, 1961; Delany and Abercrombie, 1986; Weigelt, 1989). The bite marks described from the AAS provide additional evidence of crocodyliform predation on dinosaurs and represents the best evidence for this behavior outside of Late Cretaceous communities (Schwimmer, 2002; Rivera-Sylva et al., 2009; Schwimmer and Harrell, 2010). Crocodyliforms may have killed unwary dinosaurs that journeyed too close to the water's edge and scavenged their carcasses when available,

possibly even dragging them to the water from further inland (Cott, 1961; Delany and Abercrombie, 1986; Weigelt, 1989). This feeding strategy is not unlike that reconstructed for the paleoecology other, much larger, Cretaceous crocodyliforms such as *Deinosuchus* and *Sarcosuchus* (Sereno et al., 2001; Schwimmer, 2002; Rivera-Sylva, Frey and Guzmán-Gutiérrez, 2009; Schwimmer and Harrell, 2010). The large Cretaceous crocodylifrom *Deinosuchus* was a 15 meter crocodyliform known to live in the coastal waters of the Big Bend region of Texas (Schwimmer, 2002). Evidence of hadrosaur bones found in Big Bend with crocodyliform bite marks supports the model of these animals being among the top predators of Cretaceous ecosystems. The addition of evidence for similar predatory behavior from the AAS shows that crocodyliforms remained the dominant large predators in and around coastal plain ecosystems throughout the Mesozoic Era.

Table 7.1 AAS fossils demonstrating crocodyliform bite marks. When multiple fragments are attributed to an individual, the count assumes each mark on each fragment is unique. The columns show the number of identifiable/questionable marks of each type. Each ID# corresponds to a fossil fragment that is grouped by individual.

UTA Specimen #	Turtle shell data	# of traces (upper/lower)	AAS Site
UTA-AASTO-125	partial limb (femoral condyle)	3/2?	Dinosaur Quarry
UTA-AASTL-001	shell (hinge w/lg break)	3/5?	Turtle Buffet (-10.8)
UTA-AASTL-002	shell (hinge w/sm break)	5/6	Turtle Buffet (-10.8)
UTA-AASTL-003	md shell (thin hinge)	2/1	Turtle Buffet (-10.8)
UTA-AASTL-004	md shell (thin, plastron?)	1/3	Turtle Buffet (-10.8)
UTA-AASTL-005	md shell (triangular, w/ traces)	4/2	Turtle Buffet (-5.3)
UTA-AASTL-006	md shell (rectangular, w/ traces)	4/?	Turtle Buffet (-3.7)
UTA-AASTL-007	lg shell (subrounded w/traces)	4/3?	Turtle Buffet (-3.9)
UTA-AASTL-009	sm shell edge (angular edge)	2/?	Turtle Buffet (-3.9)
UTA-AASTL-010	sm shell edge (subrectanuglar)	?/?	Turtle Buffet (-3.9)
UTA-AASTL-011	md shell (angular w/traces)	24?/?	The Nursery (-14.6)
UTA-AASTL-012	lg carapace (angular hinge)	2/4?	Turtle Buffet (-10.8)
UTA-AASTL-013	sm shell (thin, cracked)	6?/?	Turtle Buffet (-10.8)
UTA-AASTL-014	sm shell (broken edge)	3?/0	Turtle Buffet (-10.8)
UTA-AASTL-015	sm shell (triangular fragment)	6?/0	Turtle Buffet (-10.8)
UTA-AASTL-018	sm shell (triangular, w/break)	1?/0	Turtle Buffet (-10.8)
UTA-AASTL-020	sm shell (angular, fragment)	1?/1?	Turtle Buffet (-10.8)
UTA-AASTL-021	sm shell (puncture)	1?/1	Turtle Buffet (-10.8)

7.10 Conclusions

Fossil turtle and dinosaur specimens from the mid-Cretaceous Woodbine Formation at the Arlington Archosaur Site (AAS) show clear evidence of tooth marks consistent with predation by a large crocodyliform. These feeding traces are attributed to a crocodyliform based on (1) the presence of bisected score marks and hook scores and lack of diagnostic marks from ziphodont teeth (such as those of theropods); (2) similar size ranges of feeding traces and crocodyliform teeth recovered from the same bed; (3) the spacing between marks, which is consistent with the distance between the largest dental alveoli on cranial material from the same bed; (4) the location and orientation of bite marks, which follows patterns of feeding behavior observed in living crocodylians (Njau and Blumenschine, 2006; Drumheller, 2007); and (5) an abundance of the crocodyliform taxon and paucity of material from other predatory taxa (including *Woodbinesuchus* and theropod dinosaurs) from the AAS and vicinity (Noto and Main, In review). The position of tooth marks and patterns of damage on turtle and dinosaur remains are consistent with feeding behavior observed in living crocodylians (Njau and Blumenschine, 2006; Milàn et al., 2010). Furthermore, the data collected here suggests that crocodyliforms were the likely apex predators of the AAS coastal ecosystem.

7.11 Acknowledgements

I thank the Huffines family, Robert Kimball at the Viridian Properties and HC LOBF of Arlington for granting land access to the property in which the AAS fossils were recovered, the Paleomap Project, the Jurassic Foundation, and the Western Interior Paleontological Society for providing funds, my coauthors and colleagues on this project Chris Noto and Stephanie Drumheller; their contributions were invaluable and greatly appreciated. Stewart and Travis Nolan for excavating AAS turtle specimens discussed, David Kledzik and the staff of the St. Augustine Alligator Farm for allowing access to the bite mark collection from their animals, Swaggerty Sausage Co., Inc and Southeastern Provisional, LLC for providing partially butchered pig and cow limbs for a modern bite mark collection. Also Jacob Horton, Fred and Janet Drumheller for helping process the modern samples, and Chris Brochu, Eric Allen, Julia McHugh, Jessica Miller-Camp, Marc Spencer, Eric Wilberg, Jennifer Nestler, Maria Gold, Michelle Stocker, and Talia Karim for helpful discussion and suggestions. Thanks to the AAS dig crew that excavated the "*Turtle Buffet*" including Roger Fry, Darlene Sumerfelt, Anissa Camp, Jason Rich, Rachell Peterson and Ronnie Colvin, a special thanks to Roger Fry for his detailed maps of the AAS and Anissa Camp for preparing the turtle specimens discussed herein. Tracy Ford created the ornithopod body outline. The alligator photos were taken by Jessie Dickso and used with her kind permission.

CHAPTER 8

DELTA PLAIN PALEOECOLOGY OF SOUTHWEST APPALACHIA (RUDRADIA) FROM THE CRETACEOUS WOODBINE FORMATION: THE ARLINGTON ARCHOSAUR SITE

"During the many years of the world, the land and water has been colonized by many hosts of living forms. What an infinite number of generations, which the mind cannot grasp, must have succeeded one another in the many rolling years."

Charles Darwin

"The reconstruction of ancient communities sounds like the right thing to do, but where does it all lead and why?"

Stephen Jay Gould

8.1 Introduction

The word "ecology" was created by the German zoologist Ernest Haeckel in the 1860's as a description of "the study of all those complex interrelations referred to by Darwin as the conditions for the struggle of life" (Kingsland, 1991; Smith, 1996). Paleoecology is the study of ancient ecosystems, the study of fossil communities in relation to their environments, and the habits and habitats of its individual members (Prothero, 1998; Wing et al., 1992). Mid-Cretaceous (Cenomanian) terrestrial vertebrate paleocommunities are rare in North America, and therefore poorly known. The Arlington Archosaur Site (AAS) is a fossil site found in the mid-Cretaceous Woodbine Formation of North Texas that preserves a coastal community that allows for a detailed study of Cenomanian terrestrial paleoecology. The AAS was a coastal ecosystem situated along a paleogeographic peninsula referred to as Rudradia that projected into the Cretaceous

intercontinental seaway of southwestern Appalachia (Fig. 8.1). The AAS ecosystem was a diverse community that consisted of both macrovertebrates and microvertebrates from a low lying coastal marsh. The macrovertebrates were principally dinosaurs (ornithopod and theropods), crocodyliforms, and turtles. The microvertebrates include a diverse assemblage of juvenile crocodyliforms, lizards, salamanders, mammals, fish, and lungfish. The fossils occur principally from two horizons, an organic rich peat bed and a clay rich paleosol (Fig. 8.). The two fossil horizons are bound by beds containing charcoal, and in the case of the paleosol, a charcoal horizon occurs within the bed (Fig. 8.2). The presence of charcoal beds both within and bounding the fossil horizons suggests that the AAS ecosystem was potentially influenced by wildfires. The influence of wildfires on an ecosystem, particularly an ecosystem known only from the fossil record, is difficult to ascertain.

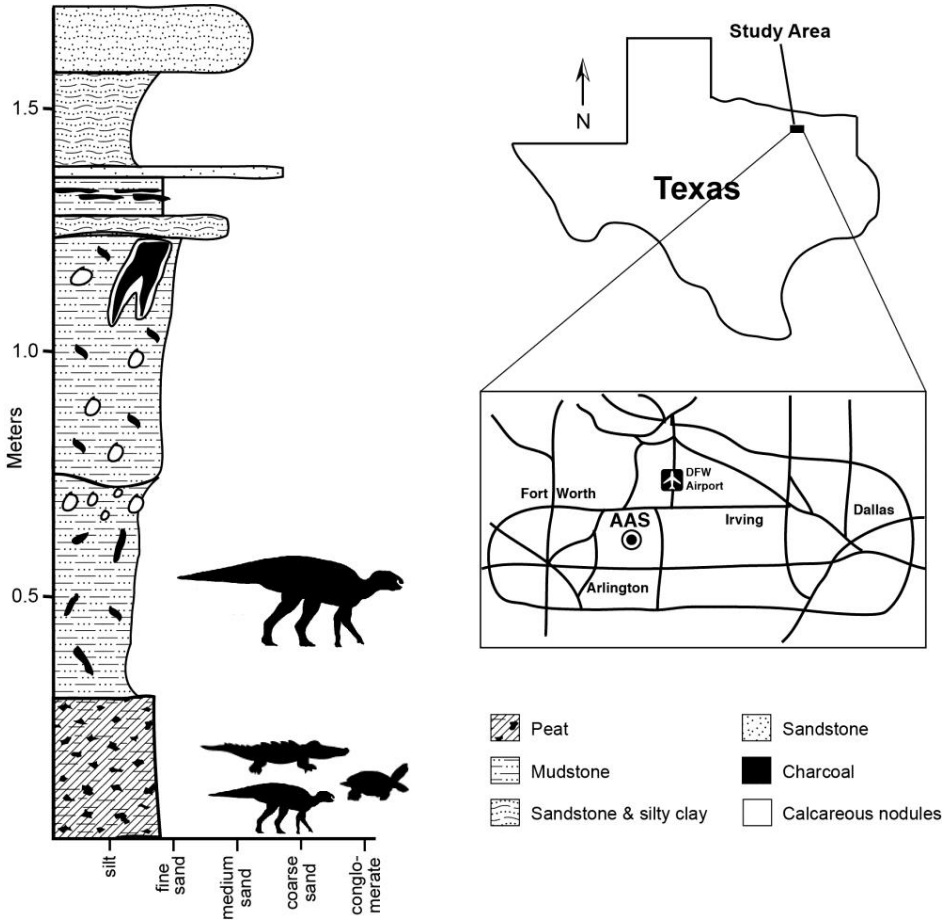

Figure 8.1 Location map of the AAS (right). A composite stratigraphic column (left); the lowermost horizon is a peat bed containing crocodyliform, turtle, and juvenile ornithopod fossils. The horizon above contained ornithopod bones and charcoal roots in a paleosol.

Wildfires are known to disturb modern ecosystems to varying degrees, and are well studied by modern ecologists concerned with the impact of fires to the ecological stabilty within given bioregions, California being a well documented example (Davis and Borchert, 2006; Fites-Kaufman et al., 2006; Keely, 2006; Shaffer et al., 2006 and Sugihara et a., 2006). There is, however, a growing volume

of work on the role of fire in the Earth system though time, with a particular interest in time frames with high fossil diversity that coincides with greenhouse climates; the Cretaceous (Brown et al., 2012). The Cretaceous has an extensive global geological record of charcoal, much of which is associated with diverse fossil horizons of both plants and vertebrates (Bond and Scott, 2010; Bowman et al., 2009; and Brown et al., 2012). Dinosaur Provincial Park in particular has yielded an abundance of charcoal in association with dinosaur remains, which allowed for the study of wildfires and their potential influence on the ecosystem (Brown et al., 2012). The interaction of disturbance mechanisms, such as wildfires, upon ecosystems allows for interesting studies of paleoecology and biodiversity in response to periodic catastrophe (Curanno et al., 2011).

AAS field work initially focused on quarrying macrovertebrates; dinosaurs and crocodyliforms. Subsequent intensive surface collecting and screen washing have since revealed a diverse microvertebrate assemblage. Chondrichthyans include an indeterminant hybodont, the lamniform *Cretodus*, the ray *Pseudohypolophus*, and the sawfish *Onchopristis*. A new species of lungfish (*Ceratodus carterii.*) has been recovered, as well as the ganoid scales of the semionotiform *Lepidotes*, the prearticular of the pycnodont cf. *Palaeobalistum*, and centra of an indeterminate amiiform (Main et al., 2012). Teleost material includes a single tooth from a tetraodontiform (cf. *Stephanodus*) and numerous unidentified centra. Salamanders and frogs are represented by a handful of

vertebrae, and a humerus and radioulna, respectively. The fresh water requirements of salamanders suggest an upstream, freshwater source for these taxa. Shell fragments of turtles (cf. *Glyptops* and Trionychoidea indet.) are common and show crocodyliform feeding traces. Lizard vertebrae are small (<4 mm) and show typical conservative morphology. Shed crocodyliform teeth are common (n>350), representing multiple taxa and growth stages. Theropod teeth are rare, but indicate at least one small (Dromaeosauridae indet.) and one large (cf. *Acrocanthosaurus*) taxon (Noto and Main, in press). A single multituberculate lower fourth premolar may represent a new taxon.

The paleoenvironments of the AAS represents an intermittently inundated delta plain that was beset by periodic storms and lightning strike wildfires. Stratigraphically, the AAS preserves a fossil rich peat from a marine-influenced wetland; a dinosaur bone bearing paleosol containing calcareous concretions and charcoal roots indicating seasonal dryness and wildfires. Each of the fossil beds is bound by fossil charcoal (fusain) bearing horizons including afossil charcoal conglomerate, a concretion bearing burned root horizon and a charcoal debris flow bed. The presence of fossil charcoal beds intermingled with the fossil horizons suggests an ecosystem that endured periodic wildfires. Thus, Woodbine ecosystems were impacted by and possibly adapted to from seasonal storms and wildfires.

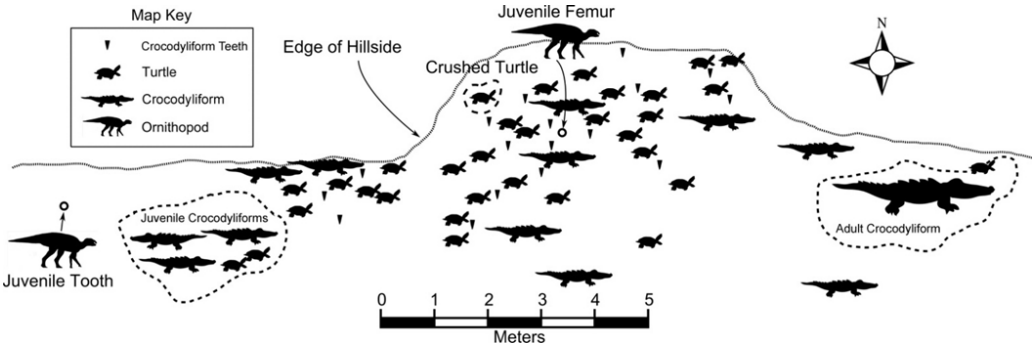

Figure 8.2 Diagram-map of theAAS excavation showing locations of crocodyliform, turtle, and ornithopod dinosaur remains within the sites referred to as Crocorama, the Turtle Buffet and the Nursery. Dense collections of fossils referable to one or more individuals are surrounded by dotted lines (occur within the"Nursery"). Crocodyliform teeth and coprolites recovered from Crocorama, Nursery and Turtle Buffet sites.

8.2 Materials and Methods

Paleoecological studies rely upon data from carefully collected, well preserved and well prepared fossils (Whittington, 1964). This study of the paleoecology of the AAS Woodbine coastal system was conducted by a large scale program of fossil collecting via prospecting and surface collection, excavation with hand tools, bulk sampling and screen washing. Surface collected fossils were photographed and notes were made of their approximate location on the property. All excavated fossils were mapped within the AAS grid system that was developed by R. Fry, photographed and documented before removal from the site (Main and Fry, 2011) (Appendix B).

All of the AAS fossil sites; the Dinosaur Quarry, the Nursery, the Turtle Buffet, Crocorama and Crocorama East occur within a well-defined metric map grid that was developed by AAS dig crew boss Roger Fry (Fig. 8.3 and 8.4). Fry established a 2.5 X 5m grid system around the initial Crocorama dig site (Fig. 8.4) (Fry and Main, 2010; Main and Fry, 2011). A Cartesian coordinate system was used to plot the locations of all fossils in 2D space. Each fossil within the grid was given an (x, y) coordinate; for example (4.5) or (-18.12), and drawn onto the maps with a brief note about the type of fossil found. This method was utilized in an effort to document both the initial identification and location of all fossils in relation to one another for future taphonomic and paleoecological purposes (Fig. 8.4). The AAS mapping methodology proved fruitful, as the final interpretation of the paleoecology of the AAS greatly relied upon these maps.

The initial map grid was established with four stakes of rebar, construction tape and a series of survey flags (Fig. 8.4). The initial grid established a perimeter; however as it was an active dig, the flags were commonly knocked over by the dig crew. This problem was noted by the author and corrected for future digs following the initial one week Crocorama excavation. In the months that followed, Fry established an extended map grid using a surveyors GeoShack tripod system (Fig. 8.3). Once lines were shot, additional rebar stakes were plotted along the base of the AAS hillside, with map grid coordinates written on the top of each stake. All fossils found within the mapped area, were added to the map by

plotting their location with measuring tape and a 0.5 m square (Fig. 8.3) (Fry and Main, 2010; Main and Fry, 2011).

The original AAS map grid was established during the Crocorama dig of 2009 and later expanded into new multiple new grids (Fig. 8.4). The original map grid was set at (0.0) and progressed to the west and ended at positive (5.5) (Fig. 8.4). As the Crocorama dig progressed, the map grid was expanded into the East, North, Northwest, and West 1 and West 2 grids. As the Crocorama site was further excavated, and expanded into the Turtle Buffet and the Nursery sites, the map grid was expanded to accommodate, however to do so the grid had to use negative coordinates; (-18.5). Ultimately by 2010, the Dinosaur Quarry was added to the map system, as was the Flying Turtle Site, with a total of 29 maps being produced, (only 21 were cited in this work as they extended beyond the areas discussed). The new maps included the North 1, North 1 East 1-2, North 1 West 1, Northeast and Northeast 1-2, Northwest 1-4, West 3-4 (Table ?). The combined AAS map grid as of the time of this writing covered a 7.5 meter wide by 70 meter long area (Table 8.1). For more on the AAS maps made by R. Fry and a full display of the mapping grid, see Appendix B.

Table 8.1 AAS Map grid information; map names, coordinates and sites covered by the AAS maps. All map coordinates are in meters (See Appendix B for AAS maps, all map data courtesy R. Fry).

Map Grid Name	**Map Coordinates**	**Site Name**
Original (Prime)	(01=>10), (01=>05)	Crocorama
East	(10=> 20), (01=>05)	Crocorama
East 1	(21=>30), (01=>05)	Crocorama East
East 2	(31=>40), (01=>05)	Crocorama East
North	(01=>10), (11=>15)	Crocorama
North 1	(01=>10), (11=>15)	Crocorama
North 1 East 1	(10=>20), (11=>15)	Crocorama East
North 1 East 2	(31=>40), (11=>15)	Crocorama East
North 1 West	(-01=>-10), (11=>15)	Crocorama
North 1 West 1	(-11=>-20), (11=>150	Turtle Buffet
North East	(10=>20), (06, =>20)	Crocorama
North East 1	(21=>30), (06=>10)	Crocorama East
Northwest	(-01=>-10), (06=>10)	Turtle Buffet
Northwest 1	(-11=>-20), (06, 10)	Turtle Buffet/Nursery
Northwest 2	(-21=>-30), (06=>10)	Nursery/Dino Quarry

Table 8.1 cont.

Northwest 3	(-31=>-40), (06=>10)	Dinosaur Quarry
Northwest 4	(-40=>-50), (06=>10)	Dinosaur Quarry
West	(-01=>-10), (01=>05)	Crocorama
West 1	(-11=>-20), (01=>05)	Turtle Buffet/Nursery
West 2	(-21=>-30), (01=>05)	Nursery/Dino Quarry
West 3	(-31=>-40), (01=>05)	Dinosaur Quarry

Figure 8.3 Roger Fry using a Geo-Shack tripod to survey the site. Then using a 0.5 m square and measuring tape to map new fossils found within the grid.

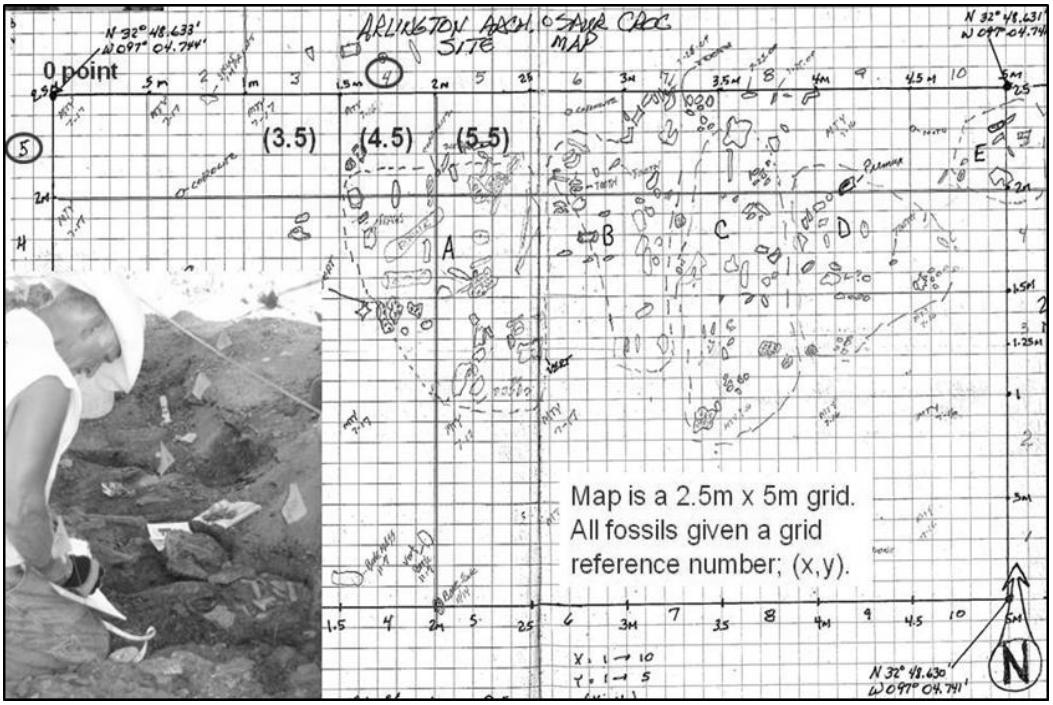

Figure 8.4 Figured map is a reproduction of R. Fry's original hand drawn map of the Crocorama Site, July 2009. See Appendix B for copies of all maps.

All fossils were photographed in situ with a metric scale bar and a north arrow to give the specimens both a size estimate and a geographic position (Fig. 8.5). This provided additional data that could be utilized for taphonomic purposes. The map coordinates were then recorded with the fossils before removal from the field. Grid coordinates were later used as a collections management technique, as all grid references were recorded on the boxes in which the fossils were stored (Fig. 8.6). The collection was then arranged based upon the map coordinates, with each shelf of fossils containing specimens from specific areas of the mapping grid

(Fig. 8.6). This method of map-based collections is new to vertebrate paleontology, as most museums store fossil specimens taxonomically.

Figure 8.5 Field data collection methods; fossil mapped in situ and photographed with a north arrow and scale.

Figure 8.6 AAS fossils in Lane cabinet, individual specimen boxes denoted with map coordinates and placed upon a shelf.

A collections database was developed by the author to catalogue all fossil specimens found at the AAS (see Appendix A). The database was primarily taxonomically ordered, with each major taxon given a collection designation based upon the year of discovery. The AAS hadrosauroid was documented within the database as UTA-AASO-2003; UTA to designate the university in which the fossils were temporarily stored (UT-Arlington), AASO to designate the site of discovery (Arlington Archosaur Site) and the taxon (Ornithopod), followed by the year of the discovery (2003). All fossil specimens from the AAS hadrosauroid were then catalogued within this taxonomic classification and given a catalogue number that began with UTA-AASO followed by an individual number (Ex: UTA-AASO-001).

The AAS crocodyliform was catalogued as UTA-AASC-2009 and all individual specimens were later logged as UTA-AASC-00# (Appendix A). The specimen number was followed by a taxonomic designation and a brief description of the fossil element (or elements in the case of multiple teeth). Other fields of data within the AAS collections database that were used was a column that featured location data to clarify where at the AAS the fossil was found. The location column included a site name; Dino-Quarry, Crocorama, Nursery or Turtle Buffet along with specific map grid coordinates (Appendix A). A collection methods column was included within the database in order to clarify if the specimen was surface collected, quarried or screen washed from a bulk

sample. Equally, a column citing the fossil discoverer was included, as some specimens may hold particular significance. Of greatest importance, a column within the database was established to notate the cabinet and drawer in which the fossil was stored in order to better facilitate locating the specimen within the collection once curated. Utilizing a combined field mapping method with a detailed collections database that links all data back to the collection itself proved an invaluable research technique for this project.

Figure 8.7 Images of the AAS excavation in the summer of 2010. By this time, the AAS reached its peak in activity and methodology. Tents were primarily used to protect the dig crew in the summer from the extreme heat. Bulks samples of excavated sediment were left out to dry before being screen washed and sorted for micro-vertebrate fossils.

Microvertebrate fossils were recovered by a complex program of bulk sampling and screenwashing of Woodbine sediment. Bulk sediment samples were taken from the AAS peat bed at the Crocorama, Turtle Buffet and Nursery sites, as well as from the Dinosaur Quarry paleosol and sand lenses. Bulk sediment samples were soaked in buckets and stirred, then poured into screens and placed into a large local water source to soak; a creek or lake (Fig. 8.8). The AAS micro-screening was conducted at two stations, a nearby creek in the woods within a ~1 km east from the AAS hillside excavation (Fig. 8.8). Referred to as "Croc Creek," the creek screen station was primarily utilized due to its close proximity to the dig, and to the shallow waters, although it commonly dried up in the summer months (Fig. 8.8). The second micro-screen station was at a lake south of the AAS hillside excavation, located at the southern edge of the property near the historic Birds Fort (Fig. 8.8). The water was deeper, and allowed for year round access (Fig. 8.8 and 8.9). Due to the common sightings of snakes at the lake, the author named it "Snake Lake."

The screens were hand built wooden frames that were 36.25 (L x W) cm x 15 H cm in diameter and had 20 mesh (2 mm) screen wire attached to the bottom (Fig. 8.9). Once sediment samples were soaked in screens for at least 24-48 hours (up to 72-96 hours), they were then screen washed (shaken) at the water source (Fig. 8.9). Once sediment was broken down and all clay was removed, screened samples were then poured onto a tarp to dry, then bagged and taken to a lab to be

sorted under a microscope (Fig. 8.9). Microvertebrate fossils found in bulk samples that were screen washed and sorted, were placed within the stratigraphic horizon from which the sample was taken. Recovered fossils (microvertebrate and macrovertebrate) were prepared for study in a lab (sediment matrix removed and preservative applied), then given an AAS collections number and logged into a collections database with key information on the element and the location at the AAS from which it was found (Appendix A). The AAS maps were used to study the lateral distributions of fossils at the site in order to understand the site taphonomy and to test hypotheses about the trophic structure of the ecosystem (Appendix B).

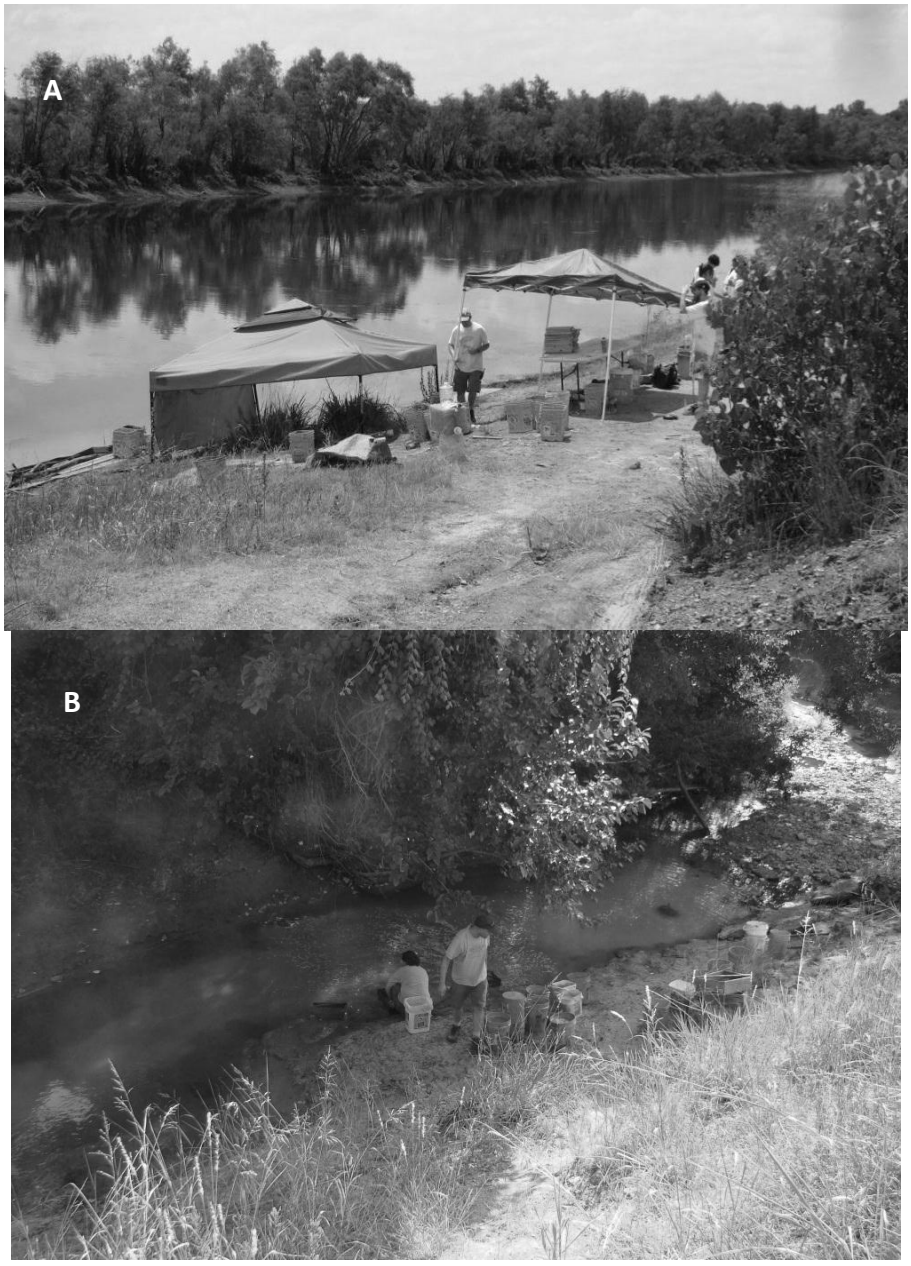

Figure 8.8 AAS Micro-screening stations. A. The “Snake Lake” micro-screening station located near the historic Birds Fort at the southern edge of the property. B. The “Croc Creek” micro-screening station at a shallow creek in the woods ~1 km to the east of the AAS hillside.

Figure 8.9 Images of AAS microvertebrate screening project. A) Woodbine sediment samples being soaked and stirred in buckets, AAS assistant N. Van Vranken stirring. B) Woodbine sample soaking in a hand built wooden screen. C) Woodbine samples being screen washed at "Snake Lake" by AAS assistant Rachel Brown and volunteers. D) Screened Woodbine samples being poured onto a tarp for drying and later sorting,
Geb Bennett.

8.3 Discussion

8.3.1Coastal Ecosystems: Crocodyliform Feeding Grounds

The Woodbine deposits at the AAS are fossil rich preserving a near complete coastal ecosystem with a variety of organisms ranging from small fish and lizards, to lungfish, turtles, crocodyliforms and dinosaurs (ornithopod and theropod) (Main, 2009). The AAS dinosaur fauna was dominanted by large herbivorous ornithopods, principally a new taxon of basal hadrosauroid (Main et al, in press). The AAS coastal ecosystem also supported a variety of small to medium range of carnivorous theropods that hunted along the coastal plain. Although theropods were present along the Rudradian coast, crocodyliforms were more common and therefore thought to be the apex predator of the system. This hypothesis is supported by numerous turtle shell remains found at the site with a variety of crocodyliform bite marks and feeding traces (Noto et al., 2012). The pattern of bite marks found in the fossils of the AAS peat bed may be utilized as an indication of the nature of the AAS coastal ecosystem as a possible feeding ground or den.

Koken (1887), Nopsca (1902), Seidlitz (1917) and Weigelt (1989) noted vertebrate fossil assemblages that are associated with remains of crocodyliforms, may be attributed to crocodyliform feeding grounds. Koken (1887) was among the first to note that fossil deposits in swamp coal beds that contain crocodyliforms tend to have diagnostic characteristics that differentiate them from

other fossil deposits. Koken (1887) noted that the fossil beds of the north German Weald coal deposits where crocodyliforms (goniopholids) were present, contained various remains of numerous taxa, many of which did not seem to be associated with one another. Koken (1887) interpreted many of the isolated fossil elements as being torn apart. Equally, among the various remains were found isolated crocodyliform teeth in great abundance (Koken, 1887). Today, modern crocodiles shed their teeth when feeding; commonly losing them among the carnage of their feeding ground (Weigelt, 1989).

Nopsca (1902) related the accumulation of saurian fossils in the mid-Cretaceous sediments of Transylvania to crocodyliform feeding grounds. Nopsca (1902) based this interpretation upon the fragmentary nature of the remains, and the presence of broken turtle shell found in great abundance. Similar crocodyliform deposits have been documented in the Gosau Formation of Austria, in the German Eocene lignite swamps, in the Oligocene oreodont beds of Nebraska and in the Miocene of Steinheim Lake (Weigelt, 1989). Seidlitz (1917) noted in the excavation of mammals from the Eocene from Seiglitz that alligator teeth occurred in abundance with the mammal fossil accumulations along with numerous alligator coprolites. Seidlitz (1917) was the first to attribute the presence of crocodilian teeth and coprolites to crocodilian feeding grounds. Since Seidlitz (1917), deposits containing the mixed remains of vertebrate carcasses, with numerous shed crocodyliform teeth and coprolites have been attributed to

feeding grounds. In all of these cases it was interpreted that the crocodyliforms were feeding, and then leaving the remains of their prey piled up, and defecating, leaving their droppings scattered among the remains (Weigelt, 1989).

The more recent work of Boyd et al. (2013), Noto et al. (2012) and Njau and Blumenschine (2006) further demonstrate how the feeding behavior of crocodyliforms may impact fossil assemblages and be used in paleoecological models. Boyd et al. (2013) and Noto et al. (2012) demonstrated that Cretaceous crocodyliforms serve as important taphonomic agents, accumulating and modifying vertebrate fossils as part of their feeding behavior. Boyd et al. (2013) documented evidence of a small crocodyliform killing and feeding upon small ornithischian dinosaurs, hypsilophodonts from the Upper Cretaceous (Campanian) Kaiparowits Formation. Boyd et al. (2013) described a series of bite marks on hypsilophodontid post cranial remains; a scapula and femur, with a partial crocodyliform tooth embedded within the limb bone. Noto et al. (2012) as part of this dissertation work, documented a series of crocodyliform bite marks, scores and punctures in turtle shell fossils. The work of Boyd et al. (2013) and Noto et al. (2012) are too date the best documented examples of Cretaceous crocodyliform feeding. The work of Njau and Blumenschine (2006) documented Cenozoic feeding traces found on mammal bones attributed to *Crocodylus niloticus* in the Plio-Pleistocene deposits of Olduvai Basin, Tanzania.

Deposits that consist of bitten, broken bones found in association with shed crocodile teeth and excrement are often found near crocodyliform dens or nests (Weigelt, 1989). In the case of dens or nests, crocodyliforms may leave the remains of meals and their excretions in great accumulations (Weigelt, 1989). This behavior has been noted among other members of the archosauria, in particular the birds. Weigelt (1989) noted numerous remains of miscellaneous vertebrates accumulated near the nests of predatory birds such as ospreys, sea eagles, merlins, gulls and owls. In the case of owls, the remains of over seven million different specimens have been recovered from the cave nest of a pair of *Strix perlata* (cave owls) (Weigelt, 1989). These patterns of feeding and nesting behavior of both modern and ancient archosaurs are important, as they may be used as an analog, or approximation for the AAS Woodbine ecosystem.

The AAS Woodbine ecosystem was dominated by crocodyliforms. Their remains were abundant at the AAS and varied in ontogeny, demonstrating growth stages from multiple individuals. The fossil remains from all of these individuals were recovered from the same horizon, the AAS Facies B peat bed at the base of the NE hillside. The remains were mapped within a 55 meter area, occurring from (32.7) to (-28. 8) on the AAS map grid. From areas at the AAS referred to as Crocorama, Crocorama East, the Turtle Buffet and the Nursery. Among the crocodyliform remains were the broken remains of turtles, some of which preserved evidence of feeding, as well as fish and lizard vertebrae, broken partial

dinosaur remains and numerous coprolites. The accumulation of fossils from the AAS peat bed is greatly reminiscent of those discussed by Weigelt (1989). The record of crocdyliform feeding at the AAS discussed in Noto et al. (2012) supports the interpretation of the AAS Woodbine ecosystem as being part of a crocodyliform feeding ground, similar to those discussed by Weigelt (1989). Therefore, the AAS ecosystem is interpreted to be representative of either a crocodyliform feeding ground, or possibly a nesting den.

In modern marsh ecosystems crocodiles exhibit complex group social behavior, and males compete for mating rights with multiple females (Lang, 1999; Magnusson et al., 1999). In the case of the Nile crocodile, *Crocodilus niloticus*, breeding occurs seasonally, at times of low water levels (Cott, 1961). Once impregnated, female crocodiles will build a nest near a source of food and water, typically near large bodies of water (Cott, 1961; Magnusson et al., 1999; Strawn, 1997). The types of nests vary from mounds constructed of foiliage to shallow, underground burrows (Magnusson et al., 1999; Strawn, 1997). In the case of *Crocodilus niloticus*, nests are dug down into the soil, typically in the mud flats of the river floodplain (Cott, 1961). Nile crocodiles will nest together in groups, exhibiting gregarious nesting behavior with as many as thirty nests in a given nesting ground (Cott, 1961). The nests are closely spaced, so much so that old, abandoned nests appear almost continuous across the floodplain (Cott, 1961). Female crocodilians will spend up to a year in, or near the nest, protecting the nest

and their young (Cott, 1961; Deitz and Hines, 1980; Magnusson et al., 1999; Strawn, 1997).

Studies of *Alligator mississippiensis* in Florida and Louisiana have repeatedly shown evidence of nesting and group behavior. Joanen (1969) documented over 300 *A. mississippiensis* nests over a five year period from Louisiana's coastal marshes. Joanen (1969) demonstrated the behavior patterns associated with alligator nesting, including male visitation and the duration at which female alligators would maintain the nest, for several months up to one year. This pattern of behavior was found to be consistent, not periodic or random. Deitz and Hines (1980) had a robust dataset via data collected from over 100 *A. mississippiensis* nests from lakes and coastal plains in Florida, principally at Paynes Prairie State Preserve, a 5,000 hectare marshy basin.

The nests at Paynes Prairie consisted of surficial nests that were constructed from sawgrass, and occurred in peat marshlands within 200 meters of levees and fresh water sources (Deitz and Hines, 1980). Nests with eggs or hatchlings were typically attended/defended by a female, not a male, but not in all instances (Deitz and Hines, 1980). The females will stay with the young in the nest for several weeks, before either carrying them out in her mouth or ultimately abandoning the nest (Deitz and Hines, 1980). In the cases of unattended nests, female turtles (*Trionyx ferax*) were found to have invaded and occupied the alligator nest for their own purposes. This behavior is particularly interesting

given the amount of turtle material found in association with crocodyliform material at the AAS.

Ogden (1978) studied thepopulation ecology, nesting and feeding behavior of the modern American crocodile, *Crocodylus acutus* from Everglades National Park and Key Largo in Florida. Ogden (1978) determined that *Crocodylus acutus* were mound nesters that had a distinct pattern of building nests in well drained coastal areas; beaches, creek banks, and abandoned canal levees. The nests were located and mapped by boat, then regularly checked during the months of the Florida breeding season, March-August. It was found that the average female produced 44-50 eggs, 44% of which survived to maturity (Ogden, 1978). Of particular interest to the AAS, is Ogden (1978) was able to show seasonal disturbance to the nesting grounds by coastal hurricanes, with nesting females leaving the nesting region, then returning to the same region on a yearly basis.

Messel and Vorlleck (1989) presented a detailed study of the ecology and behavior of the massive Australian crocodile; *Crocodylus porosus*. The modern saltwater crocodile is among the largest alive in the world today. It has an extensive biogeographic range that extends from Sri Lanka to the west coast of India, to the Philippines, New Guinea and Australia (Messel and Vorlleck, 1989). The nesting and feeding behavior of the Australian saltwater crocs was studied over a 15 year time frame in northern Australia. It was found that *Crocodylus porosus* had a distinct nesting, feeding distribution along the Australian coast,

and that environmental parameters such as salinity, wetness/dryness, and topography had an influence on their distribution, but all essentially preferred to nest within coastal swamps (Messel and Vorlleck, 1989). The work of Messel and Vorlleck (1989) established a classification for the areas within northern Australia's swamps, based on salinity and ecology (Type 1-3; Mangrove, Floodplain and Freshwater Swamp). Saltwater croc nests were common in the swamp, most of which occurred near a fresh water source and varied in size (~50 cm tall/160 cm diameter) and composition, although most were constructed from mud and vegetable debris with a mix of swamp peat and roots (Messel and Vorlleck, 1989).

Of greatest interest of the work of Messel and Vorlleck (1989) with Australian saltwater crocs that may have relevance to the AAS ecosystem is a well documented size distribution along the Australian coast, in which adults' occupied distinct regions within the swamp, separate from sub-adults and juveniles. The separation of the adults from the juveniles established distinct food preferences and separate feeding grounds. Once adults established a feeding ground, sub-adults and juveniles were forced further down the river/swamp system. The AAS does not appear to support this size differentiation, but it is worth noting. The work of Messel and Vorlleck (1989), Ogden (1978), Deitz and Hines (1980), Joanen (1969) and Campbell (1972) have shown a habitat preference and a regular pattern of behavior in Crocodylinae behavior that is

evolutionarily distinct, and may perhaps be used as a model to trace similar behavior back to the Cretaceous.

Cases of reptile nesting are well recorded among other archosauria from the fossil record, most notably from Cretaceous dinosauria. The first case of dinosaur eggs and nests was reported by the famous archeaologist Roy Chapman Andrews while exploring the Flaming Cliffs of Mongolia (Novacek et al., 1994). Since Andrews, there has been a renaissance of dinosaur egg nest discoveries reported from numerous sites (Carpenter and Alf, 1994; Carpenter, 1999). Among the egg nest discoveries are; oviraptor nests from China (Norell et al., 1995), sauropod nests from India (Sahini, 1997), theropod nests from Argentina (Salgado et al., 2007), dinosaur egg nests from Uruguay (Faccio, 1994), baby hadrosaur nests from Alberta Canada (Fanti an Mihashita, 2009), hadrosaur egg nests from Romania (Grigorescu et al., 1994), the first dinosaur egg site found in France (Cousin et al,. 1994) ,and sauropod nest sites in Spain (Sander et al., 1998) as well as evidence of dinosaurs nesting on tidal flats in Spain (Lopez-Martinez, 2000). Dinosaur egg nest sites have been documented globally, from the Upper Cretaceous deposits of nearly every continent (Carpenter and Alf, 1994). Among the more famous dinosaur egg nest sites studied was the *Maiasaura* nesting colonies from the Late Cretaceous of Montana (Horner, 1982; Horner., 1983; Horner, 1984c; Horner and Dobb, 1997).

Maiasaura, the "good Mother lizard" was a duck-billed hadrosaur discovered in the Late Cretaceous (Campanian) Two Medicine River Formation of western Montana in 1978 (Horner, 1982; Horner, 1984c; Horner, 1983). It was found to occur with multiple fossil egg nests and young in variable growth stages (Horner, 1982; Horner., 1983; Horner, 1984c; Horner and Dobb, 1997). The egg nests were numerous and occurred in an anticline, hence the name of the site, Egg Mountain (Horner, 1982). The egg nests occurred within the mudstones of an ancient floodplain, and were found spaced regularly at about 7 meter intervals (Horner, 1982; Horner, 1984c). As the estimated length of adult hadrosaurs is approximately 6-7 meters, it was interpreted by Horner (1982) that the Two Medicine River Maiasaura site was a colonial nesting ground occupied periodically by gregarious nesting hadrosaurs (Horner, 1982; Horner., 1983; Horner and Dobb, 1997). Of interesting note, the *Maiasaura* egg nest colony documented at the Egg Mountain site occurred within floodplain deposits, a similar paleoenvironmental placement that was documented at numerous other dinosaur egg nest sites. This floodplain nesting pattern demonstrates a habitat preference among the dinosauria, similar to that documented with modern crocodilians (Campbell, 1972; Carpenter, 1999; Deitz and Hines, 1980).

Given the record of archosauria nesting behavior from the modern to the ancient, it is plausible that the AAS crocodyliforms were nesting along the Rudradian coast of southwest Appalachia much like modern alligators do today in

the Florida everglades and in the extensive marshlands of Louisiana. As crocodyliforms are the most common fossil element found at the AAS, it would appear that they were the prominent component of the ecosystem (possible taphonomic bias aside). Equally, the presence of juvenile crocodyliforms recovered from the same fossil horizon as large adult skeletons, and within 10 meters of one another, implies a possible nest or den (Fig. 8.10) (Appendix B). To date, at least three juvenile crocodyliform individuals are confirmed at the AAS by the presence of three left mandibles, and numerous juvenile remains that suggest other juvenile individuals (Fig. 8.10). However, to date no fossil eggs or egg shells have been recovered from the AAS Woodbine peat bed. With the extensive micro-sampling and screen washing project at the AAS, egg shell fragments should have been detected, but were not. Therefore, it is difficult to ascertain with certainty that the AAS was a crocodyliform nesting site.

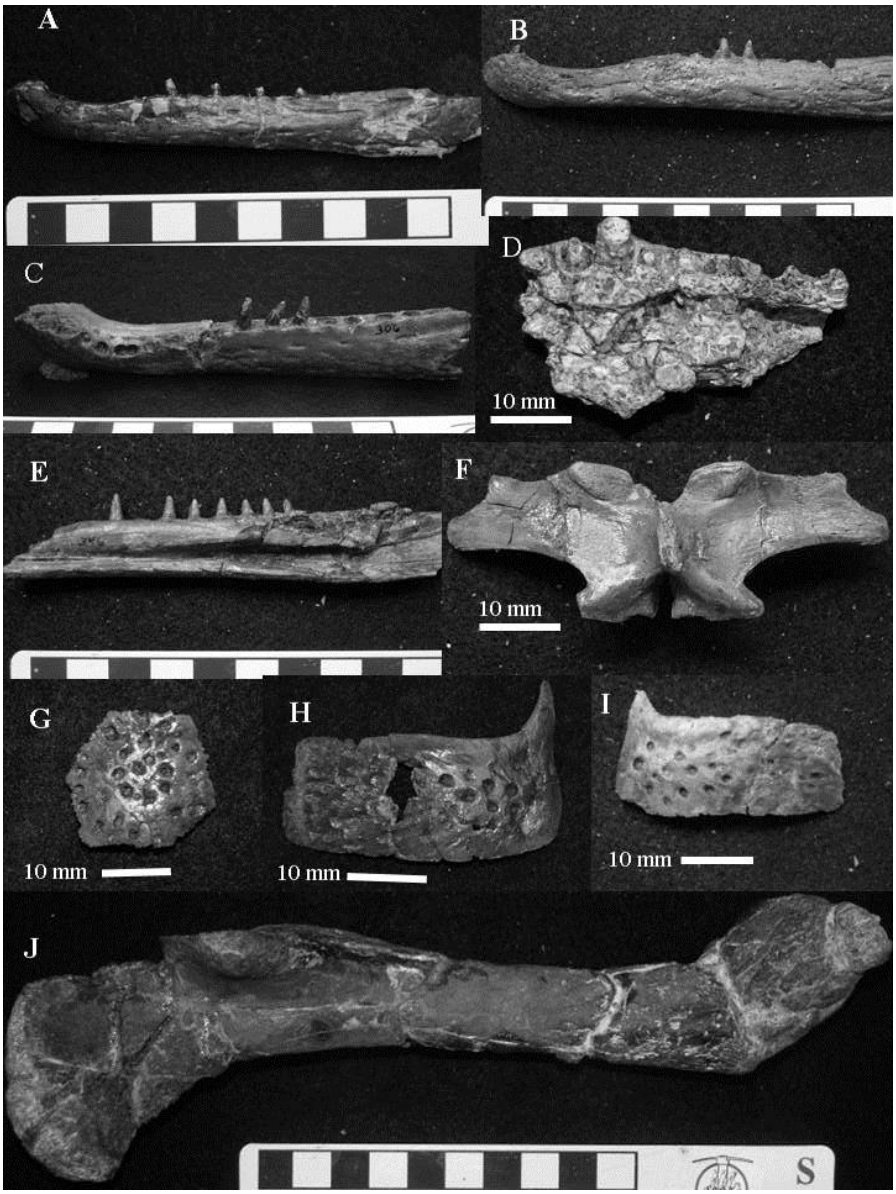

Figure 8.10 AAS juvenile crocodyliform remains. A. UTA-AASC-207 a juvenile left mandible. B. UTA-AASC-354 a juvenile left mandible. C. UTA-AASC-306 a juvenile left mandible. D. UTA-AASC-390 a partial juvenile left maxilla. E. UTA-AASC-346 a partial juvenile right mandible. F. UTA-AASC-390 a juvenile neural arch in ventral view. G. UTA-AASC-394 a juvenile ventral osteoderm. H. UTA-AASC-408 a juvenile dorsal osteoderm. I. UTA-AASC-341 a juvenile dorsal osteoderm. J. UTA-AASC-444 a sub-adult right humerus.

Although juvenile crocodyliform remains are common at the AAS, fossil eggs and egg shell have not been recovered from the AAS as yet. Therefore, with the data currently available, the feeding ground interpretation is a more tenable hypothesis. The feeding ground interpretation of the AAS is supported by the presence of numerous broken and bitten remains of turtles along with reptilian (crocodyliform) coprolites found at the site (Main et al., 2012 and 2013; Noto et al., 2012). The bitten and broken turtle shell remains were recovered from the site known as the Turtle Buffet and mapped to occur near the Crocorama site with other broken and bitten remains, including the remains of juvenile dinosaurs (see Appendix B). The bite marks were interpreted as being made by a crocodyliform and occurred in section with numerous shed crocodyliform teeth (Noto et al., 2012). The number of crocodyliform teeth and the size ranges present has been documented as evidence of crocodyliform feeding grounds in cases from both the modern world and the fossil record (Bennett, 2012; Main et al., 2012; Taylor and Neal, 1984). The abundance of bitten, discarded remains of turtle and dinosaur, along with numerous shed teeth occurring within swamp deposits, fits the description of crocodilian feeding grounds from both the modern and fossil record (Koken, 1887; Nopsca, 1902; Seidlitz, 1917 and Weigelt, 1989).

Living crocodilians are known for their voracious feeding habits (Cott, 1961; Pooley, 1999). They principally consume turtles, which have been found to make up the majority of stomach contents in large alligators and crocodiles (Cott,

1961; Milàn et al., 2010; Pooley, 1999). It has been shown that the body of the turtle can be consumed while leaving the carapace and plastron intact (Milàn et al., 2010). The abundance of shell remains and lack of turtle skeletal material at the AAS may reflect this feeding behavior. The AAS likely was part of an active crocodyliform feeding area, possibly a feeding ground associated with a breeding ground. This behavior occurred for an extended time, as shown by the > 350 isolated crocodyliform teeth (see Table 8.1) and numerous feeding traces recovered to date, a feature typical of localities with intense crocodilian activity (Njau, 2006; Weigelt, 1989). The teeth were collected by excavation and screen washing. The sizes of the shed teeth varied greatly, representing the feeding of more than one individual, and various growth stages (Table 8.1). The presence of numerous individuals of varying ages implies group feeding behavior in the region (Pooley, 1999; Taylor and Neal, 1984; Taylor, 1999; Weigelt, 1989) (Fig. 8.10 and 8.11). Areas of intense crocodyliform feeding are not unlike the paleoecology reconstructed for other Cretaceous crocodyliforms; *Deinosuchus* and *Sarcosuchus* (Main et al., 2012; Sereno et al., 2001; Schwimmer, 2002; Schwimmer and Harrell, 2010).

Table 8.1 Shed Crocodyliform tooth measurement data (Height, Width, FABL and Base Circumference), all measuremetns in mm.

Specimen #	Height	Width Carinae	FABL	Base Circumference
UTA-AASC-051	42.96	13.38	13.95	41
UTA-AASC-052	37.88	11.88	15.75	46
UTA-AASC-053	31.38	14.86	14.25	47
UTA-AASC-054	37.61	15.42	15.69	49
UTA-AASC-055	31.64	N/A	N/A	N/A
UTA-AASC-056	21.81	10.97	N/A	N/A
UTA-AASC-057	29.62	11.15	12.39	37
UTA-AASC-058	31.32	13.14	13.7	43
UTA-AASC-059	29.87	N/A	N/A	N/A
UTA-AASC-060	25.41	10.23	11.68	34
UTA-AASC-061	20.41	9.7	10.22	30
UTA-AASC-062	23.14	11.59	N/A	32
UTA-AASC-062	7	2.75	2.5	N/A
UTA-AASC-063	7	3	6	N/A
UTA-AASC-064	11.25	N/A	N/A	N/A
UTA-AASC-065	6	3	2	N/A
UTA-AASC-066	8	N/A	N/A	N/A
UTA-AASC-067	6	4.5	3	N/A
UTA-AASC-068	8	5.25	5	16
UTA-AASC-069	9	5	5	15
UTA-AASC-070	8	5	N/A	N/A
UTA-AASC-071	13	11	8	30
UTA-AASC-072	26	15	N/A	N/A
UTA-AASC-073	12	6	N/A	N/A
UTA-AASC-074	12	N/A	N/A	N/A
UTA-AASC-075	8	N/A	N/A	N/A
UTA-AASC-076	7	7	6	20

Table 1 cont.

UTA-AASC-077	7	7	6.5	N/A
UTA-AASC-078	16.25	N/A	9	N/A
UTA-AASC-079	12	7	6.5	21
UTA-AASC-080	15	7	N/A	N/A
UTA-AASC-081	13	5	5	16
UTA-AASC-082	14	7	6.5	N/A
UTA-AASC-083	11.5	6	6	18
UTA-AASC-084	11.5	7.5	7	23
UTA-AASC-085	19.5	5.5	5	16
UTA-AASC-086	8	N/A	N/A	34
UTA-AASC-087	11	N/A	N/A	14
UTA-AASC-088	12	N/A	N/A	N/A
UTA-AASC-089	12.5	N/A	N/A	N/A
UTA-AASC-090	12	5.25	3	N/A
UTA-AASC-091	17	N/A	N/A	N/A
UTA-AASC-092	23	N/A	N/A	N/A
UTA-AASC-093	23.5	N/A	N/A	N/A
UTA-AASC-094	17	N/A	N/A	N/A
UTA-AASC-095	29	N/A	N/A	N/A
UTA-AASC-096	27.25	11	N/A	N/A
UTA-AASC-097	20	N/A	N/A	62
UTA-AASC-098	8	4	4.5	14
UTA-AASC-099	18	8	7.5	23
UTA-AASC-100	7.25	3	3	too small
UTA-AASC-101	5	3.5	3	too small
UTA-AASC-102	18.5	6	6	18
UTA-AASC-118	13	5	5.5	21

UTA-AASC-123	27	N/A	N/A	N/A
UTA-AASC-124	14	N/A	N/A	N/A

UTA-AASC-129	10.75	N/A	3.25	11
UTA-AASC-130	12.25	12.25	12.75	21
UTA-AASC-131	19.25	7	7	23

Table 1 cont.

UTA-AASC-134	14.5	N/A	N/A	41
UTA-AASC-135	13	8.75	9	24
UTA-AASC-136	10.5	5.25	5.5	17
UTA-AASC-137	6.5	3.25	3	10
UTA-AASC-138	9.5	N/A	N/A	23
UTA-AASC-139	7.5	2.75	2.5	8
UTA-AASC-140	14	6.25	6.75	20
UTA-AASC-141	10	5	4.75	15
UTA-AASC-142	14.25	N/A	N/A	15
UTA-AASC-143	8.25	N/A	N/A	13
UTA-AASC-144	12	7	7	22
UTA-AASC-145	7.25	N/A	N/A	29
UTA-AASC-146	7	3.5	2.25	9
UTA-AASC-147	16	N/A	N/A	24
UTA-AASC-148	7.5	3.25	3.25	10
UTA-AASC-149	12.5	8	7.75	25
UTA-AASC-150	3	2	1.5	5.5
UTA-AASC-151	10	N/A	N/A	13
UTA-AASC-152	9.75	3.75	3.25	11
UTA-AASC-153	16.25	8	6.5	23
UTA-AASC-154	15	N/A	N/A	N/A
UTA-AASC-155	8	N/A	N/A	11
UTA-AASC-156	13.25	6.25	5.25	18
UTA-AASC-157	17.25	6.25	N/A	N/A
UTA-AASC-158	12.5	5	4.5	15
UTA-AASC-159	10.5	N/A	N/A	16
UTA-AASC-160	9.75	6.25	7	21
UTA-AASC-161	7.5	4.25	3.5	12
UTA-AASC-162	3.5	1.5	1	4
UTA-AASC-163	13	N/A	N/A	N/A
UTA-AASC-164	23	N/A	N/A	17
UTA-AASC-165	21.5	7	6	20
UTA-AASC-166	7.25	2.75	3	9

UTA-AASC-167	7.25	N/A	N/A	N/A
UTA-AASC-171	14.5	5.25	5.25	17
UTA-AASC-172	11.5	5	4.5	14
UTA-AASC-173	15.5	6.5	6.75	21
UTA-AASC-179	8	4.25	4	14
UTA-AASC-181	46.29	17.97	N/A	60
UTA-AASC-185	20.25	7.25	7.5	22
UTA-AASC-186	24	8	N/A	N/A
UTA-AASC-187	13	9.5	9.75	31
UTA-AASC-188	18.5	11.5	N/A	N/A
UTA-AASC-189	21	10	5	22
UTA-AASC-190	3	2	2	6
UTA-AASC-191	13	5.75	5	18
UTA-AASC-192	7.5	3.75	3.5	7
UTA-AASC-132	10	3.25	3	9

Bennett (2012) demonstrated that shed crocodyliform teeth can be used to study community structure in ancient coastal wetlands. Modern crocodilian populations coexisting on a feeding ground show high numbers of juvenile and sub-adult shed teeth occurring with adult teeth, although reduced in occurrence, as healthy populations support more young than old (Taylor and Neal, 1984; Taylor, 1999). Bennett (2012) sampled shed crocodyliform teeth from multiple sites within the Late Cretaceous Hell Creek Formation. The teeth were identified as belonging to more than one species, which implied niche partitioning in the Hell Creek (Bennett, 2012). The Hell Creek teeth were then measured and the data was plotted to view the percentage of juveniles to adults. Bennett (2012) confirmed a similar parrtern of shed crocodyliform teeth from the Cretaceous Hell Creek

Formation of Montanna as was noted by Taylor and Neal (1984) and Taylor (1999) for crocodilian populations in the modern world.

In order to better ascertain if the AAS was a crocodyliform feeding ground, the methodology of Bennett (2012) was applied to this project. A random sample of shed crocodyliform teeth collected from the AAS were measured and counted as a test of population structure and ecosystem dynamics. A random sample of 115 out of the 350 collected shed teeth was studied and measured (Table 8.1) (Fig. 8.11). The measurements taken were the same used by Bennett (2012), the tooth height, width of the carinae, FABL and base circumference (Fig. 8.12). The tooth height data was used to create a standard scatter plot in order to see the size distribution (Fig.8.13). It was found that the majority of crocodyliform teeth were <20 mm in height, thus representing juvenile or sub-adult crocodyliforms (Fig. 8.13). Based upon the previous work of Bennett (2012), Taylor and Neal (1984) and Taylor (1999), this data supports the interpretation of the AAS peat bed as being part of a coastal crocodyliform feeding ground (Main et al., 2013).

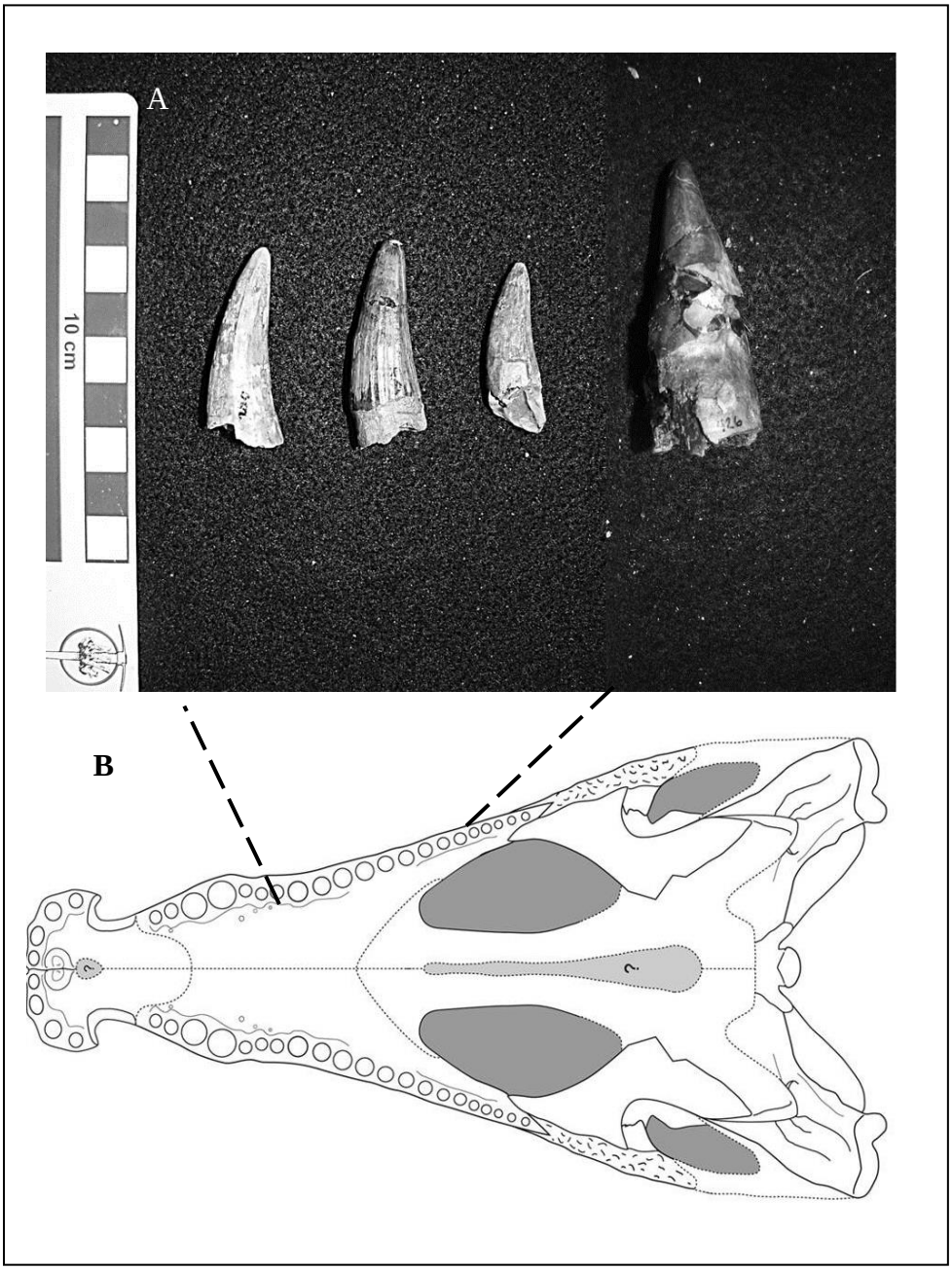

Figure 8.11 A. Size ranges of shed crocodyliform teeth collected at the AAS, sub adult to large adult, juvenile not shown. B. Shed teeth are interpreted as upper maxillary teeth (skull diagram courtesy C. R. Noto).

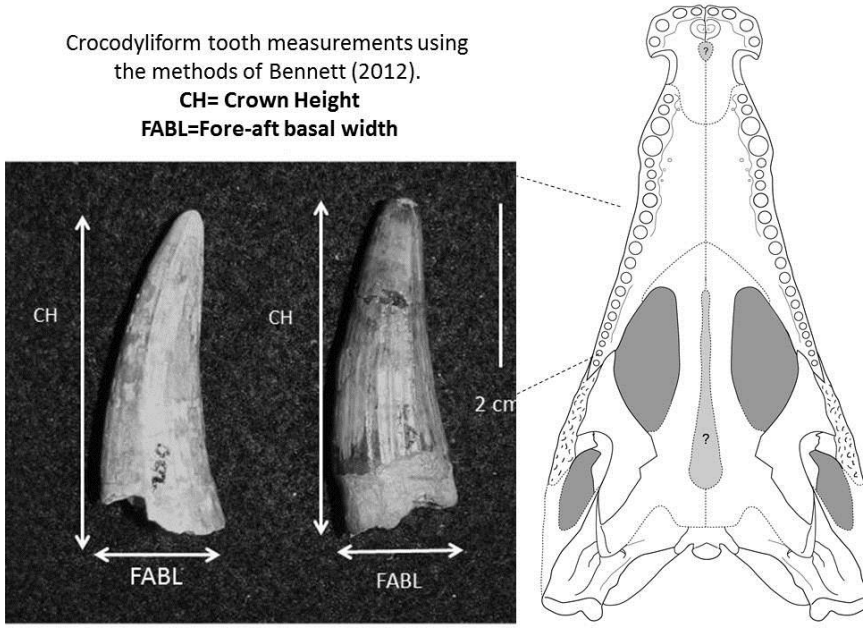

Figure 8.12 Tooth measurements utilized in this study; CH = Crown Height and FABL= Fore-aft basal width (after Bennett, 2012).

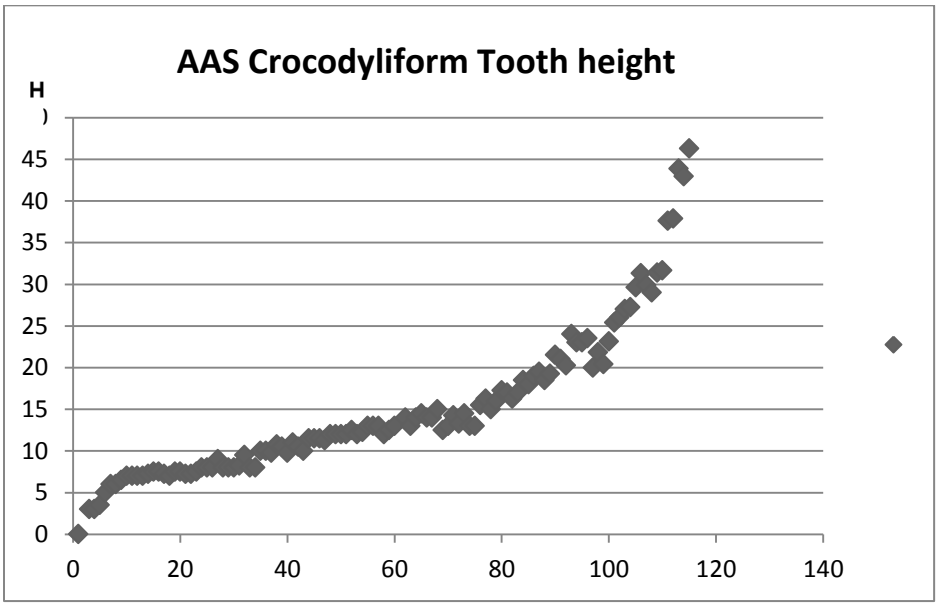

Figure 8.13 Scatter plot of the height of shed AAS crocodyliform teeth showing that the proportions of juvenile and sub-adult crocodyliforms are greater than adults among the AAS Woodbine coastal population.

8.3.2 Feeding Grounds and Coprolite Data

The feeding ground interpretation of the AAS ecosystem is supported by the presence of numerous coprolites that were recovered from the AAS, both surface collected and excavated (Main et al., 2013). The excavated coprolites were recovered primarily from a single horizon, the Facies B peat bed, and were mapped in situ in association with vertebrate remains (Fig. 8.21). Coprolites have been used since the time of Mantell and his study of *Iguanodon* to aid in the understanding of ancient ecosystems and the diet of extinct animals (Chin, 1996; Thulborn, 1991). Coprolites that were foundat the AAS in situ, excavated and then mapped, were included within this study. Over 150 (nearly 200) coprolites were recovered from the AAS, but not all were catalogued within the AAS collections database, as preference was given to mapped specimens. AAS coprolites utilized in this study may be referenced in Table 2 and Appendix A. The coprolites varied in morphology and size, but were principally classified as; Ovoid, Cylindrical/Scroll and Spiral (Sawyer, 1981and 1998; Thulborn, 1991).

Coprolite morphology may be used to identify the animal that excreted it, and thus may be used in ecological studies (Chin, 1996 and 2007; Coy, 1995; Sawyer, 1981 and 1998; Thulborn, 1991). Coprolite morphology is broadly divided into isopolar and anisopolar (Thulborn, 1991). Isopolar coprolites have ends of a similar shape; anisopolar coprolites have dissimilar ends, with one end being much larger than the other (Thulborn, 1991). Anisopolar coprolites are

typically ovoid in shape, and are attributed to large reptiles; dinosauria (Chin, 1996: Thulborn, 1991). Isopolar coprolites commonly occur as cylindrical, spiral and scroll (Thulborn, 1991). Cylidrical, Spiral and Scroll coprolite morphologies are associated with fish, sharks and crocodilians and are identified based upon size and content (Sawyer, 1981 and 1998; Thulbron, 1991). Sawyer (1998) classified coprolites from the Clapp Creek site in the Paleocene Black Mingo Group as crocodilian (crocodyliform) based on the morphology of the recovered specimens; all exhibited one of the following external shapes: Teardrop, Ovoid, or Dome/Cylinder.The classification scheme of Sawyer (1998) and Thulborn (1991) was applied to the AAS coprolites.

The AAS coprolites demonstrate all of the above mentioned morphologies, although most have either the broad Spiral or Scroll morphology, with the Dome/Cylinder classification of Sawyer (1998) being the most common. Small (< 5 cm) spiral coprolites were attributed to fish and sharks, principally the shark *Hybodus* (Thulborn, 1991) (Fig. 8.14). Large (> 6cm) Spiral and Scroll coprolites with a Dome/Cylinder morphology were attributed to crocodyliforms (Sawyer, 1998) (Fig. 8.15 and 8.16). Large (>10 cm) Ovoid coprolites were attributed to herbivorous dinosaurs (Chin 1996 and 2007) (Fig. 8.14 and 8.20). Although many of the AAS coprolites demonstrated a similar morphology, many were of variable size (22 mm L to 170 mm L). This size variance was attributed to reptile ontogeny, as juvenile crocodyliforms would not produce as large an

excrement as would an adult. Similar patterns were noted by Sawyer (1998). A list of measurements for the AAS coprolites may be referenced in Table 8.2.

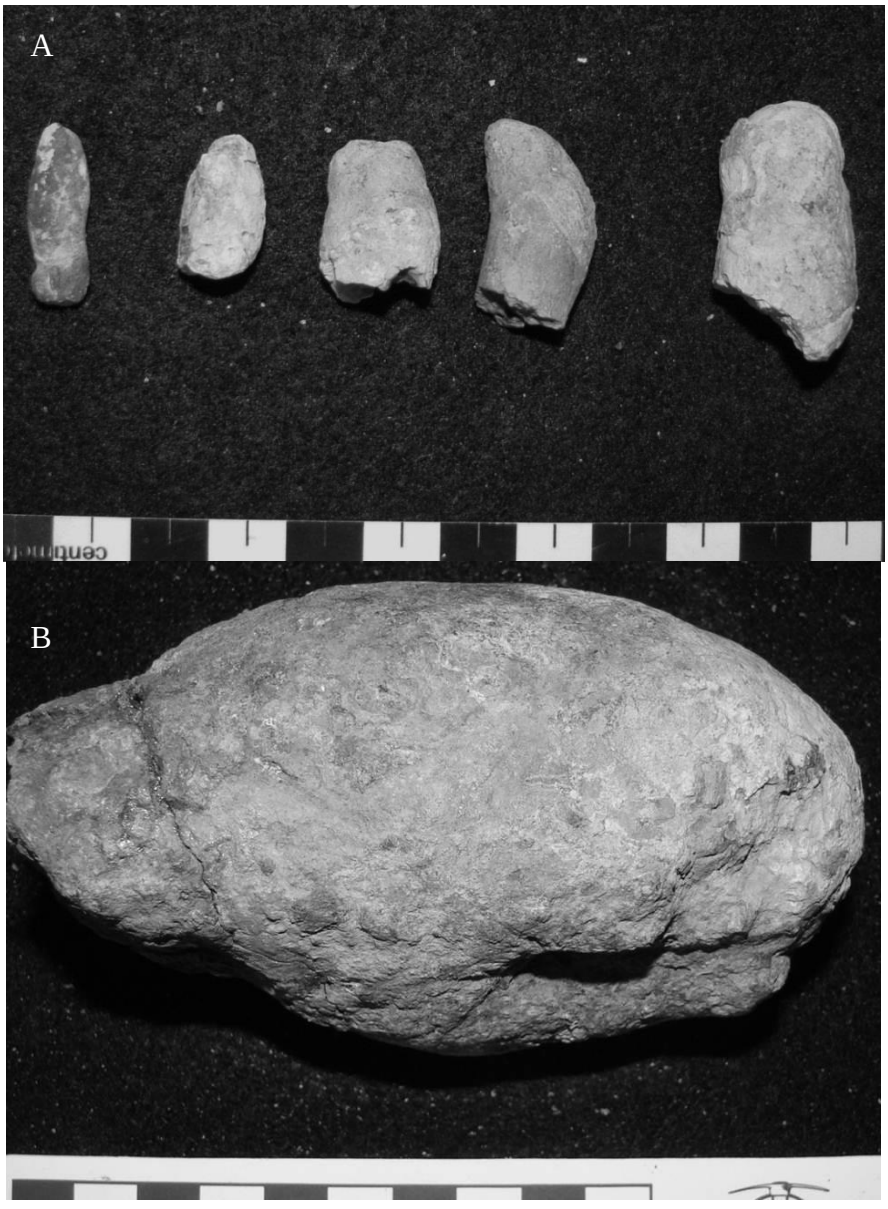

Figure 8.14 AAS Scroll, Spiral and Ovoid coprolites. A. Small Spiral and Scroll coprolites attributed to fish and sharks due to morphology and small size. B. UTA-AASCP-009 a large Ovoid coprolite attributed to a large reptile, likely dinosaurian.

Table 8.2. AAS Woodbine coprolite data (all measurements in mm).

AAS Specimen #	Fossil ID & Description	Measurements
UTA-AASCP-001	Reptilian (crocodyliform?)-spiral	84 L x 26 W
UTA-AASCP-002	Reptilian (crocodyliform?)-spiral	76 L x 28 W
UTA-AASCP-003	Reptilian (crocodyliform)-scroll	98 L x 33 W
UTA-AASCP-004	Reptilian (crocodylifrom)-scroll	78 L x 34 W
UTA-AASCP-005	Reptilian (dino)-ovoid/inclusion	195 L x 105W
UTA-AASCP-006	Reptilian (crocodyliform)-scroll	70 L x 30 W
UTA-AASCP-007	Reptilian (crocodyliform)-scroll	84 L x 52 W
UTA-AASCP-008	Reptilian (crocodyliform)-cylindrical	95L x 44 W
UTA-AASCP-009	Reptilian (dinosaur)-ovoid	108 L x 62W
UTA-AASCP-010	Reptilian (crocodyliform?)-lg scroll	88 L x 36 W
UTA-AASCP-011	Reptilian (crocodyliform)-scroll	62 L x 24 W
UTA-AASCP-012	Reptilian (crocodyliform)-scroll	72 L x 30 W
UTA-AASCP-013	Reptilian (crocodyliform?)-spiral	36 L x 15 W
UTA-AASCP-014	Crab pellets in sandstone	8 L x 7 W
UTA-AASCP-015	Reptilian (?) – partial teardrop	30 L x 28 W
UTA-AASCP-016	Reptilian (crocodyliform)-scroll	170 L x 60 W
UTA-AASCP-017	Reptilian (crocodyliform)-scroll	98 L x 42 W
UTA-AASCP-018	Reptilian (crocodyliform) –scroll	84 L x 33 W

Table 8.2 cont.

UTA-AASCP-019	Reptilian (crocodyliform)-lg partial scroll	86 L x 56 W
UTA-AASCP-020	Reptilian (crocodyliform) –scroll	106 L x 36 W
UTA-AASCP-021	Reptilian (crocodyliform)-partial scroll	72 L x 38 W
UTA-AASCP-022	Reptilian (crocodyliform)-lg partial scroll	53 L x 51 W
UTA-AASCP-023	Reptilian (crocodyliform) –scroll	78 L x 32 W
UTA-AASCP-024	Reptilian (crocodyliform)-lg partial scroll	72 L x 48 W
UTA-AASCP-025	Reptilian (crocodyliform?)-pt spiral/scroll	54 L x 42 W
UTA-AASCP-026	Reptilian (crocodyliform)-lg teardrop	62 L x 48 W
UTA-AASCP-027	Reptilian (crocodyliform)-partial scroll	71 L x 41 W
UTA-AASCP-028	Reptilian (crocodyliform)-lg partial scroll	68 L x 42 W
UTA-AASCP-029	Reptilian (crocodyliform)-partial scroll	64 L x 38 W
UTA-AASCP-030	Reptilian (crocodyliform)-partial scroll	66 L x 42 W
UTA-AASCP-031	Reptilian (crocodyliform)-partial scroll	72 L x 43 W
UTA-AASCP-032	Reptilian (crocodyliform)-partial scroll	70 L x 40 W
UTA-AASCP-033	Reptilian (crocodyliform)-partial scroll	51 L x 39 W
UTA-AASCP-034	Reptilian (crocodyliform)-partial scroll	48 L x 36 W
UTA-AASCP-035	Reptilian (crocodyliform)-partial scroll	50 L x 38 W
UTA-AASCP-036	Reptilian (crocodyliform)-partial scroll	40 L x 36 W
UTA-AASCP-037	Reptilian (crocodyliform)-lg partial scroll	66 L x 44 W

Table 8.2 cont.

UTA-AASCP-038	Reptilian (crocodyliform)- partial scroll	42 L x 34 W
UTA-AASCP-039	Reptilian (crocodyliform)- partial scroll	44 L x 46 W
UTA-AASCP-040	Reptilian (crocodyliform?)-teardrop	42 L x 36 W
UTA-AASCP-041	Reptilian (crocodyliform?)-teardrop	40 L x 35 W
UTA-AASCP-042	Reptilian (crocodyliform)- partial scroll	56 L x 32 W
UTA-AASCP-043	Reptilian (crocodyliform?)- partial spiral	57 L x 35 W
UTA-AASCP-044	Reptilian (crocodyliform?)-spiral	62 L x 28 W
UTA-AASCP-045	Reptilian (crocodyliform?)-spiral/scroll	63 L x 29 W
UTA-AASCP-046	Shark (*Hybodus?*)-partial spiral	38 L x 22 W
UTA-AASCP-047	Shark (*Hybodus?*)-partial spiral	34 L x 23 W
UTA-AASCP-048	Shark (*Hybodus?*)-partial spiral	48 L x 22 W
UTA-AASCP-049	Reptilian (crocodyliform)- scroll	55 L x 27 W
UTA-AASCP-050	Reptilian (crocodyliform)- ovoid	67 L x 33 W
UTA-AASCP-051	Reptilian (crocodyliform)- scroll	73 L x 35 W
UTA-AASCP-052	Shark (*Hybodus?*)-partial spiral	51 L x 23 W
UTA-AASCP-053	Reptilian (crocodyliform?)-teardrop	27 L x 21 W
UTA-AASCP-054	Reptilian (crocodyliform?)-teardrop	28 L x 25 W
UTA-AASCP-055	Reptilian (crocodyliform)- partial scroll	37 L x 31 W
UTA-AASCP-056	Reptilian (crocodyliform)- partial scroll	40 L x 38 W

Table 8.2 cont.

UTA-AASCP-057	Reptilian (crocodyliform)- partial scroll	44 L x 34 W
UTA-AASCP-058	Reptilian (crocodyliform)- partial scroll	62 L x 34 W
UTA-AASCP-059	Reptilian (crocodyliform)- partial scroll	55 L x 31 W
UTA-AASCP-060	Reptilian (crocodyliform)- dome	37 L x 27 W
UTA-AASCP-061	Reptilian (crocodyliform)- partial scroll	32 L x 24 W
UTA-AASCP-062	Reptilian (crocodyliform)-teardrop	34 L x 28 W
UTA-AASCP-063	Reptilian (crocodyliform)-teardrop	38 L x 30 W
UTA-AASCP-064	Reptilian (crocodyliform?)-teardrop	40 L x 24 W
UTA-AASCP-065	Reptilian (crocodyliform)-teardrop	34 L x 24 W
UTA-AASCP-066	Reptilian (crocodyliform)-teardrop	26 L x 24 W
UTA-AASCP-067	Reptilian (crocodyliform?)-teardrop	32 L x 26 W
UTA-AASCP-068	Reptilian (crocodyliform)- partial scroll	45 L x 34 W
UTA-AASCP-069	Reptilian (crocodyliform)- partial scroll	26 L x 36 W
UTA-AASCP-070	Reptilian (crocodyliform?)- dome	28 L x 32 W
UTA-AASCP-071	Reptilian (crocodyliform)- partial scroll	22 L x 32 W
UTA-AASCP-072	Reptilian (crocodyliform)- partial scroll	40 L x 28 W
UTA-AASCP-073	Reptilian (crocodyliform?)- partial scroll	38 L x 28 W
UTA-AASCP-074	Reptilian (crocodyliform?)- ovoid	48 L x 32 W
UTA-AASCP-075	Reptilian (crocodyliform?)- dome	32 L x 24 W

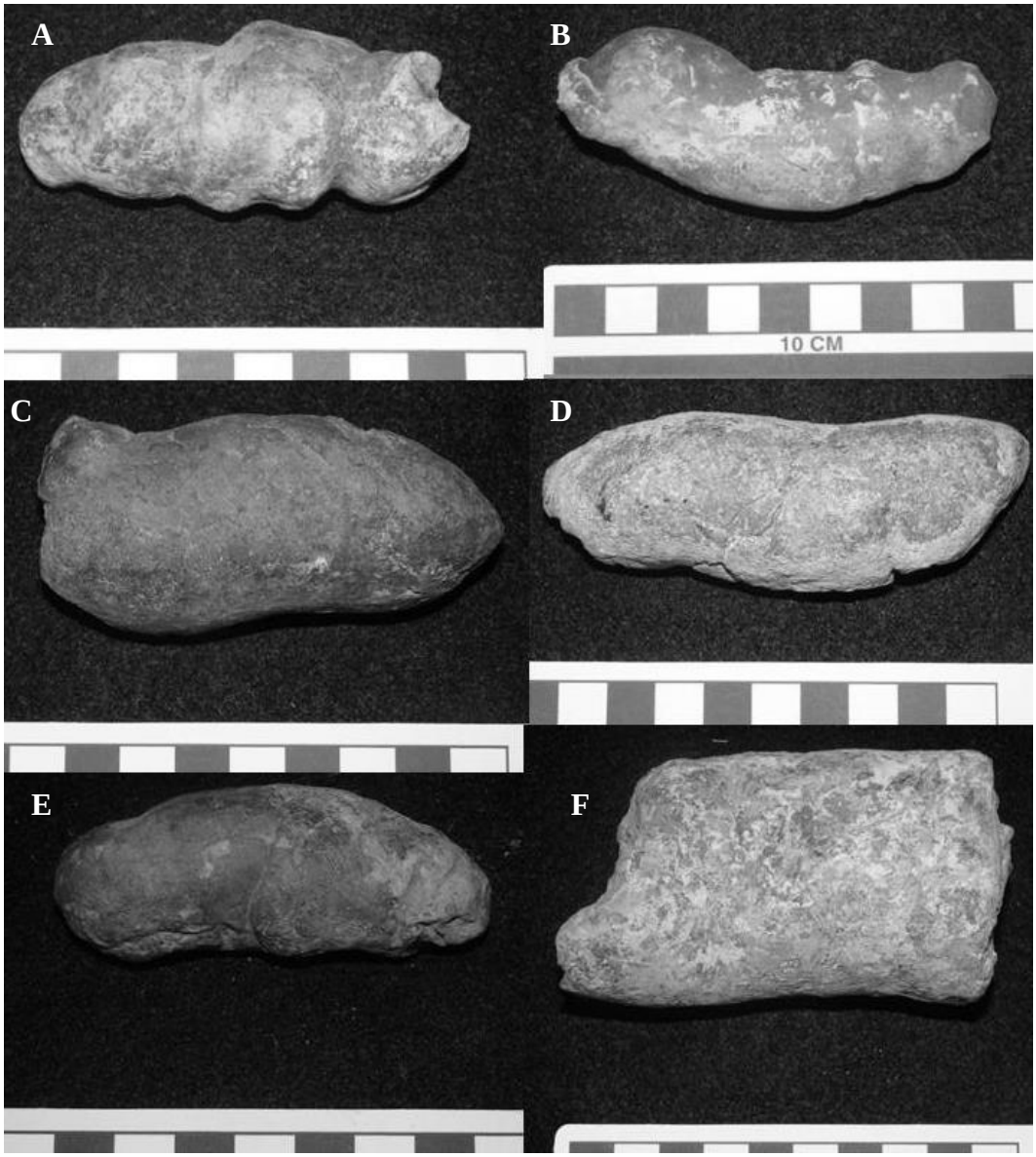

Figure 8.15 AAS Crocodyliform and reptile Scroll coprolites recovered from the AAS hill; Crocorama and the Turtle Buffet. All specimens demonstrate Spiral, Scroll or Cylindrical morphology. A. UTA-AASCP-002 a reptilian (crocodyliform?) spiral. B. UTA-AASCP-001 a reptilian (crocodyliform?) spiral. C. UTA-AASCP-004 a reptilian (crocodyliform) scroll. D. UTA-AASCP-003 a reptilian (crocodyliform) scroll. E. UTA-AASCP-006 a reptilian (crocodyliform) scroll. F. UTA-AASCP-007 a crocodyliform colonite.

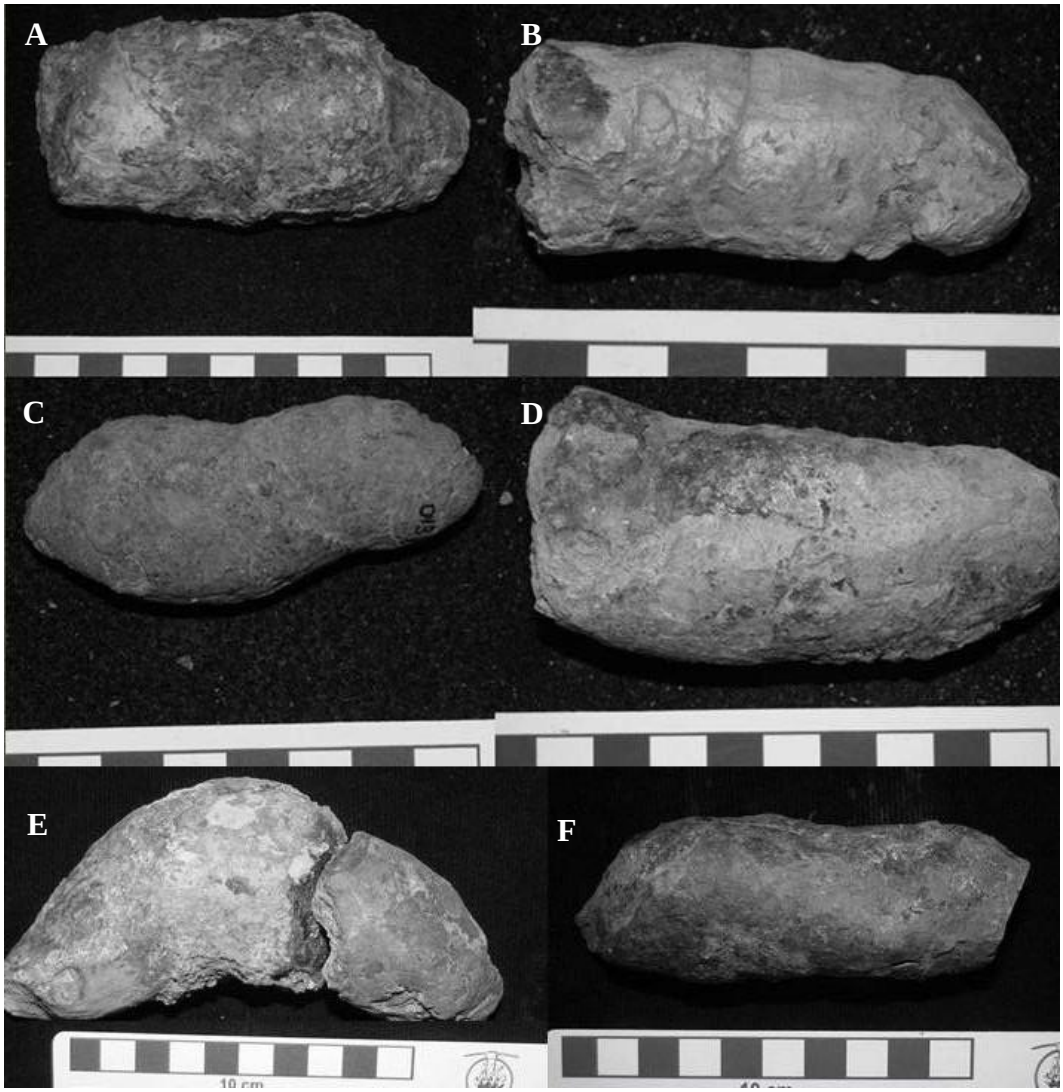

Figure 8.16 AAS Crocodyliform coprolites (scrolls) recovered from the AAS hillside excavations; Crocorama and the Turtle Buffet. A. UTA-AASCP-008 a reptilian scroll, possible crocodyliform. B. UTA-AASCP-011 a reptilian spiral coprolite; crocodyliform. C. UTA-AASCP -013 a reptilian spiral coprolite, possible crocodyliform. D. UTA-AASCP-010 a large crocodyliform scroll. E. UTA-AASCP-016 a large reptilian (crocodyliform) scroll. F. UTA-AASCP-020 a reptilian (crocodyliform) scroll. All scale bars are in centimeters.

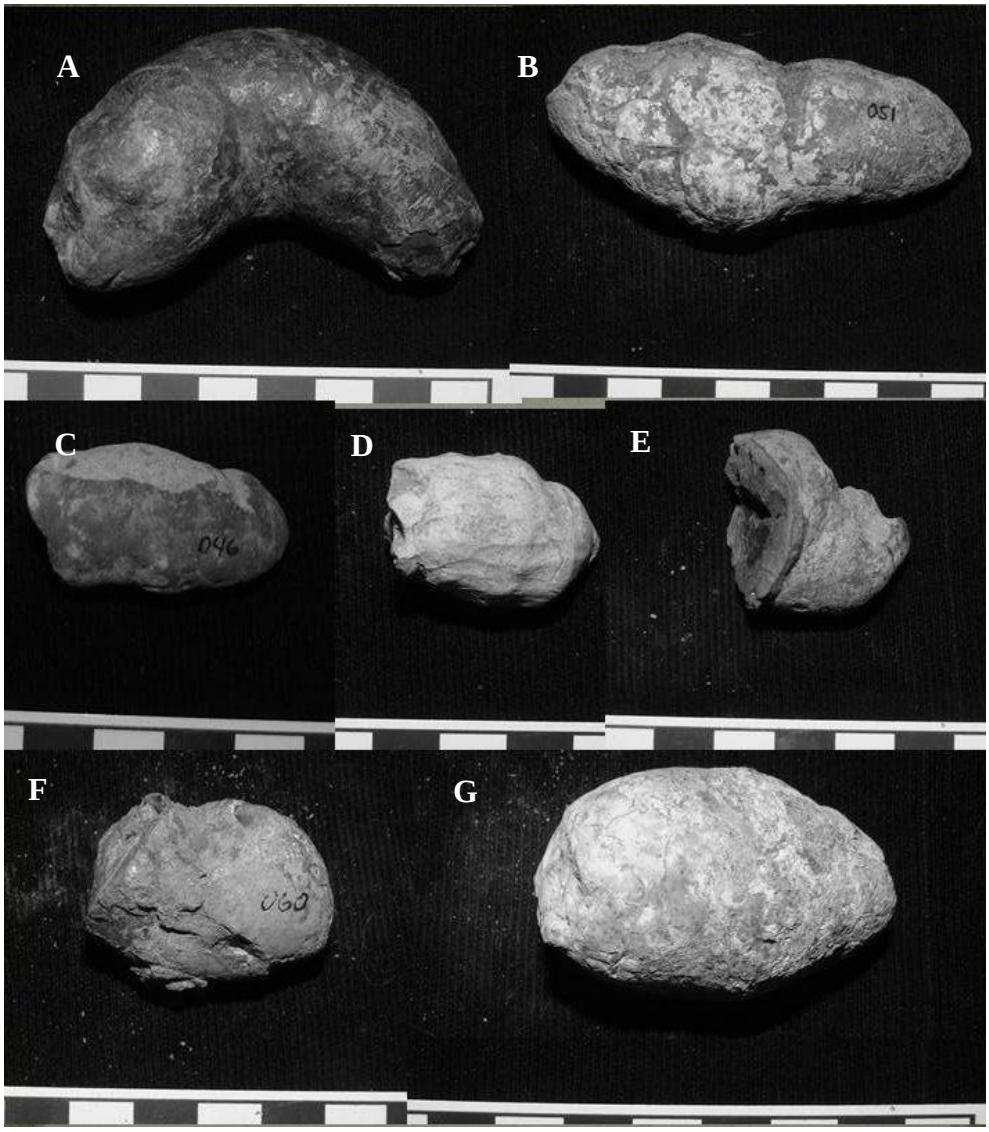

Figure 8.17 AAS Crocodyliform and reptile coprolites recovered from the AAS hillside; Crocorama and the Turtle Buffet. All specimens demonstrate Spiral, Scroll, Teardrop or Ovoid morphology. A. UTA-AASCP-050 a reptilian (crocodyliform) curled ovoid-scroll. B. UTA-AASCP-051 a reptilian (crocodyliform) scroll. C. UTA-AASCP-046 a shark (*Hybodus?*) partial spiral. D. UTA-AASCP-047 a shark (*Hybodus?*) partial spiral. E. UTA-AASP- 054 a reptilian (crocodyliform?) partial scroll/teardrop shape. F. UTA-AASCP-060 a reptilian (crocodyliform) dome. G. UTA-AASCP-074 a large reptilian (crocodyliform) ovoid form. All scale bars are in centimeters.

A sample of the reptilian scroll coprolites attributed to crocodyliform were cut into thin sections and scanned (Fig. 8.18 and 8.19). This procedure was done in an attempt to view the contents of the coprolites in an effort to identify the animal's diet. However, few structures were visible other than vesicules and fragmentary debris (Fig. 8.18 and 8.19). The lack of partially digested materials within the reptilian scrolls was accepted as further evidence of this particular excrement being the remains of crocodyliforms, as modern crocodilians have highly acidic stomachs, leaving few materials to survive the digestive tract (Cott, 1961; Milan, et al., 2010; and Pooley, 1999). Only under exceptional circumstances may bone material consumed by crocodilians survive the highly acidic digestive processes of the crocodilian digestive tract. Fisher (1981) reported partially digested teeth found within coprolites and microvertebrate fossil assemblages. In some cases, the enamel of teeth with its low organic content may survive digestion (Fisher, 1981). At the time of this writing, however, no such teeth had as yet been found within or associated with AAS crocodyliform coprolites.

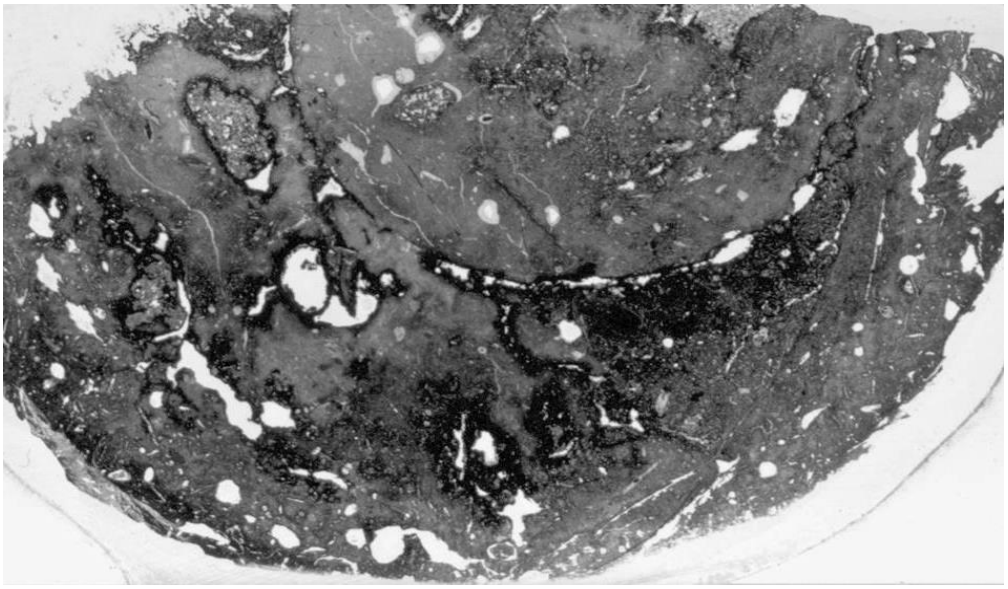

.

Figure 8.18 An AAS reptile (crocodyliform) coprolite in thin section, cross sectional view showing vesicules and fragmentary debris.

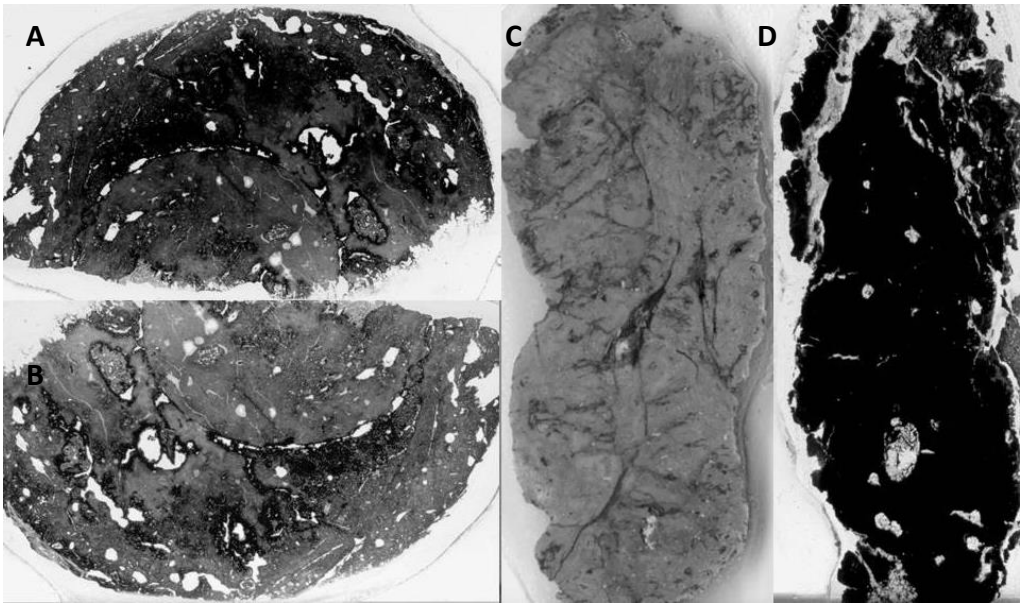

Figure 8.19 AAS scroll crocodyliform coprolite thin sections s in cross sectional (A and B) and longitudinal view (C and D), vesicules and fragmentary debris present in all specimens, although no determinant bone material present.

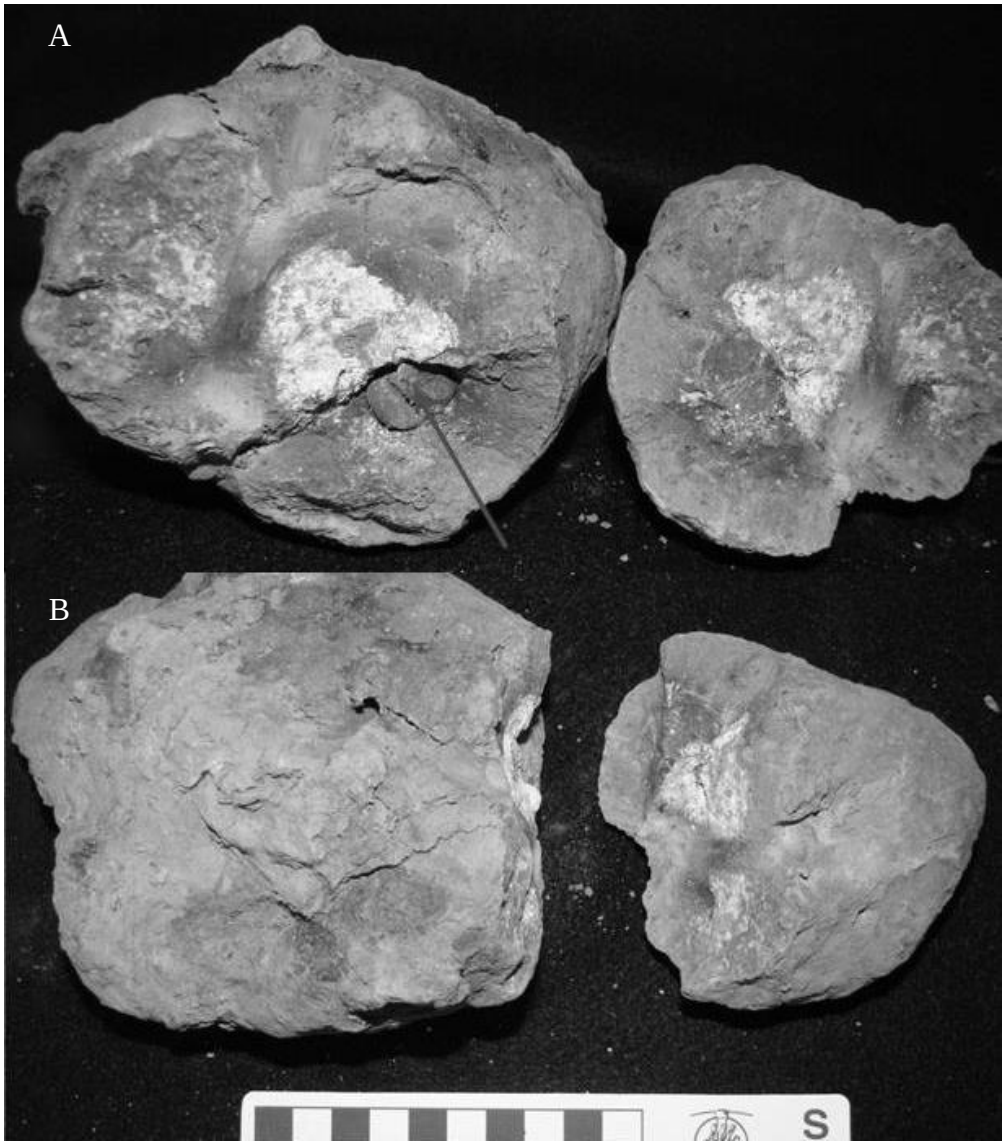

Figure 8.20 UTA-AASCP-005 a large reptilian (dinosaur) coprolite. A. Cross sectional view with gastropod inclusion (denoted by arrow) and fragmentary plant remains. B. Coprolite in plan view showing ovoid shape. Recovered near the AAS Dinosaur Quarry and interpreted as the discard of a large herbivorous dinosaur; an ornithopod.

Dinosaur coprolites were recovered from the AAS, although they were rare and low in abundance compared to crocodyliform excrement. All AAS dinosaur coprolites were surface collected, thus no stratigraphic data is available. UTA-AASCP-005 was the largest, best preserved of the collected dinosaur excrement specimens (Fig. 8.20). It was identified as a dinosaur coprolite utilizing the methods of Chin (1996 and 2007), principally based upon the ovoid morphology and large size. When split open to view the interior structure, plant debris was discovered along with a large gastropod (Fig. 8.20). Plant and wood debris have been documented to occur within herbivorous dinosaur coprolites from the Cretaceous Two Medicine Formation (Chin, 2007). The gastropod inclusion however was an unusual discovery. It may have burrowed into the coprolite after defecation, however, as it is near the center of the coprololite and surrounded by plant remains (Fig. 8.20). Thus, it is interpreted to be a case of accidental death. It is possible that a foraging ornithopod swallowed the gastropod by mistake as it muzzled a large mouth full of swamp vegetation with the gastropod innocently attached to a leaf, and consumed it. This hypothesis is of course untestable.

Of the coprolites collected from the AAS, those that are attributed to crocodyliform are most prominent. The coprolites identified as reptilian scrolls and crocodyliform were recovered and mapped from the AAS excavation in direct association with numerous crocodyliform vertebrate fossil remains (Fig. 8.21 and

8.22). Previous researchers have used the close association of reptilian scroll and crocodyliform coprolites with crocodilyform vertebrate remains as an indication of both the origins of the excretor and as inference to paleoecology (Hantzschel, 1968, Sawyer, 1998 and Waldman and Hopkin, 1970). Sawyer (1998) in particular used the association of crocodilian fossil remains with numerous reptilian and crocodilian coprolites found together at the Clapp Creek site in the Paleocene Black Mingo Group of South Carolina as an indicator of both the excretor and of the regional paleoecology. A similar pattern was observed at the AAS and applied to the paleoecological interpretation of the site.

The presence of crocodyliform coprolites found in association with shed teeth, and bitten, broken turtle remains supports the model of the AAS as a crocodyliform feeding ground (Noto et al., 2012). Numerous bitten and broken turtle shell were recovered and mapped in association with shed crocodyliform teeth (Main et al., 2013; Noto et al., 2012) (Fig. 8.21 and 8.22). The pattern and association of crocodyliform coprolites with shed teeth and broken bitten turtle shell was a prominent feature of the AAS excavation, many of which occurred within 10-20 cm of one another, often occurring together in clusters (Fig. 8.21, 8.22 and 8.23). An example of this pattern is evident in AAS map grid sections North West (-01=>-10), North West I (-11=>-20), and North East (21=>30) with coprolite, shed teeth and turtle shell associations denoted with circles (Fig. 8.21, 8.22 and 8.23).

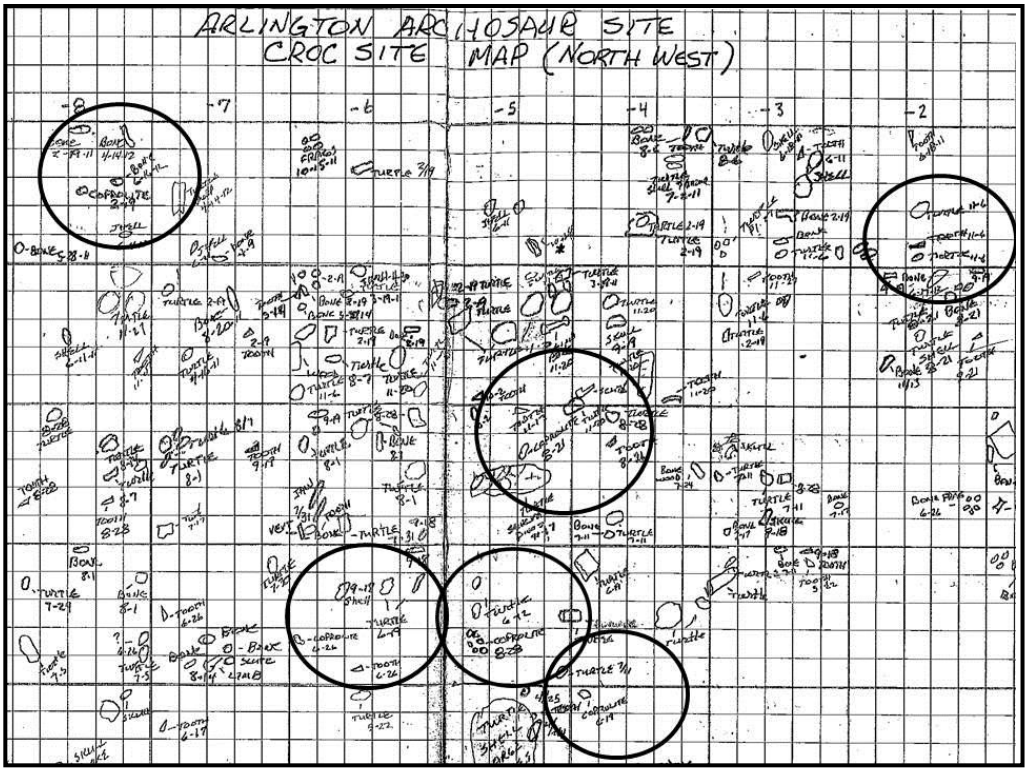

Figure 8.21 Scanned portion of AAS map North West (-01=>-10) demonstrating pattern and association of crocodyliform coprolites with shed teeth and broken bitten turtle shell, many of which occurred within 10-20 cm of one another, often occurring together in clusters, denoted with circles (map courtesy R. Fry).

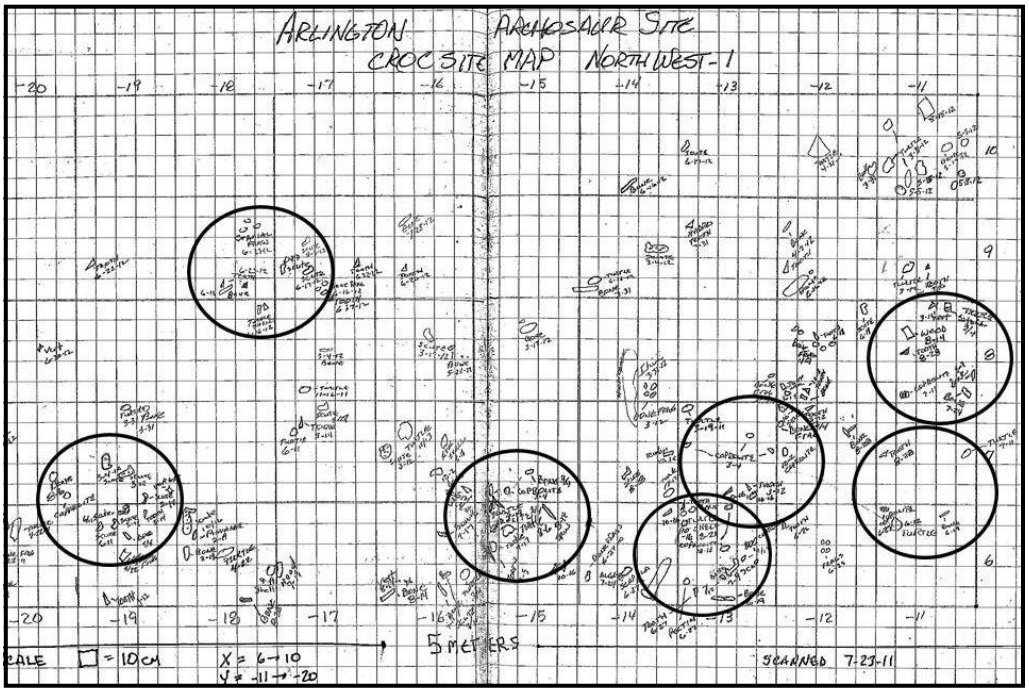

Figure 8.22 AAS map North West 1 (-11=>-20) demonstrating pattern and association of crocodyliform coprolites with shed teeth and broken turtle shell, occurring together in clusters, denoted with circles (map courtesy R. Fry).

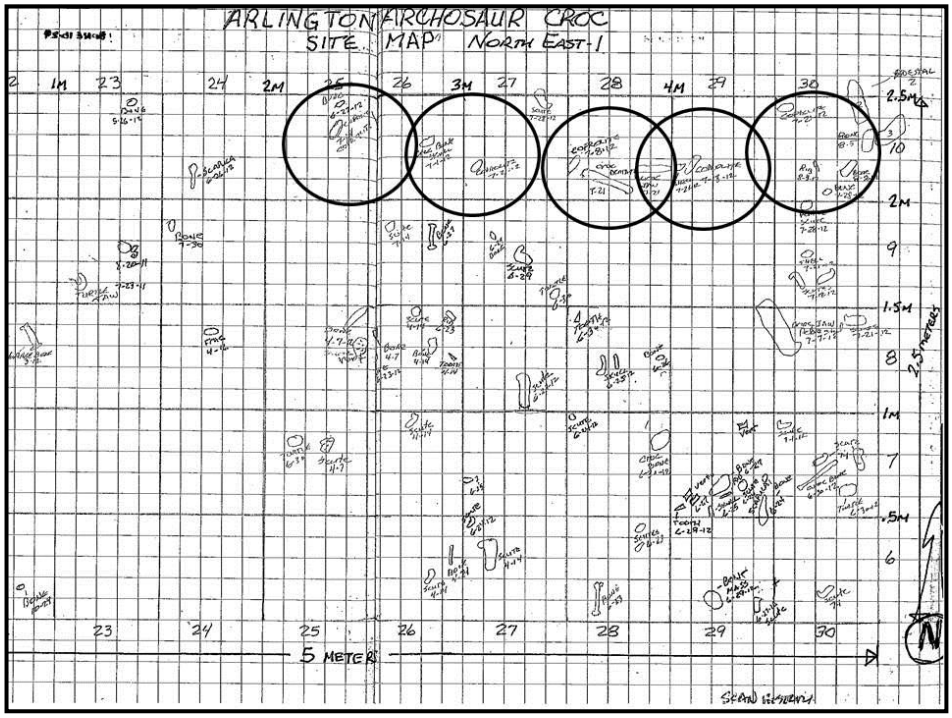

Figure 8.23 Scanned portion of AAS map North East (21=>30) demonstrating pattern and association of crocodyliform coprolites with shed teeth and turtle shell, occurring together in clusters, denoted with circles (map courtesy R. Fry).

8.3.3 AAS Delta Plain Paleoecology

In an effort to accurately reconstruct the AAS Woodbine ecosystem, from the smallest component, to the largest, bulk sediment samples were taken from multiple stratigraphic horizons, screen washed and sorted under microscopes for microvertebrate fossils. The fossils recovered ranged from brackish water shark, and marine reptiles, to fresh water fish, turtles, and crocodyliforms, to small amphibians, lizards and mammals. The AAS shark fauna is represented by hybodont spines, *Cretodus* sp. teeth and misc vertebrae that can be designated as

shark (Fig. 8.31 and 8.32). The AAS marine reptile fauna is represented by a small partial dentary, and a vertebral centrum that has the general morphology noted in the plesiosauridea (Fig. 8.24) (Caldwell, 1999; Huxley, 1858; Sollas, 1881). Although the dentary is only represented by a partial fragment, it does demonstrate a subtriangular morhphology that is typical of the plesiosauridae, and it appears to lack an intermandibular symphasis (Caldwell, 1999). The AAS plesiosaur vertebra is a weathered centrum that is amphicoelus and demonstrates the elliptical morphology of the caudal series noted by Huxley (1858) and Sollas (1881). All of the AAS shark and marine reptile material were surface collected from the Birds Fort Lake (BFL) locality to the south of the AAS hillside, and have little to no stratigraphic data.

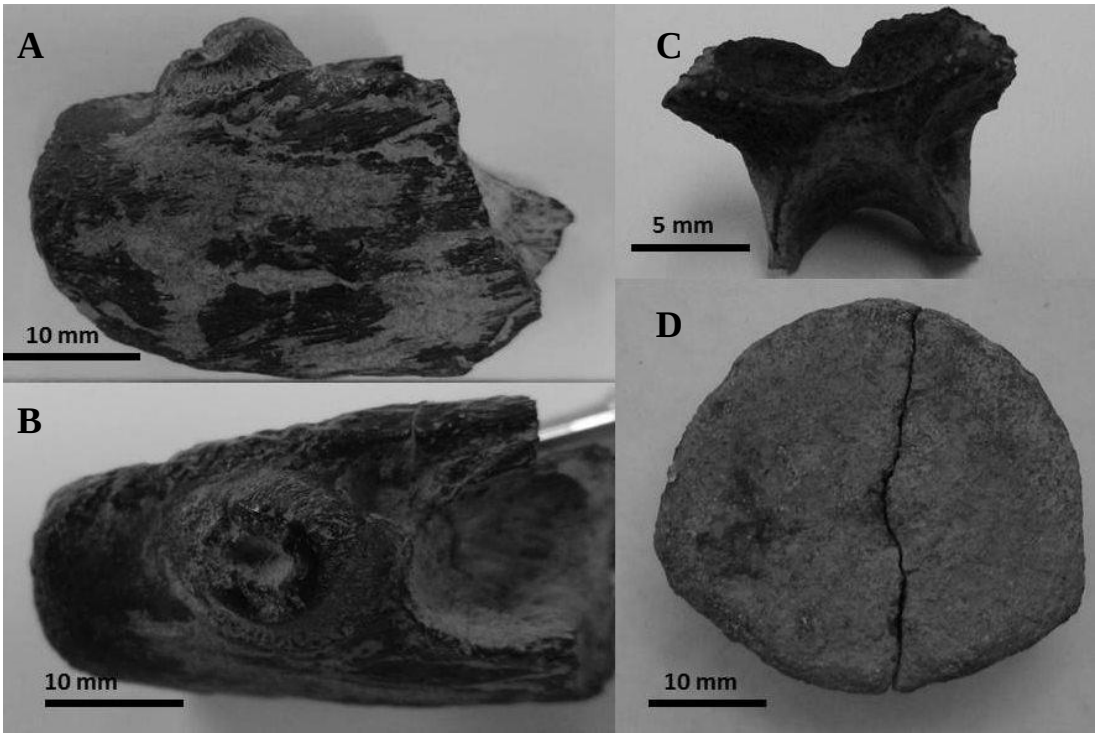

Figure 8.24 AAS marine reptiles recovered by surface collection, bulk sampling and screen washing. A. UTA-AASM-014 marine reptile, partial dentary, lateral view. B. UTA-AASM-014 marine reptile, partial dentary, dorsal view. C. UTA-AASM-333 a reptile neural arch in posterior view. D. UTA-AASM-031 a marine reptile vertebral centrum assigned to plesiosauridae. (Photos A-C courtesy Geb Bennett).

Numerous crocodyliform teeth were recovered from the AAS by surface collection, bulk sampling and screen washing. Of the recovered specimens, there was a wide range of morphological variance that can be attributed primarily to ontogeny (Fig. 8.11 and 8.25). However, there were three morphologies that were attributed to distinct taxa; *Bernisartia*, *Deltasuchus* and *Woodbinesuchus* (Lee, 1997a) (Fig. 8.25).Thus, the AAS Woodbine coastal ecosystem supported at least three taxa of crocodyliforms. It is not unusual for a coastal ecosystem to support multiple species of crocodilians. In modern ecosystems, crocodilians are known to share there territories with other species. In Florida the American alligator (*Alligator mississippiensis*) lives alongside the American crocodile (*Crocodylus acutus*) and the spectacled caiman (*Caiman crocodilus*) in the Florida everglades (Heinrich and Walsh, 2012; Lang, 1999).

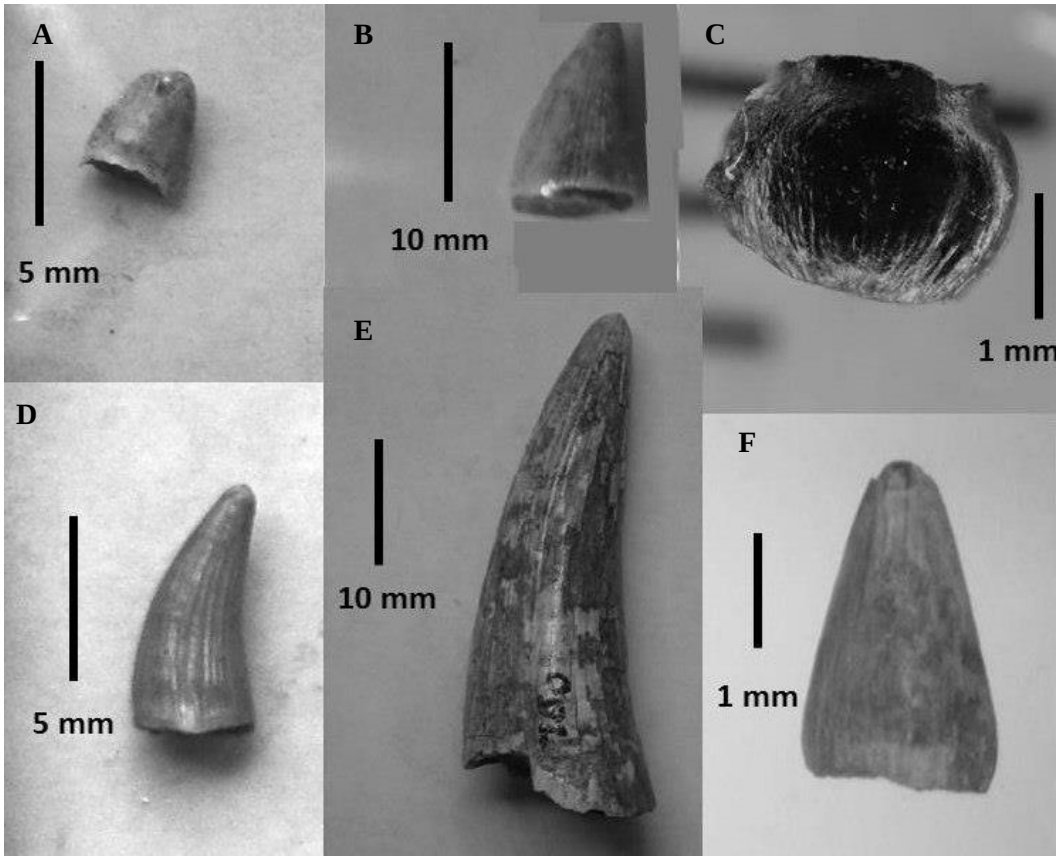

Figure 8.25 AAS microvertebrate crocdyliform teeth recovered by bulk sampling and screening. A. UTA-AASC-067 a juvenile crocodyliform tooth. B. UTA-AASC069 a juvenile crocodyliform tooth attributed to *Deltasuchus*. C. UTA-AASM-079 a small *Bernisartia* tooth. D. UTA-AASC-063 a a juvenile crocodyliform tooth. E. UTA-AASC-180 a sub-adult crocodyliform tooth. F. A small *Woodbinesuchus byersmauricei* tooth. Longitudinally striated and laterally compressed, previously known from the SMU holotype (Lee, 1997a) (Photo C courtesy K. Anderson).

Hadrosaurid crania are distinguished by their well developed dental batteries that supported up to 53 tooth positions, with up to 8 teeth per position that produced jaws with over 400 teeth (Weishampel, 1983). Their feeding behavior was a form of mastication that wore down the crowns of the teeth. As old, worn teeth lost their enamel surface, they were pushed out of the dental battery by the underlying replacement teeth (Weishampel, 1983). Thus, shed hadrosaurid teeth are commonly found in Late Cretaceous deposits.

Over forty ornithopod (Dinosauria: Ornithischia) teeth were recovered from the AAS by surface collecting, bulk sampling and screen washing at multiple localities. The ornithopod teeth were worn shed teeth representing numerous individuals from various ontogenetic stages (Fig. 8.26). Although the teeth represent variable ontogenetic stages, they all demonstrate the characteristic wear patterns associated with the masticating chewing patterns of hadrosauroids (Weishampel, 1983; Weishampel and Maria Jianu, 2000) (Fig. 8.26). Many of the shed hadrosauroid teeth were lacking crowns, and were worn to the roots (Fig. 8.26). Only one complete tooth crown was recovered, UTA-AASO-160 (Fig. 8.26). The distribution, and size range of the teeth suggests numerous hadrosauroid individuals living on the Woodbine Rudradian coast.

Given the number of teeth per hadrosaurid jaw, and the mechanism of feeding that discards old, worn teeth, the number of teeth found at the AAS seems quite low. In comparison, over 350 shed crocodyliform teeth representing various

ontogenetic stages were recovered from the same localities at the study area that only produced 40 hadrosauroid teeth (Fig. 8.26). If these numbers are taken as a representative count of the actual number of animals living along the coast, then it would seem that crocodyliforms were the more prominent component of the AAS coastal ecology.

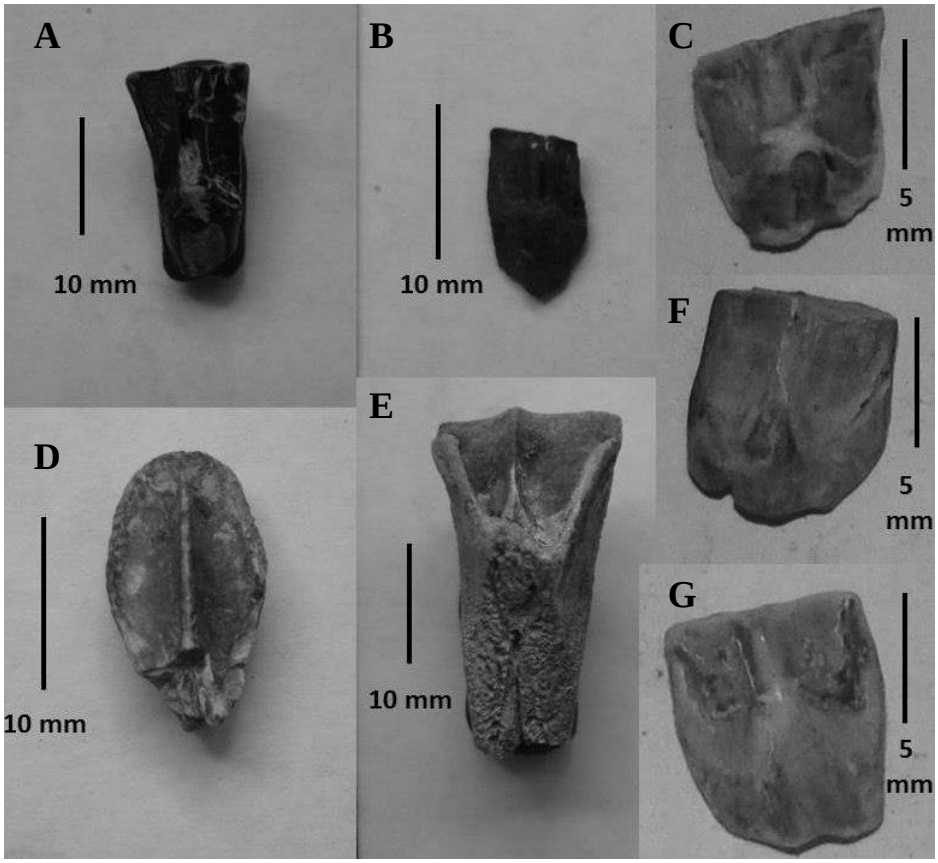

Figure 8.26 AAS shed hadrosauroid teeth recovered by surface collecting, bulk sampling and screening. All specimens, other than E, are attributed to juvenile or sub-adult hadrosauroids. All specimens, other than D (UTA-AASO-160), show signs of wear from hadrosauroid feeding via the shearing - masticating motion of the hadrosauroid jaw. Specimens C, F and G are completely worn, nearly to the root.

Microvertebrate remains of amphibians and reptiles were recovered at the AAS by the bulk sampling and screening project. Screen washed samples that were sorted under light microscopes produced small fossils that would not have been detected by traditional surface collecting methods. The microverebrate amphibian and reptile remains are too fragmentary to assign them to either a genus or species, but some could be assigned to the family level. UTA-AASM-187 is a small, robust vertebra attributed to *Cryptobranhidae indet* (Fig. 8.27). Crytopbranchids are large salamanders that have maintained a conservative body form since the Cretaceous, attaining their greatest size in the Eocene (Carroll, 2009). Cryptobranchids are common in Cenozoic sediments and rare in the Cretaceous (Carroll, 2009). Therefore, a reported cryptobranchid from the AAS Woodbine is significant. Some cryptobranchid forms survive today, the modern North American cryptobranchid is *Cryptobracnhus alleganiensis*, commonly called the Hellbender (originating from the famous phrase "anything that ugly surely came from hell.") (Holman, 2006). They have robust, flat wide skulls and conservative body forms (Holman, 2006). The AAS vertebra (UTA-AASM-187) has a 8 mm long x 5 mm wide centrum that is deeply amphicoelus and roughly circular in outline, with prominent thick transverse processes extending laterally from the centrum and connecting to the base of a stout neural arch. (Fig. 8.27).

Other components of the AAS micro-fauna are small, fragmentary remains that may be broadly assigned to small reptiles and amphibians (Fig. 8.28). UTA-

AASM-146 is a small vertebral centrum that is 4 mm in L and 2 mm W; it is assigned to sauria indet (Fig. 8.28). UTA-AASM-054 is a small salamander vertebra assigned to caudate indet, it is < 4 mm L and 1 mm W (Fig. 8.28). UTA-AASM-207 is a partial radioulna assigned to anura indet; it is 5 mm L and 2 mm W and has a deeply concave articular facet (Holman, 2006) (Fig. 8.28). UTA-AASM-239 is a partial proximal humerus assigned to anura indet; it is 9 mm L and 2 mm W at the distal shaft (Holman, 2006) (Fig. 8.28).

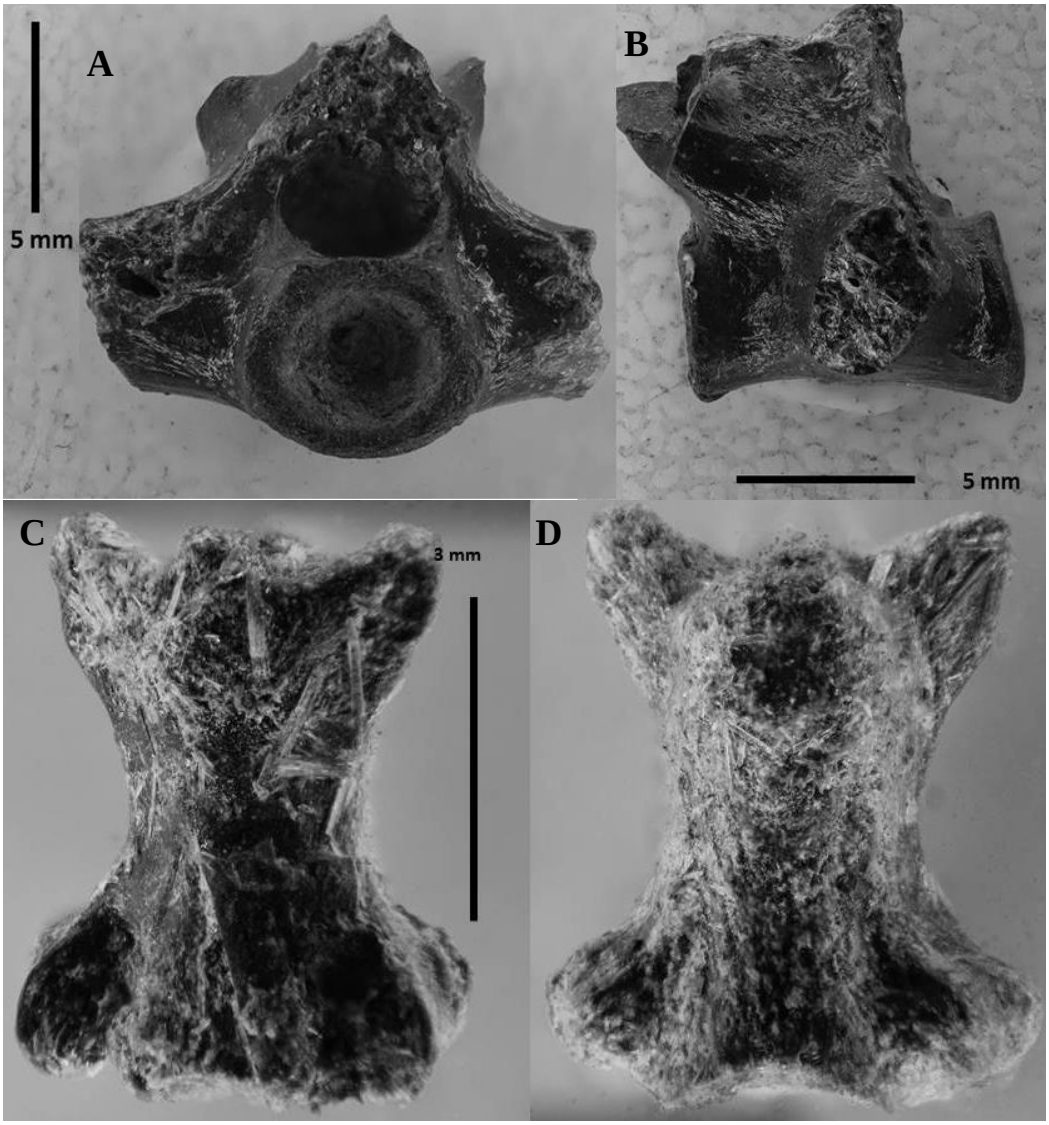

Figure 8.27 AAS microvertebrate amphibian and reptile vertebrae recovered by bulk sampling and screening. A. UTA-AASM-187 Cryptobranchidae indet. in anterior view. B. UTA-AASM-187 in lateral view. C. UTA-AASM-146 sauria indet. in dorsal view. D. UTA-AASM-146 in ventral view (Photos courtesy K. Anderson).

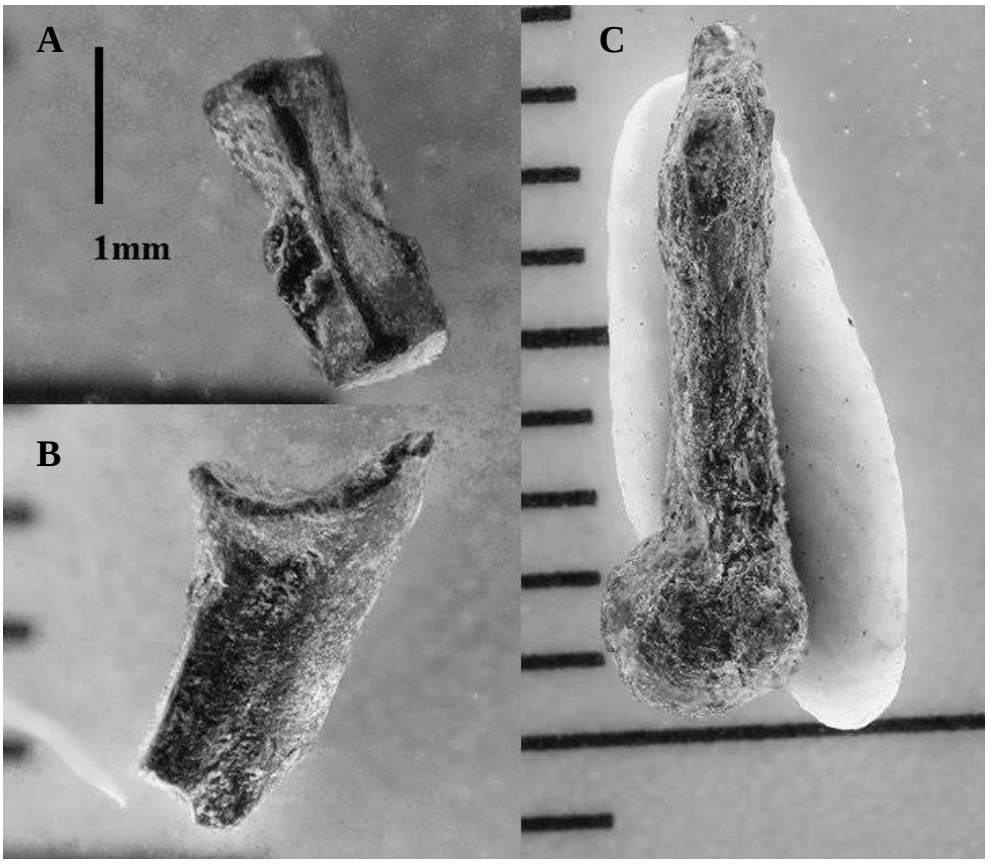

Figure 8.28 AAS microvertebrates recovered by bulk sampling and screening; anura indet. A. UTA-AASM-054 caudata indet (salamander) caudal vertebra. B. UTA-AASM-207 anura indet partial radioulna (scale in mm). C. UTA-AASM-239 anura indet proximal humerus (scale in mm). (Photos courtesy K. Anderson).

The AAS fish fauna is represented by twenty eight recovered specimens that vary in size and preservation, but are principally represented by assorted teeth, scales and vertebrae (Appendix A) (Fig. 8.29 and 8.30). The AAS fish were recovered by surface collection, bulk sampling and screen washing. Numerous pycnodont teeth (>50) were found in the screen washed sediment samples. However, only two partial jaws were recovered, one of which was preserved well enough to identify (Fig. 8.29). UTA-AASM-005 is a partial pycnodont jaw assigned to *Paleobalistum geiseri* (Heckel, 1856) (Fig. 8.29). The jaw is a typical durophagous dentition that is common among pycnodonts, it is 17 mm L x 11 mm W with 18 individual teeth preserved within the pallete (Poyato-Ariza, and Wenz, 2002) (Fig. 8.29). UTA-AASM-010 is a small, complete left prearticular plate from the lungfish *Ceratodus carterii* (Main et al., in press) (Fig 8.29). UTA-AASM-026 is one of eleven gar scales recovered by screen washing sediments at the site. It has a diamond shaped morphology with a medial slant on the left lateral surface and is assigned to *Lepidotes* sp. (Agassiz, 1832).

Among the more interesting of the AAS fish fauna are several partial sawfish rostral jaw sections. UTA-AASM-020 is one of three partial sawfish rostal jaw sections; they are assigned to *Onchopristis dunklei* (McNulty and Slaughter, 1962; McNulty, 1968). UTA-AASM-033 is a partial fish jaw; it is a small fragment, only 18 mm long with two partial worn teeth protruding from the mandibular surface (Fig. 8.29). As it is not a complete specimen, and the teeth are

so poorly preserved, a more precise designation is impossible. Seven small vertebrae were recovered from the site; most demonstrate the flat, disc like morphology associated with fish centra (Carroll, 1988; Poyato-Ariza, and Wenz, 2002). Among the better preserved specimens are UTA-AASM-008 a pycnodont fish vertebra, and UTA-AASM-001A and 001B are fish vertebrae assigned to the Cretaceous fish; *Osteichthyes* sp. (Poyato-Ariza, and Wenz, 2002) (Fig. 30).UTA-AASM-009 are a series of fish vertebrae encased within a mudstone matrix, they are assigned to the Teleostei indet (Fig. 8.31).

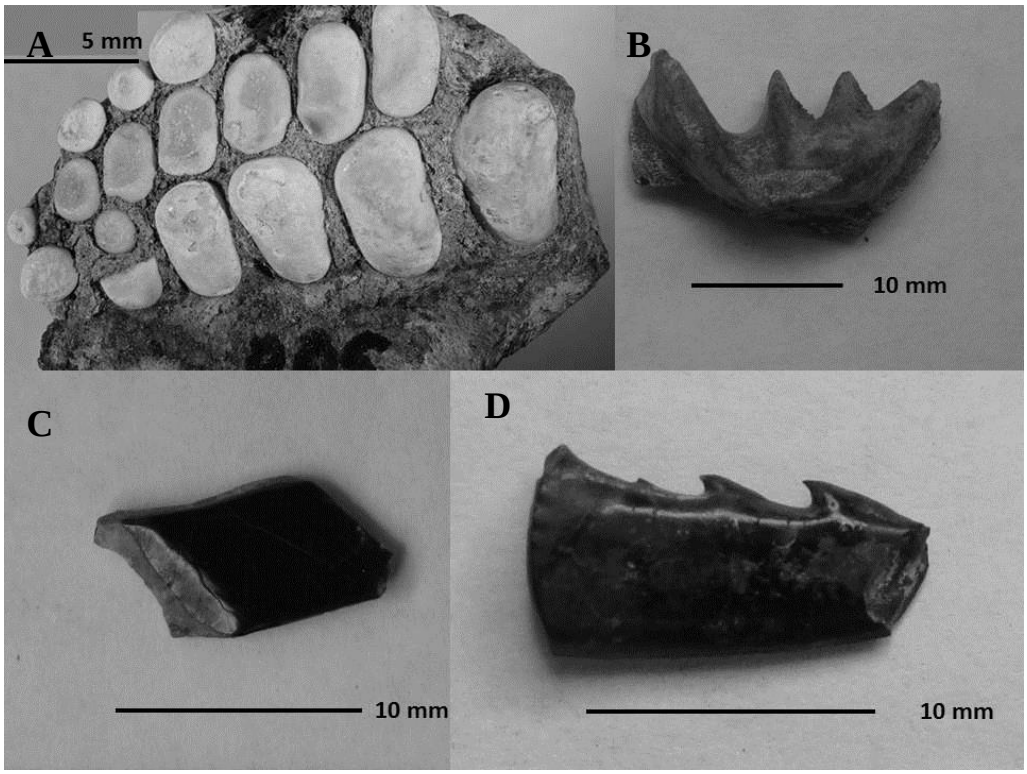

Figure 8. 29 AAS microvertebrate fish fauna recovered by surface collection, bulk sampling and screening. A. UTA-AASM-005 a pycnodont prearticular tooth pallete; Cf. *Paleobalistum geiseri*. B. UTA-AASL-010 a lungfish tooth plate; *Ceratodus carteri*. C. UTA-AASM-026 one of five gar scales assigned to *Lepidotes* sp. D. UTA-AASM-020 one of three partial sawfish rostal jaw sections; *Onchopristis dunklei.* (Photos A and D courtesy K. Anderson).

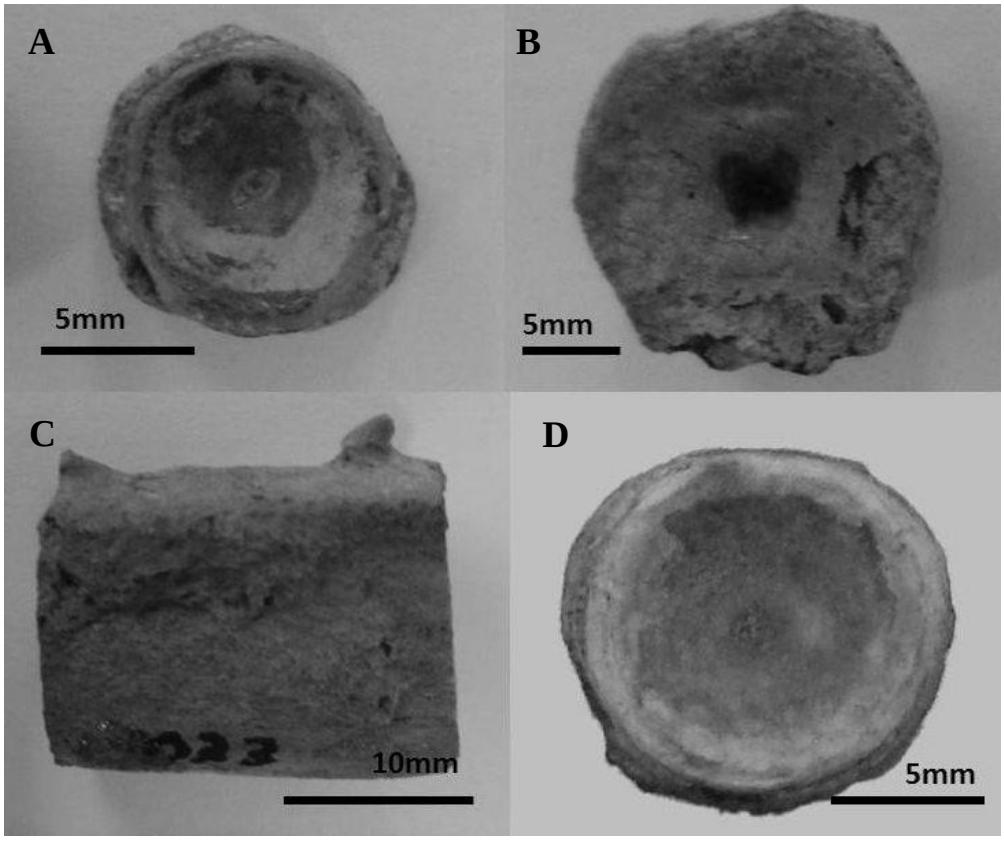

Figure 8.30 AAS microvertebrate fish material recovered by bulk sampling and screen washing. A. UTA-AASM-001a *Osteichthyes* vertebra. B. UTA-AASM-001b *Osteichthyes* vertebra. C. UTA-AASM-033 partial fish jaw. D. UTA-AASM-008 a pycnodont fish vertebra. (Photos courtesy Geb Bennett).

Other aquatic components of the AAS ecosystem are brackish water elasmobranchs that are represented by several partial teeth and spines. UTA-AASM-006 is a shark tooth from the order Lamniformes and is identified as belonging to the genus *Cretodus sp.* by the parallel secondary rdiges projecting laterally away from the central tooth crown (Dixon, 1850; Sokolov, 1965) (Fig. 8.24). *Cretodus* was a common mid-Cretaceous shark, with isolated specimens

being reported globally from Cenomanian-Turonian aged strata (Welton and Farrish, 1993). *Cretodus* was originally named *Oxyrhinus* by Dixon (1850), and later renamed *Cretodus* by Sololov (1965). UTA-AASM-043 is a small elasmobranch toothe assigned to *Pseudohyphlophus* based upon its broad, flat, sub-angular crown (Welton and Farrish, 1993) (Fig. 8.31). UTA-AASM-037 a partial *Stephanodus* shark tooth was recovered; only a 1.5 mm section of the crown was recovered, but may be indentified by the subtriangular morphology of the base crown (Welton and Farrish, 1993) (Fig. 8.31).

Axial elements of elasmobranchs are rare in the fossil record, as the post cranial skeleton is composed of cartilaginous material (Carroll, 1988). However, elasmobranch vertebrae may be found, although they are rare in the Texas Cretaceous (Thurmond, 1972; Welton and Farrish, 1993). Several vertebrae that were attributed to sharks were recovered at the AAS. UTA-AASM-004A and 004 B are small, thin discs that are concave on the anterior and posterior faces of the centra, and two pairs of openings on the circumerential surfaces of the centra (Welton and Farrish, 1993) (Fig. 8.32). UTA-AASM-004A and 004B are assigned to *Cretodus sp.* (Welton and Farrish, 1993) (Fig. 8.32). UTA-AASM-061 and UTA-AASM-104 are small partial vertebrae tentatively assigned to an unidentified fish (Fig. 8.32). UTA-AASM-024 is the head spine of a hybodont shark, it is 22 mm long with a spine that deflects at a 60˚ away from the base

(Maisey, 1982b) (Fig. 8.32). Hybodont sharks were common in the Triassic and in the Jurassic, but were rare in the Cretaceous (Carroll, 1988).

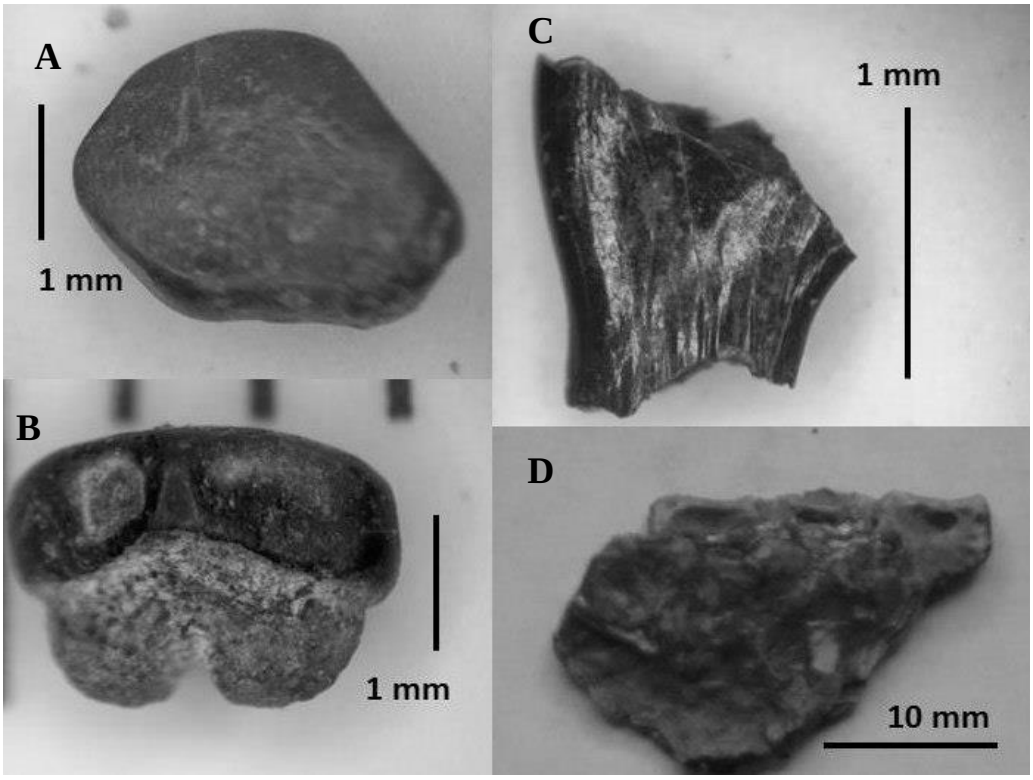

Figure 8.31 AAS microvertebrate shark and fish fauna recovered by surface collection, bulk sampling and screening. A. UTA.AASM-043 *Pseudohypholophus* in dorsal view. B. UTA.AASM-043 *Pseudohypholophus* in lateral view. C. UTA-AASM-037 a partial *Stephanodus* shark tooth in lateral view. D. UTA-AASM-009 Teleostei indet, three vertebrae in matrix. (Photos A-C courtesy K. Anderson)

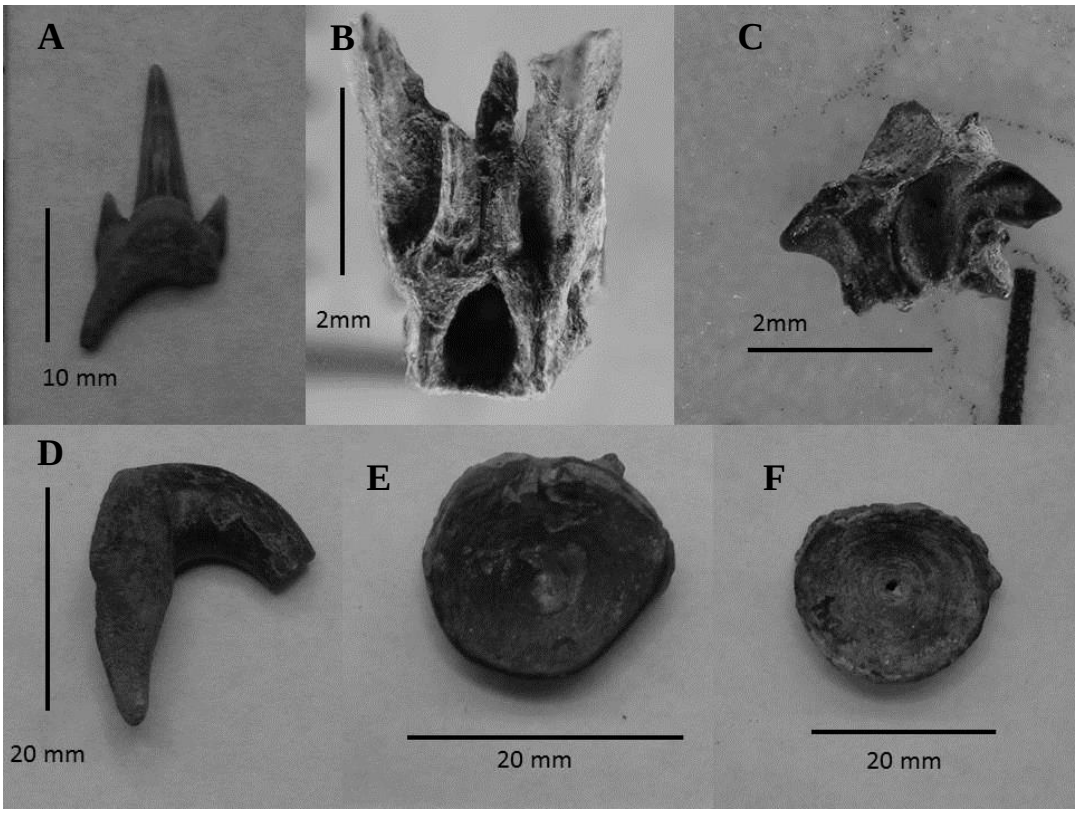

Figure 8.32 AAS microvertebrate shark and fish fauna recovered by surface collection, bulk sampling and screening. A. UTA-AASM-006 a *Cretodus* shark tooth. B. UTA-AASM-061 unidentified fish vertebra (basioccipital). C. UTA-AASM-104 a partial vertebra of a possible fish (or caudata?) D. UTA-AASM-024 a hybodont shark spine. E and F. UTA-AASM-004A and 004B *Cretodus* shark vertebra. (Photos B and C courtesy K. Anderson).

Another prominent component of the AAS coastal ecosystem is the presence of chelonia. Numerous fragmentary and complete turtle shell (carapace and plastron) remains were recovered from the AAS by excavation, surface collection, bulk sampling and screen washing. Of the turtle remains, broken shell fragments were the most common, crania, axial and appendicular elements were rare (Fig. 8.33). The turtle shell fragments range in size from 20 mm to 60 mm in length (Fig. 8.33). Many of the turtle remains recovered from the Facies B peat preserved the bite marks of crocodyliforms that were interpreted as feeding traces (Noto, et al., 2012). However, not all of the AAS turtle remains demonstrated crocodyliform feeding traces, most were merely represented by broken and fragmentary shell. Zangerl (1969) established a methodology for identifying fragmentary turtle remains by studying the pittings on the dorsal surface and relating the preserved morphology of the shell pieces to specific regions within the turtle carapace and plastron.

A study of the pittings on the dorsal surface of the AAS carapace material demonstrated at least three morphologies, thus representing at least three chelonian species present in the AAS Woodbine ecosystem (Fig. 8.33). Among the AAS chelonian fauna are; Baenidae indet, Trionichidae indet (UTA-AASM-338) and the primitive *Glytops* sp. (UTA-AASM-339), a relict of the Jurassic that has also been reported from the Mussentuchit Member of the Cedar Mountain Formation (Kirkland et al., 1999; Cifelli et al., 1999) (Fig. 8.33). It should be

noted that one nearly complete turtle was recovered from the AAS Facies B peat, affectionately referred to as the "Flying Turtle" due to the manner in which it was transported to UTA campus.

The "Flying Turtle" earned its name, and its wings, as it was accidently launched out the back of a flat bed truck while in transport to UTA. In the fall of 2010 the turtle was discovered by student John Thomason in the AAS peat facies, along the AAS hillside within 5 meters west of the AAS Dino-Quarry. The specimen was excavated over a two day weekend dig and loaded into the back of Roger Fry's truck for transport. Unfortunately, the turtle specimen was only jacketed with plaster on one side. Equally unfortunate, the specimen was not strapped down to the bed of the truck for transport. While enroute to UTA, the tailgate of Fry's truck opened and the turtle "flew" out of the back and landed on the road, incurring substantial damage. This incident became known as the "Flying Turtle."

The "Flying Turtle" is represented by a preserved plastron and carapace with axial, and appendicular material preserved within the shell, compressed to one corner. In the lab, AAS volunteers Pat and Marge Kline determined that the criteria for preparation and conservation of the specimen should be systematic, accurately mapped/plotted, and completed with a goal of reconstruction of all of the elements preserved. The Klines established four planes of reference: the carapace, internal skeletal, plastron, and surrounding matrix. An individual axis

system for each plane was established, the carapace and plastron are two dimensional, but the skeletal and surrounding matrix is three dimensional. To define each plane, four reference points were secured to the underling base support which established a lateral and centerline axis. Utilizing this axis system, a grid was measured out in centimeter squares allowing precise mapping and documentation (Fig. 8.34). To achieve a depth measurement, the four reference points are of equal height and the third dimension is calibrated by measuring down from these points. The resulting grid-coordinate mapping method devised for each plane as well as the fossil sorting and storage using commonly available materials represents a creative, yet quantitative approach to preserving small complete specimens (Fig. 8.34).

At the time of this writing the "Flying Turtle" was still under preparation and study in the lab, thus will not be described in detail, or formally named in this work. It should be noted that the both the fossil specimen, and the lab methods developed by the Klines in the conservation of the turtle, holds scientific value (Fig. 8.34). Equally, as turtles are a prominent component of the AAS coastal ecosystem, a brief discussion of the specimen will be made.

Preliminary study of the AAS "Flying Turtle" specimen places it within the Baenidae. This tentative designation is based upon the the broad, rounded morphology of the skull with deep emarginations to the posterior with a long thin crista supraoccipitalis, the subrounded morphology of the shell and general lack

of openings or separations along the peripherals and marginals of the carapace as well as the lack of separation between the plastron and hypoplastron (Fig. 8.34). The “Flying Turtle” specimen is represented by a near complete skull, carapace and plastron, a complete series of cervical and dorsal vertebrae, a left and right scapula and coracoid, a left and right humerus, a radius and ulna, several phalanges, an ilium, ischium and pubis, and a right femur (Fig. 8.35 and 8.36). For a complete list of turtle specimens and measurements, see Table 8.3.

It should also be noted that limb bones, humeri and femora from other individuals represent later ontogentic growth stages and were recovered from separate sites at the AAS (Fig. 8.36). The humeri of individuals UTA-AASTL-036 and UTA-AASTL-037 are nearly three times as large as the humeri of the “Flying Turtle” specimen (UTA-AASTL-038) (Fig. 8.36). This feature distinctly implies that the “Flying Turtle” was not full grown, but rather was a sub adult, or a juvenile individual. The sizes of the humeri from specimens UTA-AASTL-036 and UTA-AASTL-037 are large, but not on the scale of large marine turtles such as *Protostega* from the Late Cretaceous of the North American Western Interior Seaway.

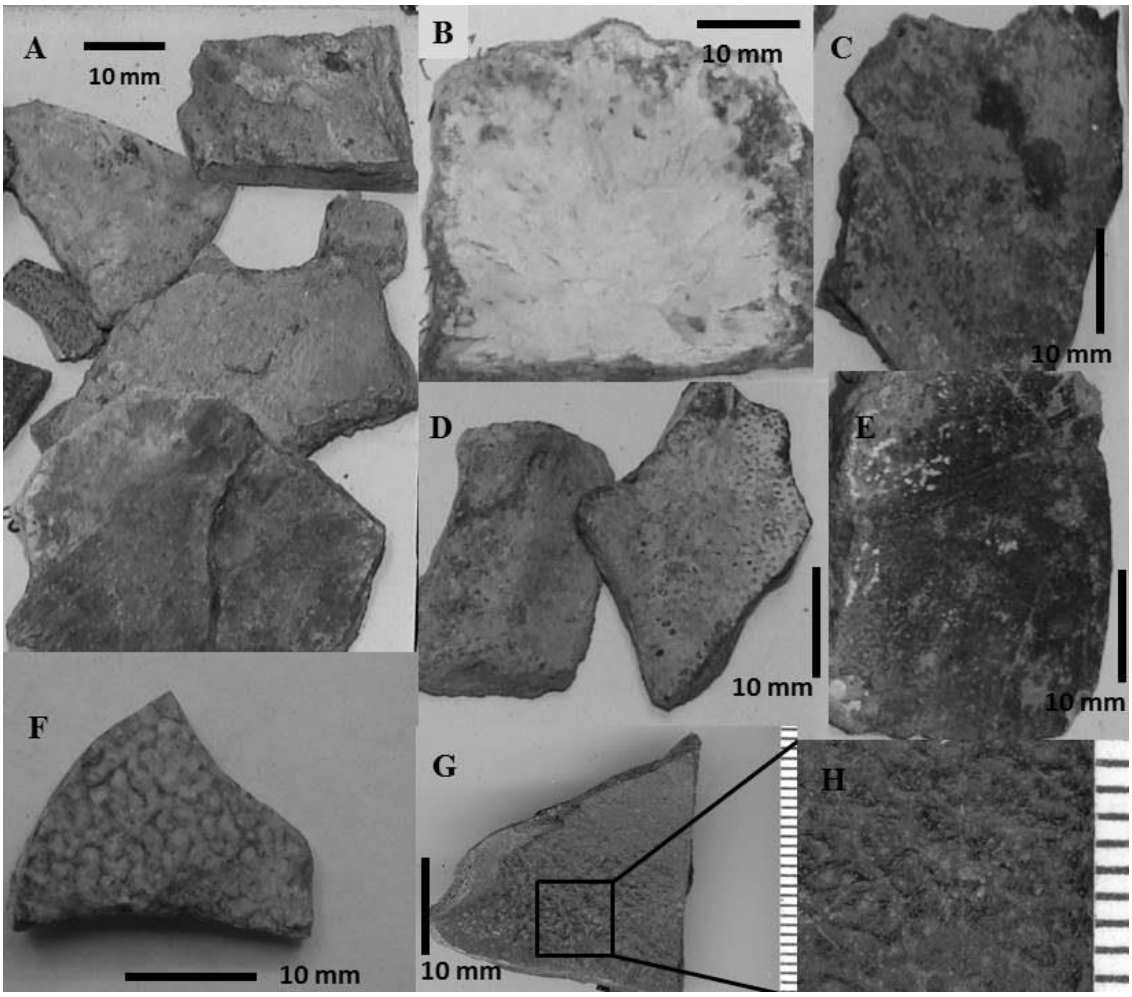

Figure 8.33 AAS Woodbine Chelonia; three turtle shell morphologies observed. A. UTA-AASTL-032 assorted surface collected shell fragments attributed to the Trionychidae. B. UTA-AASTL-034 a second pleural plate from a disarticulated turtle carapace (Trionychidae indet?). C. UTA-AASTL-033 a carapace fragment from a soft shelled turtle. D. UTA-AASTL-035 *Glytops* sp. shell fragments. E. UTA-AASTL-036 a carapace section from a soft shelled turtle with possible bite marks. F. UTA-AASM-338 a Trionychidae indet shell fragment with characteristic sculpture pattern. G. UTA-AASM-339 a *Glytops* sp. shell fragment. H. *Glytops* sp. shell fragment expanded view to highlight characteristic sculpture pattern. (Photos G and H courtesy Geb Bennett).

Figure 8.34 The AAS "Flying Turtle" specimen. A. The plastron placed in a sandbox for reconstruction (note line for grid). B. The carapace in a sandbox for reconstruction. C. The carapace removed from the sandbox and placed in a foam cradle for storage and study (note map).

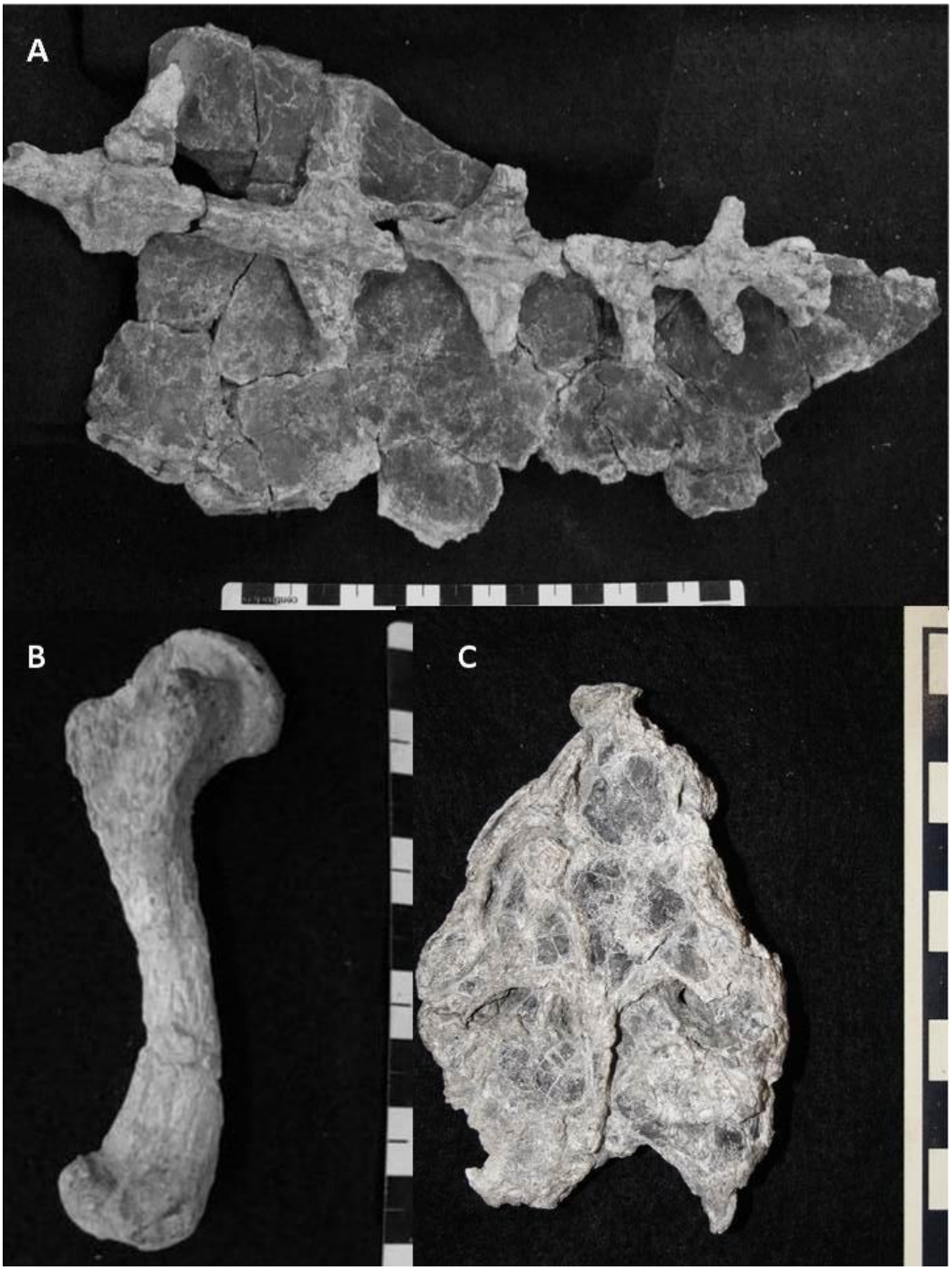

Figure 8.35 AAS “Flying Turtle” specimens. A. Dorsal vertebrae on a partial carapace segment in ventral view. B. UTA-AASTL-043, a complete right femur. C. UTA-AASTL-053 a complete, compressed skull in dorsal view.

Figure 8.36 AAS turtle humeri. A. Humeri from four individuals, the "Flying Turtle" is the smallest element on the left (UTA-AASTL-038), followed by increasingly larger elements from other individuals (UTA-AASTL-039, 036 and 037). B. UTA-AASTL-038, the "Flying Turtle" humerus scaled up to match larger individuals (C). For element measurements see Table 8.3.

Table 8.3 AAS turtle fossil specimen measurements (L x W).

AAS Specimen #'s	Element ID	Measurements (L x W)
UTA-AASTL-036	Humerus	178mm L x 72mm W
UTA-AASTL-037	Humerus	202mm L x 70mm W
UTA-AASTL-038	Humerus	76mm L x 32mm W
UTA-AASTL-039	Humerus	48mm L x 52mm W
UTA-AASTL-040	Left Scapula (inc.)	74mm L x 12mm W
UTA-AASTL-041	Coracoid	58mm L x 30mm W
UTA-AASTL-042	Ulna	77mm L x 36mm W
UTA-AASTL-043	Femur	85mm L x 33mm W
UTA-AASTL-044	Metapodial	32mm L x 6mm W
UTA-AASTL-045	Rht Scapula	90mm L x 15mm W
UTA-AASTL-046	Metapodial	24mm L x 10mm W
UTA-AASTL-047	Cervical 1	10mm L x 6mm W
UTA-AASTL-048	Cervical 2	8mm L x 4mm W
UTA-AASTL-049	Cervical 3	14mm L x 6mm W
UTA-AASTL-050	Cervical 4	12mm L x 6mm W
UTA-AASTL-051	Cervical 5	14mm L x 6mm W
UTA-AASTL-052	Dorsal	54mm L x 12mm W
UTA-AASTL-053	Skull	75mm L x 60mm W

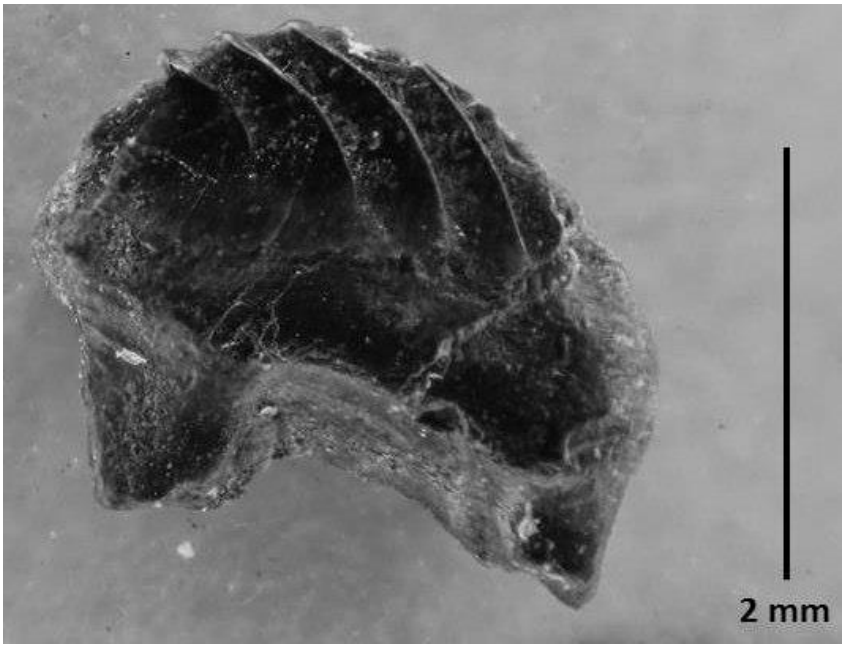

Figure 8.37 The AAS mammal; UTA-AASM-199 a multituberculate tooth, lower fourth premolar (photo courtesy K. Anderson).

The AAS has to date one recovered mammal specimen, represented by a single tooth that was recovered from the AAS Facies B peat during the screen washing and micro sorting program (Fig, 8.37). UTA-AASM-199 is single multituberculate lower fourth premolar that represents a new taxon. It is small, 3mm L x 2.5 mm H, with four preserved ridge crests that recurve gently to the posterior of the crown (Fig. 8.37). Mammals have previously been reported from the Woodbine Formation by Jacobs and Winkler (1998) and Winkler et al., (1995). Jacobs and Winkler (1998) described the lower right first molar of a marsupial (SMU 74642) that they correlated to *Kokopellia juddi* from the Cenomanian Mussentuchit Member of the Cedar Mountain Formation of Utah

and to *Pariadens kirklandi* of the middle Cenomanian Dakota Formation (Cifelli et al., 1999., and Kirkland et al., 1999). This multituberculate tooth is important as it represents a new taxon and expands what is known of the Woodbine mammal fauna, but will not be addressed in greater detail within this work.

Other fossil components of the AAS coastal ecosystem are nearly thirty plant leaf and petrified wood specimens. The plant specimens were recovered by surface collection, and excavation, the best preserved specimens were found in situ while excavating. All of the plant leafs are angiosperms and were identified using the descriptions of MacNeal (1958) for the Woodbine plant fauna previously studied from the Lewisville Member in Denton County. MacNeal (1958) described 82 species of plant fossils, all angiosperms from Woodbine sandstone and shale of the upper part of the Lewisville Member. The sampled fauna consisted of plant taxa that are attributed temperate to subtropical environments, based upon leaf morphology. Among the plant families previously described from the Lewisville Member are: Araucariaceae, Cornaceae, Osmundiceae, and Polypodiceae; all are representative of subtropical, climate zones (MacNeal, 1958). MacNeal (1958) correlated the Denton County plant fauna to similar fossils from other stratigraphic units and concluded that the Woodbine fauna was most similar to that of the Cenomanian Dakota Group, as reported by Ende (1991).

The state of preservation of the AAS plant fauna is highly variable, ranging from poor preservation to near lagerstatten, depending upon the strata and area of the site in which they were found. UTA-AASP-001, an indeterminate leaf imprint in sandstone, was recovered by surface collection along the AAS hillside and therefore has not provincial data (Fig. 8.38). UTA-AASP-002 is a partial leaf assigned to the Cornaceae; *Nyssa woodbinesis*. (MacNeal, 1958) (Fig. 8.38). The leaf is a partial imprint with a preserved length of 48 mm and width of 26 mm, it has a broad base and elliptical morphology that is typical of *N. woodbinesis* (MacNeal, 1958) (Fig. 8.38). UTA-AASP-003 is a small indeterminate leaf imprint in sandstone (Fig. 8.38). UTA-AASP-005 a near lagerstatten elongate leaf in a sandy siltstone assigned to *Ternstroemites texensis* (MacNeal, 1958) (Fig. 8.38). It is a 72 mm L and 18 mm W lanceolate form with a well preserved midrib; it has an acute apex and wide base, with well defined medial ridges along the leaf margin. UTA-AASP-006 is a partial elongate leaf in siltstone that is assigned to *Andromeda sp*. (MacNeal, 1958). It is 102 cm L with an indeterminate width, as the left margin is missing from the base to the apex. It is a lanceolate form with a thick, well defined midrib, it has an acute apex and base. UTA-AASP-008 is a partial broad leaf imprint assigned to *Liriodendron giganteum* based upon the broad, rounded leaf margins and thick midrib (MacNeal, 1958). Only the middle portion of the specimen was recovered, the base and apex were damaged during field collection.

The leaf morphologies of the AAS plant fossils are all are representative of subtropical climates and brackish coastal plain environments. The plant fossil data of the AAS Woodbine paleoenvironments correlates well with the recovered vertebrate and invertebrate fauna and with the Cretaceous climate models of Goswami (2011) that predict subtropical climate envelopes for southern Appalachia in the Mid-Cretaceous. Equally, the AAS plant fauna shows low diversity, similar to the angiosperm fauna reported from the Oligocene deposits of the Chilga Basin, which was attributed to an ecosystem adapted to disturbance by wildfires (Currano et al., 2011). The AAS Woodbine leaf fossils provide another source of ecological data that may be utilized to further confirm the paleoclimate and paleoenvironments of the Rudradian coast.

AAS plant fossils UTA-AASP-005 and 006 were the best preserved specimens, exhibiting near lagerstatten conditions of preservation. Plant specimens UTA-AASP-005, 006 and 008 were all collected from the same stratigraphic horizon at a site found at the far eastern most extent of the Viridian property on which the AAS is situated. The sediments are delta plain deposits of siltstone and shale that correlate to the middle AAS stratigraphic section of carbonaceous shale (peat), mudstone and siltstone. The plant fossil site, referred to as the “Mangrove” site, is located at Texas Hwy 360 and the Trinity Express Railway bridge.

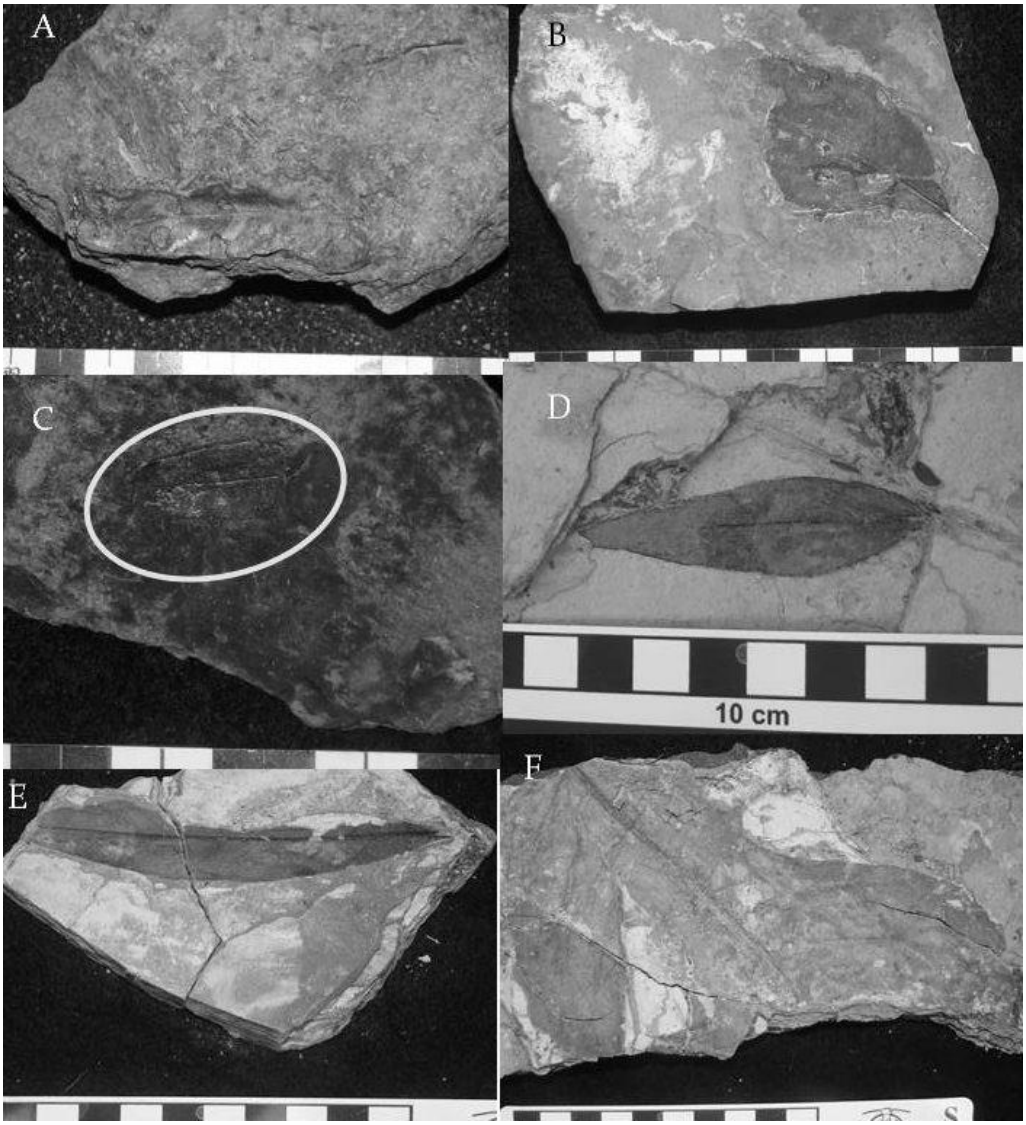

Figure 8.38 AAS Woodbine angiosperms recovered from the AAS hillside and the Texas Hwy360 "Mangrove" site at the eastern edge of the Viridian property. A. UTA-AASP-001 an indeterminate leaf imprint in sandstone. B. UTA-AASP-002 a partial leaf assigned to *Cinnamomum sp*. C. UTA-AASP-003 a small indeterminate leaf imprint in sandstone (circle denotes leaf). D. UTA-AASP-005 an elongate leaf in siltstone; *Ternstroemites texensis* (MacNeal, 1958). E. UTA-AASP-006 a partial elongate leaf assigned to *Andromeda sp*. F. UTA-AASP-008 a partial broad leaf imprint assigned to *Liriodendron giganteum* (MacNeal, 1958).

Fossil wood was recovered from the AAS at several sites on the Viridian property (Fig. 8.39). The AAS hillside produced rare, intermittent specimens that were principally surface collected, thus there is little stratigraphic or provincial data. Only one petrified branch was recovered in situ; UTA-AASP-030. It was found in situ, lying horizontally along the bedding plane of the upper paleosol horizon along the eastern wall of the AAS Dinosaur Quarry at (-28.8). The branch was in a near lagerstatten state of preservation, with bark and small wood knots visible. UTA-AASP-030 is a 54 cm L x 6 cm W branch; it is brownish-tan on the surface with intermittent sulphur stains and a black coalified texture on the interior. UTA-AASP-030 was the only large petrified wood sample recovered as all other AAS wood was found as coalified as vitrain logs and were mapped from the lower AAS peat bed. UTA-AASP-010 is a cylindrical branch segment, it is 105 mm L x 14 mm W (Fig. 8.39). This petrified branch was recovered from the AAS hillside; it exhibits lagerstatten preservation as it has bark and woody tissue structure preserved at the surface (Fig. 8.39). It is the best wood sample collected from the AAS, however, as it was surface collected from the AAS hillside, there is no stratigraphic data.

UTA-AASP-011 is a 72 mm L x 12mm W cylindrical lagerstatten branch segment with preserved bark that was surface collected from the AAS hillside (Fig. 8.39). UTA-AASP-012 is a large lagerstatten segment of petrified wood found at the “Mangrove” site off Texas Hwy 360 at the eastern most boundary

of the Viridian property. It was excavated from a carbonaceous shale bed, and was associated with numerous wood segments and plant leafs (Fig. 8.39). UTA-AASP-012 is a large, 17 cm L x 12 cm W bifurcating section of wood, that has bark preserved at the surface and is highly friable (Fig. 8.39). UTA-AASP-016 is a segment of fossil wood that was surface collected from the AAS hillside, its state of preservation is unremarkable, however it does have *Teredolites* trace burrows on one surface (Fig. 8.39). *Teredolites* burrows have previously been reported occurring in the Woodbine Formation by Main (2005), and are attributed to wood burrowing molluscs that are typical of brackish water estuaries, and coastal plain environments (Bromley et al., 1984; Hasiotis, 2002). As the AAS plant leafs are angiosperms, all of the AAS wood samples are attributed to angiosperm trees.

The lagerstatten wood recovered from the AAS Woodbine deposits are excellent specimens, and are relatively rare in the Woodbine Formation. High quality, lagerstatten wood is not rare in the fossil record, although spectacular preservation is rare. One of the best reported examples of pristine fossil wood was recently reported by Wolfe et al. (2012) from Eocene kimberlite deposits in the Slave Province of Northern Canada. The Slave Province kimberlite wood samples were so well preserved, that they were relatively unpermineralized and had genuine cellulose and occluded amber (Wolfe et al., 2012). The excellent state of preservation allowed for the conclusive genus designation of the wood as

Metasequoia and allowed for isotopic samples to be taken and utilized for paleoclimate data (Wolfe, et al. 2012). As yet, the Woodbine Formation wood has not been studied, and a taxonomic classification of the wood has not been established. The excellent state of preservation of the AAS wood samples would perhaps facilitate a taxonomic classification of the Woodbine tree fauna at a later date. The AAS plant leaf and wood specimens does currently allow for a brief expansion of the ecological data available for the Woodbine, demonstrating a sub-tropical, coastal plain.

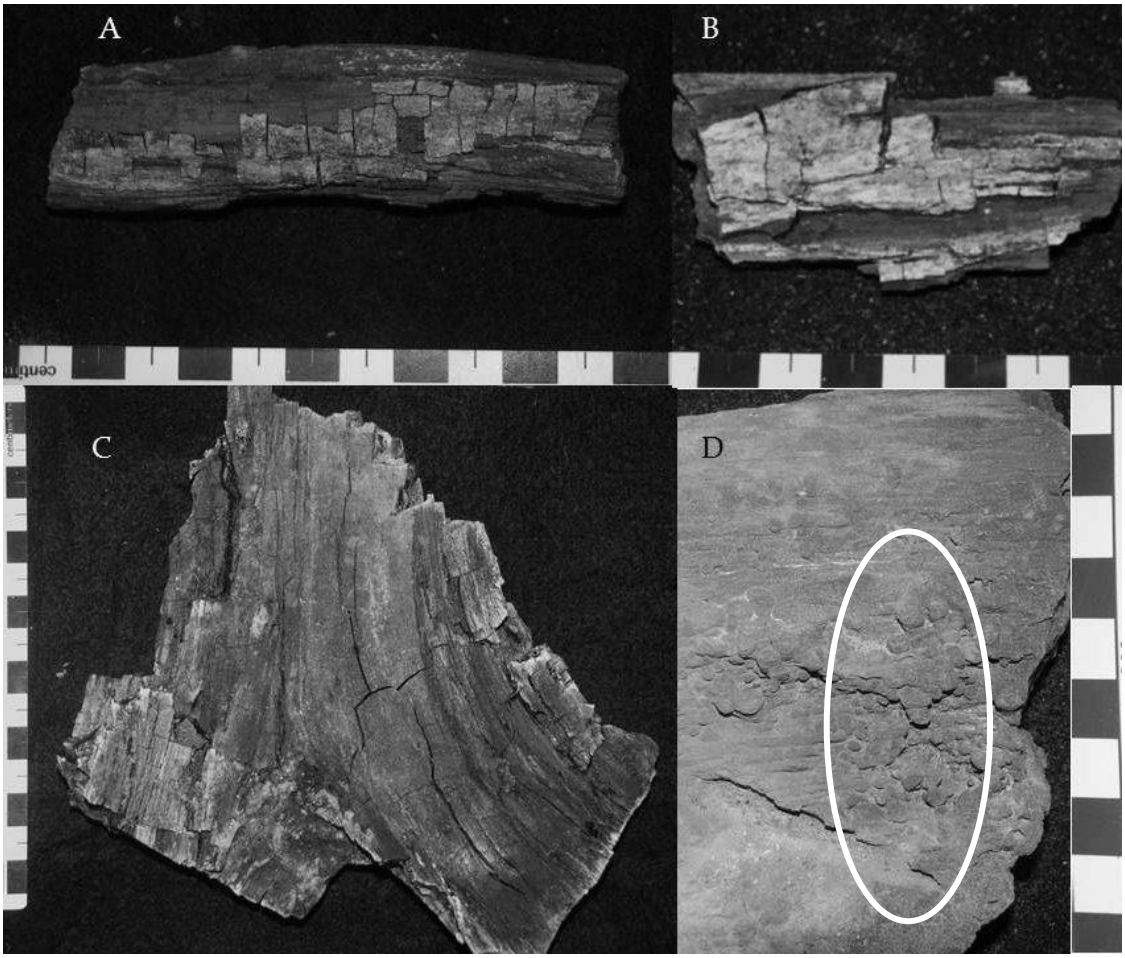

Figure 8.39 AAS Woodbine petrified wood fossils recovered from the AAS hillside and the "Mangrove" site. A. UTA-AASP-010 a lagerstatten branch segment. B. UTA-AASP-011 a lagerstatten petrified branch segment. C. UTA-AASP-012 a lagerstatten segment of bifurcating petrified wood from the "Mangrove" site. D. UTA-AASP-016 Fossil wood with *Teredolites* trace burrows (denoted with circles).

Four sediment samples were taken from AAS outcrops in November 2011. The samples were collected from the Facies B peat and the Facies C Paleosol muds at (-4.9), (7-9), (12.9), and (20.9) in the map grid and sent to Ellington & Associates, Inc. lab in Houston, Texas, where they were processed for calcareous nannofossils and foraminifers. A split from the samples was sent to National Petrographic Service, Inc. in Houston, Texas, where it was processed for palynomorphs and palynofacies. Jamie Shamrock analyzed the calcareous nannofossils at 630-1250x magnification. All samples were barren of calcareous nannofossils as well as fragments of larger calcareous microfossils. Nancy Engelhardt-Moore analyzed the residue samples for foraminifers and other microfossils. No foraminifers were observed, only common carbonized "wood" fragments and large spores.

Sediments consisted of clay, quartz, opaque minerals and organic material, with little to no indication of marine influence. Quartz and clay components decrease up-section. Significant opaque material was present in Sample 3 from map grid section (12.9), but decreases in Sample 4 at map grid section (20.9), with a relative increase in organic material. Niall Paterson analyzed the palynology slides. A total of eight slides were mounted, one kerogen slide and one oxidized slide for each sample. Kerogen slides were analyzed primarily for

the purposes of palynofacies; the oxidized slides provided ‘cleaner’ assemblages useful for palynostratigraphy. Palynomorph assemblages recovered from the AAS samples were of low to moderate diversity and relatively low abundance. Palynomorphs and organic matter were well preserved.

The palynomorph assemblages were dominated by miospores. Species present in studied samples included; *Appendicisporites erdmanii, Appendicisporites matesovae, Cicatricosisporites venustus, Cyathidites* sp.,*Camerozonosporites* sp., and *Pilosisporites ericius* (Fig. 8.40). Angiosperm pollen was also present but is less abundant than the miospores. Species include: *Dichastopollenites dunveganensis , Stellatopollis largissimus* and *Retitricolpites* cf. *R. maximus* (Fig. 8.40). Dinoflagellate cysts were also present in the sampled AAS assemblage, but they were very rare. Poor preservation precluded definitive identification, however, specimens were provisionally assigned to (?), *Florentinia* sp. and (?) *Oligosphaeridium* sp.

The processed samples were used to help establish a biostratigraphic age for the AAS. Based upon the occurrence of *Dichastopollenites dunveganensis*, the palynomorph assemblage wasinterpreted to be of mid-Cenomanian age. This interpretation is supported by the presence of another species of angiosperm pollen which is restricted to the Cenomanian, *Stellatopollis largissimus*. This age interpretation is consistent with the known range of the miospores: *Appendicisporites erdmanii* and *Cicatricosisporites venustus* (Barremian -

Cenomanian/ Turonian), *Appendicisporites matesovae* (Albian – Turonian), and *Pilosisporites ericius* (Berriasian – Cenomanian).

The Facies B peat assemblage was dominated by terrestrial plant fragments (leaf cuticle, tracheid tissues, coal precursor macerals) and terrestrial palynomorphs, (miospores) (Fig. 8.41). Dinocysts were present in the assemblage, but rare. The high abundance of terrestrial palynomorphs and organic matter relative to the low abundance of dinoflagellate cysts indicates that deposition occurred in a paleoenvironment that was dominantly fluvial – with a minor marine input, a coastal-plain swamp (delta plain) or an estuarine environment. This interpretation is consistent with the absence of nannofossils and foraminifers.The high abundance of miospores in the assemblages is a strong indication that the plant community around the AAS at time of deposition was dominated by various types of ferns. The ferns probably occupied the river banks and higher ground between the deltas distributary channels. Angiosperm pollen is also present but is less common than the ferns. This observation either indicates that angiosperms occupied a less dominant position in the ecosystem, or were transported further out by the deltas distributary networks and deposited at another point on the coastal plain.

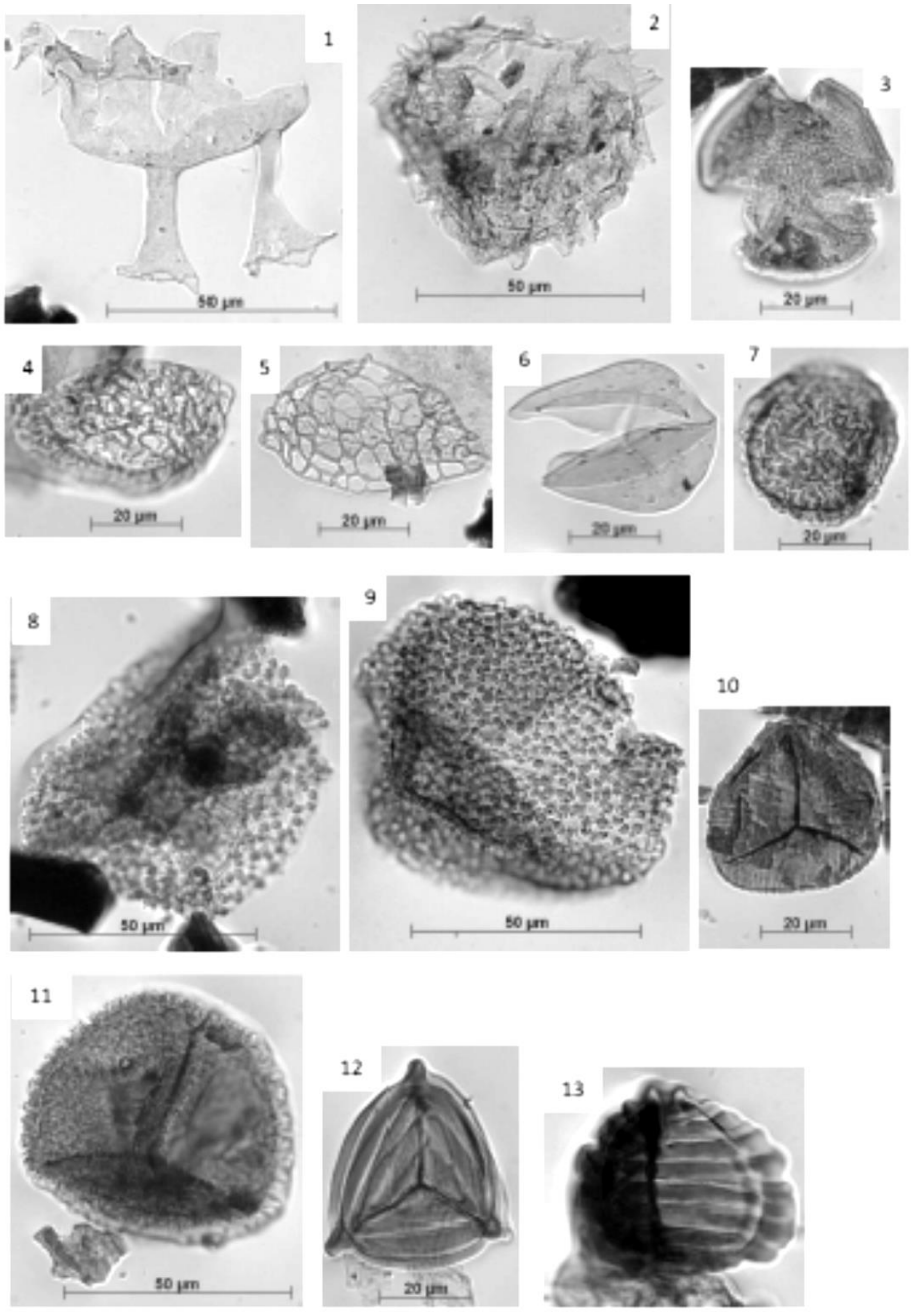

Figure 8.40 AAS palynomorph assemblage, miospores, angiosperm pollen and dinocysts. 1) *Oligosphaeridium* sp., 2) *Florentinia* sp. 3) *Retitriocolpites*, 4 & 5) *Dichastopollenites dunveganensis*, 6) *Cyathidites*, 7) *Camerozonosporites* sp., 8 and 9) *Stellatpollis largissimus*, 10) *Cicatricosisporites venustus*, 11) *Pilosisporites ericius*, 12) *Appendicisporites erdmanii*, 13) *Appendicisporities matesovae.*

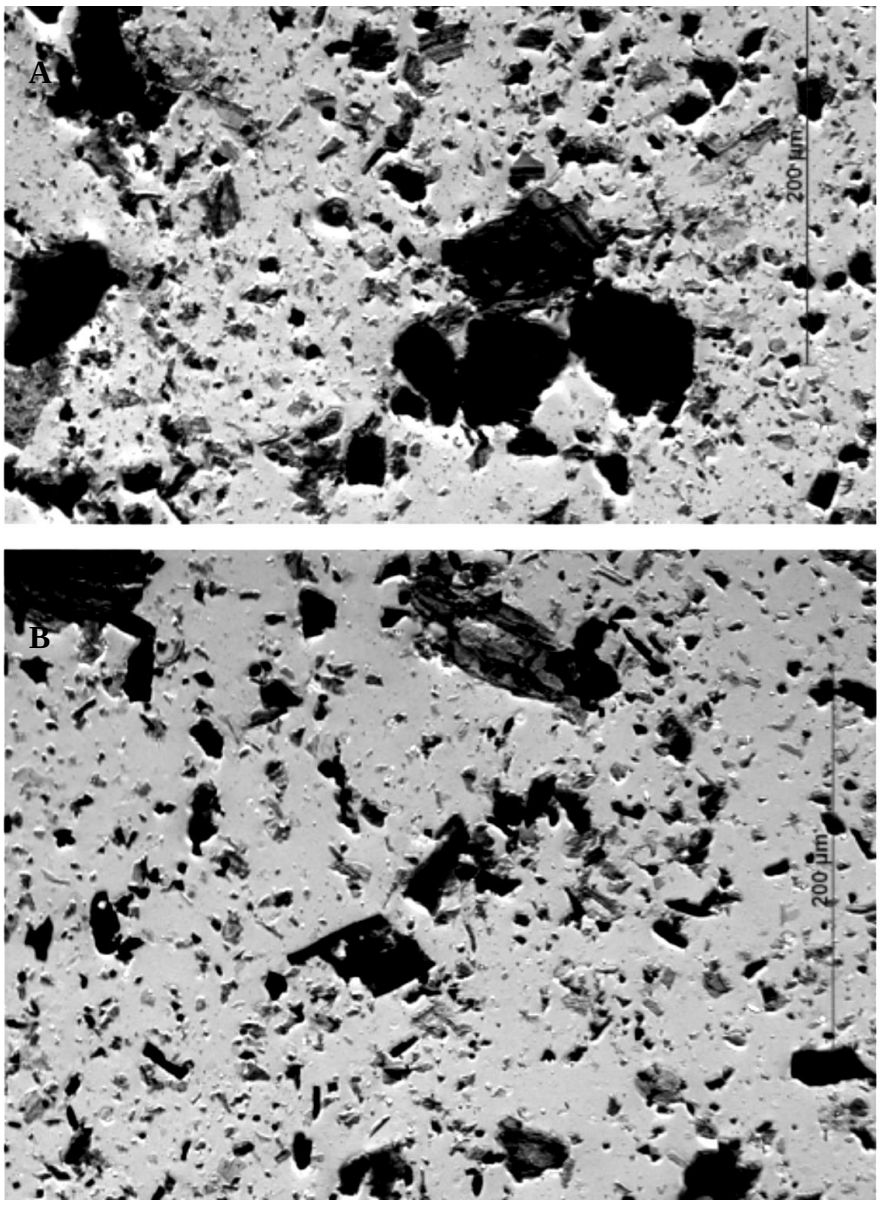

Figure 8.41 Organic matter assemblage found within the AAS Facies B peat. A. Peat sample organics from map grid (-4. 9), black particles are gelified wood fragments, grey particles are leaf cuticles. B. Peat sample organics from map grid (7. 9), black particles are charcoal, grey particles are leaf cuticles and tracheid. Note, the dominance of terrestrially derived plant matter (as expected for a delta plain).

Table 8.4 AAS Woodbine Paleoecology-Faunal List

AAS Fauna-Taxonomy	Facies	Reports in the literature
Chondrichthyes		
Hybodontiformes		
Hybodus sp.	A	McNulty and Slaughter, 1968.
Ptychodus sp.	A	
Laminformes		
Cretodus sp.	A/B	McNulty and Slaughter, 1968.
Squalicorax sp.	A	McNulty and Slaughter, 1968.
Rajiformes		
Onchopristis dunklei	A	McNulty and Slaughter, 1968.
Myliobatiformes		
Pseudohypolophus (*Hypolophus mcnultyi*)	A	McNulty and Slaughter, 1968.
Osteichthyes		
Ceradontiformes		
Ceratodus carteri	A/B	Main et al., 2012
Pycnodontiformes		
cf. *Paleobalistum geiseri*	A	McNulty and Slaughter, 1968.
Pycnodontidae indet.	A/B	McNulty and Slaughter, 1968.
Semionotiformes		
Lepidotes sp.	A	McNulty and Slaughter, 1968.
Tetraodontiformes		
Stephanodus sp.	A	
Lissamphibia		
Caudata		
Caudata indet	B	Winkler and Jacobs, 2002
Cryptobranhidae indet	B	
Anura		
Anura indet	B	Winkler and Jacobs, 2002
Reptilia		
Chelonia		
Baenidae indet	B	
Glyptops sp.	A/B	
Trionichidae indet	A/B/C/D	Noto et al., 2012
Trionichid new gen. sp.	B	
Squamata		
Plesiosauridae (?)	A	

Table 4 cont.

Crocodyformes			
	Bernessartia sp.	A/B	Lee, 1997a
	Deltasuchus motherali	A/B/C	Main et al., in press
	Goniophilidae indet	A/B/C/D	Noto et al., 2012
	Woodbinesuchus sp.	A/B	Lee, 1997a
Dinosauria			
Theropoda			
	Allosauroid	A/B	Noto and Main, in press
	Dromaeosaurida indet	B	Noto and Main, in press
	cf. Richardoestesia	A/B	Noto and Main, in press
	Tetanurae indet	B	Noto and Main, in press
Ornithopoda			
	Hadrosauridae indet	A/B/C/D	
	Protohadros	B/C	Main et al., in press
Mammalia			
Multituberulata			
	Multituberculate indet	B	Jacobs and Winkler, 1998

Table 8.5 Total count of vertebrate fossils recovered from the AAS, separated by facies and size classification (micro and macro). Table constructed from a sample of fossils taken from the AAS collections database (specimens lacking stratigraphic data, along with fragmentary or unidentified specimens were not included in this data set). It should also be noted that the catalogued AAS specimens represent about 2/3 of the total fossils recovered, as many have yet to be catalogued or studied. All specimen data may be referenced in the AAS Collections Database in Appendix A.

AAS Facies A-D	**334 Micro Specimens**	**538 Macro Specimens**
Facies A- Sandstone	76	52
Facies B- Peat	262	582
Facies C- Paleosol	17	128
Facies D- Siderite	18	24
Facies D- Heterolithics	26	16

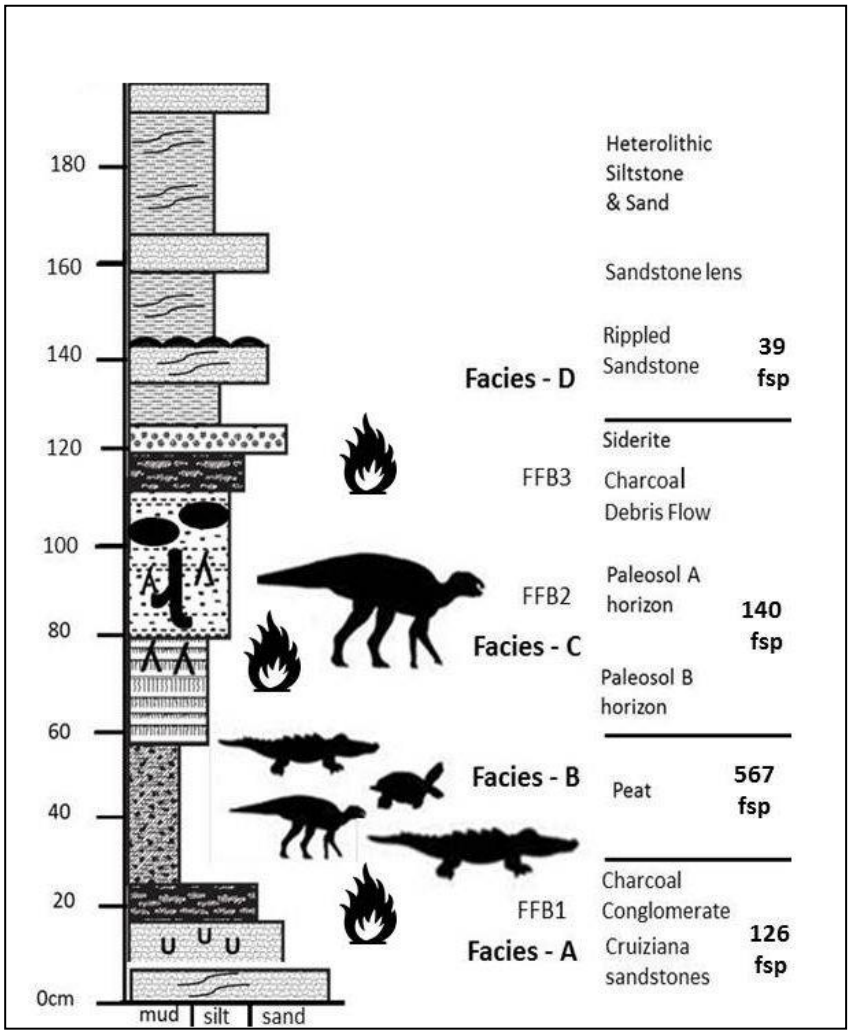

Strat Symbol Key:

Nodules =

Plant roots =

Ripple lamination =

Charcoal roots/stumps =

Fossil taxa =

Figure 8.42 Paleoecology & stratigraphy; AAS composite section. The peat bed is fossil rich with logs and vertebrates. Facies A-D and FFB1-FFB3 denoted to the side. Microvertebrates were recovered from Facies A and B. Total count of fossil specimens collected denoted with "fsp."

8.4 Conclusions

The Arlington Archosaur Site (AAS) is a productive mid-Cretaceous (Cenomanian) ecosystem located in North Texas that preserves a coastal marshland ecology that represents a unique and poorly understood time frame in Earth history. The AAS ecosystem preserves a wide range of vertebrates including; fish, lungfish, shark, amphibian, marine reptile, turtle, crocodyliform, dinosaur (theropod and ornithopod), and mammals, along with numerous coalified logs and minor plant leaf remains belonging to the angiospermidae. Among the AAS fauna are several animals that are new to science; a new species of lungfish *Ceratodus carteri*, a new chelonian, a new amphibian, a new multituberculate mammal, a new taxon of crocodyliform *Deltasuchus motherali*, and a basal hadrosauroid (*Protohadros sp.?*) (Main et al., 2012; Main et al., in press; Noto et al, 2012). All of the AAS fauna are relict in nature, or primitive, and denote the transition between older Early Cretaceous forms to those characteristic of the Late Cretaecous.

The AAS Woodbine ecosystem was located on the Rudradian peninsula in southwestern Appalachia. The coastal margin of the Rudradian peninsula formed an extensive coastal flat that was covered with a sub tropical forest canopy, or mangrove, similar to the modern Mahakam River Delta of Kalimantam Indonesia, or the modern Mississippi River Delta of the Gulf Coast (Aslan et al., 2005; Dunbar et al., 1994; Gastaldo, 1992; Roberts, 1998). The AAS fauna were

isolated on the Rudradian peninsula. This hypothesis is supported by paleogeographic studies of the Greenhorn interior seaway and by the relatively primitive, or relict nature of the AAS fauna (Elder and Kirkland, 1994; Main et al., in press). As Rudradia projected outwards into the Greenhorn interior seaway, its coasts were potentially impacted with periodic hurricanes. Coastal storms are attributed to initiating wildfires that burned the AAS coastal plain and in so doing potentially disturbed the ecosystem.

Figure 8.43 Ink drawing of the AAS delta plain with a sub adult hadrosauroid carefully wandering across the swamps of the Rudradian coast (art courtesy of Clinton Crowley).

The plant fauna recovered from the AAS was relatively low in diversity, principally angiosperm megafossils and gymnosperm palynomorph (no leaves) taxa recovered to date. The low diversity AAS plant fauna could be attributed to a fire adapted coastal community. Similar low plant diversity patterns were reported from the fossil charcoal beds of the Cobham lignite in England and the angiosperm fauna reported from the Oligocene deposits of the Chilga basin, both were attributed to an ecosystem adapted to repeated disturbance by wildfires (Collinson et al., 2007 and Currano et al., 2011).

The AAS coastal ecosystem was dominated by crocodyliforms and was likely either a breeding ground or a feeding ground for crocodyliforms. The presence of numerous juvenile remains recovered from the Facies B peat along with adults within a relatively small area is suggestive of a possible breeding ground (Appendix B). However, neither fossil eggs nor eggshell have been recovered from the site to date. The presence of multiple broken bones and bitten turtle shell remains from Facies B in association with adult crocodyliform remains is suggestive of a feeding ground (Boyd et al., 2013; Nopsca, 1902; Noto et al., 2012; Weigelt, 1989). Equally, numerous crocodyliform coprolites found in association with crocodyliform and bitten, broken turtle remains is supportive of a feeding ground interpretation (Weigelt, 1989). In the case of the feeding ground hypothesis, the presence of juvenile crocodyliforms could be interpreted as the

discarded remains of an adult meal, as modern adult saltwater crocodiles feed upon the young of rivals (Pooley, 1999). Although none of the AAS juvenile crocodyliform material shows signs of feeding via breakage patterns on the bone, or bite marks, this observation would negate entirely the breeding ground hypothesis of the AAS.

Boyd et al. (2013) and Noto et al. (2012) demonstrated that Cretaceous crocodyliforms serve as important taphonomic agents, accumulating and modifying vertebrate fossils as part of their feeding behavior. Boyd et al. (2013) documented evidence of a small crocodyliform killing and feeding upon small ornithischian dinosaurs, hypsilophodonts from the Upper Cretaceous (Campanian) Kaiparowits Formation. Boyd et al. (2013) described a series of bit marks on hypsilophodontid post cranial remains; a scapula and femur, with a partial crocodyliform tooth embedded within the limb bone. Noto et al. (2012), as part of this dissertation work, documented a series of crocodyliform bite marks, scores and punctures in turtle shell fossils. The work of Boyd et al. (2013) and Noto et al. (2012) are too date the best documented examples of Cretaceous crocodyliform feeding.

With the abundance of crocodyliform remains recovered from the AAS, the coastal ecosystem was likely dominated by crocodyliforms that potentially functioned as the apex predator of the region. Theropod remains are relatively infrequent at the AAS, which is suggestive of a crocodyliform dominated coast

(Noto and Main, in press). Equally, as hadrosauroid remains are more prominently found rather than theropods, hadrosauroids may have merely been a food source of the AAS crocodyliform (Main et al, in press). As migrating herds of hadrosauroids may have wandered too close to the crocodyliform feeding grounds and juveniles were brought down by the AAS crocs as prey (Fig. 8.43). This interpretation is supported by the presence of crocodyliform bitten hadrosauroid fossils recovered among bitten turtle shells from the AAS peat (Main et al., 2013; Noto et al., 2012).

Figure 8.44 Artist Jacek Major's reconstruction of the AAS coastal ecosystem. A. *Deltasuchus* lunges out of the water to attack a small herd of *Protohadros,* grabbing an unlucky sub-adult individual by the snout.

The Woodbine Formation and the AAS coastal fauna can be correlated to other mid-Cretaceous (Cenomanian) stratigraphic units and ecosystems in North America. The Dakota Formation and the Mussentuchit Member of the upper part of the Cedar Mountain Formation of Utah are both Late Cenomanian units that are stratigraphically and ecologically equivalent to the Woodbine Formation, although they are located on the western margin of the Greenhorn interior seaway (Cifelli, 1999; Eaton, et al., 1999; Kirkland, 1998; Kirkland et al., 1999; McDonald et al., 2010 and 2012). The Dakota Formation of the Kaiparowits Plateau consists of fluvial, lacustrine and brackish water deposits similar to those of the Woodbine Formation along with a similar fossil fauna (Eaton et al., 1999). The Dakota Formation fauna consists of the primitive fishes *Ceratodus sp*, and *Lepidotes sp*, as well as the relict Jurassic turtle *Glyptops sp*., all of which have been recovered from the AAS Woodbine fauna (Eaton et al., 1999).

The Mussentuchit Member of the upper most Cedar Mountain Formation is similar in age and environments of deposition to the Woodbine with an interestingly parallel fossil fauna as well (Cifelli, 1999; Eaton, et al., 1999; Kirkland, 1998; Kirkland et al., 1999; McDonald et al., 2010 and 2012). Among the Mussentuchit Member's fauna are; the fishes *Ceratodus sp*, Pycnodontidae indet, and Lepisostedeidae indet, the shark *Hybodus sp*., Lissamphibians; Caudata indet and Anura indet, chelonian that include Baenidae indet and the primitive *Glytops sp*., crocodyliforms that include *Bernissartia* sp. and the goniopholid

Dakosuchus sp., and a dinosaur fauna that includes ceratopsians, nodosaurids, dromaeosaurids, tyrannosaurids, hesperornithiform birds and most notably a fauna of basal hadrosauroids that includes the derived iguanodontian *Eolambia* (Cifelli, 1999; Eaton, et al., 1999; Kirkland, 1998; Kirkland et al., 1999; McDonald et al., 2010 and 2012). To date, the Mussentuchit Member supports a vastly more diverse fossil fauna than that of the Woodbine Formation, but there are similarities. The presence of the primitive lungfish *Ceratodus,* along with Pycnodontidae indet, and Lepisostedeidae indet, the shark *Hybodus sp*., the primitive turtle *Glytops sp*., and crocodyliforms that include *Bernissartia sp.* and the goniopholid *Dakosuchus* and the basal hadrosauroid *Eolambia* may all be correlated to the AAS Woodbine Formation fauna (Cifelli, 1999; Kirkland, 1998; Kirkland et al., 1999; McDonald et al., 2012). Of particular interest are *Dakosuchus* and *Eolambia* which bear morphologic similarities that place them phylogenetically close to to *Deltasuchus* and *Protohadros* of the AAS fauna.

With the similarities between the AAS ecosystem and those of the stratigraphically equivalent Dakota Formation and the Mussentuchit Member of the Cedar Moutain Formation it is likely that the faunas are paleobiogeographically linked as well. Kirkland et al. (1999) and McDonald et al. (2012) discussed the similarity of the Cedar Mountain dinosaur faunas to those of Early Cretaceous Eurasia, which they interpreted as evidence of a Eurasian migration across Beringia into North America in the Albian-Aptian.

Following this paleobiogeographic model, the AAS fauna could have been seeded by Cedar Mountain migrants that became isolated in North Texas by the Cenomanian eusatic highstand (Elder and Kirkland, 1994; Hancock and Kaufman, 1979; Haq et al., 1987). Once isolated along the Rudradian coast of the southern Greenhorn seaway, allopatric speciation could have produced a new fauna, with old relict origins.

8.5 Acknowledgements

I thank the Huffines, Robert Kimball at the Viridian Properties and HC LOBF of Arlington for granting access to the Viridian property in which the AAS study area occurs upon. I thank my friend and colleague Geb Bennett for his assistance with the AAS Micro-vertebrate project, with him all things small at the AAS would not have been found. Geb donated screens to the AAS, built new screens after my crew destroyed the old ones, and spent many a long hour screen washing and sorting Woodbine sediment samples. I thank the following AAS crew for assisting with the micro-vertebrate project: Kevin Anderson, Rachel Peterson, Coralyn Bingman, Nathan Campbell, Angela Maxwell, Albert Miramontes, Stewart Nolan, Jason Rich, Nathan Van Vranken, and Jan Weisner. Kevin Anderson and Rachell Peterson get a special thanks for their many long hours sitting in “Croc Creek” screening sediment samples, and equally many long hours in the UTA-AAS lab sorting bulk samples in search of micro fossils, and as if that

were not enough, Kevin was kind enough to bring in his professional camera gear to UTA and photograph many of the AAS fossils used in this dissertation. Brad Carter, Phil Kirchhoff and Art Sahlstein for donating coprolites found at the AAS. Kevin Anderson, Brad Carter, Anissa Camp, Phil Kirchhoff, and Art Sahlstein for donating micro-fossils found at the site via surface collecting. I thank my colleague Lorin King and fellow UTA student Lisa Moran for assisting with the identification and classification of the AAS coprolites. A special thanks to Karen Chin for taking time to discuss coprolite morphology at a busy SVP meeting, and to Bonnie Jacobs for discussing Cretaceous plant fossils with the author and providing much needed reference materials. Equally, a note of thanks to Nancy Engelhardt-Moore and Jamie Shamrock for their microfossil analyzes, Ellington & Associates, Inc., Houston, Texas for processing the nannofossils and foraminifera, and National Petrographic Service, Inc., Houston, Texas for processing the palynomorphs. A special note of thanks goes to Niall Paterson for analysis and photography of the palynomorphs, and providing much needed data on the plant paleoecology and biostratigraphy. I also thank Clinton Crowley and Jacek Major for providing arwork that helped the author visualize what the AAS Rudradian coast may have once looked like. The following provided much needed funds in support of this work; the Dallas Paleontological Society, Earthwatch Institute, Jurassic Foundation, Paleomap Project, UTA Graduate School Dissertation Fellowship and the Western Interior Paleontological Society.

Chapter 9

CONCLUSIONS

"In all works of Natural History, we constantly see the marvelous adaptation of animals to their food, their habitats, and the regions in which they are found."

Alfred Russel Wallace

The purpose of this dissertation was to document a coastal ecosystem from the mid-Cretaceous Woodbine Formation of North Texas using a variety of data sets, both macro and micro-vertebrates along with invertebrates, plant fossils (macro and micro), trace fossils, coprolites and sedimentological data. As the AAS presented a variety of preserved fossil data, a holistic approach was taken in which all of the fossils were studied and then placed into a stratigraphic and paleoecological context. Using this broad based approach, a larger view of the mid-Cretaceous coastal ecosystem preserved at the AAS was able to be presented. This broad based methodology is unusual for a lone research to attempt, but much of the work was accomplished through numerous collaborations and a large volunteer program (see acknowledgements). Of greatest utility to this project was the mapping grid that was established by volunteer Roger Fry. Maps of the fossils recovered from the AAS allowed for an accurate and detailed taphonomic and paleoecologic interpretation of the site. The work conducted at the AAS over the course of this dissertation is of value to research paleontologists, as mid-Cretaceous vertebrate ecosystems are still relatively poorly known.

The mid-Cretaceous, or Cenomanian is a unique time frame in Earth history that deserves more attention from researchers and further study. It was one of the warmest times in Earth history and a point in which vertebrate faunas underwent significant transition. In North America, Early Cretaceous iguanodontian-gymnosperm dominated ecosystems were replaced in the mid-Cretaceous by basal hadrosaur-angiosperm dominated ecosystems that were likely the descendants of Asian immigrants. These pivotal transitions are recorded in the mid-Cretaceous strata of North America.

The Cenomanian of North America is represented by only a few stratigraphic units, of which even fewer preserve the remains of vertebrate ecosystems. Among those Cenomanian units are the Dakota Formation and the Mussentuchit Member of the Cedar Mountain Formation of Utah, and the Woodbine Formation of North Texas. The Woodbine Formation has received intermittent attention since it was named by R. T. Hill over a century ago. McNulty and Slaughter (1968) published the first work on Woodbine vertebrate ecoystems. The most recent work includes the discovery and naming of a new crocodyliform by Lee (1997), a basal hadrosauroid by Head (1998) and a new mammal by Jacobs and Winkler (1998). However, many aspects of the Woodbine remained unanswered, until the discovery of a productive fossil site in North Arlington.

The Arlington Archosaur Site (AAS), a fossil site in the Woodbine Formation exposures of North Arlington, Tarrant County, discovered in 2003, has offered more data on the Cenomanian of Appalachia than any other site known today. Since its discovery in 2003, the AAS has provided an abundance of fossil data from the Woodbine Formation that can be used to address questions about the North American Cenomanian. In particular, the AAS preserves a coastal community that allows for a detailed study of Cenomanian terrestrial paleoecology of southern Appalachia (Rudradia), a relatively poorly studied paleogeographic region.

The AAS was a coastal ecosystem situated in southern Appalachia along a paleogeographic peninsula referred to as Rudradia that projected into the Greenhorn intercontinental seaway of the southwestern most Appalachia (Fig. 9.1). The AAS ecosystem was a diverse community that consisted of both macrovertebrates and microvertebrates from a low lying coastal marsh. The macrovertebrates were principally dinosaurs (ornithopod and theropods), crocodyliforms, and turtles. The microvertebrates include a diverse assemblage of juvenile crocodyliforms, lizards, salamanders, mammals, fish, lungfish and sharks.

The AAS aquatic fauna consists of the sharks *Hybodus sp., Cretodus sp.*, *Pseudohypholophus* and *Stephanodus sp.*, a partial dentary assigned to the mosasauridae, turtle shell attributed to *Glyptops sp.*, Baenidae indet, and

Trionichidae indet., along with teeth and vertebrae assigned to the pycnodont fish *Paleobalistum geiser*, partial sawfish rostal jaw sections assigned to *Onchopristis dunklei* and seven tooth plates assigned to a new species of *Ceratodus; C. carteri* (Main et al., 2012). *Ceratodus carteri* is named in honor of the discoverer Brad Carter and represented by seven tooth plates: the holotypic adult pterygopalatine plate, four adult prearticular plates, and two juvenile prearticular plates. All of the Woodbine *Ceratodus* specimens have high, sharp ridge crests that are interpreted as an adaptation for a slicing, or cutting feeding style. The upper tooth plate is relatively small compared to those of other North American ceradontids, smaller than *C. guentheri*. However, the primitive morphology of *C. carteri* is reminiscent of earlier North American ceradontids such as *C. guentheri*, but differs in size. Lungfish typically live in fresh water habitats; however, the AAS Woodbine lungfish likely lived on a delta plain. The modern South American lungfish *Lepidosiren paradoxa* lives in the Amazon River basin and delta marshes, and thus serves as a reasonable modern analogue for *Ceratodus carteri* (Main et al., 2012).

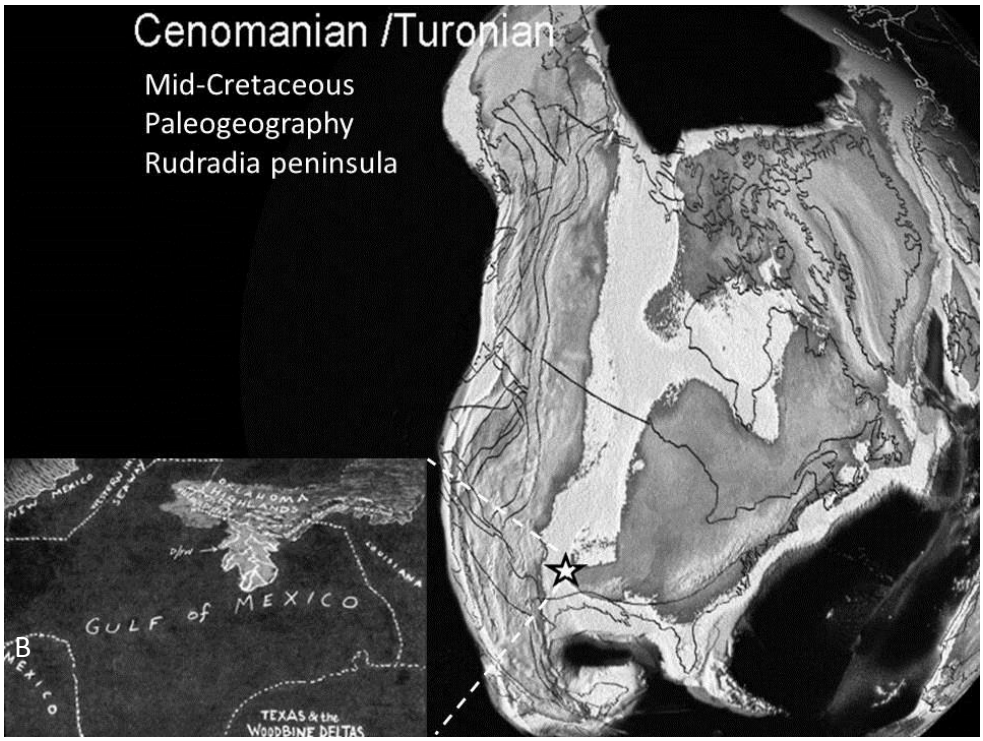

Figure 9.1 A. Cretaceous (Cenomanian-Turonian) North American paleogeographic map, AAS denoted with a star on the Rudradian peninsula of North Texas(modified from Scotese, 2005). B. Expanded view of Rudradia and the Woodbine delta system (art courtesy of Clinton Crowley).

Of the dinosaur fauna, a nearly complete basal hadrosauroid was discovered. It is an important basal hadrosauroid that presents one of the most complete post cranial skeletons of a Cenomanian hadrosauroid from Appalachia. It is morphologically similar to *Protohadros*, the only other known hadrosauroid in the Woodbine Formation and *Eolambia* from the Mussentuchit Member of the Cedar Mountain Formation (Head, 1998; McDonald et al., 2012). If the AAS hadrosauroid is indeed *Protohadros*, then it is the most complete skeleton of a *Protohadros* that has ever been recovered and allows for a greater resolution of

phylogenetic study of the taxa. In particular, the AAS hadrosauroid (*Protohadros ?*) hosts characters similar to the Eurasian hadrosauroids *Probactrosaurus, Bactrosaurus, Tethyshadros* and *Telmatosaurus* (Weishampel et al., 1993). If the AAS hadrosauroid is indeed a *Protohadros,* then for the sake of distinguishing the AAS specimen from the SMU type specimen, the author suggests using the commong name "Olivia" for the AAS *Protohadros*. The name "Olivia" is in honor of the daughter of one of the AAS discoverers, Art Sahlstein.

The similarity in character states of "Olivia" with Asian hadrosauroid taxa implies a Eurasian origins for Cenomanian North American hadrosauroids, likely from an Early Cretaceous (late Albian) dispersal across a north polar land bridge; Beringia. The Mussentuchit –Woodbine faunas of mid-Cretaceous (Cenomanian) Utah and North Texas bear strong resemblance and were likely sourced from a common origin. The *Eolambia-Protohadros* ornithopod fauna of the Mussentuchit-Woodbine fauna has sufficient similarity to the Early Cretaceous (Aptian-Albian) ornithopod faunas of Asia to support an Asian-American dispersal (Fig. 9.4).

Among the AAS coastal fauna is a new large mesoeucrocodylian crocodyliform: *Deltasuchus motherali*. *Deltasuchus* was named in honor of the discoverer, young Austin Motheral who discovered it while using his father's tractor to excavate at the AAS in the summer of 2009. This new taxon is based on multiple disarticulated but associated cranial and post cranial elements of both

adult and juveniles representing a wide ontogenetic range. As such, *Deltasuchus* represents an ecomorphotype not previously reported from the formation. Remains consist predominately of a disarticulated partially complete skull and considerable postcranial material from a single large adult individual and additional disarticulated material from a second adult, at least one sub-adult, and several juveniles, elucidating a partial growth series. Phylogenetic analysis of *Deltasuchus* following Turner and Buckley (2008) and Allen (2010) recovers the AAS crocodyliform as a sister to Eusuchia and Goniopholididae, united primairly by skull morphology and squamosals which overhang the temporo-orbital opening. This result is weakly supported as the taxon retains numerous pleisomorphic and homoplastic characters, such as goniopholidid paravertebral osteoderms and extensive polygonal ventral osteoderms, which make precise phylogenetic placement difficult. The taxon represents a previously unsampled lineage of mesoeusuchia and helps to elucidate relationships among crocodyliforms, particularly the placement of problematic clades such as the goniopholidids.

Skeletal material aside, numerous crocodyliform teeth along with broken and bitten turtle shell were recovered from the AAS. Crocodyliforms exhibit thecodont dentition, with most taxa possessing conical teeth. Teeth are continually replaced throughout life, preventing precise occlusion, but do interlock between upper and lower jaws. Tooth shape varies depending on ontogenetic stage of the

individual, thus many of the AAS teeth are attributed to juveniles. Tooth roots are resorbed and shed each successive tooth grows larger than its predecessor, with replacement slowing through life (Poole, 1961; Njau and Blumenschine, 2006). Juveniles use their teeth for piercing and grasping small, fast prey such as insects, crustaceans, amphibians, and fish. As they grow, the development of stronger jaws and robust teeth in adults are used for crushing and tearing of larger prey items such as turtles and juvenile dinosaurs. Along with the variation in tooth wear and eruption pattern, the tips of new teeth are easily chipped, which can lead to a variety of tooth marks being created by a single individual (Njau and Blumenschine, 2006).

Nopsca (1902) was among the first to note crocodylian feeding grounds as a potential source of bone accumulation in the fossil record. He attributed the accumulated remains of reptiles in Upper Cretaceous sediments of Romania to the feeding habits of crocodyliforms (Nopsca, 1902). He related the accumulation of saurian fossils in the mid-Cretaceous sediments of Transylvania to crocodyliform feeding grounds. Nopsca (1902) based this interpretation upon the fragmentary nature of the remains, and the presence of broken turtle shell found in great abundance. Similar crocodyliform deposits have been documented in the Gosau Formation of Austria, in the German Eocene lignite swamps, in the Oligocene oreodont beds of Nebraska and in the Miocene of Steinheim Lake (Weigelt, 1989).

Since the initial work of Nopsca (1902), the taphonomic contribution of crocodyliform feeding behavior to vertebrate assemblages' wetland ecosystems has only recently regained attention (Njau, 2006). Living crocodylians usually attack prey in water or near the water's edge, dragging the carcass into water to be consumed (Cott, 1961; Weigelt, 1989; Njau and Blumenschine, 2006). In some instances they travel inland to capture or scavenge prey. Most bones and teeth consumed by crocodylians are destroyed through digestion, removing them from the fossil record (Fisher, 1981). Remains too large to swallow may simply be ignored, or cached for later consumption. Such activities introduce vertebrate remains to depositional environments, thus enhancing their preservation potential. As opportunistic predators, crocodylians act as wide samplers of the surrounding fauna, especially smaller, or juvenile individuals (Cott, 1961; Delany and Abercrombie, 1986; Weigelt, 1989). This vertebrate material may be aggregated into relatively small areas (Weigelt, 1989; Njau, 2006), possibly forming bone beds that eventually attract the attention of paleontologists. In many ways then, crocodyliforms play a positive role in the formation of the vertebrate record of the areas they inhabit.

Associated with the accumulation of crocodyliform teeth are numerous broken and bitten turtle remains. A total of 31 bone fragments demonstrated tooth marks (2 ornithopod, 29 turtle). Eighty definitive tooth marks were identified along with numerous possible marks. Nearly 60% of turtle fragments showed

tooth marks, whereas only 1% of ornithopod bones were similarly marked. A total of 54 pits were observed on 16 different fragments. Turtle shell fragments include pieces of carapace and plastron referable to at least two individuals and smaller fragments of several others. All represent relatively large individuals (35–45+ cm carapace length), and include at least two different taxa. The turtle material was found in close association to the remains of *Deltasuchus*. Thus, the bite marks were attributed to *Deltasuchus* and were used to interpret crocodyliform feeding behavior along the ancient AAS coastal plain (Noto et al., 2012). The presence of the broken and bitten turtle remains were also found in association with numerous coprolites.

The coprolites varied in shape and size; however, many exhibit reptilian scroll morphology. Cylidrical, Ovoid, Spiral and Scroll coprolite morphologies are associated with fish, sharks and crocodilians based upon size and content (Sawyer, 1981 and 1998; Thulbron, 1991). The AAS coprolites demonstrate all of these morphologies, although most have either a Spiral or Scroll morphology and are quite large. Small (< 5 cm) Spiral coprolites were attributed to fish and sharks, principally the shark *Hybodus* (Thulborn, 1991). Large (> 6 cm) Spiral and Scroll coprolites were attributed to crocodyliforms. Large (>15 cm) Ovoid coprolites were attributed to herbivorous dinosaurs (Chin, 1996). The reptilian scroll coprolites were found in abundance in association with the remains of *Deltasuchus* (bones and shed teeth) as well as with many of the fragmentary turtle

remains that were documented with bite marks; scores and pits. The presence of coprolites in association with crocodilian remains and fragmentary vertebrate debris was previously acknowledged by Nopsca (1902) and Weigelt (1989) as being attributed to crocodilian feeding grounds.

The accumulation of fossils at the AAS is greatly reminiscent of those discussed by Nopsca (1902) and Weigelt (1989). The detailed maps of the AAS made by R. Fry show the distribution of the fossils and their association/relationship with one another, which allowed for an ecological interpretation of the site (see Appendix B). The presence of numerous coprolites attributed to crocodyliforms, many of which were found and mapped in association with *Deltasuchus* and its discarded meals, broken, bitten turtle shell, along with coprolites found with fragmentary bone and shed crocodyliform teeth supports the interpretation of the AAS Woodbine ecosystem as being part of a crocodyliform feeding ground, similar to the sites discussed by Nopsca (1902) and Weigelt (1989). Therefore, the AAS ecosystem is interpreted to be representative of either a crocodyliform feeding ground, or possibly even a nesting den (Fig. 9.2 and 9.3). Equally, as crocodyliforms are the predominant component of the AAS ecosystem, they are interpreted to be the prominent predator at the AAS, with *Deltasuchus* filling the role of the apex predator along the Rudradian coastal plain.

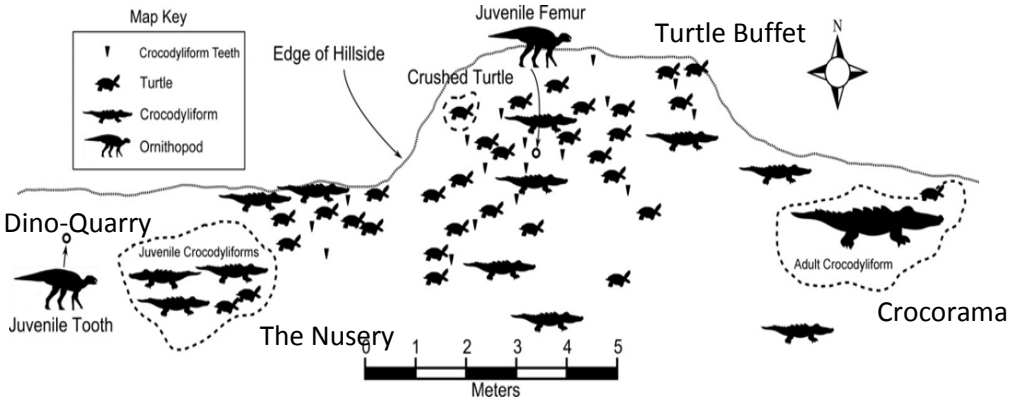

Figure 9.2 Evidence of a Crocodyliform feeding ground. Diagramatic-map of theAAS excavation showing locations of crocodyliform, turtle, and ornithopod dinosaur remains within the sites referred to as Crocorama, the Turtle Buffet and the Nursery. Dense collections of fossils referable to one or more individuals are surrounded by dotted lines. Fragmentary, bitten turtle remains and coprolites were recovered from the Turtle Buffet.

All of the components of the AAS ecosystem retain primitive characters from Late Jurassic and Early Cretaceous predecessors. The dominant AAS crocodyliform *Deltasuchus* demonstrates a mix of characters reminiscent of Late Jurassic goniopholids and Early Cretaceous pholidosaurs. The AAS ornithopod equally retains primitive characters of Late Jurassic iguanodontians and Early Cretaceous basal hadrosauroids; *Camptosaurus, Probactrosaurus* and *Bactrosaurus*. Although lungfish are conservative vertebrates, *Ceratodus carteri* retains primitive characters associated with the Late Jurassic lungfish *C. guentheri.* As the mid-Cretaceous was a time of faunal transition, it is not surprising that the AAS Woodbine fauna displays characters that record this

transition. However, the predominant retention of relict characters in the AAS fauna implies isolation, or endemism. Other cases of endemism and the effects of isolation were noted for the Late Cretaceous European ornithopods *Tethyshadros* and *Telmatosaurus* (Dalla-Vechia, 2006; Weishampel et al., 1993). Both *Tethyshadros* and *Telmatosaurus* retained primitive or relict traits due to isolation in Europe during one of the eustatic highstands of the Late Cretaceous (Dalla-Vechia, 2006; Weishampel et al., 1993). Using the isolated Late Cretaceous dinosaur faunas of Europe as a model, the AAS is interpreted as representing an endemic fauna. As the AAS ecosystem was relatively isolated on the Rudradian peninsula, the components of the ecosystem retained primitive features from Early Cretaceous predecessors.

The fossils of the AAS ecosystem occur principally from two stratigraphic beds, or facies, an organic rich peat bed and an overlying clay rich paleosol (a Histic Gleysol). The two fossil horizons are bound by beds containing charcoal, and in the case of the paleosol, a charcoal horizon occurs within the bed. The presence of fossil charcoal beds both within and bounding the fossil horizons suggests that the AAS ecosystem was potentially influenced by wildfires.

The first forest fire bed (FFB1) recorded at the AAS is a charcoal conglomerate at the base of the section and is associated with a siderite rich sandstone. Directly overlying FFB1 is the fossil rich AAS peat bed. The peat bed was found to have the greatest diversity of fossils at the AAS. Factors such as

collecting bias and preservational bias taken into consideration, the increase in diversity could be interpreted as a result of coastal wildfires and periodic disturbance to the ecosystem. Overlying the peat facies is another bone bearing horizon of clay rich paleolsol that contains vertical burned roots and stumps, referred to as FFB2. The presence of the burned roots and stumps in the paleosol demonstrates the commensurate nature of the wildfires at the time of the occupation of the region by dinosaurs. The bone bearing, burned root bed is overlain by FFB3, a forest fire debris flow bed.

Over time it would appear that regional forest fires had an adverse effect on the AAS Rudradian ecosystem. The upper heterolithic strata of the Woodbine Formation exposed and studied at the AAS produced fewer fossils than the lower strata of paleosols and peat. Taphonomic and collecting bias aside, the decrease in fossil abundance noted as occurring upwards in section at the AAS is interpreted as possible evidence of an ecosystem that was adversely affected by wildfires that occurred more frequently than what the coastal ecosystem could recover from. Over time environmental and ecological stress may have become too great for the coastal ecosystem that would later be called the AAS to survive.

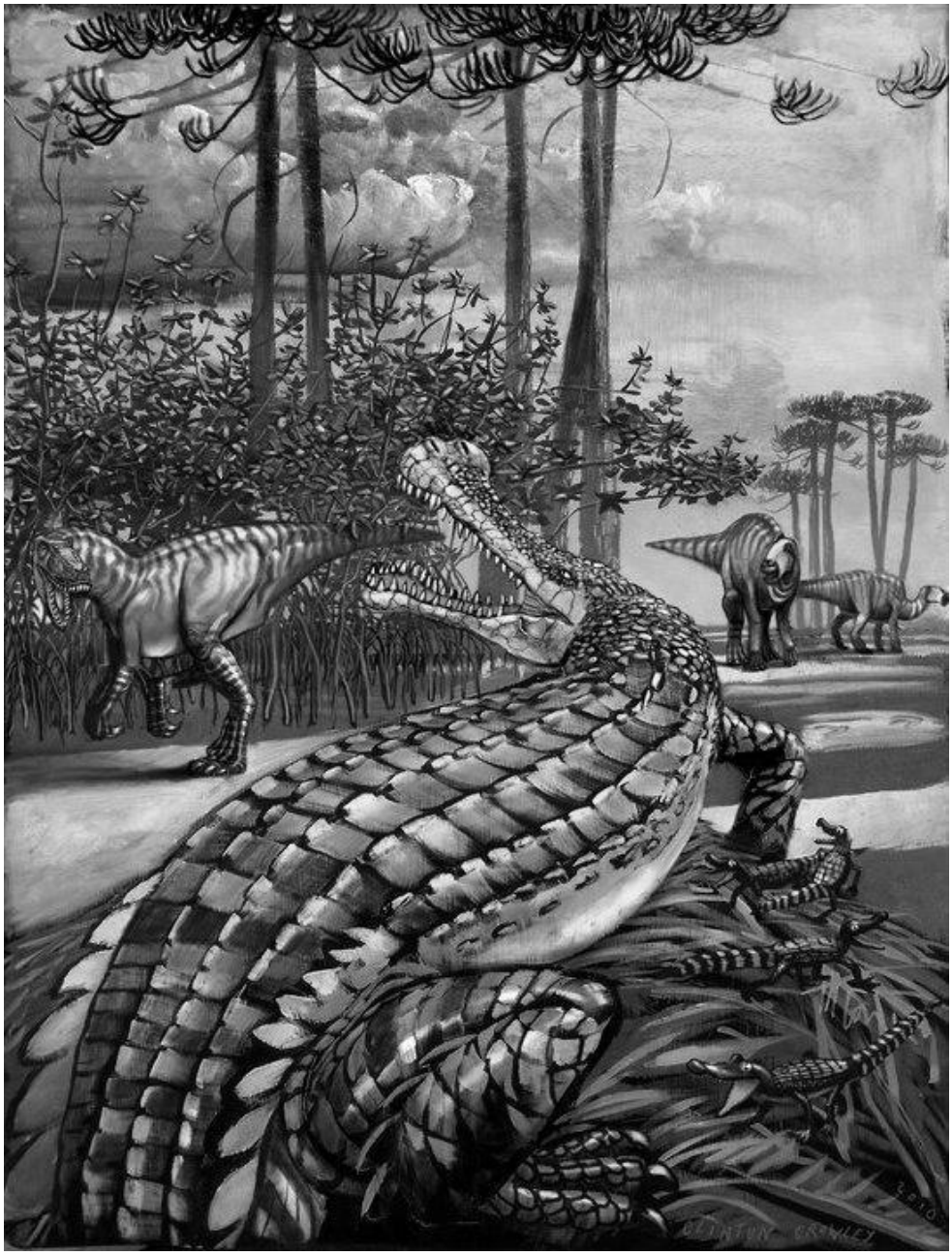

Figure 9.3 Artist Clinton Crowleys interpretation of the Arlington Archosaur Site; a female *Deltasuchus* defends her nest from dinosaurs roaming the Rudradian coastal plain.

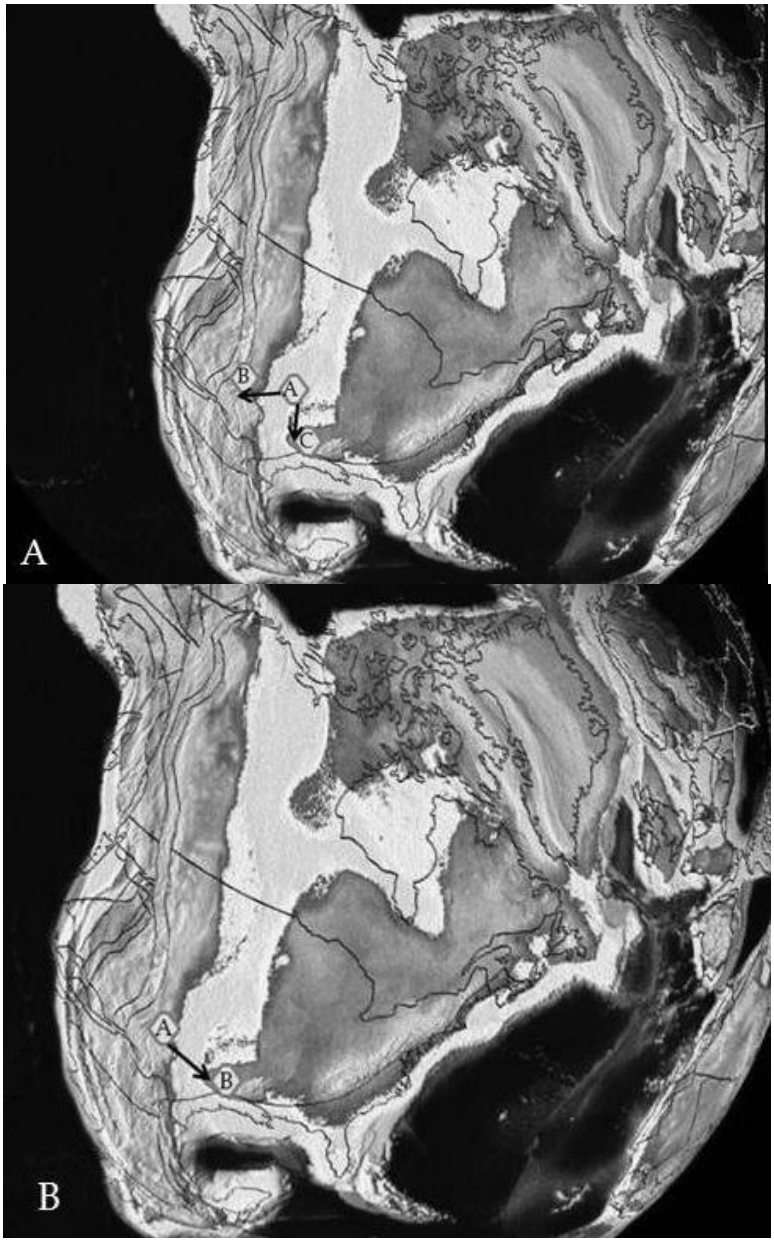

Figure 9.4 Paleobiogeographic models for origins of mid-Cretaceous ecosystems in North America. Asian migrants' entered North America via dispersal across Beringia A. Possible common ancestral population was divided by migrating coastlines, and split into the Mussentuchit and Woodbine faunas. B. The Mussentuchit fauna was the parent fauna of the Woodbine, of which was later isolated by the Cenomanian highstand.

A special note of thanks to all of the volunteers of the Arlington Archosaur Site, affectionately called the "Archosaurs." If not for them, much of what has happened and what will happen at the the AAS would not be possible. Thank you, each and every one of you.

Figure 9.5 The AAS dig crew (The "Archosaurs") August 2010, from left to right: Phil Scoggins, Art Sahlstein, Roger Fry, Chris Noto, Ronnie Colvin, Darlene Sumerfelt, Teresa Thornton, David White, Anissa Camp, Derek Main, Emily and Daniel Flores and Frankie Frazer

.

APPENDIX A

PART I

ARLINGTON ARCHOSAUR SITE COLLECTIONS DATABASE

AAS Collections #	Designation	Description	Location
Dipnoi			
UTA-AASL-001	*Ceratodus carterii*	tooth plate	AAS-Birds Fort Lake (BFL)
UTA-AASL-002	*Ceratodus carterii*	tooth plate	AAS BFL
UTA-AASL-003	*Ceratodus carterii*	tooth plate	AAS-BFL
UTA-AASL-004	*Ceratodus carterii*	juvy tooth plate	AAS hill
UTA-AASL-005	*Ceratodus carterii*	tooth plate	AAS hill
UTA-AASL-006	*Ceratodus carterii*	tooth plate	AAS
UTA-AASL-007	*Ceratodus carterii*	juvy tooth plate	AAS
UTA-AASL-008	*Ceratodus carterii*	tooth plate	AAS-BFL
UTA-AASL-009	*Ceratodus carterii*	tooth plate	AAS-BFL
Micro-samples			
UTA-AASM-001	Osteichthyes indet.	3 centra	AAS-Birds Fort (BFL)
UTA-AASM-002	*Cretodus* sp.	3 teeth & 1 partial	AAS-Birds Fort (BFL)
UTA-AASM-003	unidentified	4 cm partial limb (croc?/turtle?)	AAS-Birds Fort (BFL)
UTA-AASM-004	Elopomorpha indet.	4 centra	AAS-Birds Fort (BFL)
UTA-AASM-005	Pycnodontiformes indet.	partial jaw (4cm)	AAS-Birds Fort (BFL)
UTA-AASM-006	Odontaspididae indet.	9 sm teeth	AAS-Birds Fort (BFL)
UTA-AASM-007	croc?	phalange	AAS-BFL
UTA-AASM-008	Osteichthyes indet.	1 centrum	AAS-BFL
UTA-AASM-009	Teleostei indet.	3 sm (~1cm) verts fused in matrix	AAS-Birds Fort (BFL)
UTA-AASM-010	Elopomorpha indet.	1 large centrum (2.5 cm; elopomorph); 1 small centrum	AAS-Arena (NW hill)
UTA-AASM-011	Pycnodontiformes indet.	25 teeth (to be measured)	AAS-BFL
UTA-AASM-012	*Cretodus*	tooth	AAS-Cruziana bed (field)
UTA-AASM-013	crocodile ? Or turtle	2 verts	AAS-BFL
UTA-AASM-014	Mosasauroidea indet.	partial jaw (~4.5cm) from near symphyseal contact	AAS-BFL
UTA-AASM-015	Pycnodontiformes indet.	14 teeth (to be measured)	AAS-BFL
UTA-AASM-016	*Cretodus?*	partial tooth	AAS-BFL
UTA-AASM-017	unidentified croc?	small vert (2cm)	AAS-BFL
UTA-AASM-018	unidentified shark	small shark vert (2cm)	AAS-BFL
UTA-AASM-019	Teleostei indet.	small caudal or posterior dorsal centrum in matrix	AAS-BFL
UTA-AASM-020	*Onchopristis*	3 partial sawfish jaws	AAS-BFL
UTA-AASM-021	unidentified	2 partial crania-jaws? (5cm L-croc?)	AAS-BFL
UTA-AASM-022	Pycnodontiformes indet.	2 partial jaws (sm-1cm)	AAS-Crocorama (6.8)

UTA-AASM-023	cf. *Lepidotes*	2 gar scales (large-3cm)	AAS-Hill
UTA-AASM-024	*Hybodus* sp.	3 cephalic spines (2cm)	AAS-BFL
UTA-AASM-025	Testudines indet.	3 sm verts (1-2cm)	AAS-BFL
UTA-AASM-026	cf. *Lepidotes*	5 gar scales (sm~ <1cm)	AAS-BFL
UTA-AASM-027	*Hybodus* sp.	3 cephalic spines (partial)	AAS-BFL
UTA-AASM-028	unidentified (croc?)	partial vert (2.5 cm L)	AAS-BFL
UTA-AASM-029	unidentified (croc/turtle?)	partial vert (1.5 cm L/badly weathered)	AAS-Hill
UTA-AASM-030	unidentified fish	fish palate	AAS-BFL
UTA-AASM-031	?Reptilia	lg vert (3cmL x 4cmW)	AAS-BFL
UTA-AASM-032	unidentified croc?	lg vert (3cmL x 2cmW)	AAS-BFL
UTA-AASM-033	Osteichthyes indet.	1 partial jaw (~1-2cmL)	AAS-BFL
UTA-AASM-034	various	1 complete and 3 partial fish centra; 1 possible coprolite; 1 ?reptile centrum; 1 tiny procoelous crocodile centrum; 1 small longbone section lacking epiphyses	AAS-BFL
UTA-AASM-035	Amber	2 sm pieces (2-3mm)	AAS-Croc Creek
UTA-AASM-036	Crocodyliformes indet.	sm croc tooth (3mm)	AAS Dino Quarry (20cm-23cm below rippled sand lens)
UTA-AASM-037	*Stephanodus*	sm tooth (~3mm)	AAS Dino Quarry (20cm-23cm below rippled sand lens)
UTA-AASM-038	Crocodyliformes indet.	sm tooth (~2mm)	AAS Dino Quarry (20cm-23cm below rippled sand lens)
UTA-AASM-039	Crocodyliformes indet.	sm tooth (~2mm)	AAS Dino Quarry (20cm-23cm below rippled sand lens)
UTA-AASM-040	unidentified (croc?)	sm tooth (~3mm)	AAS Dino Quarry (20cm-23cm below rippled sand lens)
UTA-AASM-041	*Pseudohypolophus*	tooth (~3mm)	AAS Dino Quarry (20cm-23cm below rippled sand lens)
UTA-AASM-042	unidentified fish?	thin curved tooth-Morphotype A (~4mm)	AAS Dino Quarry (20cm-23cm below rippled sand lens)
UTA-AASM-043	*Pseudohypolophus*	tooth (~3mm)	AAS Dino Quarry (20cm-23cm below rippled sand lens)
UTA-AASM-044	Teleostei indet.	7 Misc (2 teleost centrum frags, undiagnostic frags)	AAS Dino Quarry (20cm-23cm below rippled sand lens)
UTA-AASM-045	*Onchopristus*	sm tooth (<1mm)	AAS Dino Quarry (20cm-23cm below rippled sand lens)
UTA-AASM-046	Osteichthyes indet.	sm tooth Morphotype A (<1mm)	AAS Dino Quarry (20cm-23cm below rippled sand lens)
UTA-AASM-047	*Pseudohypolophus*	sm tooth (<1mm)	AAS Dino Quarry (20cm-23cm below rippled sand lens)
UTA-AASM-048	Teleostei indet.	sm vert (>3mm)	AAS-Dino Quarry (20cm-30cm below rippled sand lens)
UTA-AASM-049	Crocodyliformes indet.	croc tooth (~6mm)	AAS-Dino Quarry (20cm-30cm below rippled sand lens)
UTA-AASM-050	Osteichthyes indet.	tooth Morphotype A: long, thin, oval in cross section, poorly preserved	AAS-Dino Quarry (20cm-30cm below rippled sand lens)
UTA-AASM-051	*Pseudohypolophus*	2 fish teeth (~2mm)	AAS-Dino Quarry (20cm-30cm below rippled sand lens)
UTA-AASM-052	cf. *Hybodus*	tooth (~3mm)	AAS-Dino Quarry (20cm-30cm below rippled sand lens)
UTA-AASM-053	Osteichthyes indet.	tooth Morphotype A (<1mm)	AAS-Dino Quarry (20cm-30cm below rippled sand lens)
UTA-AASM-054	Caudata indet.	caudal vert (~2mm)	AAS-Dino Quarry (20cm-30cm below rippled sand lens)
UTA-AASM-055	Teleostei indet.	sm vert (~4mm)	AAS-Dino Quarry (20cm-30cm below rippled sand lens)
UTA-AASM-056	unidentified	Misc bone frags	AAS-Crocorama (peat bed)
UTA-AASM-057	unidentified fish?	Scale	AAS-Crocorama
UTA-AASM-058	Teleostei indet.	sm vert (~3mm)	AAS-Crocorama

UTA-AASM-059	Crocodyliformes indet.	tooth (~1cm)	AAS Dino-Quarry (Siderite layer, (4)buckets)
UTA-AASM-060	Pycnodontiformes indet.	sm tooth (~1-2mm)	AAS Dino-Quarry (Siderite layer, (4)buckets)
UTA-AASM-061	unidentified fish?	sm vert (~4mm)-basioccipital	AAS Dino-Quarry (Siderite layer, (4)buckets)
UTA-AASM-062	croc?	sm tooth (~3-4mm)	AAS Dino-Quarry (Siderite layer, (4)buckets)
UTA-AASM-063	unidentified invert	sm shell (~2mm)	AAS Dino-Quarry (Siderite layer, (4)buckets)
UTA-AASM-064	unidentified shark/fish?	denticle (~3mm)	AAS Dino-Quarry (Siderite layer, (4)buckets)
UTA-AASM-065	unidentified shark/fish?	tooth (~3mm)	AAS Dino-Quarry (Siderite layer, (4)buckets)
UTA-AASM-066	unidentified shark/fish?	tooth (~3mm)	AAS Dino-Quarry (Siderite layer, (4)buckets)
UTA-AASM-067	unidentified shark/fish?	tooth (~3mm)	AAS Dino-Quarry (Siderite layer, (4)buckets)
UTA-AASM-068	Pycnodontiformes indet.	1 tooth (~3mm); 1 tooth fragment	AAS Dino-Quarry (Siderite layer, (4)buckets)
UTA-AASM-069	croc	tooth (~3mm)	AAS-Dino Quarry (45cm-60cm below top of Carbonaceous shale)
UTA-AASM-070	croc	tooth (~9mm)	AAS-Dino Quarry (20cm-30cm below rippled sand lens)
UTA-AASM-071	*Pseudohypolophus*	tooth (~3mm)	AAS-Dino Quarry (20cm-30cm below rippled sand lens)
UTA-AASM-072	unidentified	unidentified	AAS-Dino Quarry (7cm-8cm below top of Carbonaceous shale)
UTA-AASM-073	*cf. Lepidotes*	scale	AAS-Crocorama?
UTA-AASM-074	unidentified plant	seed?	AAS-Crocorama
UTA-AASM-075	unidentified	unidentified	AAS-Crocorama
UTA-AASM-076	Crocodyliformes indet.	sm tooth (~3mm)	AAS-Crocorama
UTA-AASM-077	snail?	sm tooth (~3mm)	AAS-Crocorama
UTA-AASM-078	unidentified	unidentified	AAS-Crocorama
UTA-AASM-079	cf. *Bernessartia*	1 sm tooth	AAS-Crocorama
UTA-AASM-080	unidentified turtle	sm shell (plastron?/~10mm)	AAS-Crocorama
UTA-AASM-081	Crocodyliformes indet.	sm tooth (~5mm)	AAS-Crocorama
UTA-AASM-082	unidentified (turtle/croc?)	sm limb bone (~2cm)	AAS-Crocorama
UTA-AASM-083	unidentified (turtle/croc?)	Misc bone frags	AAS-Crocorama
UTA-AASM-084	Holostei indet.	sm scale (~5mm)	AAS-Crocorama (-17.5)
UTA-AASM-085	Crocodyliformes indet.	tooth + 3 other fragments that need to be split into other catalog numbers	AAS-Crocorama
UTA-AASM-086	Crocodyliformes indet.	4 teeth	AAS-Crocorama
UTA-AASM-087	Crocodyliformes indet.	2 teeth	AAS-Crocorama
UTA-AASM-088	Teleostei indet.	4 verts (<1mm/fish?)	AAS-Crocorama? (no data)
UTA-AASM-089	various micro	possible salamander centrum fragments, amphibian jaw section, 1 partial Lepidotes scale, other fragments	AAS-Crocorama? (no data)
UTA-AASM-090	?Osteichthyes	1 tooth (~11mm crown height)	AAS-Crocorama? (no data)
UTA-AASM-091	Crocodyliformes indet.	1 tooth (~5mm, fish?)	AAS-Crocorama? (no data)
UTA-AASM-092	Crocodyliformes indet.	2 sm teeth (~3mm, fish?)	AAS-Crocorama? (no data)
UTA-AASM-093	cf. *Bernessartia*	1 sm tooth (~4mm, fish-pycnodont?)	AAS-Crocorama? (no data)
UTA-AASM-094	unidentified invert	1 sm gastopod & 2 twigs	AAS-Crocorama? (no data)

UTA-AASM-095	unidentified	1 sm tooth?	AAS-Crocorama? (no data)
UTA-AASM-096	unidentified	2 sm teeth? (<2mm)	AAS-Dino Quarry (32cm-40cm below top)
UTA-AASM-097	unidentified	Misc unidentified	AAS-Crocorama ?
UTA-AASM-098	Crocodyliformes indet.	Tooth	AAS Dino-Quarry Paleosol, (3) buckets
UTA-AASM-099	Teleostei indet.	3 centra	AAS Dino-Quarry Paleosol, (3) buckets
UTA-AASM-100	unidentified	sm tooth?	AAS Dino-Quarry Paleosol, (3) buckets
UTA-AASM-101	Teleostei indet.	2 sm verts (~2mm)	AAS Dino-Quarry Paleosol, (3) buckets
UTA-AASM-102	Crocodyliformes indet.	2 sm teeth (~2-3mm)	AAS Dino-Quarry Paleosol, (3) buckets
UTA-AASM-103	?Crocodyliformes	Unidentified	AAS Dino-Quarry Paleosol, (3) buckets
UTA-AASM-104	Caudata indet. & Teleostei indet.	5 sm verts (~2mm)	AAS Dino-Quarry Paleosol, (3) buckets
UTA-AASM-105	unidentified	bone frag	AAS Dino-Quarry Paleosol, (3) buckets
UTA-AASM-106	Teleostei indet.	1 vert (~3mm)	AAS Dino-Quarry Paleosol, (3) buckets
UTA-AASM-107	Teleostei indet.	3 sm verts (~2-3mm)	AAS-Crocorama? (no data)
UTA-AASM-108	Crocodyliformes indet.	2 teeth (~4-6mm)	AAS-Crocorama? (no data)
UTA-AASM-109	unidentified	bone frag	AAS-Crocorama? (no data)
UTA-AASM-110	Sauria indet.	1 sm vert (~4mm)	AAS-Crocorama? (no data)
UTA-AASM-111	Crocodyliformes indet.	2 sm teeth (~5-6mm)	AAS-Crocorama? (no data)
UTA-AASM-112	Crocodyliformes indet.	8 sm teeth and 2 tooth fragments	AAS-Crocorama? (no data)
UTA-AASM-113	Osteichthyes indet.	2 sm teeth (~2-4mm)	AAS-Crocorama? (no data)
UTA-AASM-114	cf. *Lepidotes*	4 sm scales (~2-5mm)	AAS-Crocorama? (no data)
UTA-AASM-115	plant-wood	sm twigs	AAS-Crocorama? (no data)
UTA-AASM-116	amber	1 sm amber sample	AAS-Crocorama? (no data)
UTA-AASM-117	Crocodyliformes indet.	4 sm teeth (~2-3mm)	AAS-Crocorama? (no data)
UTA-AASM-118	Osteichthyes indet.	2 sm scales (~2-4mm)	AAS-Crocorama? (no data)
UTA-AASM-119	Crocodyliformes indet.	1 sm thin tooth fragment (~3-4mm)	AAS-Crocorama? (no data)
UTA-AASM-120	Sauria indet.	2 sm verts (~3-4mm)	AAS-Crocorama? (no data)
UTA-AASM-121	Caudata indet., Lepidotes & indet.	1 cf. Lepidotes scale; 2 possible salamander centrum fragments; 1 salamander prezygopophysis; 6 other fragments	AAS-Crocorama
UTA-AASM-122	various	1 croc tooth, Morphotype A; 1 croc tooth, Morphotype unknown; 1 broken ?teleost centrum fragment	AAS-Crocorama
UTA-AASM-123	Crocodyliformes indet.	1 tooth (~4-5mm)	AAS-Crocorama
UTA-AASM-124	Crocodyliformes indet.	1 tooth (~4mm)	AAS-Crocorama
UTA-AASM-125	?Amiiformes	1 vert (~4mm)	AAS-Crocorama
UTA-AASM-126	Teleostei indet.	2 sm vert (~2-3mm)	AAS-Crocorama
UTA-AASM-127	Teleostei indet.	2 sm verts (~2mm)	AAS-Crocorama
UTA-AASM-128	unidentified	unidentified fragments	AAS-Crocorama
UTA-AASM-129	Crocodyliformes indet.	1 tooth (~1cm)	AAS-Crocorama
UTA-AASM-130	unidentified	2 misc bone frags	AAS-Crocorama

UTA-AASM-131	Crocodyliformes indet.	1 osteoderm fragment; 3 unidentified fragments	AAS-Crocorama
UTA-AASM-132	Sauria indet.	1 sm vert (~4mm)	AAS-Crocorama
UTA-AASM-133	Teleostei indet.	1 sm vert (~2-3mm)	AAS-Crocorama
UTA-AASM-134	?Caudata	1 possible salamander centrum fragment; 5 unidentifiable fragments	AAS-Crocorama
UTA-AASM-135	Crocodyliformes indet.	1 sm tooth (~4mm)	AAS-Crocorama?
UTA-AASM-136	Osteichthyes indet.	2 sm verts (~3mm)	AAS-Crocorama?
UTA-AASM-137	Crocodyliformes indet.	1sm tooth	AAS-Crocorama?
UTA-AASM-138	Sauria indet.	1sm vert (~3mm-good)	AAS-Crocorama
UTA-AASM-139	Teleostei indet.	1sm vert (~2mm)	AAS-Crocorama
UTA-AASM-140	Caudata indet.	1sm vert (~2mm)	AAS-Crocorama
UTA-AASM-141	wood fragment - discard	wood frag	AAS-Crocorama
UTA-AASM-142	?Osteichthyes	1 sm tooth (~1mm)	AAS-Crocorama
UTA-AASM-143	amber?	1 sm frag? (~1mm)	AAS-Crocorama
UTA-AASM-144	Osteichthyes indet.	1sm vert (~1mm)	AAS-Crocorama
UTA-AASM-145	?Crocodyliformes	1sm tooth (~1.5 mm)	AAS-Crocorama
UTA-AASM-146	Sauria indet.	1sm vert (~2-3 mm)	AAS-Crocorama
UTA-AASM-147	Sauria indet.	1sm vert (~2-3 mm)	AAS-Crocorama
UTA-AASM-148	Teleostei indet.	1sm vert (~2 mm)	AAS-Crocorama
UTA-AASM-149	Crocodyliformes indet.	1sm vert (~2 mm)	AAS-Crocorama
UTA-AASM-150	Teleostei indet.	1sm vert (~2 mm)	AAS-Crocorama
UTA-AASM-151	Crocodyliformes indet.	1 (?)sm vert (~2-3 mm)	AAS-Crocorama
UTA-AASM-152	Crocodyliformes indet.	1 broken tooth (~1cm)	AAS-Crocorama
UTA-AASM-153	Crocodyliformes indet.	1 broken tooth (~1.2cm)	AAS-Crocorama
UTA-AASM-154	Crocodyliformes indet.	1 broken tooth (~8 mm)	AAS-Crocorama
UTA-AASM-155	ornithopod	1 shed -worn tooth (~7 mm)	AAS-Crocorama
UTA-AASM-156	?Crocodyliformes	1 worn tooth (~1cm)	AAS-Crocorama
UTA-AASM-157	cf. Lepidotes	1 worn scale (<1cm)	AAS-Crocorama
UTA-AASM-158	Teleostei indet.	1sm vert (~2-3 mm)	AAS-Crocorama
UTA-AASM-159	?Crocodyliformes	1sm tooth (~6 mm)	AAS-Crocorama
UTA-AASM-160	Crocodyliformes indet.	1 tooth (~1 cm)	AAS-Crocorama
UTA-AASM-161	Crocodyliformes indet.	1 tooth (croc~6-7 mm)	AAS-Crocorama
UTA-AASM-162	?Amiiformes	1 vert (~4mm)	AAS-Crocorama
UTA-AASM-163	Reptilia indet.	1 tooth (~4mm)	AAS-Crocorama
UTA-AASM-164	Crocodyliformes indet.	1 tooth (~3mm)	AAS-Crocorama
UTA-AASM-165	Reptilia indet. (possibly bird)	sm limb bone (~4mm)	AAS-Crocorama (-9, 10)
UTA-AASM-166	Sauria indet.	sm vert (~8mm)-(lizard?)	AAS-BFL
UTA-AASM-167	Teleostei indet.	vert centrum (~2cm)	AAS-BFL
UTA-AASM-168	Teleostei indet.	vert centrum	AAS-Crocorama
UTA-AASM-169	unidentified	sm shell (?)	AAS-Crocorama
UTA-AASM-170	*Pseudohypolophus*	sm ray tooth	AAS-Crocorama

UTA-AASM-171	*Hybodus* sp.	shark or ornithopod tooth frag?	AAS-Crocorama
UTA-AASM-172	Tetrapoda indet.	1 longbone epiphysis	AAS-Crocorama
UTA-AASM-173	Tetrapoda indet.	1 longbone epiphysis	AAS-Crocorama
UTA-AASM-174	Crocodyliformes indet.	1 baby croc tooth	AAS-Crocorama (5.6)
UTA-AASM-175	plant-wood	wood frag	AAS-Crocorama
UTA-AASM-176	Crocodyliformes indet.; cf. Lepidotes	1 croc osteoderm fragment; 1 cf. Lepidotes scale	AAS-Crocorama
UTA-AASM-177	Crocodyliformes indet.	juvy croc tooth	AAS-Crocorama
UTA-AASM-178	?Amiiformes	jaw fragment with 1 styliform tooth	AAS-Crocorama
UTA-AASM-179	unidentified	longbone or rib shaft	AAS-Crocorama
UTA-AASM-180	Crocodyliformes indet.	1 partial scale	AAS-Crocorama
UTA-AASM-181	Osteichthyes indet.	vert centrum	AAS-Crocorama
UTA-AASM-182	Teleostei indet.	1 fish fragment	AAS Dino Quarry (20cm-23cm below rippled sand lens)
UTA-AASM-183	?Osteichthyes	unidentified frag	AAS-Crocorama
UTA-AASM-184	unidentified	1 caudal centrum	AAS-Crocorama
UTA-AASM-185	Sauria indet.	1 centrum	AAS-Crocorama
UTA-AASM-186	Teleostei indet.	vert centrum	AAS-Crocorama
UTA-AASM-187	?Sauria indet.	1 large centrum	AAS-Crocorama (4.6)
UTA-AASM-188	Crocodyliformes indet.	baby croc tooth	AAS-Crocorama
UTA-AASM-189	Crocodyliformes indet.	baby croc tooth	AAS-Crocorama
UTA-AASM-190	Teleostei indet.	2 vert centra	AAS-Crocorama
UTA-AASM-191	Teleostei indet.	vert centrum	AAS-Crocorama
UTA-AASM-192	?Osteichthyes	Fragment	AAS-Crocorama
UTA-AASM-193	Teleostei indet.	3 complete centra & 1 partial centrum	AAS-Crocorama
UTA-AASM-194	cf. *Lepidotes*	sm scale	AAS-Crocorama
UTA-AASM-195	Teleostei indet.	1 centrum	AAS-Crocorama
UTA-AASM-196	?Sauria	1 lizard ?metatarsal or metacarpal	AAS-Crocorama
UTA-AASM-197	Teleostei indet.	1 centrum	AAS-Crocorama
UTA-AASM-198	unidentified	misc frag	AAS-Crocorama
UTA-AASM-199	Multituberculata indet.	1 lower 4th premolar	AAS-Crocorama
UTA-AASM-200	unidentified	misc frag	AAS-Crocorama
UTA-AASM-201	Crocodyliformes indet.	1 tooth	AAS-Crocorama
UTA-AASM-202	Teleostei indet.	1 centrum	AAS-Crocorama
UTA-AASM-203	Chondrichthyes indet.	small ray tooth	AAS-Crocorama
UTA-AASM-204	unidentified	Frag	AAS-Crocorama
UTA-AASM-205	Osteichthyes indet.	1 styliform tooth (?pycnodont)	AAS-Crocorama
UTA-AASM-206	?Crocodyliformes	1 tooth	AAS-Crocorama
UTA-AASM-207	Anura indet.	1 radioulna	AAS-Crocorama
UTA-AASM-208	unidentified	bone frag?	AAS-Crocorama (1.8)
UTA-AASM-209	Teleostei indet.	4 complete centra; 2 partial centra	AAS-Crocorama
UTA-AASM-210	Teleostei indet.	1 partial centrum	AAS-Crocorama

UTA-AASM-211	?Plantae	seed fragment?	AAS-Crocorama
UTA-AASM-212	Crocodyliformes indet.	baby tooth	AAS-Crocorama
UTA-AASM-213	bone fragment		AAS-Crocorama
UTA-AASM-214	bone fragment	shell frag	AAS-Crocorama
UTA-AASM-215	Caudata indet.	1 centrum fragment	AAS-Crocorama
UTA-AASM-216	bone fragment		AAS-Crocorama
UTA-AASM-217	?Reptilia	1 tooth fragment	AAS-Crocorama
UTA-AASM-218	amber	amber	AAS-Crocorama
UTA-AASM-219	unidentified	bone frag (limb?)	AAS-Crocorama
UTA-AASM-220	?Crocodyliformes	baby tooth	AAS-Crocorama
UTA-AASM-221	Caudata indet.	1 broken prezygopophysis	AAS-Crocorama
UTA-AASM-222	?Crocodyliformes	partial baby tooth	AAS-Crocorama
UTA-AASM-223	unidentified	partial baby tooth	AAS-Crocorama
UTA-AASM-224	Crocodyliformes indet.	partial baby tooth	AAS-Crocorama
UTA-AASM-225	cf. *Lepidotes*	scale	AAS-Crocorama
UTA-AASM-226	wood	wood frags	AAS-Crocorama
UTA-AASM-227	unidentified	bone frag	AAS-Crocorama
UTA-AASM-228	?Amiiformes	sm vert centrum	AAS-Crocorama
UTA-AASM-229	Crocodyliformes indet.	1 tooth	AAS-Crocorama
UTA-AASM-230	Crocodyliformes indet.	1 tooth	AAS-Crocorama
UTA-AASM-231	?Amiiformes	1 centrum	AAS-Crocorama
UTA-AASM-232	Caudata indet.	1 vertebra	AAS-Crocorama
UTA-AASM-233	Osteichthyes indet.	1 centrum	AAS-Crocorama
UTA-AASM-234	Crocodyliformes indet.	1 tooth	AAS-Crocorama
UTA-AASM-235	Crocodyliformes indet.	tooth (long & thin)	AAS-Crocorama
UTA-AASM-236	Crocodyliformes indet.	baby croc tooth (short/stout)	AAS-Crocorama
UTA-AASM-237	Teleostei indet.	1 centrum	AAS-Crocorama
UTA-AASM-238	Teleostei indet.	2 vert centra	AAS-Crocorama
UTA-AASM-239	Anura indet.	1 proximal humerus	AAS-Crocorama
UTA-AASM-240	Crocodyliformes indet.	baby croc tooth (short/stout)	AAS-Crocorama
UTA-AASM-241	Crocodyliformes indet.	baby croc tooth (stout)	AAS-Crocorama
UTA-AASM-242	Osteichthyes indet.	sm tooth	AAS-Crocorama
UTA-AASM-243	Osteichthyes indet.	1 centrum	AAS-Crocorama
UTA-AASM-244	Crocodyliformes indet.	baby croc tooth	AAS-Crocorama
UTA-AASM-245	Crocodyliformes indet.	croc tooth (long/thin)	AAS-Crocorama
UTA-AASM-246	cf. *Lepidotes*	scale	AAS-Crocorama
UTA-AASM-247	Osteichthyes indet.	1 scale fragment	AAS-Crocorama
UTA-AASM-248	cf. *Lepidotes*	1 scale	AAS-Crocorama
UTA-AASM-249	Reptilia indet.	1 tooth	AAS-Dino quarry
UTA-AASM-250	Teleostei indet.	1 centrum	AAS-Dino quarry
UTA-AASM-251	cf. *Lepidotes*	1 scale	AAS-Crocorama
UTA-AASM-252	Crocodyliformes indet.	1 tooth	AAS-Crocorama

UTA-AASM-253	Osteichthyes indet.	1 tooth	AAS-Dino quarry
UTA-AASM-254	?Crocodyliformes	1 ?distal metatarsal	AAS-Crocorama
UTA-AASM-255	Pycnodontiformes indet.	1 palatal tooth	AAS-hillside
UTA-AASM-256	cf. *Lepidotes*	1 large scale	AAS-hillside
UTA-AASM-257	Crocodyliformes indet.	1 sm tooth	AAS-Crocorama
UTA-AASM-258	plant	Seed	AAS-Crocorama
UTA-AASM-259	Pycnodontiformes indet.	1 sm tooth	AAS-Crocorama
UTA-AASM-260	cf. Lepidotes	1 md scale	AAS-Crocorama
UTA-AASM-261	unidentified vertebrate	1 bone fragment	AAS-BFL
UTA-AASM-262	unidentified vertebrate	1 bone frag	AAS-BFL
UTA-AASM-263	Crocodyliformes indet.	1 sm tooth	AAS-Crocorama
UTA-AASM-264	Crocodyliformes indet.	1 sm thin tooth	AAS-Crocorama
UTA-AASM-265	cf. Lepidotes	1 md scale	AAS-Crocorama
UTA-AASM-266	unidentified vertebrate	2 bone frags (limbs?)	AAS-Crocorama
UTA-AASM-267	Pycnodontiformes indet.	1 sm tooth	AAS-Crocorama
UTA-AASM-268	unidentified vertebrate	scale?	AAS-Crocorama
UTA-AASM-269	unidentified vertebrate	1 partial ?fin spine; 2 bone fragments	AAS-Crocorama
UTA-AASM-270	Teleostei indet.	2 centra	AAS-Crocorama
UTA-AASM-271	plant?	Unknown	AAS-Crocorama
UTA-AASM-272	Amber	sm amber frag	AAS-BFL
UTA-AASM-273	Crocodyliformes indet.	sm croc tooth (2mm)	AAS-Crocorama
UTA-AASM-274	Crocodyliformes indet.	sm croc tooth (2mm)	AAS-Crocorama
UTA-AASM-275	cf. Lepidotes	?scale	AAS-Crocorama
UTA-AASM-276	amber	Amber	AAS-Crocorama
UTA-AASM-277	vertebrate indet	sm bone frag	AAS-Crocorama
UTA-AASM-278	Crocodyliformes indet.	sm croc tooth	AAS-Crocorama
UTA-AASM-279	Teleostei indet.	sm vert centrum	AAS-Crocorama
UTA-AASM-280	Pycnodontiformes indet.	3 teeth	AAS-Long Lake
UTA-AASM-281	vertebrate indet	bone fragment	AAS-Crocorama
UTA-AASM-282	Crocodyliformes indet.	sm croc tooth	AAS-Crocorama
UTA-AASM-283	Sauria indet.	1 centrum	AAS-Crocorama
UTA-AASM-284	plant	Seed	AAS-Crocorama
UTA-AASM-285	vertebrate indet	bone fragment	AAS-Crocorama
UTA-AASM-286	vertebrate indet	bone fragment	AAS-Crocorama
UTA-AASM-287	Teleostei indet.	1 centrum	AAS-Crocorama
UTA-AASM-288	vertebrate indet	bone frag (spine?)	AAS-Crocorama
UTA-AASM-289	amber (fire drop?)	amber with carbon inclusions (forest fire?)	AAS-Crocorama
UTA-AASM-290	amber	amber embedded in carbon	AAS-Crocorama
UTA-AASM-291	plant	plant -stem	AAS-Crocorama
UTA-AASM-292	plant	plant -stem	AAS-Crocorama

UTA-AASM-293	plant	plant -stem	AAS-Crocorama
UTA-AASM-294	vertebrate indet	limb bone frag?	AAS-Crocorama
UTA-AASM-295	amber	amber	AAS-Crocorama
UTA-AASM-296	plant	seed	AAS-Crocorama
UTA-AASM-297	plant	fragments	AAS-Crocorama
UTA-AASM-298	vertebrate indet	misc bone frag?	AAS-Crocorama
UTA-AASM-299	plant indet	misc seed frag?	AAS-Crocorama
UTA-AASM-300	?Amiidae	?coranoid tooth plate with complete teeth	AAS-Crocorama
UTA-AASM-301	Amber	amber (with one burned frag?)	AAS-Crocorama
UTA-AASM-302	plant?	unknown	AAS-Crocorama
UTA-AASM-303	invertebrate-trace indet (?)	possible nematode burrow?	AAS-Crocorama
UTA-AASM-304	Osteichthyes indet.	4 partial fin spines	BFL
UTA-AASM-305	?Osteichthyes (possibly shark)	1 centrum	AAS-Long Lake
UTA-AASM-306	?Elopomorpha	1 centrum	AAS-Long Lake
UTA-AASM-307	unidentified vertebrate	1 centrum	AAS-Long Lake
UTA-AASM-308	Osteichthyes indet.	1 centrum	AAS-Birds Fort (BFL)
UTA-AASM-309	Osteichthyes indet.	1 centrum	AAS-Birds Fort (BFL)
UTA-AASM-310	Osteichthyes indet.	1 centrum	AAS-Birds Fort (BFL)
UTA-AASM-311	Osteichthyes indet.	1 centrum	AAS-Birds Fort (BFL)
UTA-AASM-312	?Elopomorpha	1 centrum	AAS-Birds Fort (BFL)
UTA-AASM-313	Osteichthyes indet.	1 centrum	AAS-Birds Fort (BFL)
UTA-AASM-314	Osteichthyes indet.	1 centrum	AAS-Birds Fort (BFL)
UTA-AASM-315	Osteichthyes indet.	1 centrum	AAS-Birds Fort (BFL)
UTA-AASM-316	Osteichthyes indet.	1 centrum	AAS-Birds Fort (BFL)
UTA-AASM-317	Osteichthyes indet.	1 centrum	AAS-Birds Fort (BFL)
UTA-AASM-318	Osteichthyes indet.	1 centrum	AAS-Birds Fort (BFL)
UTA-AASM-319	Osteichthyes indet.	1 centrum	AAS-Birds Fort (BFL)
UTA-AASM-320	unidentified vertebrate	1 bone fragment (prezygopophysis?)	AAS-Birds Fort (BFL)
UTA-AASM-321	Osteichthyes indet.	1 centrum fragment	AAS-Birds Fort (BFL)
UTA-AASM-322	Crocodyliformes indet.	1 centrum	AAS-Birds Fort (BFL)
UTA-AASM-323	Crocodyliformes indet.	1 partial centrum	AAS-Birds Fort (BFL)
UTA-AASM-324	Crocodyliformes indet.	1 tooth	AAS-Crocorama peat
UTA-AASM-325	Crocodyliformes indet.	1 juvenile osteoderm	AAS-Crocorama peat
UTA-AASM-326	Crocodyliformes indet.	1 jaw fragment with complete tooth	AAS-Birds Fort (BFL)
UTA-AASM-327	Pycnodontiformes indet.	1 tooth	AAS-Croc Cove
UTA-AASM-328	Pycnodontiformes indet.	1 tooth	AAS-Croc Cove
UTA-AASM-329	Pycnodontiformes indet.	2 teeth	AAS-Hill West (siderite bed)
UTA-AASM-330	Crocodyliformes indet.	1 partial tooth	AAS-Hill West (siderite bed)
UTA-AASM-331	Crocodyliformes indet.	1 partial tooth	AAS-Birds Fort (BFL)
UTA-AASM-332	Crocodyliformes indet.	5 centra; 1 unidentified	AAS-Birds Fort (BFL)

UTA-AASM-333	?Sauria indet.	1 large neural arch	AAS-Birds Fort (BFL)
UTA-AASM-334	Crocodyliformes indet.	1 neural arch	AAS Crocorama East
UTA-AASM-335	Crocodyliformes indet.	1 complete caudal vertebra	AAS Dino Quarry
UTA-AASM-336	cf. Cretodus	1 tooth embedded in siderite	AAS Hill West (Siderite layer)
UTA-AASM-337	cf. Hybodus	1 cephalic spine	AAS Dino Quarry
Dinosauria (theropoda)			
UTA-AAST-001	*dromaeosaur*	partial tooth	AAS-Birds Fort (BFL)
UTA-AAST-002	*Acrocanthosaurs cf*	partial tooth	AAS
UTA-AAST-003	theropod ident.	Phalange	AAS
UTA-AAST-004	theropod ident.	misc limb shafts	AAS
UTA-AAST-005	theropod ident.	small claw	AAS-Nursery
UTA-AAST-006	theropod ident.	small tooth	AAS
UTA-AAST-007	*Acrocanthosaurs cf*	proximal partial claw	AAS-Birds Fort (BFL)
UTA-AAST-008	theropod ident.	partial tooth	AAS
UTA-AAST-009	theropod ident.	partial tooth (worn)	AAS-Dino-Quarry
UTA-AAST-010	theropod ident.	tooth (worn)	AAS-Dino-Quarry debris pile
UTA-AAST-011	theropod ident.	tooth (worn)	AAS-BFL
Dinosauria (ornithopoda)			
UTA-AASO-001	Ornithopoda (*Protohadros*)	partial right juvy dentary (posterior)	AAS
UTA-AASO-002	Ornithopoda (*Protohadros*)	Tooth	AAS
UTA-AASO-003	Ornithopoda (*Protohadros*)	Tooth	AAS
UTA-AASO-004	Ornithopoda (*Protohadros*)	Tooth	AAS-hill near Dino Quarry
UTA-AASO-005	Ornithopoda (*Protohadros*)	shed teeth (~20)	AAS-Birds Fort (BFL)
UTA-AASO-006	Ornithopoda (*Protohadros*)	shed teeth (~18)	AAS-hill; Dino Quarry
UTA-AASO-007	Ornithopoda (*Protohadros*)	shed teeth (2)	AAS-arena NW hill
UTA-AASO-008	Ornithopoda (*Protohadros*)	Scapula	AAS-Dino Quarry
UTA-AASO-009	Ornithopoda (*Protohadros*)	Coracoid	AAS-Dino Quarry
UTA-AASO-010	Ornithopoda (*Protohadros*)	prepubis	AAS-Dino Quarry
UTA-AASO-011	Ornithopoda (*Protohadros*)	ischium	AAS-Dino Quarry
UTA-AASO-012	Ornithopoda (*Protohadros*)	ilium	AAS-Dino Quarry
UTA-AASO-013	Ornithopoda (*Protohadros*)	rib	AAS-Dino Quarry
UTA-AASO-014	Ornithopoda (*Protohadros*)	rib	AAS-Dino Quarry
UTA-AASO-015	Ornithopoda (*Protohadros*)	rib	AAS-Dino Quarry
UTA-AASO-016	Ornithopoda (*Protohadros*)	rib	AAS-Dino Quarry

UTA-AASO-017	Ornithopoda (*Protohadros*)	partial prox rib (cervicals?)	AAS-Dino Quarry
UTA-AASO-018	Ornithopoda (*Protohadros*)	partial prox rib (cervicals?)	AAS-Dino Quarry
UTA-AASO-019	Ornithopoda (*Protohadros*)	partial prox rib	AAS-Dino Quarry
UTA-AASO-020	Ornithopoda (*Protohadros*)	partial prox rib	AAS-Dino Quarry
UTA-AASO-021	Ornithopoda (*Protohadros*)	partial rib shaft	AAS-Dino Quarry
UTA-AASO-022	Ornithopoda (*Protohadros*)	rib	AAS-Dino Quarry
UTA-AASO-023	Ornithopoda (*Protohadros*)	partial rib shaft	AAS-Dino Quarry
UTA-AASO-024	Ornithopoda (*Protohadros*)	partial rib shaft	AAS-Dino Quarry
UTA-AASO-025	Ornithopoda (*Protohadros*)	rib	AAS-Dino Quarry
UTA-AASO-026	Ornithopoda (*Protohadros*)	partial distal rib	AAS-Dino Quarry
UTA-AASO-027	Ornithopoda (*Protohadros*)	partial rib	AAS-Dino Quarry
UTA-AASO-028	Ornithopoda (*Protohadros*)	partial distal rib	AAS-Dino Quarry
UTA-AASO-029	Ornithopoda (*Protohadros*)	partial rib shaft	AAS-Dino Quarry
UTA-AASO-030	Ornithopoda (*Protohadros*)	partial prox rib	AAS-Dino Quarry
UTA-AASO-031	Ornithopoda (*Protohadros*)	unidentified (partial prox rib?/crania?)	AAS-Dino Quarry
UTA-AASO-032	Ornithopoda (*Protohadros*)	partial prox rib (near cervicals?)	AAS-Dino Quarry
UTA-AASO-033	Ornithopoda (*Protohadros*)	partial prox rib & shaft	AAS-Dino Quarry
UTA-AASO-034	Ornithopoda (*Protohadros*)	partial rib shaft	AAS-Dino Quarry
UTA-AASO-035	Ornithopoda (*Protohadros*)	partial distal rib shaft	AAS-Dino Quarry
UTA-AASO-036	Ornithopoda (*Protohadros*)	partial distal rib shaft	AAS-Dino Quarry
UTA-AASO-037	Ornithopoda (*Protohadros*)	partial prox rib?	AAS-Dino Quarry
UTA-AASO-038	Ornithopoda (*Protohadros*)	partial rib shaft	AAS-Dino Quarry
UTA-AASO-039	Ornithopoda (*Protohadros*)	partial prox rib?	AAS-Dino Quarry
UTA-AASO-040	Ornithopoda (*Protohadros*)	partial rib shaft in mudstone	AAS-Dino Quarry
UTA-AASO-041	Ornithopoda (*Protohadros*)	partial rib shaft in mudstone	AAS-Dino Quarry
UTA-AASO-042	Ornithopoda (*Protohadros*)	partial prox rib	AAS-Dino Quarry
UTA-AASO-043	Ornithopoda (*Protohadros*)	partial distal rib	AAS-Dino Quarry
UTA-AASO-044	Ornithopoda (*Protohadros*)	partial rib shaft	AAS-Dino Quarry
UTA-AASO-045	Ornithopoda (*Protohadros*)	partial rib shaft	AAS-Dino Quarry
UTA-AASO-046	Ornithopoda (*Protohadros*)	partial rib shaft	AAS-Dino Quarry
UTA-AASO-047	Ornithopoda (*Protohadros*)	partial rib	AAS-Dino Quarry
UTA-AASO-048	Ornithopoda (*Protohadros*)	partial rib (2 sections)	AAS-Dino Quarry
UTA-AASO-049	Ornithopoda (*Protohadros*)	partial distal rib	AAS-Dino Quarry

UTA-AASO-050	Ornithopoda (*Protohadros*)	partial proximal rib (good)	AAS-Dino Quarry
UTA-AASO-051	Ornithopoda (*Protohadros*)	partial rib shaft	AAS-Dino Quarry
UTA-AASO-052	Ornithopoda (*Protohadros*)	partial rib shaft	AAS-Dino Quarry
UTA-AASO-053	Ornithopoda (*Protohadros*)	partial rib shaft	AAS-Dino Quarry
UTA-AASO-054	Ornithopoda (*Protohadros*)	partial rib shaft	AAS-Dino Quarry
UTA-AASO-055	Ornithopoda (*Protohadros*)	partial rib shaft	AAS-Dino Quarry
UTA-AASO-056	Ornithopoda (*Protohadros*)	partial distal rib	AAS-Dino Quarry
UTA-AASO-057	Ornithopoda (*Protohadros*)	partial rib	AAS-Dino Quarry
UTA-AASO-058	Ornithopoda (*Protohadros*)	partial rib	AAS-Dino Quarry
UTA-AASO-059	Ornithopoda (*Protohadros*)	partial rib	AAS-Dino Quarry
UTA-AASO-060	Ornithopoda (*Protohadros*)	partial rib shaft	AAS-Dino Quarry
UTA-AASO-061	Ornithopoda (*Protohadros*)	partial rib shaft	AAS-Dino Quarry
UTA-AASO-062	Ornithopoda (*Protohadros*)	partial rib	AAS-Dino Quarry
UTA-AASO-063	Ornithopoda (*Protohadros*)	partial proximal rib	AAS-Dino Quarry
UTA-AASO-064	Ornithopoda (*Protohadros*)	partial rib	AAS-Dino Quarry
UTA-AASO-065	Ornithopoda (*Protohadros*)	partial rib	AAS-Dino Quarry
UTA-AASO-066	Ornithopoda (*Protohadros*)	partial rib	AAS-Dino Quarry
UTA-AASO-067	Ornithopoda (*Protohadros*)	partial rib	AAS-Dino Quarry
UTA-AASO-068	Ornithopoda (*Protohadros*)	partial rib	AAS-Dino Quarry
UTA-AASO-069	Ornithopoda (*Protohadros*)	partial rib	AAS-Dino Quarry
UTA-AASO-070	Ornithopoda (*Protohadros*)	partial rib	AAS-Dino Quarry
UTA-AASO-071	Ornithopoda (*Protohadros*)	partial rib	AAS-Dino Quarry
UTA-AASO-072	Ornithopoda (*Protohadros*)	partial rib	AAS-Dino Quarry
UTA-AASO-073	Ornithopoda (*Protohadros*)	partial proximal rib	AAS-Dino Quarry
UTA-AASO-074	Ornithopoda (*Protohadros*)	partial rib	AAS-Dino Quarry
UTA-AASO-075	Ornithopoda (*Protohadros*)	Dorsal rib (good)	AAS-Dino Quarry
UTA-AASO-076	Ornithopoda (*Protohadros*)	Misc rib fragments (in box)	AAS-Dino Quarry
UTA-AASO-077	Ornithopoda (*Protohadros*)	partial rib	AAS-Dino Quarry
UTA-AASO-078	Ornithopoda (*Protohadros*)	partial rib shaft	AAS-Dino Quarry
UTA-AASO-079	Ornithopoda (*Protohadros*)	partial rib-proximal	AAS-Dino Quarry
UTA-AASO-080	Ornithopoda (*Protohadros*)	partial rib	AAS-Dino Quarry
UTA-AASO-081	Ornithopoda (*Protohadros*)	partial rib	AAS-Dino Quarry
UTA-AASO-082	Ornithopoda (*Protohadros*)	partial rib-distal?	AAS-Dino Quarry

UTA-AASO-083	Ornithopoda (*Protohadros*)	partial rib shaft	AAS-Dino Quarry
UTA-AASO-084	Ornithopoda (*Protohadros*)	partial rib	AAS-Dino Quarry
UTA-AASO-085	Ornithopoda (*Protohadros*)	partial rib (3 parts: A-C)	AAS-Dino Quarry
UTA-AASO-086	Ornithopoda (*Protohadros*)	partial rib (thin)	AAS-Dino Quarry
UTA-AASO-087	Ornithopoda (*Protohadros*)	partial rib	AAS-Dino Quarry
UTA-AASO-088	Ornithopoda (*Protohadros*)	partial rib-distal	AAS-Dino Quarry
UTA-AASO-089	Ornithopoda (*Protohadros*)	partial rib	AAS-Croc creek
UTA-AASO- 090	Ornithopoda (*Protohadros*)	axis (excellent condition)	AAS-Dino Quarry
UTA-AASO- 091	Ornithopoda (*Protohadros*)	cervical (distorted w/slickenslides)	AAS-Dino Quarry
UTA-AASO- 092	Ornithopoda (*Protohadros*)	cervical arch	AAS-Dino Quarry
UTA-AASO- 093	Ornithopoda (*Protohadros*)	cervical centrum	AAS-Dino Quarry
UTA-AASO- 094	Ornithopoda (*Protohadros*)	partial cervical centrum	AAS-Dino Quarry
UTA-AASO- 095	Ornithopoda (*Protohadros*)	cervical (complete centrum, partial arch)	AAS-Dino Quarry
UTA-AASO- 096	Ornithopoda (*Protohadros*)	cervical centrum	AAS-Dino Quarry
UTA-AASO- 097	Ornithopoda (*Protohadros*)	cervical centrum w/partial arch	AAS-Dino Quarry
UTA-AASO- 098	Ornithopoda (*Protohadros*)	caudal (complete-good)	AAS-Dino Quarry
UTA-AASO- 099	Ornithopoda (*Protohadros*)	cervical centrum (weathered)	AAS-Dino Quarry
UTA-AASO- 100	Ornithopoda (*Protohadros*)	proximal caudal (complete-good)	AAS-Dino Quarry
UTA-AASO- 101	Ornithopoda (*Protohadros*)	dorsal (near complete: 3 parts)	AAS-Dino Quarry
UTA-AASO- 102	Ornithopoda (*Protohadros*)	caudal (near complete)	AAS-Dino Quarry
UTA-AASO- 103	Ornithopoda (*Protohadros*)	dorsal (partial; missing left trans)	AAS-Dino Quarry
UTA-AASO- 104	Ornithopoda (*Protohadros*)	dorsal (near complete-good/slickenslides)	AAS-Dino Quarry
UTA-AASO- 105	Ornithopoda (*Protohadros*)	dorsal centrum (puck)	AAS-Dino Quarry
UTA-AASO- 106	Ornithopoda (*Protohadros*)	dorsal centrum (puck)	AAS-Dino Quarry
UTA-AASO- 107	Ornithopoda (*Protohadros*)	caudal (complete centra and arch)	AAS-Dino Quarry
UTA-AASO- 108	Ornithopoda (*Protohadros*)	centra (partial-puck/poor)	AAS-Dino Quarry
UTA-AASO- 109	Ornithopoda (*Protohadros*)	centra (partial-puck)	AAS-Dino Quarry
UTA-AASO- 110	Ornithopoda (*Protohadros*)	centra (puck w/partial arch)	AAS-Dino Quarry
UTA-AASO- 111	Ornithopoda (*Protohadros*)	dorsal centrum (puck w/partial arch)	AAS-Dino Quarry
UTA-AASO- 112	Ornithopoda (*Protohadros*)	dorsal neural arch	AAS-Dino Quarry
UTA-AASO- 113	Ornithopoda (*Protohadros*)	caudal (partial-weathered/broken)	AAS-Dino Quarry
UTA-AASO- 114	Ornithopoda (*Protohadros*)	caudal (partial)	AAS-Dino Quarry
UTA-AASO- 115	Ornithopoda (*Protohadros*)	neural spine or transverse?	AAS-Dino Quarry

UTA-AASO- 116	Ornithopoda (*Protohadros*)	partial neural spine	AAS-Dino Quarry
UTA-AASO- 117	Ornithopoda (*Protohadros*)	partial neural arch	AAS-Dino Quarry
UTA-AASO- 118	Ornithopoda (*Protohadros*)	partial neural arch (weathered)	AAS-Dino Quarry
UTA-AASO- 119	Ornithopoda (*Protohadros*)	partial centrum (weathered puck)	AAS-Dino Quarry
UTA-AASO- 120	Ornithopoda (*Protohadros*)	neural arch (near complete)	AAS-Dino Quarry
UTA-AASO- 121	Ornithopoda (*Protohadros*)	partial neural arch (weathered)	AAS-Dino Quarry
UTA-AASO- 122	Ornithopoda (*Protohadros*)	small partial neural arch (broken)	AAS-Dino Quarry
UTA-AASO- 123	Ornithopoda (*Protohadros*)	partial neural spine or rib? (in mudstone)	AAS-Dino Quarry
UTA-AASO- 124	Ornithopoda (*Protohadros*)	misc fragments in box	AAS-Dino Quarry
UTA-AASO- 125	Ornithopoda (*Protohadros*)	partial femur (right proximal w/bite marks, ~21.6cm L/partial shaft)	AAS-Dino Quarry
UTA-AASO- 126	Ornithopoda (*Protohadros*)	partial fibula?	AAS-Dino Quarry
UTA-AASO- 127	Ornithopoda	sacral rib	AAS-Dino Quarry
UTA-AASO- 128	Ornithopoda	partial limb (unidentified)	AAS-Dino Quarry
UTA-AASO- 129	Ornithopoda	partial metatarsal (?)	AAS-Dino Quarry
UTA-AASO- 130	Ornithopoda	neural spine (partial)	AAS-Dino Quarry
UTA-AASO- 131	Ornithopoda	ossified tendons (misc in box)	AAS-Dino Quarry
UTA-AASO- 132	Ornithopoda	3 vertebrae (small/juvy?)	AAS-Birds Fort (BFL)
UTA-AASO- 133	Ornithopoda	small digit (toe)	AAS Dino Quarry
UTA-AASO- 134	Ornithopoda	small partial digit (?)	AAS Dino Hill
UTA-AASO- 135	Ornithopoda	small partial rib (?)	AAS Dino Quarry
UTA-AASO-136	Ornithopoda	small partial limb?	AAS field
UTA-AASO-137	Ornithopoda (*Protohadros*)	small partial juvy humerus (12cm)	Crocrama (12.8)
UTA-AASO-138	Ornithopoda	caudal vert (centrum)	AAS Hill (over Dino-Quarry)
UTA-AASO-139	Ornithopoda	caudal vert (partial neural arch/charcoal)	AAS Forest Fire Bed 1
UTA-AASO-140	Ornithopoda	partial exoccipital?	AAS-Dino Quarry
UTA-AASO-143	Ornithopoda	juvy humerus	AAS-Nursery
UTA-AASO- 147	Ornithopoda	partial vert in mud-matrix	AAS-Dino Quarry
UTA-AASO-148	Ornithopoda	partial juvy teeth (4 pieces)	AAS-Nursery (-17.3)
UTA-AASO-149	Ornithopoda	juvy humerus (122 mm L)	AAS-Nursery (22.8)
UTA-AASO-150	Ornithopoda	shed tooth (worn)	Dino-Quarry
UTA-AASO-151	Ornithopoda	femoral shaft frag	AAS- Crocorama (4.6)
UTA-AASO-152	Ornithopoda	femoral condyle frag	AAS- Crocorama (4.6)
UTA-AASO-153	Ornithopoda	juvy femoral condyle	AAS- Crocorama (4.7)
UTA-AASO-154	Ornithopoda	distal adult femur	AAS- Crocorama (-26.6)
UTA-AASO-155	Ornithopoda	juvenile ilium	AAS- Crocorama (??)
UTA-AASO-156	Ornithopoda	caudal neural spine	AAS- The Nursery (-14.6)
UTA-AASO-157	Ornithopoda	cervical neural arch	AAS-Crocorama (-12.8)
UTA-AASO-158	*Ornithopod*	1 juvenile ulna	AAS-Crocorama (13.10

UTA-AASO-159	*Ornithopoda*	1 juvenile ulna	AAS- Crocorama (-5.9)
UTA-AASO-160	*Ornithopoda*	1 tooth crown	AAS-Crocorama (-13.9)
UTA-AASO-161	*Ornithopoda*	1 complete juvenile dentary	AAS-Dino Quarry

Crocodyliforms

UTA-AASC-001	*Deltasuchus motherali*	osteoderm (cervical?)	AAS-Mr. Croc Site
UTA-AASC-002	*Deltasuchus motherali*	osteoderm (cervo-cranial?)	AAS-Mr. Croc Site
UTA-AASC-003	*Deltasuchus motherali*	osteoderm (cervo-cranial?)	AAS-Mr. Croc Site
UTA-AASC-004	*Deltasuchus motherali*	osteoderm (cervo-cranial?)	AAS-Mr. Croc Site
UTA-AASC-005	*Deltasuchus motherali*	osteoderm (cervo-2 peices?)	AAS-Mr. Croc Site
UTA-AASC-006	crocodyliform	misc (2 peices)	AAS-Mr. Croc Site
UTA-AASC-007	crocodyliform	misc (2 pieces-scute? & vert)	AAS-Mr. Croc Site
UTA-AASC-008	crocodyliform	misc (8 pieces-scutes?)	AAS-Mr. Croc Site
UTA-AASC-009	crocodyliform	misc (2 pieces-crania?)	AAS-Mr. Croc Site
UTA-AASC-010	crocodyliform	misc (2 pieces-crania?)	AAS-Mr. Croc Site
UTA-AASC-011	crocodyliform	misc (2 pieces)	AAS-Mr. Croc Site
UTA-AASC-012	crocodyliform	misc (9 pieces)	AAS-Mr. Croc Site
UTA-AASC-013	crocodyliform	misc (9 pieces)	AAS-Croc Cove
UTA-AASC-014	*Deltasuchus motherali*	osteoderm (cervo-dorso?; 2 peices)	AAS-Mr. Croc Site
UTA-AASC-015	*Deltasuchus motherali*	osteoderm (cervo-crania?; 3 peices)	AAS-Mr. Croc Site
UTA-AASC-016	*Deltasuchus motherali*	osteoderm (crania?)	AAS-Mr. Croc Site
UTA-AASC-017	*Deltasuchus motherali*	osteoderm	AAS-Mr. Croc Site
UTA-AASC-018	*Deltasuchus motherali*	misc (15 pieces)	AAS-Mr. Croc Site
UTA-AASC-019	*Deltasuchus motherali*	osteoderm (2 pieces)	AAS-Mr. Croc Site
UTA-AASC-020	*Deltasuchus motherali*	osteoderm (crania?)	AAS-Mr. Croc Site
UTA-AASC-021	*Deltasuchus motherali*	osteoderm (3 pieces)	AAS-Mr. Croc Site
UTA-AASC-022	*Deltasuchus motherali*	osteoderm (2 pieces)	AAS-Mr. Croc Site
UTA-AASC-023	*Deltasuchus motherali*	osteoderm (crania?)	AAS-Mr. Croc Site
UTA-AASC-024	*Deltasuchus motherali*	osteoderm (crania?)	AAS-Mr. Croc Site
UTA-AASC-025	*Deltasuchus motherali*	osteoderm	AAS-Mr. Croc Site
UTA-AASC-026	*Deltasuchus motherali*	misc (3 pieces)	AAS-Mr. Croc Site
UTA-AASC-027	*Deltasuchus motherali*	crania?	AAS-Mr. Croc Site
UTA-AASC-028	*Deltasuchus motherali*	crania?	AAS-Mr. Croc Site
UTA-AASC-029	*Deltasuchus motherali*	misc.	AAS-Mr. Croc Site
UTA-AASC-030	*Deltasuchus motherali*	vertebra	AAS-Mr. Croc Site
UTA-AASC-031	*Deltasuchus motherali*	partial limb	AAS-Mr. Croc Site
UTA-AASC-032	*Deltasuchus motherali*	vertebra	AAS-Croc Cove
UTA-AASC-033	*Deltasuchus motherali*	partial vertebra (centrum)	AAS-Mr. Croc Site
UTA-AASC-034	*Deltasuchus motherali*	partial limb (?)	AAS-Mr. Croc Site
UTA-AASC-035	*Deltasuchus motherali*	partial limb (?)	AAS-Mr. Croc Site

UTA-AASC-036	*Deltasuchus motherali*	partial vertebra (centrum)	AAS-Mr. Croc Site
UTA-AASC-037	*Deltasuchus motherali*	partial limb	AAS-Mr. Croc Site
UTA-AASC-038	*Deltasuchus motherali*	partial limbs	AAS-Mr. Croc Site
UTA-AASC-039	*Deltasuchus motherali*	partial vertebra (arch?)	AAS-Mr. Croc Site
UTA-AASC-040	*Deltasuchus motherali*	partial vertebra (centrum)	AAS-Mr. Croc Site
UTA-AASC-041	*Deltasuchus motherali*	partial limb	AAS-Mr. Croc Site
UTA-AASC-042	*Deltasuchus motherali*	partial limb	AAS-Mr. Croc Site
UTA-AASC-043	*Deltasuchus motherali*	caudal vertebra	AAS-Mr. Croc Site
UTA-AASC-044	*Deltasuchus motherali*	partial vertebra (centrum)	AAS-Mr. Croc Site
UTA-AASC-045	*Deltasuchus motherali*	partial limb bone	AAS-Mr. Croc Site
UTA-AASC-046	*Deltasuchus motherali*	partial limb bones (3)	AAS-Mr. Croc Site
UTA-AASC-047	*Deltasuchus motherali*	partial limb bone (digit-phalange)	AAS-Mr. Croc Site
UTA-AASC-048	*Deltasuchus motherali*	caudal vertebrae (2)	AAS-Mr. Croc Site
UTA-AASC-049	*Deltasuchus motherali*	partial limb bones (2)	AAS-Mr. Croc Site
UTA-AASC-050	*Deltasuchus motherali*	partial limb bone (large, sheared)	AAS- Croc Cove
UTA-AASC-051	crocodyliform	Tooth	AAS- Dino Quarry
UTA-AASC-052	crocodyliform	teeth (2)	AAS-Mr. Croc Site/Crocorama
UTA-AASC-053	crocodyliform	tooth	AAS-Croc Cove
UTA-AASC-054	crocodyliform	Tooth	AAS- Dino Quarry
UTA-AASC-055	crocodyliform	partial tooth	AAS- Mr Croc Site
UTA-AASC-056	crocodyliform	partial tooth	AAS- Mr Croc Site
UTA-AASC-057	crocodyliform	Tooth	AAS- Mr Croc Site
UTA-AASC-058	crocodyliform	Tooth	AAS- Mr Croc Site
UTA-AASC-059	crocodyliform	partial tooth	AAS- Mr Croc Site
UTA-AASC-060	crocodyliform	Tooth	AAS- Mr Croc Site
UTA-AASC-061	crocodyliform	Tooth	AAS- Mr Croc Site
UTA-AASC-062	crocodyliform	Tooth	AAS- Mr Croc Site
UTA-AASC-063	crocodyliform	small tooth	AAS-Birds Fort (BFL)
UTA-AASC-064	crocodyliform	Tooth	AAS-Birds Fort (BFL)
UTA-AASC-065	crocodyliform	small tooth	AAS-Birds Fort (BFL)
UTA-AASC-066	crocodyliform	small tooth	AAS-Birds Fort (BFL)
UTA-AASC-067	crocodyliform	small partial tooth	AAS-Birds Fort (BFL)
UTA-AASC-068	crocodyliform	small tooth	AAS-Birds Fort (BFL)
UTA-AASC-069	crocodyliform	small tooth	AAS-Birds Fort (BFL)
UTA-AASC-070	crocodyliform	small tooth	AAS-Birds Fort (BFL)
UTA-AASC-071	crocodyliform	partial tooth	AAS-Birds Fort (BFL)
UTA-AASC-072	crocodyliform	partial tooth (large)	AAS-Birds Fort (BFL)
UTA-AASC-073	crocodyliform	partial tooth	AAS-Birds Fort (BFL)
UTA-AASC-074	crocodyliform	partial tooth	AAS-Birds Fort (BFL)
UTA-AASC-075	crocodyliform	partial tooth	AAS-Birds Fort (BFL)
UTA-AASC-076	crocodyliform	partial tooth	AAS-Birds Fort (BFL)
UTA-AASC-077	crocodyliform	partial tooth	AAS-Birds Fort (BFL)

UTA-AASC-078	crocodyliform	Tooth	AAS-Birds Fort (BFL)
UTA-AASC-079	crocodyliform	Tooth	AAS-Birds Fort (BFL)
UTA-AASC-080	crocodyliform	Tooth	AAS-Birds Fort (BFL)
UTA-AASC-081	crocodyliform	Tooth	AAS-Birds Fort (BFL)
UTA-AASC-082	crocodyliform	Tooth	AAS-Birds Fort (BFL)
UTA-AASC-083	crocodyliform	Tooth	AAS-Birds Fort (BFL)
UTA-AASC-084	crocodyliform	Tooth	AAS-Birds Fort (BFL)
UTA-AASC-085	crocodyliform	Tooth	AAS-Birds Fort (BFL)
UTA-AASC-086	cf.	rounded tooth?	AAS-Birds Fort (BFL)
UTA-AASC-087	crocodyliform	small partial tooth	AAS-Birds Fort (BFL)
UTA-AASC-088	crocodyliform	small partial tooth (unusual morphos)	AAS-Birds Fort (BFL)
UTA-AASC-089	not croc	small partial tooth	AAS-Birds Fort (BFL)
UTA-AASC-090	crocodyliform	small partial tooth	AAS-Birds Fort (BFL)
UTA-AASC-091	crocodyliform	small partial 1/2 tooth	AAS-Birds Fort (BFL)
UTA-AASC-092	crocodyliform	tooth?	AAS-Birds Fort (BFL)
UTA-AASC-093	crocodyliform	large partial tooth	AAS-Birds Fort (BFL)
UTA-AASC-094	crocodyliform	partial tooth	AAS-Birds Fort (BFL)
UTA-AASC-095	crocodyliform	partial tooth (weathered)	AAS-Birds Fort (BFL)
UTA-AASC-096	crocodyliform	tooth	AAS- Dino Quarry
UTA-AASC-097	crocodyliform	rounded tooth	AAS- Mr Croc Site
UTA-AASC-098	crocodyliform	claw-ungual	AAS- Mr Croc Site
UTA-AASC-099	crocodyliform	misc (2limbs?-sacral rib?)	AAS-Dino Quarry
UTA-AASC-100	crocodyliform	partial jaw (2pieces-weathered)	AAS-Mr. Croc Site
UTA-AASC-101	crocodyliform	partial vertebra	AAS-Mr. Croc Site
UTA-AASC-102	crocodyliform	vertebra (weathered)	AAS-Mr. Croc Site
UTA-AASC-103	crocodyliform	misc (3 pieces-quadrate?)	AAS-Mr. Croc Site
UTA-AASC-104	crocodyliform	partial premaxilla	AAS-Mr. Croc Site
UTA-AASC-105	crocodyliform	misc (3 pieces)	AAS-Mr. Croc Site
UTA-AASC-106	crocodyliform	phalange	AAS-Mr. Croc Site
UTA-AASC-107	crocodyliform	phalange	AAS-Mr. Croc Site
UTA-AASC-108	crocodyliform	misc (8 pieces-frags)	AAS-Mr. Croc Site
UTA-AASC-109	crocodyliform	misc (9 pieces)	AAS-Mr. Croc Site
UTA-AASC-110	crocodyliform	partial jaw	AAS-Mr. Croc Site
UTA-AASC-111	crocodyliform	partial pelvis?	AAS-Mr. Croc Site
UTA-AASC-112	*Deltasuchus motherali*	teeth (2)	AAS-Cromorama (15.6)
UTA-AASC-113	crocodyliform	misc (3 pieces; misc, vert & digit?)	AAS-Mr. Croc Site
UTA-AASC-114	crocodyliform	misc (6 pieces)	AAS-Mr. Croc Site
UTA-AASC-115	crocodyliform	vertebra (centrum)	AAS-Mr. Croc Site
UTA-AASC-116	crocodyliform	teeth (3 small)	AAS-Birds Fort (BFL)
UTA-AASC-117	crocodyliform	tooth	AAS-Birds Fort (BFL)
UTA-AASC-118	crocodyliform	tooth	AAS-Birds Fort (BFL)

UTA-AASC-119	crocodyliform	tooth	AAS-Birds Fort (BFL)
UTA-AASC-120	crocodyliform	small tooth	AAS-Birds Fort (BFL)
UTA-AASC-121	crocodyliform	small tooth	AAS-Birds Fort (BFL)
UTA-AASC-122	crocodyliform	tooth (weathered)	AAS-Birds Fort (BFL)
UTA-AASC-123	crocodyliform	partial tooth (weathered)	AAS-Birds Fort (BFL)
UTA-AASC-124	crocodyliform	partial tooth (badly weathered)	AAS-Birds Fort (BFL)
UTA-AASC-125	crocodyliform	small tooth	AAS-Birds Fort (BFL)
UTA-AASC-126	crocodyliform	partial tooth (badly weathered)	AAS-Birds Fort (BFL)
UTA-AASC-127	crocodyliform	small tooth	AAS-Birds Fort (BFL)
UTA-AASC-128	crocodyliform	small tooth	AAS-Birds Fort (BFL)
UTA-AASC-129	crocodyliform	partial tooth	AAS-Birds Fort (BFL)
UTA-AASC-130	crocodyliform	tooth	AAS-Birds Fort (BFL)
UTA-AASC-131	crocodyliform	partial tooth	AAS-Birds Fort (BFL)
UTA-AASC-132	crocodyliform	partial tooth	AAS-Birds Fort (BFL)
UTA-AASC-133	crocodyliform	tooth	AAS-Birds Fort (BFL)
UTA-AASC-134	*Deltasuchus motherali*	partial rounded tooth	AAS-Crocorama (-1.6)
UTA-AASC-135	crocodyliform	partial tooth	AAS- Byrds Fort
UTA-AASC-136	*Deltasuchus motherali*	partial tooth	AAS- Crocorama (-6.7)
UTA-AASC-137	*Deltasuchus motherali*	small partial tooth	AAS- Crocorama (-10.3)
UTA-AASC-138	crocodyliform	partial tooth	AAS- Field
UTA-AASC-139	*Deltasuchus motherali*	small partial tooth	AAS- Crocorama (-9.6)
UTA-AASC-140	*Deltasuchus motherali*	partial tooth	AAS- Crocorama (-7.8)
UTA-AASC-141	*Deltasuchus motherali*	small tooth	AAS- Crocorama (3.6)
UTA-AASC-142	*Deltasuchus motherali*	weathered tooth	AAS- Crocorama (5.4)
UTA-AASC-143	*Deltasuchus motherali*	small tooth	AAS- Crocorama (1.-2)
UTA-AASC-144	*Deltasuchus motherali*	tooth	AAS- Crocorama (5.6)
UTA-AASC-145	*Deltasuchus motherali*	partial rounded tooth (?)	AAS- Crocorama (5.4)
UTA-AASC-146	*Deltasuchus motherali*	small tooth	AAS- Crocorama (-16.4)
UTA-AASC-147	*Deltasuchus motherali*	cracked tooth	AAS- Crocorama (-21.5)
UTA-AASC-148	*Deltasuchus motherali*	small tooth	AAS- Crocorama (-18.3)
UTA-AASC-149	*crocodyliform*	tooth	AAS- theropod site (west hill)
UTA-AASC-150	*Deltasuchus motherali*	small tooth	AAS-Crocorama?
UTA-AASC-151	*Deltasuchus motherali*	small tooth	AAS- Crocorama (8.6)
UTA-AASC-152	*Deltasuchus motherali*	small tooth	AAS- Crocorama (-1.8)
UTA-AASC-153	*Deltasuchus motherali*	tooth	AAS- Crocorama (-11.4)
UTA-AASC-154	*Deltasuchus motherali*	partial tooth	AAS- Crocorama (-4.8)
UTA-AASC-155	*Deltasuchus motherali*	small tooth	AAS- Crocorama (-8.3)
UTA-AASC-156	*Deltasuchus motherali*	tooth	AAS- Crocorama (screened)
UTA-AASC-157	*Deltasuchus motherali*	tooth	AAS- Crocorama (2.-7)
UTA-AASC-158	*Deltasuchus motherali*	tooth	AAS- Dino-Quarry (Coal bed)
UTA-AASC-159	*Deltasuchus motherali*	weathered tooth	AAS- Crocorama (-9.4)
UTA-AASC-160	*Deltasuchus motherali*	weathered partial tooth	AAS- Crocorama (-7.9)

UTA-AASC-161	*Deltasuchus motherali*	small tooth	AAS- Crocorama (6.10)
UTA-AASC-162	*Deltasuchus motherali*	micro- tooth	AAS- Crocorama (-15.5)
UTA-AASC-163	*Deltasuchus motherali*	partial tooth	AAS- Crocorama (Block A)
UTA-AASC-164	*Deltasuchus motherali*	curved tooth	AAS- Crocorama (-7.5)
UTA-AASC-165	*Deltasuchus motherali*	tooth	AAS- Crocorama (debris)
UTA-AASC-166	*Deltasuchus motherali*	small tooth	AAS- Crocorama (-1.-2)
UTA-AASC-167	*Deltasuchus motherali*	small partial tooth	AAS- Crocorama (-20.4)
UTA-AASC-168	*Deltasuchus motherali*	small tooth	AAS- Crocorama (-20.4)
UTA-AASC-169	*Deltasuchus motherali*	small partial tooth	AAS- Crocorama (-20.4)
UTA-AASC-170	*Deltasuchus motherali*	tooth	AAS- Dino-Quarry (-38.3)
UTA-AASC-171	*Deltasuchus motherali*	tooth	AAS- Crocorama (-18.3)
UTA-AASC-172	*Deltasuchus motherali*	tooth	AAS- Crocorama (-10.4)
UTA-AASC-173	*Deltasuchus motherali*	tooth	AAS- Crocorama (-2.5)
UTA-AASC-174	*Deltasuchus motherali*	partial tooth (eroded)	AAS- Crocorama (-18.5)
UTA-AASC-175	*Deltasuchus motherali*	tooth (rounded)	AAS- Crocorama (-15.5)
UTA-AASC-176	*Deltasuchus motherali*	partial tooth	AAS- Crocorama (2.8)
UTA-AASC-177	*Deltasuchus motherali*	partial tooth (large)	AAS- Crocorama (2.7)
UTA-AASC-178	*Deltasuchus motherali*	tooth (large)	AAS- Crocorama (-15.6)
UTA-AASC-179	*Deltasuchus motherali*	tooth (large/long)	AAS- Crocorama (-6.8)
UTA-AASC-180	*Deltasuchus motherali*	tooth (good pres)	AAS- Crocorama (-13.6)
UTA-AASC-181	*Deltasuchus motherali*	tooth (small)	AAS- Crocorama (-8.5)
UTA-AASC-182	*crocodyliform*	tooth (large, fish?)	AAS- Crocorama (-7.5)
UTA-AASC-183	*crocodyliform*	tooth	AAS- Crocorama (-15.5)
UTA-AASC-184	*Deltasuchus motherali*	tooth	AAS- Crocorama?
UTA-AASC-185	*Deltasuchus motherali*	tooth	AAS- Crocorama (-7.5)
UTA-AASC-186	*Deltasuchus motherali*	tooth	AAS- Crocorama (-11.8)
UTA-AASC-187	*Deltasuchus motherali*	tooth (round)	AAS- Crocorama (-8.8)
UTA-AASC-188	*Deltasuchus motherali*	tooth (large-eroded)	AAS- Crocorama (-8.6)
UTA-AASC-189	*Deltasuchus motherali*	tooth (large)	AAS- Crocorama (-3.7)
UTA-AASC-190	*Deltasuchus motherali*	tooth (small)	AAS- Crocorama (3.6)
UTA-AASC-191	*Deltasuchus motherali*	tooth (small)	AAS- Crocorama (-7.6)
UTA-AASC-192	*Deltasuchus motherali*	tooth	AAS- Crocorama ?
UTA-AASC-193	*Deltasuchus motherali*	tooth (med)	AAS- Crocorama (-3,5)
UTA-AASC-194	*Deltasuchus motherali*	tooth	AAS- Crocorama (-10,6)
UTA-AASC-195	*Deltasuchus motherali*	tooth (med)	AAS- Crocorama (-20,4)
UTA-AASC-196	*Deltasuchus motherali*	tooth (med/broken)	AAS- Crocorama (-10,7)
UTA-AASC-197	*Deltasuchus motherali*	osteoderm	AAS- Crocorama (10,0)
UTA-AASC-198	*Deltasuchus motherali*	misc bone	AAS- Crocorama (12,2)
UTA-AASC-199	*Deltasuchus motherali*	misc bone (spine?)	AAS- Crocorama (10,8)
UTA-AASC-200	*Deltasuchus motherali*	Ilium (left)	AAS- Crocorama (10,5)
UTA-AASC-201	*Deltasuchus motherali*	3 Misc sm bone (crania & rib?)	AAS- Crocorama (10,9)
UTA-AASC-202	*Deltasuchus motherali*	misc bones (3 peices, possible crania?)	AAS- Crocorama (11,6)

UTA-AASC-203	*Deltasuchus motherali*	limb bone	AAS- Crocorama (12.5)
UTA-AASC-204	*Deltasuchus motherali*	partial limb bone (?)	AAS- Crocorama (13.5)
UTA-AASC-205	*Deltasuchus motherali*	large partial limb bone (ulna-fibula?)	AAS- Crocorama (13.6)
UTA-AASC-206	*Deltasuchus motherali*	partial limb bone (?)	AAS- Crocorama (13.7)
UTA-AASC-207	*Deltasuchus motherali*	juvy dentary	AAS- Crocorama (14.6)
UTA-AASC-208	*Deltasuchus motherali*	Phalange (208a) & bassioccipital condyle (208b)	AAS- Crocorama (18.5)
UTA-AASC-209	*Deltasuchus motherali*	Phalange & small vert (centrum)	AAS- Crocorama (18.6)
UTA-AASC-210	*Deltasuchus motherali*	partial scute (adult/with peg)	AAS- Crocorama (8.4)
UTA-AASC-211	*Deltasuchus motherali*	partial distal scapula (broken)	AAS- Crocorama (8.4)
UTA-AASC-212	*Deltasuchus motherali*	Misc (distal caudal, 2 phalanges, & a tooth)	AAS- Crocorama (8.4)
UTA-AASC-213	*Deltasuchus motherali*	Misc (thin slivers//crania?// & a tooth)	AAS- Crocorama (8.4)
UTA-AASC-214	*Deltasuchus motherali*	Postorbital (left dorsal skull)	AAS- Crocorama (8.4)
UTA-AASC-215	*Deltasuchus motherali*	Two rib frags	AAS- Crocorama (8.4)
UTA-AASC-216	*Deltasuchus motherali*	Two rib frags	AAS- Crocorama (8.4)
UTA-AASC-217	*Deltasuchus motherali*	limb bone (radius?)	AAS- Crocorama (8.5)
UTA-AASC-218	*Deltasuchus motherali*	right quadrate	AAS- Crocorama (8.5)
UTA-AASC-219	*Deltasuchus motherali*	partial scapula/coracoid?	AAS- Crocorama (8.5)
UTA-AASC-220	*Deltasuchus motherali*	Misc frags (tooth & weird things)	AAS- Crocorama (8.5)
UTA-AASC-221	*Deltasuchus motherali*	11 Misc ribs & frags (rib frags & misc)	AAS- Crocorama (8.5)
UTA-AASC-222	*Deltasuchus motherali*	Misc frags (3 small pieces)	AAS- Crocorama (8.6)
UTA-AASC-223	*Deltasuchus motherali*	2 frags (ribs/crania?)	AAS- Crocorama (9.4)
UTA-AASC-224	*Deltasuchus motherali*	Left Surangular	AAS- Crocorama (9.4)
UTA-AASC-225	*Deltasuchus motherali*	Misc (5 pieces, ribs? & 1 phalange)	AAS- Crocorama (9.4)
UTA-AASC-226	*Deltasuchus motherali*	Misc (10 pieces, ribs? & 2 teeth)	AAS- Crocorama (9.6)
UTA-AASC-227	*Deltasuchus motherali*	osteoderm (crania?) & frags	AAS- Crocorama (9.6)
UTA-AASC-228	*Deltasuchus motherali*	jaw piece (tooth sockets) & crania frags	AAS- Crocorama (9.6)
UTA-AASC-229	*Deltasuchus motherali*	osteoderm, partial phalange & 2 frags	AAS- Crocorama (6.9)
UTA-AASC-230	*Deltasuchus motherali*	8 Misc Frags (crania?)	AAS- Crocorama (7.3)
UTA-AASC-231	*Deltasuchus motherali*	14 Misc Frags	AAS- Crocorama (7.3)
UTA-AASC-232	*Deltasuchus motherali*	Misc frags (crania?)	AAS- Crocorama (7.4)
UTA-AASC-233	*Deltasuchus motherali*	2 osteoderms	AAS- Crocorama (7.4)
UTA-AASC-234	*Deltasuchus motherali*	Osteoderm (large-dorsal)	AAS- Crocorama (7.4)
UTA-AASC-235	*Deltasuchus motherali*	Caudal vert	AAS- Crocorama (7.5)
UTA-AASC-236	*Deltasuchus motherali*	Neural spine-partial	AAS- Crocorama (7.5)
UTA-AASC-237	*Deltasuchus motherali*	premax (lft)	AAS- Crocorama (7.5)
UTA-AASC-238	*Deltasuchus motherali*	cervical rib & 2 misc pieces	AAS- Crocorama (7.5)
UTA-AASC-239	*Deltasuchus motherali*	limb bone	AAS- Crocorama (7.7)

UTA-AASC-240	*Deltasuchus motherali*	sm distal caudal	AAS- Crocorama (7.7)
UTA-AASC-241	*Deltasuchus motherali*	7 Misc: crania (?), 2 teeth, & frags	AAS- Crocorama (7.7)
UTA-AASC-242	*Deltasuchus motherali*	5 Misc: partial phalange & frags	AAS- Crocorama (7.7)
UTA-AASC-243	*Deltasuchus motherali*	4 Misc: partial jaw & frags	AAS- Crocorama (8.3)
UTA-AASC-244	*Deltasuchus motherali*	3 Misc: partial limb, tooth & rib frag?	AAS- Crocorama (8.3)
UTA-AASC-245	*Deltasuchus motherali*	6 Misc: 3 scutes, partial limb, & rib frags?	AAS- Crocorama (8.3)
UTA-AASC-246	*Deltasuchus motherali*	partial vert, centra (poor condition)	AAS- Crocorama (5.3)
UTA-AASC-247	*Deltasuchus motherali*	partial limb bone	AAS- Crocorama (5.3)
UTA-AASC-248	*Deltasuchus motherali*	jugal (and 8 frags)	AAS- Crocorama (5.3)
UTA-AASC-249	*Deltasuchus motherali*	caudal vert (near complete)	AAS- Crocorama (5.3)
UTA-AASC-250	*Deltasuchus motherali*	maxilla (partial right, & 2 frags)	AAS- Crocorama (5.4)
UTA-AASC-251	*Deltasuchus motherali*	maxilla (partial left)	AAS- Crocorama (5.4)
UTA-AASC-252	*Deltasuchus motherali*	partial rib & small limb (phalange)	AAS- Crocorama (5.4)
UTA-AASC-253	*Deltasuchus motherali*	small vert (centra)	AAS- Crocorama (5.4)
UTA-AASC-254	*Deltasuchus motherali*	7 Misc: 1 vert (centra), 1 tooth, 5 misc (copro & frags)	AAS- Crocorama (6.4)
UTA-AASC-255	*Deltasuchus motherali*	small dorsal osteoderm	AAS- Crocorama (5.8)
UTA-AASC-256	*Deltasuchus motherali*	left dentary (12.2cm L)	AAS- Crocorama (5.5)
UTA-AASC-257	*Deltasuchus motherali*	right dentary (~14cm L)	AAS- Crocorama (9.5)
UTA-AASC-258	*Deltasuchus motherali*	caudal vert	AAS- Crocorama (6.3)
UTA-AASC-259	*Deltasuchus motherali*	vert neural arch & 2 frags	AAS- Crocorama (6.4)
UTA-AASC-260	*Deltasuchus motherali*	caudal vert & partial phalange	AAS- Crocorama (6.4)
UTA-AASC-261	*Deltasuchus motherali*	Adult Atlas & 3 misc frags	AAS- Crocorama (6.4)
UTA-AASC-262	*Deltasuchus motherali*	partial crania (jaw?)	AAS- Crocorama (6.4)
UTA-AASC-263	*Deltasuchus motherali*	small tooth	AAS- Crocorama (6.5)
UTA-AASC-264	*Deltasuchus motherali*	med partial tooth	AAS- Crocorama (6.5)
UTA-AASC-265	*Deltasuchus motherali*	9 Misc thin frags	AAS- Crocorama (6.5)
UTA-AASC-266	*Deltasuchus motherali*	5 Misc small frags; (2 teeth, small vert)	AAS- Crocorama (6.5)
UTA-AASC-267	*Deltasuchus motherali*	cervical rib & 2 misc pieces (prox rib)	AAS- Crocorama (6.5)
UTA-AASC-268	*Deltasuchus motherali*	partial crania (2 pieces)	AAS- Crocorama (6.7)
UTA-AASC-269	*Deltasuchus motherali*	4 Misc pieces	AAS- Crocorama (6.5)
UTA-AASC-270	*Deltasuchus motherali*	tooth	AAS- Crocorama (6.5)
UTA-AASC-271	*Deltasuchus motherali*	phalange	AAS- Crocorama (6.5)
UTA-AASC-272	*Deltasuchus motherali*	8 Misc (2 worn teeth)	AAS- Crocorama (6.6)
UTA-AASC-273	*Deltasuchus motherali*	tooth	AAS- Crocorama (6.6)
UTA-AASC-274	*Deltasuchus motherali*	trace fossil (?)	AAS- Crocorama (6.10)
UTA-AASC-275	*Deltasuchus motherali*	vert centra (split)	AAS- Crocorama (1.6)
UTA-AASC-276	*Deltasuchus motherali*	osteoderm (dorsal)	AAS- Crocorama (2.5)
UTA-AASC-277	*Deltasuchus motherali*	small (3.5cm) prepubis (?)	AAS- Crocorama (2.8)

UTA-AASC-278	*Deltasuchus motherali*	caudal vert (nearly complete)	AAS- Crocorama (2.10)
UTA-AASC-279	*Deltasuchus motherali*	2 Misc pieces (long thin frags)	AAS- Crocorama (3.1)
UTA-AASC-280	*Deltasuchus motherali*	Axis (odontoid)	AAS- Crocorama (3.6)
UTA-AASC-281	*Deltasuchus motherali*	3 Misc (parietal? & cerv rib?)	AAS- Crocorama (3.6)
UTA-AASC-282	*Deltasuchus motherali*	tooth (partial-med size)	AAS- Crocorama (3.6)
UTA-AASC-283	*Deltasuchus motherali*	crania (?) & proximal rib	AAS- Crocorama (3.8)
UTA-AASC-284	*Deltasuchus motherali*	crania (2 pieces)	AAS- Crocorama (4.4)
UTA-AASC-285	*Deltasuchus motherali*	humerus (complete)	AAS- Crocorama (4.4)
UTA-AASC-286	*Deltasuchus motherali*	maxilla (partial-right)	AAS- Crocorama (4.4)
UTA-AASC-287	*Deltasuchus motherali*	left exoccipital	AAS- Crocorama (5.5)
UTA-AASC-288	*Deltasuchus motherali*	Crania	AAS- Crocorama (5.4)
UTA-AASC-289	*Deltasuchus motherali*	crania? & ribs? (8 sm pieces)	AAS- Crocorama (5.6)
UTA-AASC-290	*Deltasuchus motherali*	caudal vert (near complete)	AAS- Crocorama (4.6)
UTA-AASC-291	*Deltasuchus motherali*	4 Misc (ribs? or crania?)	AAS- Crocorama (4.4)
UTA-AASC-292	*Deltasuchus motherali*	limb bone (partial)	AAS- Crocorama (4.4)
UTA-AASC-293	*Deltasuchus motherali*	Axis- centra	AAS- Crocorama (4.6)
UTA-AASC-294	*Deltasuchus motherali*	Coronoid	AAS- Crocorama (4.6)
UTA-AASC-295	*Deltasuchus motherali*	Misc (scute frag)	AAS- Crocorama (4.7)
UTA-AASC-296	*Deltasuchus motherali*	cervical rib	AAS- Crocorama (4.7)
UTA-AASC-297	*Deltasuchus motherali*	2 Misc (thin pieces)	AAS- Crocorama (4.7)
UTA-AASC-298	*Deltasuchus motherali*	caudal vert	AAS- Crocorama (4.6)
UTA-AASC-299	*Deltasuchus motherali*	Tooth	AAS- Crocorama (4.6)
UTA-AASC-300	*Deltasuchus motherali*	tooth (small)	AAS- Crocorama (4.6)
UTA-AASC-301	crocodyliform	partial femora	Mr. Croc Site
UTA-AASC-302	*Deltasuchus motherali*	3 misc (2 thin frags & scute)	AAS- Crocorama (7.5)
UTA-AASC-303	*Deltasuchus motherali*	tooth (small)	AAS- Crocorama (-3.6)
UTA-AASC-304	*Deltasuchus motherali*	crania (juvy premax?)	AAS- Crocorama (-6.6)
UTA-AASC-305	*Deltasuchus motherali*	crania (left surangular/angular?)	AAS- Crocorama (-6.5)
UTA-AASC-306	*Deltasuchus motherali*	juvy dentary	AAS- Crocorama (-6.8)
UTA-AASC-307	*Deltasuchus motherali*	2 Misc (frags)	AAS- Crocorama (-8.3)
UTA-AASC-308	*Deltasuchus motherali*	Lacrimal	AAS- Crocorama (-7.5)
UTA-AASC-309	*Deltasuchus motherali*	Atlas (left-neural arch)	AAS- Crocorama (-7.5)
UTA-AASC-310	*Deltasuchus motherali*	Phalange	AAS- Crocorama (-7.7)
UTA-AASC-311	*Deltasuchus motherali*	basioccipital condyle	AAS- Crocorama (-8.6)
UTA-AASC-312	*Deltasuchus motherali*	crania (left prefrontal)	AAS- Crocorama (-8.6)
UTA-AASC-313	*Deltasuchus motherali*	4 Misc frags (partial tooth)	AAS- Crocorama (-12.6)
UTA-AASC-314	*Deltasuchus motherali*	Angular (?)-subadult	AAS- Crocorama (-9.3)
UTA-AASC-315	Deltasuchus motherali	juvenile radius	AAS-Crocorama (16.5)
UTA-AASC-316	*Deltasuchus motherali*	2 smal ribs	AAS- The Nursery (-15.3)

UTA-AASC-317	*Deltasuchus motherali*	Small tooth	AAS- The Nursery (-14.5)
UTA-AASC-318	*Deltasuchus motherali*	Med tooth	AAS- The Nursery (-14.5)
UTA-AASC-319	*Deltasuchus motherali*	small limb (ulna?-hooked)	AAS- The Nursery (-15.5)
UTA-AASC-320	*Deltasuchus motherali*	juvy cervical rib, (angular frag?) & sm bone frag	AAS- The Nursery (-16.5)
UTA-AASC-321	*Deltasuchus motherali*	small juvy ulna	AAS- The Nursery (-16.3)
UTA-AASC-322	*Deltasuchus motherali*	6 Misc (scutes, copro & sm bone frags)	AAS- The Nursery (-16.5)
UTA-AASC-323	*Deltasuchus motherali*	3 Misc (sm scute & sm bone frags)	AAS- The Nursery (-16.6)
UTA-AASC-324	*Deltasuchus motherali*	sm juvy coracoid (1 of 2, see #340)	AAS- The Nursery (-16.6)
UTA-AASC-325	*Deltasuchus motherali*	small juvy jaw (splenial and 2 frags)	AAS- The Nursery (-15.6)
UTA-AASC-326	*Deltasuchus motherali*	partial mandible (4 sockets/teeth broken at root)	AAS- Crocorama (5.4)
UTA-AASC-327	*Deltasuchus motherali*	partial crania (right nasal/& 1 frag)	AAS- Crocorama (4.4)
UTA-AASC-328	*Deltasuchus motherali*	partial crania (leftt nasal)	AAS- Crocorama (4.4)
UTA-AASC-329	*Deltasuchus motherali*	partial crania (sm~8cm)	AAS- Crocorama (5.4)
UTA-AASC-330	*Deltasuchus motherali*	partial crania (lg-18cm elongate)	AAS- Crocorama (4.4)
UTA-AASC-331	*Deltasuchus motherali*	ectopterygoid (left-sm-triangular w/sutures)	AAS- Crocorama (5.4)
UTA-AASC-332	*Deltasuchus motherali*	dorsal vert (near complete)	AAS- Crocorama (11.8)
Nursery (juvy crocs)			
UTA-AASC-333	*Deltasuchus motherali*	Crania ? (small~5.4cm w/knob)	AAS- Crocorama/Nursery (-16.7)
UTA-AASC-334	*Deltasuchus motherali*	partial juvy scute & limb	AAS- Nursery (-17.4)
UTA-AASC-335	*Deltasuchus motherali*	partial juvy femur (and misc)	AAS- Nursery (-17.4)
UTA-AASC-336	*Deltasuchus motherali*	small crania (surangular?)	AAS- Nursery (-19.5)
UTA-AASC-337	*Deltasuchus motherali*	small misc crania (6 pieces) & ribs	AAS- Nursery (-17.5)
UTA-AASC-338	*Deltasuchus motherali*	small crania (snout)	AAS- Nursery (-17.5)
UTA-AASC-339	*Deltasuchus motherali*	partial dorsal scute	AAS- Nursery (-18.3)
UTA-AASC-340	*Deltasuchus motherali*	juvy coracoid (~5.6cm)(1 of 2, see # 324)	AAS- Nursery (-18.3)
UTA-AASC-341	*Deltasuchus motherali*	2 small scutes (ventral/hex & dorsal/rect)	AAS- Nursery (-18.3)
UTA-AASC-342	*Deltasuchus motherali*	small (~5.4cm) scute (dorsal/rectangular)	AAS- Nursery (-18.3)
UTA-AASC-343	*Deltasuchus motherali*	small (~4cm) scute (dorsal/rectangular)	AAS- Nursery (-18.3)
UTA-AASC-344	*Deltasuchus motherali*	small (~2.6cm) scute (ventral/hex)(copro&misc)	AAS- Nursery (-18.3)
UTA-AASC-345	*Deltasuchus motherali*	small juvy ribs	AAS- Nursery (-18.6)
UTA-AASC-346	*Deltasuchus motherali*	small juvy jaw	AAS- Nursery (-19.3)
UTA-AASC-347	*Deltasuchus motherali*	small juvy misc	AAS- Nursery (-19.4)
UTA-AASC-348	*Deltasuchus motherali*	small juvy crania?	AAS- Nursery (-20.1)
UTA-AASC-349	*Deltasuchus motherali*	juvy crania (nares?)	AAS- Nursery (-20.2)
UTA-AASC-350	*Deltasuchus motherali*	juvy crania (braincase?)	AAS- Nursery (-20.2)
UTA-AASC-351	*Deltasuchus motherali*	cervical rib	AAS- Nursery (-20.2)

UTA-AASC-352	*Deltasuchus motherali*	sm (1.8cm) juvy vert centra	AAS- Nursery (-20.2)
UTA-AASC-353	*Deltasuchus motherali*	sm juvy misc (scute, rib & frags)	AAS- Nursery (-20.2)
UTA-AASC-354	*Deltasuchus motherali*	sm (~15.6cm) juvy jaw (dentary)	AAS- Nursery (-20.2)
UTA-AASC-355	*Deltasuchus motherali*	juvy angular, surangular	AAS- Nursery (-20.2)
UTA-AASC-356	*Deltasuchus motherali*	3 sm centra (1.6cm)	AAS- Nursery (-20.2)
UTA-AASC-357	*Deltasuchus motherali*	sm (~3.6cm) juvy scute (dorsal)	AAS- Nursery (-20.2)
UTA-AASC-358	*Deltasuchus motherali*	sm (~5.6cm) juvy scute (dorsal)	AAS- Nursery (-20.2)
UTA-AASC-359	*Deltasuchus motherali*	3 misc	AAS- Nursery (-20.2)
UTA-AASC-360	*Deltasuchus motherali*	juvy basioccipital	AAS- Nursery (-18.5)
UTA-AASC-361	*Deltasuchus motherali*	juvy scute (~4.6cm)/misc frags	AAS- Nursery (-18.5)
UTA-AASC-362	*Deltasuchus motherali*	misc juvy (frags)	AAS- Nursery (-20.5)
UTA-AASC-363	*Deltasuchus motherali*	misc juvy (2 ribs/frags)	AAS- Nursery (-20.5)
UTA-AASC-364	*Deltasuchus motherali*	juvy fibula (or radius?)	AAS- Nursery (-20.5)
UTA-AASC-365	*Deltasuchus motherali*	neural arch & frags	AAS- Nursery (-19.3)
UTA-AASC-366	*Deltasuchus motherali*	sm juvy scute (?)	AAS- Nursery (-21.5)
UTA-AASC-367	*Deltasuchus motherali*	juvy neural arch & transverse	AAS- Nursery (-20.4)
UTA-AASC-368	*Deltasuchus motherali*	juvy neural arch	AAS- Nursery (-20.4)
UTA-AASC-369	*Deltasuchus motherali*	sm juvy centra (~1.5cm) & frags	AAS- Nursery (-20.4)
UTA-AASC-370	*Deltasuchus motherali*	sm juvy post-dentary (angular/surangular)	AAS- Nursery (-21.1)
UTA-AASC-371	*Deltasuchus motherali*	juvy neural arch	AAS- Nursery (-21.1)
UTA-AASC-372	*Deltasuchus motherali*	juvy scute (~5.2cm)	AAS- Nursery (-21.1)
UTA-AASC-373	*Deltasuchus motherali*	juvy rib (~7.2cm)	AAS- Nursery (-20.3)
UTA-AASC-374	*Deltasuchus motherali*	2 juvy centra (~1.6cm)	AAS- Nursery (-20.3)
UTA-AASC-375	*Deltasuchus motherali*	4 juvy scutes (?)	AAS- Nursery (-20.3)
UTA-AASC-376	*Deltasuchus motherali*	juvy rib (5.6cm)	AAS- Nursery (-20.3)
UTA-AASC-377	*Deltasuchus motherali*	4 misc (scutes & crania)	AAS- Nursery (-20.3)
UTA-AASC-378	*Deltasuchus motherali*	juvy neural arch	AAS- Nursery (-21.3)
UTA-AASC-379	*Deltasuchus motherali*	2 juvy ribs	AAS- Nursery (-21.3)
UTA-AASC-380	*Deltasuchus motherali*	juvy neural arch & tooth	AAS- Nursery (-21.3)
UTA-AASC-381	*Deltasuchus motherali*	Misc frags	AAS- Nursery (-21.3)
UTA-AASC-382	*Deltasuchus motherali*	partial crania & misc frags	AAS- Nursery (-22.3)
UTA-AASC-383	*Deltasuchus motherali*	juvy neural arch	AAS- Nursery (-22.2)
UTA-AASC-384	*Deltasuchus motherali*	2 juvy vert centra	AAS- Nursery (-21.2)
UTA-AASC-385	*Deltasuchus motherali*	sm (4.5cm) juvy scute (dorsal)	AAS- Nursery (-21.2)
UTA-AASC-386	*Deltasuchus motherali*	sm (2.5cm) juvy scute (ventral)	AAS- Nursery (-21.2)
UTA-AASC-387	*Deltasuchus motherali*	Quadrate-juvy (Misc frags-crania/ribs?)	AAS- Nursery (-21.2)
UTA-AASC-388	?Ichthyodectiform	fin spine; coprolite; fragments	AAS- Nursery (-21.2)
UTA-AASC-389	*Deltasuchus motherali*	Juvy Crania-partial palatine & maxilla	AAS- Nursery (-21.2)

UTA-AASC-390	*Deltasuchus motherali*	Crania-partial juvy maxilla	AAS- Nursery (-21.2)
UTA-AASC-391	*Deltasuchus motherali*	Misc (scute frags)	AAS- Nursery (-21.2)
UTA-AASC-392	*Deltasuchus motherali*	juvy neural arch	AAS- Nursery (-22.2)
UTA-AASC-393	*Deltasuchus motherali*	juvy centra	AAS- Nursery (-22.1)
UTA-AASC-394	*Deltasuchus motherali*	2 juvy scutes (ventral)	AAS- Nursery (-22.1)
UTA-AASC-395	*Deltasuchus motherali*	2 juvy centra	AAS- Nursery (-22.4)
UTA-AASC-396	*Deltasuchus motherali*	juvy scute (ventral)	AAS- Nursery (-22.4)
UTA-AASC-397	*Deltasuchus motherali*	misc	AAS- Nursery (-22.4)
UTA-AASC-398	*Deltasuchus motherali*	juvy centrum	AAS- Nursery (-23.4)
UTA-AASC-399	*Deltasuchus motherali*	juvy neural arch	AAS- Nursery (-23.4)
UTA-AASC-400	*Deltasuchus motherali*	juvy neural arch & transverse	AAS- Nursery (-25.5)
UTA-AASC-401	*Deltasuchus motherali*	partial juvy neural arch	AAS- Nursery (-25.5)
UTA-AASC-402	*Deltasuchus motherali*	partial juvy post dentary	AAS- Nursery (-25.5)
UTA-AASC-403	*Deltasuchus motherali*	phalange	AAS- Crocorama (4.4)
UTA-AASC-404	*Deltasuchus motherali*	maxilla (left)	AAS- Crocorama (5.4)
UTA-AASC-405	*Deltasuchus motherali*	ectopterygoid (right)	AAS- Crocorama (5.4)
UTA-AASC-406	*Deltasuchus motherali*	right exocippital	AAS- Crocorama (5.4)
UTA-AASC-407	*Deltasuchus motherali*	juvy scute (~5.5cm)	AAS- Nursery (-22.5)
UTA-AASC-408	*Deltasuchus motherali*	juvy scute (~5.5cm)	AAS- Nursery (-23.5)
UTA-AASC-409	*Deltasuchus motherali*	juvy right frontal (~5cm)	AAS- Crocorama (11.9)
UTA-AASC-410	*Deltasuchus motherali*	sm croc (?) limb bone (partial shaft)	AAS- Crocorama (5.4)
UTA-AASC-412	*Deltasuchus motherali*	1 sm croc (?) vert	AAS- Crocorama (-5.9)
UTA-AASC-413	*Deltasuchus motherali*	1 sm odd croc (?) bone (triangular shape)	AAS- Crocorama (-5.9)
UTA-AASC-414	*Deltasuchus motherali*	basioccipital condyle (adult)	AAS- Crocorama (5.3)
UTA-AASC-415	*Deltasuchus motherali*	adult phalange	AAS- Crocorama (8.5)
UTA-AASC-416	*Deltasuchus motherali*	vert centrum	AAS- Crocorama (2.5)
UTA-AASC-417	*Deltasuchus motherali*	limb shaft	AAS- Crocorama (2.6)
UTA-AASC-418	*Deltasuchus motherali*	vert centrum	AAS- Crocorama (2.6)
UTA-AASC-419	*Deltasuchus motherali*	Atlas (partial right Neural arch)	AAS- Crocorama (-2.9)
UTA-AASC-420	*Deltasuchus motherali*	sm limb bone	AAS- Crocorama (-21.5)
UTA-AASC-421	*Deltasuchus motherali*	sm vert (~1cm)	AAS- Crocorama (-1.8)
UTA-AASC-422	*Deltasuchus motherali*	3 misc (limb shaft, seed? & copro?)	AAS- Crocorama (-15.5)
UTA-AASC-423	*Deltasuchus motherali*	sm vert	AAS- Crocorama (-16.6)
UTA-AASC-424	*Deltasuchus motherali*	tooth plate?	AAS- Crocorama (-16.6)
UTA-AASC-425	*Deltasuchus motherali*	misc	AAS- Crocorama (-16.5)
UTA-AASC-426	*Deltasuchus motherali*	large adult tooth (~6cm)	AAS- Crocorama (-5.5)
UTA-AASC-427	*Deltasuchus motherali*	small limb or rib, & proximal process	AAS- Crocorama (6.10)
UTA-AASC-428	*Deltasuchus motherali*	small juvy centra	AAS- Dino-Quarry
UTA-AASC-429	*Deltasuchus motherali*	partial left quadrate	AAS-Crocorama (8.5)

UTA-AASC-430	*Deltasuchus motherali*	partial left spleenial (inner jaw)-sub adult	AAS-Crocorama (-5.5)
UTA-AASC-431	*Deltasuchus motherali*	Right Squamosal-juvy	AAS-Crocorama (15.8)
UTA-AASC-432	*Deltasuchus motherali*	pterygoid (right)	AAS-Crocorama (10.5)
UTA-AASC-433	*Deltasuchus motherali*	juvy crania?	AAS-Crocorama (-12.7)
UTA-AASC-434	*Deltasuchus motherali*	sm juvy verts (~1cm)	AAS-Crocorama (-6.8)
UTA-AASC-435	*Deltasuchus motherali*	sm misc (juvy?)	AAS-Crocorama (-22.5)
UTA-AASC-436	*Deltasuchus motherali*	specimen removed from collection (Missidentified)	AAS-Crocorama (12.8)
UTA-AASC-437	*Deltasuchus motherali*	2 misc (frag & vert centra)	AAS-Crocorama (7.10)
UTA-AASC-438	*Deltasuchus motherali*	juvy right maxilla	AAS-Crocorama (13.10)
UTA-AASC-439	*Deltasuchus motherali*	bassioccipital condyle	AAS-Crocorama (18.5)
UTA-AASC-440	*Deltasuchus motherali*	left squamosal	AAS-Crocorama (13.10)
UTA-AASC-441	*Deltasuchus motherali*	Scute	AAS-Crocorama (-12.9)
UTA-AASC-443	*Deltasuchus motherali*	juvy premax-max	AAS-Crocorama (-7.2)
UTA-AASC-444	*Deltasuchus motherali*	juvy right femur	AAS-Mutant Turtle site
UTA-AASC-445	*Deltasuchus motherali*	squamosal (right)	AAS-Crocorama (8.4)
UTA-AASC-446	*Deltasuchus motherali*	crania (sm element)	AAS-Crocorama (-3.7)
UTA-AASC-447	*Deltasuchus motherali*	crania (ectopterygoid)	AAS-Crocorama (-20.6)
UTA-AASC-448	*Deltasuchus motherali*	left premaxilla (adult)	AAS-Crocorama (5.5)
UTA-AASC-449	*Deltasuchus motherali*	crania (sm misc)	AAS-Mr Croc Site
UTA-AASC-450	*Deltasuchus motherali*	dentary (juvy)	AAS-Crocorama (??)
UTA-AASC-451	*Deltasuchus motherali*	left transverse process	AAS-Crocorama (10.5)
UTA-AASC-452	*Deltasuchus motherali*	cervical centrum	AAS-Crocorama (4.5)
UTA-AASC-453	*Deltasuchus motherali*	juvy cervical (atlas)	AAS-Crocorama (4.5)
UTA-AASC-454	*Deltasuchus motherali*	Phalange	AAS-Crocorama (4.5)
UTA-AASC-455	*Deltasuchus motherali*	phalange	AAS-Crocorama (4.5)
UTA-AASC-456	*Deltasuchus motherali*	juvy cervical (atlas)	AAS-Crocorama (4.5)
UTA-AASC-457	*Deltasuchus motherali*	juvenile/subadult femur (left)	Crocorama East (28, 6)

Chelonia

UTA-AASTL-001	unnamed Chelonian	large turtle shell (~20cm-bitten?)	AAS-Turtle Buffet (-10.8)
UTA-AASTL-002	unnamed Chelonian	large turtle shell (~15cm-bitten?)	AAS-Turtle Buffet (-10.8)
UTA-AASTL-003	unnamed Chelonian	turtle shell (~14cm-bitten?)	AAS-Turtle Buffet (-10.8)
UTA-AASTL-004	unnamed Chelonian	turtle plastron (~15cm, curved)	AAS-Turtle Buffet (-10.8)
UTA-AASTL-005	unnamed Chelonian	turtle shell (~11cm, bitten)	AAS-Turtle Buffet (-5.3)
UTA-AASTL-006	unnamed Chelonian	turtle shell (~11cm, bitten)	AAS-Turtle Buffet (-3.7)
UTA-AASTL-007	unnamed Chelonian	Lg thin & flat turtle carapace (~20cm, bitten)	AAS-Turtle Buffet (-3.9)
UTA-AASTL-008	unnamed Chelonian	turtle shell (~10cm/curved edge)	AAS-Turtle Buffet (-10.8)
UTA-AASTL-009	unnamed Chelonian	turtle shell (~11.5cm, bitten)	AAS-Turtle Buffet (-3.9)
UTA-AASTL-010	unnamed Chelonian	turtle shell (~10cm)	AAS-Turtle Buffet (-3.9)

UTA-AASTL-011	unnamed Chelonian	thin turtle shell (~10cm, rectangular, w bites/marks)	AAS-Turtle Buffet/Nursery(-14.6)
UTA-AASTL-012	unnamed Chelonian	turtle carapace (~17cm, curved) & misc frags	AAS-Turtle Buffet (-10.8)
UTA-AASTL-013	unnamed Chelonian	turtle shell (~11cm, thin plastron?)	AAS-Turtle Buffet (-10.8)
UTA-AASTL-014	unnamed Chelonian	turtle carapace (~8cm)	AAS-Turtle Buffet (-10.8)
UTA-AASTL-015	unnamed Chelonian	turtle carapace (~7cm, triangular)	AAS-Turtle Buffet (-10.8)
UTA-AASTL-016	unnamed Chelonian	sm turtle shell frag (~6cm)	AAS-Turtle Buffet (-10.8)
UTA-AASTL-017	unnamed Chelonian	sm turtle vert (~2.5cm)	AAS-Turtle Buffet (-10.8)
UTA-AASTL-018	unnamed Chelonian	turtle carapace (~7cm, bitten/bent)	AAS-Turtle Buffet (-10.8)
UTA-AASTL-019	unnamed Chelonian	turtle carapace	AAS-Turtle Buffet (-10.8)
UTA-AASTL-020	unnamed Chelonian	sm turtle carapace (jagged breaks)	AAS-Turtle Buffet (-10.8)
UTA-AASTL-021	unnamed Chelonian	sm turtle carapace (broken/punctured?)	AAS-Turtle Buffet (-4.8)
UTA-AASTL-022	unnamed Chelonian	sm turtle carapace (curved edge)	AAS-Turtle Buffet (-4.8)
UTA-AASTL-023	unnamed Chelonian	turtle carapace (curved edge)	AAS-Turtle Buffet (-10.3)
UTA-AASTL-024	unnamed Chelonian	turtle shell (bitten)-surface collect	AAS hillside
UTA-AASTL-025	unnamed Chelonian	turtle shell (~9cm/triangular edge)	AAS-Turtle Buffet (-10.8)
UTA-AASTL-026	unnamed Chelonian (?)	small rib	AAS-Turtle Buffet (2.8)
UTA-AASTL-027	unnamed Chelonian (?)	small shell frag	AAS-Crocorama (15.9)
UTA-AASTL-028	unnamed Chelonian (?)	small vert	AAS-Crocorama (15.9)
UTA-AASTL-029	unnamed Chelonian (?)	turtle shell with bite marks (unpublished)	AAS-Crocorama (-7.9)
UTA-AASTL-030	cf. *Helopanoplia* sp.	2 ?costal fragments; 1 shell fragment	AAS-surface-no other data
UTA-AASTL-031	unnamed Chelonian	jaw (mandible-dentary)	AAS-Crocorama (no other data)

AAS Flying Turtle

UTA-AASTL-032	unnamed Chelonian	Turtle carapace	AAS-Flying Turtle Site
UTA-AASTL-033	unnamed Chelonian	Turtle carapace	AAS-Flying Turtle Site
UTA-AASTL-034	unnamed Chelonian	Turtle carapace	AAS-Flying Turtle Site
UTA-AASTL-035	unnamed Chelonian	Turtle carapace	AAS-Flying Turtle Site
UTA-AASTL-036	unnamed Chelonian	Turtle carapace	AAS-Flying Turtle Site
UTA-AASTL-037	unnamed Chelonian	Turtle carapace	AAS-Flying Turtle Site
UTA-AASTL-037	unnamed Chelonian	Turtle carapace	AAS-Flying Turtle Site
UTA-AASTL-038	unnamed Chelonian	Turtle carapace	AAS-Flying Turtle Site
UTA-AASTL-039	unnamed Chelonian	Turtle carapace	AAS-Flying Turtle Site
UTA-AASTL-040	unnamed Chelonian	Turtle carapace	AAS-Flying Turtle Site
UTA-AASTL-041	unnamed Chelonian	Turtle plastron	AAS-Flying Turtle Site
UTA-AASTL-042	unnamed Chelonian	Turtle plastron	AAS-Flying Turtle Site
UTA-AASTL-043	unnamed Chelonian	Turtle plastron	AAS-Flying Turtle Site
UTA-AASTL-044	unnamed Chelonian	Turtle plastron	AAS-Flying Turtle Site
UTA-AASTL-045	unnamed Chelonian	Turtle plastron	AAS-Flying Turtle Site

UTA-AASTL-046	unnamed Chelonian	Turtle plastron	AAS-Flying Turtle Site
UTA-AASTL-047	unnamed Chelonian	Turtle plastron	AAS-Flying Turtle Site
UTA-AASTL-048	unnamed Chelonian	Scapula	AAS-Flying Turtle Site
UTA-AASTL-049	unnamed Chelonian	limb bone	AAS-Flying Turtle Site
UTA-AASTL-050	unnamed Chelonian	crania (near complete skull)	AAS-Flying Turtle Site
UTA-AASTL-051	unnamed Chelonian	vertebrae (cervical)	AAS-Flying Turtle Site
UTA-AASTL-052	unnamed Chelonian	vertebrae (caudal)	AAS-Flying Turtle Site
UTA-AASTL-053	unnamed Chelonian	pelvic material	AAS-Flying Turtle Site
UTA-AASTL-054	unnamed Chelonian	limb bone	AAS-Flying Turtle Site
UTA-AASTL-055	unnamed Chelonian	limb bone	AAS-Flying Turtle Site

AAS Coprolites

UTA-AASCP-001	Reptile (crocodyliform)	crocodyliform -spiral	AAS-Crocorama (8.4)
UTA-AASCP-002	Reptile (crocodyliform)	crocodyliform -spiral	AAS-Crocorama (2.5)
UTA-AASCP-003	Reptilian (dinosaur)	scroll-curved	AAS-Crocorama (3.6)
UTA-AASCP-004	Reptile (possible dino)	scroll-possible dinosaur	AAS-hillside
UTA-AASCP-005	Reptilian (dinosauria)	lg copro with gastropod & plant inclusion	AAS-hillside
UTA-AASCP-006	Reptilian (scroll)	curved scroll	AAS-Crocorama (-6. 7)
UTA-AASCP-007	Reptile (crocodyliform)	colonite-intestinal tract	AAS-hillside
UTA-AASCP-008	Reptilian (scroll)	scroll-cylindrical	AAS-hillside
UTA-AASCP-009	Reptilian (dinosauria)	ovoid-dinosaur?	AAS-hillside
UTA-AASCP-010	Reptilian (scroll)	scroll-cylindrical	AAS-hillside
UTA-AASCP-011	Reptilian (scroll)	scroll-sprial	AAS-Crocorama (2.5)
UTA-AASCP-012	Reptilian (scroll)	scroll-sprial	AAS-Crocorama (-10.4)
UTA-AASCP-013	Shark	possible inclusions	AAS-hillside
UTA-AASCP-014	crab pellets	multiple pellets in sand	AAS-field
UTA-AASCP-015	Reptilian (cone)	conical frag (incomplete)	AAS-Crocorama (-10.4)
UTA-AASCP-016	Reptile (crocodyliform)	small -cylidrical	AAS-Crocorama (-10.5)
UTA-AASCP-017	Reptile (crocodyliform)	small -conical	AAS-Crocorama (-8.6)
UTA-AASCP-018	Reptile (crocodyliform)	small -conical	AAS-Crocorama (-15.5)
UTA-AASCP-019	Reptile (crocodyliform)	Lg –curved	AAS-Crocorama (-6.4)
UTA-AASCP-020	Reptile (crocodyliform)	Med –conical	AAS-Crocorama (5.6)
UTA-AASCP-021	Reptile (crocodyliform)	Partial scroll	AAS-Crocorama (6.10)
UTA-AASCP-022	Reptile (crocodyliform)	partial scroll	AAS-Crocorama (6.10)
UTA-AASCP-023	Reptile (crocodyliform)	scroll	AAS-Crocorama (-12.7)
UTA-AASCP-024	Reptilian scroll (crocodyliform)	lg partial scroll	AAS-Crocorama (6.10)
UTA-AASCP-025	Reptilian (crocodyliform)	artial scroll/spiral	AAS-Crocorama (10.5)
UTA-AASCP-026	Reptilian (crocodyliform)	teardrop	AAS-Crocorama (4.6)
UTA-AASCP-027	Reptilian (crocodyliform)	partial sroll	AAS-Crocorama (4.7)

UTA-AASCP-028	Reptilian (crocodyliform)	lg partial scroll	AAS-Turtle Buffet (-10.8)
UTA-AASCP-029	Reptilian scroll (crocodyliform)	partial scroll	AAS-Turtle Buffet (-12.8)
UTA-AASCP-030	Reptilian scroll (crocodyliform)	partial scroll	AAS-Turtle Buffet (-4.8)
UTA-AASCP-031	Reptilian scroll (crocodyliform)	partial scroll	AAS-Turtle Buffet (25.10)
UTA-AASCP-032	Reptilian scroll (crocodyliform)	partial scroll	AAS-Turtle Buffet (18.13)
UTA-AASCP-033	Reptilian scroll (crocodyliform)	partial scroll	AAS-Turtle Buffet (-4.8)
UTA-AASCP-034	Reptilian scroll (crocodyliform)	partial scroll	AAS-Crocorama (6.5)
UTA-AASCP-035	Reptilian sroll (crocodyliform)	partial scroll	AAS-Crocorama (-5.8)
UTA-AASCP-036	Reptilian scroll (crocodyliform)	partial scroll	AAS-Turtle Buffet (-8.10)
UTA-AASCP-037	Reptilian scroll (crocodyliform)	lg partial scroll	AAS-Turtle Buffet (-4.9)
UTA-AASCP-038	Reptilian scroll (crocodyliform)	partial scroll	AAS-Turtle Buffet (-6.10)
UTA-AASCP-039	Reptilian scroll (crocodyliform)	partial scroll	AAS-Turtle Buffet (20.6)
UTA-AASCP-040	Reptilian (crocodyliform?)	teardrop	AAS-Crocorama (8.6)
UTA-AASCP-041	Reptilian (crocodyliform?)	teardrop	AAS-Crocorama (5.5)
UTA-AASCP-042	Reptilian scroll (crocdyliform)	partial scroll	AAS-Crocorama (15.10)
UTA-AASCP-043	Reptilian scroll (crocodyliform)	partial scroll	AAS-Turtle Buffet (-8.12)
UTA-AASCP-044	Reptilian scroll (crocodyliform)	spiral	AAS-Turtle Buffet (11.8)
UTA-AASCP-045	Reptilian scroll (crocodyliform)	spiral/scroll	AAS-Turtle Buffet (20.6)
UTA-AASCP-046	Shark (Hybodus?)	sm partial spiral	AAS hillside
UTA-AASCP-047	Shark (Hybodus?)	partial spiral	AAS-Nursery (-22.4)
UTA-AASCP-048	Shark (Hybodus?)	sm partial spiral	AAS-hillside/field
UTA-AASCP-049	Reptilian scroll (crocodyliform)	scroll	AAS-Turtle Buffet (-4.10)
UTA-AASCP-050	Reptilian scroll (crocodyliform)	ovoid	AAS-Turtle Buffet (-10.8)
UTA-AASCP-051	Reptilian scroll (crocodyliform)	scroll	AAS-Crocorama (-9.3)
UTA-AASCP-052	Shark (Hybodus?)	partial scroll	AAS hillside
UTA-AASCP-053	Reptilian (crocodyliform)	teardrop	AAS-Crocorama (2.5)
UTA-AASCP-056	Reptilian scroll (crocodyliform)	partial scroll	AAS-Nursery (-21.6)
UTA-AASCP-057	Reptilian scroll (crocodyliform)	partial scroll	AAS Nursery (-21.3)
UTA-AASCP-058	Reptilian scroll (crocodyliform)	partial scroll	AAS-Nursery (-25.4)

UTA-AASCP-059	Reptilian scroll (crocodyliform)	partial scroll	AAS Nursery (-27.4)
UTA-AASCP-060	Reptilian scroll (crocodyliform)	partial scroll	AAS Nursery (-29.6)
UTA-AASCP-061	Reptilian scroll (crocodyliform)	partial scroll	AAS Turtle Buffet (28.10)
UTA-AASCP-062	Reptilian (crocodyliform)	teardrop	AAS Crocorama (-5.7)
UTA-AASCP-063	Reptilian (crocodyliform)	teardrop	AAS Crocorama (9.7)
UTA-AASCP-064	Reptilian (crocodyliform)	teardrop	AAS Crocorama (-8.10)
UTA-AASCP-065	Reptilian (crocodyliform)	teardrop	AAS Crocorama (-11.6)
UTA-AASP-066	Reptilian (crocodyliform)	teardrop	AAS Crocorama (5.10)
UTA-AASP-067	Reptilian (crocodyliform)	teardrop	AAS Crocorama (5.10)
UTA-AASP-068	Reptilian (crocodyliform)	partial scroll	AAS Crocorama (-4.6)
UTA-AASCP-069	Reptilian (crocodyliform)	partial scroll	AAS Crocorama (-6.7)
UTA-AASCP-070	Reptilian (crocodyliform)	dome	AAS Turtle Buffet (29.10)
UTA-AASCP-071	Reptilian (crocodyliform)	partial scroll	AAS Crocorama (-13.7)
UTA-AASCP-072	Reptilian scroll (crocodyliform)	partial scroll	AAS Crocorama (-13.7)
UTA-AASCP-073	Reptilian scroll (crocodyliform)	partial scroll	AAS Crocorama (-13.7)
UTA-AASCP-074	Reptilian (crocodyliform)	ovoid	AAS Crocodyliform (30.10)
UTA-AASCP-075	Reptilian (crocodyliform)	dome	AAS Crocodyliform (-12.7)

APPENDIX A

PART II

ARLINGTON ARCHOSAUR SITE COLLECTIONS DATABASE SUBDIVIDED BY FACIES

AAS Facies A Microvertebrate Collection

UTA-AASL-001	*Ceratodus carterii*	tooth plate
UTA-AASL-002	*Ceratodus carterii*	tooth plate
UTA-AASL-003	*Ceratodus carterii*	tooth plate
UTA-AASL-004	*Ceratodus carterii*	juvy tooth plate
UTA-AASL-005	*Ceratodus carterii*	tooth plate
UTA-AASL-006	*Ceratodus carterii*	tooth plate
UTA-AASL-007	*Ceratodus carterii*	juvy tooth plate
UTA-AASL-008	*Ceratodus carterii*	tooth plate
UTA-AASL-009	*Ceratodus carterii*	tooth plate
UTA-AASM-001	Osteichthyes indet.	3 centra
UTA-AASM-002	*Cretodus* sp.	3 teeth & 1 partial
UTA-AASM-003	unidentified	4 cm partial limb (croc?/turtle?)
UTA-AASM-004	Elopomorpha indet.	4 centra
UTA-AASM-005	Pycnodontiformes indet.	partial jaw (4cm)
UTA-AASM-006	Odontaspididae indet.	9 sm teeth
UTA-AASM-007	croc?	phalange
UTA-AASM-008	Osteichthyes indet.	1 centrum
UTA-AASM-009	Teleostei indet.	3 sm (~1cm) verts fused in matrix
UTA-AASM-010	Elopomorpha indet.	1 large centrum (2.5 cm)
UTA-AASM-011	Pycnodontiformes indet.	25 teeth (to be measured)
UTA-AASM-012	*Cretodus*	Tooth
UTA-AASM-013	crocodile ? Or turtle	2 verts
UTA-AASM-014	Mosasauroidea indet.	partial jaw (~4.5cm)
UTA-AASM-015	Pycnodontiformes indet.	14 teeth (to be measured)
UTA-AASM-016	*Cretodus?*	partial tooth
UTA-AASM-017	unidentified croc?	small vert (2cm)
UTA-AASM-018	unidentified shark	small shark vert (2cm)
UTA-AASM-019	Teleostei	small caudal centrum in matrix
UTA-AASM-020	*Onchopristis*	3 partial sawfish jaws
UTA-AASM-021	Unidentified	2 partial crania-jaws? (5cm L-croc?)
UTA-AASM-023	cf. *Lepidotes*	2 gar scales (large-3cm)
UTA-AASM-024	*Hybodus* sp.	3 cephalic spines (2cm)
UTA-AASM-025	Testudines indet.	3 sm verts (1-2cm)
UTA-AASM-026	cf. *Lepidotes*	5 gar scales (sm~ <1cm)
UTA-AASM-027	*Hybodus* sp.	3 cephalic spines (partial)

UTA-AASM-028	unidentified (croc?)	partial vert (2.5 cm L)
UTA-AASM-029	unidentified (croc/turtle?)	partial vert (1.5 cm L)
UTA-AASM-030	unidentified fish	fish palate
UTA-AASM-031	?Reptilia	lg vert (3cmL x 4cmW)
UTA-AASM-032	unidentified croc?	lg vert (3cmL x 2cmW)
UTA-AASM-033	Osteichthyes indet.	1 partial jaw (~1-2cmL)
UTA-AASM-034	various	1 complete & 3 partial centra
UTA-AASM-166	Sauria indet.	sm vert (~8mm)-(lizard?)
UTA-AASM-167	Teleostei indet.	vert centrum (~2cm)
UTA-AASM-166	Sauria indet.	sm vert (~8mm)-(lizard?)
UTA-AASM-167	Teleostei indet.	vert centrum (~2cm)
UTA-AASM-280	Pycnodontiformes indet.	3 teeth
UTA-AASM-304	Osteichthyes indet.	4 partial fin spines
UTA-AASM-305	?Osteichthyes (possibly shark)	1 centrum
UTA-AASM-306	?Elopomorpha	1 centrum
UTA-AASM-307	unidentified vertebrate	1 centrum
UTA-AASM-308	Osteichthyes indet.	1 centrum
UTA-AASM-309	Osteichthyes indet.	1 centrum
UTA-AASM-310	Osteichthyes indet.	1 centrum
UTA-AASM-311	Osteichthyes indet.	1 centrum
UTA-AASM-312	?Elopomorpha	1 centrum
UTA-AASM-313	Osteichthyes indet.	1 centrum
UTA-AASM-314	Osteichthyes indet.	1 centrum
UTA-AASM-315	Osteichthyes indet.	1 centrum
UTA-AASM-316	Osteichthyes indet.	1 centrum
UTA-AASM-317	Osteichthyes indet.	1 centrum
UTA-AASM-318	Osteichthyes indet.	1 centrum
UTA-AASM-319	Osteichthyes indet.	1 centrum
UTA-AASM-320	unidentified vertebrate	1 bone fragment (prezygopo?)
UTA-AASM-321	Osteichthyes indet.	1 centrum fragment
UTA-AASM-322	Crocodyliformes indet.	1 centrum
UTA-AASM-323	Crocodyliformes indet.	1 partial centrum
UTA-AASM-326	Crocodyliformes indet.	1 jaw fragment with tooth
UTA-AASM-331	Crocodyliformes indet.	1 partial tooth
UTA-AASM-332	Crocodyliformes indet.	5 centra; 1 unidentified
UTA-AASM-333	?Sauria indet.	1 large neural arch
UTA-AAST-001	*dromaeosaur*	partial tooth
UTA-AAST-002	*Acrocanthosaurs cf*	partial tooth

UTA-AAST-006	theropod ident.	small tooth
UTA-AAST-007	*Acrocanthosaurs cf*	proximal partial claw
UTA-AAST-011	theropod ident.	tooth (worn)
UTA-AASC-063	crocodyliform	small tooth
UTA-AASC-064	crocodyliform	Tooth
UTA-AASC-065	crocodyliform	small tooth
UTA-AASC-066	crocodyliform	small tooth
UTA-AASC-067	crocodyliform	small partial tooth
UTA-AASC-068	crocodyliform	small tooth
UTA-AASC-069	crocodyliform	small tooth
UTA-AASC-070	crocodyliform	small tooth
UTA-AASC-071	crocodyliform	partial tooth
UTA-AASC-072	crocodyliform	partial tooth (large)
UTA-AASC-073	crocodyliform	partial tooth
UTA-AASC-074	crocodyliform	partial tooth
UTA-AASC-075	crocodyliform	partial tooth
UTA-AASC-076	crocodyliform	partial tooth
UTA-AASC-077	crocodyliform	partial tooth
UTA-AASC-078	crocodyliform	Tooth
UTA-AASC-079	crocodyliform	Tooth
UTA-AASC-080	crocodyliform	Tooth
UTA-AASC-081	crocodyliform	Tooth
UTA-AASC-082	crocodyliform	Tooth
UTA-AASC-083	crocodyliform	Tooth
UTA-AASC-084	crocodyliform	Tooth
UTA-AASC-085	crocodyliform	Tooth
UTA-AASC-086	Crocodyliform	rounded tooth?
UTA-AASC-087	Crocodyliform	small partial tooth
UTA-AASC-088	Crocodyliform	small partial tooth
UTA-AASC-089	not croc	small partial tooth
UTA-AASC-090	Crocodyliform	small partial tooth
UTA-AASC-091	Crocodyliform	small partial 1/2 tooth
UTA-AASC-092	Crocodyliform	tooth?
UTA-AASC-093	Crocodyliform	large partial tooth
UTA-AASC-094	Crocodyliform	partial tooth
UTA-AASC-095	Crocodyliform	partial tooth (weathered)
UTA-AASC-116	Crocodyliform	teeth (3 small)
UTA-AASC-117	Crocodyliform	tooth

UTA-AASC-118	Crocodyliform	tooth
UTA-AASC-119	Crocodyliform	tooth
UTA-AASC-120	Crocodyliform	small tooth
UTA-AASC-121	Crocodyliform	small tooth
UTA-AASC-122	Crocodyliform	tooth (weathered)
UTA-AASC-123	Crocodyliform	partial tooth (weathered)
UTA-AASC-124	Crocodyliform	partial tooth (weathered)
UTA-AASC-125	Crocodyliform	small tooth
UTA-AASC-126	Crocodyliform	partial tooth (weathered)
UTA-AASC-127	Crocodyliform	small tooth
UTA-AASC-128	Crocodyliform	small tooth
UTA-AASC-129	Crocodyliform	partial tooth
UTA-AASC-130	Crocodyliform	tooth
UTA-AASC-131	Crocodyliform	partial tooth
UTA-AASC-132	Crocodyliform	partial tooth
UTA-AASC-133	Crocodyliform	tooth

AAS Facies B Microvertebrate Collection

UTA-AASM-022	Pycnodontiformes indet.	2 partial jaws (sm-1cm)
UTA-AASM-056	unidentified	Misc bone frags
UTA-AASM-057	unidentified fish?	Scale
UTA-AASM-058	Teleostei indet.	sm vert (~3mm)
UTA-AASM-073	*cf. Lepidotes*	Scale
UTA-AASM-074	unidentified plant	seed?
UTA-AASM-075	unidentified	unidentified
UTA-AASM-076	Crocodyliformes indet.	sm tooth (~3mm)
UTA-AASM-077	snail?	
UTA-AASM-078	unidentified	unidentified
UTA-AASM-079	cf. *Bernessartia*	1 sm tooth
UTA-AASM-080	unidentified turtle	sm shell (plastron?)
UTA-AASM-081	Crocodyliformes indet.	sm tooth (~5mm)
UTA-AASM-082	unidentified (turtle/croc?)	sm limb bone (~2cm)
UTA-AASM-083	unidentified (turtle/croc?)	Misc bone frags
UTA-AASM-084	Holostei indet.	sm scale (~5mm)
UTA-AASM-085	Crocodyliformes indet.	tooth + 3 other frags
UTA-AASM-086	Crocodyliformes indet.	4 teeth

UTA-AASM-087	Crocodyliformes indet.	2 teeth
UTA-AASM-088	Teleostei indet.	4 verts (<1mm/fish?)
UTA-AASM-089	various micro	salamander centrum
UTA-AASM-090	?Osteichthyes	1 tooth
UTA-AASM-091	Crocodyliformes indet.	1 tooth (fish?)
UTA-AASM-092	Crocodyliformes indet.	2 sm teeth (fish?)
UTA-AASM-093	cf. *Bernessartia*	1 sm tooth (fish)
UTA-AASM-094	unidentified invert	1 sm gastopod & twigs
UTA-AASM-095	unidentified	1 sm tooth?
UTA-AASM-107	Teleostei indet.	3 sm verts
UTA-AASM-108	Crocodyliformes indet.	2 teeth (~4-6mm)
UTA-AASM-110	Sauria indet.	1 sm vert
UTA-AASM-111	Crocodyliformes indet.	2 sm teeth
UTA-AASM-112	Crocodyliformes indet.	8 sm teeth
UTA-AASM-113	Osteichthyes indet.	2 sm teeth (~2-4mm)
UTA-AASM-114	cf. *Lepidotes*	4 sm scales (~2-5mm)
UTA-AASM-115	plant-wood	sm twigs
UTA-AASM-116	amber	1 sm amber
UTA-AASM-117	Crocodyliformes indet.	4 sm teeth (~2-3mm)
UTA-AASM-118	Osteichthyes indet.	2 sm scales (~2-4mm)
UTA-AASM-119	Crocodyliformes indet.	1 sm thin tooth
UTA-AASM-120	Sauria indet.	2 sm verts
UTA-AASM-121	Caudata indet., Lepidotes & indet.	1 cf. Lepidotes
UTA-AASM-122	various	1 croc tooth
UTA-AASM-123	Crocodyliformes indet.	1 tooth (~4-5mm)
UTA-AASM-124	Crocodyliformes indet.	1 tooth (~4mm)
UTA-AASM-125	?Amiiformes	1 vert (~4mm)
UTA-AASM-126	Teleostei indet.	2 sm vert
UTA-AASM-127	Teleostei indet.	2 sm verts (~2mm)
UTA-AASM-129	Crocodyliformes indet.	1 tooth (~1cm)
UTA-AASM-130	unidentified	2 misc bone frags
UTA-AASM-131	Crocodyliformes indet.	1-3 osteoderm
UTA-AASM-132	Sauria indet.	1 sm vert (~4mm)
UTA-AASM-133	Teleostei indet.	1 sm vert (~2-3mm)
UTA-AASM-134	?Caudata	1 salamander
UTA-AASM-135	Crocodyliformes indet.	1 sm tooth (~4mm)
UTA-AASM-136	Osteichthyes indet.	2 sm verts (~3mm)

UTA-AASM-137	Crocodyliformes indet.	1sm tooth
UTA-AASM-138	Sauria indet.	1sm vert (-good)
UTA-AASM-139	Teleostei indet.	1sm vert (~2mm)
UTA-AASM-140	Caudata indet.	1sm vert (~2mm)
UTA-AASM-141	wood fragment - discard	wood frag
UTA-AASM-142	?Osteichthyes	1 sm tooth (~1mm)
UTA-AASM-144	Osteichthyes indet.	1sm vert (~1mm)
UTA-AASM-145	?Crocodyliformes	1sm tooth
UTA-AASM-146	Sauria indet.	1sm vert (~2-3 mm)
UTA-AASM-147	Sauria indet.	1sm vert (~2-3 mm)
UTA-AASM-148	Teleostei indet.	1sm vert (~2 mm)
UTA-AASM-149	Crocodyliformes indet.	1sm vert (~2 mm)
UTA-AASM-150	Teleostei indet.	1sm vert (~2 mm)
UTA-AASM-151	Crocodyliformes indet.	1 (?)sm vert (2 mm)
UTA-AASM-152	Crocodyliformes indet.	1 broken tooth
UTA-AASM-153	Crocodyliformes indet.	1 broken tooth
UTA-AASM-154	Crocodyliformes indet.	1 broken tooth
UTA-AASM-155	ornithopod	1 shed -worn tooth
UTA-AASM-156	?Crocodyliformes	1 worn tooth (~1cm)
UTA-AASM-157	cf. Lepidotes	1 worn scale (<1cm)
UTA-AASM-158	Teleostei indet.	1sm vert (~2-3 mm)
UTA-AASM-159	?Crocodyliformes	1sm tooth (~6 mm)
UTA-AASM-160	Crocodyliformes indet.	1 tooth (~1 cm)
UTA-AASM-161	Crocodyliformes indet.	1 tooth (croc 7 mm)
UTA-AASM-162	?Amiiformes	1 vert (~4mm)
UTA-AASM-163	Reptilia indet.	1 tooth (~4mm)
UTA-AASM-164	Crocodyliformes indet.	1 tooth (~3mm)
UTA-AASM-165	Reptilia indet. (possibly bird)	sm limb bone
UTA-AASM-168	Teleostei indet.	vert centrum
UTA-AASM-169	unidentified	sm shell (?)
UTA-AASM-170	*Pseudohypolophus*	sm ray tooth
UTA-AASM-171	*Hybodus* sp.	Shark tooth
UTA-AASM-172	Tetrapoda indet.	1 longbone epiphysis
UTA-AASM-173	Tetrapoda indet.	1 longbone epiphysis
UTA-AASM-174	Crocodyliformes indet.	1 baby croc tooth
UTA-AASM-175	plant-wood	wood frag
UTA-AASM-176	Crocodyliformes indet.; cf. Lepidotes	1 osteoder
UTA-AASM-177	Crocodyliformes indet.	juvy croc tooth

UTA-AASM-178	?Amiiformes	jaw frag with 1 tooth
UTA-AASM-179	unidentified	longbone or rib
UTA-AASM-180	Crocodyliformes indet.	1 partial scale
UTA-AASM-181	Osteichthyes indet.	vert centrum
UTA-AASM-183	?Osteichthyes	unidentified frag
UTA-AASM-184	unidentified	1 caudal centrum
UTA-AASM-185	Sauria indet.	1 centrum
UTA-AASM-186	Teleostei indet.	vert centrum
UTA-AASM-187	?Sauria indet.	1 large centrum
UTA-AASM-188	Crocodyliformes indet.	baby croc tooth
UTA-AASM-189	Crocodyliformes indet.	baby tooth
UTA-AASM-190	Teleostei indet.	2 vert centra
UTA-AASM-191	Teleostei indet.	vert centrum
UTA-AASM-192	?Osteichthyes	Fragment
UTA-AASM-193	Teleostei indet.	3 complete centra
UTA-AASM-194	cf. *Lepidotes*	sm scale
UTA-AASM-195	Teleostei indet.	1 centrum
UTA-AASM-196	?Sauria	1 bone
UTA-AASM-197	Teleostei indet.	1 centrum
UTA-AASM-198	unidentified	misc frag
UTA-AASM-199	Multituberculata indet.	1 lower 4th premolar
UTA-AASM-200	unidentified	misc frag
UTA-AASM-201	Crocodyliformes indet.	1 tooth
UTA-AASM-202	Teleostei indet.	1 centrum
UTA-AASM-203	Chondrichthyes indet.	small ray tooth
UTA-AASM-204	unidentified	
UTA-AASM-205	Osteichthyes indet.	1 styliform tooth
UTA-AASM-206	?Crocodyliformes	1 tooth
UTA-AASM-207	Anura indet.	1 radioulna
UTA-AASM-208	unidentified	bone frag
UTA-AASM-209	Teleostei indet.	4 complete centra
UTA-AASM-210	Teleostei indet.	1 partial centrum
UTA-AASM-211	?Plantae	seed?
UTA-AASM-212	Crocodyliformes indet.	baby tooth
UTA-AASM-215	Caudata indet.	1 centrum fragment
UTA-AASM-216	bone fragment	
UTA-AASM-217	?Reptilia	1 tooth frag
UTA-AASM-218	amber	

UTA-AASM-219	unidentified	bone frag (limb?)
UTA-AASM-220	?Crocodyliformes	baby tooth
UTA-AASM-221	Caudata indet.	1 broken prezygop
UTA-AASM-222	?Crocodyliformes	partial baby tooth
UTA-AASM-223	unidentified	partial baby tooth
UTA-AASM-224	Crocodyliformes indet.	partial baby tooth
UTA-AASM-225	cf. *Lepidotes*	Scale
UTA-AASM-228	?Amiiformes	sm vert centrum
UTA-AASM-229	Crocodyliformes indet.	1 tooth
UTA-AASM-230	Crocodyliformes indet.	1 tooth
UTA-AASM-231	?Amiiformes	1 centrum
UTA-AASM-232	Caudata indet.	1 vertebra
UTA-AASM-233	Osteichthyes indet.	1 centrum
UTA-AASM-234	Crocodyliformes indet.	1 tooth
UTA-AASM-235	Crocodyliformes indet.	tooth (long & thin)
UTA-AASM-236	Crocodyliformes indet.	baby croc tooth
UTA-AASM-237	Teleostei indet.	1 centrum
UTA-AASM-238	Teleostei indet.	2 vert centra
UTA-AASM-239	Anura indet.	1 proximal humerus
UTA-AASM-240	Crocodyliformes indet.	baby croc tooth
UTA-AASM-241	Crocodyliformes indet.	baby croc tooth
UTA-AASM-242	Osteichthyes indet.	sm tooth
UTA-AASM-243	Osteichthyes indet.	1 centrum
UTA-AASM-244	Crocodyliformes indet.	baby croc tooth
UTA-AASM-245	Crocodyliformes indet.	croc tooth (long/thin)
UTA-AASM-246	cf. *Lepidotes*	Scale
UTA-AASM-247	Osteichthyes indet.	1 scale fragment
UTA-AASM-248	cf. *Lepidotes*	1 scale
UTA-AASM-251	cf. *Lepidotes*	1 scale
UTA-AASM-252	Crocodyliformes indet.	1 tooth
UTA-AASM-254	?Crocodyliformes	1 ?distal metatarsal
UTA-AASM-257	Crocodyliformes indet.	1 sm tooth
UTA-AASM-259	Pycnodontiformes indet.	1 sm tooth
UTA-AASM-260	cf. Lepidotes	1 md scale
UTA-AASM-263	Crocodyliformes indet.	1 sm tooth
UTA-AASM-264	Crocodyliformes indet.	1 sm thin tooth
UTA-AASM-265	cf. Lepidotes	1 md scale
UTA-AASM-266	unidentified vertebrate	2 bone frags (limbs?)

UTA-AASM-267	Pycnodontiformes indet.	1 sm tooth
UTA-AASM-268	unidentified vertebrate	
UTA-AASM-269	unidentified vertebrate	1 partial ?fin spine;
UTA-AASM-270	Teleostei indet.	2 centra
UTA-AASM-273	Crocodyliformes indet.	sm croc tooth
UTA-AASM-274	Crocodyliformes indet.	sm croc tooth
UTA-AASM-275	cf. Lepidotes	?scale
UTA-AASM-276	amber	
UTA-AASM-277	vertebrate indet	sm bone frag
UTA-AASM-278	Crocodyliformes indet.	sm croc tooth
UTA-AASM-279	Teleostei indet.	sm vert centrum
UTA-AASM-281	vertebrate indet	bone fragment
UTA-AASM-282	Crocodyliformes indet.	sm croc tooth
UTA-AASM-283	Sauria indet.	1 centrum
UTA-AASM-284	plant	Seed
UTA-AASM-285	vertebrate indet	bone fragment
UTA-AASM-286	vertebrate indet	bone fragment
UTA-AASM-287	Teleostei indet.	1 centrum
UTA-AASM-288	vertebrate indet	bone frag (spine?)
UTA-AASM-289	amber (fire drop?)	amber with carbon
UTA-AASM-290	amber	
UTA-AASM-291	plant	plant –stem
UTA-AASM-292	plant	plant –stem
UTA-AASM-294	vertebrate indet	limb bone frag?
UTA-AASM-295	amber	
UTA-AASM-296	plant	Seed
UTA-AASM-298	vertebrate indet	misc bone frag?
UTA-AASM-300	?Amiidae	?coranoid tooth
UTA-AASM-301	Amber	
UTA-AASM-324	Crocodyliformes indet.	1 tooth
UTA-AASM-325	Crocodyliformes indet.	1 juvenile osteoderm
UTA-AASM-334	Crocodyliformes indet.	1 neural arch
UTA-AAST-005	theropod ident.	small claw
UTA-AAST-009	theropod ident.	partial tooth (worn)

AAS Facies C Microvertebrate Collection

UTA-AASM-098	Crocodyliformes indet.	Tooth
UTA-AASM-099	Teleostei indet.	3 centra
UTA-AASM-100	unidentified	sm tooth?
UTA-AASM-101	Teleostei indet.	2 sm verts (~2mm)
UTA-AASM-102	Crocodyliformes indet.	2 sm teeth (~2-3mm)
UTA-AASM-103	?Crocodyliformes	Unidentified
UTA-AASM-104	Caudata indet. & Teleostei indet.	5 sm verts (~2mm)
UTA-AASM-105	unidentified	bone frag
UTA-AASM-106	Teleostei indet.	1 vert (~3mm)
UTA-AASM-249	Reptilia indet.	1 tooth, laterally compressed (theropod)
UTA-AASM-250	Teleostei indet.	1 centrum
UTA-AASM-253	Osteichthyes indet.	1 tooth; unusual elongate laterally compressed and lacks carinae & striations
UTA-AASM-255	Pycnodontiformes indet.	1 palatal tooth
UTA-AASM-256	cf. *Lepidotes*	1 large scale
UTA-AASM-335	Crocodyliformes indet.	1 complete caudal vertebra

AAS Facies D Microvertebrate Collection

UTA-AASM-036	Crocodyliformes indet.	sm croc tooth (3mm)
UTA-AASM-037	*Stephanodus*	sm tooth (~3mm)
UTA-AASM-038	Crocodyliformes indet.	sm tooth (~2mm)
UTA-AASM-039	Crocodyliformes indet.	sm tooth (~2mm)
UTA-AASM-040	unidentified (croc?)	sm tooth (~3mm)
UTA-AASM-041	*Pseudohypolophus*	tooth (~3mm)
UTA-AASM-042	unidentified fish?	thin curved tooth-Morpho A
UTA-AASM-043	*Pseudohypolophus*	tooth (~3mm)
UTA-AASM-044	Teleostei indet.	7 Misc (2 teleost centrum
UTA-AASM-045	*Onchopristus*	sm tooth (<1mm)
UTA-AASM-046	Osteichthyes indet.	sm tooth Morphotype A
UTA-AASM-047	*Pseudohypolophus*	sm tooth (<1mm)
UTA-AASM-048	Teleostei indet.	sm vert (>3mm)
UTA-AASM-049	Crocodyliformes indet.	croc tooth (~6mm)
UTA-AASM-050	Osteichthyes indet.	tooth Morphotype A

UTA-AASM-051	*Pseudohypolophus*	2 fish teeth (~2mm)
UTA-AASM-052	cf. *Hybodus*	tooth (~3mm)
UTA-AASM-053	Osteichthyes indet.	tooth Morphotype A
UTA-AASM-054	Caudata indet.	caudal vert (~2mm)
UTA-AASM-055	Teleostei indet.	sm vert (~4mm)
UTA-AASM-069	croc	tooth (~3mm)
UTA-AASM-070	croc	tooth (~9mm)
UTA-AASM-071	*Pseudohypolophus*	tooth (~3mm)
UTA-AASM-072	unidentified	unidentified
UTA-AASM-182	Teleostei indet.	1 fish fragment
Facies D Siderite bed		
UTA-AASM-059	Crocodyliformes indet.	tooth (~1cm)
UTA-AASM-060	Pycnodontiformes indet.	sm tooth (~1-2mm)
UTA-AASM-061	unidentified fish?	sm vert (~4mm)-basioccipital
UTA-AASM-062	croc?	sm tooth (~3-4mm)
UTA-AASM-063	unidentified invert	sm shell (~2mm)
UTA-AASM-064	unidentified shark/fish?	denticle (~3mm)
UTA-AASM-065	unidentified shark/fish?	tooth (~3mm)
UTA-AASM-066	unidentified shark/fish?	tooth (~3mm)
UTA-AASM-067	unidentified shark/fish?	tooth (~3mm)
UTA-AASM-068	Pycnodontiformes indet.	1 tooth (~3mm); 1 tooth frag
UTA-AASM-329	Pycnodontiformes indet.	2 teeth
UTA-AASM-330	Crocodyliformes indet.	1 partial tooth
UTA-AASM-336	cf. Cretodus	1 tooth embedded in siderite
UTA-AASM-337	cf. Hybodus	1 cephalic spine

APPENDIX B

ARLINGTON ARCHOSAUR SITE
GRID MAPS

(COURTESY R. FRY)

AAS Map Grid Key

Map Grid Name	Map Coordinates (meters)	Site Name
Original (Prime)	(01=>10), (01=>05)	Crocorama
East	(10=> 20), (01=>05)	Crocorama
East 1	(21=>30), (01=>05)	Crocorama East
East 2	(31=>40), (01=>05)	Crocorama East
North	(01=>10), (11=>15)	Crocorama
North 1	(01=>10), (11=>15)	Crocorama
North 1 East 1	(10=>20), (11=>15)	Crocorama East
North 1 East 2	(31=>40), (11=>15)	Crocorama East
North 1 West	(-01=>-10), (11=>15)	Crocorama
North 1 West 1	(-11=>-20), (11=>150)	Turtle Buffet
Northeast	(10=>20), (06, =>20)	Crocorama
Northeast 1	(21=>30), (06=>10)	Crocorama East
Northwest	(-01=>-10), (06=>10)	Turtle Buffet
Northwest 1	(-11=>-20), (06, 10)	Turtle Buffet/Nursery
Northwest 2	(-21=>-30), (06=>10)	Nursery/Dino Quarry
Northwest 3	(-31=>-40), (06=>10)	Dinosaur Quarry
Northwest 4	(-40=>-50), (06=>10)	Dinosaur Quarry
West	(-01=>-10), (01=>05)	Crocorama
West 1	(-11=>-20), (01=>05)	Turtle Buffet/Nursery

AAS Prime Map (01=>10), (01,=>05)

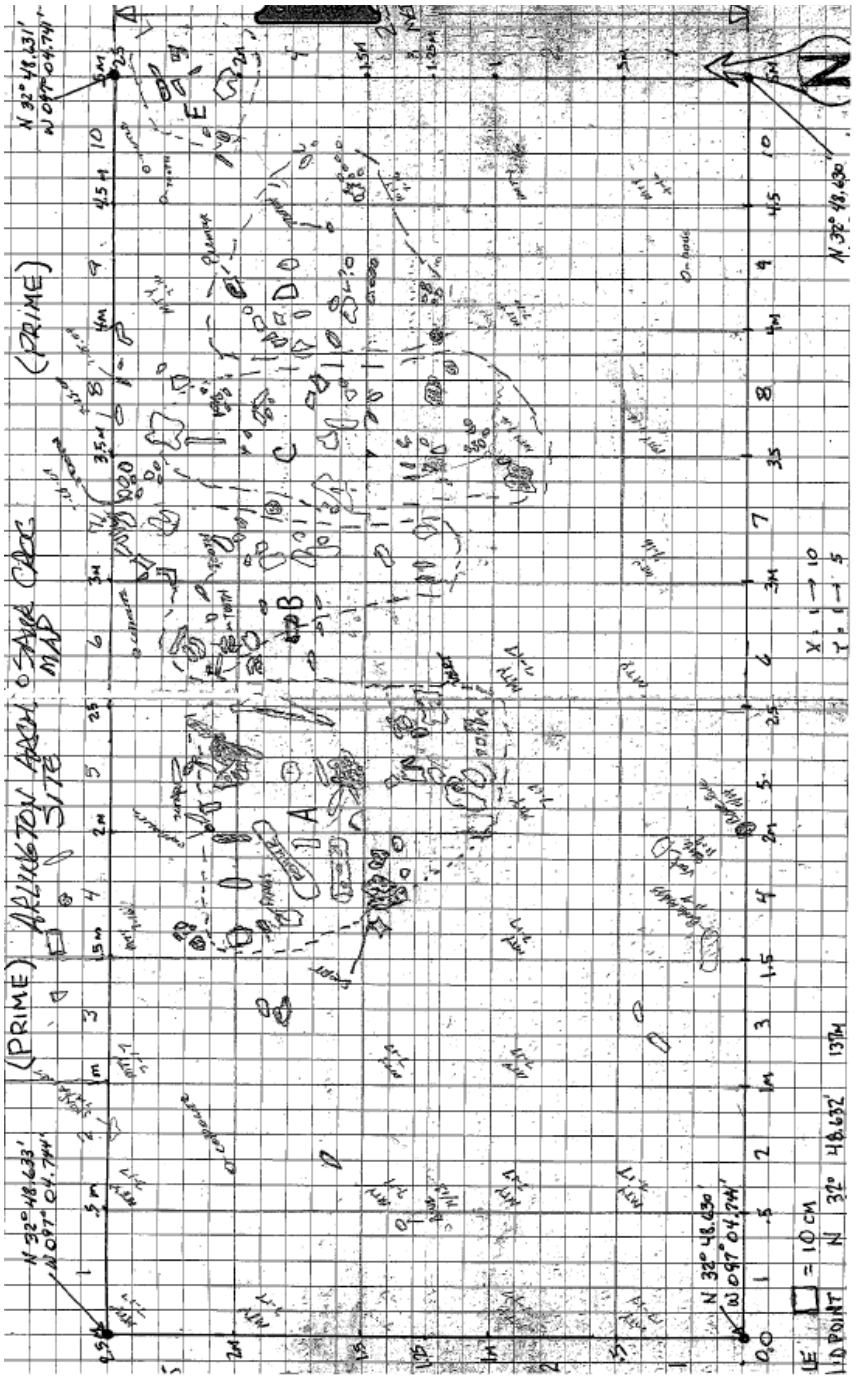

AAS West 1 Map (-11=>-20), (01=>05)

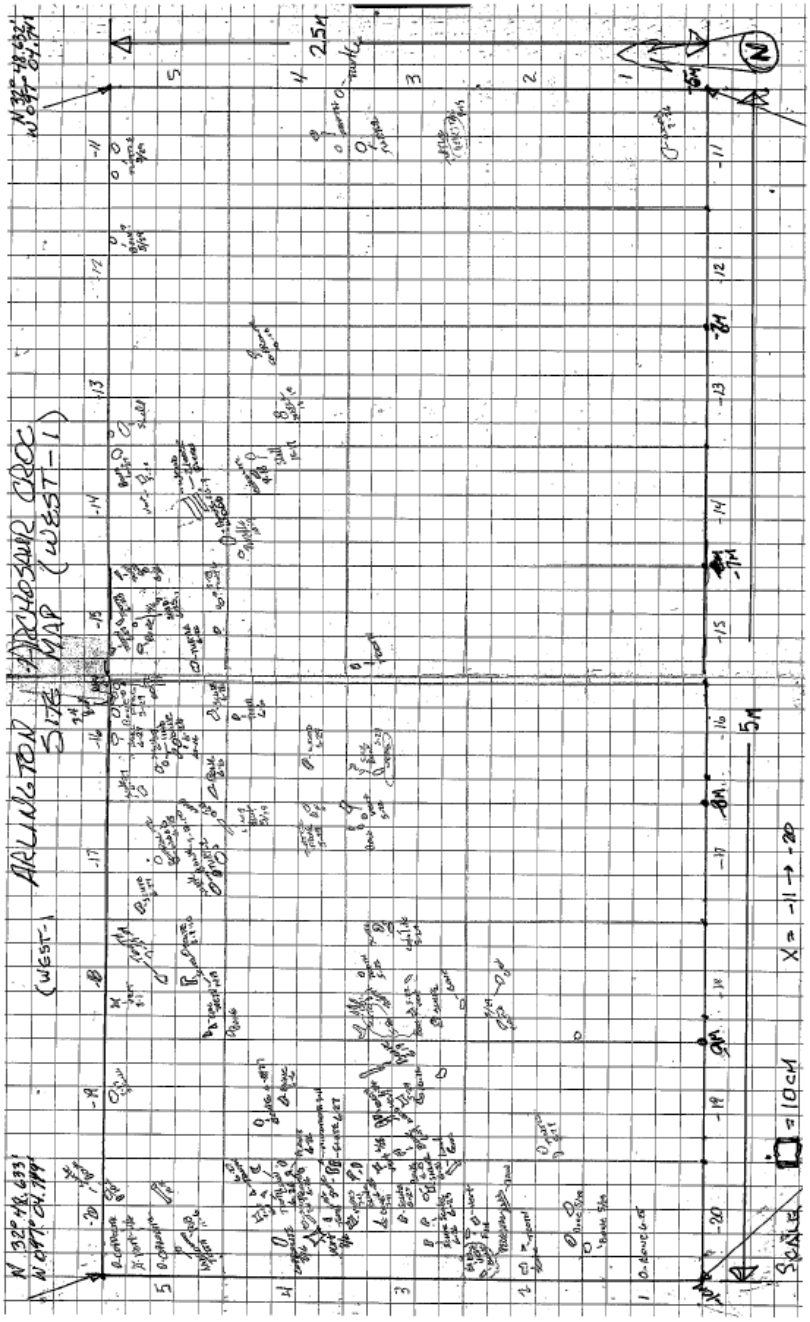

AAS West 1 Map (-11=>-20), (01=>05)

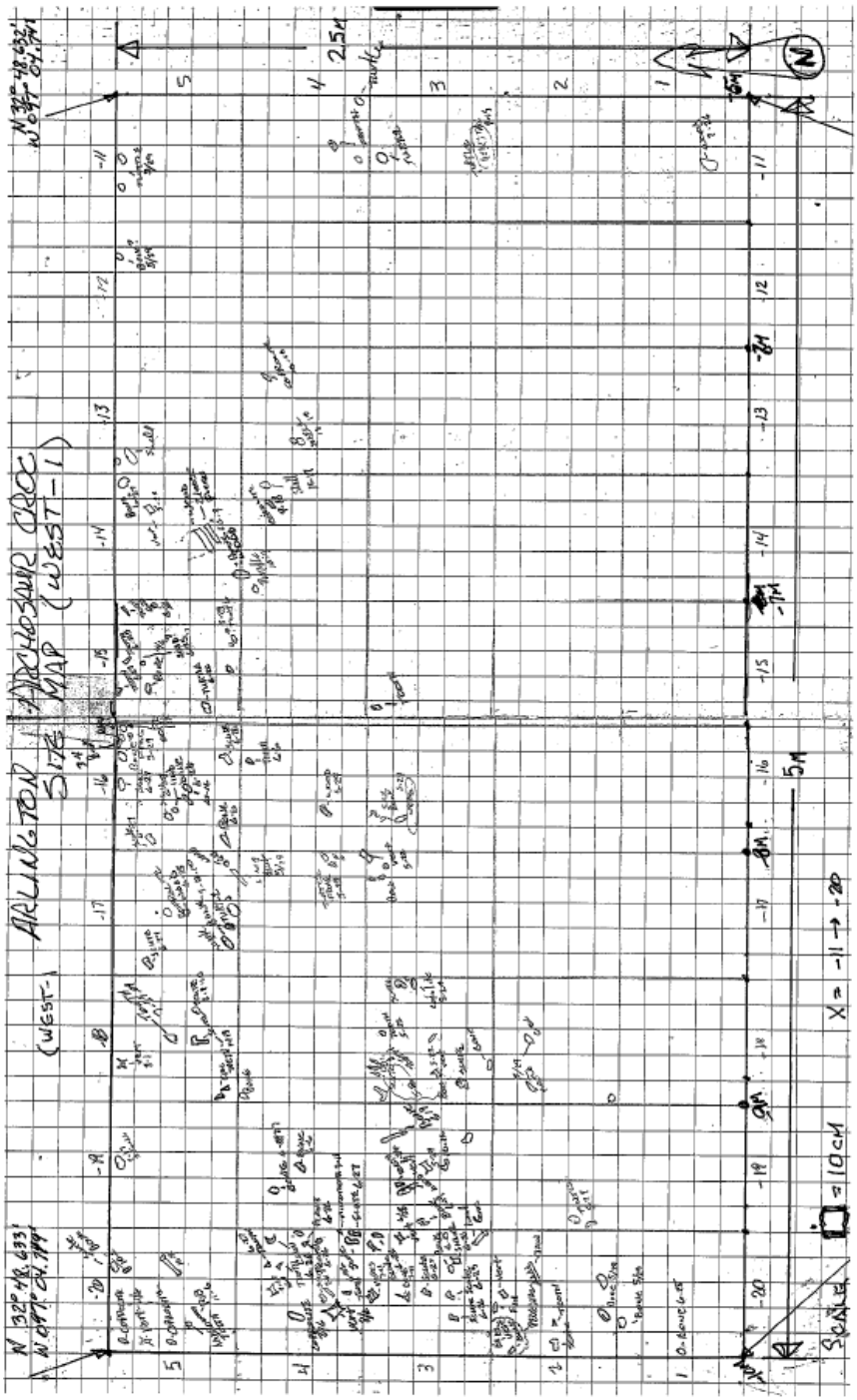

AAS West 2 Map(-21=> -20), (01=>05)

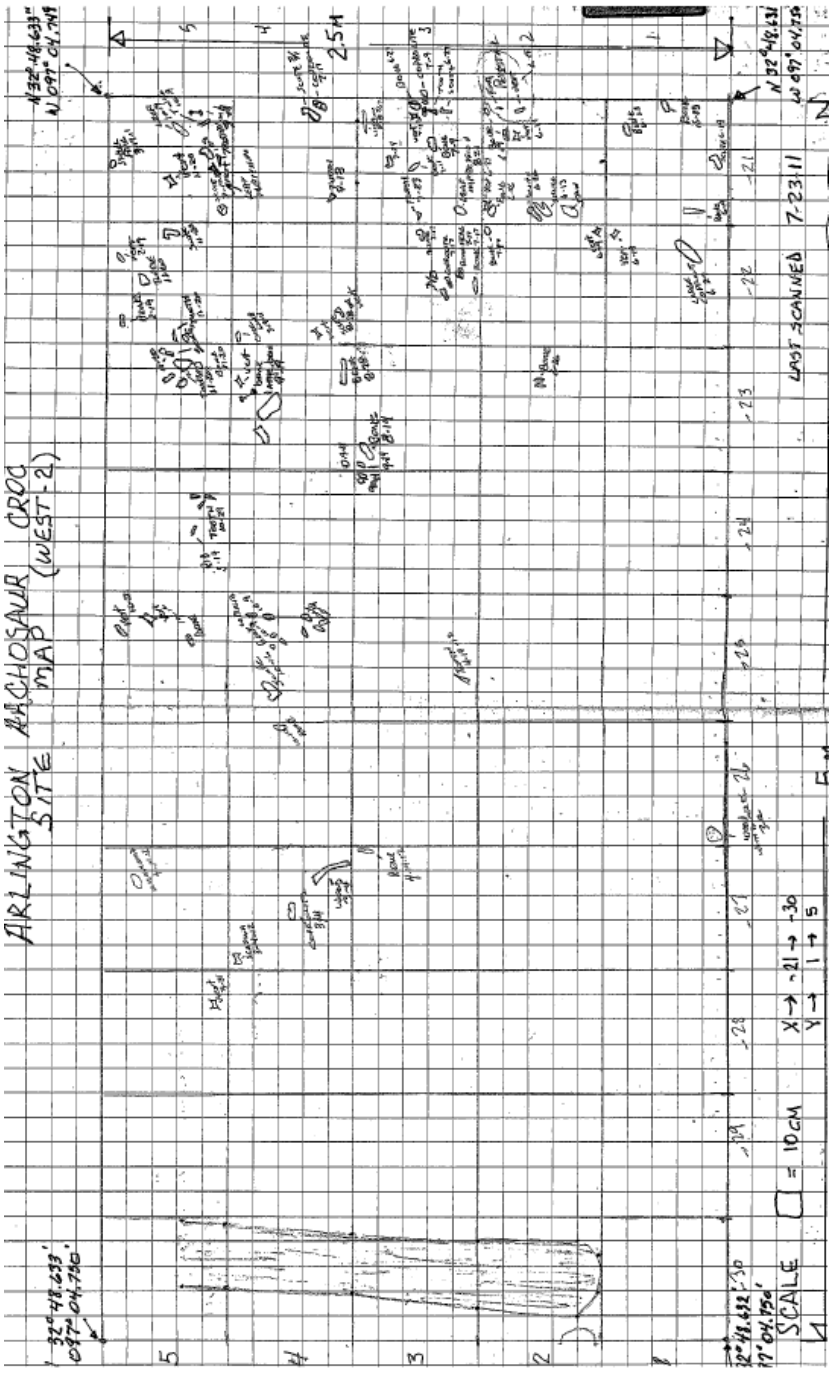

AAS West 3 (-31, =>-40). (01=>05)

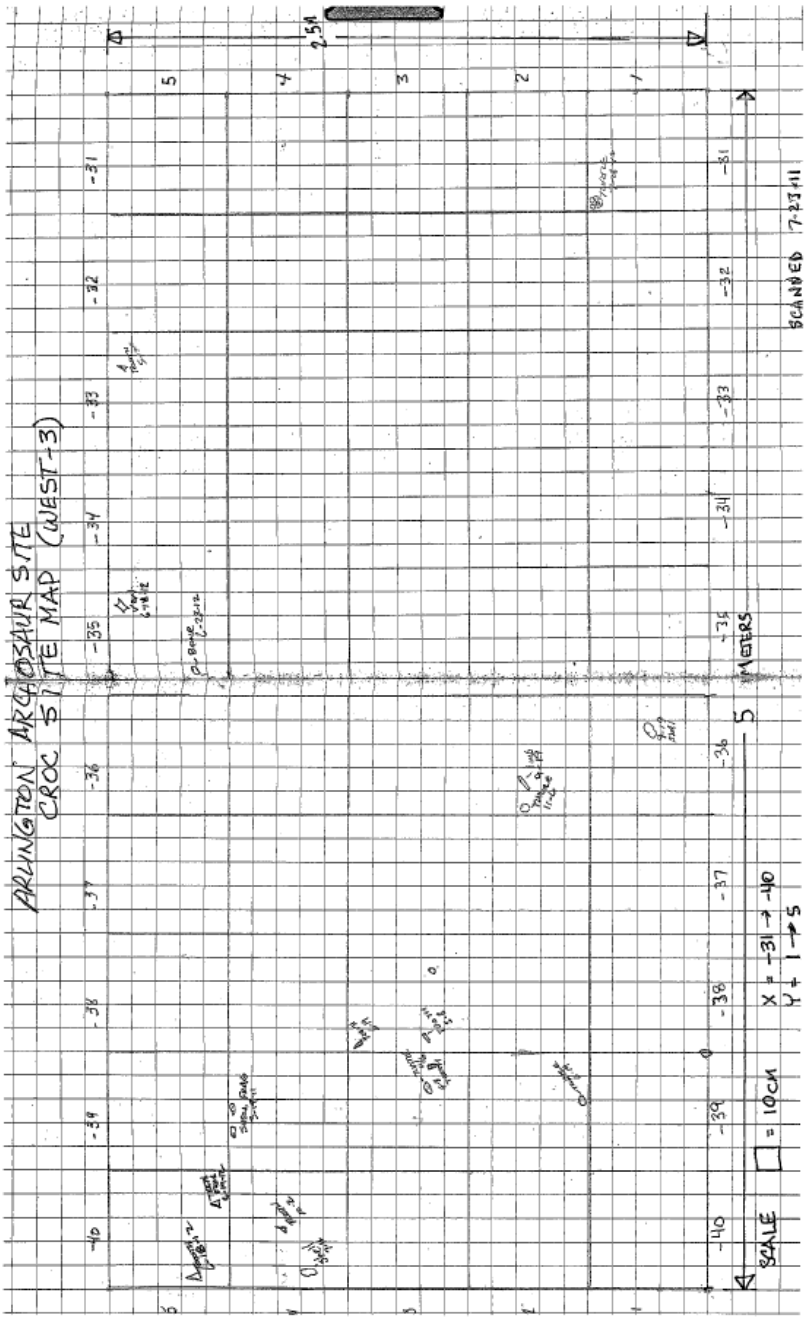

AAS West 4 Map (-41=.-50), (01=>05)

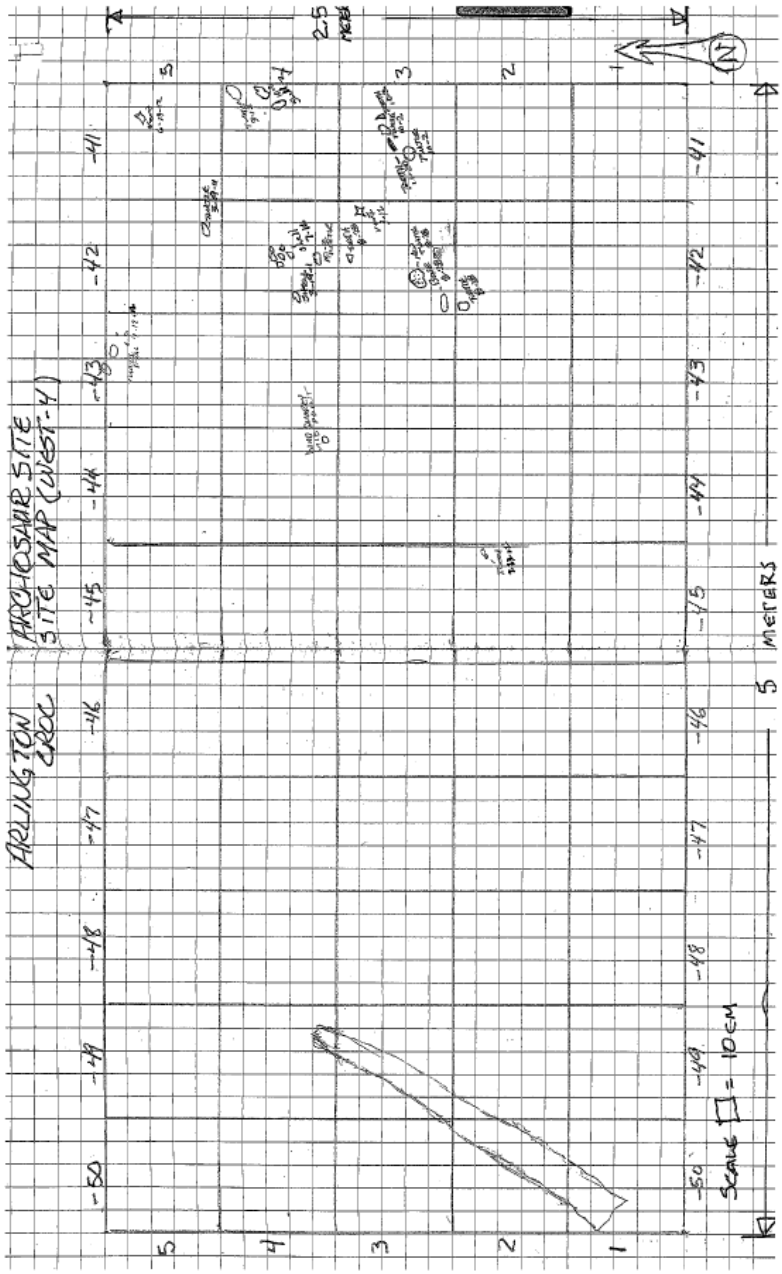

AAS East Map (10, =>20), (01=>05)

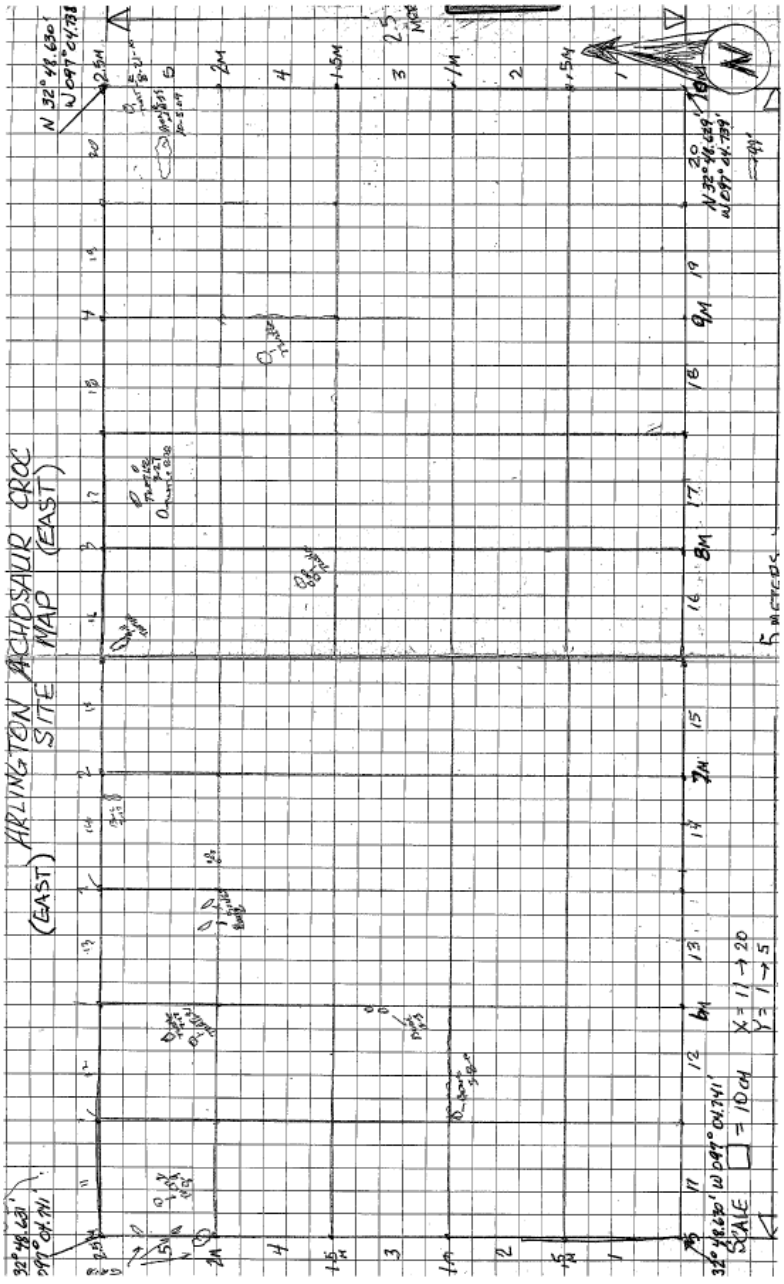

AAS East Map 1 (10, =>20), (01=>05)

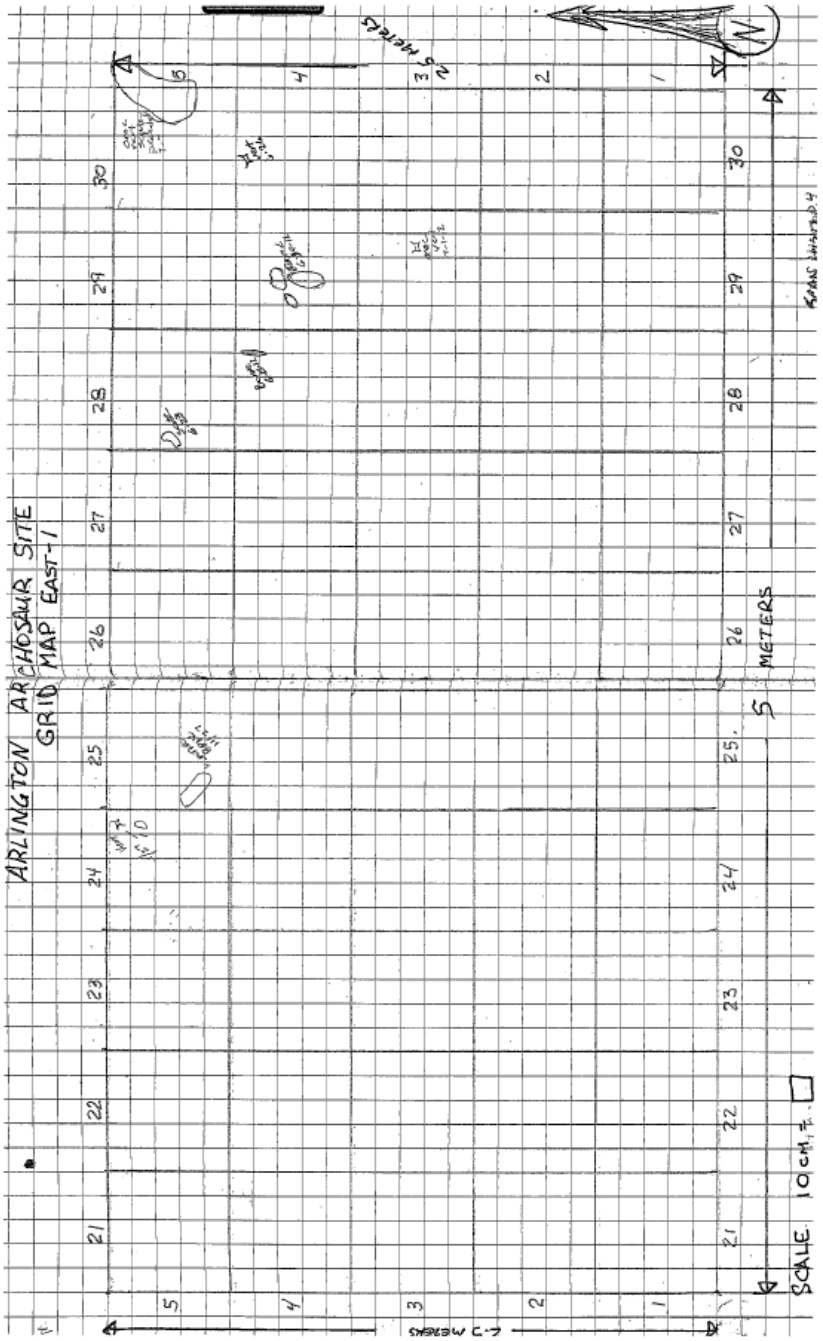

AAS East Map 2 (21, =>20), (01=>05)

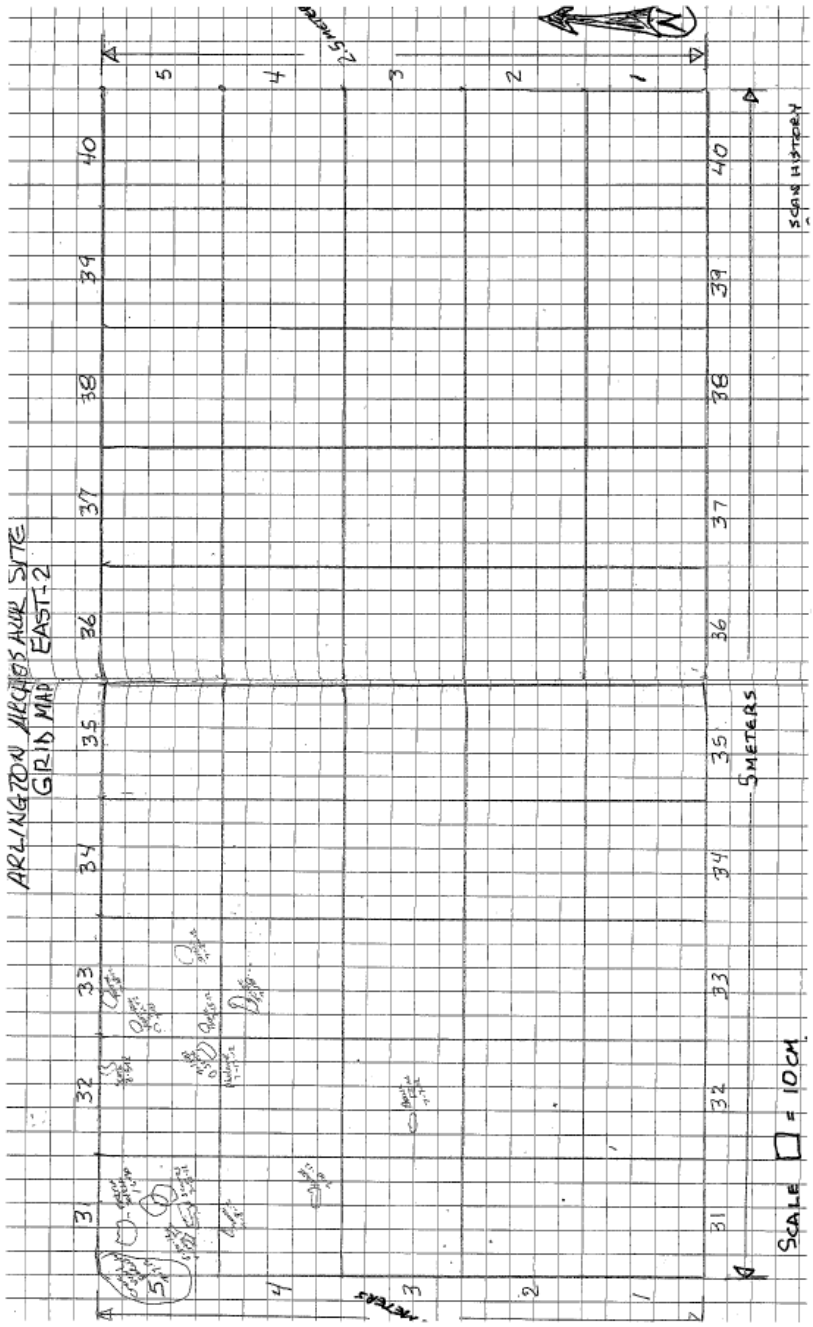

AAS North Map (01=>10), (06=>10)

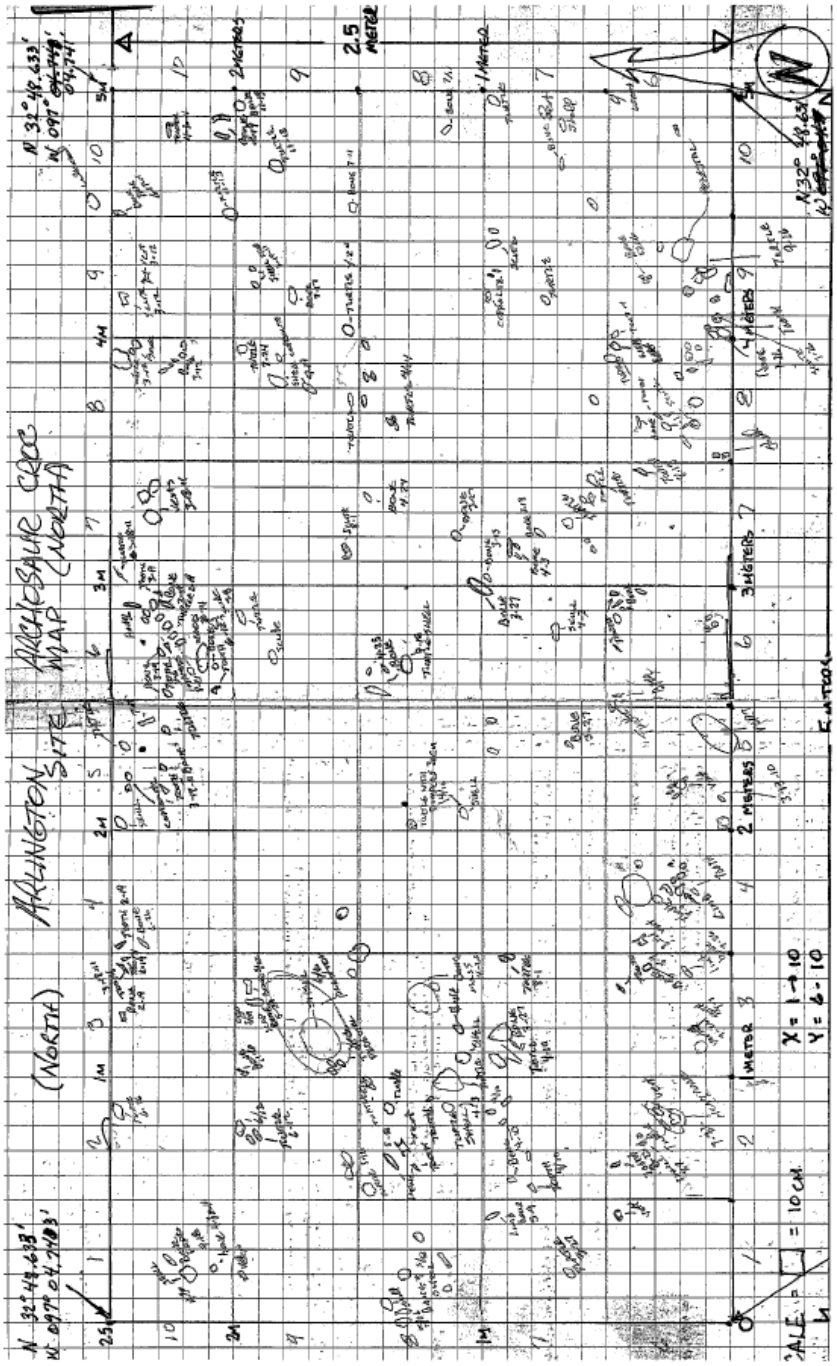

AAS Northwest Map (-01=>10), (06=>10)

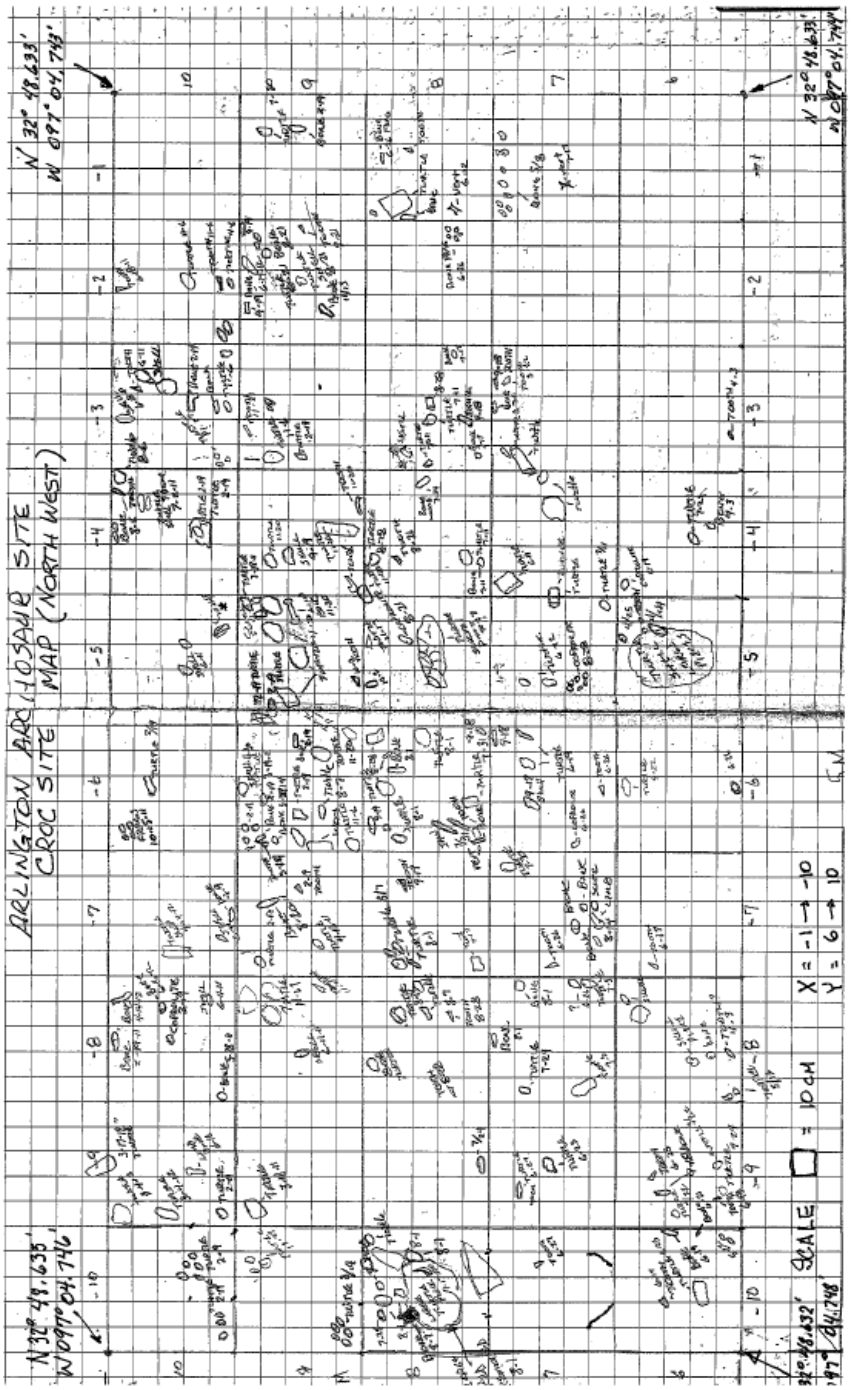

AAS Northwest 1 Map (-11=>20), (06=>10)

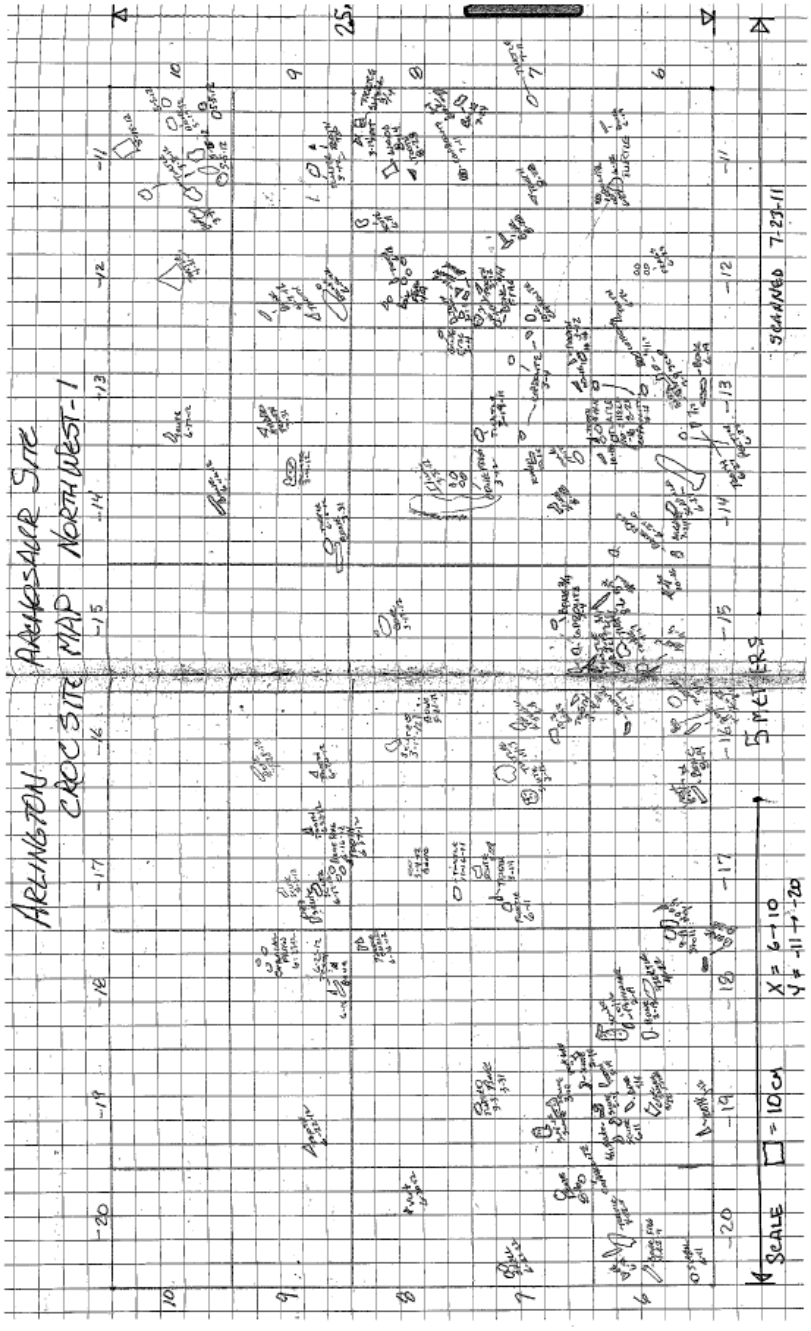

AAS Northwest 2 Map (-21=>30), (06=>10)

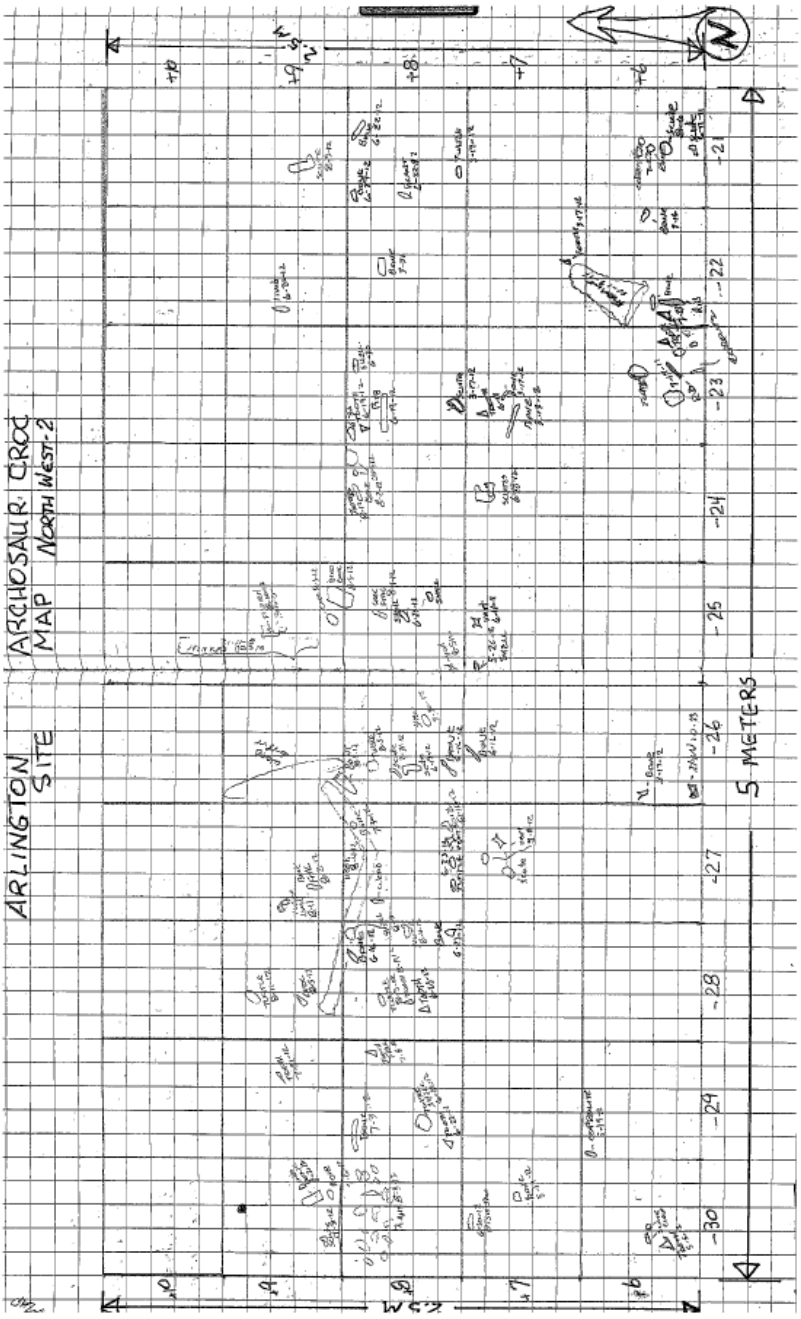

AAS Northwest 3 Map (-31, =>40), (06=>10)

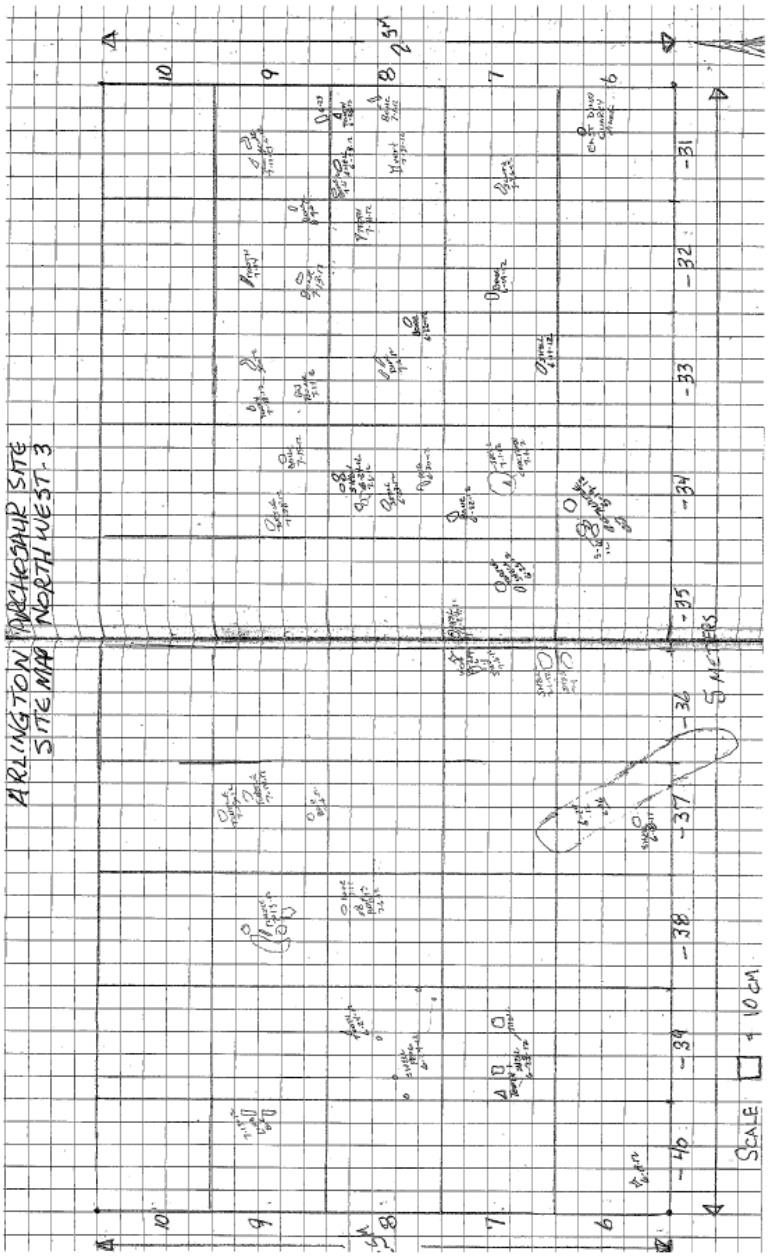

AAS Northeast Map (10, =>20), (06,=>10)

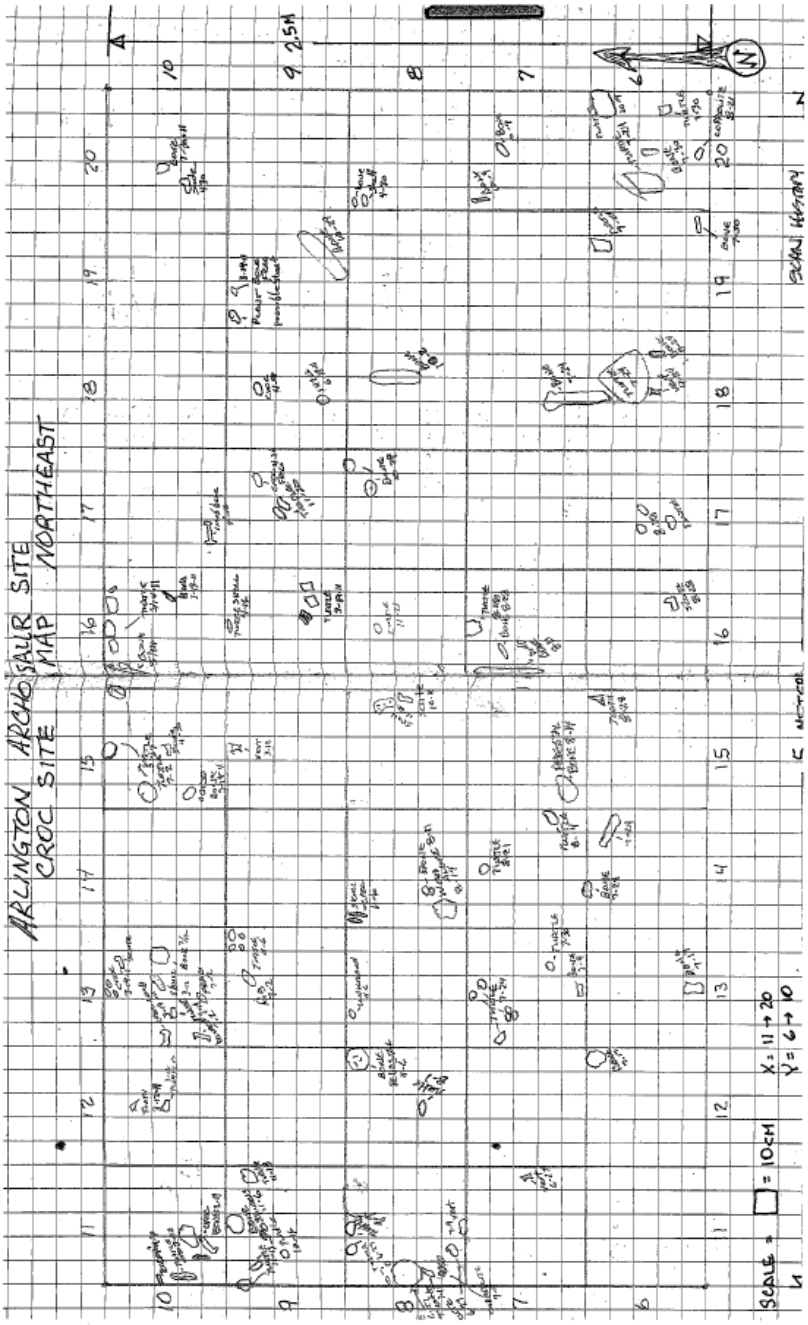

AAS Northeast-1 Map (21, =>30), (06,=>10)

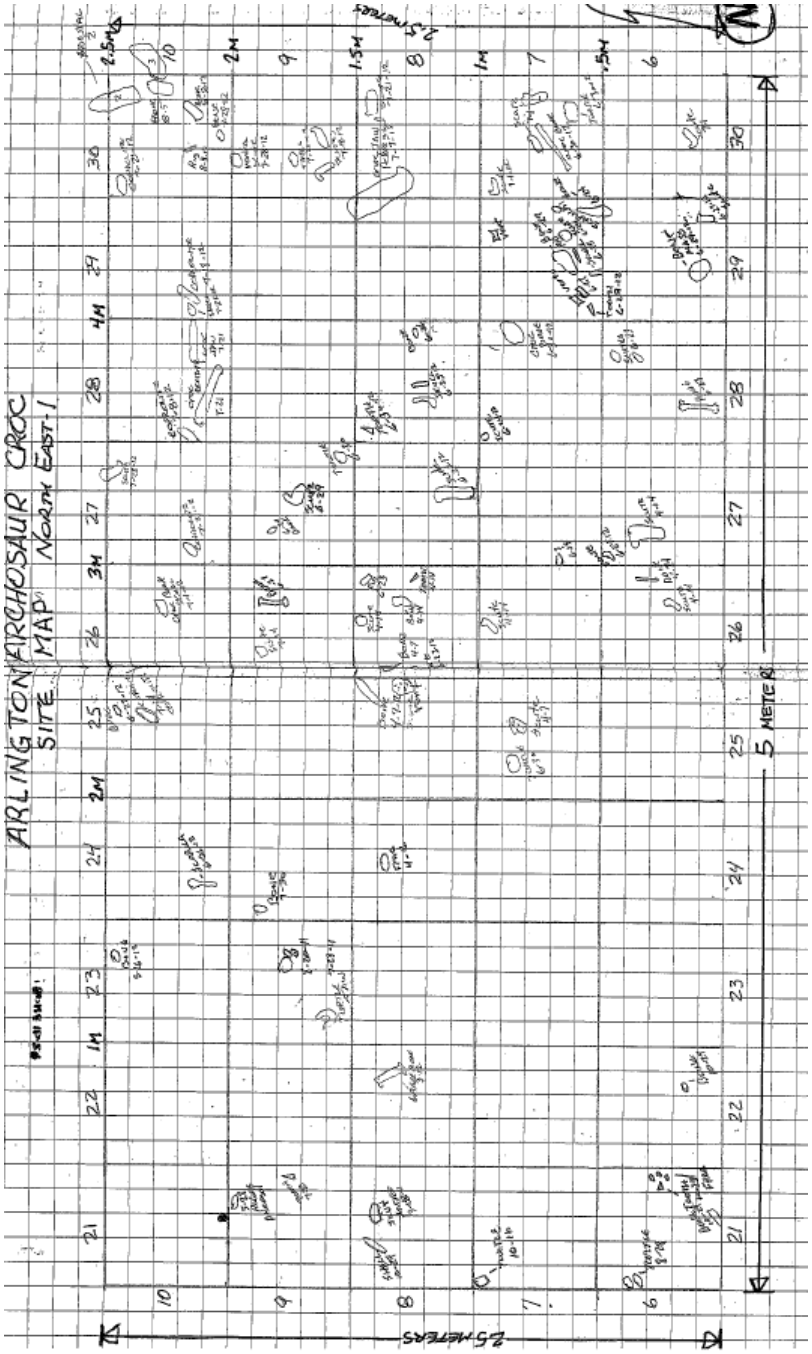

AAS Northeast-2 Map (31, =>40), (06=>10)

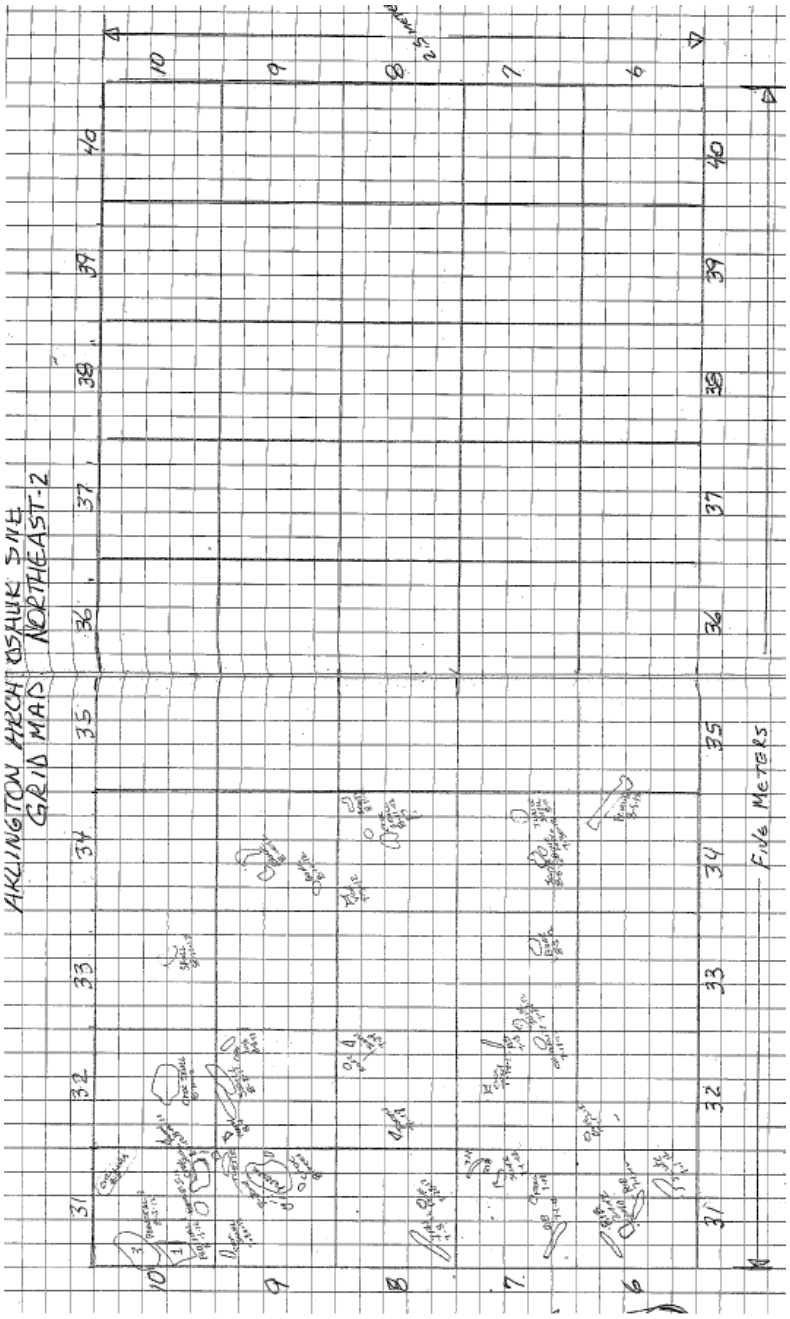

AAS North 1 Map (01=>10), (11=>15)

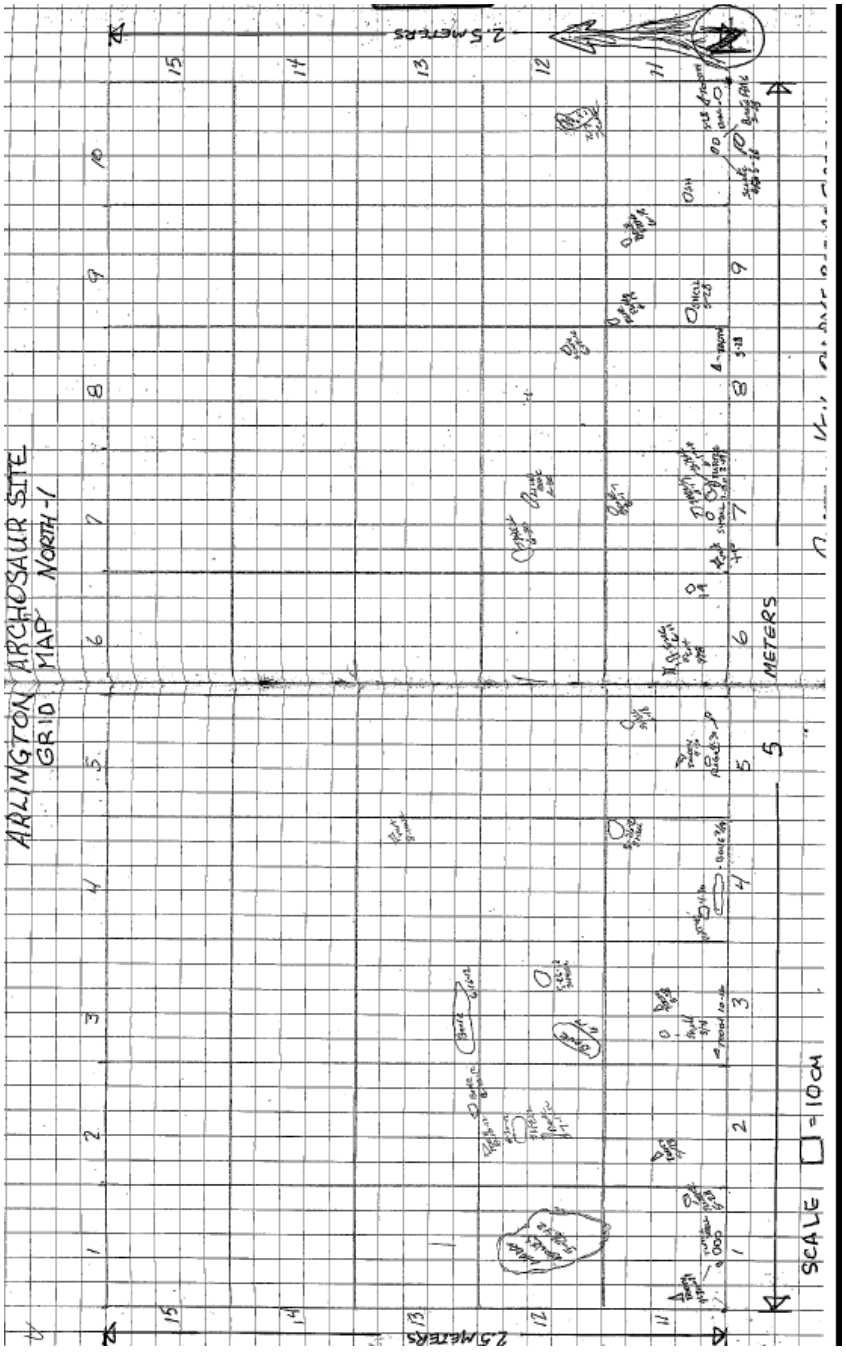

AAS North 1 West Map (01=>10), (11=>15)

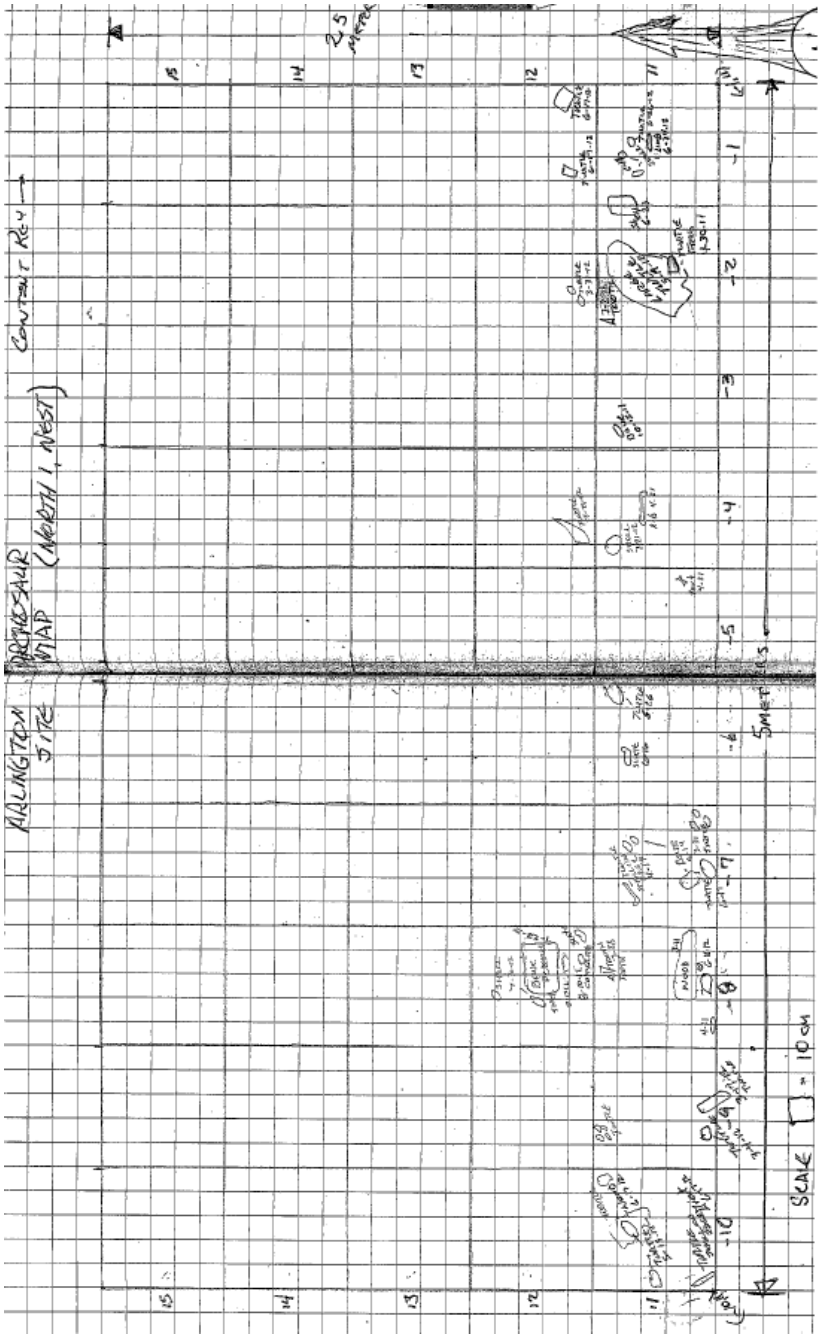

AAS North 1 West 1 Map (-11=>-20), (11=>15)

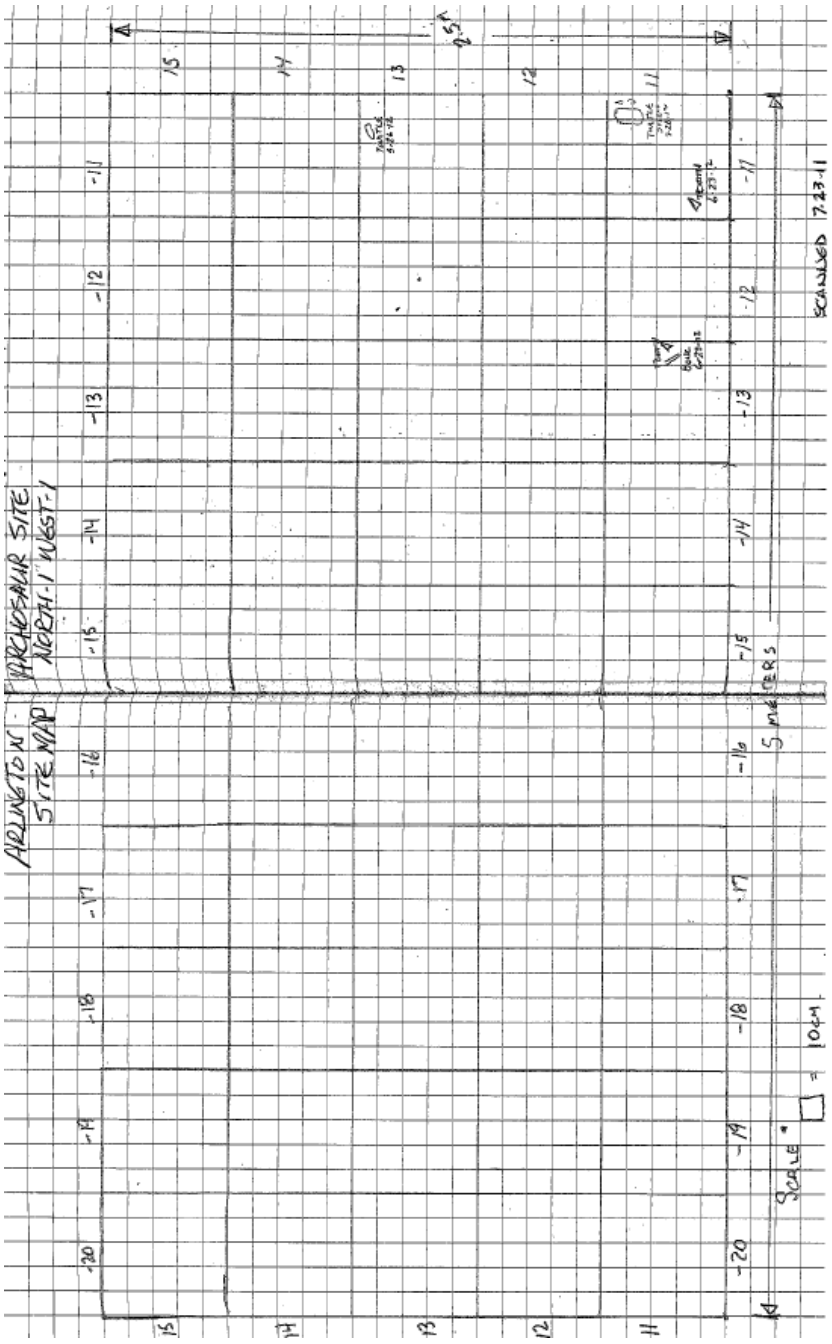

AAS North 1 East 1 Map (-21=>-30),(11=>15)

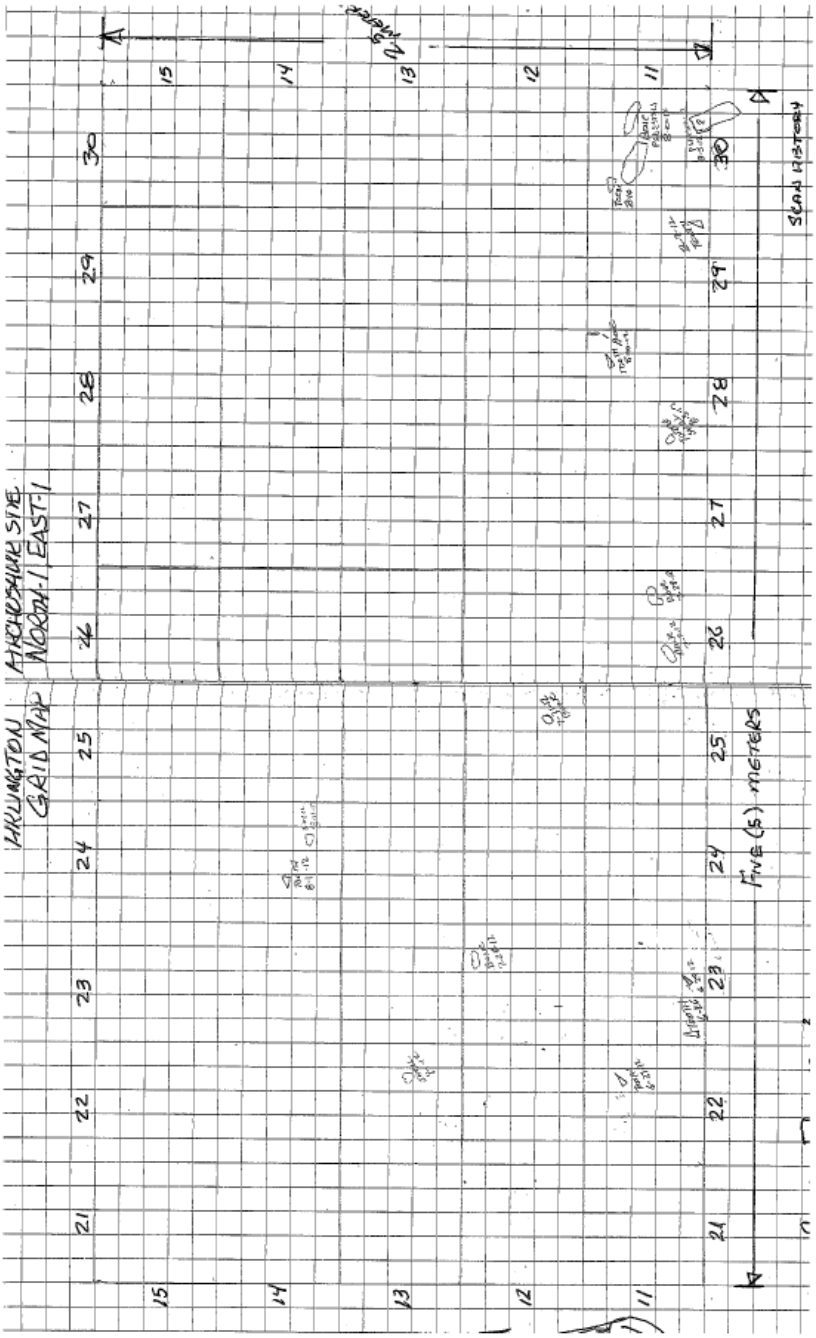

AAS North 1 East Map (10=>20), (11=>15)

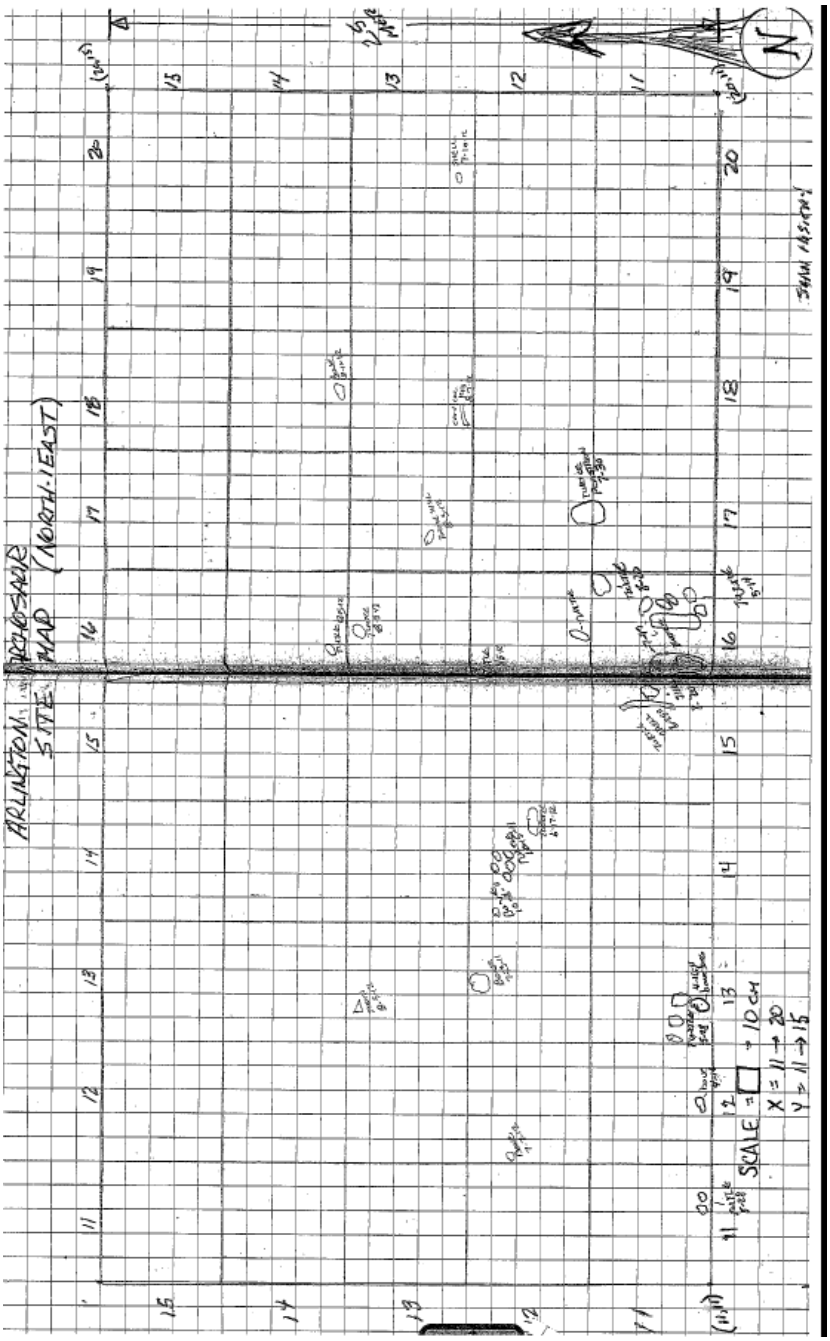

REFERENCES

Adams, T. L., Polcyn, M. J., Mateus, O., Winkler, D. A., and Jacobs, L. L. 2011. First Occurrence of the Long-Snouted Crocodyliform Terminonaris (Pholidosauridae) from the Woodbine Formation (Cenomanian) of Texas: Journal of Vertebrate Paleontology, (31), 712-716.

Agassiz, L. 1837. *Researches sur les Poissons Fossils*, (5), 1-1420.

Agassiz, L. 1882. Untersuchungen iber die fossilen Fishce der Lias Formation. Neus Jahrbuch fur Mineralogie, Geognosie, Geologie and Peterfaktenkunde (3), 139-149.

Algner, T. 1985. Storm Depositional Systems-Dynamic Stratigraphy in Modern and Ancient Shallow Marine Sequences. Lecture notes in Earth Science. Vol. 3. Springer Verlag, Berlin. 1-174.

Allen, E. 2010. Phylogenetic analysis of goniopholid crocodyliforms of the Morrison Formation. Journal of Paleontology, Supplement 30(2): 52A.

Allen, E., Main, D. J., and Noto, C. R. 2011. A New Crocodyliform from the Mid Cretaceous Woodbine Formation of Texas. Journal of Vertebrate Paleontology, Supplement. 31 (2): 61.

Amiot, R., Buffetaut, E., Tong, L. Boudad L, and Kabiri, L. 2004. Isolated theropod teeth from the Cenomanian of Morocco and their paleobiogeographical significance. Revue dePaleobiologie, volume spécial 9, 143-149.

Andrade, M. B., Edmonds, R., Benton, M. J., and Schouten, E. 2011. A new Berriasian species of Goniopholis (Mesoeucrocodylia, Neosuchia) from England and a review of the genus Zoological Journal of the Linnean Society, (163), 66-108.

Aslan, A., Autin, W. J., and Blum, M. D. 2005. Causes of river avulsion; insights from the late Holocene avulsion history of the Mississippi River, USA. Journal of Sedimentary Research, (75), 650-664.

Bader, K. S., Hasiotis, S. T., and Martin, L. D. 2009. Application of forensic science techniques to trace fossils on dinosaur bones from a quarry in the Upper Jurassic Morrison Formation, northeastern Wyoming: Palaios, (24), 140-158.

Bakker, R. T., Williams, M., and Currie, P. 1988. Nanotyrannus, a new genus of pygmy tyrannosaurus from the Latest Cretaceous of Montana. Hunteria, 1(5). 1-30.

Basham, A. L. 1989. The Origins and Development of Classical Hinduism. Zysk, K. (ed). New York: Oxford University Press. 1-15.

Behrensmeyer, A. K. 1978. Taphonomic and ecologic information from bone weathering: Paleobiology, (4) 150-162.

Behrensmeyer, A. K., Western, D., and Dechant Boaz, D. E., 1979. New perspectives invertebrate paleoecology from a recent bone assemblage: Paleobiology, (5) 12-21.

Behrensmeyer, A. K. and Hook, R.W. 1992. Paleoenvironmental contexts and taphonomic modes, *In* Behrensmeyer, A. K., Damuth, J. D., DiMichele, W. A., Potts, R., Sues, H.-D., and Wing, S. L., eds., Terrestrial ecosystems through time: evolutionary paleoecology of terrestrial plants and animals: University of Chicago Press, Chicago, 15-136.

Bennett, G. E. 2012. Community structure and paleoecology of crocodyliforms from the upper Hell Creek Formation (Masstrichtian) of eastern Montna, based on shed teeth. Jeffersonia, (28), 1-15.

Bennett, G. E., Main, D. J., Noto, C., and Anderson, K. B. 2011. Microvertebrate Paleoecology, Wildfires and Biodiversity of Coastal Appalachia from the Cretaceous (Cenomanian) Woodbine Formation at the Arlington Archosaur Site, North Central Texas. Journal of Vertebrate Paleontology, Supplement. 2012b.

Berg, L. S. 1940. Classification of fishes, both recent and fossil. *Trudy Zool. Inst. Leningrad* (51), 1-517.

Bergquist, H. R. 1949. The Woodbine Formation of Cooke, Grayson and Fannin Counties, Texas.USGS Oil and Gas Inventory. Preliminary Map 98.

Bhattacharya, J. P. and Walker, R. G. 1991. River and wave dominated depositional systems of the Upper Cretaceous Dunvegan Formation, northwestern Alberta. Bulletin of Canadian Peteroleum Geology, (39). 165-191.

Bhattacharya, J. P. and Walker, R. G. 1992. Deltas. Walker, R. G. and James, N. P. (eds.) *In* Facies Models, Response to Sea Level Change. Geological Association of Canada, 157-177.

Bhattacharya, J. P. and Walker, B. J. 2001. Lowstand deltas in the Frontier Formation, Powder River Basin, Wyoming: Implications for sequence stratigraphic models. AAPG Bulletin, 85 (2), 261-292.

Binford, L. R. 1981. Bones: Ancient Men and Modern Myths: Academic Press, New York. 21-30.

Boggs, S. 1995. Physical Properties of Sedimentary Rocks, Sedimentary Structures. *In* Principles of Sedimentology and Stratigraphy 2nd edition. Prentice Hall. 78-154.

Boyd, C. A., Drumheller, S. K., and Gates, T. A. 2013. Crocodyliform Feeding Traces on Juvenile Ornithischian Dinosaurs from the Upper Cretaceous (Campanian) Kaiparowits Formation, Utah. PLoS One 8 (2). e57605. doi:10.1371/journal.pone.0057605.

Brewer, R. and Sleeman, J. R. 1964. Glaebules; Their definition, classification and interpretation. Journal of Soil Science, (15). 66-78.

Brett-Surman, M. K. 1979. Phylogeny and paleobiogeography of the hadrosaurian dinosaurs. Nature, 277. 560-562.

Brett-Surman, M. K. and Wagner, J. R. 2007. Discussion of Character Analysis of

the Appendicular Anatomy in Campanian and Maastrichtian North American hadrosaurids-Variation and Ontogeny. *In* Carpenter, K. (ed.), Horns and Beaks, Ceratopsian and Ornithopod Dinosaurs. Indiana University Press. 135-169.

Brinkman, D. L, Cifelli, R. L., and Czapleski, N. J. 1998. First occurrence of *Deinonychus antirrhopus* (Dinosauria: Theropoda) from the Antlers Formation (Lower Cretaceous: Aptian-Albian) of Oklahoma. Oklahoa Geological Survey Bulletin, (146), 1-27.

Brinkman, D. B., Russell, A. P., Eberth, D. A., and Peng, J. 2004. Vertebrate paleocommunities of the lower Judith River (Campanian) of southeastern Alberta, Canada, as interpreted from vertebrate microfossil assemblages. Paleogeography, Paleoclimatiligy, Paleoecology, (213), 295-313.

Brochu, C. A. 2001. Crocodylian snouts in space and time: Phylogenetic approaches toward adaptive radiation: American Zoology, (41) 564-585.

Brochu, C. A. 2003. Phylogenetic Approaches toward Crocodylian History: Annual Review of Earth & Planetary Sciences, (31), 357-397.

Brochu, C. A., Njau, J. Blumenschine, R. J., and Densmore, L. D. 2010. A new hornedcrocodile from the Plio-Pleistocene hominid sites at Olduvai Gorge, Tanzania: PLoS One, (5), p. e9333, doi: 10.1371/journal.pone.0009333.

Bromley, S., Pemberton, G., and Rahmani, R. A. 1984. A Cretaceous woodground; the *Teredolites* ichnofacies. Journal of Paleontology, 58 (2). 488-498.

Brown, B. 1907. The Hell Creek Beds of the Upper Cretaceous of Montana: their relation to the contiguous deposits, with faunal and floral lists and a discussion of their correlation. Bulletin of the American Museum of Natural History, 55.1, 77 (78.6), 823-845.

Brown, S. A. E., Scott, A. C., Glasspool, I. J., and Margaret, E. C. 2012. Cretaceous wildfires and their impact on the Earth system. Cretaceous Research (2012), 1-29.

Bruton, M. N. 2003. Lungfishes and Coelacanths. *In:* Paxton, J. R. and W. N. Eschmeyer, Encyclopedia of Fishes. 70-73.

Buffetaut, E. and M. Ouaja. 2002. A new specimen of *Spinosaurus* (Dinosauria, Theropoda)From the Lower Cretaceous of Tunisia, with remarks on the evolutionary history of the Spinosauridae. Bulletin de la Societe Geologique de France (173), 415-421.

Byers, S. N. 2005. Introduction to forensic anthropology: a textbook: Pearson, Allyn and Bacon, New York. 1-246.

Caceres, I. and Alisna, J. M. 2012. A detailed event by event analysis of suspended sediment concentrations in the swash zone. Continental Shelf Research. In press.

Caldwell, M. W. 1999. Squamate phylogeny and the relationships of snakes and mosasaurids. Zoological Journal of the Linnean Society, (125), 115- 147.

Campbell, H. W. 1972. Ecological or phylogenetic interpretations of crocodilian

nesting habits. Nature, (238), 404-405.

Carpenter, K. and Lindsey, D. 1980. The dentary of *Brachychampsa montana* Gilmore (Alligatorinae; Crocodylidae), a Late Cretaceous turtle-eating alligator: Journal of Paleontology, (54), 1213-1217.

Carpenter, K. and Alf, K. 1994. Global distribution of dinosaur eggs, nests and babies. *In* Dinosaur Eggs and Babies. Carpenter, K., Kirsch, K. and Horner, J. (eds). Cambridge University Press. 15-30.

Carpenter, K. 1998. Evidence of predatory behavior by carnivorous dinosaurs: GAIA, (15), 135-144.

Carpenter, K. 1999. The Nest. *In* Eggs, Nests and Baby Dinosaurs, a Look at Dinosaur Reproduction. Indiana University Press. 152-178.

Carpenter, K., Miles, C., and Cloward, K. 2005a. New small theropod from the Upper Jurassic Morrison Formation of Wyoming. *In* Kenneth Carpenter (ed.), The Carnivorous Dinosaurs. Indiana University Press, Bloomington, Indiana. 23-48.

Carpenter, K., Miles, C., Ostrom, J. H., and Cloward, K.. 2005b. Redescription of the small maniraptoran theropods *Ornitholestes* and *Coelurus* from the Upper Jurassic Morrison Formation of Wyoming. *In* Kenneth Carpenter (ed.), The Carnivorous Dinosaurs. Indiana University Press, Bloomington, Indiana. 49-71.

Carpenter, K. and Wilson, Y. 2008. A new Species of *Camptosaurus*

(Ornithopoda: Dinosauria) from the Morrison Formation (Upper Jurassic) of Dinosaur National Monument, Utah and a Biomechanical Analysis of its Forelimbs. Annals of the Carnegie Museum, 76 (4), 227-263.

Carr, D. A. 1991. Facies and depositional environments of the coal bearing upper carbonaceous member of the Wepo Formatiom (Upper Cretaceous), northeastern Black Mesa, Arizona. Geological Society of America Special Paper 260, 161-188.

Carroll, R. 1988. Vertebrate Paleontology and Evolution. McGill University. W. H. Freeman and Company. 1-696.

Carroll, R. 2009. The Ancestry of Salamanders. *In* The Rise of the Amphibians, 365 Million Years of Evolution. Johns Hopkins University Press. Baltimore, Maryland. 267-290.

Casanovas, M. L., Suberbiola, X. P., Santafe, J. V., and Weishampel, D. B. 1999. First lambeosaurine hadrosaurid from Europe: paleobiological implications. Geol. Mag, 136 (2), 205-211.

Chapman, R. E. and Brett-Surman, M. K. 1990. Morphometric observations on hadrosaurid dinosaurs. *In* K. Carpenter and P. J. Currie (eds.), Dinosaur Systematics: Approaches and Perspectives. Cambridge University Press. 163-177.

Chin. K. 1996.The paleobiological implications of herbivorous dinosaur coprolites: ichnologic, petrographic and organic geochemical investigations. Dissertation, University of Califronia Santa Barbara. 1-171.

Chin, K. 2007. The paleobiological implications of herbivorous dinosaur coprolites from the Upper Cretaceous Two Medicine Formation of Montana: why eat wood?: Palaios, (22), 554-566.

Chin, K., Eberth, D. A., Schweitzer, M. H., Rando, T. A., Sloboda, W. J., and Horner, J. R. 2003. Remarkable preservation of undigested muscle-tissue within a Late Cretaceous tyrannosaurid coprolite from Alberta, Canada: Palaios, (18), 286-294.

Chure, D. J., Fiorillo, A. R., and Jacobsen, A. 1998. Prey bone utilization by predatory dinosaursin the Late Jurassic of North America, with comments on prey bone use by dinosaurs throughout the Mesozoic: GAIA (15), 227–232.

Cifelli, R. L., Nydam, R. L., Gardner, J. D., Weil, A. Eaton, J. G., Kirkland, J. I., and Madsen, S. K. 1999. Medial Cretaceous Verteberates from the Cedar Mountain Formation, Emery County Utah; the Mussentuchit Local Fauna. *In* Vertebrate Paleontology in Utah. Gillette, D. G. (ed.) Utah Geological Survey Publication 99-1, 219-238.

Cleuren, J. and De Vree, F. 2000. Feeding in crocodilians, *In* Schwenk, K., ed., Feeding: form, function, and evolution in tetrapod vertebates: Academic Press, San Diego. 337–358.

Collins, M. E. and Kuel, R. J. 2001. Organic Matter Accumulation and Organic Soils. *In* Wetland Soils; Genesis, Hydrology, Landscapges and Classification. Richardson, J. L. and Vepraskas, M. J. (eds) CRC Press. 137-162.

Collinson, J. D. 1969. The sedimentology of the Grindslow Shales and the Kinderscout Grit; a deltaic complex in the Namurian of northern England: Journal of Sedimentary Petrology, (39), 194-221.

Collinson, M. E., Steart, D. C., Glasspool, I. J., and Hooker, J. J. 2007. Episodic fire, runoff and deposition at the Paleocene-Eocene boundary. Journal of the Geological Society of London, (164), 87-97.

Cope, E. D. 1875. Ckeck-list of North American Batrachia and Reptilia with a systematic list of the higher groups and an essay on geographical distribution based on the specimens in the U.S. National Museum: Bulletin of the United States National Museum, (1), 1-104.

Cott, H. B. 1961. Scientific results of an inquiry into the ecology and economic status of the Nile Crocodile (Crocodilus niloticus) in Uganda and Northern Rhodesia: The Transactions of the Zoological Society of London, (29), 211-356.

Cousin, R., Breton, G., Fournier, R., and Watte, J. P. 1994. Dinosaur egglaying and nesting in France. *In* Dinosaur Eggs and Babies. Carpenter, K., Kirsch, K. and Horner, J. (eds). Cambridge University Press. 56-74.

Coy, C. E. 1995. The First Record of Sprial Coprolites from the Dinosaur Park Formation (Judith River Group, Upper Cretaceous) Southern Alberta, Canada. Journal of Paleontology, (69), 1191-1194.

Curanno, E. D., Jacobs, B. F., Pan, A. D., and Tabor, N. J. 2011. Inferring ecological disturbance in the fossil record: A case study from the Oligocene of Ethiopia. Paleogeography, Paleoclimatology, and Paleoecology, (309). 242-252.

Currie, P. 1987. Theropods from the Judith River Formation of Dinosaur National Provincial Park, Alberta, Canada. Tyrell Museum of Paleontology, Occasional Paper 3:52-60.

Currie, P., Rigby, K., and Sloan, R. E 1990. Theropod teeth from the Judith River Formation of Southern Alberta, Canada; *In* P. Currie and K. Carpenter (eds.), Dinosaur Systematics, Approaches and Perspectives. Cambridge University Press, New York, New York. 107-125.

Currie, P. and Carpenter, K. 2000. A new specimen of *Acrocanthosaurus atokensis* (Theropoda, Dinosauria) from the Lower Cretaceous Antlers Formation (Lower Cretaceous, Aptian) of Oklahoma, USA. Geodiversitas 22: 207-246.

Dalla Vechia, F. M. 2009. *Tethyshadros insularis*, a New Hadrosauroid (Dinosauria: Ornithischia) from the Upper Cretaceous of Italy. Journal of Vertebrate Paleontology 29 (4), 1100-1116.

Dalrymple, R. W. 1992. Tidal Depositional Systems. *In* Walker, R. and James, N. P. (eds.) Facies Models; Response to Sea Level Change, 195-218.

Davies-Vollum, K. S. and Smith, N. D. 2008. Factors Affecting the Accumulation of Organic Rich Deposits in a Modern Avulsive Floodplain: Examples from the Cumberland Marshes, Saskatchewan, Canada. Journal of Sedimentary Research, (78). 683-692.

D'Amore, D. C. and Blumenschine, R. J. 2009. Komodo monitor (*Varanus komodoensis*) feeding behavior and dental function reflected through tooth marks on bone surfaces, and the application to ziphodont paleobiology: Paleobiology, (35), 525-552.

Davidson, I. and Solomon, S. 1990. Was OH7 the victim of a crocodile attack?, *In* Solomon,S., Davidson, I., and Watson, D., (eds.), Problem Solving in Taphonomy: Archaeological and Palaeontological Studies from Europe, Africa and Oceania: Tempus, St. Lucia, Queensland. 197–206.

Davies, K. L. 1983. Hadrosaurian Dinosaurs of Big Bend National Park, Brewster County Texas. Unpublished M. S. Thesis University of Texas at Austin. 1-235.

Day, J. W., Britsch, L. D., Hawes, S. R., Shaffer, G. P., Reed, D. J., and Cahoon, D. 2000. Pattern and process of land loss in the Mississippi Delta:A spatial and temporal analysis of wetland habitat change. Estuaries, (23). 425-438.

Deitz, D. C. and Hines, T. C. 1980. Alligator Nesting in North Central Florida. Copeia, 1980 (2), 249-258.

Delany, F. and Abercrombie, C. L. 1986. American alligator food habits in northcentral Florida: The Journal of Wildlife Management, (50), 348-353.

Delfino, M., Piras, P., and Smith, T. 2005. Anatomy and phylogeny of the gavialoid crocodylian *Eosuchus lerichei* from the Paleocene of Europe: Acta Palaeontologica Polonica, (50), 565-580.

Delfino, M. and Smith, T. 2009. A reassessment of the morphology and taxonomic status of Crocodylus depressifrons Blaineville, 1855 (Crocodylia, Crocodyloidea) based on the Early Eocene remains of Belgium. Zoological Journal of the Linnean Society. (156), 140-167.

de Raaf, J. F. M., Reading, H. G., and Walker, R. G. 1965. Cyclic sedimentation in the Lower Westphalian of North Devon, England. Sedimentology, (4) 1-52.

DiMichele, W. A., Tabor, N. J.; Chaney, D. S., and Nelson, W. J. 2006. From wetlands to wetspots: Environmental tracking and the fate of Carboniferous elements in Early Permian tropical floras. Greb, S. F. and

DiMichelle, W. A. (eds.), *In* Wetlands Through Time. Geological Society of America Special Paper 399, 223-248.

Dixon, F. 1850. Geology and fossils of the Teriary and Cretaceous formations of Sussex. 1-422.

Dodge, C. F. 1952. Stratigraphy of the Woodbine Formation in the Arlington area, Tarrant Co., Texas. Field and Lab. 66-78.

Dodge, C. F. 1968. Stratigraphic Nomenclature of the Woodbine Formation Tarrant County, Texas. *In* C.F. Dodge (ed.), Field trip Guidebook, South Central Section, Stratigraphy of the Woodbine Formation, The Geological Society of America. 107-125.

Dodge, C. F. 1969. Stratigraphic Nomenclature of the Woodbine Formation Tarrant County, Texas. The Texas Journal of Science, (21), 43-62.

Dott, R. H. 1983. SEPM Presidential Address: Episodic Sedimentation-How Normal is Average and How Rare is Rare. Does it Matter? Journal of Sedimentary Petrology, 53 (1), 5-23.

Dunbar, J. D., Blaes, M. R., Duitt, S. E., May, J. R., and Stroud, K.W. 1994. *Geological Investigation of the Mississippi River Deltaic Plain*, Technical Report GL-84-15, U.S.Army Engineer Waterways Experiment, Vicksburg MS. 1-46.

Drumheller, S. 2007. Experimental taphonomy and microanalysis of crocodylian feeding traces: Microscopy and Microanalysis, (13), 510-511.

Dyson, I. A. 2007. Significance of hummocky cross stratification and quasi planar lamination in the Lower Devonian Walhalla Group at Cape Liptral, Victoria. Australian Journal of Earth Sciences An International Geoscience Journal of the Geological Society of Australia, 43 (2), 189-199.

Dyman, T. S., Cobban, W. A., Titus, A. L., Obradovich, J. D., Davis, L. E., Eves, R. L., Pollock, G. L., Takahashi, K. I., and Hester, T. C., 2002. New biostratigraphic and radiometric ages for Albian-Turonian Dakota Formation and Tropic Shale at Grand Staircase Escalante National Monument and Iron Springs Formation near Cedar City, Parowan, and Gunlock in SW Utah: Geological Society of America Abstracts with Programs, 34 (4), 13.

Eaton, J. G., Cifelli, R. L., Hutchinson, J. H., Kirkland, J. H., and Parrish, J. M. 1999. Cretaceous vertebrate faunas of the Kaiparowits Basin (Cenomanian-Campanian), southern Utah. *In* D. Gillette, (ed.). *Vertebrate Paleontology in Utah*, Utah Geological Survey. Miscellaneous Publication 99-1. 345-353.

Edmonds, D. A., Hoyal, D. C. J. D., Sheets, B. A., Slingerland, R. L. 2009. Predicting delta avulsions: Implications for coastal wetland restoration. Geology, 37 (8), 759-762.

Eberth, D. A., Braman, D. R., and Tokaryk, T. T. 1990. Stratigraphy,

sedimentology and vertebrate paleontology of the Judith River Formation (Campanian) near Muddy Lake, west central Saskatchewan. Bulletin of Canadian Petroleum Geology, 38 (4), 387-406.

Eberth, D. A. 2005. The Geology. *In* Phil Currie and Eva Koppelhus (eds.) Dinosaur Provincial Park; A Spectacular Ancient Ecosystem Revealed. Indiana University Press. 54-82.

Elder, W. P. and Kirkland, J. I. 1994. Cretaceous Paleogeography of the Southern Interior Region. *In* Mesozoic Systems of the Rocky Mountain Region, USA. Caputo, M. V., Peterson, J. A. and Franczyk, K. J. (eds). 415-440.

Ende, B. A. 1991. Depositional environments, palynology and age of the Dakota Formation, south central Utah. Nations, J. D. and Eaton J. G. (eds). *In* Stratigraphy, depositional environments and sedimentary tectonics of the western margin, Cretaceous Interior Seaway. Geological Society of America, Special Paper 260, 65-83.

Erickson, G. M. and Olson, K. H. 1996. Bite marks attributable to *Tyrannosaurus rex*: Preliminary description and implications: Journal of Vertebrate Paleontology, (16), 175-178.

Erickson, G. M., Lappin, K. H., and Vliet, K. A. 2003. The ontogeny of bite-force performance in American alligator (Alligator mississippiensis): Journal of Zoology, (260), 317-327.

Faccio, G. 1994. Dinosaurian eggs from the Upper Cretaceous of Uruguay. *In*

Dinosaur Eggs and Babies. Carpenter, K., Kirsch, K., and Horner, J. (eds). Cambridge University Press, 56-74.

Fanti, F. and Miyashita, T. 2009. A high latititude vertebrate fossil assemblage from the Late Cretaceous of west –central Alberta, Canada: evidence for dinosaur nesting and vertebrate latitudinal gradient. Paleogeography, Paleoclimatology, and Paleoecology, (275), 37-53.

Farlow, J. O. 1976. A Consideration of the Trophic Dynamics of a Late Cretaceous Large Dinosaur Community (Oldman Formation). Ecology, 57 (5), 841-857.

Farlow, J. O. 1993. The Dinosaurs of Dinsoaur Valley State Park. Texas Parks and Wildlife Department. 1-32.

Fastovsky, D. E. 1987. Paleoenvironments of Vertebrate Bearing Strata during the Cretaceous Paleogene transition of Eastern Montana and Western North Dakota. Palaios, (2), 282-295.

Fiorillo, A. R. 1988. Taphonomy of Hazard Homestead Quarry (Ogallala Group), Hitchcock County, Nebraska: Rocky Mountain Geology, (26), 57-97.

Fiorillo, A. R. 1989. The Vertebrate Fauna from the Judith River Formation (Late Cretaceous) of Wheatland and Golden Valley Counties, Montana. The Mosasaur, (4), 127-142.

Fiorillo, A. R. 1991a. Prey bone utilization by predatory dinosaurs: Palaeogeography,Palaeoclimatology, Palaeoecology, (88), 157-166.

Fiorillo, A. R. 1991b.Taphonomy and depositional setting of Careless Creek Quarry (Judith River Formation), Wheatland County, Montana, U.S.A.: Palaeogeography Palaeoclimatology, Palaeoecology, (81), 281-311.

Fiorillo, A. R. and P. Currie. 1994. Theropod teeth from the Judith River Formation (Upper Cretaceous) of south central Montana. Journal of Vertebrate Paleontology, (14), 74-80.

Fiorillo, A. R., Padian, K., and Musikasinthorn, C. 2000.Taphonomy and Depositional Setting of the Placerias Quarry (Chinle Formation: Late Triassic, Arizona): Palaios, (15), 373-386.

Fisher, D. C. 1981. Crocodilian scatology, microvertebrate concentrations, and enamel-less teeth: Paleobiology, (7), 262-275.

Forrest, R. 2003. Evidence for scavenging by the marine crocodile *Metriorhynchus* on the carcass of a plesiosaur: Proceedings of the Geologists' Association, (114), 363-366.

Fowler, D. W. and Sullivan, R. M. 2006. A ceratopsid pelvis with toothmarks from the Upper Cretaceous Kirtland Formation, New Mexico: evidence of late Campanian tyrannosaurid feeding behavior: New Mexico Museum of Natural History and Science Bulletin, (35), 127-130.

Fry, R. and Main, D. J. 2010. Mapping and recording the excavation of a Mid-

Cretaceous crocodile (Archosauria: Goniopholidae) at an urban dig utilizing a Cartesian mapping system: the Arlington Archosaur Site, Arlington TX. Journal of Vertebrate Paleontology Supplement, 3 (30). 126

Frey, E., Buchy, M. C., Stinnesbeck, W., and Lopez-Olivia, J. G. 2002. *Geosaurus vignaudi* n. sp. (Crocodyliformes: Thalatosuchia), first evidence of metriorhynchid crocodilians in the Late Jurassic (Tithonian) of central – east Mexico (State of Puebla). Canadian Journal of Earth Sciences, (39). 1467-1483.

Fuentes, E. J. 2003. Predación crocodiliana a quelonios. Un Neochelys (Pelomedusidae), del Eoceno de Zemora, lisiando por un *Asiatosuchus*: Studia Geologica Salmanticensia, (39), 1101-1123.

Galton, P. M. and P. Taquet. 1982. *Valdosaurus*, a hypsilophodontid dinosaur from the Lower Cretaceous of Europe and Africa. Geobios (15), 147-159.

Gangloff, R. 1998. Arctic Dinosaurs with emphasis on the Cretaceous Record of Alaska and the Eurasian-North American Connection. Lucas, S. G., Kirkland, J. I., Estep, J.W. (eds.), *In* Lower and Middle Cretaceous Terrestrial Ecosystems. New Mexico Museum of Natural History and Science Bulletin (14). 211-220.

Gasparini, Z., Diego, P., and Spalletti, L. A. 2006. An Unusual Marine Crocodyliform from the Jurassic-Cretaceous Boundary of Patagonia. Science express, (311), 71-73.

Gastaldo, R. A. 1992. Sediment Facies, Depositional Environments, and Distribution of Phytoclasts in the Recent Mahakam River Delta, Kalimantan, Indonesia. Palaios, (7), 574-590.

Gill, T. 1872. Arrangement of the families of fishes, or classes, Pisces, Marsipobranchii, and Leptocardii: Smithsonian Miscellaneous Collections (11), 1-49.

Gilmore, C. W. 1919. Reptilian Faunas of the Torrejon, Puerco and underlying Upper Cretaceous Formations of San Juan County, New Mexico. Department of the Interior, U. S. Geological Survey Professional Paper 119. 1-96.

Gilmore, C. W. 1933a. On the dinosaurian fauna from the Iren Dabasu Formation. Bulletin of the American Museum of Natural History. (67), 27-78.

Gilpin, D., DiCroce, T., and Carpenter, K. 2007. A Possible New Basal Hadrosaur from the Lower Cretaceous Cedar Mountain Formation of Eastern Utah. *In* K. Carpenter (ed.), Horns and Beaks, Ceratopsian and Ornithopod Dinosaurs, Indiana University Press. 79-89.

Godefroit, P., Dong, Z. M., Bultynck, L., Li, H., and Feng, Lu. 1998. Cretaceous Dinosaurs and Mammals from Inner Mongolia. New *Bactrosaurus* (Dinosauria: Hadrosauridae) material from Iren Dabasu (Inner Mongolia, P. R. China). Bulletin de l'Institute Royal des Sciences Naturelles de Belgique Supp. 68. 3-70.

Goswami, A. 2011. Predicting the Geographic Distribution of Ancient Soils with Special Reference to the Cretaceous. Ph. D. Dissertation. University of Texas at Arlington. 1-362.

Gould, H. R. 1970. "The Mississippi Delta Complex" *Deltaic Sedimentation: Modern and Ancient, SEPM Special Publication 15,* Morgan, J. P. (ed.), Society of Economic paleontologists and Mineralogists, Tulsa Oklahoma, 3-30.

Grigorescu, D., Weishampel, D. W., Norman, D., Seclamen, M., Rusu, M., Blatres, A., and Teodorescu, V., 1994. Late Maastrichtian dinosaur eggs from the Hateg Basin (Romania). *In* Dinosaur Eggs and Babies. Carpenter, K., Kirsch, K. and Horner, J. (eds). Cambridge University Press. 75- 87.

Hancock, J. M. and Kauffman, E. G. 1979. The great transgressions of the Late Cretaceous. Journal of the Geological Society of Lonon. (136). 175-186.

Hantzschel, W., el-Baz, F., and Amstutz, G. C. 1968. Coprolites: an annotated bibliography. Geological Society of America, Memoir 108, Boulder, Colorado. 1-121.

Hasiotis, S. T. 2002. Continental Trace Fossils. SEPM Short Course Notes, (51), 1-131.

Hatcher, J. B. 1893. The Ceratopsiabeds of Converse County, Wyoming, American Journal of Science, (3), 395-402.

Hatcher, J. B. 1903. Relative age of the Lance Creek (Ceratops) beds of Converse

County, Wyoming., the Judith River Beds of Montana and the Belly River beds of Canada. American Geology, (31), 369-375.

Haq, B. U., Hardenbol, J. and Vail, P. R. 1987. Chronology of Fluctuating Sea Level Since the Triassic. Science, (235), 1156-1168.

Heckel, J. 1856. Beitrage zur Kenntniss der fossilen Fische Osterreichs, Denkschriften des kaiserlichen Akademie der Wissenschaften, Mathematicsch-Naturewissenchaftliche Klasse XI. 187-214.

Heinrich, G. L. and Walsh, T. J. 2012. American Alligator of the Southern United States. A Guide to its Natural History. Quick Reference Publishing. 1-14.

Head, J. 1998. A new species of basal hadrosaurid (Dinosauria, Ornithischia) from the Cenomanian of Texas. Journal of Vertebrate Paleontology (18), 718-738.

Hernandez-Divers, S. J., Hensel, P., Gladden, J., Hernandez-Divers, S. M., Buhlmann, K. A.,Hagen, C., Sanchez, S., Latimer, K. S., Ard, M., and Camus, A. C. 2009. Investigation of shell disease in map turtles (*Graptemys* spp.): Journal of Wildlife Diseases, (45), 637-652.

Hill, R. T. 1901. Geography and geology of the Black and Grand Prairies, Texas: with detailed descriptions of the Cretaceous formations and special reference to artesian waters: U.S. Geological Survey, 21st Annual Report 1899-1900, 1-666.

Hedlund, R. W. 1966. Palynology of the Red Branch Member of the Woodbine Formation. Oklahoma Geological Survey, Bulletin 112, 6-42.

Holbrook, J. and Dunbar, R. W. 1992. Depositional history of Lower Cretaceous strata in northeastern New Mexico: Implications for regional tectonics and depositional sequences. Geological Society of America Bulletin, (104), 802-813.

Holbrook, J. M. 1996. Complex Fluvial Response to Low Gradients at Maximum Regression: A Genetic Link Between Smooth Sequence Boundary Morphology and Architecture of Overlying Sheet Sandstone. Journal of Sedimentary Research, 66 (4), 713-722.

Holbrook, J, M. 2001. Origin, genetic relationships and stratigraphy over the continuum of fluvial channel form bounding surfaces:an illustration from middle Cretaceous strata, southeastern Colorado. Sedimentary Geology, (144), 179-222.

Holland, W. J. 1905. A New Crocodile from the Jurassic of Wyoming. Annals of the Carnegie Museu, (3), 430-434.

Holman, J. A. 2006. Fossil Salamander of North America. Indiana University Press. 1-232.

Holtz, T. R. Jr. 2002. Theropod predation: evidence and ecomorphology. *In*: P.H. Kelly, M. Koweleski, and T.A. Hansen (eds.), Predator−Prey Interactions

in the Fossil Record. Topics in Geobiology 17, Kluwer, Plenum, New York. 325–340.

Hooley, R. W. 1907. On the skull and greater portions pf the skeleton of Goniopholis crassidens from the Wealdon shales of Atherfield (Isle of Wight). Quarterly Journal of the Geological Society, (63), 50-63.

Horner, J. R. 1982. Evidence of colonial nesting and site fidelity among ornithischian dinosaurs. Nature, 297 (24), 675-676.

Horner, J. R. 1983. Cranial Osteology and Morphology of the Type Specimen of Maiasaura Peeblesorum (Ornithischia: Hadrosauridae), with discussion of its Phylogenetic Position. Journal of Vertebrate Paleontology, 3 (1), 29-38.

Horner, J. R. 1984c. The nesting behavior of dinosaurs. Scientific American, (250), 130–137.

Horner, J. R. and Lessem, D. 1993. The Complete T. rex. Simon and Schuster. New York. 1-238.

Horner, J. R. and Dobb, E. 1997. Dinosaur Lives. Harvest Books. 1-244.

Horner, J. R., Weishampel, D. B., and Forster, C. A. 2004. Hadrosauridae. Weishampel, D., Dodson, P., and Osmolska, H. (eds.), *In* The Dinosauria 2nd edition, University of California Press, Berkeley. 438- 463.

Horner, J. R., Goodwin, M. B., and Myhrvold, N. 2011. Dinsoaur census reveals

abundant *Tyrannosaurus* and rare ontogenetic stages in the Upper Cretaceous Hell Creek Formation (Maastrichtian) Montana, USA. PLoS One, 6 (2), 1-9.

Hua, S., Buffetaut, E., Legall, C., and Rogron, P. 2007. *Oceanosuchus boecensis* n. gen, n. sp., a marine pholidosaurid (Crocodylia, Mesosuchia) from the Lower Cenomanian of Normandy (western France): Bulletin de la Societe Geologique de France, (178), 503-513.

Huxley, T. H. 1858. On a New species of Plesiosaurus from Street, near Glastonbury; with Remarks on the Structure of the Atlas and Axis vertebrae, and the cranium in that genus. Quarterly Journal of the Geological Society, (14), 281-294.

Jacobs, L. L. and D. A. Winkler. 1998. Mammals, archosaurs and the early to lateCretaceous transition in North-Central Texas; *In* Y. Tomida, L. J. Flynn and L. L. Jacobs (eds.), Advances in Vertebrate Paleontology and Geochronology. National Science Museum Monographs 14, 253-280.

Jacobsen, A. R. 2001. Tooth-marked small theropod bone: an extremely rare trace, *In* Tanke, D.H., and Carpenter, K., (eds.), Mesozoic Vertebrate Life: Indiana University Press, Bloomington, 58-63.

Jamniczky, H. A., Brinkman, D. B., and Russel, A. P. 2003. Vertebrate microsite sampling: how much is enough?: Journal of Vertebrate Paleontology, (23), 725-734.

Joanen, T. 1969. Nesting ecology of alligators in Louisiana. Proc. Ann. Conf. Southeast Assn. Game and Fish Commision, (23), 141-151.

Johnson, R. O. 1974. Lithofacies and depositional environments of the Rush Creek Member of the Woodbine Formation (Gulfian) of North Central Texas. Masters Thesis, University of Texas at Arlington. 1-158.

Karl, T. R., Melilo, J. M., Peterson, T. C., and Hassol, S. J. 2009. Global Climate Change Impacts on the United States. Cambridge University Press. 1-192.

Kauffman, E. G. 1969. Cretaceous marine cycles in the Western Interior. The Mountain Geologist, (6), 227-245.

Kemp, A. 1997. A revision of Australian Mesozoic and Cenozoic lungfish of the family Neoceratodontidae (Osteichthys: Dipnoi), with a description of four new species. Journal of Paleontology, (71), 713-733.

Kemp, A., 1998. Skull structure in post-Paleozoic lungfish. Journal of Vertebrate Paleontology, 18 (1), 1-43.

Kemp, A. 2002. Unique Dentition of Lungfish. Microscopy Research and Technique, (59), 435-448.

Kennedy, W. J. and Cobban, W. A. 1990. Cenomanian ammonite faunas from the Woodbine Formation and lower part of the Eagle Ford Group, Texas. Paleontology, (33), 75-154.

Kingsland, S. E. 1991. Foundational Papers: Defining Ecology as a Science.

Foundations of Ecology, Classic Papers with Commentaries. Real, L. A. and Brown, J. H. (eds). The University of Chicago Press. 1-13.

Kirkland, J. I. 1987. Upper Jurassic and Cretaceous Lungfish Tooth Plates from the Western Interior, the Last Dipnoan Faunas of North America. Hunteria, (2), 1-16.

Kirkland, J. I. 1996. Paleontology of the Greenhorn cylcothem (Cretaceous: late Cenomanian to middle Turonian) at Black Mesa, northeastern Arizona. New Mexico Museum of Natural History and Science. Bulletin 9, 1-122.

Kirkland, J. I., Britt, B., Burge, D. L., Carpenter, K., Cifelli, R., Decourten, F., Eaton, J., Hasiotis, S., and Lawton, T. 1997. Lower to Middle Cretaceous Dinosaur Faunas of the Colorado Plateau; Key to Understanding 35 Million years of Tectonics, Sedimentology, Evolution and Biogeography. BYU Geology Studies, 42 (2), 69- 103.

Kirkland, J. I. 1998. Morrison Fishes. Modern Geology. Pp. 503-533.

Kirkland, J. I. 1998. A new hadrosaurid from the Upper Cedar Mountain Formation (Albian-Cenomanian: Cretaceous) of Eastern Utah-The oldest known hadrosaurid (Lambeosaurine?). *In* Lower and Middle Cretaceous Terrestrial Ecosystems. Lucas, S. G., Kirkland, J. I. and Estep, J. W. (eds.), New Mexico Museum of Natural History and Science Bulletin, (14), 283-302.

Kirkland, J. I., Cifelli, R. L., Britt, B. B., Burge, D. L., DeCourten, F. L., Eaton, J.

G., and Parrish, J. M. 1999. Distribution of Vertebrate faunas in the Cedar Mountain Formation, East Central Utah. *In* Vertebrate Paleontology in Utah. Gillette, D. G. (ed.) Utah Geological Survey Publication 99-1, 201-217.

Kirkland, J. I. 2005. Utah's newly recognized dinosaur record from the Early Cretaceous Cedar Mountain Formation. Utah Geological Survey Notes. 37 (1), 1-5.

Kirkland, J. I. and Madsen, S. K. 2007. The Lower Cretaceous Cedar Mountain Formation, Eastern Utah: The View up an always interesting learning curve. Field Trip Guide. Geological Society of America Rocky Mountain Section Annual Meeting.Utah Geological Association Publication 35. 1-108.

Koken, E. 1887. Die Dinosaurier, Crocodiliden und Sauropterygier des norddeutschen Wealden.Geol. Palaont. Abh. (3), 311-419.

Kolb, C. R. and Van Lopik, J. R. (1958). *Geology of the Mississippi River Deltaic Plain,Southern Louisiana,* Technical Report No. 3-483, U.S. Army Engineer Waterways Eperiment Station, Vicksburg , MS. 1-39.

Kumar, N. and Sanders, J. E. 1976. Characteristics of shoreface storm deposits: modern and ancient examples. Journal of Sedimentary Petrology. (46), 145-162.

Kraus, M. J. 1996. Avulsion Deposits in Lower Eocene Alluvial Rocks, Bighorn

Basin, Wyoming. Journal of Sedimentary Research, 66 (2), 354-363.

Lang, J. W. 1999. Social Behavior. *In* Crocodiles and Alligators. Ross, C. A. (ed) Facts on File. New York. 102-117.

Lee, Y. N. 1997a. Bird and dinosaur footprints in the Woodbine Formation (Cenomanian), Texas. Cretaceous Research, (18), 840-864.

Lee, Y. N. 1997b. The archosauria from the Woodbine Formation (Cenomanian) in Texas. Journal of Paleontology, 71(6), 1147-1156.

Leeds, E. T. 1908. On the Metriorhynchus brachyrhynchus (Deslong) from the Oxford Clay near Peterborough. Quarterly Journal of the Geological Society. (64), 345-357.

Lehman, T. and Coulson, A. B. 2002. A juvenile specimen of the sauropod dinosaur *Alamosaurus sanjuanensis* from the Upper Cretaceous of Big Bend National Park, Texas. Journal of Paleontology, 76 (1), 156-172.

Lehman, T. M., McDowell, F. W., and Connelly, J. N. 2006. First isotopic (U-PB) age for the Late Cretaceous *Alamosaurus* vertebrate fauna of west Texas and its significance as a link between two faunal provinces. Journal of Vertebrate Paleontology, 26 (4). 922-928.

Liu, K. B. and Fearn, M. L. 1993. Lake-sediment record of late Holocene hurricane activities from coastal Alabama. *Geology,* (21), 793-796.

Liu, K. B. and Fearn, M. L. 2000a. Reconstruction of Preshistoric Landfall

Frequencies of Catastrophic Hurricanes in Northwestern Florida from Lake Sediment Records, Florida. Quaternary Research, 54 (2). 238-245.

Liu, K. B. and Fearn, M.L. 2000b. Holocene history of catastrophic hurricane landfalls along the Gulf of Mexico coast reconstructed from coastal lake and marsh sediments. *In* Current Stresses and Potential Vulnerabilities, Implications of Global Change for the Gulf Coast Region of the United States. Z. H. Ning and Abdollahi, K. (eds.), Baton Rouge, Franklin Press. 38-47.

Liu., K. B. 2004. Paleotempestology; principles, methods and examples from Gulf coast lake sediments. *In* Murnane, R. J. and Liu., K. B. eds. Hurricanes and Typhoons; Past, Present and Future. New York: Colubia University Press. 13-57.

Lockley, M. G., Young, B. H. and Carpenter, K. 1982. Hadrosaur locomotion and herding behavior: evidence from footprints in the Mesaverde Formation Grande Mesa Coal Field, Colorado. The Mountain Geologist. Vol. 20. (1). 5-14.

Lopez-Martin, N., Moratall, J. J., and Sanz., J. L., 2000. Dinosaurs nesting on tidal flats. Paleogeography, Paleoclimatology, and Paleoecology, (160), 153-163.

Lubkin, S. R. 1997. On pattern formation in reptilian dentition: Journal of Theoretical Biology, (186), 145-157.

Lucas, S. G. and Sullivan, R. M. 2003. A new crocodyliform from the Upper Cretaceous of the San Juan Basin, New Mexico. N. Jb. Geol. Palaont. Mh. 109-119.

Ludvigson, G. A., Gonzalez, L. A., Metzger, R. A., Witzke, B. J., Brenner, R. L., Murillo, A. P., and White, T. S. 1998. Meteoric spahaerosiderite lines and their use for paleohydrology and paleoclimatology. Geological Society of America. Geology, 26 (11), 1039-1042.

Lull, R. S. and Wright, N. E. 1942. Hadrosaurian Dinosaurs of North America. Geological Society of America Special Papers 4, 1-239.

Lutterschmidt, W. I., and Wasko, D. K. 2006. Seasonal activity, relative abundance and size class structure of the American Alligator (Alligator mississippiensis) in a highly distrubed inland lake. The Southwestern Naturalist, 51 (3), 346-351.

Lyman, R. L. and Fox, G. L. 1989. A critical evaluation of bone weathering as an indication of bone assemblage formation: Journal of Archaeological Science, (16), 293-317.

Mack, G. H., James, W. C., and Monger, H. C. 1993. Classification of Paleosols. Geological Society of America Bulletin, (105), 129-136.

MacNeal, D. L. 1958. The Flora and Fauna of the Upper Cretaceous Woodbine Formation Sand in Denton County, Texas. Monographs of the Academy of Natural Sciences of Philidelphia. 1-152.

Maddison, W. P. and Maddison D. R. 2011. Mesquite: A modular system for evolutionary analysis. Version 2.75. http://mesquiteproject.org

Magnusson, W. E., Vliet, K. A., Pooley, A. C., and Whitaker, R. 1999. Crocodile Reproduction. *In* Crocodiles and Alligators. Ross, C. A. (ed.) Facts on File, New York. 118-135.

Main, D. J. and Fiorillo, A. R. 2003. Report of new Cenomanian Hadrosaur (Dinosauria: Ornithischia) post crania from the Woodbine Formation of North Texas. Journal of Vertebrate Paleontology Supplement, 3 (23), 32.

Main, D. J. 2004. New Archosaur Sites in the Cenomanian Woodbine Formation of North Texas: The Discovery of Arlington's First Dinosaur. Geological Society of America Abstracts with Programs. 36 (1), 5.

Main, D. J. 2005. Paleoenvironments and Paleoecology of the Cenomanian Woodbine Formation of Texas: Paleobiogeography of the Hadrosaurs (Dinosauria: Ornithischia). Unpublished Masters Thesis. 1-304.

Main, D. J., 2009. Delta plain environments and ecology of the Cretaceous (Cenomanian) Woodbine Formation at the Arlington Archosaur Site, North Texas, Geological Society of America, Abstracts with Programs, 41 (7), 103.

Main, D. J. and Fry. R. 2009. Preliminary report of a new dinosaur tracksite in the

Lower Cretaceous of Parker County, North Central Texas. Main, D. J. (ed.) Occassional Papers of the Dallas Paleontological Society, (8), 35-47.

Main, D. J. 2010. Delta Plain Bloat and Float Taphonomy in the Cretaceous (Cenomanian) Woodbine Formation at the Arlington Archosaur Site Dinosaur Quarry, North Texas. Geological Society of America Abstracts with Programs, 42 (2), 40.

Main, D. J., Noto, C. R., and Scotese, C. R. 2010. Coastal Cretaceous Forest Fires, Paleosols, Dinosaur Paleoecology from the Arlington Archosaur Site, North Texas. Geological Society of America Abstracts with Programs. Vol. 42. No 5. Pp. 175.

Main, D. J. and Fry, R. 2011. Excavating Cretaceous Crocodyliforms from the Woodbine Formation (95 Mya) at the Arlington Archosaur Site; a North Texas Crocorama. Occasional Papers of the Dallas Paleontological Society, Main, D. J. (ed.), (9), 61-73.

Main, D. J., Noto, C. R., Weishampel, D. B., and Scotese, C. R. 2011. New Basal Hadrosauroid Postcrania from the Cretaceous (Cenomanian) Woodbine Formation at the Arlington Archosaur Site, North Texas. The Royal Tyrrell Museum of Paleontology Hadrosaur Symposium. 81-86.

Main, D. J., D. Parris, B. Grandstaff, and B. Carter. 2012. A New lungfish (Dipnoi:Ceratodontidae) from the Cretaceous Woodbine Formation,

Arlington Archosaur Site, North Texas. Texas Journal of Science, (56), 112-126.

Main, D. J., Noto, C. R., and Drumheller, S. K. 2012b. Crocodiles of the Texas Cretaceous: The Campanian of Big Bend to the Cenomanian of North Central Texas, a Comparison of Great Size, Feeding Behavior and Paleoecology. Geological Society of America Abstracts with Programs. 44 (1), 3.

Main, D. J., Noto, C. R., Drumheller, S. K., and King, L. 2013. Coastal Plain Paleoecology, an Example of Crocodyliform Feeding Grounds from the Cretaceous Woodbine Formation of North Texas. Geological Society of America Abstracts with Programs. 45 (3), 69.

Maisey, J. G. 1982b. The anatomy and interrelationships of Mesozoic hybodont sharks. American Museum of Natural History Noviates, 2724, 1-48.

Marsagalia, K. M. and Klein, G. D. 1983. The Paleogeography of Paleozoic and Mesozoic Storm Depostional Systems. The Journal of Geology, 91 (2), 117-142.

Martin, M. 1980. Revision of *Ceratodus concinnus*. Plieninger. Stuttgarter Beitrage zur Naturkunde (B) 56, 15.

Martin, M., Signogneu-Russel, D., Coupatez, P., and Wouters, G. 1981. Les Ceratodontides (Dipnoi) du Rhetien de Saint-Nicolas-de-Port (Meurthe-et-Moselle). Geobios 14, 773–791.

Martin, M. 1982a. Nouvelles donnee sur la phylogenie et la systematique des Dipneustes Postpaleazoiques, Consequences stratigraphiques et paleogeographiquea. Geobios Memoire Special 6, 53-64.

Martin, M. 1982b. Nouvelles donnes sur la phylogenie et la systematique des Dipneustes Postpaleazoiques, C.R. Academie Sciences Paris, (II) 294, 611-614.

Martin, M., 1984. Revision des arganodontides et des neoceratodontides (Dipnoi,Ceratodontiformes) du Cretace africain. Neues jahrbuch geologische und paleontologishe abhangen. (169), 225-260.

Martin, R. E. 1999. Taphonomy a Process Approach. Cambridge Paleobiology Series 4. Cambridge University Press. 1-508.

Maryanska, T. and Osmolska, H. 1984. Postcranial Anatomy of *Saurolophus angustirostris* with comments on other hadrosaurs. Paleontologia Polonica, (46), 119-141.

Mawamba, M. J. and Torres, R. 2002. Rainfall effects on marsh sediment redistribution North Inlet, South Carolina, USA. Marine Geology, (189), 267-287.

McCloskey, T. A. and G. Keller. 2009. 5000 year sedimentary record of hurricane strikes on the central coast of Belize. Quaternary International (195); 53–68.

McDonald, A. T., Wolfe, D. G., and Kirkland, J. I., 2010, A new basal hadrosauroid (Dinosauria: Ornithopoda) from the Turonian of New Mexico: Journal of Vertebrate Paleontology, 30 (3), 799-812.

McDonald, A. T., Kirkland, J. I., DeBlieux, D. D., Madsen, S., Cavin, J., Milner, A. R. C., Panzarin, L. 2010. New Basal Iguanodonts from the Cedar Mountain Formation of Utah and the Evolution of Thumb Spiked Dinosaurs. PLoS One, 5 (11). E 14075. 1-35.

McDonald, A. T.; Bird, J. Kirkland, J. I., and Dodson, P. 2012. Osteology of the basal hadrosaouroid *Eolambia caroljonesa* (Dinosauria: Ornithopoda) from the Cedar Mountain Formation of Utah. PLoS One, 1-86.

McKenna, M. C., 1962, Collecting small fossils by washing and screening: Curator: The Museum Journal, (5), 221-235.

McNulty, C. L. and Slaughter, B. H. 1962. A New Sawfish from the Woodbine Formation (Cretaceous) of Texas, Copeia, 775-776.

McNulty, C. L. and Slaughter, B. H. 1968. Fishbed conglomerate fauna, Arlington Member, Woodbine Formation (Cenomanian) of Texas. Fieldtrip Guidebook, South-Central Section, Stratigraphy of the Woodbine Formation, Tarrant County, Texas. The Geological Society of America, 68-73.

Mead, J., Cubero, R., Zamora, A., Swift, S., Laurito, C., and Gomez, L. 2006. Plio

Pleistocene *Crocodylus* (Crocodylia) from southwestern Costa Rica: Studies on Neotropical Fauna and Environment, (41), 1-7.

Messel., H. and Vorllcek, G. 1989. Ecology of *Crocodylus porosus* in Northern Australia. *In* Crocodiles: Their Ecology, Management and Conservation. Special Publications of the Crocodile Specialist Group, ICUN Publications. 164-183.

Mikulas, R., Kadlecova, E., Fejfar, O., and Dvorak, Z. 2006. Three new ichnogenera of biting and gnawing traces on reptilian and mammalian bones: a case study from the Miocene of the Czech Republic: Ichnos, (13), 113-127.

Milàn, J., Kofoed, J., and Bromley, R. G., 2010, Crocodylian-chelonian carnivory: bite traces of dwarf caiman, *Paleosuchus palpebrosus*, in red-eared slider, *Trachemys scripta*, carapaces *In* Milàn, J., Lucas, S.G., Lockley, M.G., and Spielmann, J.A., (eds.), Crocodyle tracks and traces, Albequerque, New Mexico Museum of Natural History & Science, (51), 195-199.

Milner, A. R. C., Harris, J. D., Lockley, M. G., Kirkland, J. L., and Matthews, N. A. 2009. Bird-like anatomy, posture, and behavior revealed by an Early Jurassic theropod dinosaur resting trace: PLoS ONE, (4), e4591.

Muller, J. 1845. Memoire sure les ganoides et sur la classification des Poissons: Annales des Sciences Naturelles, 603-607.

Mook, C. C. 1942a. *Anglosuchus*, a new genus of Teleosauroid Crocodilians. American Museum Novitates, (1217), 144-145.

Mook, C. C. 1964. A New Species of Goniopholis from the Morrison of Oklahoma. Contriburtions to the Osteology, Affinities and Distribution of the Crocodilia. (48), 283-287.

Njau, J. K. 2006. The relevance of crocodiles to Oldowan hominin paleoecology at Olduvai Gorge, Tanzania: Ph.D Dissertation, Rutgers, The State University of New Jersey, New Brunswick. 1-347.

Njau, J. K., and Blumenschine, R. J., 2006, A diagnosis of crocodile feeding traces on larger mammal bone, with fossil examples from the Plio-Pleistocene Olduvai Basin, Tanzania: Journal of Human Evolution, (50), 142-162.

Nopsca, F.V., 1902, Ueber das Vorkommen der Dinosaurier von Szentpéterfalva: Zeitschrift der deutschen geologischen Gesellschaft, (54), 34-39.

Norman, D. B. 2004. Basal Iguanodontia. Weishampel, P. Dodson, and H. Osmolska (eds.), *In* The Dinosauria 2nd edition, University of California Press, Berkeley. 438- 463.

Norman, D. B. 2002. On Asian ornithopods (Dinosauria: Ornithischia). 4. *Probactrosaurus* Rozhdestvensky, 1966. Archosaurian anatomy and paleontology. Essays in memory of Alick D. Walker. Norman, D. B. and

Glower, D. J. (eds). Zoological Journal of the Linnean Society. (36), 113-144.

Norman, D. B. 1980. On the Ornithischian Dinosaur *Iguanodon bernissarartensis* from the Lower Cretaceous of Bernissart Belgium. Institut Royal des Sciences Naturalles de Belgique Memoire 178, 1-99.

Norell, M. A., Clark, J. M. Chiappe, L. M., and Dashzeveg, D. 1995. A nesting dinosaur. Nature, (378), 774-776.

Noto, C. R., Main, D. J., Moore, T., Scotese, C. R., and Goswami, A. 2010. Untangling the relationship between climate and biodiversity in Mesozoic terrestrial vertebrates. Geological Society of America Abstracts with Programs 44 (5), 173.

Noto, C. R.. Drumheller, S. K., Main, D. J., and Allen, E. R. 2011. Life and Death in a Cretaceous Coastal Swamp: Example from the Woodbine Formation of Texas. Journal of Vertebrate Paleontology, Supplement, 46.

Noto, C. R., Main, D. J., and Drumheller, S. R. 2012. Feeding Traces and Paleobiology of a Cretaceous (Cenomanian) Crocodyliform: Example from the Woodbine Formation of Texas. Palaios, 27 (2), 105-115.

Noto, C. R. and Main, D. J., In review, Paleoecologic and paleobiogeographic implications of new theropod material from the Cretaceous (Cenomanian) Woodbine Formation of North Central Texas. PLoS One.

Novacek, M., Norell, M. McKenna, M. C., Clark, J. 1994. Fossils of the Flaming

Cliffs. Scientific American, 271 (6), 60-69.

Ogden, J. C. 1978. Status and Nesting Biology of the American Crocodile, *Crocodylus acutus*, (Reptilia, Crocodilidae) in Florida. Journal of Herpetology. 12 (2) 183-196.

Oliver, W. B. 1971. Depositional systems within the Woodbine Formation (Upper Cretaceous), northeast Texas: Reports of Investigations. Bureau of Economic Geology. The University of Texas at Austin, 73, 1-28.

Osborn, H. F. 1905. *Tyrannosaurus* and other Cretaceous carnivorous dinosaurs. Bulletin of the American Museum of Natural History, (21), 259-265.

Ostrom, J. H. 1961. A New Species of Hadrosaurian Dinosaur from the Cretaceous of New Mexico. Journal of Paleontology, 35 (3), 575-577.

Owen, R. 1841, On British fossil reptiles: Report of the British Association for the Advancement of Science, (11), 60-204.

Owen, R. 1878, Monograph of the fossil Reptila of the Wealden and Purbeck Formations. Supplement IX (Goniopholis, Petrosuchus, and Suchosaurus). Paleontological Society Monographs, London, (32), 1-15.

Palangues, A., Guillen, J., Puig, P., and Madron X. D. 2008. Storm driven shelf to canyon suspended sediment transport at the southwestern Gulf of Lions. Continental Shelf Research, 1947-1966.

Parks, W. A. 1920. The Osteology of the Trachodont Dinosaur *Kritosaurus*

incurvimanus. Univ. of Toronto Geol. Series, (11), 1-72.

Pardo, J. D., Huttenlocker, A. K., Small, B. J., and Gorman, M. A. II. 2010 The cranial morphology of a new genus of lungfish (Osteichthyes: Dipnoi) from the Upper Jurassic Morrison Formation of North America. Journal of Vertebrate Paleontology 30 (5), 1352-1359.

Parris, D. C., Grandstaff, B. S., and Gallagher, W. B. 2004. A Lungfish (Dipnoan) from the Upper Cretaceous of New Jersey. The Mosasau, 65-68.

Parris, D. C. Grandstaff, B., and Banks, N. T. 2007. Dental function in lungfishes (Ceratodontidae) from the Cretaceous of North Texas. Journal of Vertebrate Paleontology, 127A.

Parris, D. C., Grandstaff, B. S., and Banks, N. T. *In press.* Lungfishes from the Trinity Group (Cretaceous) of North Texas. Texas Journal of Science.

Paul, G. S. 2007. Turning the Old into the New: A Separate Genus for the Gracile Iguanodont from the Wealden of England. *In* Carpenter, K. (ed.), Horns and Beaks, Ceratopsian and Ornithopod Dinosaurs. Indiana University Press. 69-77.

Pepper, D. A. and Stone, G. W. 2004. Hydrodynamic and sedimentary response to two contrasting winter storms on the inner shelf of the northern Gulf of Mexico. Marine Geology, (210), 43-66.

Pettijohn, F. J. 1957. Nonclastic Sediments (Excluding Limestones). *In*

Sedimentary Rocks. Harper & Brothers, NY. 470-492.

Peyer, K. 2006. A Reconsideration of *Compsognathus* from the Upper Tithonian of Canjuers Southeastern France. Journal of Vertebrate Paleontology, (26), 879-896.

Poole, D. F. G. 1961. Notes on tooth replacement in the Nile crocodile *Crocodilus niloticus*: Proceedings of the Zoological Society of London, (136), 131-140.

Poole, K. E. 2008. A New Specimen of Iguanodontian Dinosaur from the Cedar Mountain Formation, Grand County, Utah. Unpublished Masters Thesis. Washington University. 1-62.

Pooley, A. C. 1999. Food and Feeding Habits. *In* Crocodiles and Alligators. Ross, C. A. (ed) Facts on File. New York. 76-91.

Potts, R. 1986. Temporal span of bone accumulations at Olduvai Gorge and implications for early hominid foraging behavior: Paleobiology, (12), 25-31.

Poyato-Ariza, F. J. and Wenz, S. 2002. A new insight into pycnodontiform Fishes. Geodiversitas, 24 (1), 139-248.

Preito-Marquez, A. 2007. Postcranial Osteology of the Hadrosaurid Dinosaur *Brachylophosaurus canadensis* from the Late Cretaceous of Montana. *In* Carpenter, K. (ed.), Horns and Beaks, Ceratopsian and Ornithopod Dinosaurs. Indiana University Press. 91-115.

Prieto-Márquez, A., Gaete, R., Rivas, G. Galobart, A., and Boada, M. 2006.

Hadrosauroid dinosaurs from the Late Cretaceous of Spain: *Pararhabdodon isonensis* revisited and *Koutalisaurus kohlerorum*, gen. et sp. nov. Journal of Vertebrate Paleontology, (26), 929–943.

Pritchard, D. W. 1967. What is an estuary: physical standpoint? *In* Lauff, G. H. (ed), Estuaries, Washington D.C., American Association for the Advancement of Science, Publication 83, 3-5.

Prothero, D. P. 1990. Coastal Environments. *In* Interpreting the Stratigraphic Record. The W. H. Freeman Series in the Geological Sciences. 75-101.

Prothero, D. 1998. Paleoecology, *In* Bringing Fossils to Life; An Introduction to Paleobiology. McGraw Hill. 118-147.

Ralston, D. K. and Stacey, M. T. 2007. Tidal and meteorological forcing of sediment transport in tributary mudflat channels. Continental Shelf Research, (27). 1510-1527.

Reisz, R. R. and Tsuji, L. A. 2006. An articulated skeleton of *Varanops* with bite marks: the oldest known evidence of scavenging among terrestrial vertebrates: Journal of Vertebrate Paleontology, (26), 1021-1023.

Retallack, G. J., Leahy, G. D., and Spoon, M. D. 1987. Evidence from paleosols for ecosystem changes across the Cretaceous/Tertiary boundary in Eastern Montana. Geology, 15 (12), 1090-1093.

Rivera-Sylva, H.E., Frey, E., and Guzmán-Gutiérrez, J.R., 2009, Evidence of predation on the vertebra of a hadrosaurid dinosaur from the Upper

Cretaceous (Campanian) of Coahuila, Mexico: Carnets de Géologie/Notebooks on Geology, Letter, (2). 155-159.

Roberts, H. H. 1998. Delta Switching, Early Responses to the Atchafalaya. Journal of Coastal Research, 14 (3), 882-899.

Rogers, R. R., Krause, D. W., and Rogers, K. C. 2003. Cannibalism in the Madagascan dinosaur *Majungatholus atopus*: Nature, (422), 515-518.

Rose, P. J. 2007. A new titanosauriform sauropod (Dinosauria: Saurischia) from the Early Cretaceous of Central Texas and its phylogentic relationships. Paleontologica Electronica. 10 (2). 8-65.

Rowe, T., Cifelli, R. I., Lehman, T. M., and Weil, A. 1992. The Campanian Terlingua Local Fauna with a Summation of the Vertebrates from the Aguja Formation, Trans Pecos Texas. Journal of Vertebrate Paleontology, 12 (4). 472-493.

Russell, D.A. 1970 Tyrannosaurs of the Late Cretaceous of western Canada. National Museum of Natural Sciences, Publications in Palaeontology (1), 1–34.

Sahini, A. 1997. Paleoenvironments of Late Cretaceous dinosaur egg nesting sites of India. Dinofest International. 291-301.

Salgado, L. Coria, R. A., Magalhaes-Ribeiro, C. M., Garrido, A. Rogers, R., Simon, M. E., Arucci, A. B., Curry Rogers, K., Carabajal, A. P., Apesteguia, S., Fernandez, M., Garcia, R. A., and Talevi, M. 2007. Upper

Cretaceous nesting sites of Rio Negro (Salitral Ojo de Agua and Salinas de Trapalco-Salitral de Santa Rosa), northern Patagonia, Argentina. Cretaceous Research, (28), 393-404.

Salisbury, S.W., Molnar, R. E., Eberhand, F., and Willis, P. M. A., 2006, The origin of modern crocodyliforms: new evidence from the Cretaceous of Australia: Proceedings of the Royal Society, (3613), 1-11.

Salisbury, S.W., Willis, P. M., Peitz, S. and Sander, P. M., 1999, The Crocodilian *Goniopholis simus* from the Lower Cretaceous of North Western Germany: Special Papers in Paleontology (60), 121-148.

Sander, P. M., Peitz, C., Gallemi, J., Cousin, R. 1998. Dinosaurs nesting on a beach? Earth and Planetary Sciences. Accademie des Sciences Paris. (337), 67-74.

Sankey, J. T., Standhardt, B. R., and Schiebout, J. A. 2005. Theropod teeth from the Upper Cretaceous (Campanian–Maastrichtian), Big Bend National Park, *In* K. Carpenter (ed.), The Carnivorous Dinosaurs. Indiana University Press, Bloomington, Indiana. 127-152.

Sankey, J. T. 2007. Vertebrate Paleoecology from microsites, Talley Mountain, upper Aguja Formation (Late Cretaceous), Big Bend National Park, Texas. *In* Vertebrate Microfossil Assemblages; their Role in Paleoecology and Paleobiogeography. Sankey, J. T. and Baszio, S. (eds.), 61-77.

Sarachik, E. S. and Cane. M. A. 2010. ENSO effects. *In* The El Nino –Southern Oscillation Phenomenon.Cambridge University Press. 49-60.

Saucier, R.T. 1994. *Geomorphology and Quaternary Geologic History of the Lower Mississippi Valley*. U.S. Army Corps of Engineers Waterways Experiment Station,Vicksburg MS. 1-34.

Sawyger, T. 1981. A study of crocodilian coprolites from Wannagan Creek Quarry (Paleocene-North Dakota), Ichnofossils II, Minnesota. Scientific Publication of the Science Museum, 5(2), 1-29.

Sawyger, T. 1998. Coprolites of the Black Mingo Group (Paleocene) South Carolina. Transactions of the American Philisophical Society. New Series. 88 (4), 221-228.

Schwimmer, D. R. 1997. Late Cretaceous dinosaurs in eastern U.S.A.: A taphonomic and biogeographic model of occurrences. Dinofest International. 203-211.

Schwimmer, D. R. 2002. King of the Crocodylians: the paleobiology of *Deinosuchus*: Bloomington, Indiana University Press, 1-220.

Schwimmer, D. R. and Harrell, S. D. 2010, Trace fossils from both ends of *Deinosuchus*: Late Cretaceous estuarine crocodylian bite marks and coprolites from West Georgia: Geological Society of America Abstracts with Programs, (42), 104.

Scotese, C. R. 2001. Earth History: Cretaceous. Paleomap Project, Department of Geology, University of Texas at Arlington. Available at www.scotese.com. Accessed July 10, 2010.

Scotese, C. R. 2005. Middle Cretaceous (Cenomanian-Turonian) Paleogeographic map-North America. Paleomap Project, Earth Atlas. Unpublished

Scotese, C. R. 2008. Early Cretaceous Paleogeographic and Paleoclimate map.Paleomap-Gandolf Project, Earth Atlas. Unpublished.

Scott, A. C. 2010. Charcoal recognition, taphonomy and uses in paleoenvironmental analysis. Paleogeography, Paleoclimatology and Paleoecology, (164), 11-39.

Seidlitz, W. 1917. Ueber ein Krokodil aus den oligocanen Braunkohlenschichten von camberg a Saale. Jb. Preuss. Geol. Landesanst, (38), 347-367.

Seilacher, A. 2007. "Burrows of Strip Miners" *In* Trace Fossil Analysis. Springer Press. 103-116.

Sereno, P. C., Larsson, H. C. E., Sidor, C. A., and Gado, B. 2001, The Giant Crocodyliform *Sarcosuchus* from the Cretaceous of Africa: Science, (294), 1516-1519.

Shuler, E. W. 1917. Dinosaur Tracks in the Glen Rose Limestone near Glen Rose Texas. American Journal of Science. 4th Ser. XLIV (CXCIV). 294-295.

Simpson, G. G. 1960. The History of Life. *In* Evolution of Life. Tax, S. (ed). University of Chicago Press. (1), 117-180.

Slingerland, R. and Smith, N. D. 2004. River avulsion and their deposits: Annual review of Earth and Planetary Sciences, (32), 257-285.

Smith, N. D., Cross, T. A., Dufficy, J. P., and Clough, S. R. 1989. Anatomy of an avulsion. Sedimentology, (36), 1-23.

Smith, R. L. 1996. Ecology: Its Meaning and Scope. *In* Ecology and Field Biology. Haper Collins College Publishers. 3-14.

Snively, E., Henderson, D. M., and Phillips, D. S. 2006. Fused and vaulted nasals of tyrannosaurid dinosaurs: Implications for cranial strength and feeding mechanics. *Acta Palaeontologica Polonica* 51 (3), 435–454.

Sokolov, M. 1965. Teeth evolution of some genera of Cretaceous sharks and reconstruction of their dentition. Moskovkoe Obshchestvo Ispytatelie Prirody, Biulleten Otodel Geologicheskii, (40), 133-134.

Sollas, W. J. 1881. On a new species of *Plesiosaurus* (*P. Conybeari*) from the Lower Lias of Charmouth; with observations on *P. megacephalus*, Stuchbury and *P. brachycephalus*, Owen. Quarterly Journal of the Geological Society, (37), 440-481.

Steadman, D. W., Franz, R., Morgan, G. S., Albury, N. A., Kakuk, B., Broad, K., Fanz, S. E., Tinker, K., Pateman, M. P., Lott, T. A., Jarzen, D. M., and Dilcher, D. L. 2007. Exceptionally well preserved late Quaternary plant and vertebrate fossils from a blue hole on Abaco, The Bahamas:

Proceedings of the National Academy of Sciences, (104), p. 1989719902, doi: 10.1073/pnas.0709572104.

Stephenson, L. W. 1952. Larger Invertebrate Fossils of the Woodbine Formation (Cenomanian) of Texas. United States Geological Survey Professional Paper 242, 1-211.

Storms, J. E. A., Hoogendoorn, R. M., Dam, R. A. C., Hoitnick, A. J. F., and Kroonenberg, S. B. 2005. Late Holocene evolution of the Mahakam delta, east Kalimantan Indonesia. Sedimentary Geology, 180 (3-4), 149-166.

Stouthhammer, E. and Berendson, H. J. A. 2000. Factors controlling the Holocene avulsion history of the Rhine-Meuse Delta, the Netherlands. Journal of Sedimentary Research, 70 (5). 1051-1064.

Stouthhamer, E. 2001. Sedimentary products of avulsion in the Rhine-Meuse Delta, the Netherlands: Sedimentary Geology, (145), 73-92.

Strawn, M. A. 1997. Alligators, Prehistoric Presence in the American Landscape. Johns Hopkins University Press. Baltimore. 1-227.

Sullivan, R.M. and Lucas, S. G. 2003. *Brachychampsa montana* Gilmore (Crocodylia, Alligatoroidea) from the Kirtland Formation (Upper Campanian), San Juan Basin, New Mexico: Journal of Vertebrate Paleontology, (23), 832-841.

Tappen, M. 1994. Bone weathering in the tropical rain forest: Journal of Archaeological Science, (21), 667-673.

Thulborn, R. A. 1991. Morphology, preservation and paleobiological significance of dinosaur coprolites. Paleogeography, Paleoclimatoogy, Paleoecology, (83), 341-366.

Thurmond, J. 1972. Cartilaginous fishes of the Trinity Group and related rocks (LowerCretaceous) of North Central Texas. Southeast Geology, 13 (4), 207-227.

Thurmond, J. T. 1974. Lower vertebrate faunas of the Trinity Division in North Central Texas. Geosciences and Man, 103-129.

Titus, A. L., Powell, J. D. Roberts, E. M., Sampson, S. D., Pollack, S. L., Kirkland. J. I., and Albright, B. L. 2005 Late Cretaceous stratigraphy, depositional environments, and macrovertebrate paleontology of the Kaiparowits Plateau, Grand Staircase-Escalante National Monument, Utah, *In* Pederson, J. and Dehler, C.M. (eds.) Interior Western United States,Geological Society of America Field Guide 6, 101-128.

Trudel, P. 1994. Strtigtraphic Sequences and Facies Architecture of the Woodbine – Eagle Ford Interval, Upper Cretaceous, North Central Texas. Unpublished Masters Thesis. Tarleton State University. 1-105.

Tornqvist, T. E. and Bridge, J. S. 2002. Spatial variation of overbank aggradation rate and its influence on avulsion frequency; Sedimentology. (49), 891-905.

Turner, A. H. and Buckley, G. A. 2008. Mahajangasuchus insignis (Crocodyliformes: Mesoeucrocodylia) cranial anatomy and new data on the origin of the Eusuchian style palate. Journal of Vertebrate Paleontology, 28 (2), 328-408.

van Breemen, N. 1982. Genesis, morphology, and classification of acid sulfate soils in coastal plains. *In* Kittrick, J. A., Fanning, D. S., and Hossner, L. R. (eds.), Acid Sulfate Weathering. Soil Sci. Soc. Am., Madison, WI, 95–108.

Varrichhio, D., Martin, A., and Katsura, Y. 2007. First trace and body fossil evidence of a burrowing, denning dinosaur: Proceedings of the Royal Society B: Biological Sciences, 1361-1368.

Varricchio, D. J. 2001. Gut contents from a Cretaceous tyrannosaurid: implications for theropod dinosaur digestive tracts: Journal of Paleontology, (75), 401-406.

Vorob'yeva, E. I. and Minikh, M. G. 1968. Experimental application of biometry to the study of ceratodontid dental plates. Paleontological Journal, Washington, 217-227.

Waldman, M. and Hopkins, W. S. 1970. Coprolites from the Upper Cretaceous of Alberta, Canada, with a description of their microflora. Canadaian Journal of Earth Scienc, 7 (1), 295-1,303.

Walker, R. G. 1983. Cardium Formation. Sedimentology and Stratigraphy in the

Garrington-Caroline area. Bulletin of Canadian Petroleum Geology, (31), 213-230.

Walker, R. G. 1984. General introduction to facies, facies sequences and facies models, *In* Walker R. G. (eds.), Facies Models, 2nd Edition. Geological Association of Canada, Geosciences Canada Reprint Series 1, 1-9.

Weigelt, J., 1989. Recent Vertebrate Carcasses and their Paleobiological Implications: Chicago, University of Chicago Press. 1-188.

Weishampel, D. B. and Weishampel, J. B. 1983. Annotated localities if ornithopod dinosaurs:implications to Mesozoic paleobiogeography. The Mosasaur: Journal of the Delaware Valley Paleontological Society. No 1, 43-88

Weishampel, D. B. 1983. Hadrosaurid Jaw Mechanics. Second Symposium on Mesozoic Terrestrial Ecosystems. Paleontologica, 28 (2), 271-280.

Weishampel, D. B and Horner, J. R. 1990. Hadrosauridae, Weishampel, D. B., Dodson, P. and Osmolska, H. (eds.), *In* The Dinosauria, University of California Press, Berkeley. 534- 561

Weishampel, D. B., Norman, D. B., and Grigorescu, D. 1993. *Telmatosaurus transsylvanicus* from the Late Cretaceous of Romania: the most basal hadrosaurid dinosaur. Paleontology, (36), 361-385.

Weishampel, D. B. and Maria Jianu. 2000. Plant eaters and ghost lineages:

dinosaurian herbivory revisited. *In* Evolution of Herbivory in Terrestrial Vertebrates. Hans Dieter Sue (ed). 123-143.

Weishampel, D. B., Jianu. C. M., Csiki, Z, and Norman, D. B. 2003. Osteology and Phylogeny of *Zalmoxes* (N. G.), and unusual Euornithopod Dinosaur from the Latest Cretaceous of Romania. Journal of Systematic Paleontology 1 (2). 65-123.

Weishampel, D. B., Barrett, P. M., Coria, R. A., Loeuff, J. L., Xing, X., Xijin, Z, Sahni, A., Gomani, E., M., P., and Noto, C. R. 2004. Dinosaur Distributions. Weishampel, D., Dodson, P., and Osmolska, H. (eds.), *In* The Dinosauria 2nd edition, University of California Press, Berkeley. 517-606.

Weishampel, D. B. and Jianu, C.-M. 2011. Transylvanian Dinosaurs. Johns Hopkins University Press, Baltimore. 1-301.

Wells, S. M. 2000. Iron concretion formation and diagenesis in the Upper Cretaceous Woodbine Formation of North Central Texas. Masters Thesis, University of Texas at Arlington. 1-88.

Welton, B. J. and Farrish, R. F. 1993. The collectors guide to fossil sharks and rays from the Cretaceous of Texas. Before Time publishing. 1-204.

White, T., Gonzalez, L., Ludvigson, G., and Poulsen, C. 2001. Middle Cretaceous greenhouse hydrologic cycle of North America. Geological Society of America. Geology, 29 (4), 363-366.

Williams, J. J. and Rose, C. P. 2001. Measured and predicted rates of sediment transport in storm conditions. Marine Geology, (179), 121-133.

Wing, S. L., Sues, H.D., Potts, R., DiMichele, W. A., Behrensmeyer, A. K. 1992. Evolutionary Paleoecology. Behrensmeyer, A. K, Damuth, J. D., DiMichele, W. A., Potts, R., Sues, H.D., Wing, S. L. (eds.) *In* Terrestrial Ecosystems through Time, Evolutionary Paleoecology of Terrestrial Plants and Animals. University of Chicago Press. 1-11.

Winkler, D. A., Murray, P. A., and Jacobs, L. J. 1990. Early Cretaceous (Comanchean) Vertebrates of Central Texas. Journal of Vertebrate Paleontology, (10), 95-116.

Winkler, D. A., Jacobs, L. L., Lee, Y. N., and Murray, P. A. 1995. Sea Level Fluctuation and Terrestrial Faunal Change in North-Central Texas. Sixth Symposium on Mesozoic Terrestrial Ecosystems and Biota. Ailing Sun and Yuanqing Wang (ed.). 175-177.

Winkler, D. A. and Jacobs, L. L. 2002. Cenomanian vertebrate faunas of the Woodbine Formation, Texas. Journal of Vertebrate Paleontology, (22), 120A.

Wright, J. L. 1999. Ichnological evidence for the use of the forelimb in iguanodontid locomotion, Cretaceous Fossil Vertebrates, 209-219.

Wolfe, A. P., Csank, A. Z., Reyes, A. V., McKellar, R. C., Tappert, R., and

Muehlenbachc, K. 2012. Pristine Early Eocene Wood Buried Deeply in Kimerlite from Northern Canada. PLoS One, 7 (9), 1-8.

Wu, X.-C., Brinkman, D. B., and Russell, A. P., 1996a, *Sunosuchus junggarensis* sp. nov. (Archosauria: Crocodyliformes) from the Upper Jurassic of Xinjiang, Peoples Republic of China: Canadian Journal of Earth Sciences, (33), 606-630.

Wu, X.-C., Russell, A. P. and Cumbaa, S. L., 2001, *Terminonaris* (Archosauria: Crocodyliformes): New Material from Saskatchewan, Canada and comments on its Phylogenetic Relationships: Journal of Vertebrate Paleontology, (21), 492-514.

Yang, B., Dalrymple, R. W. and Chun. S. 2006. The Significance of Hummocky Cross Stratification (HCS) wavelengths; evidence from an open coast tidal flat, South Korea. Journal of Sedimentary Research, (76), 2-8.

Zangerl, R. 1969. The Turtle Shell. Bulletin of the Field Museum, Chicago Press. 309-324.

Zanno, L. E. and Mackovicky, P. J. 2011. On the earliest record of Cretaceous tyrannosauroids in western North America: implications for an Early Cretaceous Laurasian interchange event. Historical Biology, (23), 317-325.

BIOGRAPHICAL INFORMATION

Derek Jason Main was born in Irving, Texas on August 8, 1971 to Norman and Jannie Main. Attending public school in Irving, he graduated from Mac Arthur High in 1989. He began college in 1989 at Northlake College in Irving, but left school to pursue a career in music. After a brief career as a musician (guitar player), he later attended Collin College in 1994. While there, he worked in the schools science labs and developed interest in geology while working with the schools rock, mineral and fossil collections.

In 1997 he transferred to the University of Texas at Dallas and declared his major as geology. As an undergraduate, he participated in the schools *Alamosaurus* excavation in Big Bend National Park. Working in Big Bend, he became fascinated with paleontology. He worked as a field assistant in Big Bend until his senior year and became a T.A. for the Age of Dinosaurs course. As an undergraduate, his involvement in the UTD Big Bend *Alamosaurus* project led to a part time fossil preparator position. He worked on *Alamosaurus* fossils at the Dallas Museum of Natural History under the guidance of preparator Geb Bennett and curator Dr. Tony Fiorillo. His experiences with *Alamosaurus* led to an interest in the sauropod dinosaurs and to a second part time job, at the Shuler Museum of Paleontology at SMU. While there, he worked on *Paluxysaurus* fossils under the guidance of preparator Kent Newman and curator Dr. Louis Jacobs.

After graduating with bachelors degree in Geology in 2001, he published his first paper and accepted a full time position in the Paleontology Dept. at the Dallas Museum of Natural History. In 2003 he began graduate work with Dr. Christopher R. Scotese at the University of Texas at Arlington. During his first year at UTA, a dinosaur was discovered in Arlington, and almost immediately became part of his graduate thesis. He completed his Masters in Geology in 2005, with a thesis on the Woodbine Formation and a discussion of dinosaurs found in Arlington and Grapevine. The Arlington dinosaur site later came to be known as the Arlington Archosaur Site, and led to a doctoral project following completion of his master's thesis work. While at UTA, he taught lecture courses on Dinosaurs, Earth History and Earth Systems and led his students on regular field trip-excavations to the Arlington Archosaur Site.

With the support of Dr. Scotese, the former UTA Paleomap Project computer lab room was converted into a fossil prep paleo lab and a portion of the Geology Dept. collections room was set aside for the AAS collection. Over the course of his doctoral work, Derek managed the AAS Paleo Lab, organizing volunteer projects and also worked as the AAS collections manager. The UTA-AAS volunteer program was largely responsible for the success of the AAS project that led to a doctorate. Derek is a strong supporter of science public outreach and programs that bridge the divide between scientists and the public.

Derek getting covered in his work at the AAS, standing at the edge of the Dino Quarry in the opening year of excavations; 2008.

Derek with his AAS project colleagues Chris Noto (middle) and Geb Bennett (left) at the AAS in the summer 2012.